
**Distribution and abundance of Larvaceans in the
Southern Ocean**

By
Margaret Caroline Murray LINDSAY
BSc. (Env. Mang. & Eco) Hons. GCAS

Submitted in fulfilment of the requirements for the Degree of
Doctor of Philosophy

University of Tasmania

June 2012

Declaration of originality

This thesis contains no material which has been accepted for a degree or diploma by the University or any other institution, except by way of background information and duly acknowledged in the thesis, and to the best of my knowledge and belief no material previously published or written by another person except where due acknowledgement is made in the text of the thesis, nor does the thesis contain any material that infringes copyright.

Margaret CM Lindsay
June 2012

Statement of authority of access

This thesis may be made available for loan and limited copying in accordance with the *Copyright Act 1968*.

Margaret CM Lindsay
June 2012

Statement regarding published work contained in the thesis

The publishers of the papers comprising Chapter 5 hold the copyright for that content, and access to the material should be sought from the respective journals. The remaining non published content of the thesis may be available for loan and limited copying in accordance with the Copyright Act 1968.

Margaret CM Lindsay
June 2012

Statement of co-authorship

The following people and institutions contributed to the publication of the work undertaken as part of this thesis:

Chapter 5: Distribution and abundance of Larvaceans in the Southern Ocean between 30° and 80°E. Published in *Deep-Sea Research II* **57** (2010) 905–15

Margaret Lindsay (candidate and first author) (70 %) and Guy Williams (co-author) (30 %) of the Institute of Low Temperature Science, Hokkaido University, Sapporo, Japan.

The author's roles were the candidate, Margaret Lindsay, developed the idea, completed the papers formalisation and development, completed the sampling and data analysis and also completed the refinement and presentation. Guy Williams (co-author) contributed to the papers formalisation and development and assisted with refinement and presentation.

We the undersigned agree with the above stated “proportion of work undertaken” for the above published peer-reviewed manuscripts contributing to this thesis.

Prof Thomas Trull
Supervisor
Institute for Marine and Antarctic Studies
University of Tasmania

Craig Johnson
Head of School
Institute for Marine and Antarctic Studies
University of Tasmania

September 2011

Abstract

Larvaceans (also known as appendicularians) are zooplankton that inhabit most oceans, coastal waters and estuaries, and are often found in abundances that are second only to copepods among the meso-zooplankton. They form a gelatinous “house” through which they circulate seawater to filter very small particles onto mucopolysaccharide mesh. This concentrates sub-micron and micron-sized protists to 100 -1000 times the ambient concentrations. The house is discarded when the mesh clogs which can occur several times per day. These contribute significantly to the large particles of marine detritus known as “marine snow”. In addition, larvaceans form tightly compacted, rapidly sinking faecal pellets that contribute to carbon “export” from surface waters. Thus larvaceans play a rather unusual role in marine microbial food-webs, by transferring matter across many orders of magnitude in organism size, and moving it into the ocean depths.

Previously there was little known about larvaceans in the Southern Ocean. The aims of this study were to increase the knowledge of the ecological role of the larvaceans species: by first determining their distribution and abundance in the Sub-Antarctic Zone (SAZ), Southern Oceans Permanently Open Ocean Zone (POOZ) and the Sea Ice Zone (SIZ) and secondly, by determining the diet of Southern Ocean larvaceans.

Larvaceans were collected during four Southern Ocean marine science voyages between 2006 and 2008 which surveyed the different zones through different seasons in the East Antarctic sector of the Southern Ocean. Larvaceans were collected using a number of sampling devices; a purpose-built ring net, Rectangular Mid-Water Trawl (RMT1), Working Party 2 (WP2) net, HYDRO-BIOS MultiNet, Visual Plankton Recorder (VPR) and the Continuous Plankton Recorder (CPR).

Larvacean distributions were complex. A significant fraction of the net hauls (55%) contained no specimens, while others obtained high abundances (maximum

57.8 ind. m⁻³). The average abundances of larvaceans from the variety of nets used were 1.4 ± 5.4 ind. m⁻³, and for the CPR were 6.4 ± 29.7 ind. m⁻³. The surveys revealed that for the period of this study larvacean abundances varied between the Southern Ocean zones with the lowest abundances in the SAZ (0.6 ± 2.6 ind. m⁻³, maximum = 15.9 ind. m⁻³), highest in the POOZ (2.8 ± 10.6 ind. m⁻³, maximum = 57.8 ind. m⁻³) and 1.4 ± 4.8 ind. m⁻³ (maximum = 49.7 ind. m⁻³) in the SIZ.

Possible controls on larvacean distributions were evaluated by comparing them to physical (latitude, longitude, water temperature, salinity, light and sea-ice) and biological (chlorophyll and total zooplankton) distributions. Significant correlations occurred with physical parameters of latitude, longitude, fluorescence, irradiance, water temperature and salinity and the biological distributions of other Southern Ocean zooplankton.

The diet of the Southern Ocean larvacean was determined using scanning electron microscopy (SEM) and stomach dissections from the samples collected from the ring net during January to March 2006. Protists ranging from 3.5 µm – 240 µm were the main food items. By considering the alignment and sizes of the largest ingested protist, *Corethron pennatum*, the inferred feeding house mesh size was 5 - 82 µm.

From this study Southern Ocean larvaceans were estimated to contribute ~10.5 million tonnes of (wet) biomass to the Southern Ocean. Comparing this to the ~250 million tonnes of copepods, which are considered to be a keystone taxon, emphasizes the need to consider the importance of larvaceans to Antarctic food webs.

Key words

Larvaceans, Appendicularians, Southern Ocean, Sub-Antarctic Zone (SAZ), Permanent Open Ocean Zone (POOZ), Sea Ice Zone (SIZ), Diet, Biomass, Carbon contribution.

Acknowledgements

A huge thanks is required for my supervisors Professor Tom Trull, Dr Graham Hosie and Dr Simon Wright – this would not have been possible without your guidance.

Thankyou.

A high level of appreciation goes to the following organisations for the logistical support provided by the Australian Antarctic Division (AAD), Kingston; Institute for Marine and Antarctic Studies (IMAS) (previously the Institute of Antarctic and Southern Ocean Studies (IASOS)), Hobart; University of Tasmania (UTas), Hobart; and the Antarctic Climate and Ecosystems Cooperative Research Centre (ACE CRC), Hobart.

The officers, crew and cadets on RSV *Aurora Australis* and TS *Umitaka Maru*, the Marine Science Support at AAD – especially Aaron Spurr, Tony Veness, Alan Poole Marine Science Voyage management and my fellow expeditioners, require special mention as without their support the successful voyages that made this a successful doctorate, would not have happened let alone been as enjoyable as they were.

The officers, crew and cadets and CEAMARC researchers on the TS *Umitaka Maru*, especially Graham Hosie, Russ Hopcroft, Dhugal Lindsay, Andrea Walters, Jean Henri and Veronica Feuntes. This voyage was made possible thanks to the International Antarctic Institute and ACE CRC travel funding.

This study would have been impossible without financial support from an Australian Postgraduate Award (UTas) and Antarctic Climate and Ecosystems Cooperative Research Centre (ACE CRC) Top-Up. The project was also supported in kind by the Australian Antarctic Division.

Thanks also goes to other key academics and scientist for their support, including, Mark Curren, Patti Virtue, Guy Williams, Karen Westwood, Steve Candy, Simon Wotherspoon, Imojen Pierce, Russ Hopcroft, Brian Griffiths, Will Howard, Andrew Moy, Donna Roberts, David McLeod, Gerry Nash, Fiona Scott, Rob King and all those that have assisted in all the ways they could.

Finally, though far from the least, my friends and relatives are thanked for remaining both friendly and related throughout the PhD journey. Especially those that were involved with insuring I remained sane enough to continue the PhD journey including my mum, Alice and my best friend and partner, Aaron, fellow students and work colleagues and all those that I have shared many adventures and cups of tea, coffee and chai with.

The deepest thanks to each and every one of you.

Margaret CM Lindsay
June 2012

“Did you know the word plankton comes from the Greek for ‘born to wander’?” he said.

I owned up to my ignorance.

“I think that is why I love the little things. They’ve got the lifestyle I’d like to adopt: wandering the seas.”

‘Plankton, huh?’

“Sure! Give me the squidgy goey things every time. Whales get all the glory. I like the proletariat of the food chain, those amorphous gelatinous things that everybody ignores. They’re fascinating.”

Roff Smith
(2002)

Life on the Ice

- *No one goes to Antarctica Alone*

Table of Contents

Title page	i
Authorship	ii
Abstract	iv
Acknowledgment and quote	vi
Table of contents	viii
List of figures	xii
List of tables	xxvi
List of appendices	xxxii
<hr/>	
1. Introduction	1
<hr/>	
1.1 Introduction	1
1.2 History of larvacean studies	2
1.3 Taxonomy	4
1.4 Form, life cycle and function	5
1.5 Ecological role	7
1.6 Distribution and abundance	8
1.7 Hypothesis and aims	11
1.8 Structure of this study	12
<hr/>	
2. Study regions and voyages	14
<hr/>	
2.1 Oceanography of the Southern Ocean	14
2.2 Southern Ocean larvacean zones	28
2.3 Survey regions	28
2.4 Purpose and structure of the voyages	31
2.4.1 BROKE-West	31
2.4.2 SAZ-Sense	33
2.4.3 SIPEX	35
2.4.4 CEAMARC – Pelagic	36
<hr/>	
3. Identification of Southern Ocean larvaceans	38
<hr/>	
3.1 Introduction	38
3.2 Methods	44
3.3 Results	47
3.3.1 BROKE-West	47
3.3.2 SAZ-Sense	49
3.3.3 SIPEX	49
3.3.4 CEAMARC-Pelagic	49
3.4 Discussion	51

4. Large-scale distribution patterns determined from the CPR	54
4.1 Introduction	54
4.2 The Continuous Plankton Recorder (CPR)	54
4.3 Existing but limited CPR data	57
4.4 Extended CPR data	59
4.5 Results	60
4.5.1 SO-CPR Survey distribution and abundance maps	60
Annual distribution and abundance of Southern Ocean Larvaceans	60
Seasonal distribution and abundance of Southern Ocean larvaceans	79
4.5.2 Annual and seasonal mean abundances of Southern Ocean larvaceans	91
4.5.3 Annual and seasonal mean abundances of Southern Ocean Zones	95
4.5.4 Relationships between larvaceans and other zooplankton in the Southern Ocean	99
4.5.5 Southern Ocean physical parameters	110
4.5.6 Summary of larvacean distribution and abundance in the Southern Ocean	114
4.5.7 Larvacean CPR database 1991 – 2008 distribution and abundance according to Generalized Additive Mixed Models (GAMM)	114
Methods	117
Results	118
4.6 Discussion	144
4.7 Conclusions from Southern Ocean CPR	149
<hr/>	
5. Distribution and abundance between 30° and 80° E	151
<hr/>	
Distribution and abundance of Larvaceans in the Southern Ocean between 30 and 80 E longitude.	
Lindsay, M and Williams, G., 2010. Deep Sea Research II 57 905-915.	
<i>Preface</i>	151
Abstract	151
Keywords	152
5.1 Introduction	152
5.2 Data and Methods	154
5.2.1 Survey region and large-scale oceanography	154
5.2.2 Sampling	156
5.2.3 Preservation and processing	158
5.2.4 Environmental parameters	159
5.3 Results	160
5.3.1 Distribution and abundances	161
5.3.1.1 Ring net larvaceans across the BROKE-West region	162
5.3.1.2 RMT1 larvaceans across the BROKE-West region	166

5.3.1.3 CPR larvaceans across the Southern Ocean	170
5.3.2 Statistics	172
5.4 Discussion	174
5. Acknowledgments	181
<hr/>	
6. Fine-scale distribution patterns determined from plankton nets	182
6.1 Introduction	182
6.2 Methods	184
6.2.1 Survey region	184
6.2.2 Plankton nets	185
Ring net	185
Ring net Subantarctic Zone (SAZ)	186
Ring net Permanent open ocean Zone (POOZ)	186
Ring net Sea Ice Zone (SIZ)	187
Rectangular Mid-water Trawl 1+8 (RMT)	187
RMT SAZ	188
RMT SIZ	189
Additional plankton nets and sampling devices	189
Working Party 2 (WP2)	190
HYDRO-BIOS MultiNet	191
Visual plankton recorder (VPR)	192
Continuous Plankton Recorder (CPR)	193
CPR deployment on BROKE-West	193
CPR deployment on SIPEX	194
CPR deployment on CEAMARC	196
6.2.3 Processing and preservation of samples	198
6.2.4 Physical parameters	199
6.2.5 Data analysis	199
6.3 Results	200
6.3.1 Distribution and abundance of larvaceans from SAZ-Sense	200
Diel distribution of larvaceans during SAZ-Sense	204
Stratified distribution of larvaceans during SAZ-Sense	205
Physical and biological parameters during SAZ-Sense	206
6.3.2 Distribution and abundance of larvaceans from BROKE-West	207
Physical and biological parameters during BROKE-West	210
6.3.3 Distribution and abundance of larvaceans from SIPEX	211
Physical and biological parameters during SIPEX	217
6.3.4 Distribution and abundance of larvaceans from	
CEAMARC-pelagic	218
Physical and biological parameters during	
CEAMARC-pelagic	222
6.3.5 Net comparisons	223
6.3.6 Physical and biological parameters of the Southern Ocean	224
6.4 Discussion	225
6.4.1 Summary of distributions and abundances of larvaceans in the	
Southern Ocean	225
6.4.2 Sub Antarctic Zone (SAZ)	228
6.4.3 Permanent Open Ocean Zone (POOZ)	230
6.4.4 Sea Ice Zone (SIZ)	230

6.5 Conclusion	232
<hr/>	
7. Feeding ecology	234
<hr/>	
7.1 Introduction	234
7.2 Background to larvacean feeding and ecology	235
Oikopleurid house and feeding behaviour	235
Fritillariid house and feeding behaviour	239
Kowalevskia house and feeding behaviour	241
Feeding house filters	241
Role in carbon flux	245
Role of larvaceans in the food web	246
7.3 Methods	249
7.3.1 Survey region and sampling device	249
7.3.2. Protist sampling and quantification	251
7.3.3. Sampling, preservation and SEM processing of larvaceans	251
7.3.4 Analysis of stomach and gut contents	252
7.3.5 Larvacean protist comparison to water column protists	252
7.3.6 Inferred mesh size	253
7.4 Results	253
7.4.1 Distribution of marine protists and larvaceans	253
7.4.2 Larvacean diet determined by scanning electron microscopy (SEM)	255
7.4.3 Inferred mesh size	258
7.5 Discussion	260
7.6 Conclusion	263
<hr/>	
8. Conclusions	265
<hr/>	
8.1 Overview	265
8.2 Abundance and distribution of larvaceans	265
8.3 Feeding ecology of larvaceans	268
8.4 Larvacean biomass and grazing estimates, and their possible contribution to carbon fluxes to the ocean interior	269
8.5 Conclusion	276
8.6 Recommendations for future studies	273
<hr/>	
Reference	275
Appendix	287

List of Figures

1. Introduction

Figure 1.1. Family tree showing the three larvacean families (blue) lineage from the Chordata phylum and urochordata subphylum. 4

Figure 1.2. Examples of the three larvacean families; A. Oikopleuridae B. Fritillariidae C. Kowalevskiidae (from Ritz et al. 2003). 5

Figure 1.3. Generalised structure of larvaceans. 1. Feeding house 2. Inlet filter 3. Escape slot 4. Trunk 5. Tail 6. Outlet 7. Filter (adapted from Flood and Deibel 1998). 6

Figure 1.4. Larvaceans carbon contribution and role in the marine ecosystem. 8

Figure 1.5. Global distribution of larvaceans. Data extent map from Ocean Biogeographic Information System Australia / C Square Mapper) (square size 1 degree). [Accessed 12 April 2010] www.iobis.org 10

Figure 1.6. The SCAR-MarBIN Distribution of larvaceans (RAMS 2010) <http://www.scarmarbin.be/AntobisMapper.php> accessed 10 May 2010) 11

2. Study regions and voyages

Figure 2.1. Circumpolar distribution of the Sub-Antarctic Front (SAF), Polar Front (PF) and Southern Antarctic Circumpolar Current Front (ACCF). Also shows the Subtropical Front (STF) and Southern Boundary of the ACC boundary (Orsi et al., 1995). 15

Figure 2.2. A schematic of the meridional overturning circulation in the Southern Ocean showing annual mean wind-stress curl (10^9 dyn cm^{-2}) (Trull et al., 2001). 16

Figure 2.3. Map of the total annual mean subduction (m year^{-1}) show high circumpolar variability The three main fronts (PF, SAF and SAF-N) of the ACC are superimposed as dark lines radiate from the South pole (*). Source: Sallée et al. (2009). 17

Figure 2.4. Map of the mean February and September sea ice, each calculated from 2006-2008 daily AMSR-E satellite data (Spreen et al., 2008). 18

Figure 2.5. Maps of mean monthly ice edge locations in East Antarctica for February 1991 to 1995 and September 1991 to 1994 (Worby et al., 1998). 19

Figure 2.6. Global sea surface temperature from the World Ocean Atlas (WOA). Data produced from the Ocean Climate Laboratory of the National Oceanographic Data Center (U.S., WOA 2005). http://en.wikipedia.org/wiki/World_Ocean_Atlas (accessed 2010) **20**

Figure 2.7. Map of dissolved (a) nitrate and (b) silicate summer average concentrations at 10m. The grey square in the centre is the location of the Southern Ocean Iron Release Experiment (SOIREE) (Trull et al., 2001). **21**

Figure 2.8. Mean chlorophyll distribution in the Southern Ocean averaged over the period from October 1997 to October 2002 (Sokolov and Rintoul, 2007). **22**

Figure 2.9. Mean summer chlorophyll concentrations south of Australia. Mean summer positions of the ACC fronts are also shown and colour – coded to show that the concentrations vary widely in the Southern Ocean (Sokolov and Rintoul, 2007). **23**

Figure 2.10. Climatological (1978 – 1986) seasonal sea surface chlorophyll for the austral seasons; winter (June to August), spring (September to November), summer (December to February) and autumn (March to May). Colour is a log scale for chlorophyll: purple = <0.06 mg Chl m⁻³, orange- red = 1 – 10 mg Chl m⁻³ (Longhurst, 1998). **24**

Figure 2.11. Distribution of principal concentrations of krill (encircled black circles) in relation to the East Wind Drift and Weddell Drift (dashed lines), Polar Front (black lines) and Southern Boundary of the Antarctic Circumpolar Current (ACC) (red line) (Tynan, 1998). **25**

Figure 2.12. Distribution of blue whale catches during January 1931/32 to 1966/67 in relation to the Southern Boundary of the Antarctic Circumpolar Current (ACC) (red line) and the mean monthly extent of sea-ice coverage (blue) for January 1979 to 1987. Grid size for the whale data is 1° latitude and 2° longitude (Tynan, 1998). **26**

Figure 2.13. Distribution and abundance (grams per square metre) of a) whales, b) seabirds and c) Antarctic krill (*Euphausia superba*) off east Antarctica during austral summer, 1996. The BROKE Survey track is indicated (Nicol et al., 2000). **27**

Figure 2.14. Map of the Southern Ocean zones and voyage tracks undertaken to determine the distribution and abundance of larvaceans. The Sub Antarctic Zone (SAZ) was surveyed during SAZ-Sense (green); the Permanent Open Ocean Zone (POOZ) during the westbound leg of the BROKE West voyage (red); the Sea Ice Zone (SIZ) during BROKE-West (red), SIPEX (blue) and CEAMARC (purple). **30**

Figure 2.15. Graph showing ordinal date and latitude for the voyages undertaken to collect larvaceans in the East Antarctic Southern Ocean. BROKE-West (red), SAZ-Sense (green), SIPEX (blue) and CEAMARC (purple). **31**

Figure 2.16. Survey region of the Baseline Research on Oceanography, Krill and the Environment – West (BROKE West) voyage from 2 January to 14 March 2006, aboard RSV *Aurora Australis*. Figure adapted from the Australian Antarctic Data Centre. **32**

Figure 2.17. Map of sample sites and process stations for the Sub-Antarctic Zone – Sensitivity (SAZ Sense) voyage from 17 January to 20 February, 2007, aboard RSV *Aurora Australis*. Figure adapted from the Australian Antarctic Data Centre. **34**

Figure 2.18. Voyage track and sample points for the Sea Ice Physics and Ecosystem eXperiment (SIPEX) from 4 September to 17 October, 2007, conducted aboard RSV *Aurora Australis*. Figure adapted from the Australian Antarctic Data Centre. **35**

Figure 2.19. Sample sites from the Collaborative East Antarctic Marine Census - Pelagic (CEAMARC – pelagic) voyage from 23 January to 17 February, 2008 aboard TRV *Umitaka Maru*. Figure adapted from the Australian Antarctic Data Centre. **37**

3. Identification of Southern Ocean larvaceans

Figure 3.1. Classification of the larvacean families and genera. The number of species per genera is indicated on the right. Parentheses indicate the number of genera including forms (compiled from Fenaux, 1998 and Hopcroft, 2005). **40**

Figure 3.2. Features used to identify larvaceans; 1. tail fin shape 2. trunk shape 3. buccal glands 4. subchordal cells (absence, or quantity and location if present), and scale (adapted from O’Sullivan, 1983). **45**

Figure 3.3. The three larvaceans families; A. Oikopleura B. Fritillaria C. Kowalevskia (from Ritz et al., 2003). **46**

Figure 3.4. Oikopleuridae A. left side view of body B. dorsal view of body C. complete larvacean **2.** Fritillaridae A. left side view of body B. ventral view of body C. tail **3.** Kowaleviskiidae A. right side view of body B. ventral view of body C. complete larvacean (from Fenaux, 1998). **46**

Figure 3.5. *Fritillaria drygalski* A. a. trunk dorsal view, b. tail. (from O’Sullivan 1983) B. Scanning Electron Microscope image (scale bar 100 µm) C. stereo dissecting microscope digital image (scale bar 100 µm). **47**

Figure 3.6. *Oikopleura gaussica* A. a. trunk lateral view, b. tail dorsal view of bend (from O’Sullivan 1983). B. Scanning Electron Microscope image (scale bar 1 mm) C. stereo dissecting microscope digital image (scale bar 1 mm). **48**

Figure 3.7. Larvaceans identified from CEAMARC-Pelagic, A. *Fritillaria borealis* f. *typica* a. trunk dorsal view, b. tail. (from O’Sullivan, 1983) B. *Oikopleura gaussica* a. trunk lateral view, b. tail dorsal view (from O’Sullivan, 1983). C. *Oikopleura vanhoeffeni* a. trunk lateral view, b. tail dorsal view (from Bückmann, 1969). **50**

Figure 3.8. VPR image of *F. borealis* during the CEAMARC-Pelagic voyage. **50**

4. Large-scale distribution patterns determined from the CPR

Figure 4.1. Schematic of CPR unit (from <http://data.aad.gov.au/>) **55**

Figure 4.2. SCAR SO-CPR Survey tows from 1990/91 to 2008. Produced by AAD data centre, published June 2008, SCAR map catalogue No. 13481. **56**

Figure 4.3. CPR atlas map for total near-surface *Oikopleura* sp. Data from 60° E to 160° E in the Southern Ocean and collected through SO-CPR Survey from 1991 to 2008. The abundance scale is relative to the size of the shaded circle representing $\log_{10}(X+1)$ transformed data displayed in 1° latitude and 2° longitude bins (McLeod et al., 2010). **58**

Figure 4.4. CPR atlas map for total near-surface *Fritillaria* sp. Data from 60° E to 160° E in the Southern Ocean and collected through SO-CPR Survey from 1991 to 2008. The abundance scale is relative to the size of the shaded circle representing $\log_{10}(X+1)$ transformed data displayed in 1° latitude and 2° longitude bins (McLeod et al., 2010). **59**

Figure 4.5 A. 1996 – 1997 CPR transects showing abundances of *Oikopleura* sp. (counts per 5 Nm). **62**

Figure 4.5 B. 1996 – 1997 CPR transects showing abundances of *Fritillaria* sp. (counts per 5 Nm). **63**

Figure 4.6 A. 1997 – 1998 CPR transects showing abundances of *Oikopleura* sp. (counts per 5 Nm). **64**

Figure 4.6 B. 1997 – 1998 CPR transects showing abundances of *Fritillaria* sp. (counts per 5 Nm). **65**

Figure 4.7 A. 1999 – 2000 CPR transects showing abundances of *Oikopleura* sp. (counts per 5 Nm). **66**

Figure 4.7 B. 1999 – 2000 CPR transects showing abundances of *Fritillaria* sp. (counts per 5 Nm). **67**

Figure 4.8 A. 2001 – 2002 CPR transects showing abundances of *Oikopleura* sp. (counts per 5 Nm). **68**

Figure 4.8 B. 2001 – 2002 CPR transects showing abundances of <i>Fritillaria</i> sp. (counts per 5 Nm).	69
Figure 4.9 A. 2003 – 2004 CPR transects showing abundances of <i>Oikopleura</i> sp. (counts per 5 Nm).	70
Figure 4.9 B. 2003 – 2004 CPR transects showing abundances of <i>Fritillaria</i> sp. (counts per 5 Nm).	71
Figure 4.10 A. 2005 – 2006 CPR transects showing abundances of <i>Oikopleura</i> sp. (counts per 5 Nm).	73
Figure 4.10 B. 2005 – 2006 CPR transects showing abundances of <i>Fritillaria</i> sp. (counts per 5 Nm).	74
Figure 4.11 A. 2006 – 2007 CPR transects showing abundances of <i>Oikopleura</i> sp. (counts per 5 Nm).	76
Figure 4.11 B. 2006 – 2007 CPR transects showing abundances of <i>Fritillaria</i> sp. (counts per 5 Nm).	77
Figure 4.12 A. 2007 – 2008 CPR transects showing abundances of <i>Oikopleura</i> sp. (counts per 5 Nm).	78
Figure 4.12 B. 2007 – 2008 CPR transects showing abundances of <i>Fritillaria</i> sp. (counts per 5 Nm).	79
Figure 4.13 A. October (spring) CPR transects showing abundances of <i>Oikopleura</i> sp. (counts per 5 Nm).	82
Figure 4.13 B. October (spring) CPR transects showing abundances of <i>Fritillaria</i> sp. (counts per 5 Nm).	83
Figure 4.14 A. December (late spring) CPR transects showing abundances of <i>Oikopleura</i> sp. (counts per 5 Nm).	84
Figure 4.14 B. December (late spring) CPR transects showing abundances of <i>Fritillaria</i> sp. (counts per 5 Nm).	85
Figure 4.15 A. February (summer) CPR transects showing abundances of <i>Oikopleura</i> sp. (counts per 5 Nm).	86
Figure 4.15 B. February (summer) CPR transects showing abundances of <i>Fritillaria</i> sp. (counts per 5 Nm).	87
Figure 4.16A. April (autumn) CPR transects showing abundances of <i>Oikopleura</i> sp. (counts per 5 Nm).	88
Figure 4.16 B. April (autumn) CPR transects showing abundances of <i>Fritillaria</i> sp. (counts per 5 Nm).	89

Figure 4.17. July (winter) CPR transects showing abundances of *Oikopleura* sp. (counts per 5 Nm). **90**

Figure 4.18. Annual mean abundance of larvaceans from the Southern Ocean. Black is *Fritillaria* sp. (ind. m⁻³, grey standard error bars), white *Oikopleura* sp. (ind. m⁻³, black standard error bars), and grey is Larvaceans (ind. m⁻³, grey standard error bars). Overall means: *Fritillaria* sp. 4.4 ind. m⁻³, *Oikopleura* sp. 1.9 ind. m⁻³, Larvaceans 6.4 ind. m⁻³. **92**

Figure 4.19. *Fritillaria* sp and *Oikopleura* sp. monthly mean abundances from SO-CPR data. Black is *Fritillaria* sp. abundance (ind. m⁻³, grey standard error bars), white *Oikopleura* sp. abundance (ind. m⁻³, black standard error bars), and grey larvacean abundance (ind. m⁻³, grey standard error bars). **94**

Figure 4.20. Southern Ocean annual mean abundances of larvaceans (ind. m⁻³) from the SO-CPR Survey. The ocean was divided into three zones; Sub Antarctic Zone (SAZ, north 48 °S, black), Permanent Open Ocean Zone (POOZ, 50 - 60 °S, grey) and the Seasonal Ice Zone (SIZ, south 62 °S, white). Blue indicates total mean larvacean abundances (ind. m⁻³) and error bars are the standard deviations. **96**

Figure 4.21. Southern Ocean monthly mean larvacean abundances (ind. m⁻³) from the SO-CPR Survey. The ocean was divided into three zones; Sub Antarctic Zone (SAZ, north 48 °S, black), Permanent Open Ocean Zone (POOZ, 50 - 60 °S, grey) and the Seasonal Ice Zone (SIZ, south 62 °S, white). Blue indicates total mean larvacean abundances (ind. m⁻³) and error bars are the standard deviations. **98**

Figure 4.22. Annual comparison of average larvacean (black) abundances and total zooplankton (grey). Data from the SO-CPR Survey. **104**

Figure 4.23. Monthly comparison of average larvacean (black) abundances and total zooplankton (white). Data from the SO-CPR Survey. **106**

Figure 4.24. Visualisation of the monthly SO-CPR Survey (1991 – 2008) abundance (count per 5Nm) data for A) total zooplankton, B) total larvacean, C) *Oikopleura* sp. and D) *Fritillaria* sp. compared to latitude (°South). Note there is no data for June. **108**

Figure 4.25. A) ggplot of the monthly average abundance (count per 5Nm) for total zooplankton compared to the difference in latitude between sample location and the sea ice extent (diffSIcelat). B) ggplot of the monthly average abundance (count per 5Nm) for total larvaceans compared to the difference in latitude between sample location and the sea ice extent (diffSIcelat). Transparency of both plots set at 0.01 and showing a smoothed mean (red line). **113**

Figure 4.26. A plot of the fitted GAMM on top of total abundance (for each of total zooplankton (A) (marginal R² 0.0405 $\sigma = 1.054$ $\phi = 59.741$) and total larvacean (B) (marginal R² 0.0098 $\sigma = 1.432$ $\phi = 4.268$) vs fitted GAMM values shown by the red points which form a line. The green points are from the

fitted loess smoother (which is independent of the individual GAMM components) using the GAMM fitted value as the x-variable and the R-function loess). **120**

Figure 4.27. A) Visualisation of the SO-CPR Survey data (1991-2008). Total zooplankton abundance (counts per 5 Nm) compared to latitude (R^2 0.0014). B) GAMM output for zooplankton CPR 1991-2008 analyses Total zooplankton (ordinate scale estimated degrees of freedom (edf)) GAMM and latitude ($^{\circ}$ South). C) ggplot of total zooplankton abundance (0 – 3500 counts per 5 Nm) compared to latitude ($^{\circ}$ S). Transparency of data points set at 0.01 and showing a smoothed mean (red line). D) ggplot of total zooplankton abundance (0 – 1000 counts per 5 Nm) compared to latitude ($^{\circ}$ S). Transparency of data points set at 0.01 and showing a smoothed mean (red line). **122**

Figure 4.28. A) Visualisation of the SO-CPR Survey data (1991-2008). Total zooplankton abundance (counts per 5 Nm) compared to water temperature ($^{\circ}$ C) (R^2 0.0069). B) GAMM output for zooplankton CPR 1991-2008 analyses Total zooplankton (ordinate scale (edf)) GAMM water temperature ($^{\circ}$ C). C) ggplot of total zooplankton abundance (0 – 1000 counts per 5 Nm) compared to water temperature ($^{\circ}$ C). Transparency of data points set at 0.01 and showing a smoothed mean (red line). **125**

Figure 4.29. A) Visualisation of the SO-CPR Survey data (1991-2008). Total zooplankton abundance (counts per 5 Nm) compared to fluorescence (R^2 0.0015). B) GAMM output for zooplankton CPR 1991-2008 analyses Total zooplankton (ordinate scale (edf)) GAMM fluorescence. C) ggplot of total zooplankton abundance (0 – 1000 counts per 5 Nm) compared to fluorescence. Transparency of data points set at 0.01 and showing a smoothed mean (red line). **126**

Figure 4.30. A) Visualisation of the SO-CPR Survey data (1991-2008). Total zooplankton abundance (counts per 5 Nm) compared to salinity (psu) (R^2 0.005). B) ggplot of zooplankton abundance (0 – 200 counts per 5 Nm) compared to salinity (psu). Transparency of data points set at 0.01 and showing a smoothed mean (red line). **127**

Figure 4.31. A) Visualisation of the SO-CPR Survey data (1991-2008). Total zooplankton abundance (counts per 5 Nm) compared to month (R^2 4e-05). B) GAMM output for zooplankton CPR 1991-2008 analyses Total zooplankton (ordinate scale (edf)) GAMM month from July (no abundances for June). C) ggplot of total zooplankton abundance (0 – 1000 counts per 5 Nm) compared to months. Transparency of data points set at 0.01 and showing a smoothed mean (red line). Note no data for the month of June. **129**

Figure 4.32. A) Visualisation of the SO-CPR Survey data (1991-2008). Total zooplankton abundance (counts per 5 Nm) compared to season (R^2 0.0018). B) GAMM output for zooplankton CPR 1991-2008 analyses Total zooplankton (ordinate scale (edf)) GAMM season. C) ggplot of total zooplankton abundance (0 – 1000 counts per 5 Nm) compared to seasons. Transparency of data points set at 0.01 and showing a smoothed mean (red line). **130**

Figure 4.33. A) Visualisation of the SO-CPR Survey data (1991-2008). Total larvacean abundance (count per 5 Nm) compared to total zooplankton abundance (counts per 5 Nm) (R^2 0.2499). B) GAMM output for Larvacean CPR 1991-2008 analyses Total larvacean (Log count per 5 Nm) (ordinate scale (edf)) GAMM total Log link zooplankton (Log count per 5Nm). C) ggplot of total zooplankton larvaceans abundance (0 – 3500 counts per 5 Nm) compared to larvaceans abundance (0 – 1800 counts per 5 Nm). Transparency of data points set at 0.01 and showing a smoothed mean (red line). D) ggplot of total zooplankton larvaceans abundance (0 – 200 counts per 5 Nm) compared to larvaceans abundance (0 – 200 counts per 5 Nm). Transparency of data points set at 0.01 and showing a smoothed mean (red line). **132**

Figure 4.34. A) Visualisation of the SO-CPR Survey data (1991-2008). Total larvacean abundance (counts per 5 Nm) compared latitude ($^{\circ}$ South) (R^2 0.007). B) GAMM output for Larvacean CPR 1991-2008 analyses Total larvacean (ordinate scale (edf)) GAMM and latitude ($^{\circ}$ South). C) ggplot of larvaceans abundance (0 – 1800 counts per 5 Nm) compared to latitude ($^{\circ}$ S). Transparency of data points set at 0.1 and showing a smoothed mean (red line). D) ggplot of larvaceans abundance (0 – 200 counts per 5 Nm) compared to latitude ($^{\circ}$ S). Transparency of data points set at 0.05 and showing a smoothed mean (red line). **135**

Figure 4.35. A) Visualisation of the SO-CPR Survey data (1991-2008). Total larvacean abundance (counts per 5 Nm) compared water temperature ($^{\circ}$ C) (R^2 0.001). B) GAMM output for Larvacean CPR 1991-2008 analyses Total larvacean (ordinate scale (edf)) GAMM water temperature ($^{\circ}$ C). C) ggplot of larvaceans abundance (0 – 200 counts per 5 Nm) compared to water temperature ($^{\circ}$ C). Transparency of data points set at 0.01 and showing a smoothed mean (red line). **137**

Figure 4.36. A) Visualisation of the SO-CPR Survey data (1991-2008). Total larvacean abundance (counts per 5 Nm) compared to fluorescence (R^2 0.0018). C) ggplot of larvaceans abundance (0 – 200 counts per 5 Nm) compared to fluorescence. Transparency of data points set at 0.01 and showing a smoothed mean (red line). **139**

Figure 4.37. A) Visualisation of the SO-CPR Survey data (1991-2008). Total larvacean abundance (counts per 5 Nm) compared to salinity (psu) (R^2 0.005). B) ggplot of larvaceans abundance (0 – 200 counts per 5 Nm) compared to salinity (psu). Transparency of data points set at 0.01 and showing a smoothed mean (red line). **140**

Figure 4.38. A) Visualisation of the SO-CPR Survey data (1991-2008). Total larvacean abundance (counts per 5 Nm) compared to month (R^2 0.0002). B) GAMM output for Larvacean CPR 1991-2008 analyses Total larvacean (ordinate scale (edf)) GAMM month from July. ggplot of larvaceans abundance (0 – 200 counts per 5 Nm) compared to months. Transparency of data points set at 0.01 and showing a smoothed mean (red line). Note no data for the month of June. **141**

Figure 4.39. A) Visualisation of the SO-CPR Survey data (1991-2008). Total larvacean abundance (counts per 5 Nm) compared to season ($R^2 = 7e-05$). B) GAMM output for Larvacean CPR 1991-2008 analyses Total larvacean (ordinate scale (edf)) GAMM season. C) ggplot of larvaceans abundance (0 – 200 counts per 5 Nm) compared to seasons. Transparency of data points set at 0.01 and showing a smoothed mean (red line). **143**

Figure 4. 40. ggplot of *Oikopleura* compared to *Fritillaria* abundance (0 – 200 counts per 5 Nm). Transparency of data points set at 0.01 and showing a smoothed mean (red line). **144**

Figure 4.41. Relative abundances of larvaceans from the SO-CPR Survey compared to physical (latitude, longitude, temperature, salinity and irradiance (light)) and biological (fluorescence and total zooplankton) parameters. **146**

5. Distribution and abundance between 30° and 80° E

Figure 5.1. Schematic of large-scale circulation and water mass boundaries for the BROKE-West survey area (60—70°S, 30—80°E) in the southwest Indian Ocean sector of East Antarctica (modified from Williams et al., (2010)). **155**

Figure 5.2. *Fritillaria drygalski* (*Fritillaria* spp.) a) Scanning Electron Microscope image (scale bar 100 μm) b) stereo dissecting microscope digital image (scale bar 100 μm). **160**

Figure 5.3. *Oikopleura gaussica* (*Oikopleura* spp.) a) Scanning Electron Microscope image (scale bar 1 mm) b) stereo dissecting microscope digital image (scale bar 1 mm). **161**

Figure 5.4 A. Distribution and abundance (ind. m^{-3}) of *Fritillaria* spp. from ring net samples. Filled and varying circle size represent abundance values, empty circles zero abundance, X CTD sites not sampled. Large dashed and small dashed lines represent the Southern Boundary and south ACC front respectively, following Orsi et al. (1995). Light arrows represent the position of the strong westward flowing Antarctic Slope Current and the dark arrows represent the respective positions of the eastern Weddell Gyre and the Prydz Bay Gyre following Heywood et al. (1999) **163**

Figure 5.4 B. Distribution and abundance (ind. m^{-3}) of *Oikopleura* spp. from ring net samples. Filled and varying circle size represent abundance values, empty circles zero abundance, X CTD sites not sampled. Large dashed and small dashed lines represent the Southern Boundary and south ACC front respectively, following Orsi et al. (1995). Light arrows represent the position of the strong westward flowing Antarctic Slope Current and the dark arrows represent the respective positions of the eastern Weddell Gyre and the Prydz Bay Gyre following Heywood et al. (1999) **164**

Figure 5.4 C. Distribution and abundance (ind. m⁻³) of total larvaceans from ring net samples. Filled and varying circle size represent abundance values, empty circles zero abundance, X CTD sites not sampled. Large dashed and small dashed lines represent the Southern Boundary and south ACC front respectively, following Orsi et al. (1995). Light arrows represent the position of the strong westward flowing Antarctic Slope Current and the dark arrows represent the respective positions of the eastern Weddell Gyre and the Prydz Bay Gyre following Heywood et al. (1999) **165**

Figure 5.5 A. As in Figure 5.4 A, but for the distribution and abundance (ind. m⁻³) of *Fritillaria* from RMT1 samples. **167**

Figure 5.5 B. As in Figure 5.4 B, but for the distribution and abundance (ind. m⁻³) of *Oikopleura* from RMT1 samples. **168**

Figure 5.5 C. As in Figure 5.4 C, but for the distribution and abundance (ind. m⁻³) of total larvaceans from RMT1 samples. **169**

Figure 5.6. Distribution and abundance (ind. m⁻³) of Southern Ocean *Fritillaria* (black) and *Oikopleura* (white) from the four Continuous Plankton Recorder (CPR) transects. Numbers represent total larvaceans abundance (ind. m⁻³) for each CPR transect. **171**

Figure 5.7. Seasonal larvacean abundances from the Southern Ocean Continuous Plankton Recorder (SO-CPR) Survey database located at the Australian Antarctic Division. Black is *Fritillaria* ind. m⁻³ (grey standard error bars) and white *Oikopleura* ind. m⁻³ (black standard error bars). **179**

6. Fine-scale distribution patterns determined from plankton nets

Figure 6.1. Ring net which was vertically deployed. Mouth area 0.8m², 150 µm mesh and a 20 L, weighted (approximately 15kg), 0.3 m wide cod-end with windows. **186**

Figure 6.2. Generalised schematic of the Rectangular Mid-water Trawl 1 (RMT1), part of an RMT1+8 system. **188**

Figure 6.3. WP2 net with 200 µm mesh used during the CEAMARC – Pelagic voyage. Hauls were vertical between 0 – 200 m. **190**

Figure 6.4. HYDRO-BIOS MultiNet with 150 µm mesh. Horizontal trawls were conducted between the surface and bottom during the CEAMARC – Pelagic voyage. **191**

Figure 6.5. The Autonomous Video Plankton Recorder deployed during CEAMARC – Pelagic. It was housed in a stainless steel frame with cameras, lights and associated sensors. Photo: JAMSTEC **192**

Figure 6.6. SO-CPR transects during the BROKE-West voyage aboard RSV *Aurora Australis*. The western transect was the southbound transect deployed in January 2006. The eastern transect was the northbound transect deployed in March 2006. A break in the northbound transect was due to the malfunction of a mechanism inside the CPR. **194**

Figure 6.7. SO-CPR transects during the SIPEX voyage aboard RSV *Aurora Australis*. The eastern transect was the southbound transect conducted in September 2007. The western transect was the northbound transect conducted in October 2007. A break in the southbound transect was due to the malfunction of a silk inside the CPR. **195**

Figure 6.8. SO-CPR transects during the CEAMARC–Pelagic voyage aboard *TRV Umitaka Maru*. The western transect was the southbound transect deployed in January 2008. The eastern transect was the northbound transect deployed in February 2008. **197**

Figure 6.9. SAZ-Sense voyage track and sample sites (circles) overlaid on a MERIS ocean colour composite image (SeaWiFS) with 1 km resolution (ESA satellite). Data is for the period 5-11 February 2007 and was processed by the PML Remote Sensing Group. The colour scale at the bottom of the image is a logarithmic scale between 0.01 and 60 μg chlorophyll *a* l^{-1} (source Bowie et al., in press). **201**

Figure 6.10. Larvacean abundances (ind. m^{-3}) determined using a ring net. Abundances were high in the west and low in the east. Data obtained during the SAZ-Sense voyage from 17 January to 20 February 2007, aboard RSV *Aurora Australis*. Figure adapted from the Australian Antarctic Data Centre. **202**

Figure 6.11 Larvaceans abundances (ind. m^{-3}) determined using RMT1 trawls. Abundances were high in the west and low in the east. Data obtained during the SAZ-Sense voyage from 17 January to 20 February 2007, aboard RSV *Aurora Australis*. Figure adapted from the Australian Antarctic Data Centre. **203**

Figure 6.12. Diel abundance of larvaceans at 20 m during the SAZ-Sense voyage. (A) process station one (B) process station two. The curved yellow line represents light availability as a relative concentration to time. **204**

Figure 6.13. Abundance of larvaceans with depth during the SAZ-Sense voyage. (A) process station one (B) process station two. **205**

Figure 6.14 A. SO-CPR BROKE-West distribution and abundance maps of Southern Ocean *Oikopleura* sp. Abundance is in counts per 5 Nm. **208**

Figure 6.14 B. SO-CPR BROKE-West distribution and abundance maps of Southern Ocean *Fritillaria* sp. Abundance is in counts per 5 Nm. **209**

Figure 6.15. Larvacean abundances (ind. m^{-3}) determined from ring net samples during the SIPEX voyage. The voyage was conducted from 4 September to 17

October 2007 aboard RSV *Aurora Australis*. Figure adapted from the Australian Antarctic Data Centre. **212**

Figure 6.16. *Oikopleura* sp. abundances (ind. m⁻³) determined from ring net samples during the SIPEX voyage. The voyage was conducted from 4 September to 17 October 2007 aboard RSV *Aurora Australis*. Figure adapted from the Australian Antarctic Data Centre **213**

Figure 6.17. *Fritillaria* sp. abundances (ind. m⁻³) determined from the ring net samples during the SIPEX voyage. The voyage was conducted from 4 September to 17 October 2007 aboard RSV *Aurora Australis*. Figure adapted from the Australian Antarctic Data Centre **214**

Figure 6.18 A. *Oikopleura* sp. abundances determined using CPR during the SIPEX voyage. Abundance is in counts per 5 Nm. **215**

Figure 6.18 B. *Fritillaria* sp. abundances determined using CPR during the SIPEX voyage. Abundance is in counts per 5 Nm. **216**

Figure 6.19. Presence or absence of larvaceans determined using the WP2 net, the HYDRO BIOS MultiNet and the VPR in the SIZ during the CEAMARC – Pelagic voyage. The voyage was conducted from 23 January to 17 February 2008 aboard *TRV Umitaka Maru*. Figure adapted from the Australian Antarctic Data Centre. **219**

Figure 6.20 A. Abundance of *Oikopleura* sp. determined using CPR during the CEAMARC – Pelagic voyage. Abundance is in counts per 5 Nm. **220**

Figure 6.20 B. Abundance of *Fritillaria* sp. determined using CPR during the CEAMARC – Pelagic voyage. Abundance is in counts per 5 Nm. **227**

Figure 6.21 Graph showing ordinal date and larvacean abundance (BROKE-West (red), SAZ-Sense (green) and SIPEX (blue) abundances as ind.m⁻³ and CEAMARC (purple) recorded as presence (1) and absence (0)) for the voyages undertaken to collect larvaceans in the East Antarctic Southern Ocean. BROKE-West (red), SAZ-Sense (green), SIPEX (blue) and CEAMARC (purple). **227**

Figure 2.22 Graph showing ordinal date and latitude for the voyages undertaken to collect larvaceans in the East Antarctic Southern Ocean. BROKE-West (red), SAZ-Sense (green), SIPEX (blue) and CEAMARC (purple). **227**

Figure 6.23. Larvacean abundances from ring net (ind.m⁻³) and chlorophyll *a* concentrations (coloured scale) during SAZ-Sense. The red line indicates the inverse relationship between larvacean abundance and chlorophyll *a*, as measure of productivity. **229**

Figure 6.24. Sea ice algal cell density from the western area of the SIPEX voyage. Station 7 is the first station that significant algal densities occurred. Data from K. Petrou. **231**

Figure 6.25. Relative abundances of larvaceans compared to physical (latitude, longitude, temperature, salinity and light) and biological (total zooplankton) distributions. 233

7. Feeding ecology

Figure 7.1. Diagram of the feeding house of *O. labradoriensis*. Dark green and light green arrows indicate water flow through the house before, and after, the passage of water through the food concentrating filter. Olive green arrow indicates the flow of trapped particles towards the mouth for consumption (modified from Flood and Diebel 1998). 237

Figure 7.2. *O. labradoriensis* feeding house inflation in successive stages (Flood and Diebel, 1998) 238

Figure 7.3. Diagram of the feeding house of *F. borealis*. Black and white arrows indicate water flow through the house before, and after, its passage through the food concentrating filter (Flood and Diebel, 1998). 240

Figure 7.4. Typical feeding cycle of *F. borealis* in relation to the inflation and deflation of the house (Flood, 2003). 240

Figure 7.5. Line drawing of *Kowalevskia tenuis* house from A) below and B) side. Fol (1872) Notes: q, coquille (house); z, three-dimensional internal cavity (Flood and Deibel, 1998). 241

Figure 7.6. Scanning electron micrographs showing the different structures of A. upper, and B. lower food concentrating filters of *Oikopleura dioica*. Magnification x12,000 (adapted from Flood and Deibel 1998). 243

Figure 7.7. Schematic of generalised feeding house showing two filters and the flow of seawater. Dark green and light green arrows indicate water flow through the house before, and after, the passage of water through the food concentrating filter. Olive green arrow indicates the flow of trapped particles towards the mouth for consumption. 244

Figure 7.8. Discarded feeding house. Photo courtesy of Debbie Steinberg and Stephanie Wilson of the Virginia Institute of Marine Science. Scale bar = 1 mm. 245

Figure 7.9. Larvacean faecal pellet size: <300 - 500 μm . Photos courtesy of Debbie Steinberg and Stephanie Wilson of the Virginia Institute of Marine Science 246

Figure 7.10. Role of larvaceans in marine ecosystem (adapted from Gorsky and Fenoux, 1998) 247

Figure 7.11. Larvaceans role in the food web. 248

Figure 7.12. Larvaceans contribution to marine snow and carbon cycling. **249**

Figure 7.13. Abundance and distribution map of larvaceans that were captured using a ring net. The location of stations 25 and 65 (squares) where protists were sampled are shown. The location of stations 28 and 67 (triangles) where larvaceans were sampled for diet studies are also shown. Station 25 and Station 28 (white shapes) were at a similar location. Station 65 and Station 67 (black shapes) were also at a similar location. **250**

Figure 7.14. Schematic summary of the method used to determine Southern Ocean larvacean diet. Marine protists identified were from water samples collected using a CTD and a “snatcher” (a rosette of Niskin bottles that collected surface waters). **251**

Figure 7.15. Marine protist distributions in relation to chlorophyll *a* ($\mu\text{g/L}$). A. Leg 1 showing the northerly location of CTDs 28 and 25, and B. Leg 5 showing the southerly location of CTDs 67 and 65 (modified after Wright et al., 2010). **255**

Figure 7.16. Antarctic marine protists found in the water column, on the surface of *O. gaussica*, or within the stomach of *O. gaussica*. A. *Corethron pennatum* (scale bar 10 μm) B. *Thalassiosira* (scale bar 1 μm) C. *Fragilariopsis* (scale bar 1 μm). **257**

Figure 7. 17. *Rhizosolenia* on the trunk of *O. gaussica* (scale bar 100 μm). **257**

Figure 7. 18. SEM stub showing gut content **257**

Figure 7.19. Size comparison between a. *O.gaussica* and b. *Corethron pennatum* (axis size range in μm) c. *Thalassiosira* (axis size range in μm) d. *Fragilariopsis* (axis size range in μm). **259**

Figure 7.20. The alignment of *Corethron pennatum* cells required for ingestion by *O. gaussica*. The inferred feeding-mesh size from this alignment is between 5 and 82 μm given the known dimensions of the protist. **260**

8. Conclusions

Figure 8.1 Relative abundances of larvaceans in the Southern Ocean compared to physical (latitude, longitude, temperature, salinity and light) and biological (total zooplankton) distributions. **267**

List of Tables

1. Introduction

Table 1.1 Major studies on larvaceans from the Southern Ocean (from O' Sullivan 1983) 3

2. Study regions, cruises and experimental approaches

Table 2.1. Summary of Southern Ocean voyages undertaken between 2006 and 2008 to examine larvaceans. The voyage dates are from departure from Australia to return to Australia. The methods used include the ring net, the Continuous Plankton Recorder (CPR), Rectangular Mid-water Trawl (RMT1), cameras from the Remote Operated Vehicle (ROV) and Surface Underwater I Trawl (SUIT), multi net and Visual Plankton recorder (VPR). 29

3. Identification of Southern Ocean larvaceans

Table 3.1. Antarctic Ocean larvaceans listed by Fenaux et al. (1998) with additional larvaceans described by O'Sullivan (1983) included in bold. * *F.borealis typica*; the only bi-polar larvacean. 42

Table 3.2. General distribution and relative abundance of 29 larvacean species in the South Atlantic Ocean, poleward of 40° S. Key; ■■■■ very rare, ---- Scarce, ===== frequent, ≡≡≡ abundant and □□□□ probable range (from Esnal 1999). 43

4. Large-scale distribution patterns determined from the CPR

Table 4.1. Pearson's *r* correlation between longitude and abundances of larvaceans in 2003 – 2004. **Bold** indicates a significant relationship (ns = not significant), $\alpha=0.05(2)$. 71

Table 4.2. Pearson's *r* correlation between abundances of *Oikopleura sp.* and *Fritillaria sp.* in 2005 – 2006. **Bold** indicates a significant relationship (ns = not significant), $\alpha=0.05(2)$. 75

Table 4.3. Southern Ocean annual mean abundances for *Fritillaria sp.*, *Oikopleura sp.*, total larvaceans and total zooplankton (ind. m⁻³) from the SO-CPR database. Sample numbers (n) and std (±) is the standard deviation 93

Table 4.4. Southern Ocean monthly mean abundances for *Fritillaria sp.*, *Oikopleura sp.*, total larvaceans and total zooplankton (ind. m⁻³) from the SO-CPR database. Sample numbers (n) and std (±) is the standard deviation 95

Table 4.5. Southern Ocean annual larvacean mean abundances (ind. m⁻³) from the SO-CPR Survey. Std (±) is the standard deviation. 97

Table 4.6. Monthly mean larvacean abundances (ind. m⁻³) for the Southern Ocean and associated zones. Data from the SO-CPR Survey. Std (±) is the standard deviation. **99**

Table 4.7. Sub Antarctic Zone (SAZ, north of 48 °S) annual mean abundances for *Fritillaria* sp., *Oikopleura* sp., total larvaceans and total zooplankton. Std (±) is the standard deviation. **100**

Table 4.8. Sub Antarctic Zone (SAZ, north of 48 °S) monthly mean abundances for *Fritillaria* sp., *Oikopleura* sp., total larvaceans and total zooplankton. Std (±) is the standard deviation. **100**

Table 4.9 Permanent Open Ocean Zone (POOZ, between 50 – 60°S) annual mean abundances for *Fritillaria* sp., *Oikopleura* sp., total larvaceans and total zooplankton. Std (±) is the standard deviation. **101**

Table 4.10. Permanent Open Ocean Zone (POOZ, between 50 – 60°S) monthly mean abundances for *Fritillaria* sp., *Oikopleura* sp., total larvaceans and total zooplankton. Std (±) is the standard deviation. **101**

Table 4.11. Seasonal Ice Zone (SIZ, south 62 °S) annual mean abundances for *Fritillaria* sp., *Oikopleura* sp., total larvaceans and total zooplankton. Std (±) is the standard deviation. **102**

Table 4.12. Seasonal Ice Zone (SIZ, south 62 °S) monthly mean abundances for *Fritillaria* sp., *Oikopleura* sp., total larvaceans and total zooplankton. Std (±) is the standard deviation. **102**

Table 4.13. Annual comparison of larvacean percentages compared to total zooplankton. **105**

Table 4.14. Monthly seasonal comparison of larvacean percentages compared to total zooplankton. **107**

Table 4.15. Seasonal underway data from the SO-CPR Survey dataset 1990 – 2008. **110**

Table 4.16. Monthly underway data from the SO-CPR Survey dataset 1990 – 2008. Std (±) is the standard deviation. **111**

Table 4.17. Southern Ocean zone underway data from the SO-CPR Survey dataset 1990 – 2008. Std (±) is the standard deviation. **111**

Table 4.18. Pearson's *r* correlations between larvacean abundances and environmental parameters. UW = underway data, and **Bold** indicates a significant relationship (ns = not significant), $\alpha=0.05(2)$. Degrees of freedom (df) for are 1000 data points or ∞ . **112**

Table 4.19. Approximate significance of smooth terms for GAMM analysis of total zooplankton abundances from the CPR database 1990-91 to 2008 (n = 25,791). **121**

Table 4.20. Approximate significance of smooth terms for GAMM analysis of total larvacean abundances from the CPR database 1990-91 to 2008 (n = 25791). **131**

5. Distribution and abundance between 30° and 80° E

Table 5.1. Abundance data for Southern Ocean larvaceans during the BROKE-West survey using three sampling devices. **161**

Table 5.2. BROKE-West CPR transect details and larvacean abundances. **172**

Table 5.3. Pearson's *r* correlation between the abundance of *Fritillaria* and *Oikopleura* for each sampling device. Bold values indicate a significant relationship ($\alpha=0.05(2)$, ns = not significant). **173**

Table 5.4. Pearson's *r* correlation between the larvacean abundances from each sampling device and environmental parameters, including latitude, longitude and corresponding underway data (UW) and shipboard hydrographic data (CTD - ring net only). Bold indicates a significant relationship (ns = not significant), $\alpha=0.05(2)$. **173**

6. Fine-scale distribution patterns determined from plankton nets

Table 6.1. Successful HYDRO-BIOS MultiNet deployment depths during CEAMARC. Depths in metres. **191**

Table 6.2. CPR tow details for BROKE-West **193**

Table 6.3. CPR tow details for SIPEX **195**

Table 6.4. CPR tow details for CEAMARC – Pelagic **196**

Table 6.5. Diel vertical migration of larvaceans during SAZ-Sense **204**

Table 6.6. Abundance of larvaceans with depth during the SAZ-Sense voyage **205**

Table 6.7. Pearson's *r* correlations between larvacean abundances from each sampling device, and environmental parameters measured during SAZ-Sense. UW = underway data, CTD = data measured using the CTD during ring net deployments. **Bold** indicates a significant relationship (ns = not significant), $\alpha=0.05(2)$. **206**

Table 6.8. BROKE-West CPR transect summary **210**

Table 6.9. Pearson's *r* correlations between larvacean abundances and environmental parameters. Data collected using a ring net and RMT1. **Bold** indicates a significant relationship (ns = not significant), $\alpha=0.05(2)$. 210

Table 6.10. Pearson's *r* correlations between larvacean abundances determined from eight CPR tows during BROKE-West, and environmental parameters determined from underway data. **Bold** indicates a significant relationship (ns = not significant), $\alpha=0.05(2)$. 211

Table 6.11. Average *Fritillaria* sp., *Oikopleura* sp. and larvacean abundances determined using CPR during the SIPEX voyage. Data are shown for each tow undertaken. 212

Table 6.12. Average *Fritillaria* sp., *Oikopleura* sp. and larvacean abundances determined using CPR during the SIPEX voyage. To determine transect averages, data from each tow within the same transect were pooled. 212

Table 6.13. Pearson's *r* correlations between larvacean abundances determined using a ring net, and environmental parameters during the SIPEX voyage. UW= underway data. **Bold** indicates a significant relationship (ns = not significant), $\alpha=0.05(2)$. 212

Table 6.14. Pearson's *r* correlations between larvacean abundances determined using CPR segments and environmental parameters determined from underway data during the SIPEX voyage. **Bold** indicates a significant relationship (ns = not significant), $\alpha=0.05(2)$. 213

Table 6.15. Average *Fritillaria* sp., *Oikopleura* sp. and larvaceans abundances determined using CPR during the CEAMARC – Pelagic voyage. Data are shown for each tow undertaken. 222

Table 6.16. Average *Fritillaria* sp., *Oikopleura* sp. and larvacean abundances determined using CPR during the CEAMARC – Pelagic voyage. To determine transect averages, data from each tow within the same transect were pooled. 222

Table 6.17. Pearson's *r* correlations between larvacean abundances determined using a ring net, and environmental parameters recorded during the CEAMARC – Pelagic voyage. **Bold** indicates a significant relationship (ns = not significant), $\alpha=0.05(2)$. 206

Table 6.18. Pearson's *r* correlations between larvacean abundances determined from CPR segments, and environmental parameters determined from underway data during the CEAMARC – Pelagic voyage. **Bold** indicates a significant relationship (ns = not significant), $\alpha=0.05(2)$. 222

Table 6.19. Averages of underway data for each oceanographic zone in the Southern Ocean and during each research voyage. 224

Table 6.20. Mean larvacean, *Oikopleura* sp. and *Fritillaria* sp. abundances for each sampling device used. Data from each research voyage were pooled. Sample size (n) represents number of net deployments. **225**

Table 6.21. Mean larvacean, *Oikopleura* sp. and *Fritillaria* sp. abundances (ind. m⁻³) within each oceanographic zone determined from net samples (excludes CPR data). Data from each research voyage were pooled. **226**

Table 6.22. Mean larvacean abundance determined using nets for each voyage in each oceanographic zone. **226**

7. Feeding ecology

Table 7. 1. Numerical data on selected larvacean species and their houses, (U) Upper filter screen (L) Lower filter screen (extracted from Flood and Diebel, 1998). The filtration rate is the bulk flow of water pumped through the house. The clearance rate is the volume of water swept clear of particulate matter (or protists), which equates to the filtration rate times the particle retention efficiency. The open area fraction is a measure of porosity. **242**

Table 7.2. Mean abundance of larvaceans and marine protist species associated with the diet of *O. gaussica* at the surveyed CTD sites. **254**

Table 7.3. Protists found in the water column, on the surface of *O. gaussica*, or within the stomach of *O. gaussica* in the Southern Ocean. Those in **bold** occurred in all three scenarios. **256**

Table 7.4. Size of protists (from Scott and Marchant 2005) associated with the diet of *O.gaussica*. Those in **bold** occurred in the water column, on the surface of *O. gaussica*, and within the stomach of *O. gaussica*. **258**

Table 7.5. Numerical data on feeding behaviour of *O. labradoriensis* and *F. borealis* (Flood and Diebel, 1998) compared to *O. gaussica* and *Fritillaria* sp. (this study). (U) Upper filter screen (L) Lower filter screen. **Bold** values are assumptions due to similar size. **263**

8. Conclusions

Table 8.1. Physical parameters that were significantly correlated with larvacean abundances for each voyage. Data was analysed using Pearson's *r* correlations. **268**

Table 8.2. Carbon-based weight specific clearance rates and ingestion rates (source Sato et al. 2005). **271**

List of Appendices

287

Appendix I. Larvacean species list (RAMS, 2010)	288
Appendix II. Larvacean taxonomic tree (RAMS, 2010)	290
Appendix III . Larvacean images submitted to SCARmarBIN	294
Appendix IV. Larvacean images submitted to WoRMS	298
Appendix V. SO-CPR Survey annual and seasonal maps	302
Appendix VI. Generalized Additive Mixed Models (GAMM) theory	323
Appendix VII. R code for mgcv	327
Appendix VIII. Mean abundances of marine protists. Raw data from Fiona Scott.	334
Appendix IX. Sizes of marine protist. (from Scott and Marchant 2005)	335
Appendix X. PDF of Lindsay, M. and Williams, G. 2010. Distribution and abundance of Larvaceans in the Southern Ocean between 30° and 80°E. <i>Deep-Sea Research II</i> 57 905–15	337

CHAPTER 1.

Introduction

1.1 Introduction

Larvaceans are an obscure group of gelatinous zooplankton and appear to represent a significant proportion of zooplankton in the Southern Ocean. Based on knowledge of larvaceans from other regions, it is likely that these organisms account for a significant amount of grazing and carbon flux in the Southern Ocean. Larvaceans may therefore have a large influence on climate change through the mediation of carbon transfer from surface waters to the ocean interior. Zooplankton are also good indicators of climate change for the following reasons (Hays et al., 2005).

1. Long-term changes can be attributed to climate change as few species of plankton are commercially exploited,
2. Tight coupling between environmental change and plankton dynamics due to short generation times of plankton,
3. Distribution can change dramatically because plankton are free-floating and increase or decrease their range to respond to changes in temperature and oceanic current systems, and
4. Plankton are a more sensitive indicator of change compared to environmental parameters.

Though Hays et al. (2005) identifies that zooplankton are good indicators of climate change, zooplankton may not be an entirely robust indicator of long-term environmental change, as a large number of zooplankton, including larvaceans, are prey of the commercially exploited species and therefore the zooplankton maybe affected indirectly by commercial fishing. Larvaceans have a short generation time thus environmental change will be reflected in larvacean dynamics. Changes in temperature and oceanic current systems may be reflected in larvacean distribution as they are free-floating and could increase or decrease their range to respond to environmental changes. Changes to environmental

parameters may be more subtle compared to changes to the larvacean distribution and abundances.

1.2 History of larvacean studies

Thus far, larvacean studies have focussed on tropical and northern hemisphere temperate species, and only cursory studies have been conducted on Southern Ocean larvacean taxonomy, abundance and distribution. Most studies on Southern Ocean zooplankton have focused on euphausiids, copepods and other crustaceans, which are relatively hard-bodied and able to withstand sampling and preservation processes. There has been little attention given to larvaceans and other gelatinous zooplankton, with the exception of salps (Nicol et al., 2000; Atkinson et al. 2004), partly because they are easily damaged or are overlooked because of their transparency and size.

Investigations into Southern Ocean zooplankton commenced with the *Challenger* expeditions in 1882 – 1886, with this and future expeditions examining taxonomy, distributional patterns and life cycles of various groups (Knox, 2007) (Table 1.1). The literature is dominated by studies of krill due to their large biomass (50% of zooplankton in some regions), ecological importance and resource potential. Hosie (2007) calculated that zooplankton contribute a biomass of over 450 million tonnes in the Southern Ocean, compared to 100 million tonnes of fish and 0.8 million tonnes of penguins.

Table 1.1 Major studies on larvaceans from the Southern Ocean (from O' Sullivan 1983)

Author	Expedition
Herdman 1888	<i>Challenger</i>
Lohmann 1892	<i>Plankton</i>
Seeliger 1895	<i>Plankton</i>
Lohmann 1896	<i>Plankton</i>
Lohmann 1905	
Herdmann 1910a	National Antarctic
Lohmann 1914	Valdivia
Büeckmann 1924	Deutschen <i>Sudpolar</i>
Lohmann and Büeckmann 1926	Deutschen <i>Sudpolar</i>
Lohmann 1928	Deutschen Antarktischen
Lohmann 1931	Deutschen <i>Tiefsee</i>
Garstang and Georgeson 1935	<i>Terra Nova</i>
Thompson 1954	BANZARE
Udvardy 1958	Swedish Antarctic
Tokioka 1961	Japanese Antarctic
Tokioka 1964	Japanese Antarctic

Gelatinous zooplankton are a group that Pugh (1989) referred to as “the forgotten fauna”. Initial publications on this group focused on species descriptions. Table 1.1 is a list of the major studies on Southern Ocean larvacean taxonomy from O' Sullivan (1983). Research by Totton (1954), Kramp (1957) and Foxton (1966) in the *Discovery Reports* provided distribution and abundance data that indicated the importance of Southern Ocean gelatinous zooplankton. Knox (2007) stated that “the ecological role of the gelatinous zooplankton has been reappraised...but data about species composition, abundance, and distribution are still scarce”. Knox (2007) goes on to say that the role of gelatinous zooplankton in the Antarctic pelagic food web has been underestimated. Boero et al. (2008) addressed the “neglected aspects” of the ecology and biology of gelatinous zooplankton, emphasising the importance of these organisms and that a lack of knowledge of their role could affect the understanding of the marine ecosystem in its entirety. Lohmann 1903 (cited by Paffenhöfer, 1973) stated that globally, larvaceans are considered to be the most numerous marine zooplankton after copepods.

1.3 Taxonomy

Larvaceans, also called appendicularians, are solitary and free-swimming gelatinous zooplankton. Larvaceans are urochordates (tunicates) that belong to the phylum Chordata (Figure 1.1). They are distinguished from the other tunicates, such as pyrosomes, salps and doliolids, by retention in the adult of a muscular tail or notochord. The Appendicularia consist of three families; Oikopleuridae, Fritillariidae and Kowalevskiidae (Figure 1.2). Sixty-five species of larvaceans have been identified to date (Hopcroft 2005). The Ocean Biogeographic Information System (OBIS) database (Accessed 12 April 2010) lists 58 species in its database (RAMS taxonomy list appendix I).

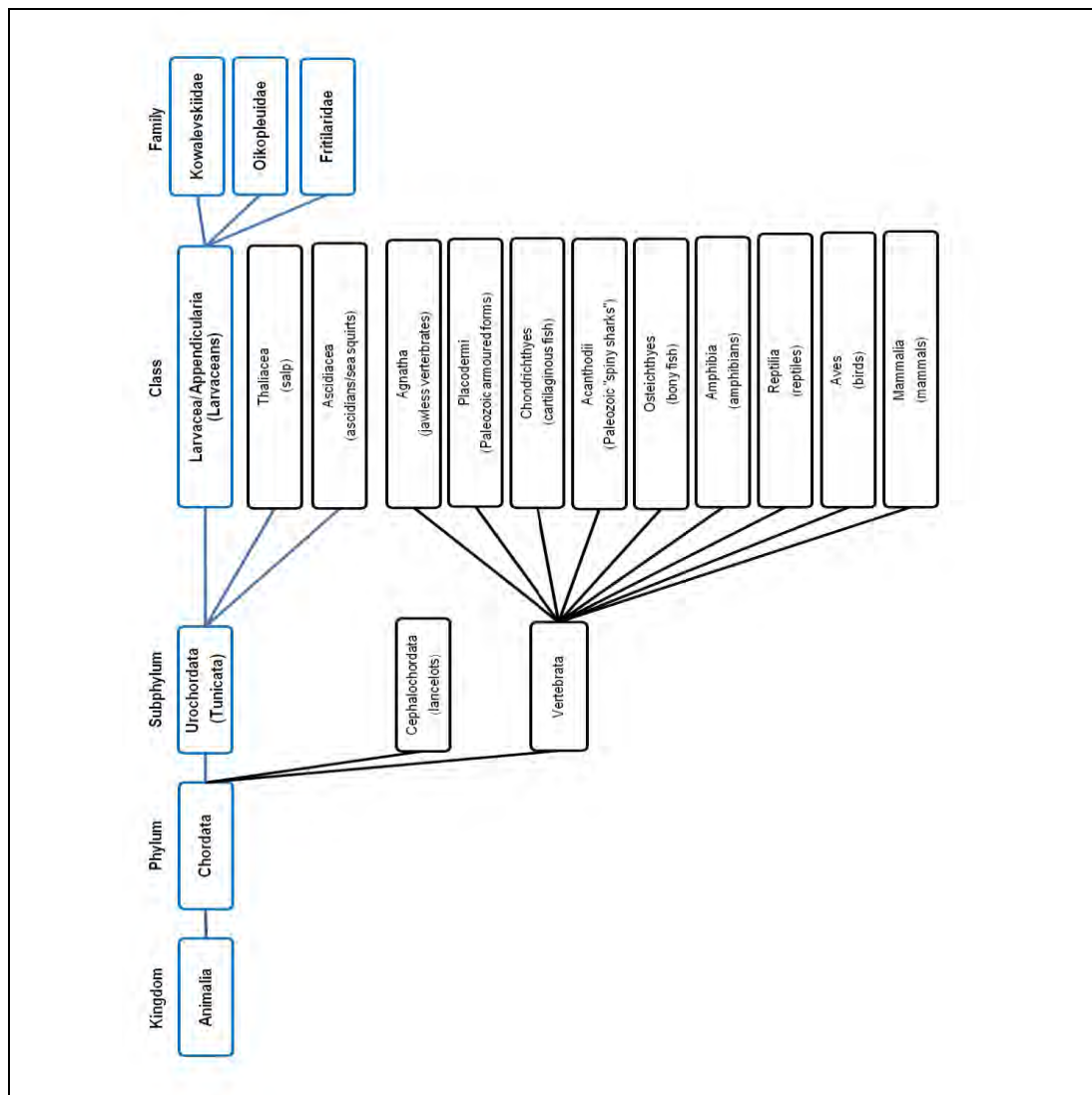


Figure 1.1. Family tree showing the three larvacean families (blue) lineage from the Chordata phylum and urochordata subphylum.

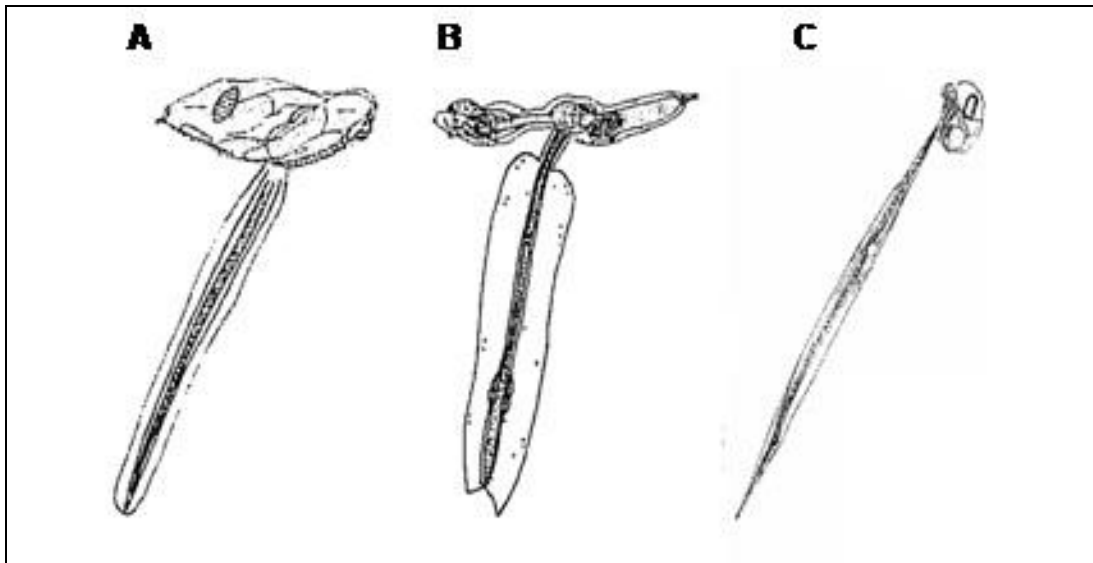


Figure 1.2. Examples of the three larvacean families; A. Oikopleuridae B. Fritillariidae C. Kowalevskiidae (from Ritz et al. 2003).

1.4 Form, life cycle and function

The tadpole-like body of larvaceans is divided into two sections - a trunk and a tail - around which a gelatinous feeding house is built, several times larger than the body (Bone, 1998). The general structure of larvaceans is represented in Figure 1.3.

Larvaceans are generally smaller than 5 mm, although one giant species, *Bathochordaeus charon*, found in the depths of the Arctic, has a feeding house occasionally up to 2 m wide (Hamner and Robison 1992).

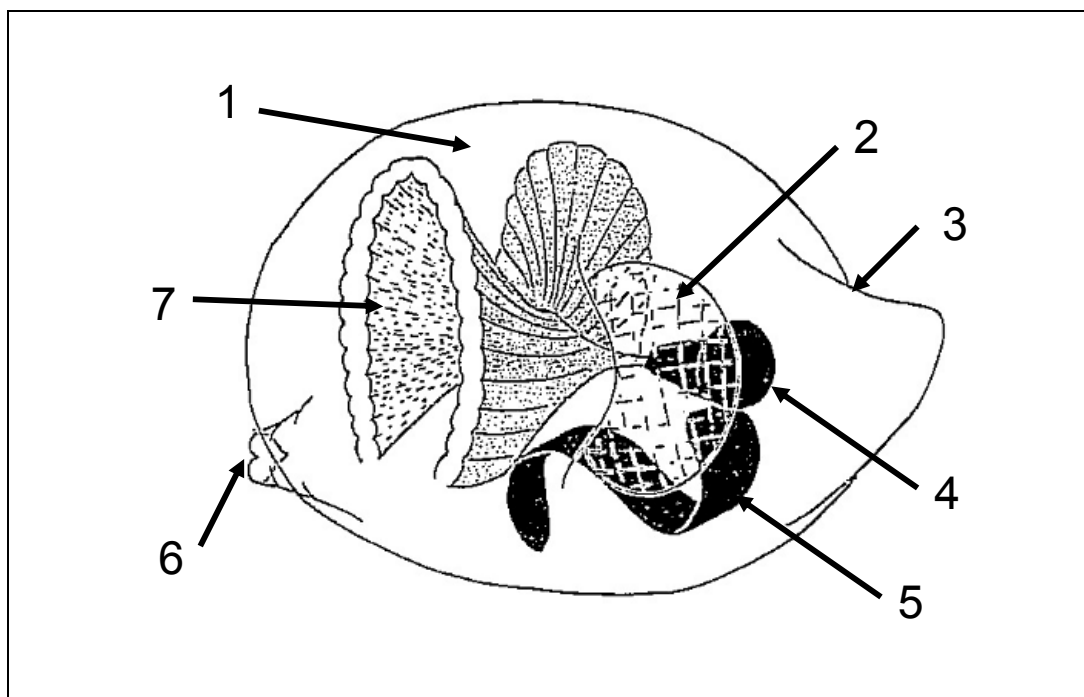


Figure 1.3. Generalised structure of larvaceans. 1. Feeding house 2. Inlet filter 3. Escape slot 4. Trunk 5. Tail 6. Outlet 7. Filter (adapted from Flood and Deibel 1998).

The life cycle of larvaceans is only known for the cosmopolitan *Oikopleura dioica* (Bone, 1998). It is divided into four distinct periods: fertilisation, hatching, shift of the tail and spawning/death. Fertilisation occurs in open water with early development of a tail and trunk. At hatching, the tail is adult-like while the trunk still requires development. The third stage, tail shift, involves the tail altering its orientation and the construction of a feeding house. Further growth occurs due to an increase in the volume of somatic cells. Spawning then occurs, followed by death from rupturing of the ovary and genital cavity wall. The life span of larvaceans is temperature dependent, with *O. dioica* living for 5 days at 22°C, and living longer in cooler waters (12 days at 14°C) (Fenaux, 1998). The generation time is not currently known for polar larvacean species.

The feeding house filters particulate matter and food, concentrating particles to approximately 100 to 1000 times ambient concentrations, with the food then being drawn through the digestive system. Larvaceans can concentrate and convert relatively small particulate matter to tissue - particles which would otherwise be too small for direct consumption by filter feeders and carnivores, e.g. copepods and krill. Whilst larvaceans are typically placed at an intermediate trophic level

within the marine food web, they differ from other intermediate zooplankton because they can “gather” a variety of food sources, from dissolved organic matter to large diatoms, using the feeding house. Waste is excreted as compact and ellipsoid faecal pellets (Aldridge, 1972 and 1976) with as many as 40 pellets produced per day.

The feeding house has two filters, an inlet filter that rejects protists that are too large, and a food concentration filter that concentrates protists for ingestion. When the feeding house becomes clogged it is discarded. *Oikopleura dioica* can produce up to 16 feeding houses per day (Sato et al., 2001). The discarded house then sinks, transporting both the house and accumulated particulate matter trapped within the filter. The feeding behaviour of larvaceans is described in more detail in Chapter 7.

1.5 Ecological role

Larvaceans are thought to play a significant role in the vertical flux of carbon from surface waters to the deep ocean (“EURAPP”, 1988; Steinberg et al., 1994) due to their disposal of feeding houses when clogged, as shown in figure 1.4. Both discarded houses and faecal pellets sink and contribute to marine snow (Aldridge 1972 and 1976). Due to the high efficiency with which larvaceans can ingest nano- and pico-plankton, their houses and faecal pellets represent a sink for small particles that would not normally fall from the euphotic (sunlit) zone, due to their low inherent sinking rates (Vargas et al., 2002).

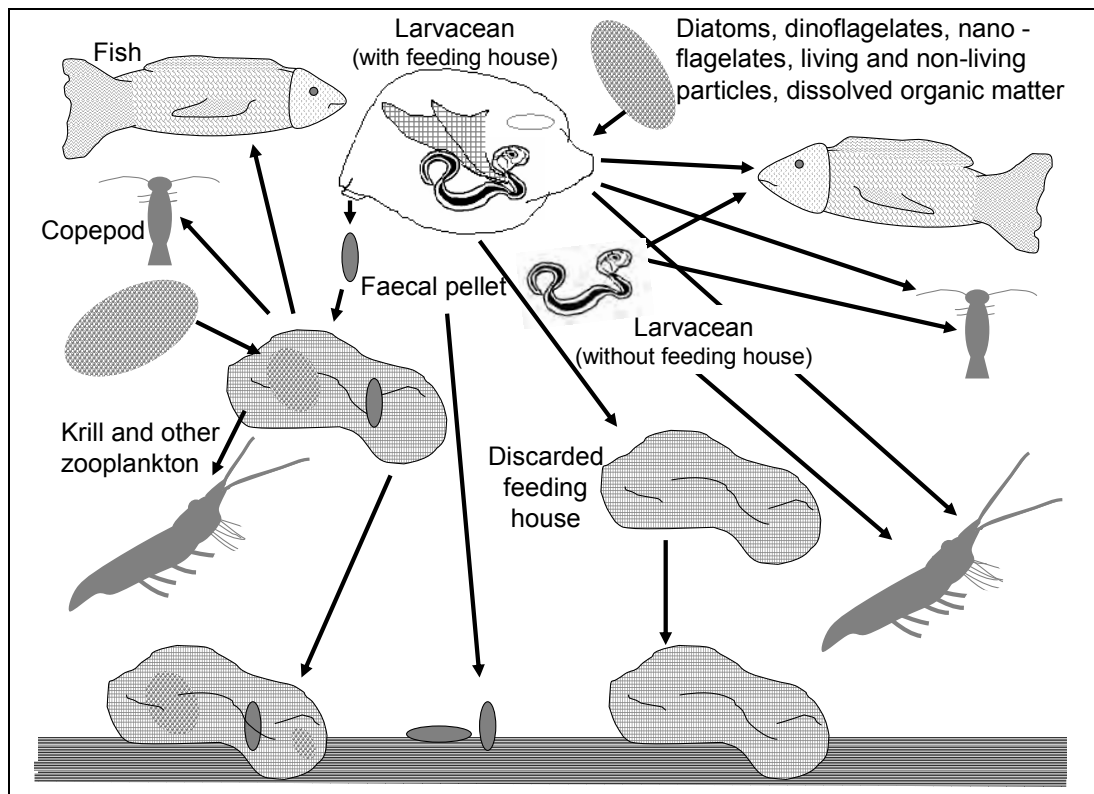


Figure 1.4. Larvaceans carbon contribution and role in the marine ecosystem.

This may have significant effects on the functioning of the biological carbon pump and particularly on the role of the Southern Ocean as a major sink for atmospheric carbon. Basic knowledge of the filtration rate and number of houses produced per day by larvaceans is required to define the trophic importance of this group. Thus far, this has not been studied in the Southern Ocean. House production rate is expected to be considerably lower in the Southern Ocean due to the lower temperatures, compared to that for tropical and temperate species, but this may be compensated for by the larger size of Southern Ocean species which produce substantially larger houses.

1.6 Distribution and abundance

Prior to this study the knowledge of the distribution and abundance of Southern Ocean larvaceans was poor. Figure 1.5 shows the global distribution of larvaceans according to the OBIS database. The map has 52 species recorded as point data, whilst 58 species in total are recorded. The OBIS database indicates that the Indian Ocean sector of the Southern Ocean has a wide distribution of larvaceans. This distribution pattern is reflected by the fact that the database includes the

Southern Ocean – Continuous Plankton Recorder (SO-CPR) Survey data. The SO-CPR Survey only records larvaceans as either *Fritillaria sp.* or *Oikopleura sp.* or as appendicularians due to the majority of samples being damaged.

SO-CPR data has shown that larvaceans are among the most common and abundant zooplankton groups (Hunt and Hosie 2003, 2006a and b). Hunt and Hosie (2006a and b) identified that larvaceans had a zonal distribution with high abundances in the Sea Ice Zone (SIZ). Tsujimoto et al. (2006) also reported high abundances of larvaceans in the SIZ. The Permanent Open Ocean Zone (POOZ) is generally considered oligotrophic, with some elevated primary production around the Polar Frontal Zone (PFZ), but not as high as in the SIZ (Banse, 1996; Atkinson, 1998; Fiala et al., 1998). Sampling in the Southern Ocean by CPR and NORPAC net has recorded mean abundances of larvaceans exceeding 50 individuals m^{-3} (Hunt and Hosie 2003, 2006a and b), representing a large fraction of total zooplankton abundance. Other dominant zooplankton in the region included small cyclopoid copepods, mainly *Oithona similis*, small calanoid copepods and small euphausiids. Pinkerton et al. (2010) identified that *O. similis*, between 1991 – 2006, occurred in 91.1 % of SO-CPR samples and constituted 55.1 % of total counts. Larvaceans are typical of oceanic oligotrophic conditions (Bone, 1998; Deibel 1998), but also occur in large numbers in the SIZ, coastal and fjordic waters.

Knox (2007) cited a study by Jazdzewski et al. (1982) to show that Southern Ocean larvaceans were mainly concentrated in the upper 100m, as shown on the Antarctic Peninsula shelf, and near the northern slopes of the South Shetlands and Palmer Archipelago. SCAR-MarBIN records on the distribution of larvaceans (RAMS, 2010) showed 483 occurrences, with the majority of observations in the Atlantic Ocean, in the vicinity of the French Antarctic station Dumont D'Urville, and in Prydz Bay (Figure 1.6).

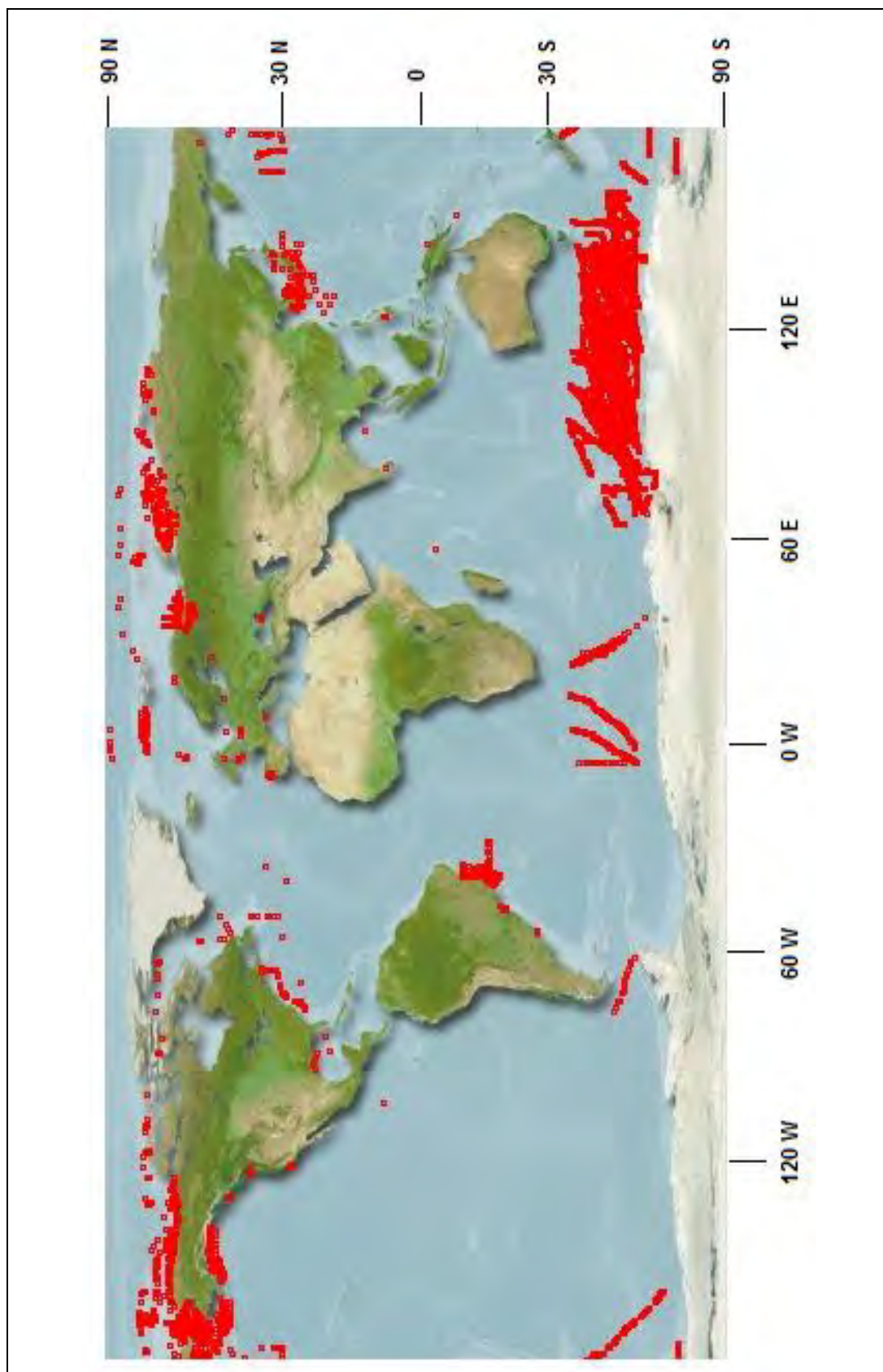


Figure 1.5. Global distribution of larvaceans. Data extent map from Ocean Biogeographic Information System Australia / C Square Mapper) (square size 1 degree). [Accessed 12 April 2010] www.iobis.org

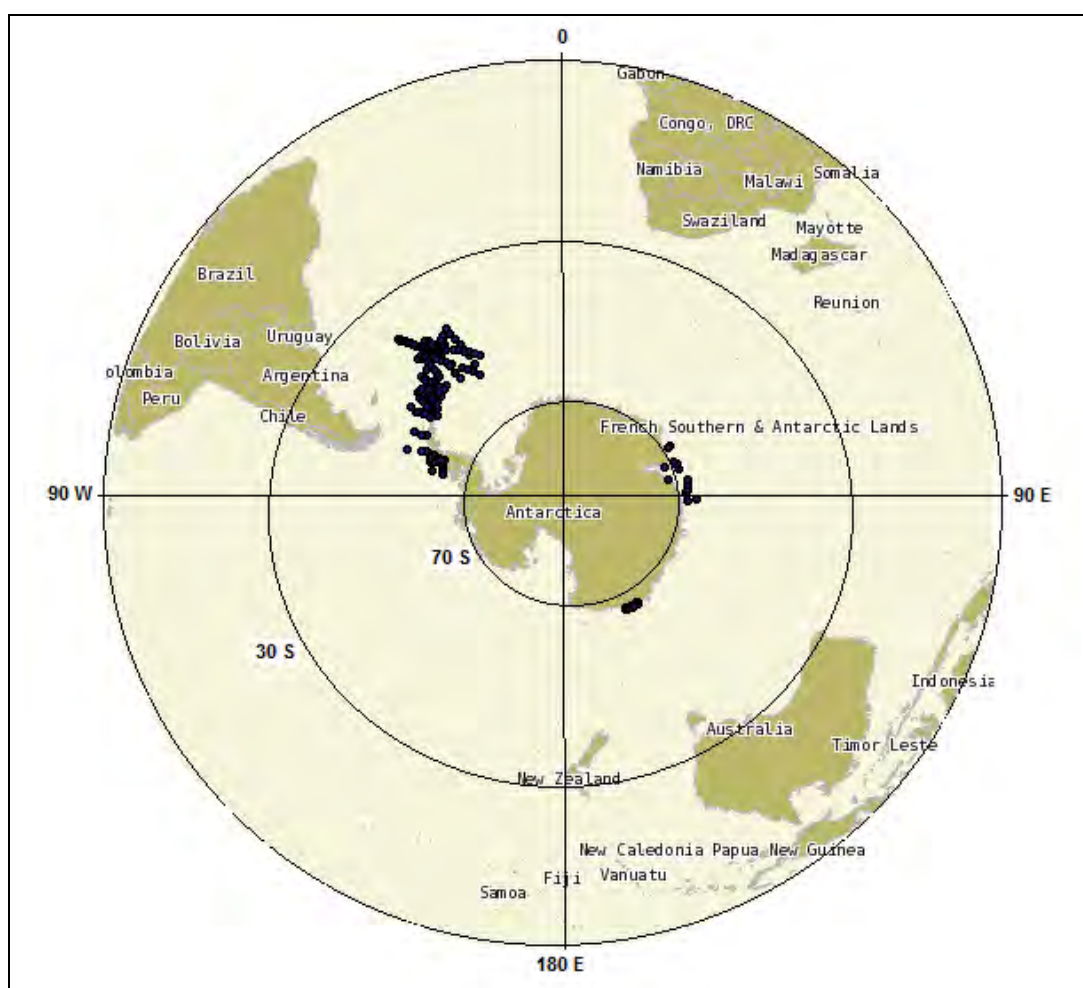


Figure 1.6. The SCAR-MarBIN Distribution of larvaceans (RAMS 2010)
<http://www.scarmarbin.be/AntobisMapper.php> accessed 10 May 2010)

1.7 Hypothesis and aims

This aim of this research is to further examine the distribution and abundance of Southern Ocean larvaceans, and to determine their ecological role. Previous studies have shown that larvaceans are widely distributed throughout the Southern Ocean and Antarctic coastal waters, and can be found in high abundances. Their capacity to ingest large quantities of nano- and pico-plankton means that they may play an unusual role in the marine microbial food-web, by transferring matter across many orders of magnitude in size, and moving it into the ocean interior. Thus, they may form an alternative link in the Antarctic food web between protists and vertebrates.

This study was conducted by identifying larvaceans, and determining their distribution and abundance in relation to biological and physical oceanographic features. Larvacean feeding ecology was also examined. The carbon flux of larvaceans in the Southern Ocean was calculated from both collected and published data.

The specific hypotheses that will be tested as part of this thesis include;

1. That the distribution and abundance of larvaceans have distinct zonation, as well as seasonal and annual variations;
2. That the distribution and abundance of larvaceans is related to physical (latitude, longitude, temperature, salinity and light) and biological (chlorophyll *a* and total zooplankton) influences;
3. That the diet of the Southern Ocean larvaceans is selective; and
4. That larvaceans contribute to carbon flux in the Southern Ocean by concentrating cells with their feeding houses, which are regularly discarded and via their faecal pellets.

1.8 Structure of this study

Chapter 2 describes the characteristics of the study region, oceanography, productivity, and the four voyages undertaken between the 2006/2006 and 2007/2008 Antarctic seasons.

Chapter 3 reviews the global taxonomic diversity of larvaceans, which are then compared with an analysis of species collected on research voyages in the present study.

Chapter 4 presents a re-analysis of a 25 year data set from the SO-CPR, focussing on the distribution and abundance of larvaceans, as well as seasonal and inter-annual patterns of abundance.

Chapter 5 is work that has already been published in Deep-Sea Research II and details the distribution of larvaceans from the BROKE-West voyage, a summer voyage to the high latitude Antarctic Ocean in 2005/2006.

Chapter 6 includes similar data from Chapter 5 for CEAMARC (2007/2008), another summer voyage in the high Antarctic, SIPEX (2007/2008), a winter voyage in the high Antarctic sea ice zone, and SAZ-SENSE (2006/2007), a summer voyage in the subantarctic zone.

Chapter 7 examines the stomach contents and morphology of the animals using scanning electron microscopy (SEM) to determine the size and species of phytoplankton that had been ingested by larvaceans. Results from this study are then compared with published data from non-Antarctic species to provide an estimate of the feeding capability of Southern Ocean larvaceans.

Finally, in Chapter 8 the estimates of distribution and abundance (Chapters 4, 5 and 6) are coupled with the inferred feeding rates (Chapter 7) to estimate the overall grazing impact and contribution to carbon flux from larvaceans in the Southern Ocean.

CHAPTER 2.

Study region and voyages

This chapter provides a brief overview of the Southern Ocean pelagic environment, followed by descriptions of each of the larvacean sampling voyages. The focus is on open ocean waters south of Australia.

2.1 Oceanography of the Southern Ocean

The Southern Ocean covers an area of approximately 50 million km² (10 % of the world's oceans) and forms a significant component of the global marine ecosystem. It consists of distinct physical and biological regimes, separated in the Pacific, Indian and Atlantic oceans by the Polar Front (PF) (Constable et al., 2003).

Five characteristics of the Southern Ocean as identified by Knox (2007), are;

1. it is a large system;
2. it is a semi-enclosed system (the Sub-Antarctic Front (SAF) forms a northern boundary and the ice edge forms the southern boundary);
3. it is an old system (its oceanic patterns are estimated to have formed 20 million years ago);
4. most of the major taxonomic groups are circumpolar, with the principal variation in distribution determined by variable productivity; and
5. it is quantitatively and qualitatively different from other oceanic systems, e.g. *Euphausia superba* (Antarctic krill) is a dominant and key species in the Southern Ocean, and not elsewhere.

The Southern Ocean is characterised by a large scale, circumpolar circulation, with currents, upwelling, overturning circulation, and connections between basins and fronts. These characteristics all play an important role in climate regulation (Orsi et al., 1995, Sallée et al., 2009). Orsi et al. (1995) defines the northern hydrographic boundary of the Southern Ocean as the Subtropical Front (STF) (Figure 2.1).

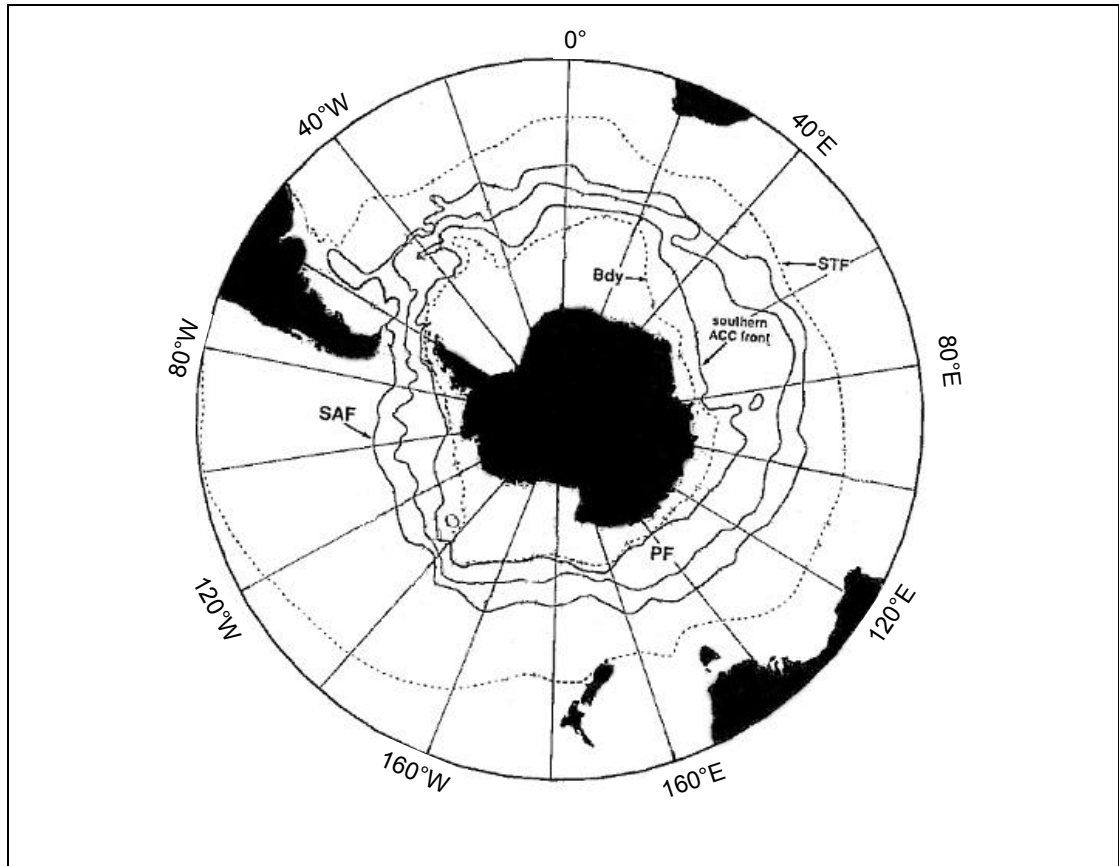


Figure 2.1. Circumpolar distribution of the Sub-Antarctic Front (SAF), Polar Front (PF) and Southern Antarctic Circumpolar Current Front (ACC front). Also shows the Subtropical Front (STF) and Southern Boundary of the ACC boundary (Orsi et al., 1995).

Recent Southern Ocean studies have identified a departure from zonal structures associated with latitude (Sallée et al., 2009). Rather, fronts are linked to overturning circulation patterns, as shown in Figure 2.2. The transition from upwelling and buoyancy gain in the south to downwelling and buoyancy loss in the north roughly coincides with the SAF. Formation of Subantarctic Mode Water (SAMW) and Antarctic Intermediate Water (AAIW) occurs north of the SAF. Antarctic Bottom Water (AABW) on the Antarctic Shelf occurs only in restricted locations. Nutrients are brought to the surface from Upper and Lower Circumpolar Deep Water (UCDW and LCDW) with increasing efficiency further south as a result of the increasingly negative wind-stress curl, as well as deep winter convection associated with sea-ice formation (Trull et al., 2001). Spatial patterns of overturning (upwelling and downwelling) circulation show high circumpolar variability (Sallée et al., 2009; Figure 2.3).

The southern and northern boundaries of the circumpolar Southern Ocean have additional complexities. The Ross/Weddell/Prydz embayments are regions recognised as having different properties than adjacent circumpolar waters. Regions characterised by the northern edge western boundary current, such as the Benguela current off Africa, and other regions such as the East Australian Current (EAC) east of Australia (Bowie et al., 2009), bring additional influences such as water temperature, salinity concentrations and current directions.

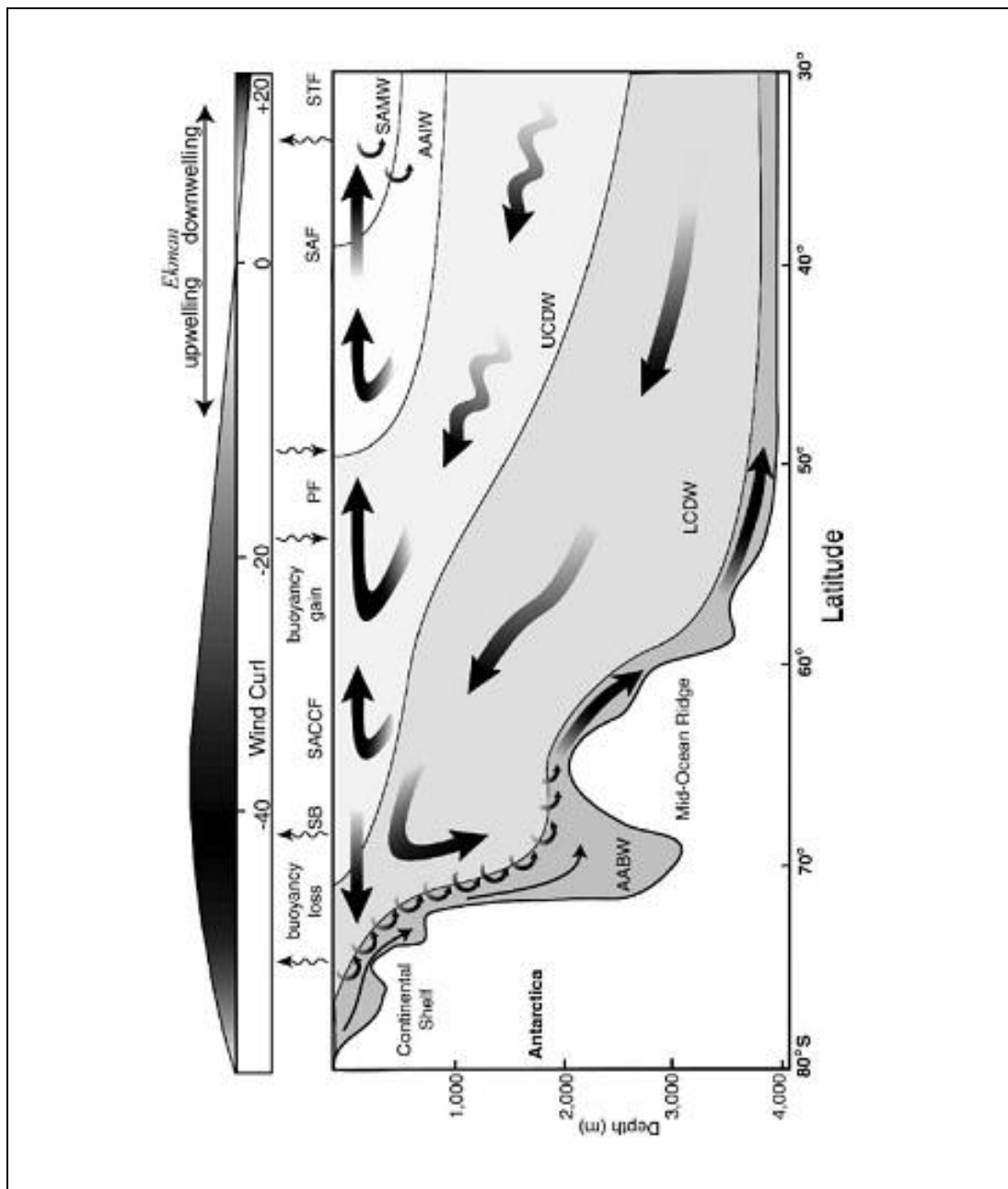


Figure 2.2. A schematic of the meridional overturning circulation in the Southern Ocean showing annual mean wind-stress curl (10^9 dyn cm^{-2}) (Trull et al., 2001).

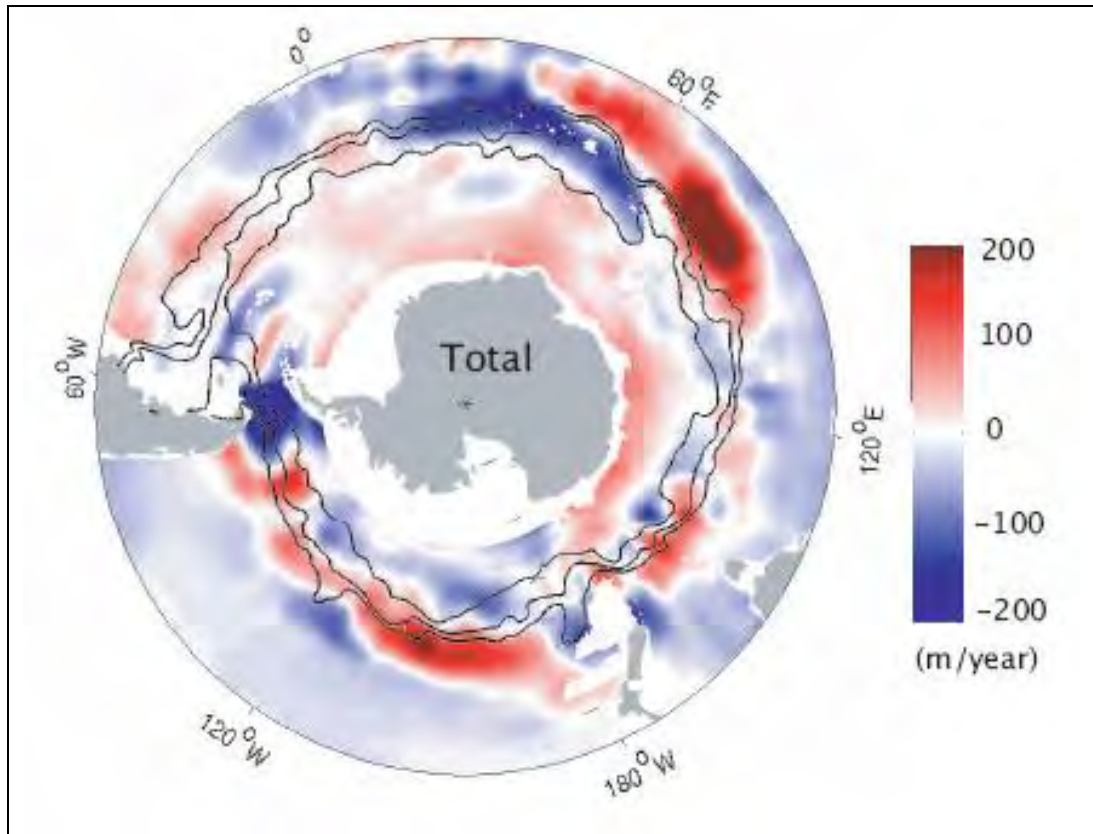


Figure 2.3. Map of the total annual mean subduction (m year^{-1}) show high circumpolar variability. The three main fronts (PF, SAF and SAF-N) of the ACC are superimposed as dark lines radiate from the South pole (*). Source: Sallée et al. (2009).

The Southern Ocean has a highly defined seasonality that governs physical and biological characteristics due to the growth and melt of sea-ice. Figure 2.4 shows the mean February (minimum) and September (maximum) sea ice extent in the Southern Ocean, each calculated from 2006-2008 daily AMSR-E satellite data (Spren et al., 2008). There are generally high levels of interannual variability in sea-ice. The 1979–2000 mean September average sea-ice extent was 18.7 million km^2 compared to the smaller February average extent of 2.9 million km^2 (NASA, 2010). In March, as the temperature drops, the ocean begins to freeze at an average of 4 km per day, extending 600 – 3000 km from the coastline by September. The winter sea-ice maximum covers an area of 22 million km^2 (twice the size of the Antarctic continent, Orsi et al., 1995). During spring and summer, the sea-ice melts to only 4 million km^2 . Figure 2.5 shows the sea-ice extent south of Australia which is the area of study for this thesis (Worby et al., 1998).

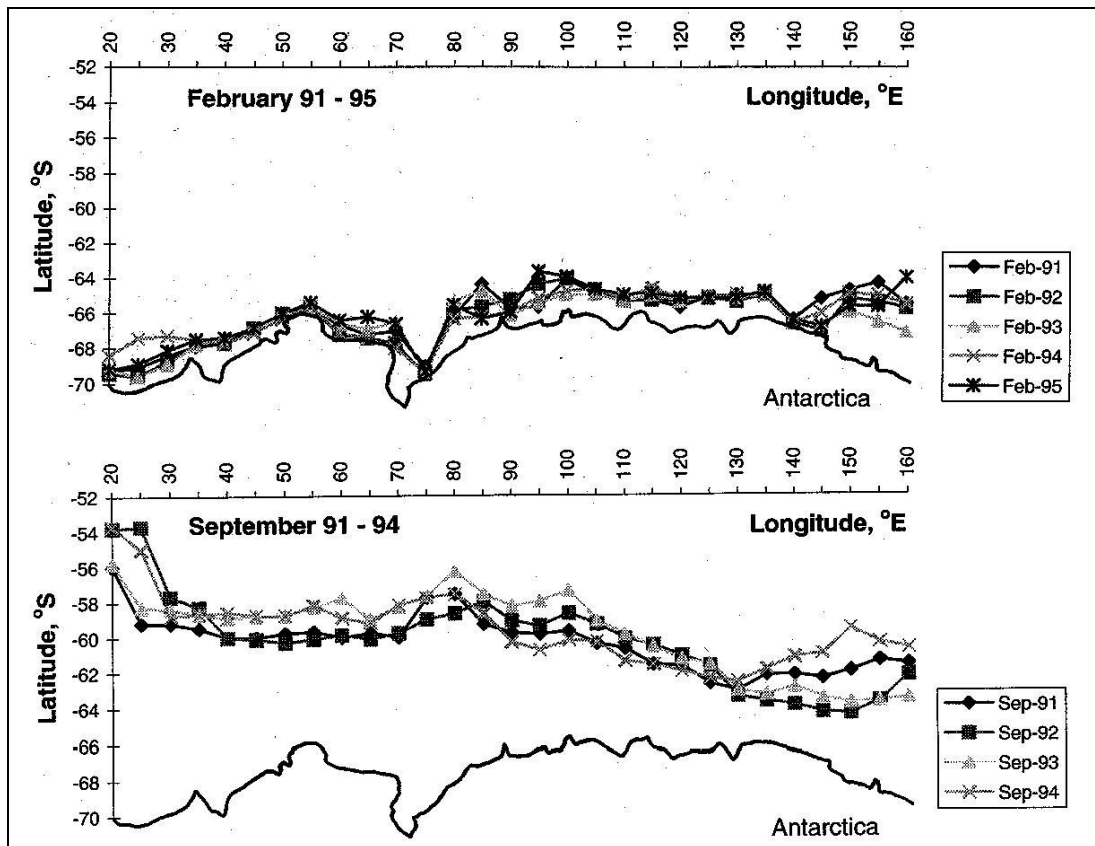


Figure 2.5. Maps of mean monthly ice edge locations in East Antarctica for February 1991 to 1995 and September 1991 to 1994 (Worby et al., 1998).

Southern Ocean oceanography and ecology are strongly influenced by sea-ice (Sallée et al., 2009), temperature (Figure 2.6, World Ocean Atlas, 2005), and light availability which is largely influenced by mixed layer depth (Sallée et al., 2009). Nutrient availability also has a strong influence on ecology. The macronutrient, nitrate, has a similar distribution to phosphate, with concentrations increasing from north to south (Figure 2.7a). Silicate concentrations (Figure 2.7b) are low in the north so that large diatom growth is generally confined to the south (Trull et al. 2001). Other species such, as cyanobacteria, tend to occur in the SAZ (Trull et al., 2001).

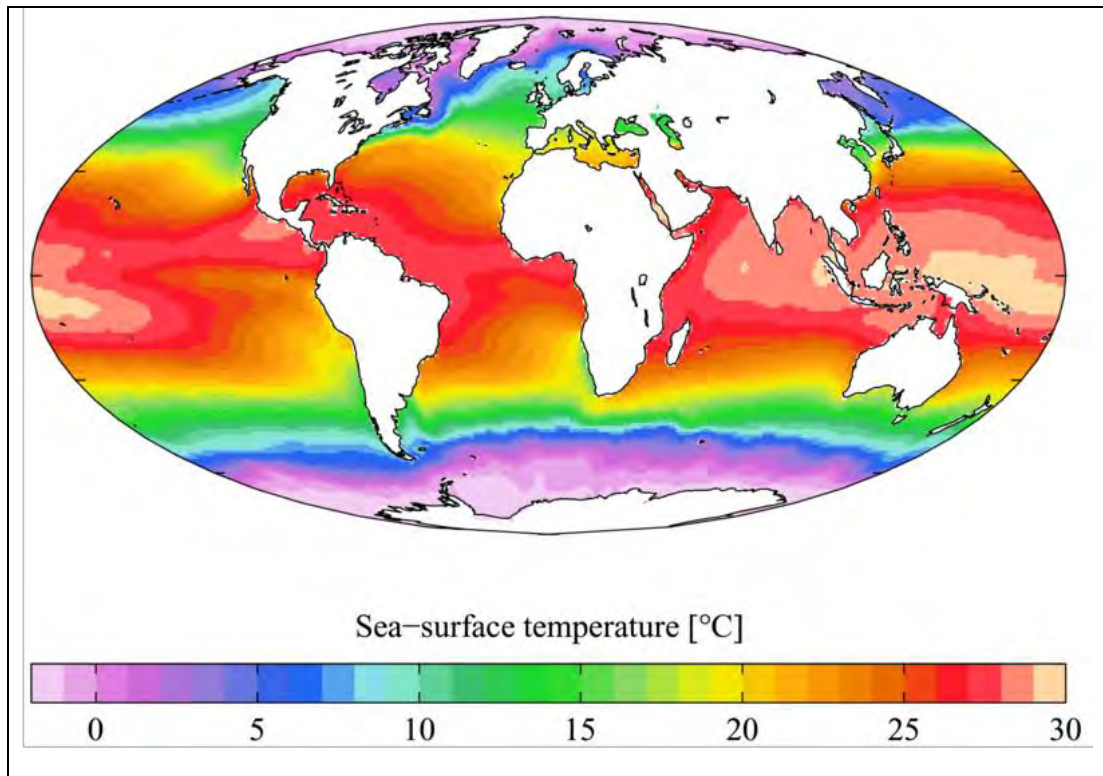


Figure 2.6. Global mean sea surface temperature from the World Ocean Atlas (WOA). Data produced from the Ocean Climate Laboratory of the National Oceanographic Data Center (U.S., WOA 2005).
http://en.wikipedia.org/wiki/World_Ocean_Atlas (accessed 2010)

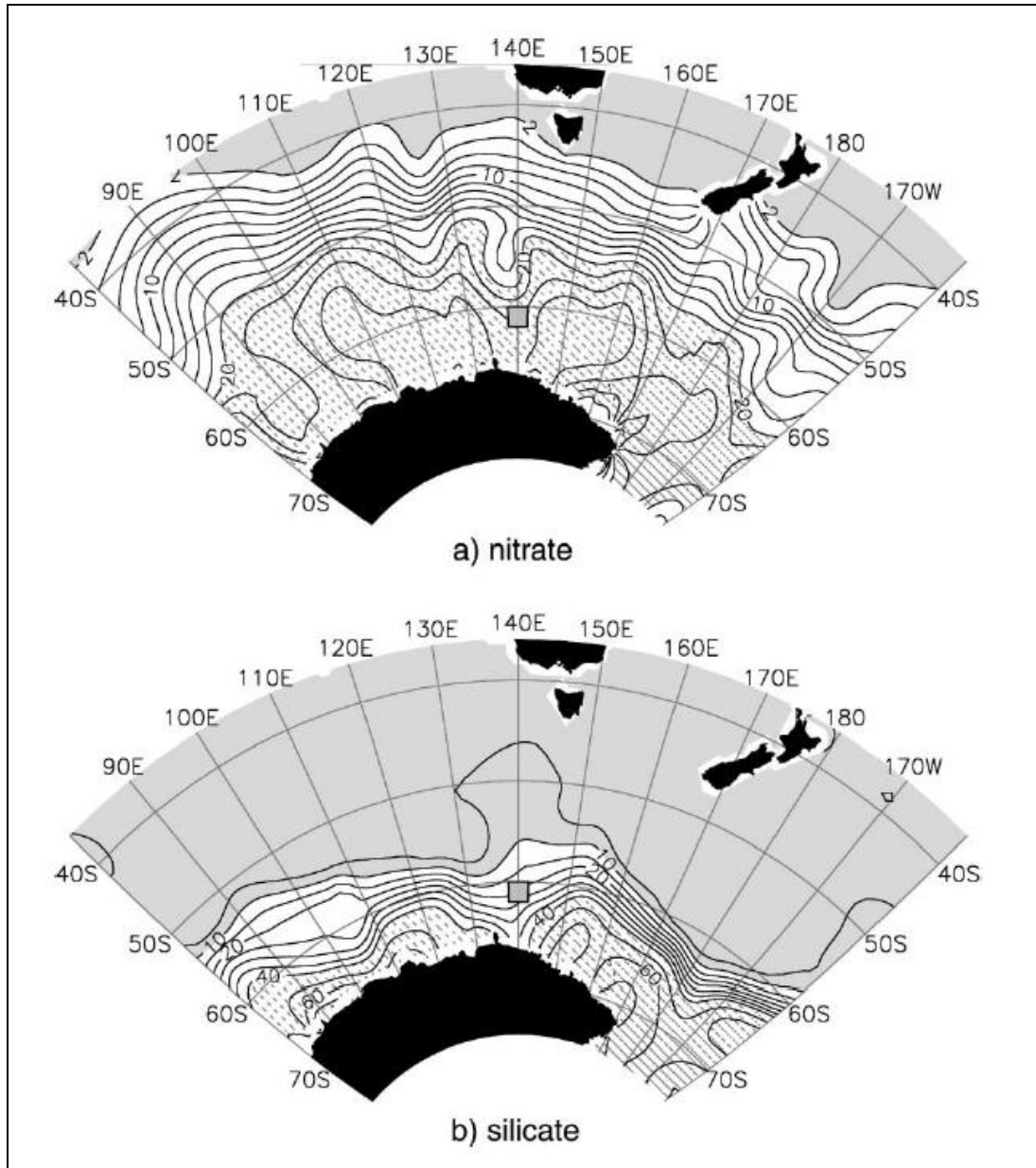


Figure 2.7. Map of dissolved (a) nitrate and (b) silicate summer average concentrations at 10m. The grey square in the centre is the location of the Southern Ocean Iron Release Experiment (SOIREE) (Trull et al., 2001).

Phytoplankton distributions and abundances vary widely in the Southern Ocean (Sokolov and Rintoul, 2007; Arrigo et al., 1998; Moore and Abbott, 2000). Figure 2.8 shows ocean colour and fronts of the Southern Ocean. Mean summer chlorophyll concentrations south of Australia, the main study area for this thesis, are mapped in Figure 2.9 (Sokolov and Rintoul, 2007).

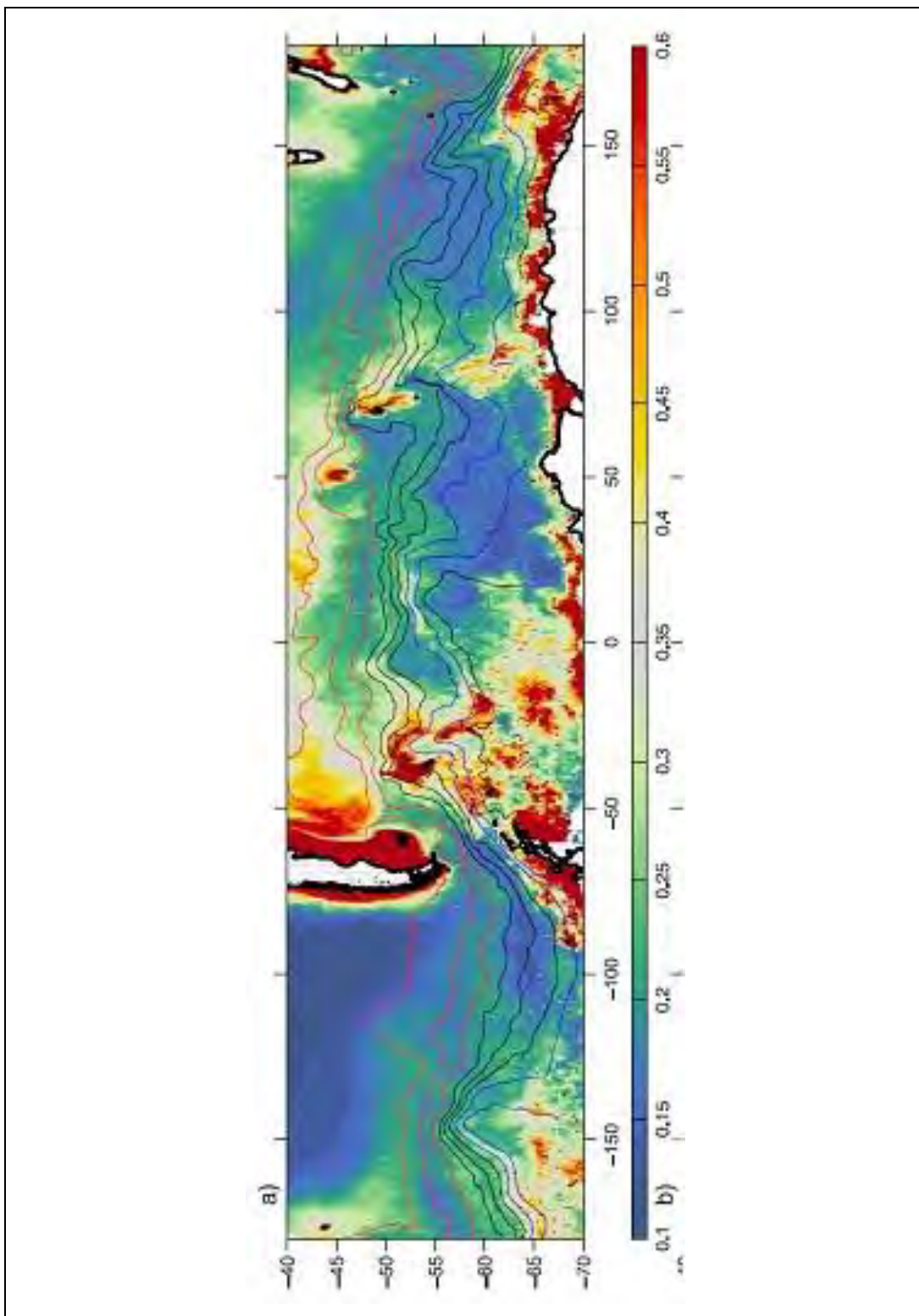


Figure 2.8. Mean chlorophyll distribution in the Southern Ocean averaged over the period from October 1997 to October 2002 (Sokolov and Rintoul, 2007).

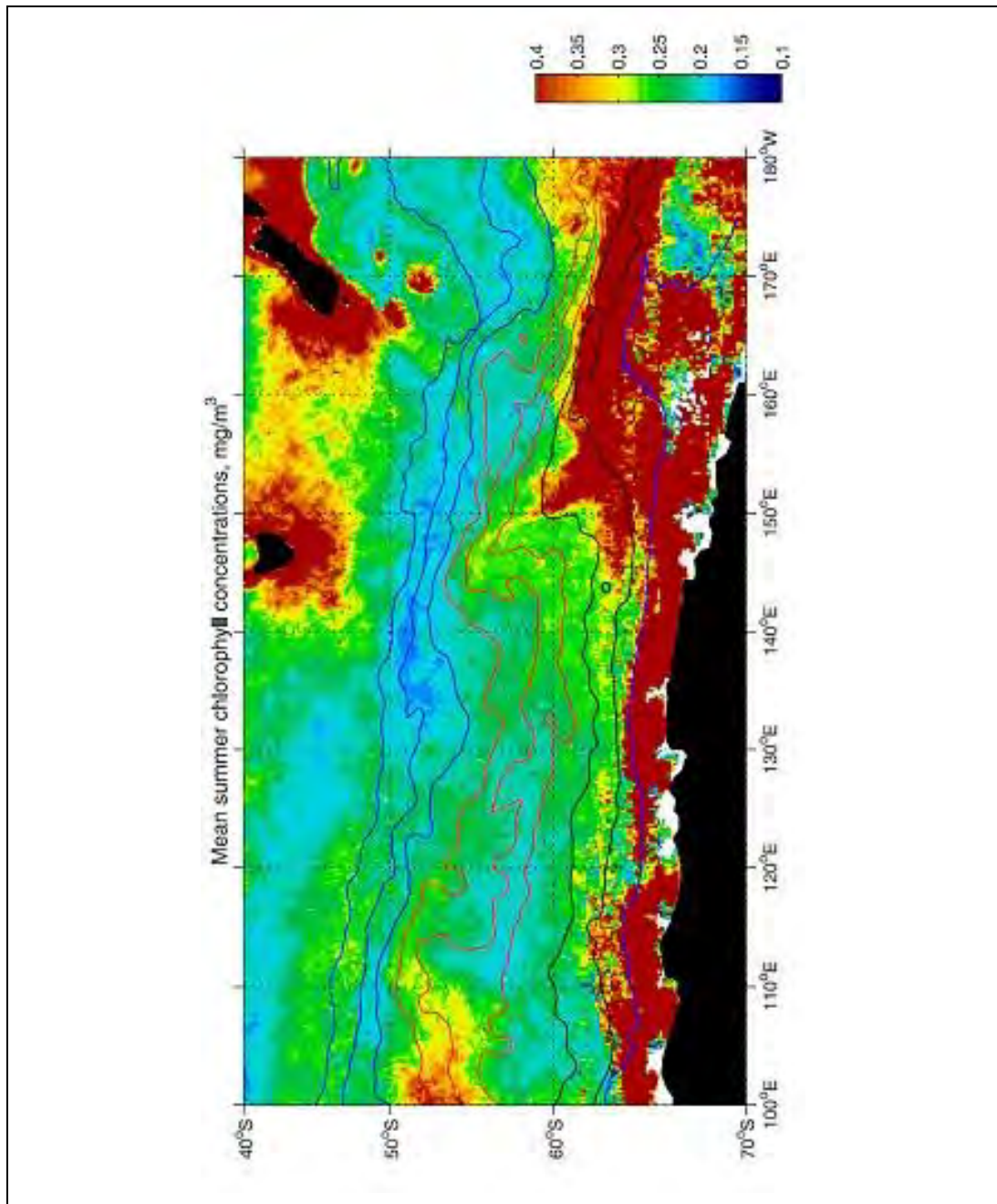


Figure 2.9. Mean summer chlorophyll concentrations south of Australia. Mean summer positions of the ACC fronts are also shown and colour – coded to show that the concentrations vary widely in the Southern Ocean (Sokolov and Rintoul, 2007).

Phytoplankton distribution is not as zonal as the physical and chemical characteristics described above. This is thought to be due to iron limitation, with the Southern Ocean considered a High Nutrient Low Chlorophyll (HNLC) region. Iron limitation has been clearly demonstrated in a number of studies, using both experimental (Boyd et al., 2008), and *in situ* iron additions (de Baar et al., 1995;

Blain et al., 2007; Pollard et al., 2009). Iron limitation has been demonstrated both south of the PF, and north of the PF in the SAZ (Bowie et al., 2009).

Figure 2.10 (Longhurst, 1998) shows the seasonal and zonal variability of sea surface chlorophyll for the Southern Ocean.

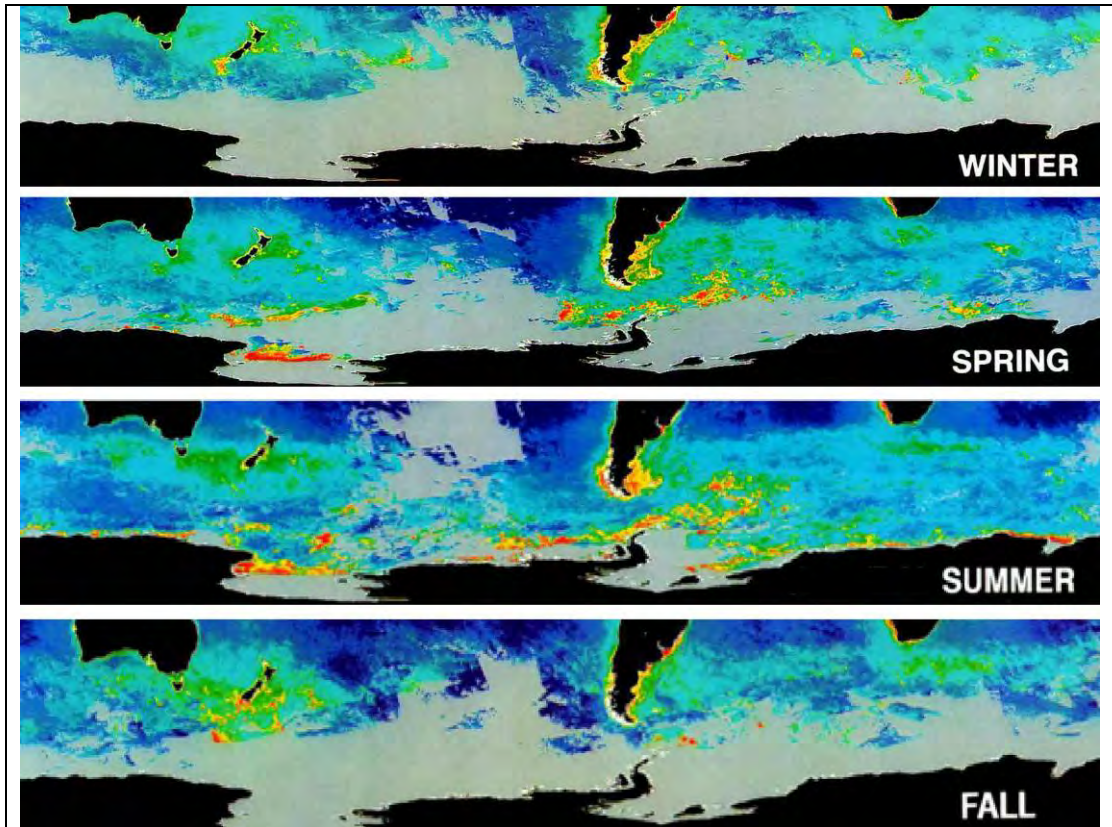


Figure 2.10. Climatological (1978 – 1986) seasonal sea surface chlorophyll for the austral seasons; winter (June to August), spring (September to November), summer (December to February) and autumn (March to May). Colour is a log scale for chlorophyll: purple = $<0.06 \text{ mg Chl m}^{-3}$, orange-red = $1 - 10 \text{ mg Chl m}^{-3}$ (Longhurst, 1998).

In contrast to phytoplankton, zooplankton distributions in the Southern Ocean tend to be more zonal. Salps and krill tend to have alternate distributions, with salps occurring in the north given that they can tolerate warmer waters (Atkinson et al., 2004). Nicol et al. (2000) also identified that salps occurred in areas where sea-ice extent was minimal. Biological zonation also occurs at higher trophic levels, e.g. with krill (Figure 2.11) and blue whale (Figure 2.12) abundances related to the East Wind Drift, Weddell Drift, Polar Front and Southern Boundary of the Antarctic Circumpolar Current (ACC) (Tynan, 1998). In addition, during the BROKE survey in 1996 (Nicol et al., 2000), whale, seabird and *E. superba*

populations (Figure 2.13) tended to be concentrated in areas where winter sea-ice extent was maximal. Primary productivity and phytoplankton were also concentrated in these areas (Nicol et al., 2000).

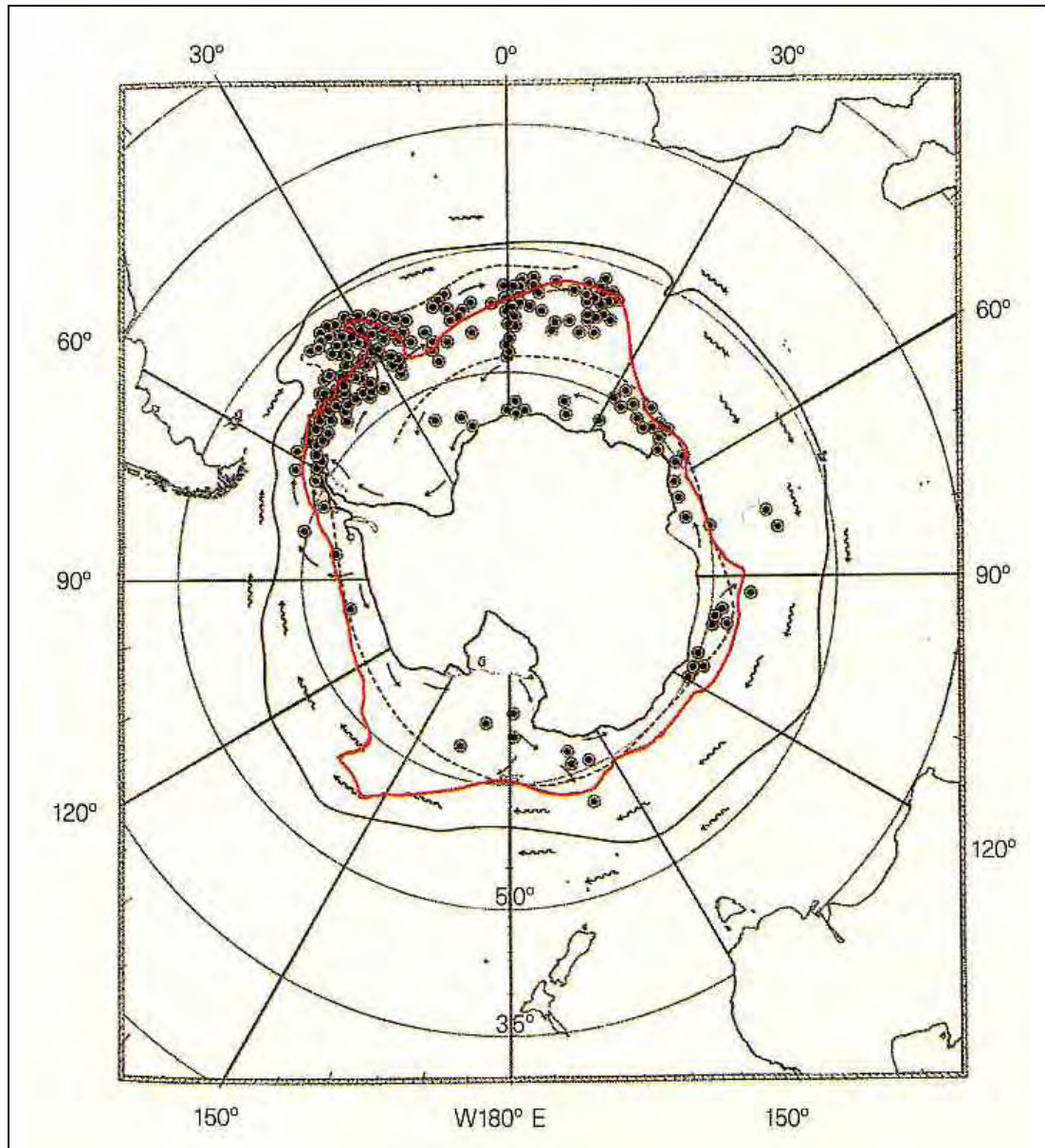


Figure 2.11. Distribution of principal concentrations of krill (encircled black circles) in relation to the East Wind Drift and Weddell Drift (dashed lines), Polar Front (black lines) and Southern Boundary of the Antarctic Circumpolar Current (ACC) (red line) (Tynan, 1998).

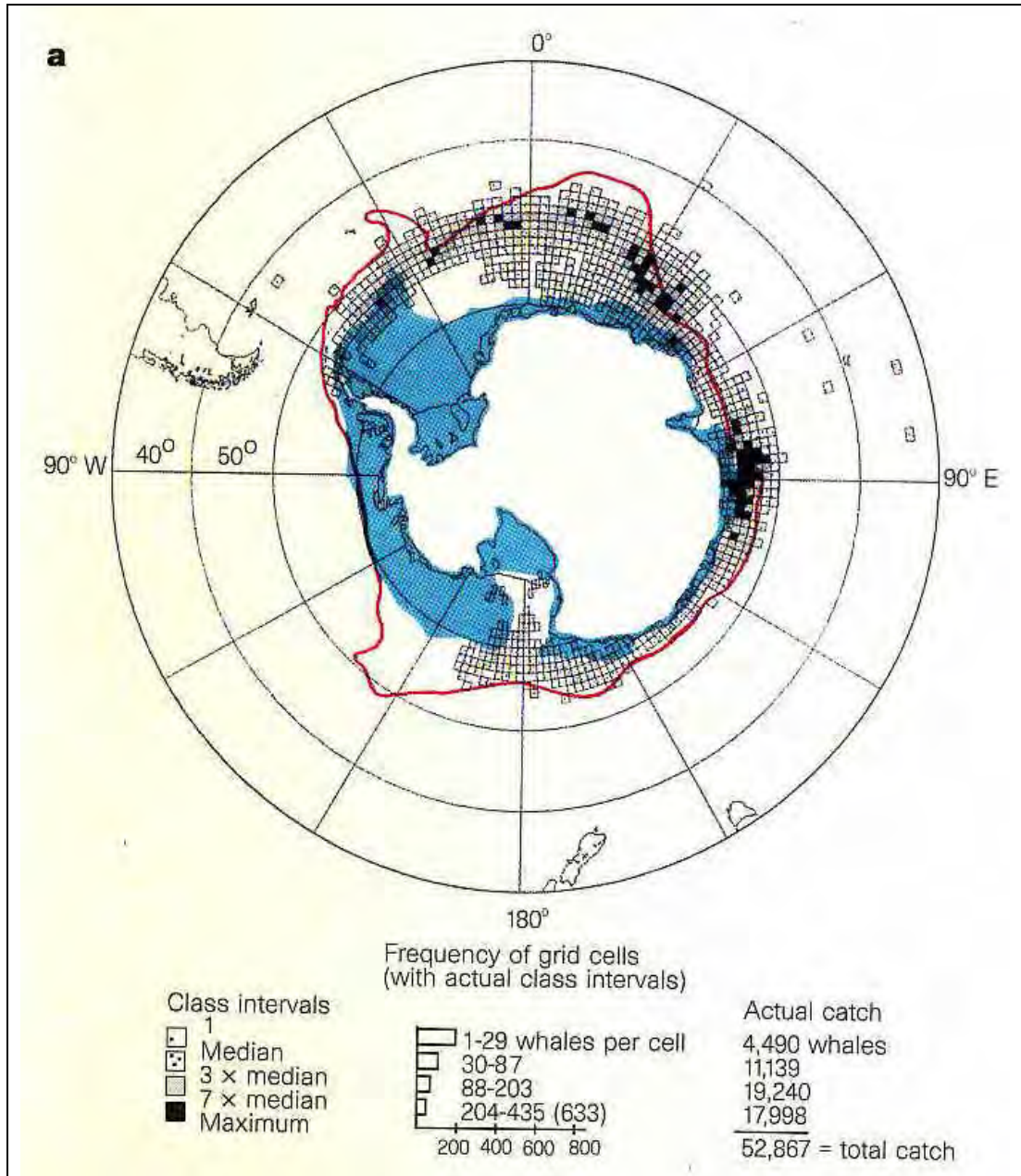


Figure 2.12. Distribution of blue whale catches during January 1931/32 to 1966/67 in relation to the Southern Boundary of the Antarctic Circumpolar Current (ACC) (red line) and the mean monthly extent of sea-ice coverage (blue) for January 1979 to 1987. Grid size for the whale data is 1° latitude and 2° longitude (Tynan, 1998).

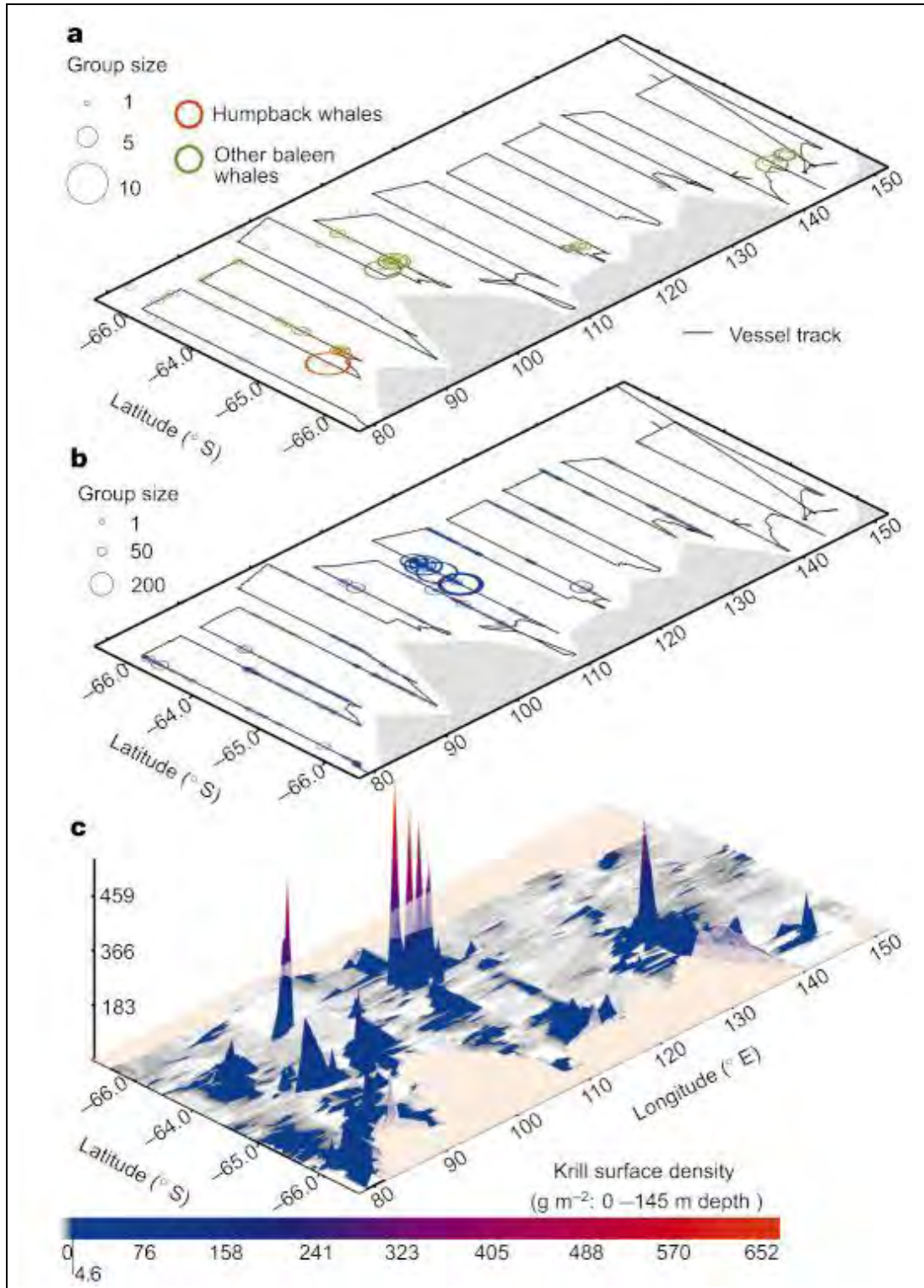


Figure 2.13. Distribution and abundance (grams per square metre) of a) whales, b) seabirds and c) Antarctic krill (*Euphausia superba*) off east Antarctica during austral summer, 1996. The BROKE survey track is indicated (Nicol et al., 2000).

2.2 Southern Ocean larvacean zones

For the purposes of this thesis, the Southern Ocean was divided into a number of zones in order to allow comparisons of distributions and abundances. All research voyages undertaken were conducted in the East Antarctic, with the Southern Ocean divided into the Sub Antarctic Zone (SAZ), Permanent Open Ocean Zone (POOZ, including the PFZ) and Sea Ice Zone (SIZ). Each zone had a 2° gap in latitude so there was no overlap. The SAZ is defined as north of 48°S, the POOZ between 50° and 60°S, and the SIZ as south of 62°S.

2.3 Survey regions

Four research voyages were undertaken between 2006 and 2008 that covered the three Southern Ocean zones defined above (Table 2.1 and Figure 2.14). Figure 2.15 is a graph showing the latitudes that were surveyed for larvaceans, in relation to time of year (ordinal date). It should be noted that the voyages were undertaken in different years in most cases (Table 2.1).

Table 2.1. Summary of Southern Ocean voyages undertaken between 2006 and 2008 to examine larvaceans. The voyage dates are from departure from Australia to return to Australia. The methods used include the ring net, the Continuous Plankton Recorder (CPR), Rectangular Mid-water Trawl (RMT1), cameras from the Remote Operated Vehicle (ROV) and Surface Underwater I Trawl (SUIT), multi net and Visual Plankton recorder (VPR).

Voyage acronym	Voyage # and zone	Full title	Period and dates	Vessel	Sampling methods	Study focus
BROKE-West	V3 POOZ and SIZ	Baseline Research on Oceanography, Krill and the Environment – West	72 days; 2 Jan – 14 March 2006	RSV <i>Aurora Australis</i>	Ring net (150 µm) CPR RMT1 (330 µm)	Distribution and abundance Diet
SAZ-Sense	V3 SAZ	Sub-Antarctic Zone – Sensitivity	35 days; 17 Jan – 20 Feb 2007	RSV <i>Aurora Australis</i>	Ring net (150 µm) RMT1 (150 µm)	Distribution and abundance Diel cycle Stratification
SIPEX	V1 SIZ	Sea Ice Physics & Ecosystem eXperiment	44 days; 4 Sept – 17 Oct 2007	RSV <i>Aurora Australis</i>	Ring net (150 µm) RMT1 (330µm) ROV – SUIT camera CPR	Distribution and abundance
CEAMARC - Pelagic	NA SIZ	Collaborative East Antarctic Marine Census	26 days; 23 Jan– 17 Feb 2008	TRV <i>Umitaka Maru</i>	WP2 net (150 µm) Multi net (150 µm) CPR VPR	Distribution (presence / absence)

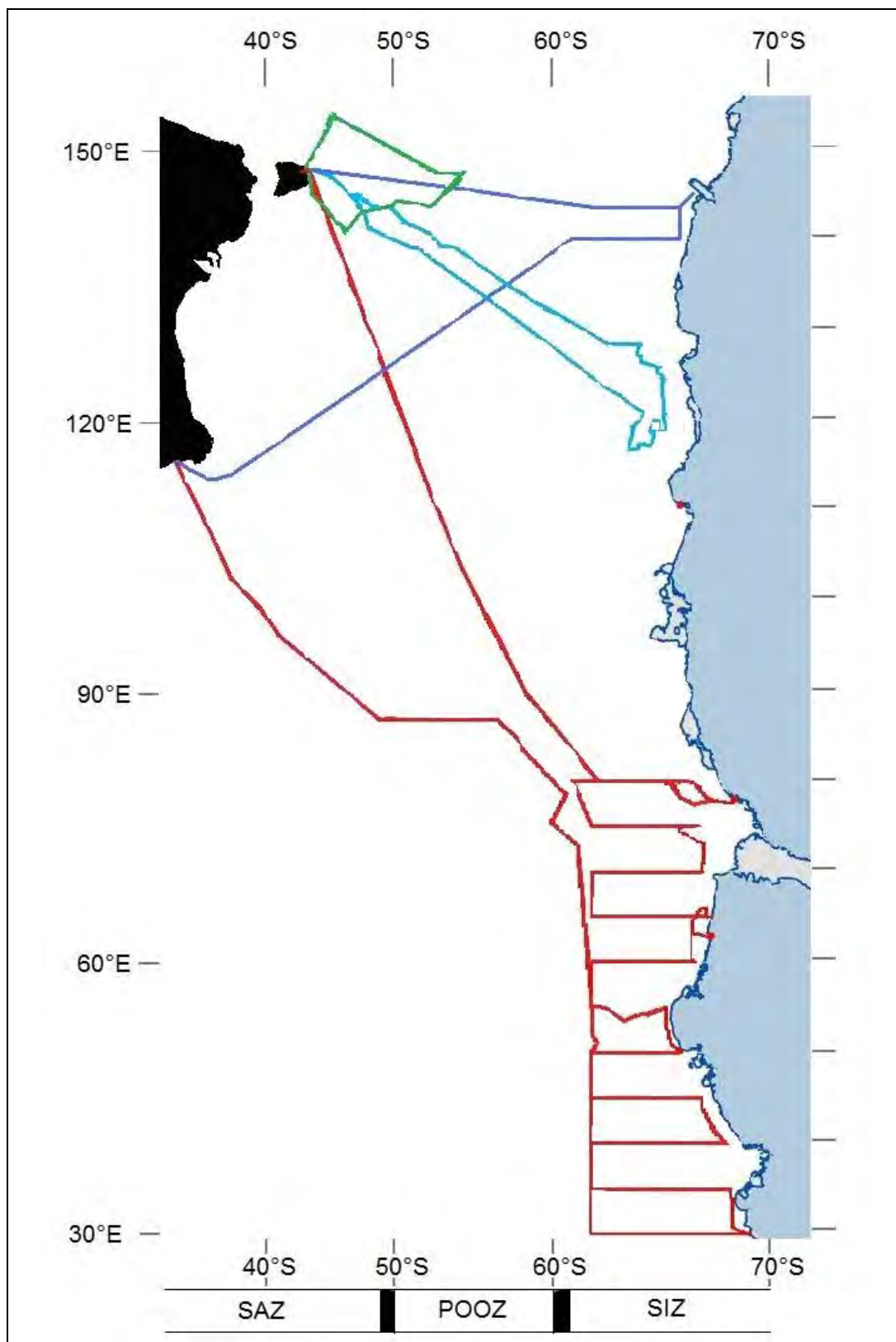


Figure 2.14. Map of the Southern Ocean zones and voyage tracks undertaken to determine the distribution and abundance of larvaceans. The Sub Antarctic Zone (SAZ) was surveyed during SAZ-Sense (green); the Permanent Open Ocean Zone (POOZ) during the westbound leg of the BROKE West voyage (red); the Sea Ice Zone (SIZ) during BROKE-West (red), SIPEX (blue) and CEAMARC (purple).

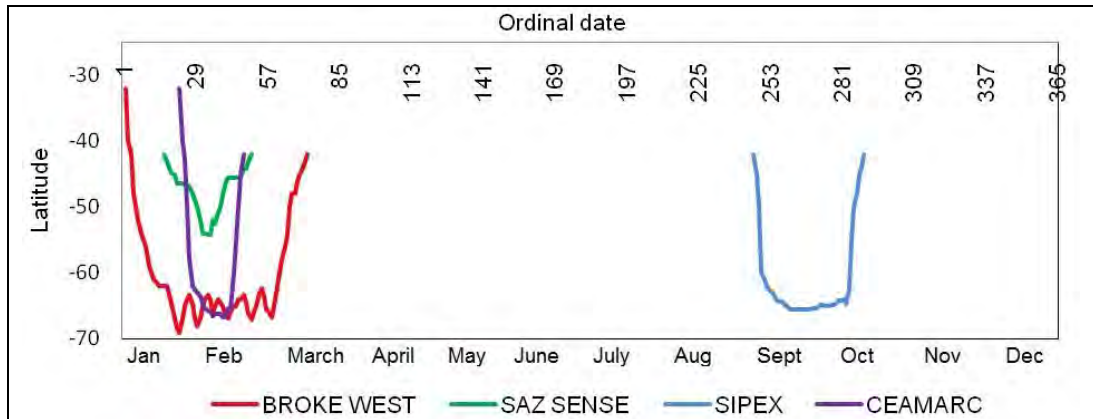


Figure 2.15. Graph showing ordinal date and latitude for the voyages undertaken to collect larvaceans in the East Antarctic Southern Ocean. BROKE-West (red), SAZ-Sense (green), SIPEX (blue) and CEAMARC (purple).

2.4 Purpose and structure of the voyages

The purpose and structure of each voyage to survey larvaceans is detailed below. The four voyages used ship-time opportunistically as they were multi-disciplinary. Aside from the voyages described below, additional oceanography and plankton studies were undertaken by the French vessel *l’Astrolabe* throughout the duration of the project (<http://mersaustrales.mnhn.fr>).

2.4.1 BROKE-West

The Baseline Research on Oceanography, Krill and the Environment – West (BROKE-West) survey (Nicol and Meiners, 2010) was conducted in austral summer, 2006. It was a comprehensive hydro-acoustic survey of the Antarctic margin, in the southwest Indian Ocean sector of the Southern Ocean. A suite of physical and biological observations were conducted, including sampling for larvaceans. Samples were collected between 10 January and 28 February, 2006, aboard the RSV *Aurora Australis*. The voyage covered an area from 60 - 70°S and 30 - 80°E (Figure 2.16). A total of twelve transects were conducted, covering 1.5 million km² of sampling area. There was one westbound transect and six southbound transects, interspersed with five northbound transects. Sampling was also conducted on the outward and return transit legs through deployment of a CPR.

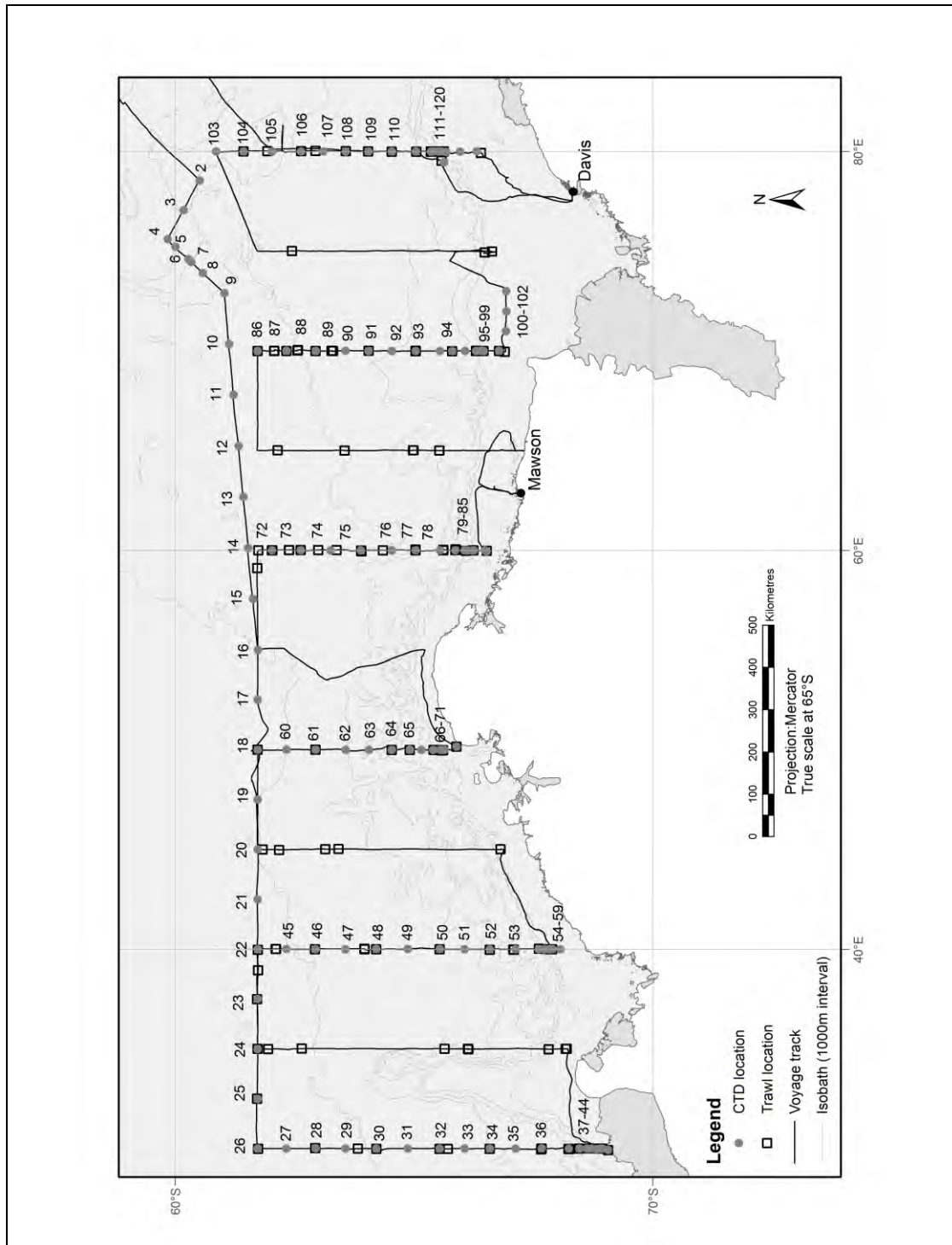


Figure 2.16. Survey region of the Baseline Research on Oceanography, Krill and the Environment – West (BROKE West) voyage from 2 January to 14 March 2006, aboard RSV *Aurora Australis*. Figure adapted from the Australian Antarctic Data Centre.

2.4.2 SAZ-Sense

The SAZ-SENSE research voyage examined the sensitivity of the Sub-Antarctic Zone (SAZ) to global change. It was a 32-day voyage that departed Hobart on 17 January and returned 20 February, 2007, conducted aboard RSV *Aurora Australis*. Oceanography, the microbial ecosystem, zooplankton, and biogeochemical processes were examined between 140°E and 160°E in the SAZ and in the Polar Frontal Zone south of the SAZ (Figure 2.17). The main aim of the voyage was to investigate SAZ productivity and carbon cycling, and to assess the region's sensitivity to climate change. This was done by comparing low productivity waters west of Tasmania with higher productivity waters to the east, focussing on the role of iron as a limiting micronutrient. The study also examined the effect of rising CO₂ levels on phytoplankton - both via regional inter-comparisons and incubation experiments (Deep Sea Research II SAZ-Sense special edition, *in prep.*; <http://www.cmar.csiro.au/datacentre/saz-sense/>).

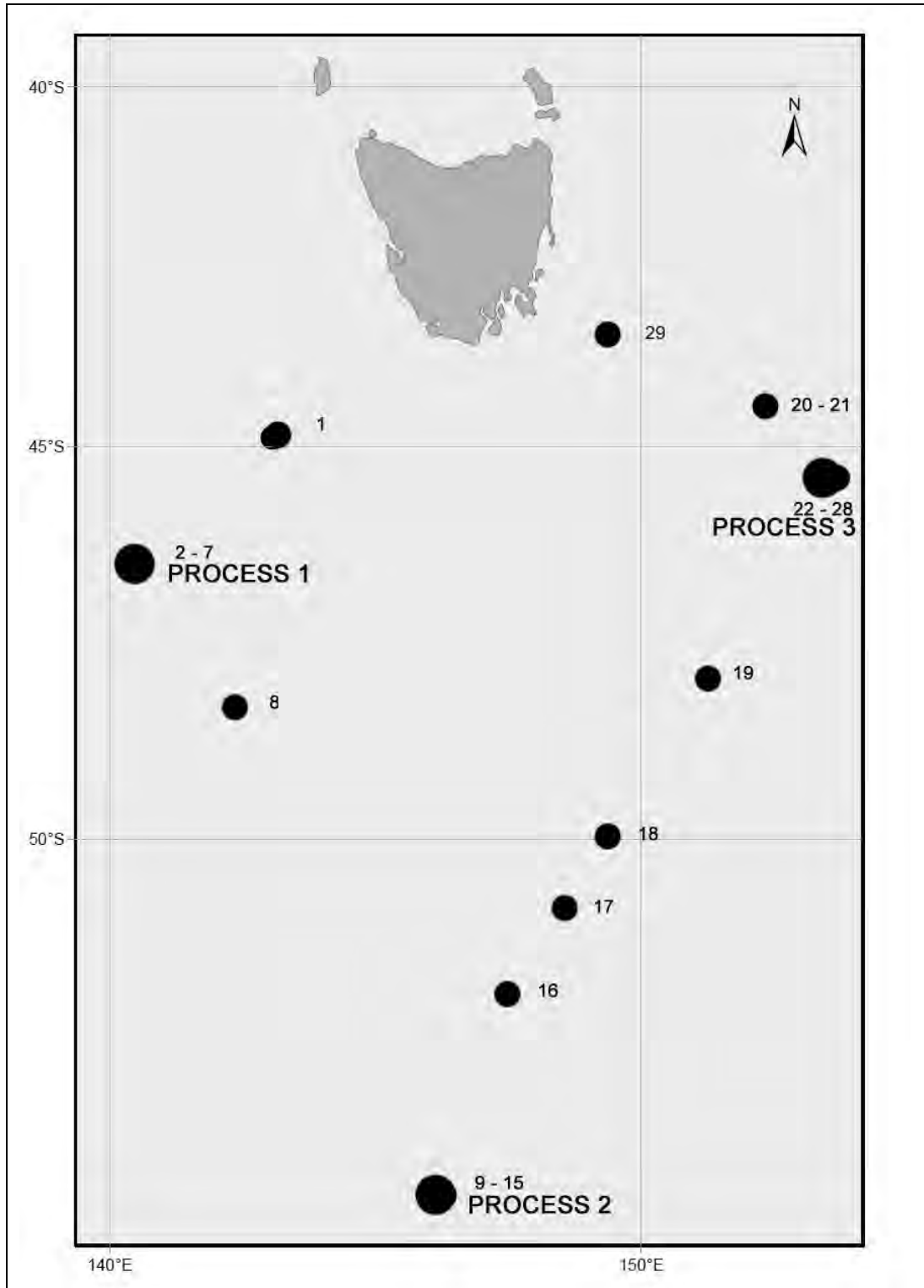


Figure 2.17. Map of sample sites and process stations for the Sub-Antarctic Zone – Sensitivity (SAZ Sense) voyage from 17 January to 20 February, 2007, aboard RSV *Aurora Australis*. Figure adapted from the Australian Antarctic Data Centre.

2.4.3 SIPEX

The Sea Ice Physics and Ecosystem eXperiment (SIPEX) research voyage was undertaken in the SIZ and was one of Australia's major contributions to the International Polar Year (IPY). The expedition concentrated on a small area of the SIZ and was undertaken from 9 September to 11 October, 2007. Samples were collected aboard RSV *Aurora Australis*, from 110°E to 130°E (Figure 2.18). A total of 15 ice stations were completed in the SIZ, with specific examination of relationships between the physical sea-ice environment and the structure of the Southern Ocean ecosystem (www.acecrc.sipex.aq).

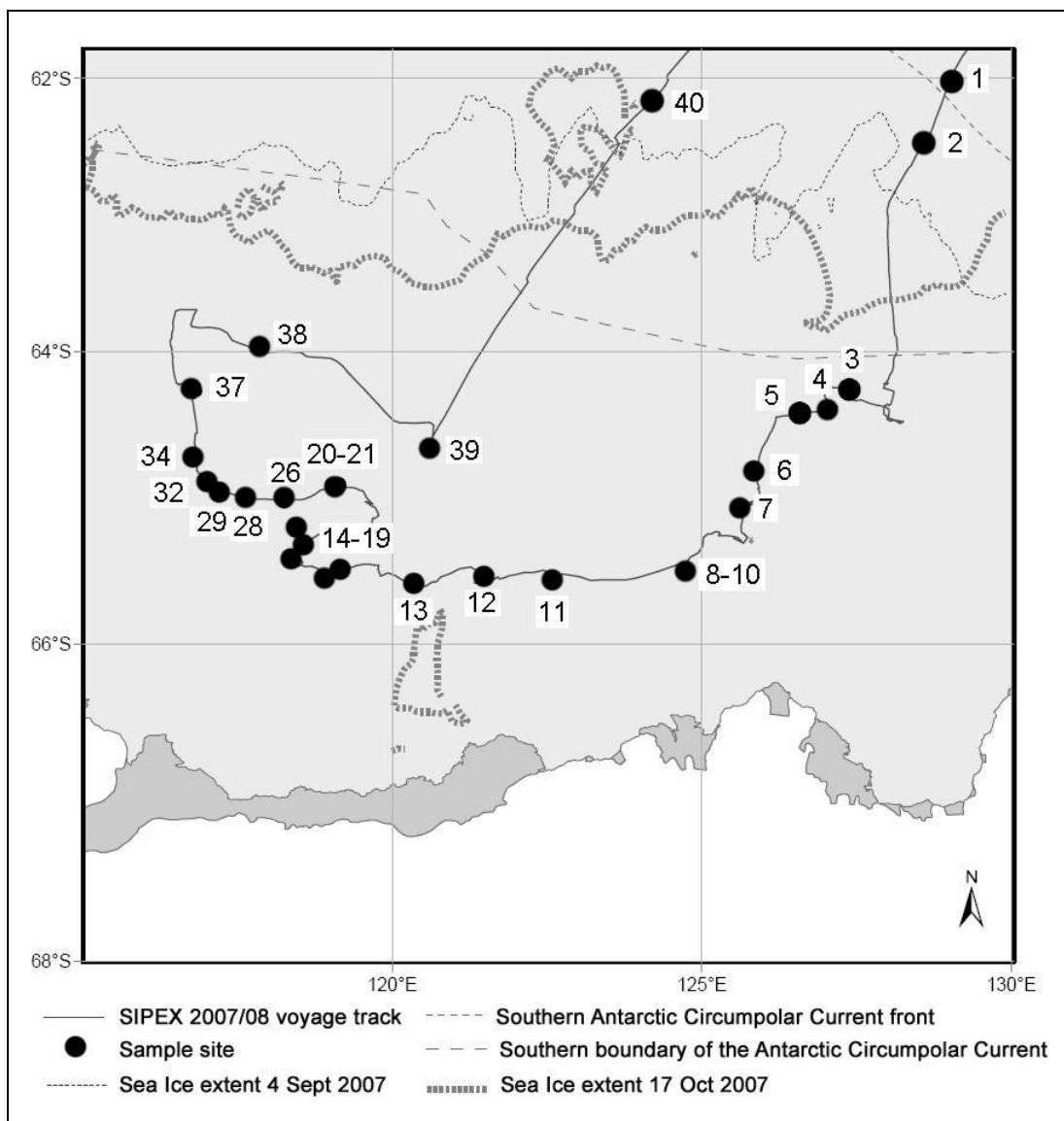


Figure 2.18. Voyage track and sample points for the Sea Ice Physics and Ecosystem eXperiment (SIPEX) from 4 September to 17 October, 2007, conducted aboard RSV *Aurora Australis*. Figure adapted from the Australian Antarctic Data Centre.

2.4.4 CEAMARC - Pelagic

The Collaborative East Antarctic Marine Census - Pelagic (CEAMARC - pelagic) voyage was conducted aboard the TRV *Umitaka Maru*. This project formed part of the Census for Antarctic Marine Life (CAML, IPY Project 53). The voyage departed Fremantle in Western Australia on the 23 January and returned to Hobart on 17 February, 2008. CEAMARC was the Australian-French-Japanese-Belgium contribution to CAML. The CEAMARC survey region covered an area north of Terre Adélie and George V Land off Eastern Antarctica (Figure 2.19). The main aim of the voyage was to examine Antarctic marine biodiversity and to understand the processes that lead to evolution and survival of the biota. In this way, responses to future change in the environment may be predicted. Both CEAMARC and CAML specifically targeted mesozooplankton and gelatinous zooplankton, the deeper pelagic populations in particular (Hosie et al., 2011) (www.caml.aq/).

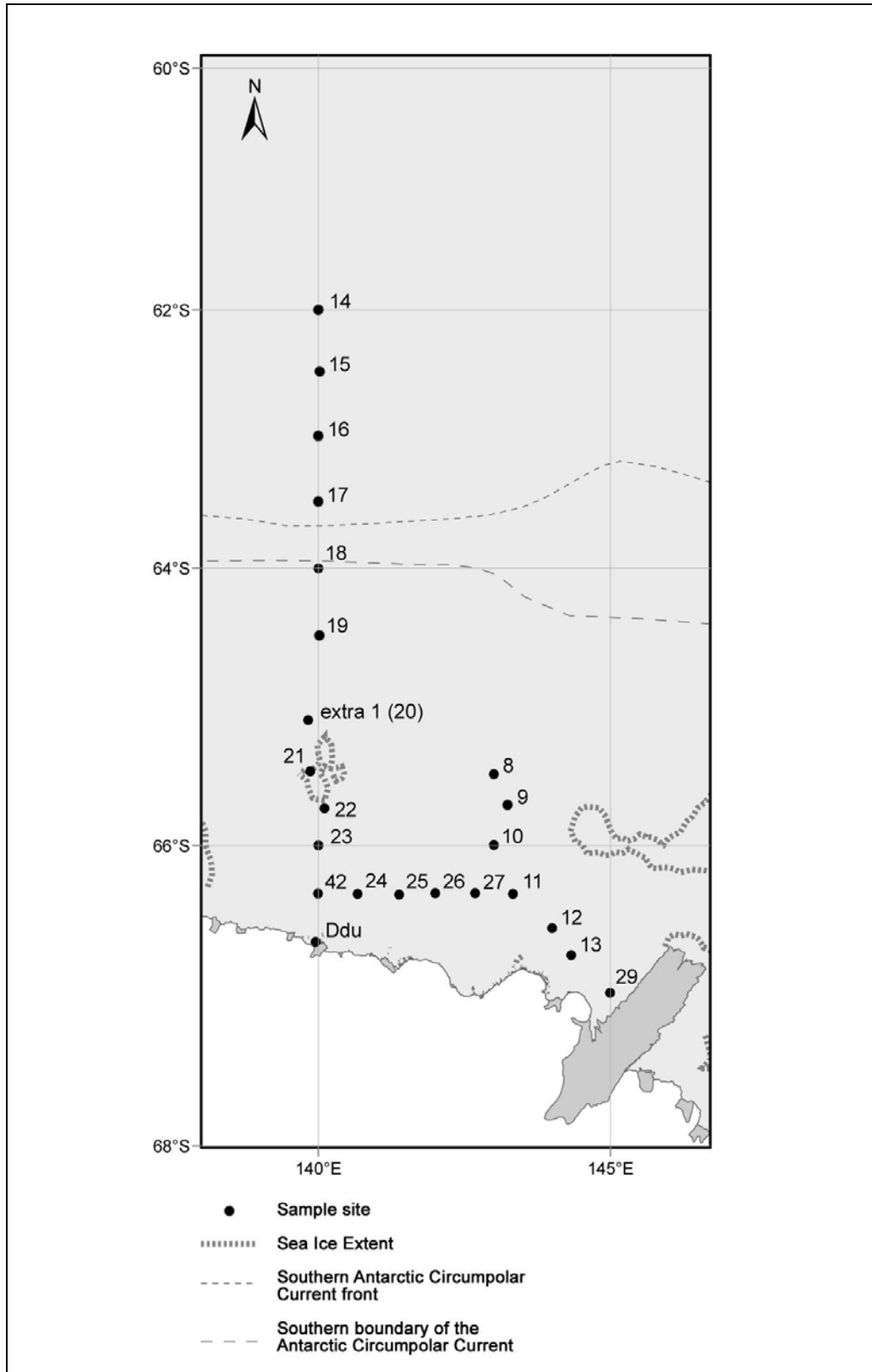


Figure 2.19. Sample sites from the Collaborative East Antarctic Marine Census - Pelagic (CEAMARC – pelagic) voyage from 23 January to 17 February, 2008 aboard TRV *Umitaka Maru*. Figure adapted from the Australian Antarctic Data Centre.

CHAPTER 3.**Identification of Southern Ocean larvaceans****3.1 Introduction**

In this chapter, the taxonomic diversity of larvaceans is reviewed and an analysis of the species collected during research voyages in the Southern Ocean provided. Knowledge of the taxonomy of larvaceans is required to determine their distribution and abundance in the Southern Ocean.

The Ocean Biogeographic Information System (OBIS) database (accessed 12 April 2010) lists only 58 larvacean species (Appendix I) occurring globally, and Hopcroft (2005) describes 65 species and suggests low diversity. Limited taxonomic diversity is thought to be due to the poor condition of specimens caused through collection methods, as well as a lack of focus on larvacean taxonomy when sampling zooplankton (Hopcroft 2005). Larvaceans are generally identified to family, or to the genera *Oikopleura* spp. or *Fritillaria* spp. The challenges associated with identification of larvaceans increase with damage, e.g. damaged *Fritillaria* can be easily mistaken for small *Oikopleura*. Larvaceans are also commonly identified as *de facto* *Oikopleura dioica* due to a lack of appropriate taxonomic efforts.

The global identification of larvaceans can historically be divided into three exploratory periods:

1. The German exploration (1870 – 1930s), with many publications produced by German researchers Lohmann and Bückmann (Lohmann 1896, 1914, 1931; Bückmann, 1924; Lohmann and Bückmann, 1926);
2. The Japanese exploration (1950 – 1960s), with publications by the Japanese researcher Tokioka (1951, 1955, 1956 and 1957); and
3. The Midwater (pelagic) exploration (1990s), with publications by Fenaux and Youngbluth (1990, 1991), Fenaux (1992, 1993), Hopcroft and Robison (1999) and Flood (2000).

Some intensive taxonomic efforts have been disregarded by Lohmann and Tokioka (e.g. Aida, 1907; Essenberg, 1926) due to errors in preservation, incomplete species descriptions, and within-species variability.

Fenaux (1998) and Hopcroft (2005) listed 15 genera that are commonly recognised, and organised them into three families within the class Larvacea/Appendicularia (Figure 3.1). A detailed taxonomic tree is provided in Appendix II. The genera *Oikopleura* and *Fritillaria* are the most diverse and dominant. In five of the 65 species described by Hopcroft (2005), multiple “forms” were recognised. Different forms were noted by Fenaux et al. (1998) and Hopcroft (2005) to co-occur within the same collection. Different forms may also occupy the tropical, temperate and polar waters, although Esnal et al. (1996) found that *Fritillaria borealis* appears to have a continuous transition of forms across oceanic water masses, making it a “polymorphic” species.

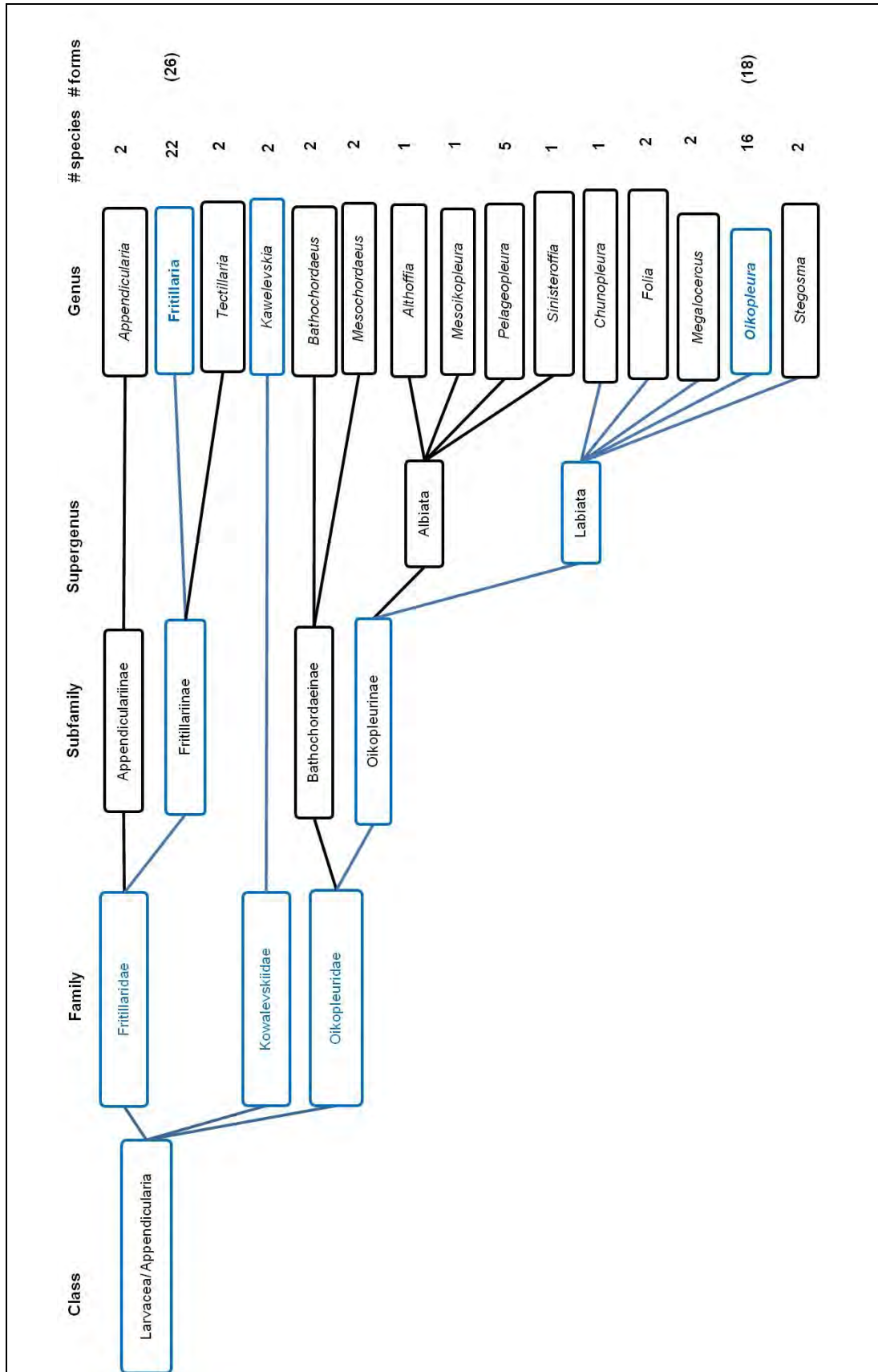


Figure 3.1. Classification of the larvacean families and genera. The number of species per genera is indicated on the right. Parentheses indicate the number of genera including forms (compiled from Fenaux, 1998 and Hopcroft,2005).

Larvaceans were first recorded in the Southern Ocean during the *Challenger* expedition in 1888 (Herdman, 1888). Studies that have focused on Antarctic larvaceans and identified them to species level include Tokioaka (1964), O'Sullivan (1983) and Esnal (1999). Lohmann and Hentschel (1939) alluded to 9 new Antarctic (or subantarctic) species, though unfortunately the samples were destroyed during World War II and were therefore never formally described.

O'Sullivan (1983) suggested that the majority of larvaceans are warm water forms, but that they do also occur in the Antarctic and Arctic oceans. A total of 23 species were described for the Antarctic Ocean, the Antarctic Ocean being defined as the water mass between the Antarctic continent and the Antarctic convergence. These species are listed in Table 3.1. Fenaux et al. (1998) lists a single *Oikopleura* species, *O. gaussica* (*syn. O. valdiviae, O. drygalskii, O. weddelli*), a single *Fritillaria* species, *F. antarctica*, and two *Pelagopleura* species, *P. magna* and *P. australis*, as larvaceans that are unique to Antarctica. The only bi-polar species is *Fritillaria borealis typica*. Warm water species that have been recorded south of the Antarctic convergence include; *Oikopleura fusiformis, O. longicauda, O. parva, Sinistereroffia scrippsi* and *Stegosoma magnum*. Warm water *Fritillaria* species that have been identified in the Antarctic Ocean include *F. aberrans, F. drygalskii, F. formica* (this may be a new subspecies, Tokioka 1964), *F. haplostoma, F. haplostoma glanularis, F. megachile, F. pellucida typica, F. tenella, F. venusta*, and a single Kowalewskidae, *Kowalevskia tenuis* (Table 3.1).

Table 3.1. Antarctic Ocean larvaceans listed by Fenaux et al. (1998) with additional larvaceans described by O’Sullivan (1983) included in bold. * *F.borealis typica*; the only bi-polar larvacean.

Species	
<i>Folia gracilis</i>	Lohmann 1896
<i>Oikopleura fusiformis</i>	Fol 1872
<i>O. longicauda</i>	Vogt 1854
<i>O. parva</i>	Lohmann 1896
<i>O. dioica</i>	Fol
<i>O. gaussica</i>	Lohmann 1905
<i>O. valdiviae</i>	Lohmann 1905
<i>O. drygalski</i>	Lohmann and Bückmann 1926
<i>O. weddelli</i>	Lohmann 1928
<i>Pelagopleura australis</i>	Bückmann 1924
<i>P. magna</i>	Lohmann 1926
<i>Sinistereroffia scrippsi</i>	Tokioka 1957
<i>Stegosoma magnum</i>	Langerhans 1880
<i>Fritillaria aberrans</i>	Lohmann 1896
<i>F. abjornseni</i>	Lohmann 1909
<i>F. antarctica</i>	Lohmann 1905
<i>F. borealis typica</i> *	Lohmann
<i>F. drygalskii</i>	Lohmann
<i>F. formica digitata</i>	Fol 1872
<i>F. haplostoma</i>	Fol 1872
<i>F. megachile</i>	Fol 1872
<i>F. pellucida typica</i>	Busch 1851
<i>F. tenella</i>	Lohmann 1896
<i>F. venusta</i>	Lohmann
<i>F. scillae</i>	Lohmann
<i>F. fraudax</i>	Lohmann 1896
<i>Kowalevskia tenuis</i>	Fol 1872

In a more recent study, Esnal (1999) compiled a list of 43 South Atlantic larvaceans in relation to relative abundances and latitude. According to this list, 29 larvacean species occurred poleward of 40° S. These species are listed according to relative abundance and latitude in Table 3.2.

Tokioka (1961) discussed taxonomic problems associated with Antarctic larvaceans, and Tokioka (1964) proposed that the oikopleurid-group, consisting of *O. gaussica*, *O. valdiviae*, *O. drygalski* and *O. weddelli*, should be considered to be a single species, *O. gaussica* (supported also by Fenaux, 1993, 1998; Capitanio et al., 2003). This was due to uncertainties associated with larvacean identification when using different sampling devices. For these reasons, *Fritillaria* have been referred to as *Fritillaria* spp. and *Oikopleura* referred to as *Oikopleura* spp.

Table 3.2. General distribution and relative abundance of 29 larvacean species in the South Atlantic Ocean, poleward of 40° S. Key; ■■■■ very rare, ---- Scarce, ===== frequent, ≡≡≡ abundant and □□□□ probable range (from Esnal 1999).

Larvacean	40°S	50°S	60°S	
<i>Kowalevskia tenuis</i>	■■■■			
<i>Folia gracilis</i>	■■■■	■■■■		
<i>Fritillaria aberrans</i>	■■■■	■■■■		
<i>Oikopleura rufescens</i>	≡≡≡			
<i>Stegosoma magnum</i>	=====			
<i>Oikopleura albicans</i>	=====	=====		
<i>Oikopleura cophocerca</i>	≡≡≡	≡≡≡		
<i>Fritillaria drygalski</i>	□□□□	□□■	■■■■	
<i>Fritillaria formica</i>	=====	=====	=====	
<i>Fritillaria haplostoma</i>	■■■■	■■■■	■■■■	
<i>Oikopleura diocia</i>	≡≡≡	=====	=====	
<i>Tectillaria fertilis</i>	■■□□	□□■	■■■■	
<i>Fritillaria fraudax</i>	=====	=====	=====	=====
<i>Fritillaria tenella</i>	----	----	■■■■	■
<i>Appendicularia sicula</i>	■■■■	■■■■	■■■■	■■■■
<i>Fritillaria borealis</i>	≡≡≡	≡≡≡	≡≡≡	≡≡≡
<i>Fritillaria megachile</i>	■■■■	■■■■	■■■■	■■■■
<i>Oikopleura cornutogastra</i>	=====	=====	=====	=====
<i>Oikopleura fusiformis</i>	≡≡≡	≡≡≡	≡≡≡	≡≡≡
<i>Oikopleura longicauda</i>	≡≡≡	≡≡≡	≡≡≡	≡≡≡
<i>Oikopleura parva</i>	----	----		
<i>Fritillaria pellucida</i>	=====	=====	■■■■	■■■■
<i>Fritillaria antarctica</i>	■■■■	■■■■	■■■■	■■■■
<i>Oikopleura drygalskii</i>	■■■■	■■■■	■■■■	■■■■
<i>Oikopleura gaussica</i>			≡≡≡	=====
<i>Oikopleura valdivia</i>	■■■■	■■■■	■■■■	■■■■
<i>Oikopleura weddelli</i>	■■■■	■■■■	■■■■	■■■■
<i>Pelagopleura australis</i>			■■■■	■■■■
<i>Pelagopleura magna</i>				■■■■

Southern Ocean CPR and RMT studies in the East Antarctic have also identified larvaceans as *Fritillaria* sp. or *Oikopleura* sp. Ideally this sector requires better identification of larvacean species for an increased understanding of the Southern Ocean ecosystem. This study aimed to identify specimens collected using fine scale nets and a visual plankton recorder (VPR) during the BROKE-West and CEAMARC-Pelagic voyages.

3.2 Methods

Larvaceans were obtained from the BROKE-West voyage using a ring net, and from the CEAMARC voyage using a Working party 2 (WP2) plankton net, HYDRO-BIOS MultiNet and VPR. Larvaceans were also collected using a CPR and RMT during the BROKE-West, SAZ-Sense and SIPEX voyages. The organisms collected were identified to genus, or recorded as ‘larvacean’, depending on the condition of the individual. Sampling methods and net specifications are provided in Chapter 5.

The contents of cod-ends from the ring net, WP2 and HYDRO-BIOS MultiNet were observed under a light microscope before disintegration of samples. During BROKE-West, visible larvaceans were separated and preserved in 2.5 % buffered formalin and 100% ethanol. A random selection of individual larvaceans from BROKE-West were also prepared for Scanning Electron Microscopy (SEM). This was achieved by post-fixing the specimens with osmium tetroxide on the ship, then later completing a dehydration sequence with a series of methanol, dry methanol, and acetone washes, before critical point drying and stud preparation in the laboratory. SEM images were taken using a JEOL JSM 840 SEM with a magnification range of 10 – 300,000 times. Additional digital images were taken through a stereo dissecting microscope.

Southern Ocean larvaceans were identified using Thompson (1948), Tokioka (1961, 1964), Bückmann (1968), O’Sullivan (1983), Esnal (1999) and Ritz et al. (2003). The features used to identify larvaceans (Figure 3.2) were the tail fin shape, trunk shape, buccal (oral) gland location, size/scale, the presence/absence of subchordal cells, and the quantity and location of subchordal cells if present.

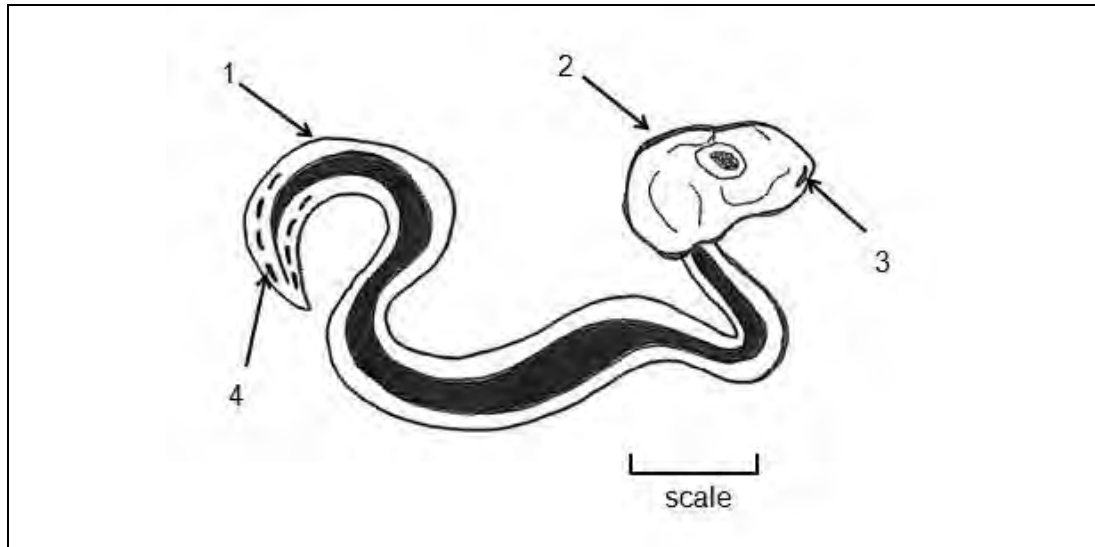


Figure 3.2. Features used to identify larvaceans; 1. tail fin shape 2. trunk shape 3. buccal glands 4. subchordal cells (absence, or quantity and location if present), and scale (adapted from O’Sullivan, 1983).

According to O’Sullivan (1983) the three larvaceans families are distinguished by the following:

OIKOPLEURIDAE

Body ovoid; endostyle (a short tube closed at both ends, located in front of the pharynx) straight; spiracles (two ciliated apertures also known as stigmata or branchial apertures) in the rectal area; tail thin and never indented at the tip. (Figure 3.3 A)

FRITILLARIDAE

Body elongated or flattened dorso-ventrally; endostyle curved; spiracles in the anterior part of the pharyngeal cavity; tail broad and short, sometimes indented in the median part of the fore edge (Figure 3.3 B).

KOWALEVSKIIDAE

Body short; endostyle and heart missing; no spiracles; elongated branchial apparatus; tail elongated with willow sliver shape (Figure 3.3 C).

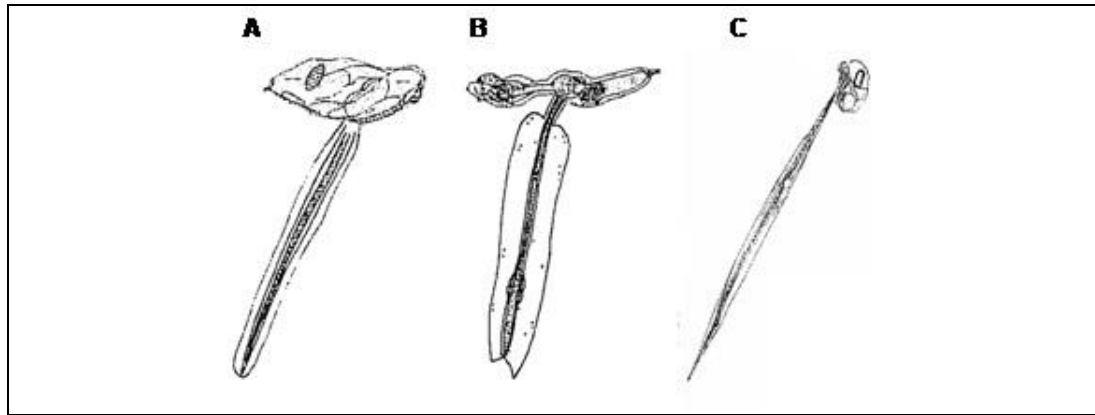


Figure 3.3. The three larvaceans families; A. Oikopleura B. Fritillaria C. Kowalevskia (from Ritz et al., 2003).

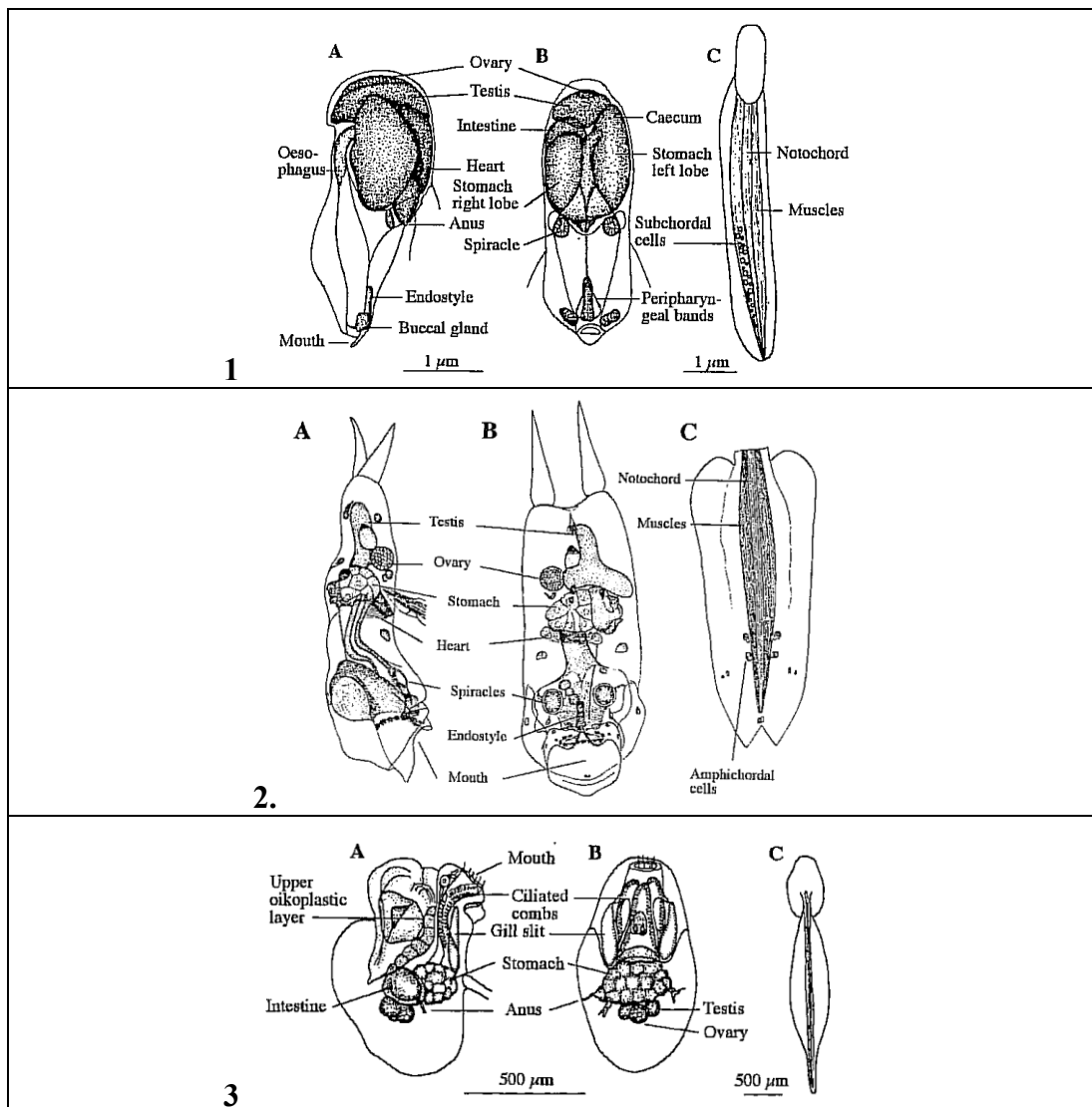


Figure 3.4. Oikopleuridae A. left side view of body B. dorsal view of body C. complete larvacean 2. Fritillaridae A. left side view of body B. ventral view of body C. tail 3. Kowalevskiidae A. right side view of body B. ventral view of body C. complete larvacean (from Fenaux, 1998).

3.3 Results

3.3.1 BROKE-West

The smaller (less than 2mm long) larvaceans from the ring net deployed during BROKE- west included *Fritillaria drygalski* (Figure 3.5), and the larger (up to 2 cm long) larvacean *Oikopleura gaussica* (Figure 3.6). The tail and body shape of larvaceans from the RMT and CPR samples identified two genus present; *Fritillaria* and *Oikopleura*.

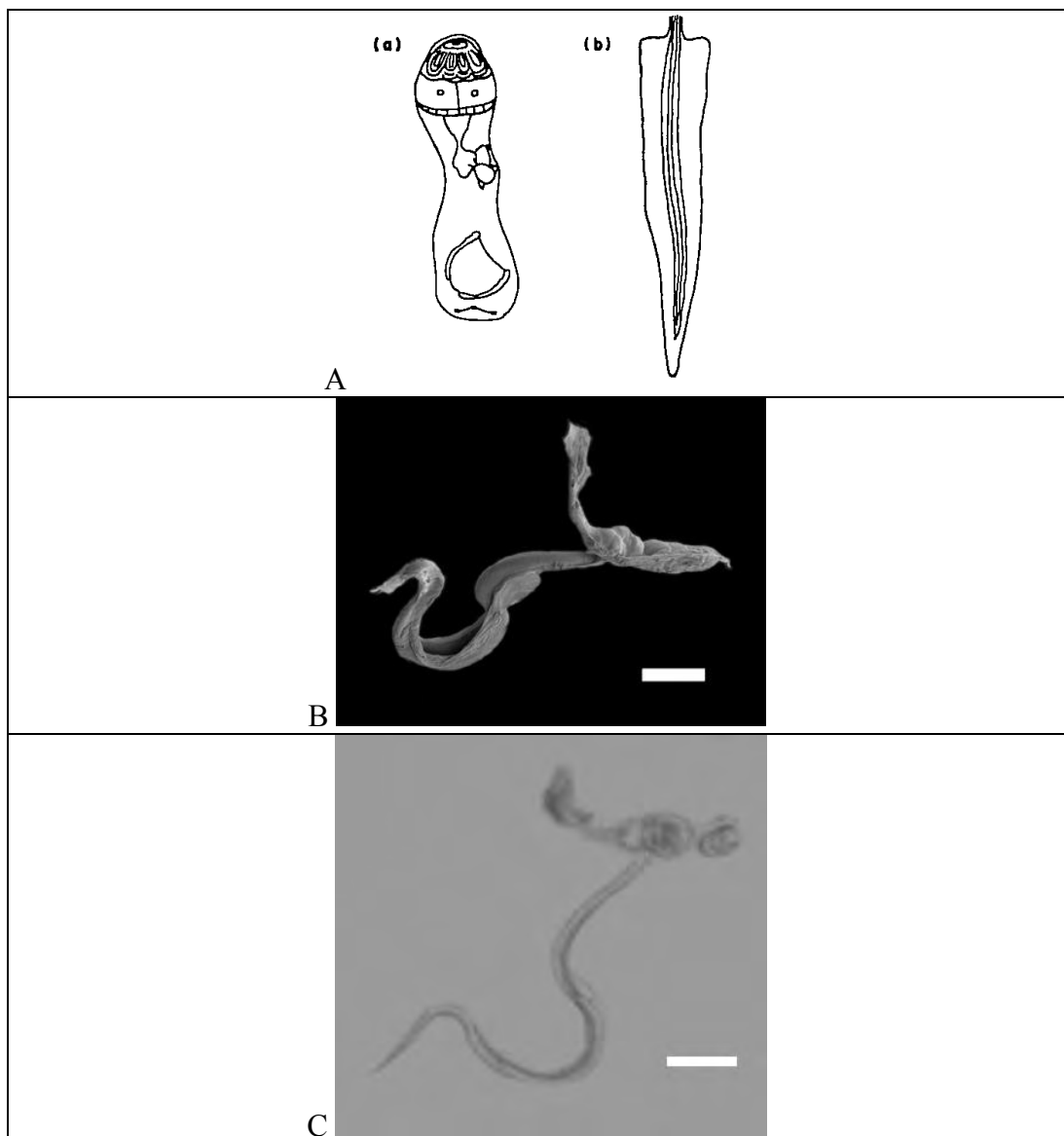


Figure 3.5. *Fritillaria drygalski* A. a. trunk dorsal view, b. tail. (from O'Sullivan 1983) B. Scanning Electron Microscope image (scale bar 100 µm) C. stereo dissecting microscope digital image (scale bar 100 µm).

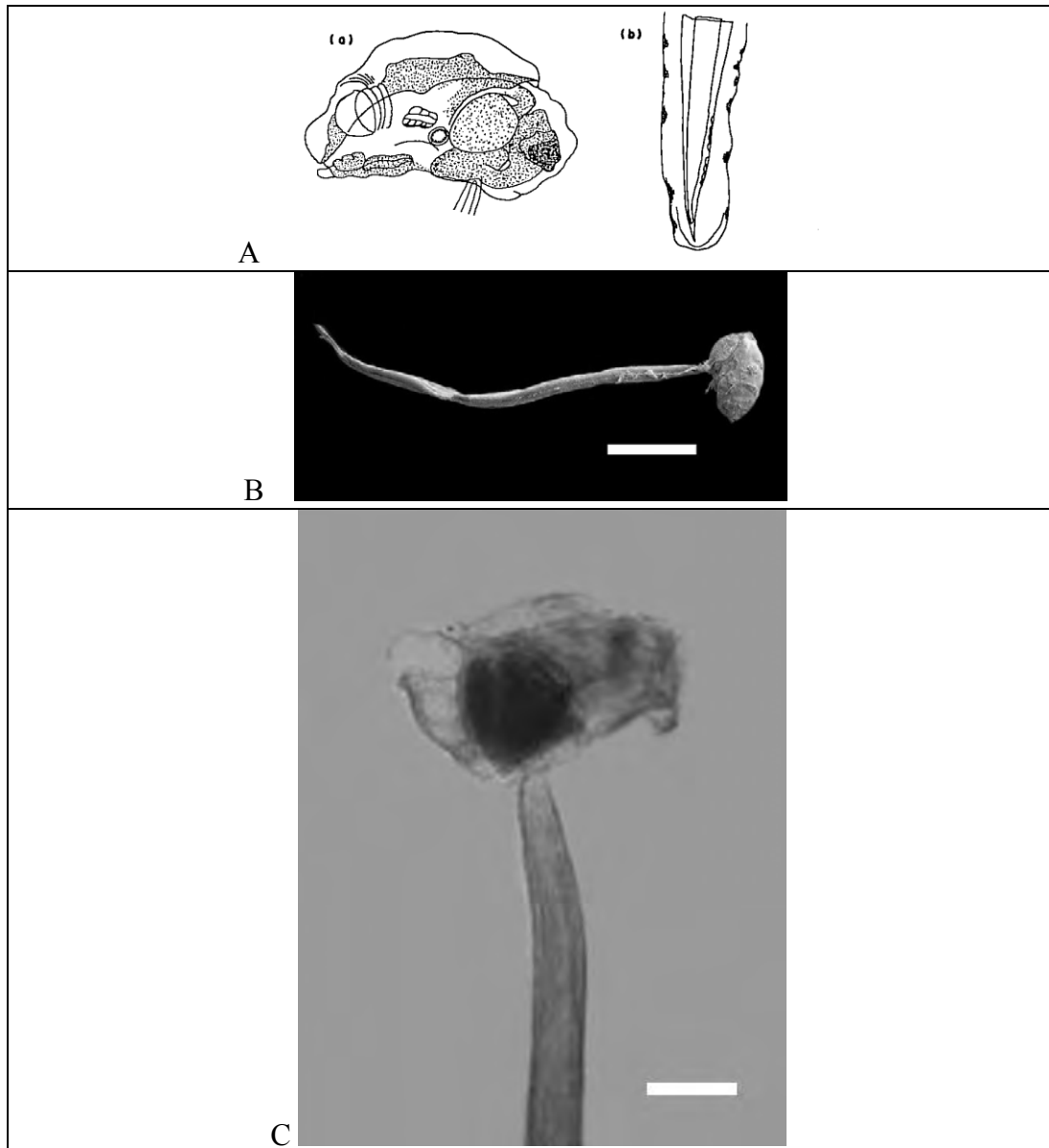


Figure 3.6. *Oikopleura gaussica* A. a. trunk lateral view, b. tail dorsal view of bend (from O’Sullivan 1983). B. Scanning Electron Microscope image (scale bar 1 mm) C. stereo dissecting microscope digital image (scale bar 1 mm).

The images from Figure 3.5 B and C and Figure 3.6 B and C have been submitted to the photo gallery for SCARmarBIN and the World Register of Marine Species (WoRMS). The submitted versions are included in Appendix III and IV, respectively.

3.3.2 SAZ-Sense

Due to the poor condition of samples from both the ring net and RMT, all larvaceans from SAZ-Sense were grouped as ‘larvaceans’ and analysed according to the plankton net used.

3.3.3 SIPEX

Samples from both the ring net and RMT used during SIPEX were also in slightly poor condition and larvaceans were identified to genus level only; *Fritillaria* sp. and *Oikopleura* sp.

3.3.4 CEAMARC-Pelagic

Larvaceans collected with the WP2 were identified as *Fritillaria borealis typica* (Figure 3.7 A) and *Oikopleura gaussica* (Figure 3.7 B). The HYDRO-BIOS MultiNet collected *Oikopleura gaussica* and *Oikopleura vanhoeffeni* (Figure 3.7 C), the latter being a deep species. A *Fritillaria* sp. was also observed using the VPR but differed from the HYDRO-BIOS Multinet samples in that it was a deep water species and larger than *F. borealis typica* (Figure 3.8).

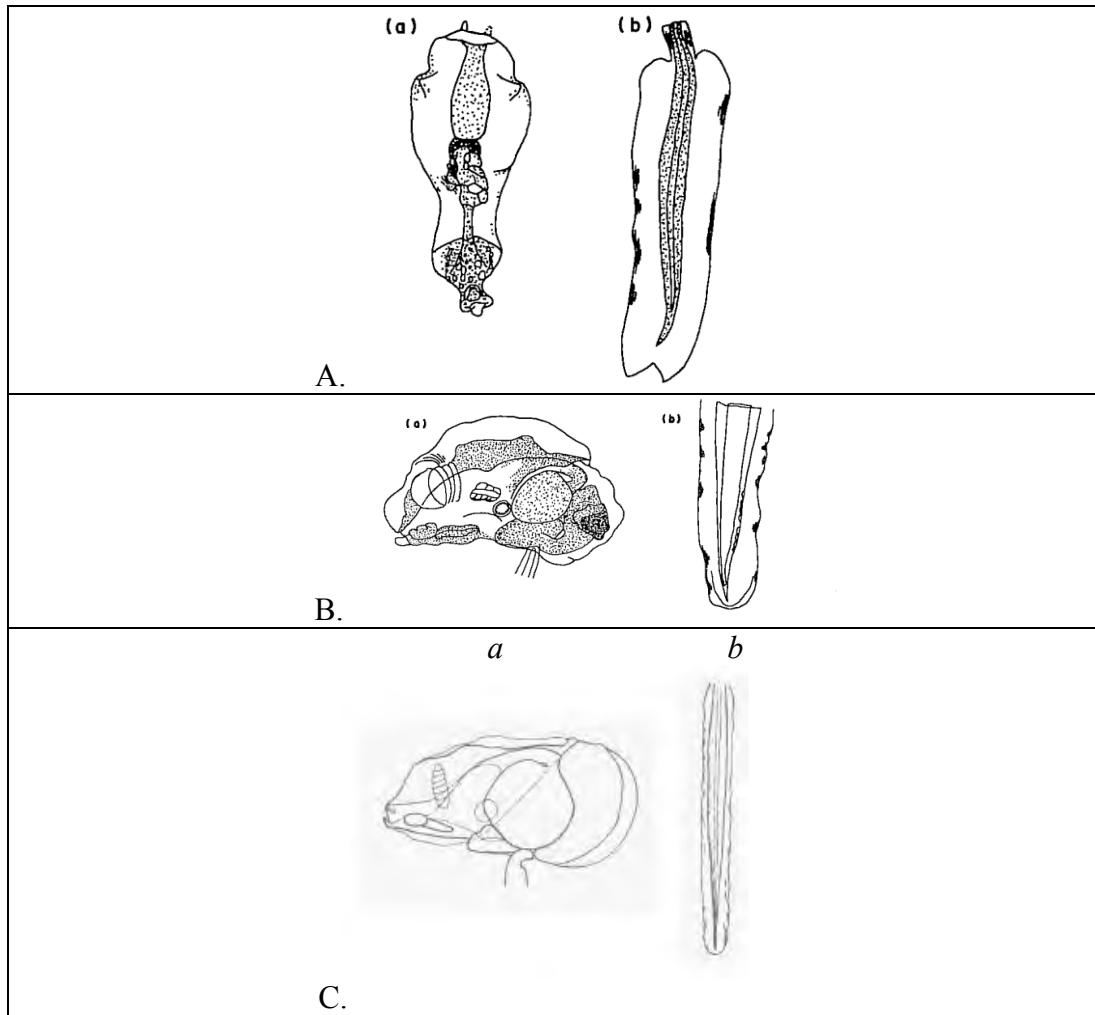


Figure 3.7. Larvaceans identified from CEAMARC-Pelagic, A. *Fritillaria borealis* f. *typica* a. trunk dorsal view, b. tail. (from O’Sullivan, 1983) B. *Oikopleura gaussica* a. trunk lateral view, b. tail dorsal view (from O’Sullivan, 1983). C. *Oikopleura vanhoeffeni* a. trunk lateral view, b. tail dorsal view (from Bückmann, 1969).

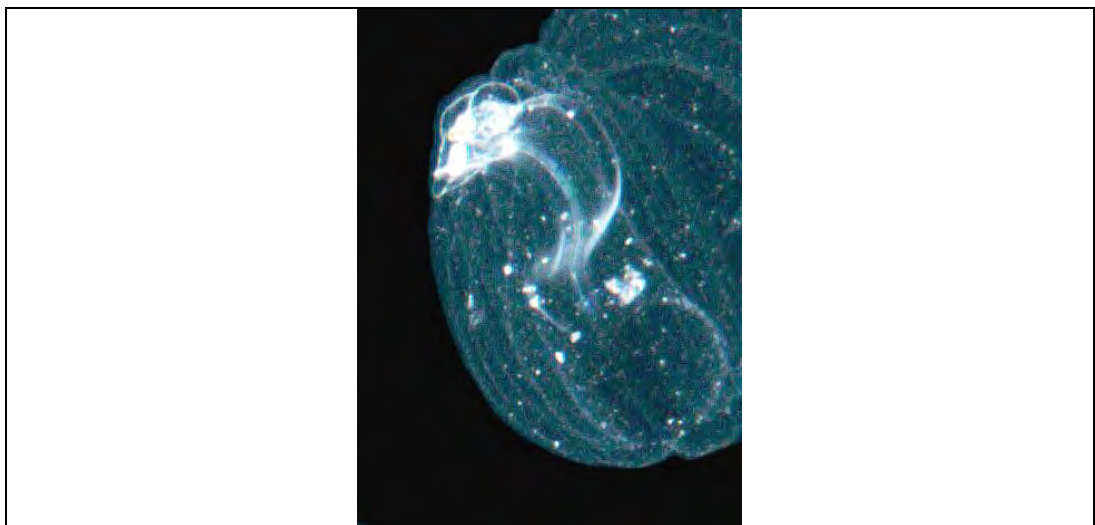


Figure 3.8. VPR image of *F. borealis* during the CEAMARC-Pelagic voyage.

3.4 Discussion

The two BROKE-West larvacean species identified from ring net samples included the smaller (less than 1mm) and more abundant *F. drygalski*, and the larger (up to 2 cm) and less abundant *O. gaussica*. Due to uncertainties associated with the collection of larvaceans using different sampling devices, *F. drygalski* was referred to as *Fritillaria* spp. and *O. gaussica* as *Oikopleura* spp.

Identification to species level was not possible for RMT samples due to the damaged condition of the larvaceans. They were identifiable to genus or family at best. Based on the ring net samples, it was assumed that all *Fritillaria* were *F. drygalski* and all *Oikopleura* were *O. gaussica*. Whilst a ring net specifically targets larvaceans, the RMT is designed for targeting krill (Euphausiacea) and zooplankton, and the CPR for robust meso-zooplankton.

O'Sullivan (1983) showed previous distributions of both of the larvaceans identified in this study; *F. drygalski* and *O. gaussica*. However, the validity of four of the species described for the Antarctic Ocean (*O. gaussica*, *O. valdiviae* Lohmann, *O. drygalski* Lohmann and Buckmann, and *O. weddelli* Lohmann) was discussed by Tokioka (1964). *O. drygalski* was described on the basis of a few imperfectly preserved specimens. It is possible that *O. drygalski* was instead an individual of *O. gaussica* or *O. valdiviae*, which was mature in spite of having a small body. Only three immature specimens of *O. weddelli* are known. This species is only separated from *O. gaussica* and *O. valdiviae* by a character which varies considerably in arrangement and structure. *O. weddelli* most closely resembles *O. valdiviae* in that it has a similar oikoplast-epithelium, and a tail characterised by capsule subchordal cells and wide musculature. The two remaining species, *O. valdivia* and *O. gaussica*, resemble each other closely, and Tokioka (1964) considered them identical. *O. gaussica* has been reported from the Southern Ocean by numerous other researchers and Tokioka (1961) considers this species to be endemic. Garstang and Georgeson (1935) detail the maturation process for this species and describe the principal gelatinous and membranous elements of the house rudiments.

Fritillaria drygalski has previously been reported from the Antarctic by Lohmann and Buckmann (1926, cited by O'Sullivan, 1983). Some investigators consider *Fritillaria drygalski* to be synonymous with *F. aequatorialis*, in which case it is likely to be a warm-water form that penetrated into Antarctic waters (Tokioka, 1961).

Larvaceans collected and identified to species level during the CEAMARC – Pelagic voyage using the WP2 were identified as *Fritillaria borealis typica* and *Oikopleura gaussica*. *Fritillaria borealis typica* was originally described by Tokioka (1964). It is a cold water form with a bi-polar distribution (Tokioka, 1940,1960; Thompson, 1948; Bückmann, 1996, cited in O'Sullivan, 1983) and has been previously found in the Antarctic by Lohmann and Bückmann (1926) and Tokioka (1964). Another larvacean was also observed during the voyage using the VPR and was also identified as a *Fritillaria* sp.. However, this *Fritillaria* was a deep water species and was larger than *F. borealis typica*.

The HYDRO-BIOS MultiNet collected *Oikopleura gaussica* and *Oikopleura vanhoeffeni* during the CEAMARC–Pelagic voyage. *Oikopleura vanhoeffeni* is known to be a deep water species and this was the very first identification of this species in Antarctic waters. This finding may have been related to the sampling of deeper water than that commonly sampled for larvaceans. Hopcroft (2005) previously stated that little to no deep water studies on larvaceans had been conducted in the Southern Ocean or other regions.

The collection of larvaceans for identification and possible cultivation proved highly difficult on all research voyages. A ring net was used specifically to collect quality specimens, but unfortunately proved too harsh. Net adaptations and adjustments in deployment rate were not able to be experimented with, as the research occurred on opportunistic ship-time and the larvacean project was never a priority study. The HYDRO-BIOS MultiNet deployed during the CEAMARC–Pelagic voyage did provide some samples for successful identification of *O. gaussica* and *O. vanhoeffeni*, though not in a condition that was suitable for subsequent cultivation. All attempts were made to use the ring net in a manner that was as gentle as possible on the larvaceans, but to no avail. Unfortunately,

methods of DNA identification mentioned by Hopcroft (2005) were unable to be utilised in this study due to funding and time constraints.

CHAPTER 4.

Large-scale distribution patterns determined from the Continuous Plankton Recorder (CPR)

4.1 Introduction

This chapter shows an overview of the Southern Ocean Continuous Plankton Recorder (SO-CPR) Survey, then presents a re-analysis of the 25 year data set. The analysis focuses on the distribution of larvaceans, as well as the seasonal and inter-annual patterns of abundance.

The SO-CPR Survey has been operating since 1991 (Hosie et al., 2003) and was established to map the biodiversity of zooplankton in the Southern Ocean. More specifically, it was designed to determine seasonal, annual and long-term variability in species composition, abundances and distribution patterns.

4.2 The Continuous Plankton Recorder (CPR)

For this study, a Type II, Mark V CPR (Figure 4.1) was used. The unit utilised a standard 270 μm mesh and was towed approximately 100 m behind the ship at normal ship's speed in ice free waters. This enabled the unit to be towed horizontally at a depth of approximately 10 m, although mixing by the ship's propeller meant that the top 20 m was likely to be sampled. Water enters the CPR through an aperture of 1.25 x 1.25 cm, then expands into a collecting tunnel of 5 x 10 cm, reducing water speed by about a factor of 30. Therefore, at 15 knots of water flow, the speed of flow across the collecting silk inside the CPR would be equivalent to 0.5 knots. There was no flow meter attached to the CPR and the filtration efficiency was assumed to be constant.

CPR silks were preserved in 10% buffered formalin in sea-water and returned to the laboratory for analysis. The CPR silks were then cut into segments representing ~ 9.3 kms (5 nautical miles), or 1.49 m^3 of sampled water, according to methods described by Hosie et al. (2003). The entire contents of each sample

were identified and counted under a stereo dissecting microscope. Zooplankton were identified to species level when possible. Soft-bodied species such as larvaceans were identified to genus level, either as *Oikopleura* or *Fritillaria*. Larvacean abundances were converted to ind. m⁻³.

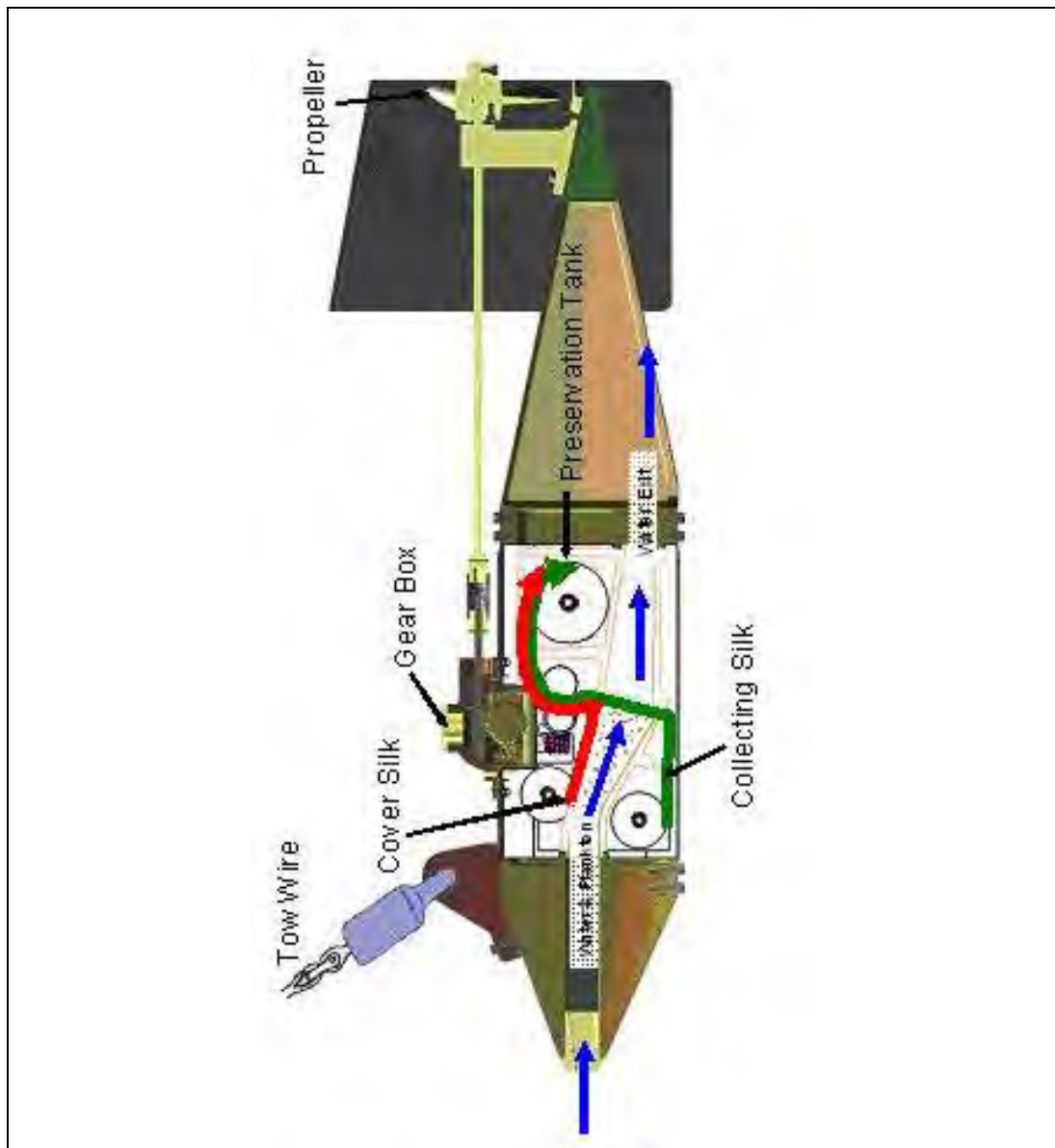


Figure 4.1. Schematic of CPR unit (from <http://data.aad.gov.au/>)

Physical oceanography data was collected during CPR deployments using underway shipboard meters. The data was logged at one minute intervals and included temperature, salinity, Photosynthetically Active Radiation (PAR) and

fluorescence measurements. PAR values from port and starboard sensors were averaged to reduce the influence of shadows.

SO-CPR data used in this study was collected from the start of the Antarctic season in 1990/91 to the end of the Antarctic season in 2008. Figure 4.2 is a map showing the SO-CPR transects for this period. The data were collected aboard nine research vessels: *Akademik Fedorov*, *Aurora Australis*, *Shirase*, *Hakuho Maru*, *Tangaroa*, *Umitaka Maru*, *Kaiyo Maru*, *Polarstern* and *Yuzhmorgeologiya*.

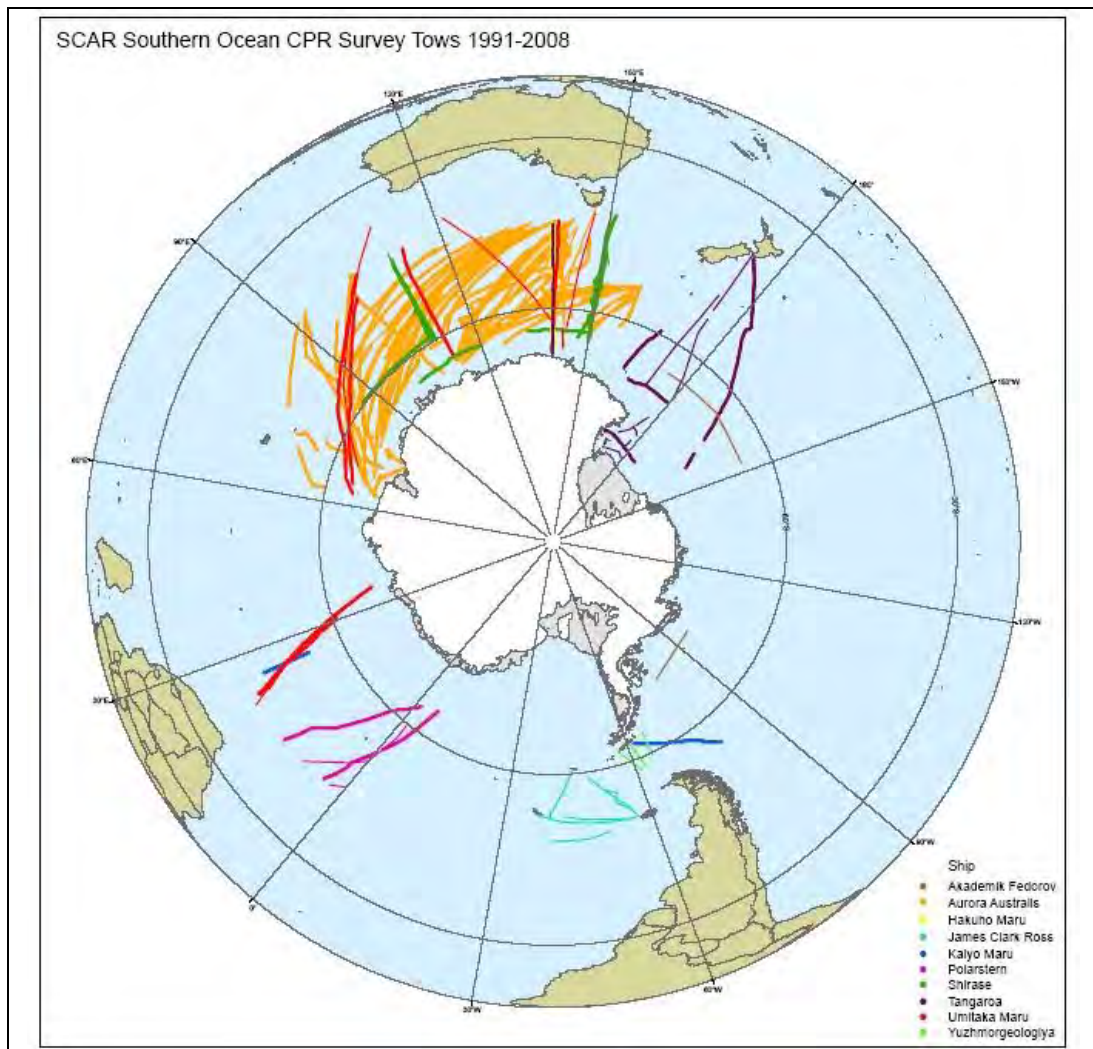


Figure 4.2. SCAR SO-CPR Survey tows from 1990/91 to 2008. Produced by AAD data centre, published June 2008, SCAR map catalogue No. 13481.

4.3 Existing but limited CPR data

Southern Ocean larvacean distribution and abundance studies have previously been undertaken by Takahashi et al. (2002), Hunt and Hosie (2003; 2005; 2006a; 2006b) and Tsujimoto et al. (2006). The majority of these studies used and/or contributed to SO-CPR Survey data. The CPR provides a survey transect that is comparable with other CPR deployments, with limited to no variation in sampling scale.

During SO-CPR Surveys conducted by three ships in 1999, larvaceans were found to be one of ten major taxa (Hosie et al., 2003). As part of this research, Hunt and Hosie (2003) reported bloom conditions of larvaceans along a 140°E, 66°S transect. In addition, abundances of *Fritillaria* and *Oikopleura* at 49°S in the SAZ were found to be 1053 and 230 per m⁻³, respectively. Similar distribution and abundance patterns were shown by Tsujimoto et al. (2006). They reported that in 2002, larvaceans were most abundant at 66° 28'S, the southern-most station sampled (Japanese Antarctic Research expedition number 43, JARE 43). This station was south of the Southern Boundary (SB), and larvaceans comprised 84 % of zooplankton with an abundance of 327.1 ind. m⁻³. Northern station abundances were 0.6 ind. m⁻³ (63° 59'S) and 1.6 ind. m⁻³ (61° 02'S). This survey was conducted along 140°E and used NORPAC nets that were deployed vertically to 150 m (330 µm mesh). Two weeks prior to the 2002 JARE 43 expedition, Hunt and Hosie (2005) reported that larvaceans had dominated the SO-CPR Survey, with most zooplankton located south of the SB. The average abundance was 192.9 ind. m⁻³.

Takahashi et al. (2002) surveyed zooplankton in relation to Antarctic Polar Front Zones using CPR aboard the *Kaiyo Maru* in 1999/2000. *Oikopleura* sp. and *Fritillaria* sp. were within the top 17 zooplankton taxa, contributing a combined 1.6 % to total zooplankton abundance. Hunt and Hosie (2003) conducted a transect along 140°E, between 51 and 62°S. The average CPR abundance was 32.1 ind. m⁻³, whilst NORPAC net abundances were 11.3, 7.7, 5.5, and 5.0 ind. m⁻³ for depths of 20, 20-50, 50-100 and 100-150 m, respectively. The most abundant region for larvaceans was between the northern and southern Polar

Front. Hunt and Hosie (2006a) repeatedly sampled along 140° E in the SIZ south of 62°S, between November 2001 and March 2002. Along this transect they found that larvaceans were common throughout the season and they demonstrated a seasonal cycle similar to other zooplankton. Peaks in abundance corresponded with seasonal warming and increased chlorophyll *a* and phytoplankton concentrations. In 2001/02 SO-CPR tows were also undertaken on the *RSV Tangaroa* (New Zealand research vessel) and a bloom of larvaceans was encountered. *Fritillaria* sp. had the highest abundance with 0-1572 ind. per 5 Nm, compared to 0-533 ind. per 5 Nm for *Oikopleura* sp. It was found that *Oikopleura* sp. had a northerly distribution and *Fritillaria* sp. a southern distribution.

McLeod et al. (2010) recently published a zooplankton atlas of the Southern Ocean which shows the near surface distribution and abundance for total near-surface *Oikopleura* sp. (Figure 4.3) and *Fritillaria* sp. (Figure 4.4).

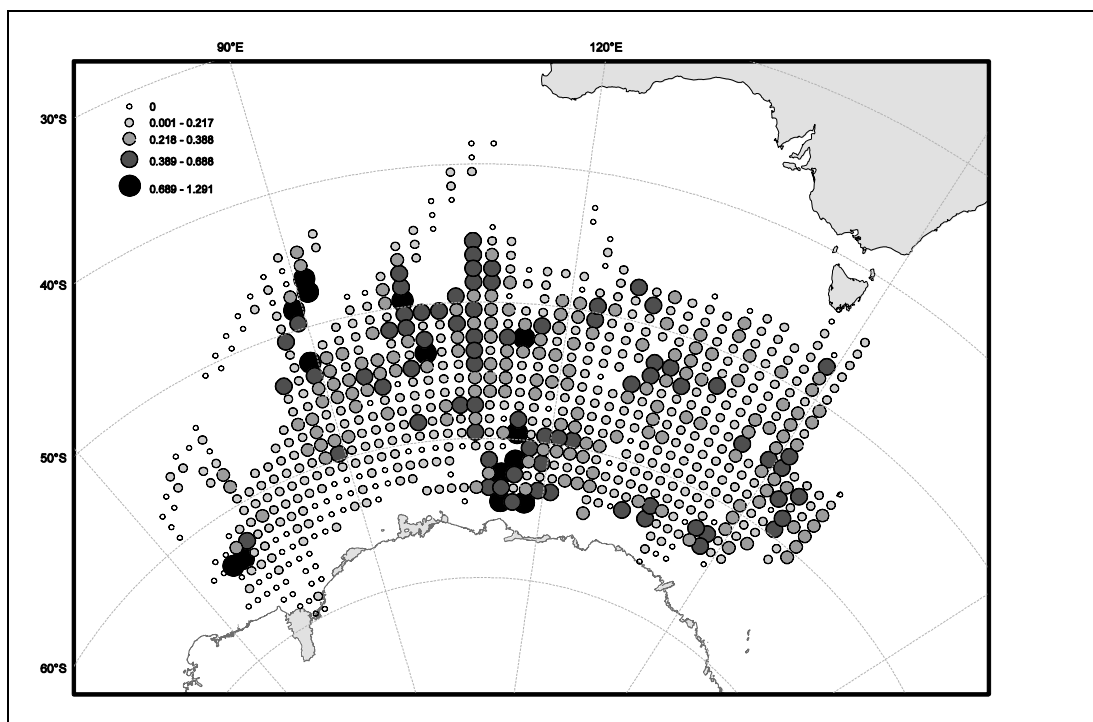


Figure 4.3. CPR atlas map for total near-surface *Oikopleura* sp. Data from 60° E to 160° E in the Southern Ocean and collected through SO-CPR Survey from 1991 to 2008. The abundance scale is relative to the size of the shaded circle representing $\log_{10}(X+1)$ transformed data displayed in 1° latitude and 2° longitude bins (McLeod et al., 2010).

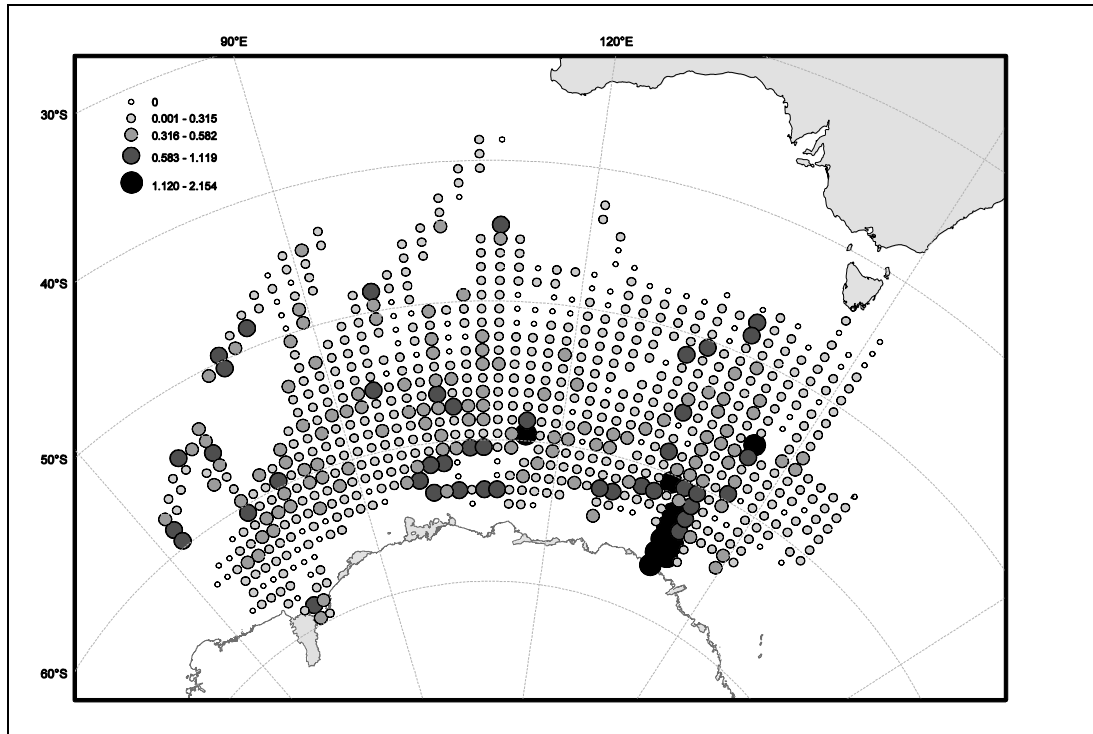


Figure 4.4. CPR atlas map for total near-surface *Fritillaria* sp. Data from 60° E to 160° E in the Southern Ocean and collected through SO-CPR Survey from 1991 to 2008. The abundance scale is relative to the size of the shaded circle representing $\log_{10}(X+1)$ transformed data displayed in 1° latitude and 2° longitude bins (McLeod et al., 2010).

SO-CPR Survey data from 1990-91 to 2004-05 showed that larvaceans and zooplankton were consistently present in most years prior to commencing this study and they occur throughout the Southern Ocean. They were not present in the survey in the first four years. This may be due to the condition of the samples and a lack of focus on larvaceans by researchers (as discussed in Chapter 3).

4.4 Extended CPR data

As described in Chapter 2, this study examines large scale larvacean distributions within three zones; the Sub Antarctic Zone (SAZ) north of 48°S, the Permanent Open Ocean Zone (POOZ) between 50 and 60°S, and the Seasonal Ice Zone (SIZ) south of 62°S. The zones are separated by a 2° gap to minimise the overlap of zones. This zonation is relative to physical and biological parameters in the East Antarctic. To examine within-season and between-season variation of larvaceans,

distribution and abundance were compared with physical and environmental parameters (fluorescence, water temperature, PAR, latitude and longitude) by applying Pearson's r correlation and a Generalised additive mixed model (GAMM).

Fluorescence is an uncalibrated relative scale measured by the Turner TD10 fluorometer. Salinity is measured in practical salinity unit (psu) and water temperature as °C. PAR is Photosynthetically Active Radiation ($\mu\text{Em}^{-2}\text{s}^{-1}$) from underway data logged at one minute intervals by shipboard meters. PAR values for port and starboard side were averaged to reduce the influence of ship shadow.

4.5 Results

4.5.1 SO-CPR Survey distribution and abundance maps

The following maps show the distribution and abundance of *Oikopleura* sp. and *Fritillaria* sp. with data presented as counts per 5 Nm (9.3 km). Note that the scale is not constant for each map since the abundance range was too variable between surveys.

Annual distribution and abundance of Southern Ocean larvaceans

Annual distribution maps over a number of years are presented in this section, and between-season maps are in Appendix V. Overall the inter-annual distribution of larvaceans shows that *Fritillaria* sp. have a more southerly distribution compared to the more central (POOZ) distribution of *Oikopleura* sp. (Figure 4.26).

There were no larvaceans recorded in the SO-CPR Survey during the first four years of the survey (1990-1991 to 1995-1996). The tows that were undertaken in these years are shown in Appendix V.1 (1990-1991), V.2 (1991-1992), and V.3 (1995-1996). There were no CPR transects recorded for the mapped area in 1993-1994.

Data from 1996 – 1997 showed the first identification of larvaceans in the SO-CPR database (Figure 4.5). There were higher abundances of *Oikopleura* sp.

compared to *Fritillaria* sp. In 1997 – 1998 (Figure 4.6) and 1998 – 1999 (Appendix V.4), the opposite result was found with lower abundances of *Oikopleura* sp. compared to *Fritillaria* sp.. However, distribution patterns were similar.

In 1999 – 2000 (Figure 4.7) *Oikopleura* sp. and *Fritillaria* sp. had more similar abundances. *Oikopleura* sp. had a south-easterly distribution, whereas *Fritillaria* sp. had a south-westerly distribution. In 2000 – 2001 (Appendix V.5), higher *Oikopleura* sp. abundances were found in the north-east compared to lower abundances of *Fritillaria* sp. in the south-west.

In 2002 – 2003 (Appendix V.6) *Oikopleura* sp. abundance was lower than *Fritillaria* sp., the latter having a south-west distribution. In the POOZ, between the Subtropical Front and the Southern Antarctic Circumpolar Current Front, the distribution tended to alternate between dominance of *Oikopleura* sp. and *Fritillaria* sp. In 2003 – 2004 (Figure 4.9) these larvaceans had a similar distribution pattern along western transects. However, in the east, *Oikopleura* sp. had a southern distribution compared to *Fritillaria* sp. which had an easterly distribution. In 2004 – 2005 (Appendix V.7), there were lower abundances of *Oikopleura* sp. compared to *Fritillaria* sp. and the distribution was similar for some transects only.

Larvacean surveys for this thesis commenced in 2005. In 2005 – 2006 (Figure 4.10) there were higher *Oikopleura* sp. abundances compared to *Fritillaria* sp. In 2006 – 2007 (Figure 4.11) there were lower *Oikopleura* sp. abundances compared to *Fritillaria* sp. The north-south transect in the west had a similar distribution pattern to the east, with *Oikopleura* sp. having a northerly distribution and *Fritillaria* sp. a southerly distribution. In 2007 – 2008 (Figure 4.12) there were again lower *Oikopleura* sp. abundances compared *Fritillaria* sp. with a number of high abundance “hot spots” occurring for *Fritillaria* sp. in the east. Overall, it appears that on the majority of the tows conducted, the distribution of the two genera alternated.

Abundance data from 1996 – 1997; the first season where larvaceans were identified in the SO-CPR database. There were higher abundances of *Oikopleura* sp. (Figure 4.5A) compared to *Fritillaria* sp. (Figure 4.5B).

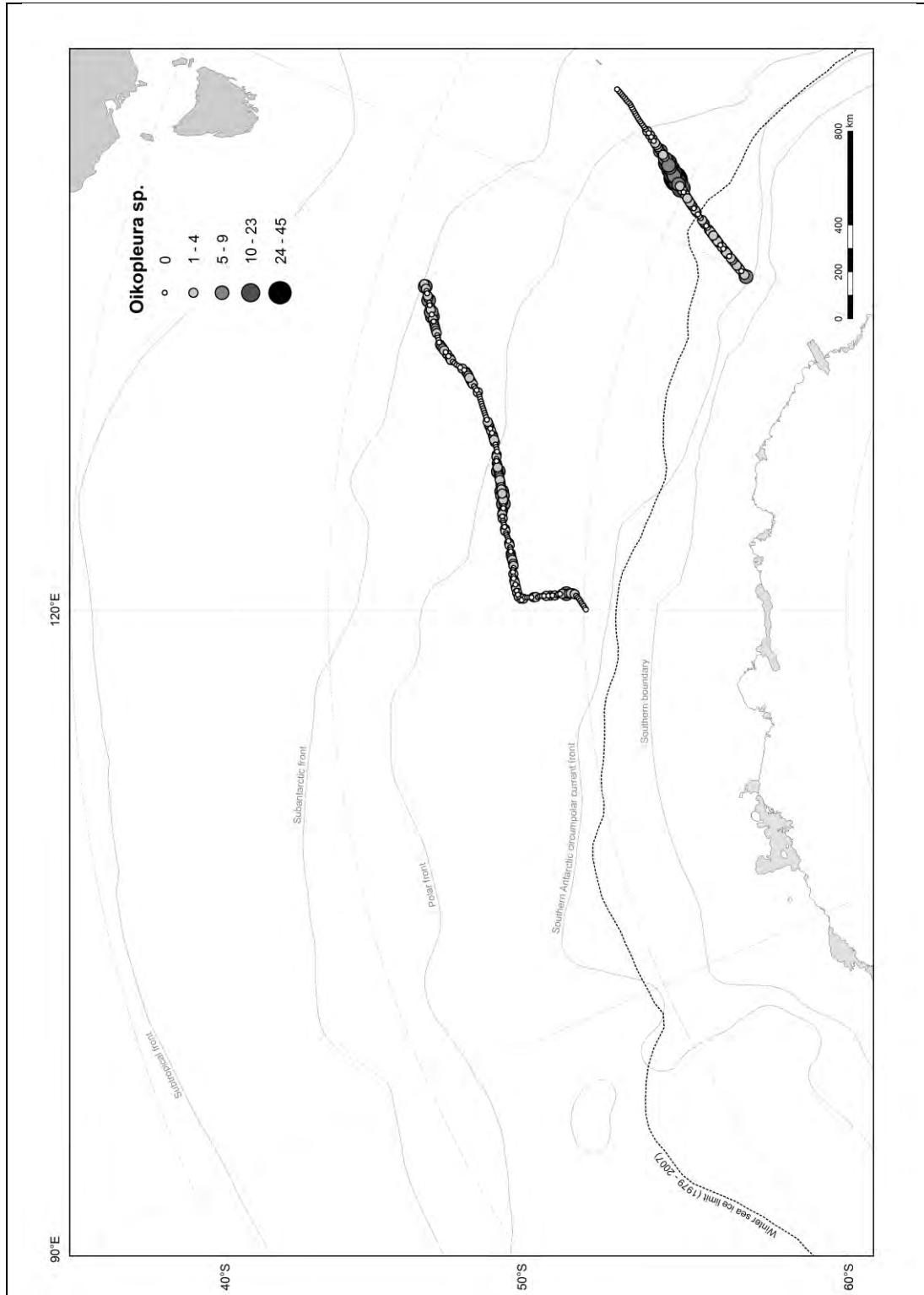


Figure 4.5 A. 1996 – 1997 CPR transects showing abundances of *Oikopleura* sp. (counts per 5 Nm).

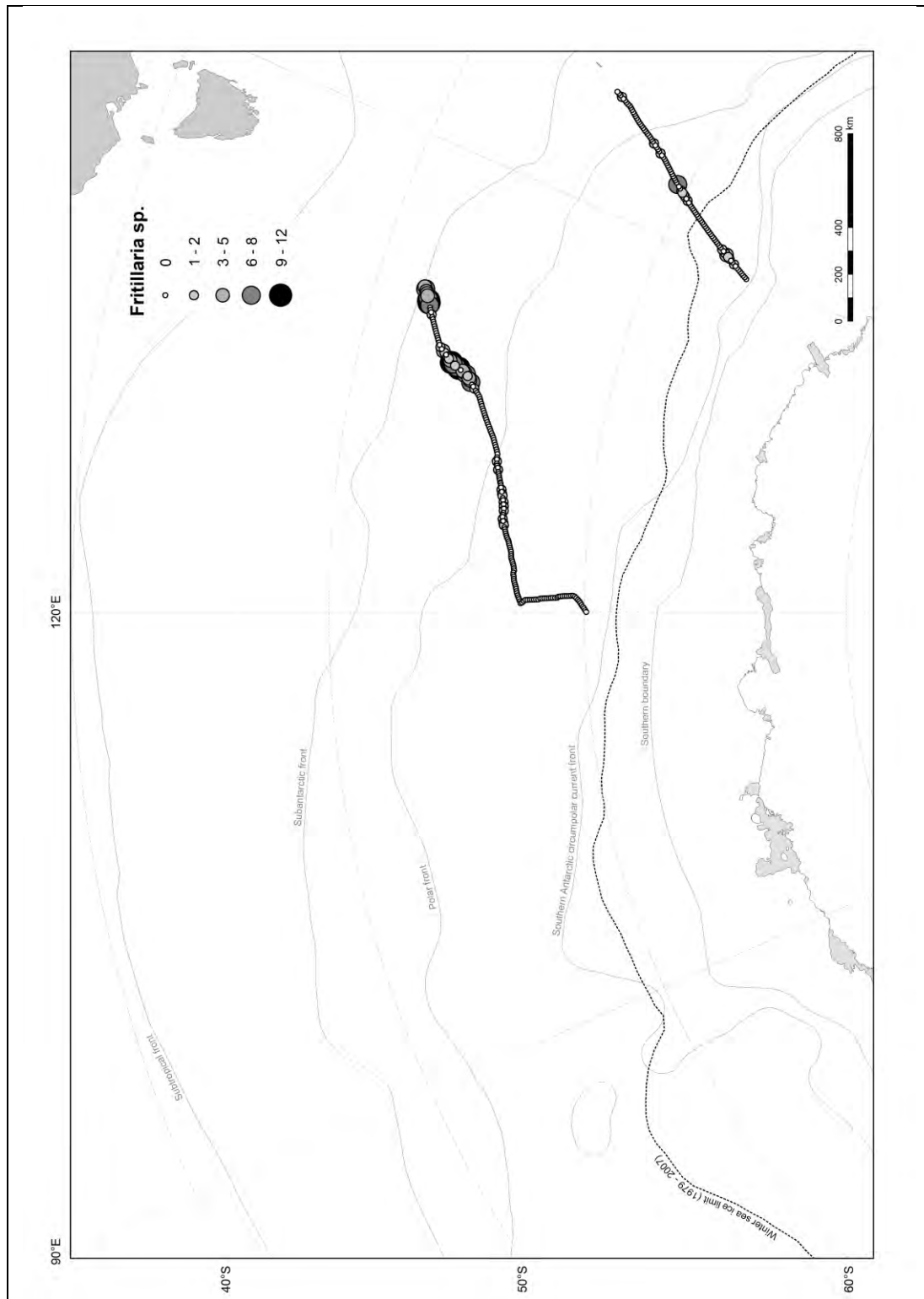


Figure 4.5 B. 1996 – 1997 CPR transects showing abundances of *Fritillaria* sp. (counts per 5 Nm).

Figure 4.6 shows that in 1997 – 1998 there were lower abundances of *Oikopleura* sp. (Figure 4.6A) compared to *Fritillaria* sp. (Figure 4.6B), though they had a similar distribution and abundance pattern.

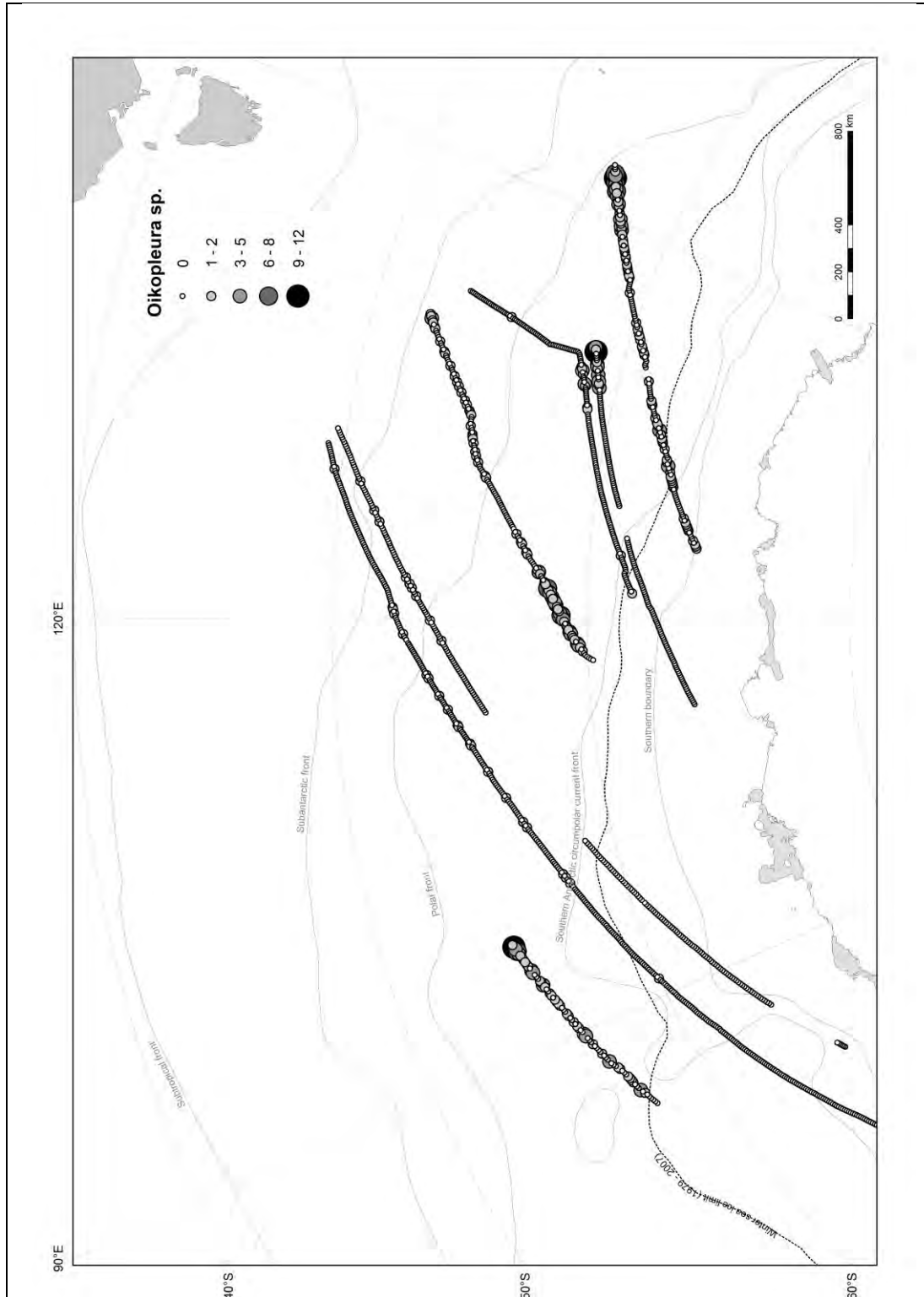


Figure 4.6 A. 1997 – 1998 CPR transects showing abundances of *Oikopleura* sp. (counts per 5 Nm).

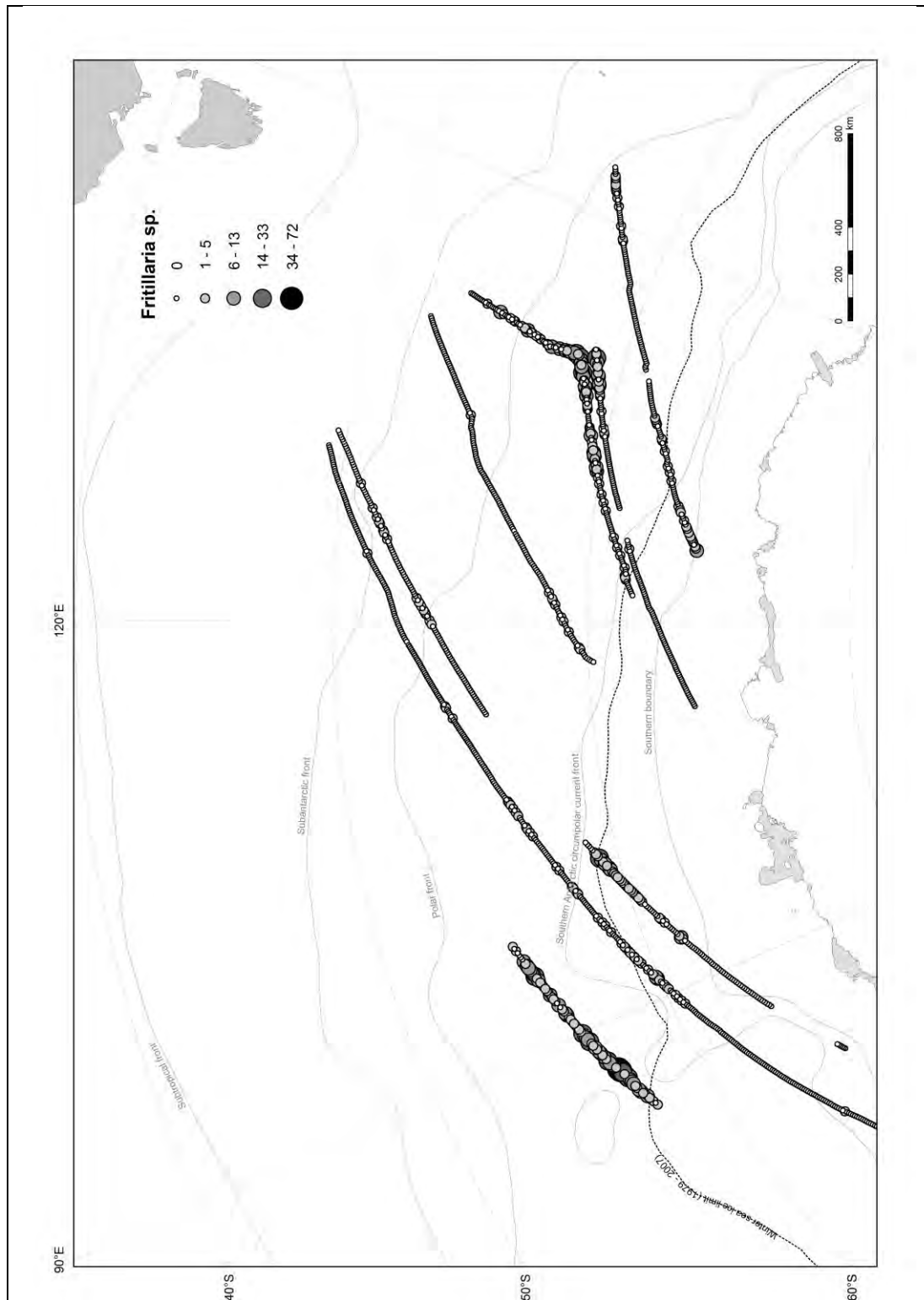


Figure 4.6 B. 1997 – 1998 CPR transects showing abundances of *Fritillaria* sp. (counts per 5 Nm).

Data from 1999 – 2000 showed that *Oikopleura* sp. (Figure 4.7A) and *Fritillaria* sp. (Figure 4.7B) had similar abundances. *Oikopleura* sp. had a south-easterly distribution and *Fritillaria* sp. a south-westerly distribution.

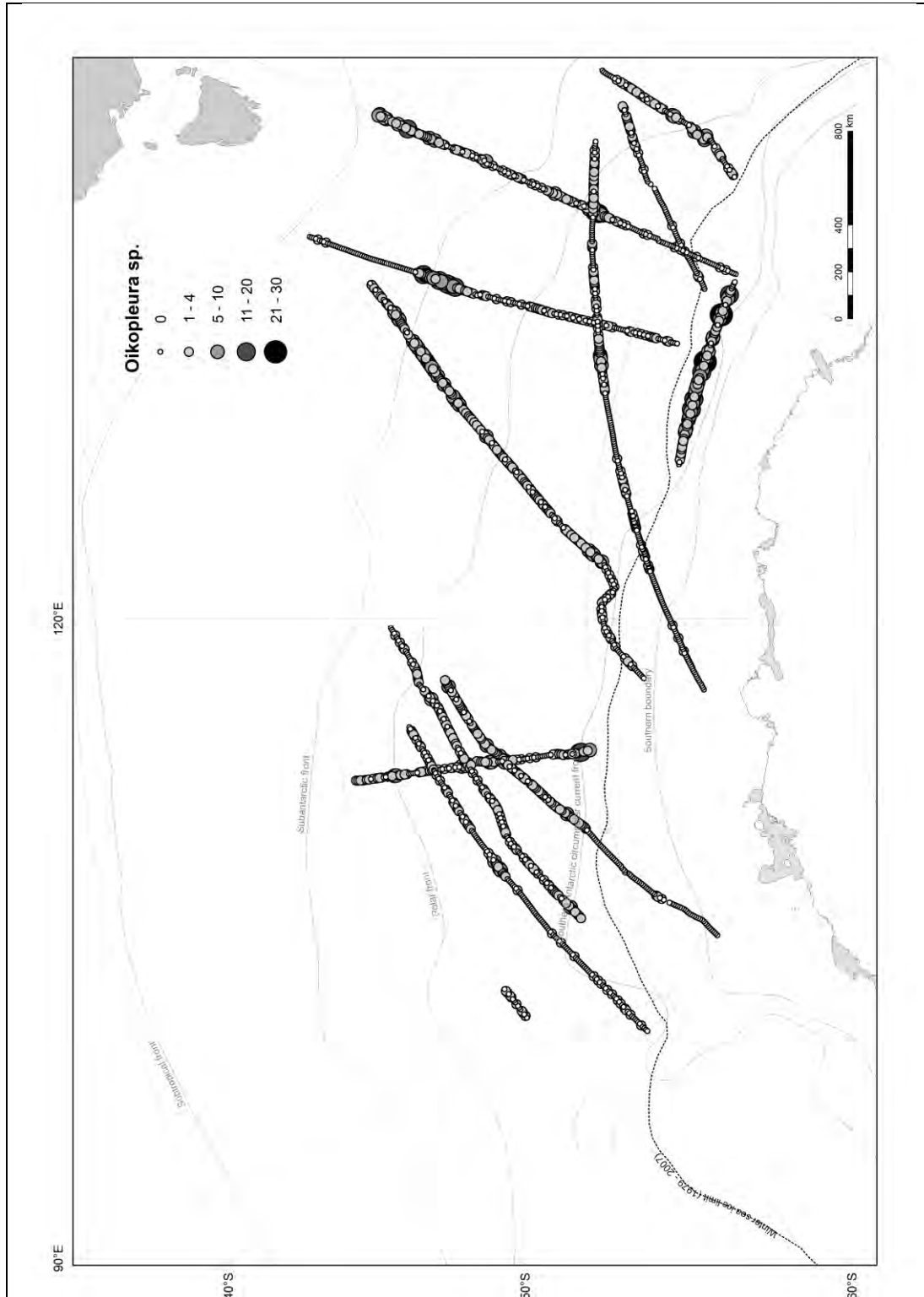


Figure 4.7 A. 1999 – 2000 CPR transects showing abundances of *Oikopleura* sp. (counts per 5 Nm).

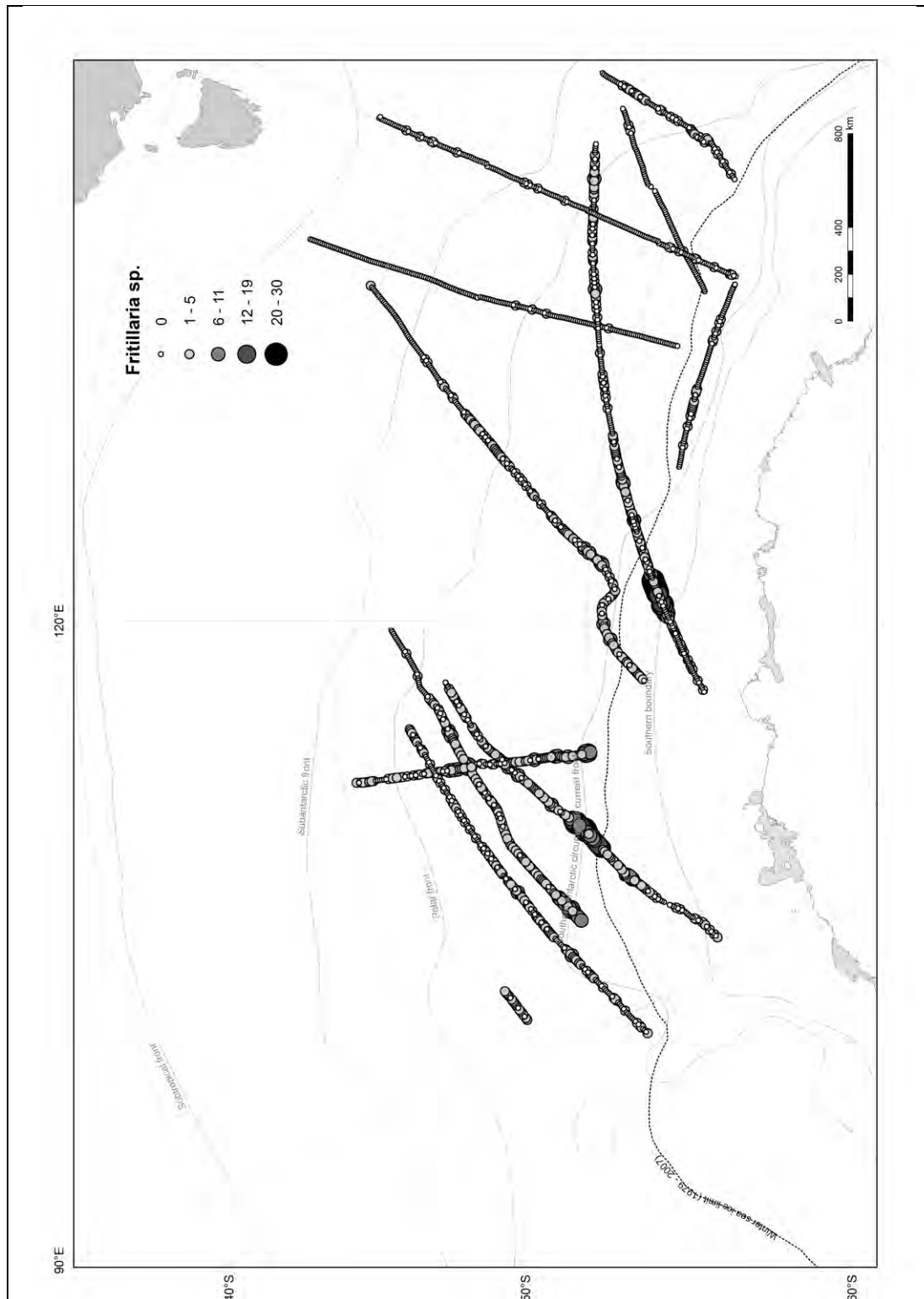


Figure 4.7 B. 1999 – 2000 CPR transects showing abundances of *Fritillaria* sp. (counts per 5 Nm).

In 2001 - 2002 (Figure 4.8) the western area had similar distributions of *Oikopleura* sp. and *Fritillaria* sp.. Data from the voyage on the *RSV Tangaroa* (red rectangle) showed highest larvacean abundances, with *Oikopleura* sp. having a northerly distribution (Figure 4.8A) and *Fritillaria* sp. a southern distribution (Figure 4.8B). *Fritillaria* sp. had a higher abundance of 0 - 1572 ind. per 5 Nm, compared to 0-533 ind. per 5 Nm for *Oikopleura* sp..

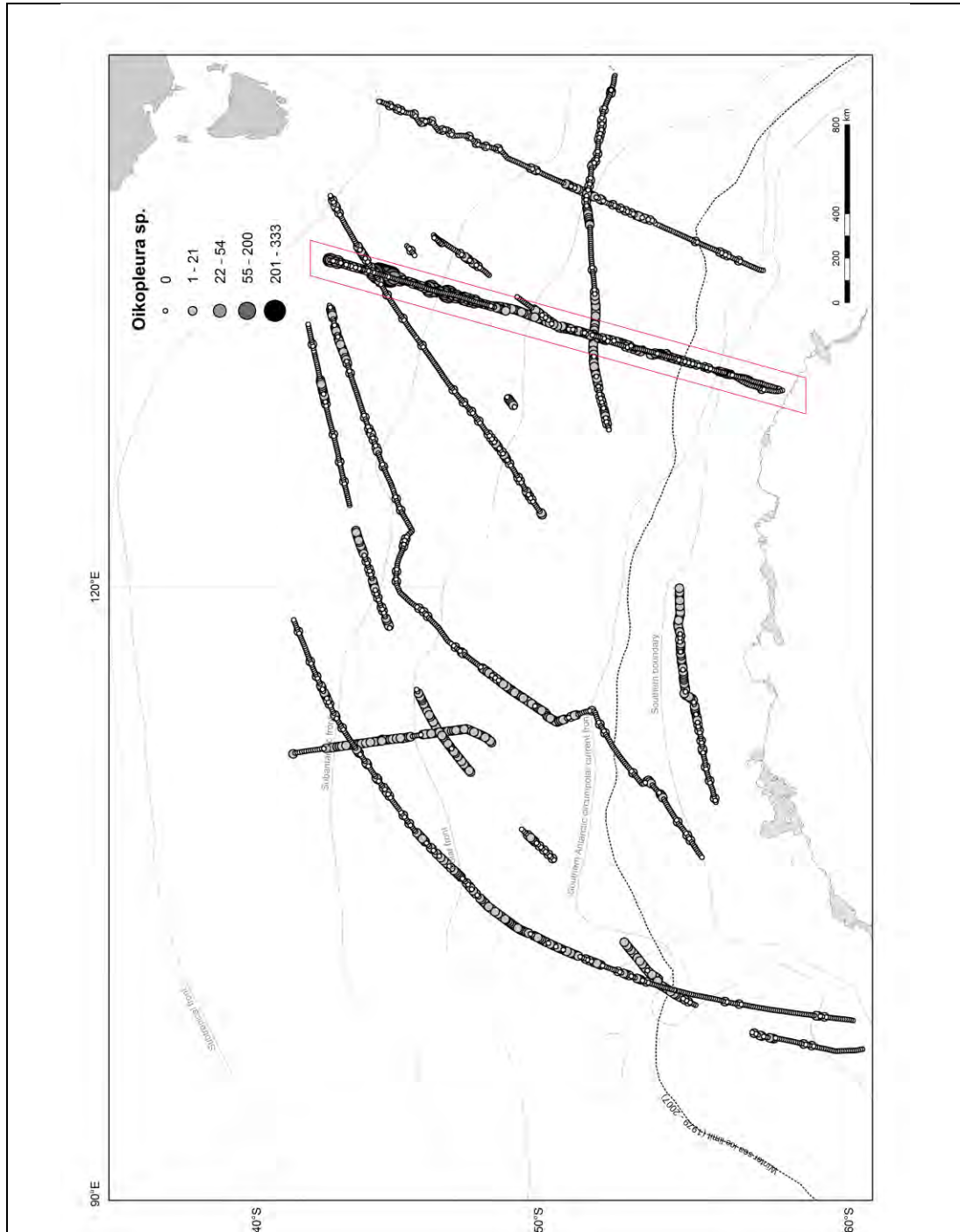


Figure 4.8 A. 2001 – 2002 CPR transects showing abundances of *Oikopleura* sp. (counts per 5 Nm).

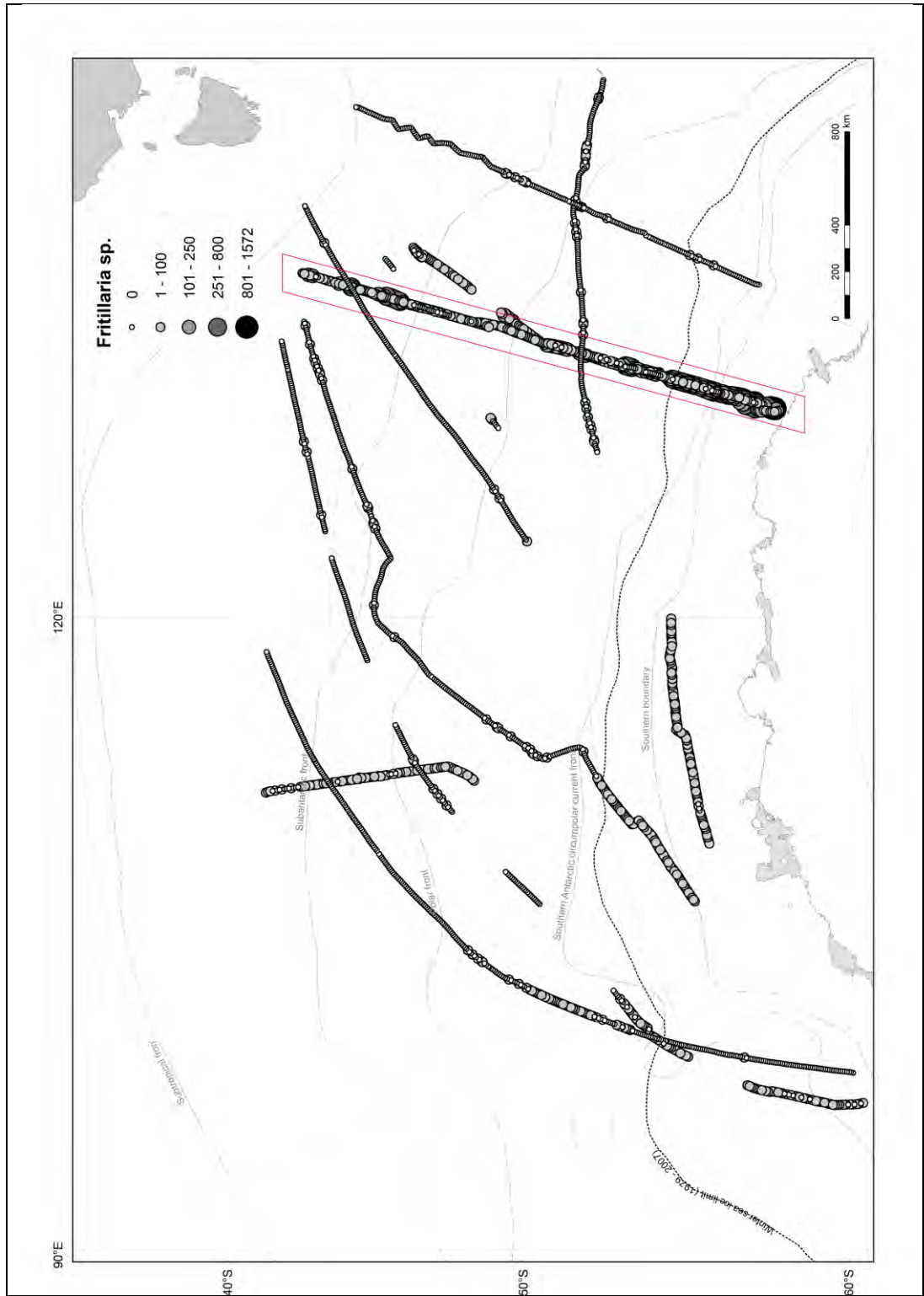


Figure 4.8 B. 2001 – 2002 CPR transects showing abundances of *Fritillaria* sp. (counts per 5 Nm).

In 2003 – 2004 the two larvacean species had a similar distribution pattern for the western transects, but in the east *Oikopleura* sp. (Figure 4.9A) had a southern distribution compared to *Fritillaria* sp. (Figure 4.9B) which had an easterly distribution. Table 4.1 shows that the Pearson’s r correlation between longitude and abundances of larvaceans from 2003 – 2004 was statistically significant.

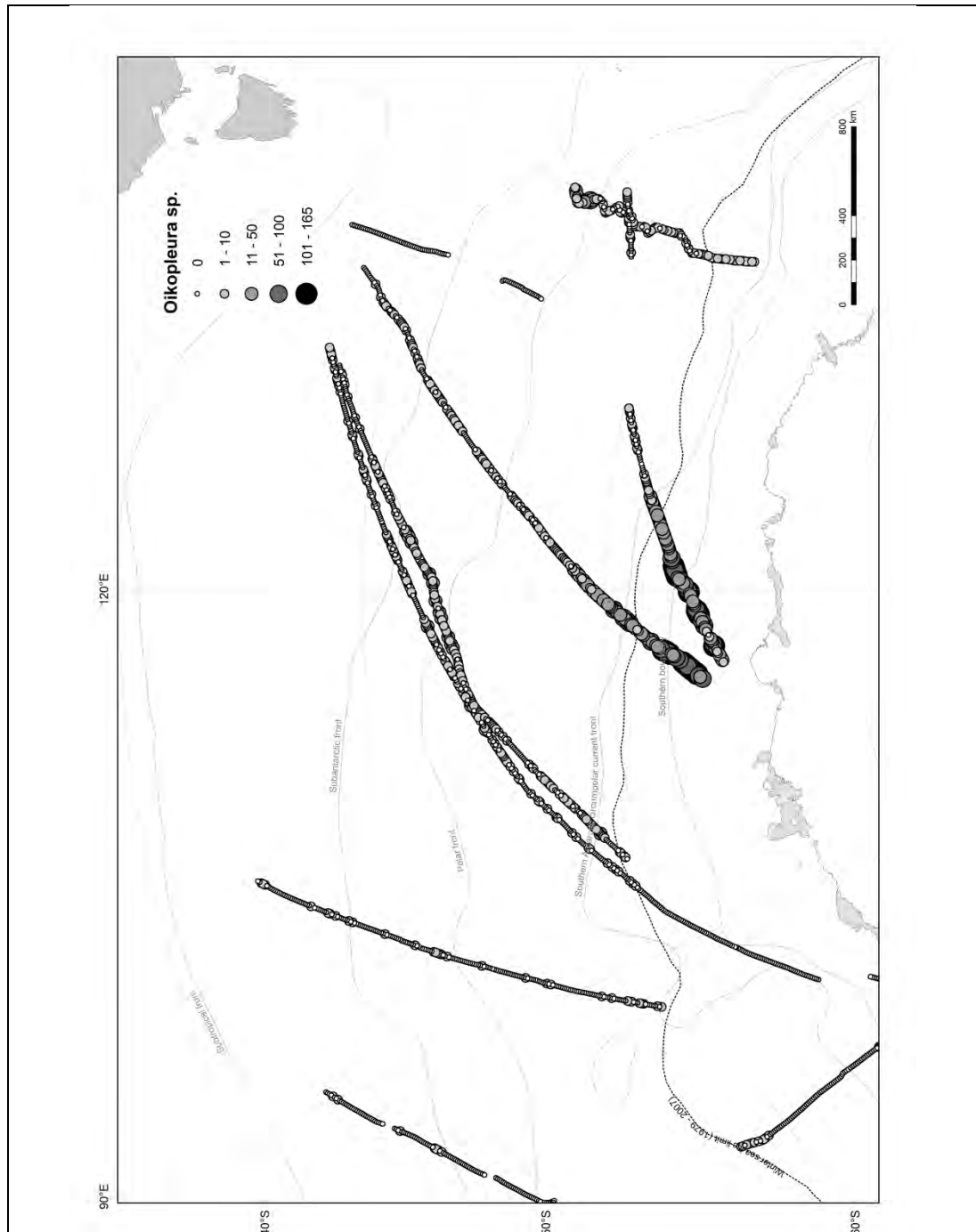


Figure 4.9 A. 2003 – 2004 CPR transects showing abundances of *Oikopleura* sp. (counts per 5 Nm).

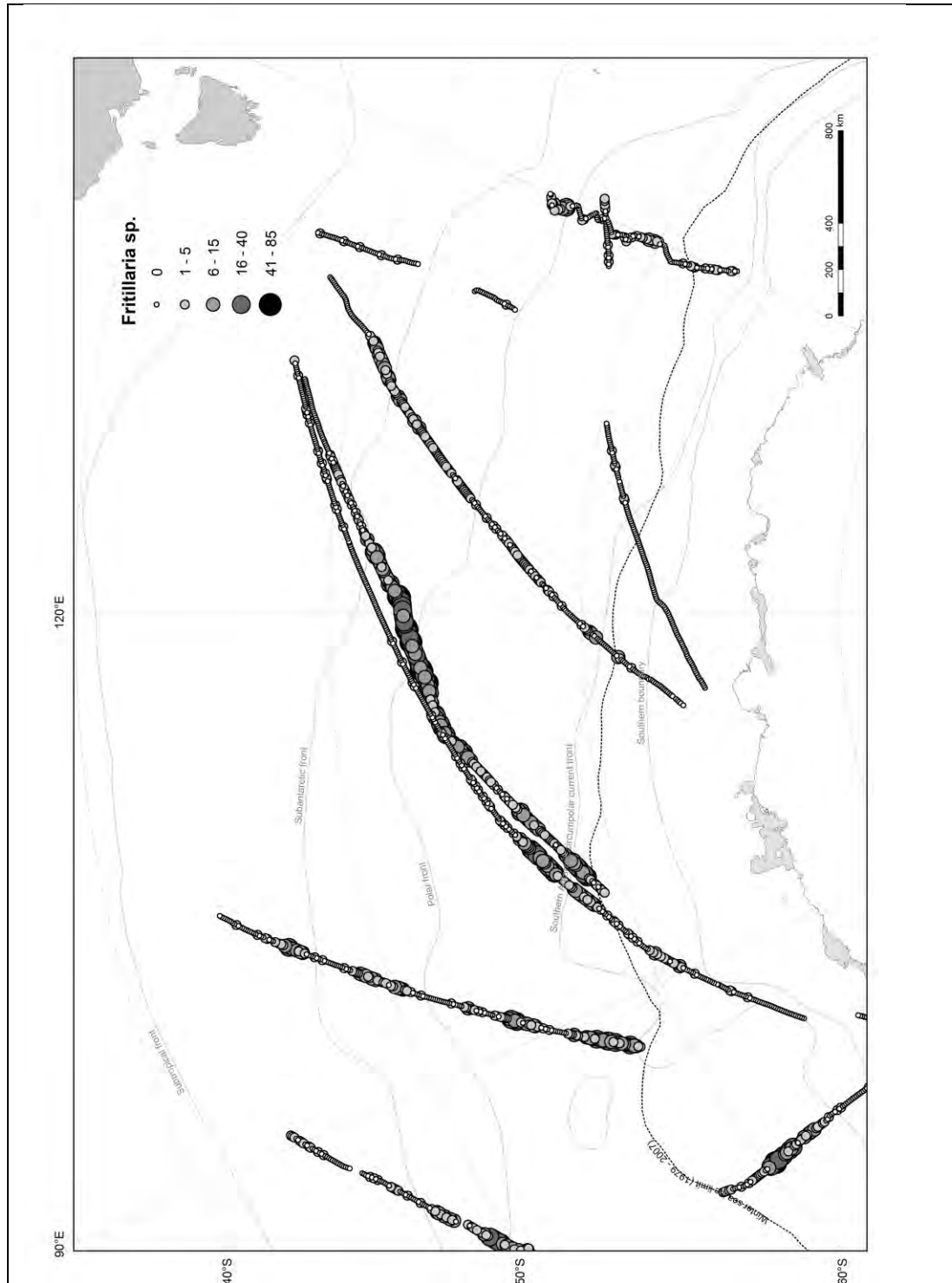


Figure 4.9 B. 2003 – 2004 CPR transects showing abundances of *Fritillaria* sp. (counts per 5 Nm).

Table 4.1. Pearson’s *r* correlation between longitude and abundances of larvaceans in 2003 – 2004. **Bold** indicates a significant relationship (ns = not significant), $\alpha=0.05(2)$.

Parameter	<i>r</i>	df	Critical <i>r</i>	<i>p</i>
Longitude and larvacean abundance	0.134	2290	0.062	0.005 < <i>p</i> < 0.01

In 2005 – 2006 there was higher *Oikopleura* sp. (Figure 4.10A) abundances compared to *Fritillaria* sp. (Figure 4.10B). This also occurred in 1997-1998. It appears that on the majority of transects the distribution of the two species alternated, indicating possible “niche separation” along transects. Pearson’s r correlation between the abundance of *Oikopleura* sp. and *Fritillaria* sp. found a statistically significant relationship (Table 4.2).

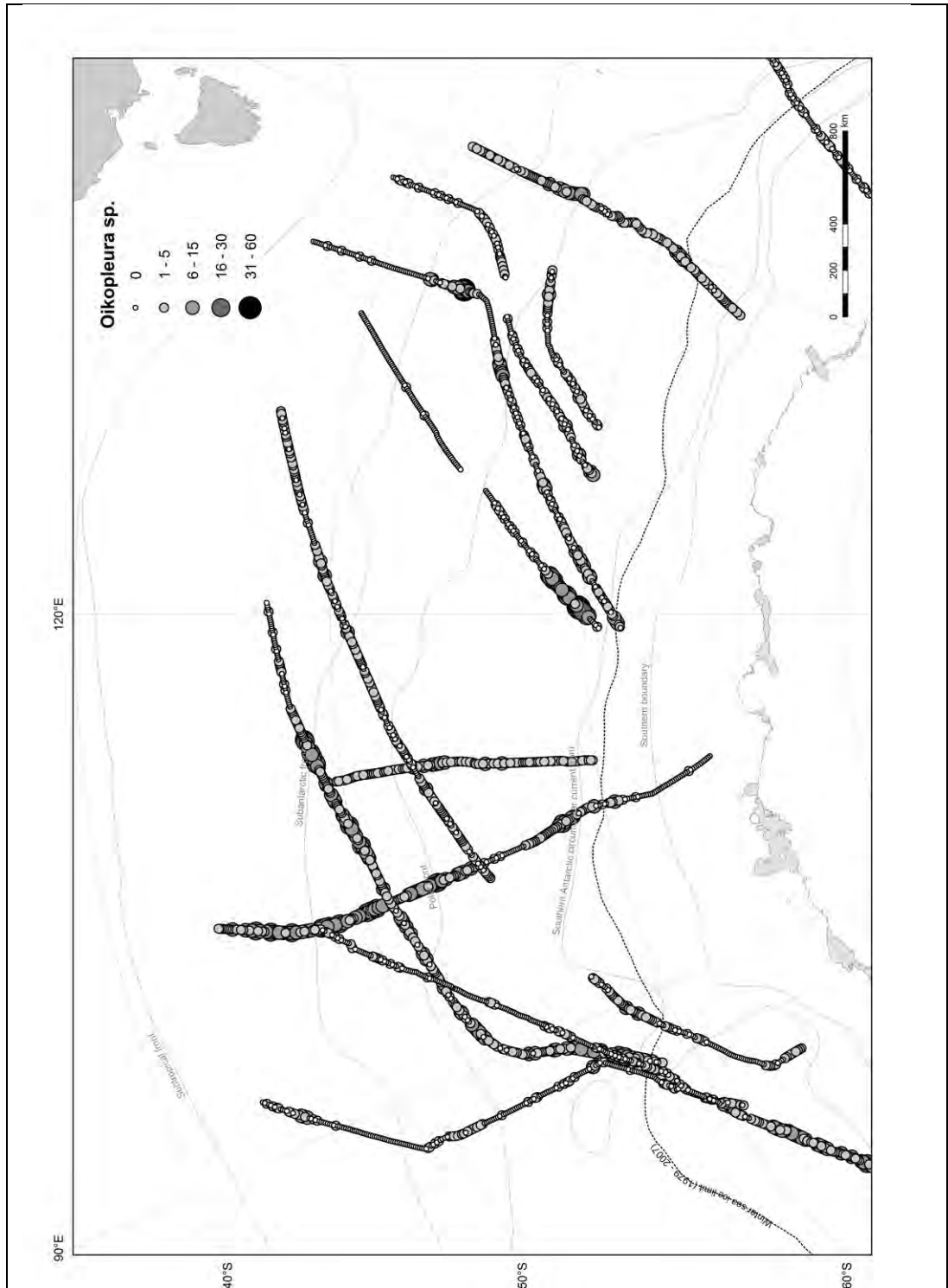


Figure 4.10 A. 2005 – 2006 CPR transects showing abundances of *Oikopleura* sp. (counts per 5 Nm).

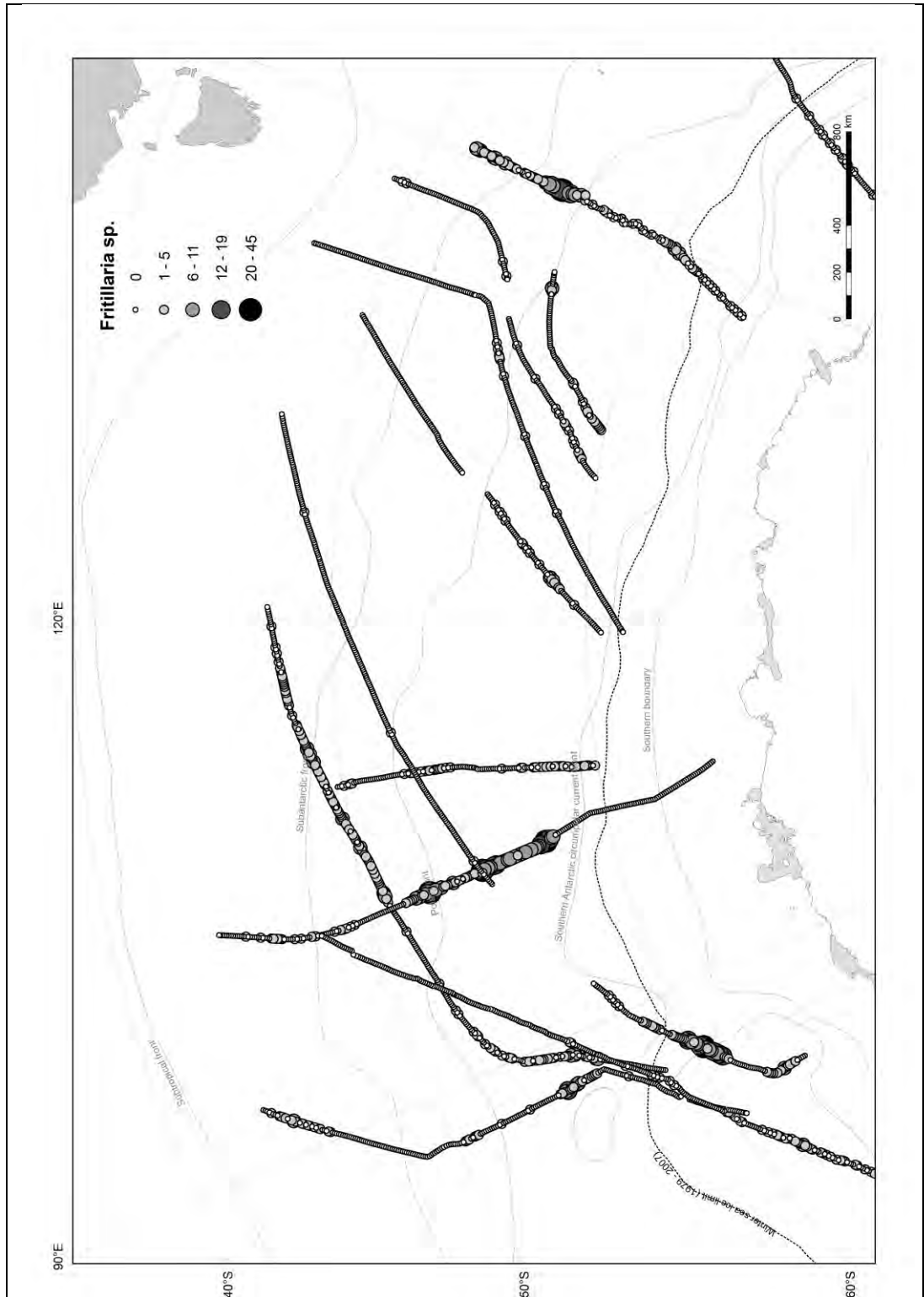


Figure 4.10 B. 2005 – 2006 CPR transects showing abundances of *Fritillaria* sp. (counts per 5 Nm).

Table 4.2. Pearson's r correlation between abundances of *Oikopleura sp.* and *Fritillaria sp.* in 2005 – 2006. **Bold** indicates a significant relationship (ns = not significant), $\alpha=0.05(2)$.

Parameter	r	df	Critical r	p
<i>Oikopleura sp.</i> and <i>Fritillaria sp.</i>	0.306	2290	0.062	0.005 < p < 0.01

In 2006 – 2007 there were lower *Oikopleura sp.* (Figure 4.11A) abundances compared to *Fritillaria sp.* (Figure 4.11B). When comparing transects for each species, there were similar distributions in the west. In the east, *Oikopleura sp.* had a northerly distribution, compared to a southerly distribution for *Fritillaria sp.*

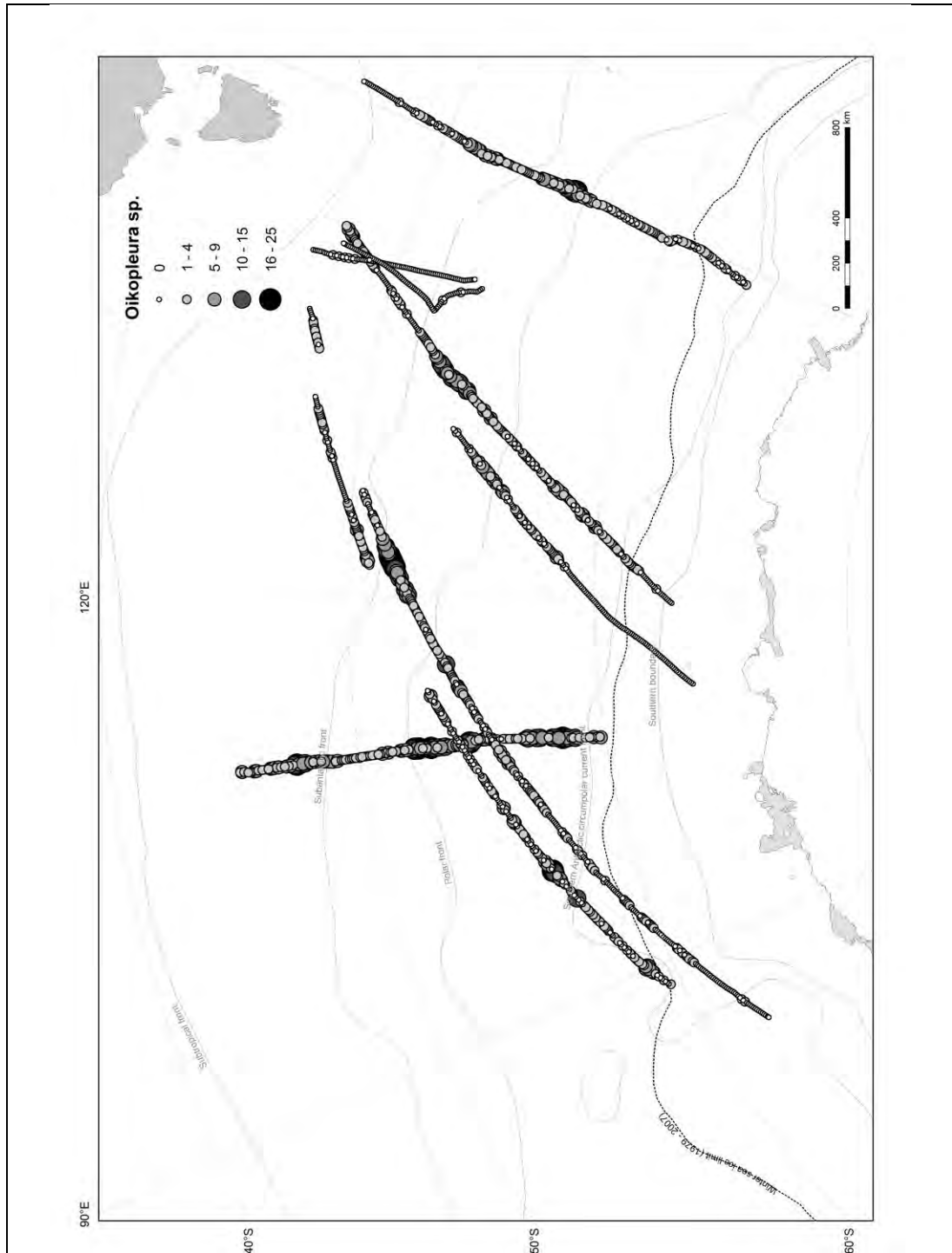


Figure 4.11 A. 2006 – 2007 CPR transects showing abundances of *Oikopleura* sp. (counts per 5 Nm).

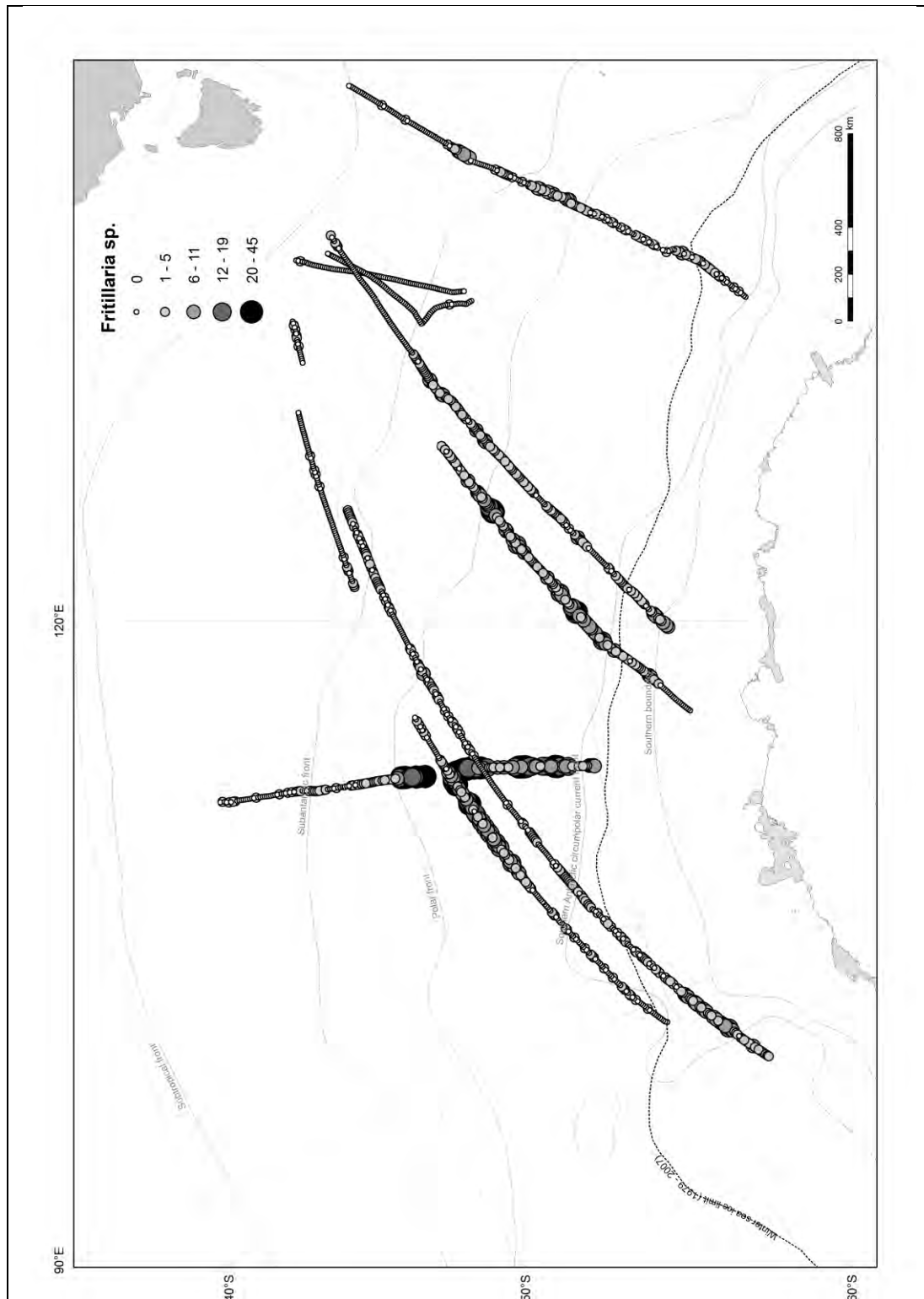


Figure 4.11 B. 2006 – 2007 CPR transects showing abundances of *Fritillaria* sp. (counts per 5 Nm).

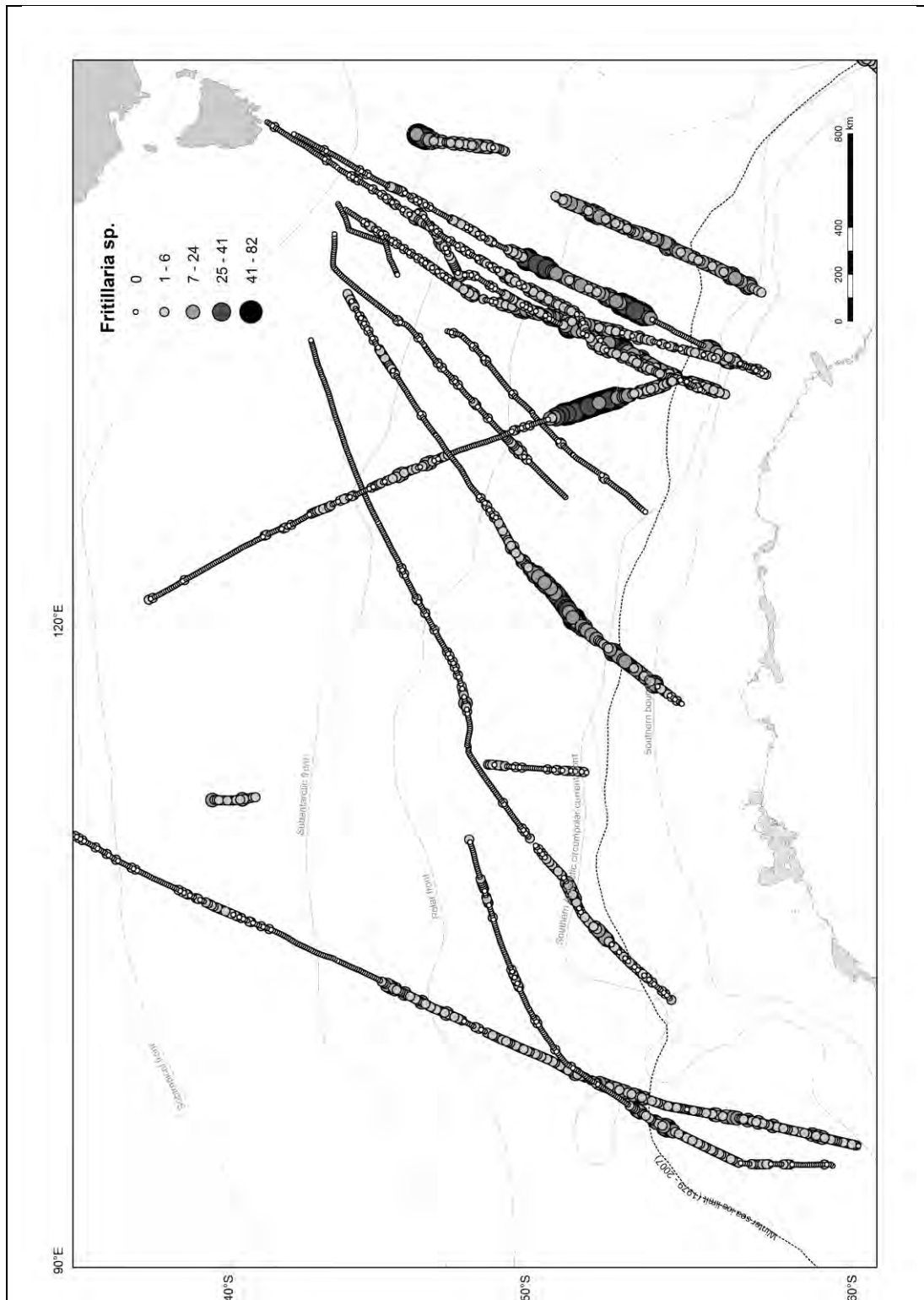


Figure 4.12 B. 2007 – 2008 CPR transects showing abundances of *Fritillaria* sp. (counts per 5 Nm).

Seasonal distribution and abundance of Southern Ocean larvaceans

Selected seasonal distribution maps are presented in this section, and the remaining seasonal maps are in Appendix V. The data suggests that season appears to have a large influence on larvacean abundance, with the highest mean abundance of 13.4 individuals per 5 Nm recorded for summer (January and February), and the lowest abundance of 1 individual per 5 Nm recorded in winter (June and July). Distributions of *Oikopleura* sp. and *Fritillaria* sp. tend to alternate along CPR transects, with *Fritillaria* sp. dominating southern regions and *Oikopleura* sp. dominating the central (POOZ) and northern regions. *Oikopleura* sp. move further south in February and return to northern regions in winter (July).

In the Southern Ocean, spring occurs in September and October, and late spring in November and December. In September (Appendix V.8), there was a low abundance of *Fritillaria* sp. at only 1-2 individuals per 5 Nm, and no recorded *Oikopleura* sp. In October (Figure 4.13), *Oikopleura* sp. were present in higher abundances compared to *Fritillaria* sp. The majority of *Oikopleura* sp. occurred in the POOZ, and *Fritillaria* sp. in the SIZ.

In November during late spring (Appendix V.9), *Oikopleura* sp. had higher abundances in the south compared to the north and there were no recorded *Fritillaria* sp. In December (Figure 4.14), there were generally higher abundances of larvaceans than early spring, and *Oikopleura* sp. had lower abundances compared to *Fritillaria* sp., although, in late spring both species had a wide latitudinal distribution.

Summer in the Southern Ocean occurs during January and February and is a season with long daylight hours of up to 24 hours of light in mid summer. In January (Appendix V.10), there were higher abundances of *Fritillaria* sp. in the south, compared to *Oikopleura* sp. in the north. Though, along some tows there appeared to be an alternate distribution between the two species. Highest annual abundances of larvaceans occurred in February (Figure 4.15), with *Fritillaria* sp. having the highest abundance at 1580 individuals per 5 Nm. For *Oikopleura* sp.,

335 individuals per 5 Nm were recorded. Higher abundances of both species occurred in the south of the survey region.

In autumn (March and April), larvacean abundances tended to decrease. In March (Appendix V.11), the distribution of both species was similar, though *Oikopleura* sp. dominated. In April (Figure 4.16), *Oikopleura* sp. had an easterly distribution and a lower abundance, compared to *Fritillaria* sp. which occurred predominantly in the west.

The short daylight hours of winter occur between May and August in the Southern Ocean with up to 24 hours of darkness in mid winter. In May (Appendix V.12), both species had low abundances. *Oikopleura* sp. again occurred in the north, and had double the abundance of *Fritillaria* sp. in the south. There were no CPR transects completed in June.

In July (Figure 4.17), *Oikopleura* sp. had a greater northerly distribution than at other times of year and no *Fritillaria* sp. were recorded. In August (Appendix V.13), both *Oikopleura* sp. and *Fritillaria* sp. occurred north of the winter sea-ice limit, but in very low abundances (1 individual per 5 Nm).

In early spring in October, *Oikopleura* sp. (Figure 4.13A) was present in higher abundances than *Fritillaria* sp. (Figure 4.13B). *Fritillaria* sp. occurred in the southern area, while the majority of *Oikopleura* sp. were in the POOZ.

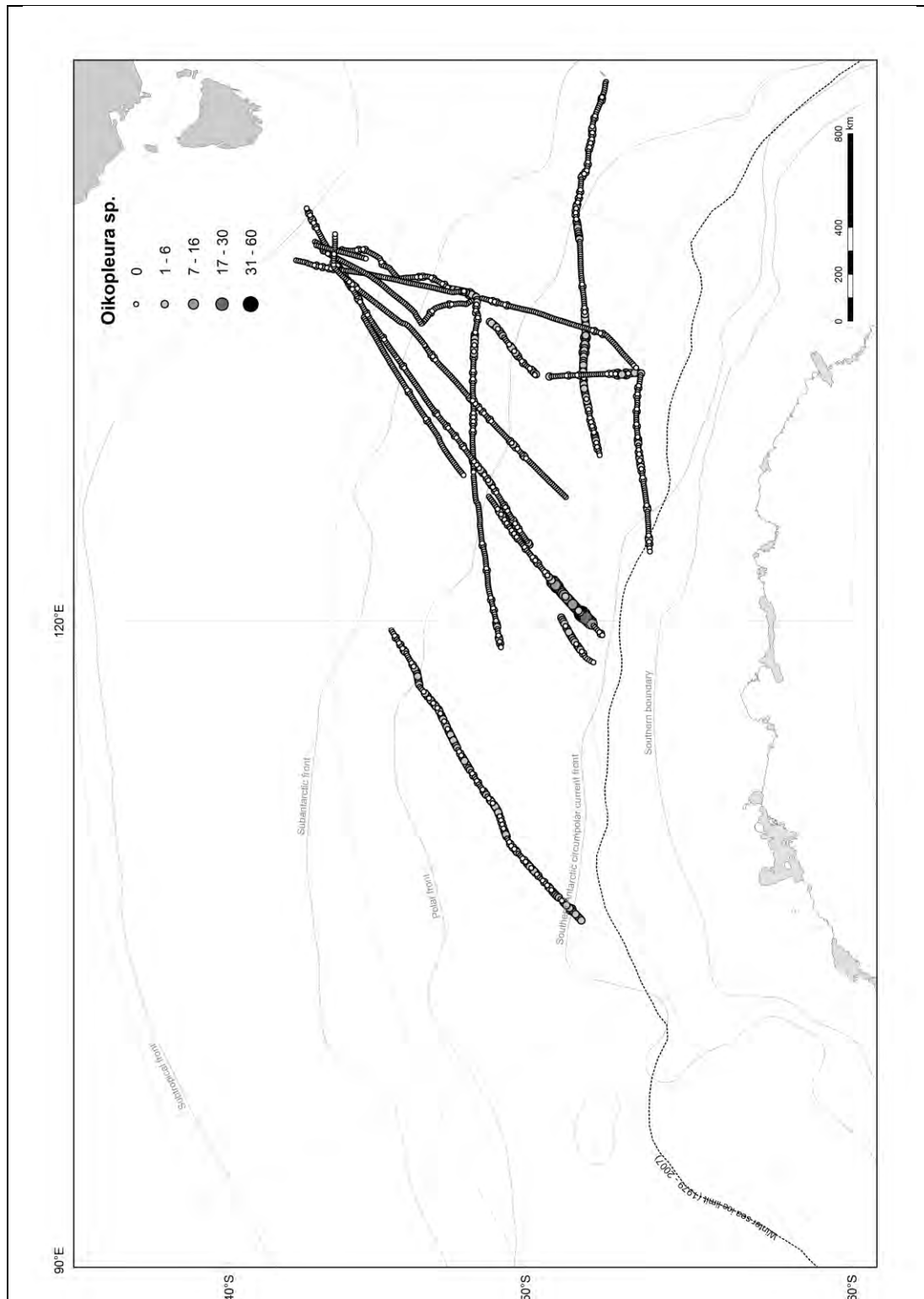


Figure 4. 13 A. October (spring) CPR transects showing abundances of *Oikopleura* sp. (counts per 5 Nm).

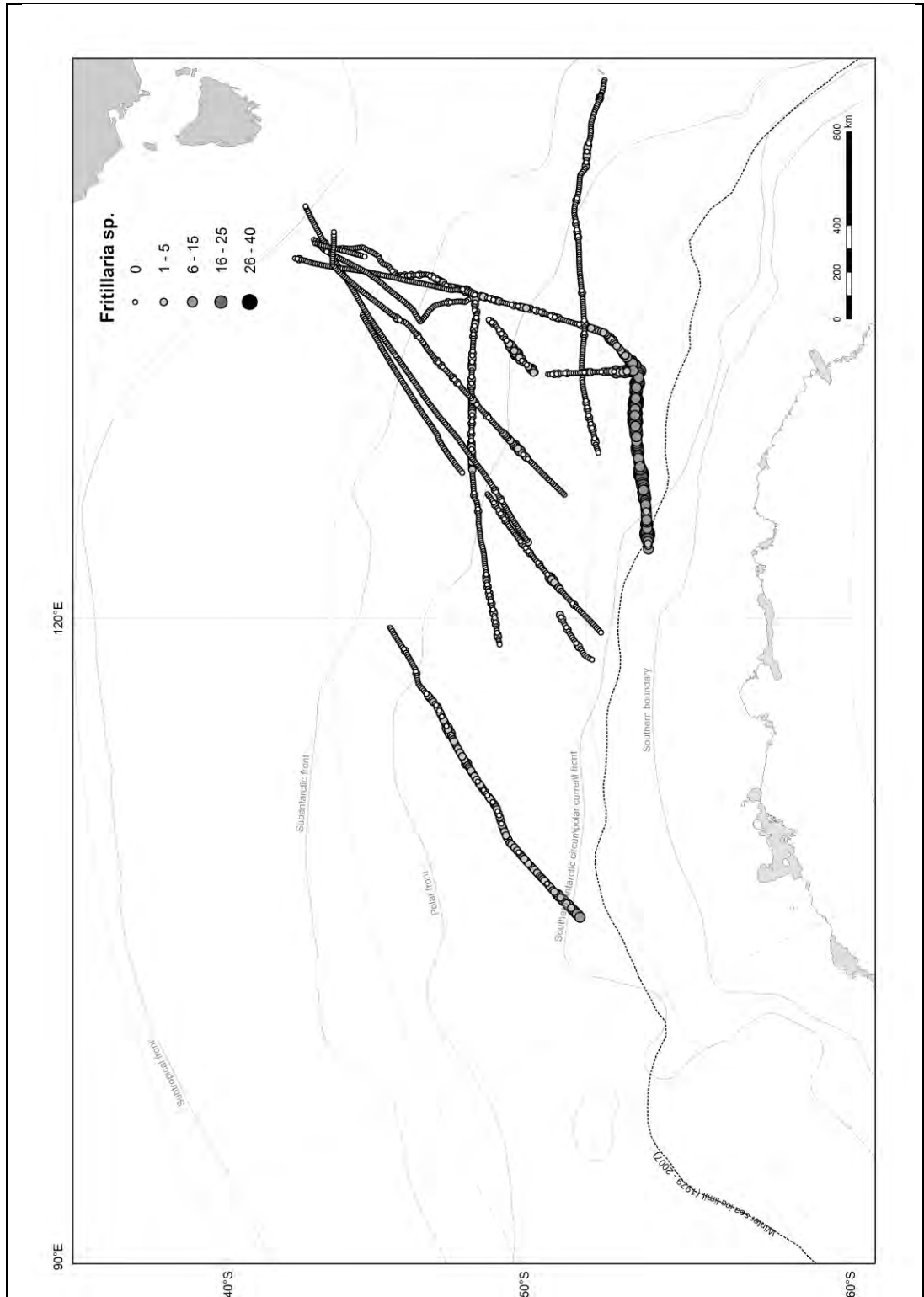


Figure 4.13 B. October (spring) CPR transects showing abundances of *Fritillaria* sp. (counts per 5 Nm).

In December (late spring) there were higher abundances of larvaceans compared to early spring. There was a lower abundance of *Oikopleura* sp. (Figure 4.14A) compared to *Fritillaria* sp. (Figure 4.14B), though both had a wide distribution.

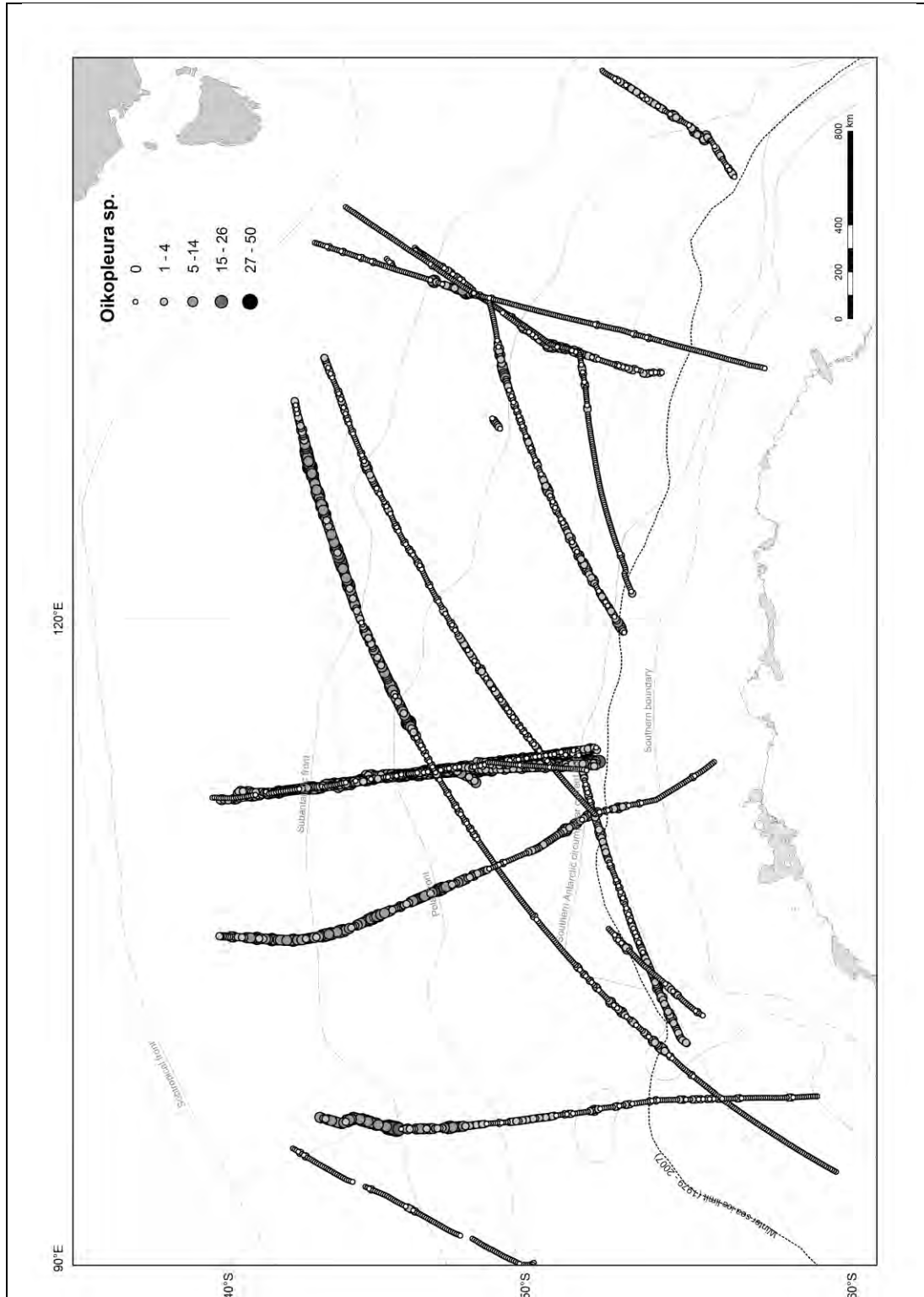


Figure 4.14 A. December (late spring) CPR transects showing abundances of *Oikopleura* sp. (counts per 5 Nm).

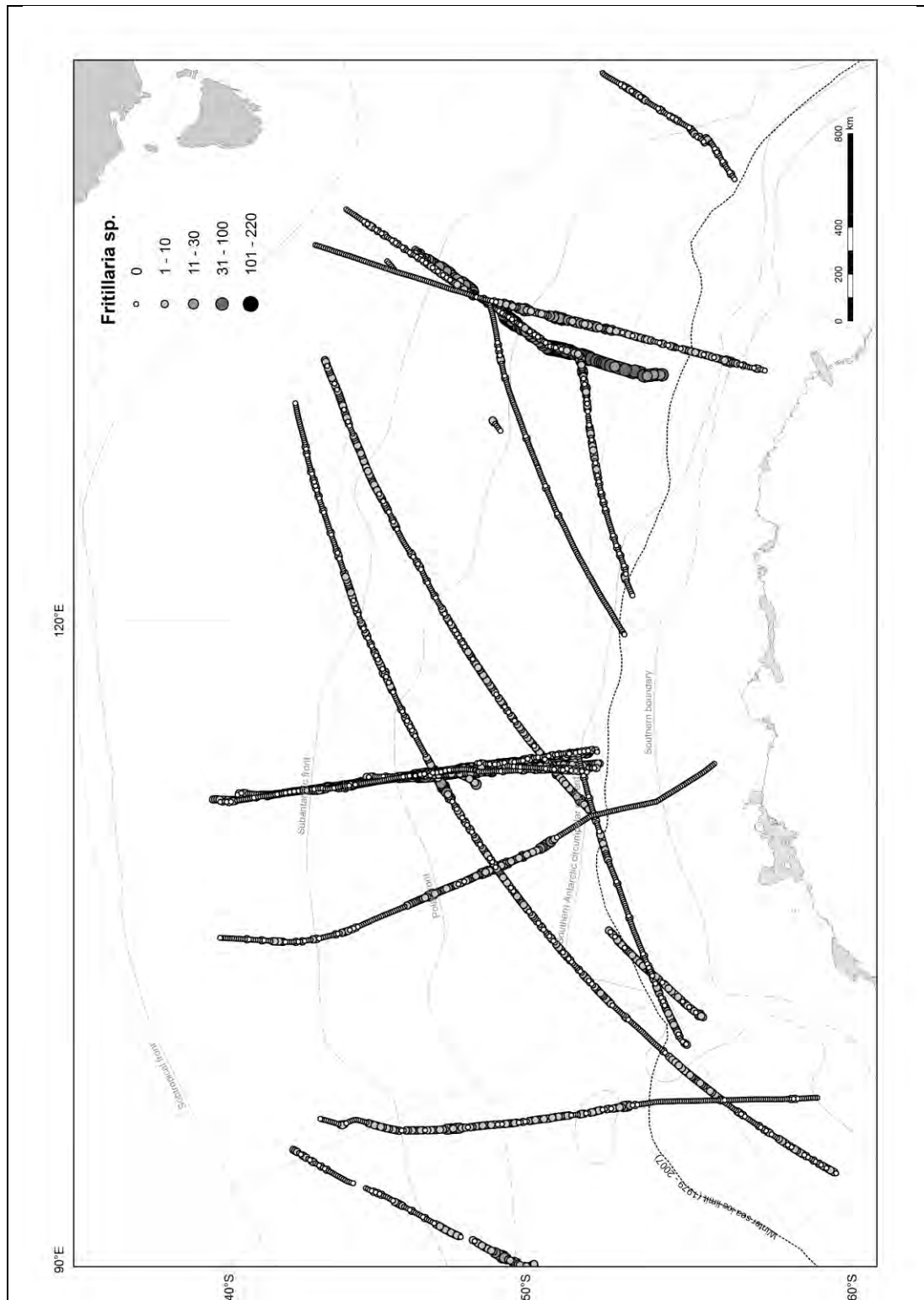


Figure 4.14 B. December (late spring) CPR transects showing abundances of *Fritillaria* sp. (counts per 5 Nm).

Highest abundances of larvaceans occurred in February (summer). *Fritillaria* sp. (Figure 4.15B) had the highest abundance at 1580 individuals per 5 Nm and *Oikopleura* sp. 335 individuals per 5 Nm (Figure 4.15A). In the south there were higher abundances of both species.

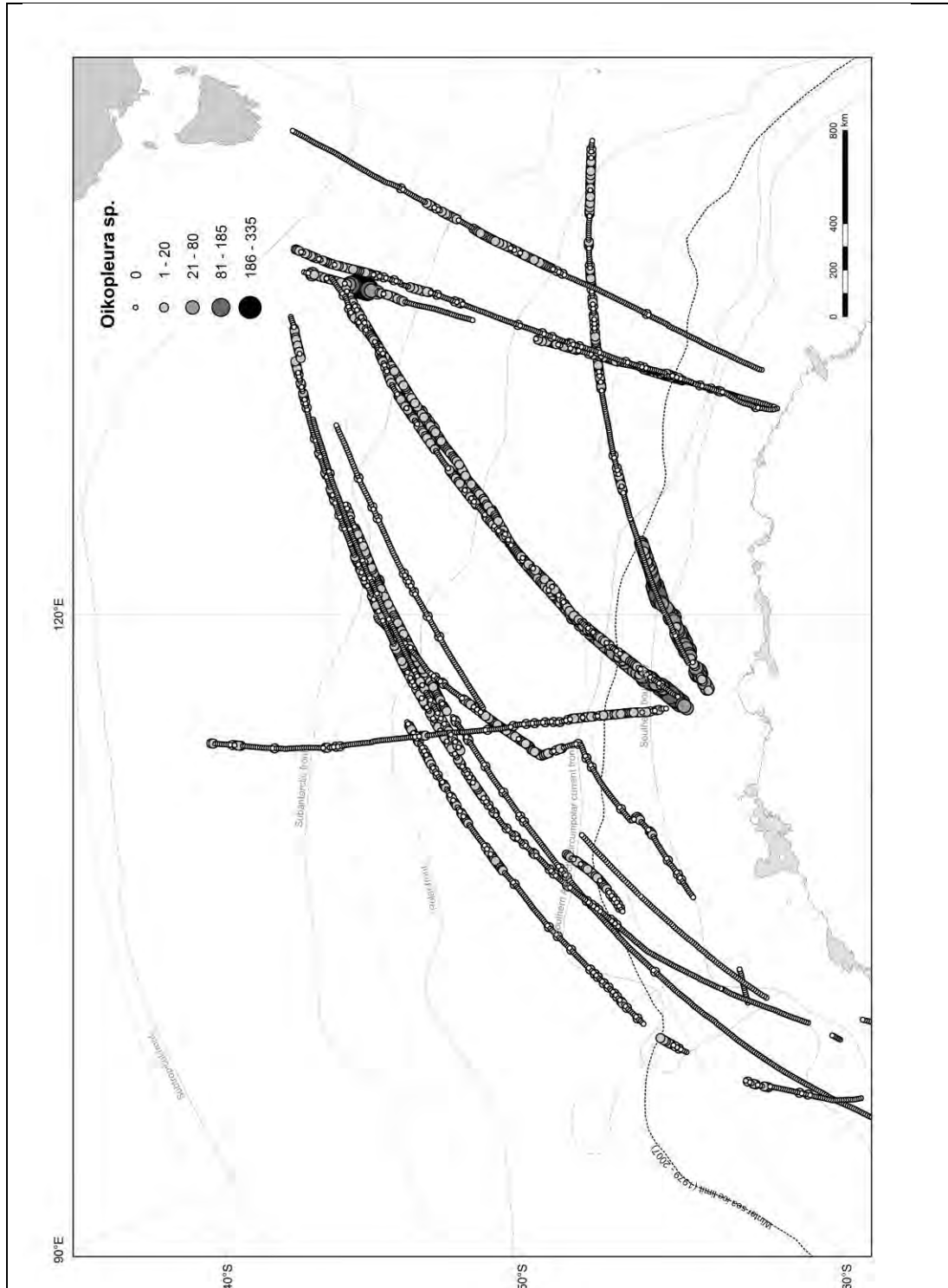


Figure 4.15 A. February (summer) CPR transects showing abundances of *Oikopleura* sp. (counts per 5 Nm).

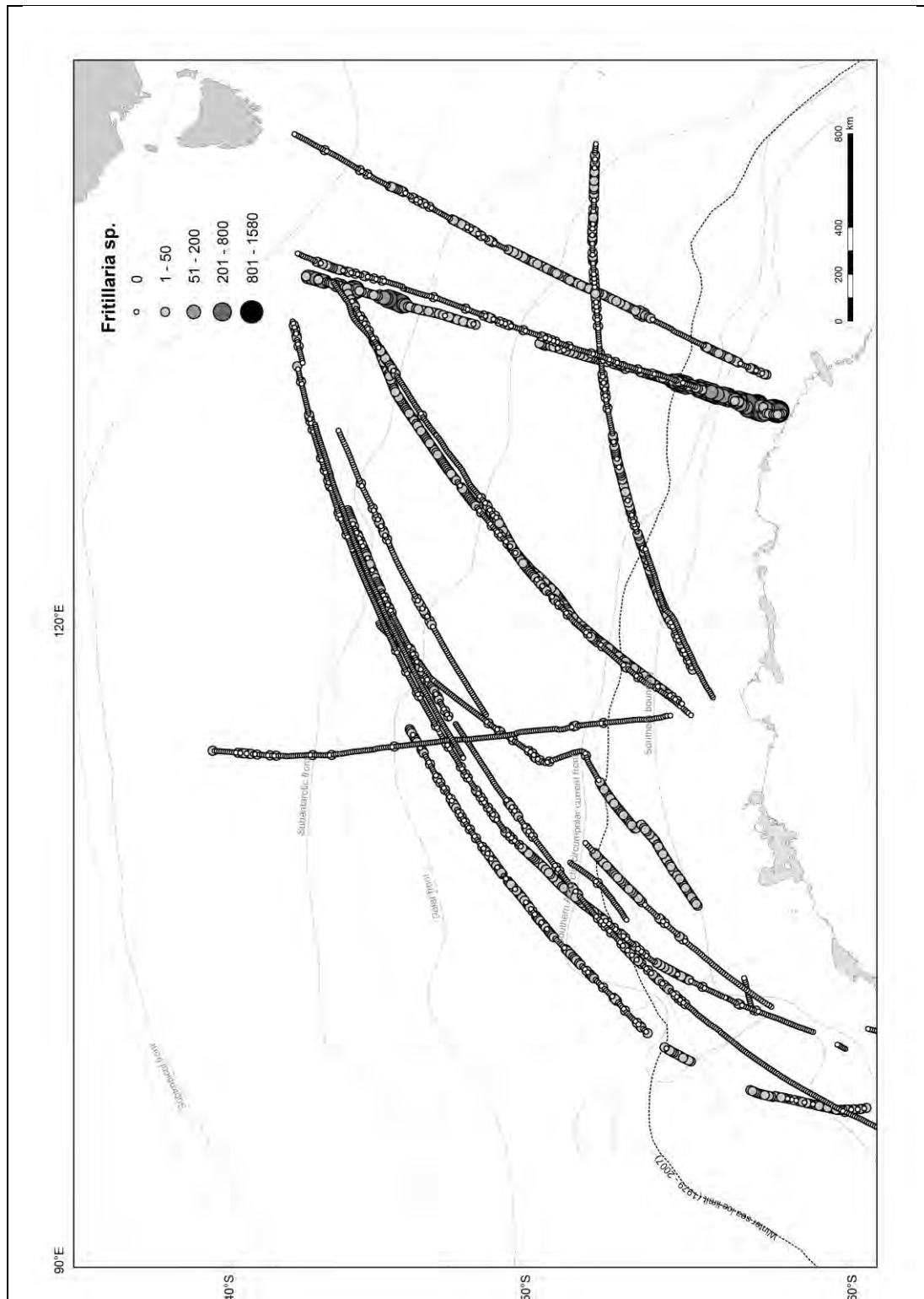


Figure 4.15 B. February (summer) CPR transects showing abundances of *Fritillaria* sp. (counts per 5 Nm).

In April (autumn), *Oikopleura* sp. (Figure 4.16A) had an easterly distribution and a lower abundance compared to *Fritillaria* sp. which had a westerly distribution (Figure 4.16B).

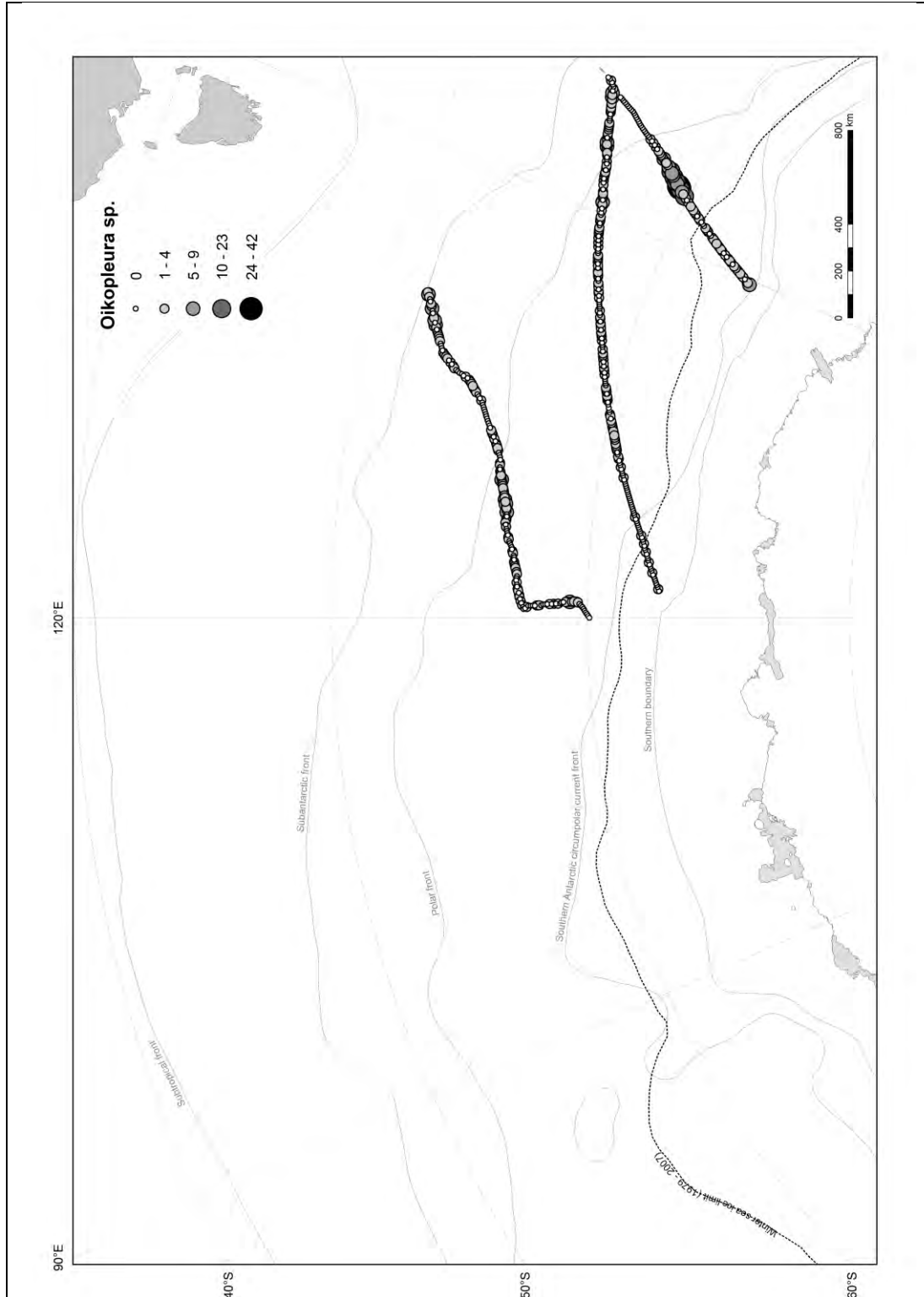


Figure 4.16A. April (autumn) CPR transects showing abundances of *Oikopleura* sp. (counts per 5 Nm).

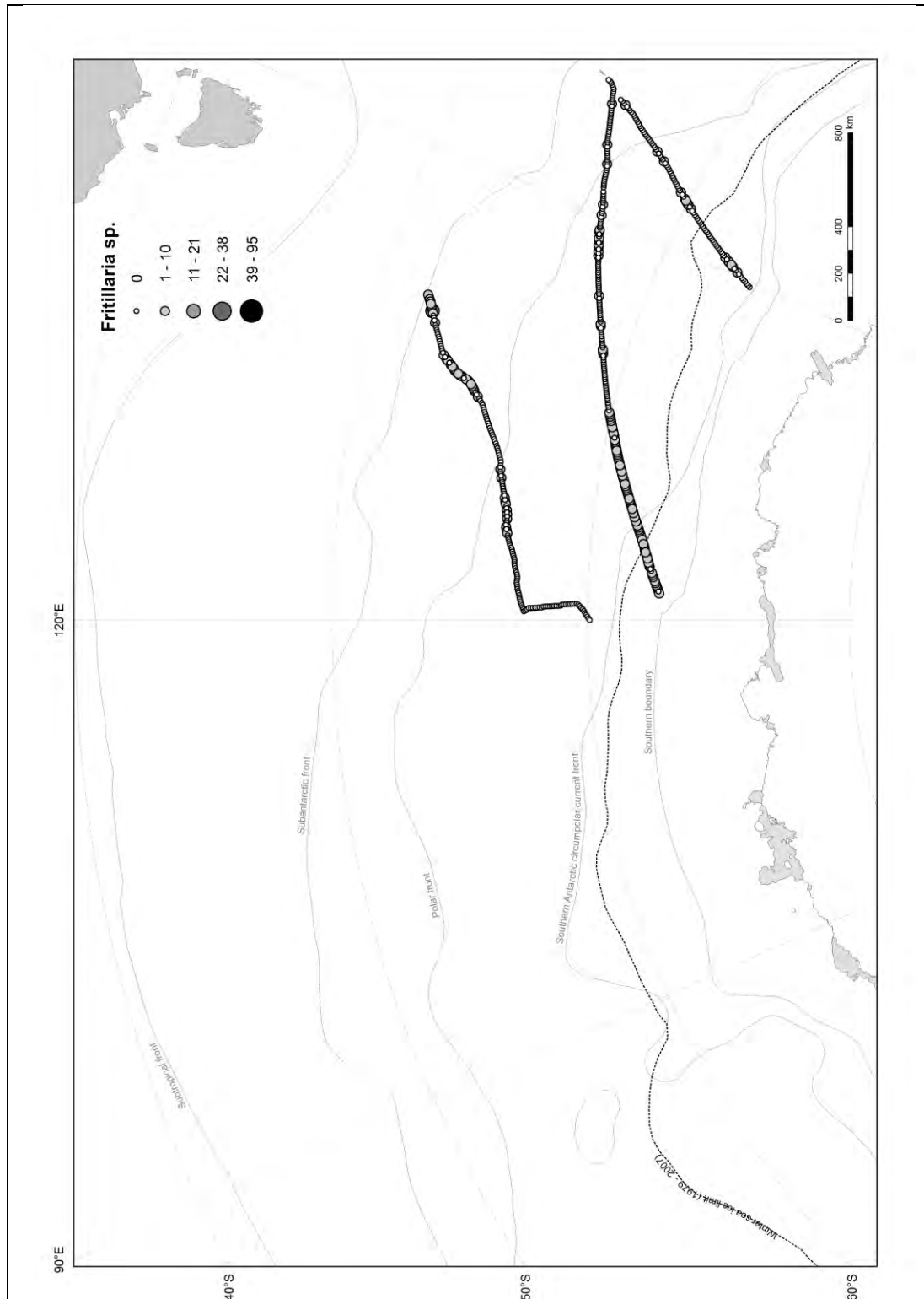


Figure 4.16 B April (autumn) CPR transects showing abundances of *Fritillaria* sp. (counts per 5 Nm).

In July (winter), *Oikopleura* sp. (Figure 4.17A) had a greater northerly distribution than at other times of the year. There were no *Fritillaria* sp. recorded.

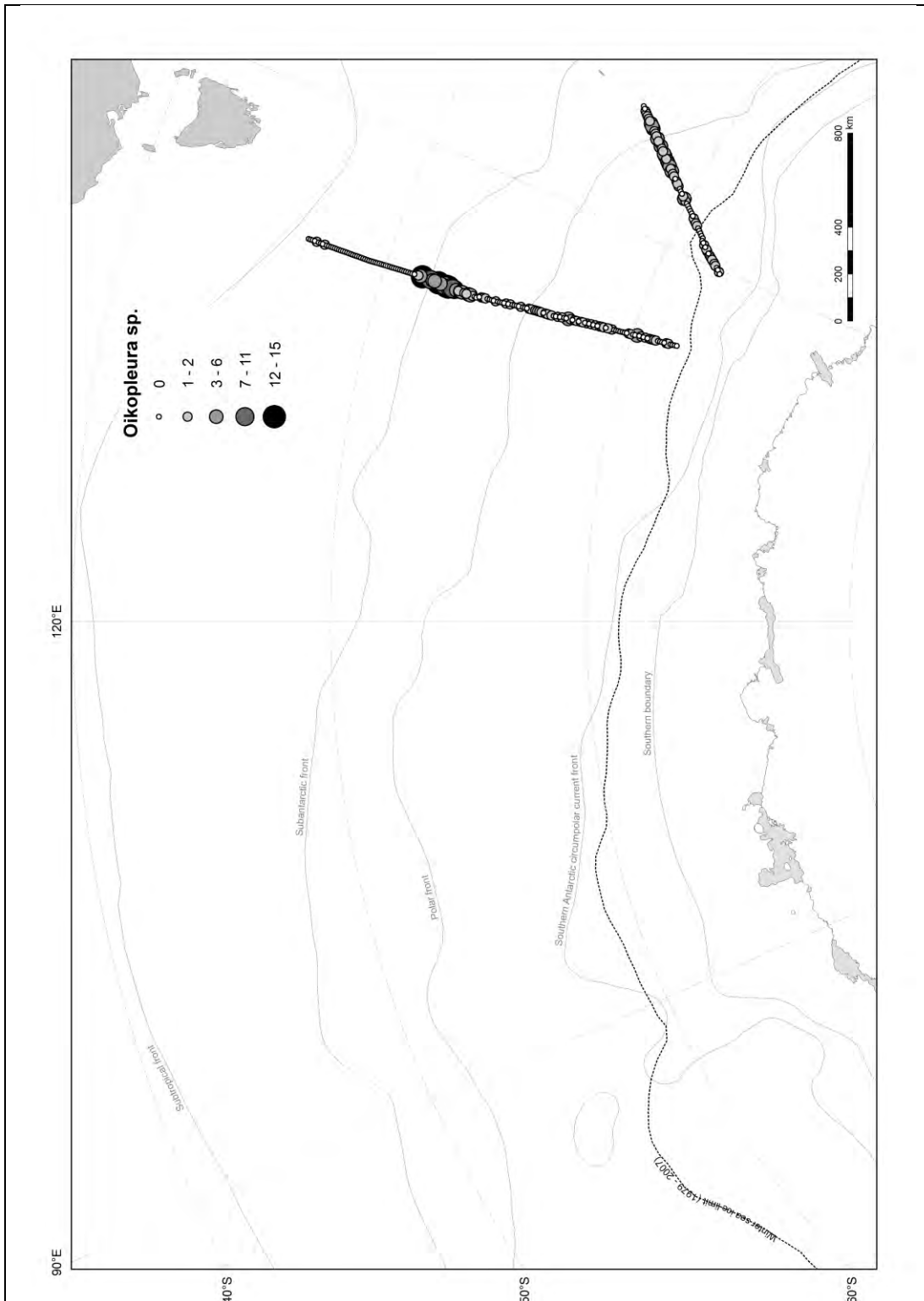


Figure 4.17. July (winter) CPR transects showing abundances of *Oikopleura* sp. (counts per 5 Nm).

4.5.2 Annual and seasonal mean abundances of Southern Ocean larvaceans

Southern Ocean annual mean abundances of larvaceans from 1990–1991 to 2007–2008 are graphed in Figure 4.18. The overall mean for all larvaceans (Table 4.3) was 6.4 ± 29.7 ind. m^{-3} . The average for *Fritillaria* sp. was 4.4 ± 28.2 ind. m^{-3} and for *Oikopleura* sp. 1.9 ± 7.6 ind. m^{-3} . The graph shows some variation between years, though *Fritillaria* sp. consistently dominates. A peak in larvaceans in the 2001–2002 season was due to the inclusion of voyage data from the *RSV Tangaroa*, discussed above. Inter-annual variations in larvacean abundances were similar to inter-annual variations in total zooplankton, as also discussed above.

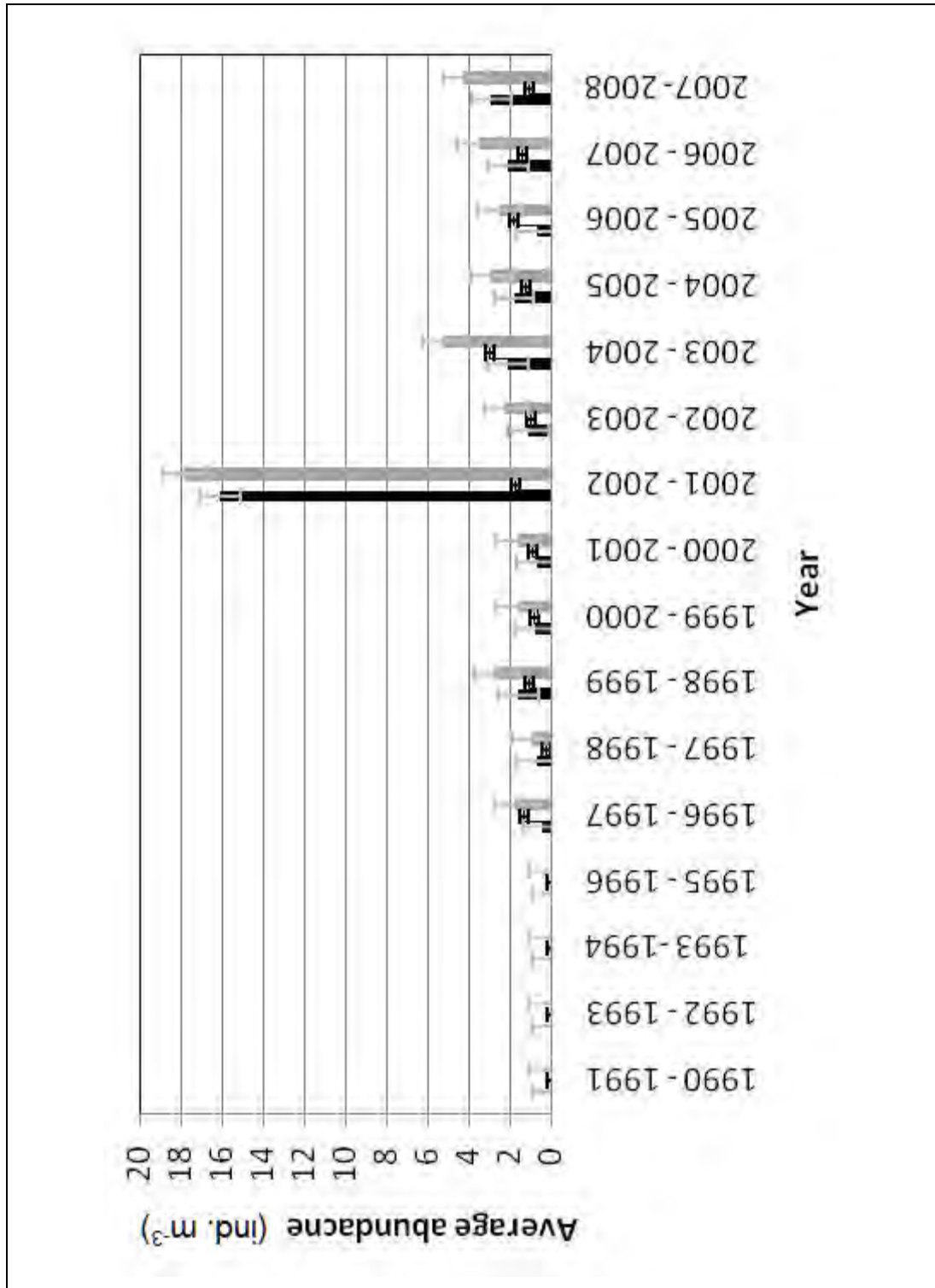


Figure 4.18. Annual mean abundance of larvaceans from the Southern Ocean. Black is *Fritillaria* sp. (ind. m⁻³, grey standard error bars), white *Oikopleura* sp. (ind. m⁻³, black standard error bars), and grey is Larvaceans (ind. m⁻³, grey standard error bars). Overall means: *Fritillaria* sp. 4.4 ind. m⁻³, *Oikopleura* sp. 1.9 ind. m⁻³, Larvaceans 6.4 ind. m⁻³.

Table 4.3. Southern Ocean annual mean abundances for *Fritillaria* sp., *Oikopleura* sp., total larvaceans and total zooplankton (ind. m⁻³) from the SO-CPR database. Sample numbers (n) and std (±) is the standard deviation

YEAR	n	<i>Fritillaria</i> sp.		<i>Oikopleura</i> sp.		Total larvaceans		Total zooplankton	
		ind. m ⁻³	std (±)	ind. m ⁻³	std (±)	ind. m ⁻³	std (±)	ind. m ⁻³	std (±)
1990 - 1991	212	0	0	0	0	0	0	29.9	101.9
1992 - 1993	0	0	0	0	0	0	0	0.9	1.5
1993 - 1994	108	0	0	0	0	0	0	4.2	4.3
1995 - 1996	94	0	0	0	0	0	0	0.9	0.9
1996 - 1997	0	0.4	1.2	1.3	2.9	1.7	3.3	63.1	84.3
1997 - 1998	87	0.7	2.3	0.2	0.7	0.9	2.5	73.9	95.1
1998 - 1999	284	1.6	4.6	1.1	2.6	2.7	7	49.6	41.8
1999 - 2000	1474	0.8	1.9	0.8	1.5	1.6	2.4	87.7	108.2
2000 - 2001	623	0.7	1.5	0.9	2	1.6	2.6	50.5	60.6
2001 - 2002	2153	16.1	57.6	1.7	10.9	17.8	58.8	133	231.4
2002 - 2003	2105	1.1	3.1	1	2.2	2.2	3.8	87.8	111.6
2003 - 2004	2651	2.1	4.6	3	11	5.2	11.7	79.3	95.9
2004 - 2005	2092	1.8	5	1.2	2.6	2.9	5.7	84.8	111.2
2005 - 2006	2291	0.7	1.9	1.8	3.1	2.5	4.1	92.2	96
2006 - 2007	2406	2.1	5.6	1.4	2.2	3.5	6.7	107.5	117.9
2007 - 2008	3216	2.9	6.8	1.1	2.4	4.2	10.2	71.5	75.5
Overall mean	25791	4.4	28.2	1.9	7.6	6.4	29.7	121.7	171.6

Monthly larvacean mean abundances from the Southern Ocean are graphed in Figure 4.19. Patterns are associated with seasonality, with a peak in February, the second month of summer. The overall mean for larvaceans in February (Table 4.4) was 8.7 ± 38.8 ind. m⁻³. *Fritillaria* sp. averaged 6.3 ± 36.9 ind. m⁻³ and *Oikopleura* sp. 2.4 ± 11.1 ind. m⁻³. The total average zooplankton abundance for February was 98.5 ± 150.6 ind. m⁻³. The highest total zooplankton abundance occurred in December with 122 ± 135.9 ind. m⁻³. Abundances of zooplankton declined during autumn, reaching lowest numbers in winter. Larvacean numbers began to increase in October (spring) through to November and December (late spring). Both larvacean species showed the same seasonal pattern. Seasonality of larvaceans appeared to lag one month behind that of total zooplankton, as shown in Table 4.4 and Figure 4.22.

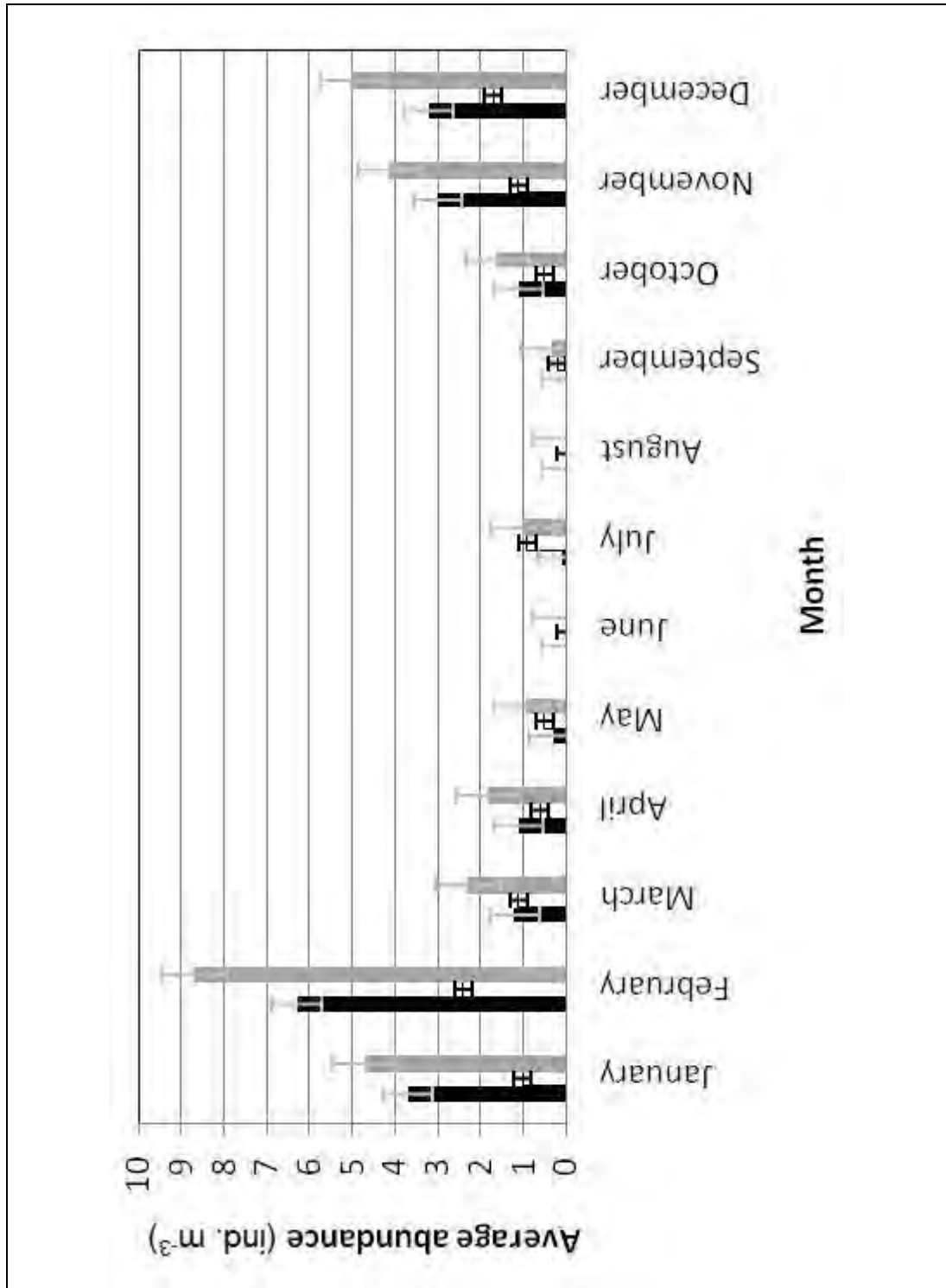


Figure 4.19. *Fritillaria* sp and *Oikopleura* sp. monthly mean abundances from SO-CPR data. Black is *Fritillaria* sp. abundance (ind. m⁻³, grey standard error bars), white *Oikopleura* sp. abundance (ind. m⁻³, black standard error bars), and grey larvacean abundance (ind. m⁻³, grey standard error bars).

Table 4.4. Southern Ocean monthly mean abundances for *Fritillaria* sp., *Oikopleura* sp., total larvaceans and total zooplankton (ind. m⁻³) from the SO-CPR database. Sample numbers (n) and std (±) is the standard deviation

MONTH	n	<i>Fritillaria</i> sp.		<i>Oikopleura</i> sp.		Total larvaceans		Total zooplankton	
		ind. m ⁻³	std (±)	ind. m ⁻³	std (±)	ind. m ⁻³	std (±)	ind. m ⁻³	std (±)
January	5201	3.7	23.3	1	2.5	4.7	23.5	95.2	141.2
February	4628	6.3	36.9	2.4	11.1	8.7	38.8	98.5	150.6
March	5983	1.2	3.2	1.1	2.8	2.3	4.6	62.9	76.3
April	939	1.1	2.2	0.6	1.8	1.8	2.8	47.9	53.1
May	230	0.3	0.7	0.5	1	0.9	1.3	34.5	2
June	0								
July	251	0.1	0.2	0.9	1.7	1	1.7	32.2	27.3
August	130	0	0.1	0	0.1	0	0.1	3.4	4.8
September	447	0	0.2	0.2	0.5	0.3	0.6	16.8	18
October	1603	1.1	3.1	0.5	2	1.6	3.7	26.6	36.3
November	2415	3	6.3	1.1	2.2	4.1	7.2	100.4	86.7
December	3964	3.2	9.4	1.7	3	5	11.5	122	135.9
Overall mean	2579	4.4	28.2	1.9	7.6	6.4	29.7	121.7	171.6

4.5.3 Annual and seasonal mean abundances of Southern Ocean zones

Inter-annual variation within each oceanic zone (Figure 4.20 and Table 4.5) was small, with highest larvacean abundances occurring in the SIZ (11.1 ± 49.3 ind. m⁻³). The POOZ averaged 6.4 ± 29.7 ind. m⁻³ and the SAZ had the lowest abundance with an average of 1.9 ± 7.6 ind. m⁻³. In seven of the survey years (1998-1999, 2000-2001, 2002-2003, 2004-2005, 2005-2006, 2006-2007 and 2007-2008) the POOZ had higher abundances than the SIZ. However, the differences in abundances were not as large as in the 4 other years when the SIZ had significantly higher abundances.

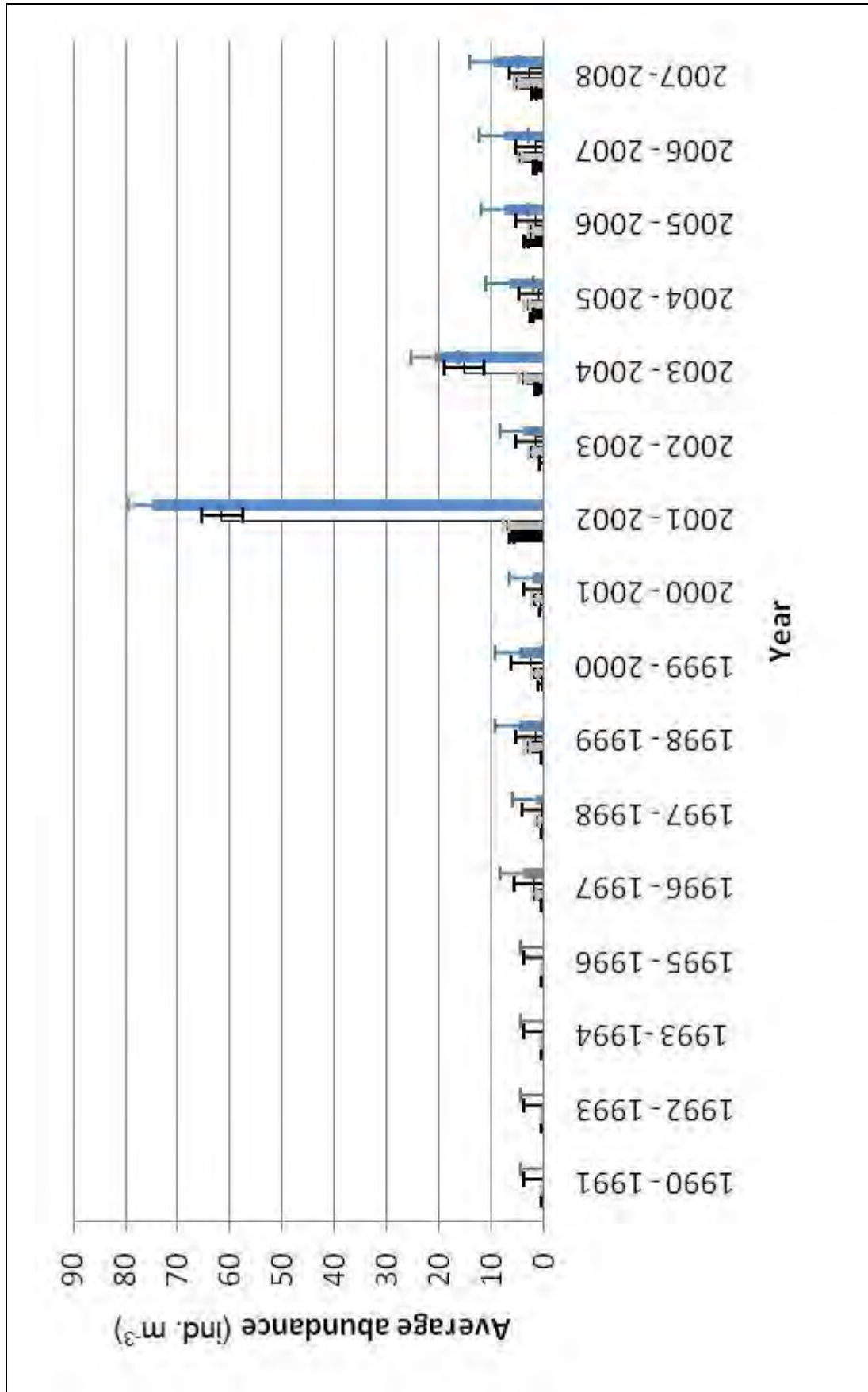


Figure 4.20. Southern Ocean annual mean abundances of larvaceans (ind. m⁻³) from the SO-CPR Survey. The ocean was divided into three zones; Sub Antarctic Zone (SAZ, north 48 °S, black), Permanent Open Ocean Zone (POOZ, 50 - 60 °S,

grey) and the Seasonal Ice Zone (SIZ, south 62 °S, white). Blue indicates total mean larvacean abundances (ind. m⁻³) and error bars are the standard deviations.

Table 4.5. Southern Ocean annual larvacean mean abundances (ind. m⁻³) from the SO-CPR Survey. Std (±) is the standard deviation.

YEAR	Southern Ocean		SAZ North 48 °S		POOZ 50 - 60 °S		SIZ South 62 °S	
	ind. m ⁻³	std (±)	ind. m ⁻³	std (±)	ind. m ⁻³	std (±)	ind. m ⁻³	std (±)
1990 - 1991	0	0	0	0	0	0	0	0
1992 - 1993	0	0	0	0	0	0	0	0
1993 - 1994	0	0	0	0	0	0	0	0
1995 - 1996	0	0	0	0	0	0	0	0
1996 - 1997	1.7	3.3	0	0	1.8	3.6	1.9	1.5
1997 - 1998	0.9	2.5	0	0	1.3	3	0.2	0.7
1998 - 1999	2.7	7	0	0	3.2	8.6	1.6	2.1
1999 - 2000	1.6	2.4	0.6	1.3	1.7	2.2	2.4	4
2000 - 2001	1.6	2.6	0.3	0.6	1.7	2.2	0.1	0.3
2001 - 2002	17.8	58.8	6.2	16.4	7.1	22.3	61.5	118.1
2002 - 2003	2.2	3.8	0.2	0.5	2.3	4	1.4	1.6
2003 - 2004	5.2	11.7	1.4	2.3	4.1	6.6	15.2	25.4
2004 - 2005	2.9	5.7	2.3	4.1	3.2	6.3	1	3.1
2005 - 2006	2.5	4.1	3.4	4.5	2.5	4.4	1.5	2.2
2006 - 2007	3.5	6.7	1.7	2.4	4.5	7.9	1.4	1.6
2007 - 2008	4.2	10.2	1.9	4.3	5.1	10.5	2.7	4.9
Overall mean	4.4	28.2	1.9	7.6	6.4	29.7	11.1	49.3

Figure 4.21 and Table 4.6 show variations in the monthly means of larvaceans in Southern Ocean zones. Seasonal variation in the SIZ was greater than that in the SAZ and POOZ. In the SAZ (4.5 ± 14.4 ind m⁻³) highest abundances occurred in February, at the same time as highest abundances in the SIZ (22 ± 71.1 ind m⁻³). In the POOZ, highest abundances occurred in December (5.6 ± 11.8 ind m⁻³).

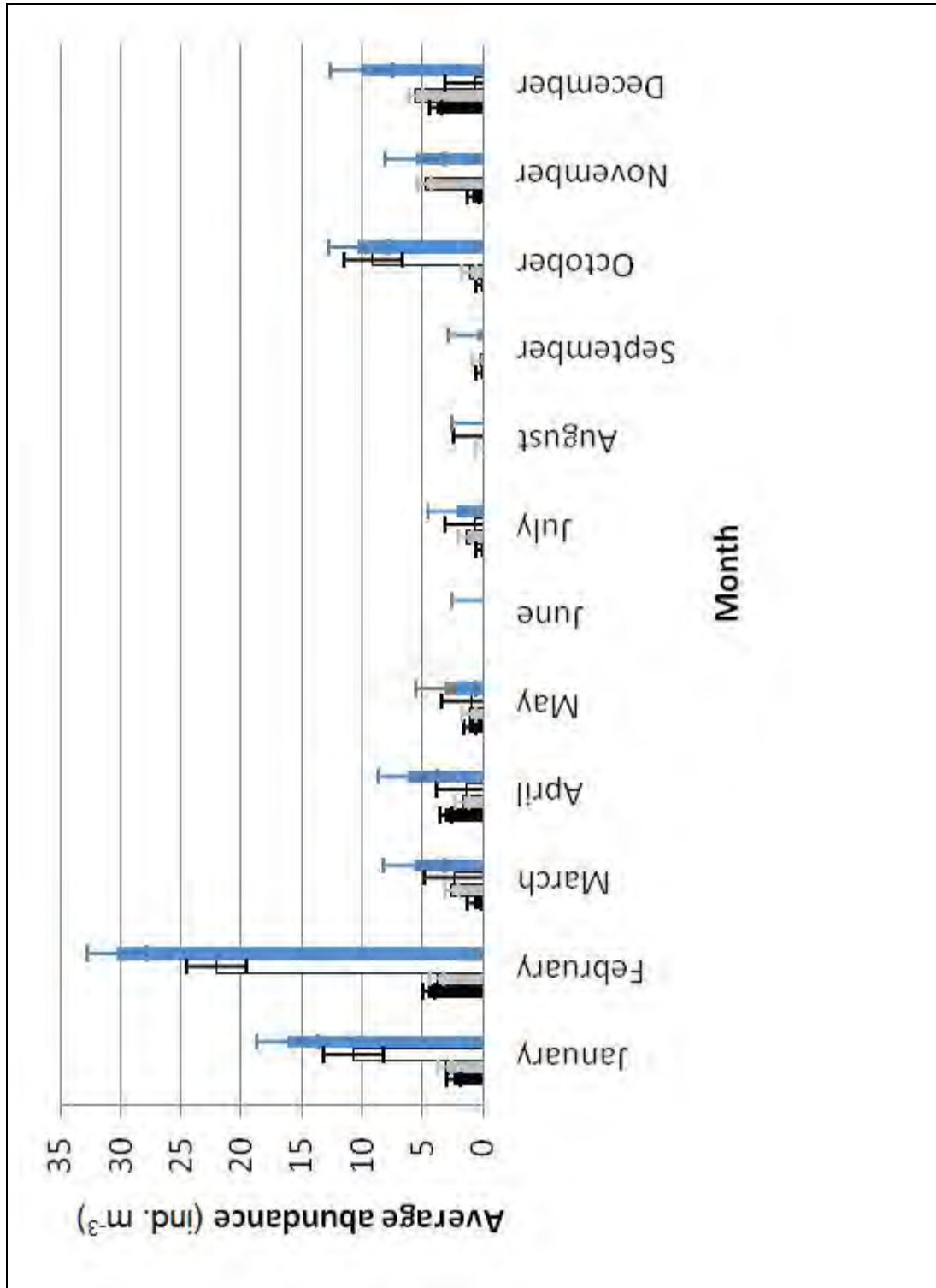


Figure 4.21. Southern Ocean monthly mean larvacean abundances (ind. m⁻³) from the SO-CPR Survey. The ocean was divided into three zones; Sub Antarctic Zone (SAZ, north 48 °S, black), Permanent Open Ocean Zone (POOZ, 50 - 60 °S, grey) and the Seasonal Ice Zone (SIZ, south 62 °S, white). Blue indicates total mean larvacean abundances (ind. m⁻³) and error bars are the standard deviations.

Table 4.6. Monthly mean larvacean abundances (ind. m⁻³) for the Southern Ocean and associated zones. Data from the SO-CPR Survey. Std (±) is the standard deviation.

MONTH	Southern Ocean		SAZ North 48 °S		POOZ 50 - 60 °S		SIZ South 62 °S	
	ind. m ⁻³	std (±)	ind. m ⁻³	std (±)	ind. m ⁻³	std (±)	ind. m ⁻³	std (±)
January	4.7	23.5	2.4	5.2	3.1	7.1	10.7	50.1
February	8.7	38.8	4.5	14.4	3.8	15.2	22	71.1
March	2.3	4.6	0.7	1.6	2.6	5	2.4	3.8
April	1.8	2.8	3.1	3.1	1.7	2.9	1.4	1.4
May	0.9	1.3	1.1	1.3	1.1	1.7	0.9	1.2
June	0	0	0	0	0	0	0	0
July	1	1.7	0.1	0.2	1.4	2	0.6	0.6
August	0	0.1	0	0	0	0.1	0	0
September	0.3	0.6	0.1	0.3	0.3	0.6	0	0
October	1.6	3.7	0.1	0.3	1.1	2.5	9.1	5.1
November	4.1	7.2	0.8	2.1	4.8	7.8	0	0
December	5	11.5	3.9	5.4	5.6	11.8	0.6	1.8
Overall mean	6.4	29.7	2.4	6.2	3.4	9.3	11.1	49.3

4.5.4 Relationships between larvaceans and other zooplankton in the Southern Ocean

Annual and monthly variations in abundances of *Fritillaria* sp., *Oikopleura* sp., total larvaceans, and total zooplankton are presented in Tables 4.7 to 4.12. Tables 4.7 and 4.8 show annual and monthly variations in the SAZ. The SAZ had little inter-annual variation and seasonal variation was similar for both larvaceans and total zooplankton.

Table 4.7. Sub Antarctic Zone (SAZ, north of 48 °S) annual mean abundances for *Fritillaria* sp., *Oikopleura* sp., total larvaceans and total zooplankton. Std (\pm) is the standard deviation.

SEASON	<i>Fritillaria</i> sp.		<i>Oikopleura</i> sp.		Total larvaceans		Total zooplankton	
	ind. m ⁻³	std (\pm)	ind. m ⁻³	std (\pm)	ind. m ⁻³	std (\pm)	ind. m ⁻³	std (\pm)
1990 - 1991	NO CPR TOWS IN THIS REGION BETWEEN 1990 AND 1999							
1992 - 1993								
1993 - 1994								
1995 - 1996								
1996 - 1997								
1997 - 1998								
1998 - 1999								
1999 - 2000	0	0	0.6	1.3	0.6	1.3	7.4	4.1
2000 - 2001	0	0	0.3	0.6	0.3	0.6	19.1	25.1
2001 - 2002	5.2	14.5	1.1	3.5	6.2	16.4	55.8	91.6
2002 - 2003	0	0	0.2	0.5	0.2	0.5	27.7	21
2003 - 2004	1.1	2.1	0.3	0.7	1.4	2.3	40.3	29.6
2004 - 2005	0.2	0.5	2.1	3.9	2.3	4.1	84.7	79.3
2005 - 2006	0.2	0.6	3.2	4.4	3.4	4.5	58.2	54.3
2006 - 2007	0.1	0.3	1.5	2.2	1.7	2.4	74.2	78.1
2007 - 2008	1	3.1	0.9	2	1.9	4.3	44.5	66.3
Overall mean	1	4.9	1.4	3	2.4	6.2	52.2	65.8

Table 4.8. Sub Antarctic Zone (SAZ, north of 48 °S) monthly mean abundances for *Fritillaria* sp., *Oikopleura* sp., total larvaceans and total zooplankton. Std (\pm) is the standard deviation.

MONTH	<i>Fritillaria</i> sp.		<i>Oikopleura</i> sp.		Total larvaceans		Total zooplankton	
	ind. m ⁻³	std (\pm)	ind. m ⁻³	std (\pm)	ind. m ⁻³	std (\pm)	ind. m ⁻³	std (\pm)
January	0.6	3	1.8	3.8	2.4	5.2	44.9	50.8
February	3.4	13.2	1.1	2.1	4.5	14.4	52.7	82.1
March	0.3	1.2	0.4	0.9	0.7	1.6	31.6	36.6
April	2.3	2.4	0.8	1.2	3.1	3.1	28.5	9.9
May	0.8	1	0.3	0.8	1.1	1.3	37.1	20.4
June	0	0	0	0	0	0	0	0
July	0	0	0.1	0.2	0.1	0.2	5.4	1.8
August	0	0	0	0	0	0	0	0
September	0	0.2	0.1	0.2	0.1	0.3	16.3	13.5
October	0	0.1	0.1	0.3	0.1	0.3	22.6	25.6
November	0.7	2.1	0.2	0.4	0.8	2.1	26.8	22.3
December	1.5	3.6	2.4	3.5	3.9	5.4	99.1	89.4
Overall mean	1	4.9	1.4	3	2.4	6.2	52.2	65.8

Table 4.9 and Table 4.10 show annual and monthly variations for the Permanent Open Ocean Zone (POOZ). Inter-annual variations and seasonal variations were similar for larvaceans and total zooplankton.

Table 4.9 Permanent Open Ocean Zone (POOZ, between 50 – 60°S) annual mean abundances for *Fritillaria* sp., *Oikopleura* sp., total larvaceans and total zooplankton. Std (\pm) is the standard deviation.

SEASON	<i>Fritillaria</i> sp.		<i>Oikopleura</i> sp.		Total larvaceans		Total zooplankton	
	ind. m ⁻³	std (\pm)	ind. m ⁻³	std (\pm)	ind. m ⁻³	std (\pm)	ind. m ⁻³	std (\pm)
1990 - 1991	0	0	0	0	0	0	43.6	65.9
1992 - 1993	0	0	0	0	0	0		
1993 - 1994	0	0	0	0	0	0		
1995 - 1996	0	0	0	0	0	0	0.9	0.9
1996 - 1997	0.5	1.3	1.3	3.2	1.8	3.6	67.9	90.7
1997 - 1998	1	2.8	0.3	0.8	1.3	3	92.3	101
1998 - 1999	1.7	5.7	1.5	3.2	3.2	8.6	51.5	44.8
1999 - 2000	0.8	1.7	0.9	1.4	1.7	2.2	99.1	110.5
2000 - 2001	0.9	1.7	0.9	1.3	1.7	2.2	56.4	56.4
2001 - 2002	5.6	21.4	1.5	4.5	7.1	22.3	115.8	164.5
2002 - 2003	1.2	3.4	1.1	2.1	2.3	4	110.9	127.4
2003 - 2004	2.9	5.4	1.1	2.6	4.1	6.6	84.2	84.5
2004 - 2005	2	5.6	1.2	2.4	3.2	6.3	94.7	126.3
2005 - 2006	0.7	2.1	1.8	3.1	2.5	4.4	100.7	101.5
2006 - 2007	2.7	6.7	1.8	2.4	4.5	7.9	126.7	133.2
2007 - 2008	3.5	7.7	1.5	2.8	5.1	10.5	86.8	78.3
Overall mean	2.1	8.2	1.3	2.7	3.4	9.3	93.3	110

Table 4.10. Permanent Open Ocean Zone (POOZ, between 50 – 60°S) monthly mean abundances for *Fritillaria* sp., *Oikopleura* sp., total larvaceans and total zooplankton. Std (\pm) is the standard deviation.

MONTH	<i>Fritillaria</i> sp.		<i>Oikopleura</i> sp.		Total larvaceans		Total zooplankton	
	ind. m ⁻³	std (\pm)	ind. m ⁻³	std (\pm)	ind. m ⁻³	std (\pm)	ind. m ⁻³	std (\pm)
January	1.9	5.1	1.1	2.3	3.1	7.1	120.1	114.3
February	2.5	14.1	1.3	2.7	3.8	15.2	98.3	118.7
March	1.1	3.2	1.5	3.3	2.6	5	68.2	78.6
April	1	2.2	0.7	2.1	1.7	2.9	50.1	60.4
May	0.2	0.4	1	1.4	1.1	1.7	39.2	36.6
June	0	0	0	0	0	0		
July	0.1	0.3	1.3	2	1.4	2	37.5	29.9
August	0	0	0	0.1	0	0.1	1.3	1.8
September	0	0.2	0.3	0.6	0.3	0.6	17.6	19.4
October	0.5	1.2	0.6	2	1.1	2.5	24.8	26.9
November	3.6	6.9	1.2	2.2	4.8	7.8	117.2	86
December	3.9	10.9	1.7	2.8	5.6	11.8	137.4	149.4
Overall mean	2.1	8.2	1.3	2.7	3.4	9.3	93.3	110

Table 4.11 and Table 4.12 show annual and monthly variations for the Seasonal Ice Zone (SIZ). Inter-annual variations and seasonal variations were similar for larvaceans and total zooplankton.

Table 4.11. Seasonal Ice Zone (SIZ, south 62 °S) annual mean abundances for *Fritillaria* sp., *Oikopleura* sp., total larvaceans and total zooplankton. Std (\pm) is the standard deviation.

SEASON	<i>Fritillaria</i> sp.		<i>Oikopleura</i> sp.		Total larvaceans		Total zooplankton	
	ind. m ⁻³	std (\pm)	ind. m ⁻³	std (\pm)	ind. m ⁻³	std (\pm)	ind. m ⁻³	std (\pm)
1990 - 1991	0	0	0	0	0	0	25.9	125.8
1992 - 1993	0	0	0	0	0	0	0.9	1.5
1993 -1994	0	0	0	0	0	0	4.2	4.2
1995 - 1996	0	0	0	0	0	0		
1996 - 1997	0.4	0.6	1.6	1.3	1.9	1.5	27.7	14.8
1997 - 1998	0.1	0.5	0.1	0.3	0.2	0.7	9.4	14.7
1998 - 1999	1.4	1.7	0.3	0.5	1.6	2.1	24.7	21.9
1999 - 2000	1.3	3.6	1.1	2.5	2.4	4	59.2	69.8
2000 - 2001	0.1	0.3	0	0.2	0.1	0.3	8.4	14.8
2001 - 2002	61.1	118.2	0.4	1.1	61.5	118.1	251.4	399.3
2002 - 2003	1.4	1.6	0	0.1	1.4	1.6	42.3	31.1
2003 - 2004	0.4	1.1	14.8	25.7	15.2	25.4	108.6	144.5
2004 - 2005	0.9	3.1	0.1	0.4	1	3.1	21.8	24.7
2005 - 2006	0.5	1.1	1	1.7	1.5	2.2	72.9	95.3
2006 - 2007	1.3	1.6	0.1	0.3	1.4	1.6	84.8	52.3
2007- 2008	2.5	4.5	0.2	1	2.7	4.9	45.2	61.7
Overall mean	9.4	48.8	1.7	8.7	11.1	49.3	75	181.1

Table 4.12. Seasonal Ice Zone (SIZ, south 62 °S) monthly mean abundances for *Fritillaria* sp., *Oikopleura* sp., total larvaceans and total zooplankton. Std (\pm) is the standard deviation.

MONTH	<i>Fritillaria</i> sp.		<i>Oikopleura</i> sp.		Total larvaceans		Total zooplankton	
	ind. m ⁻³	std (\pm)	ind. m ⁻³	std (\pm)	ind. m ⁻³	std (\pm)	ind. m ⁻³	std (\pm)
January	10.5	50.1	0.2	1.1	10.7	50.1	72	216.9
February	17.8	70.5	4.2	14.8	22	71.1	113.2	228.8
March	1.7	3.4	0.7	1.8	2.4	3.8	50.2	73.8
April	1	1.3	0.4	0.9	1.4	1.4	20.2	26
May	0.5	0.9	0.4	0.6	0.9	1.2	33.3	15.1
June	0	0	0	0	0	0		
July	0.3	0.4	0.3	0.4	0.6	0.6	43.4	18.4
August	0	0	0	0	0	0	4.8	
September	0	0	0	0	0	0		
October	8.9	5	0.2	0.3	9.1	5.1	32.3	10.7
November	0	0	0	0	0	0		
December	0.6	1.7	0	0.1	0.6	1.8	27	34.3
Overall mean	9.4	48.8	1.7	8.7	11.1	49.3	75	181.1

Overall, larvaceans were found to consist on average 5.2% of the total zooplankton population. The highest percentage of larvaceans (13.4 %) occurred in 2001-2002 in the year that high abundances were recorded during the New Zealand *Tangora* voyage. Annual mean abundances of larvaceans and total zooplankton are graphed in Figure 4.22, and as percentages in Table 4.13.

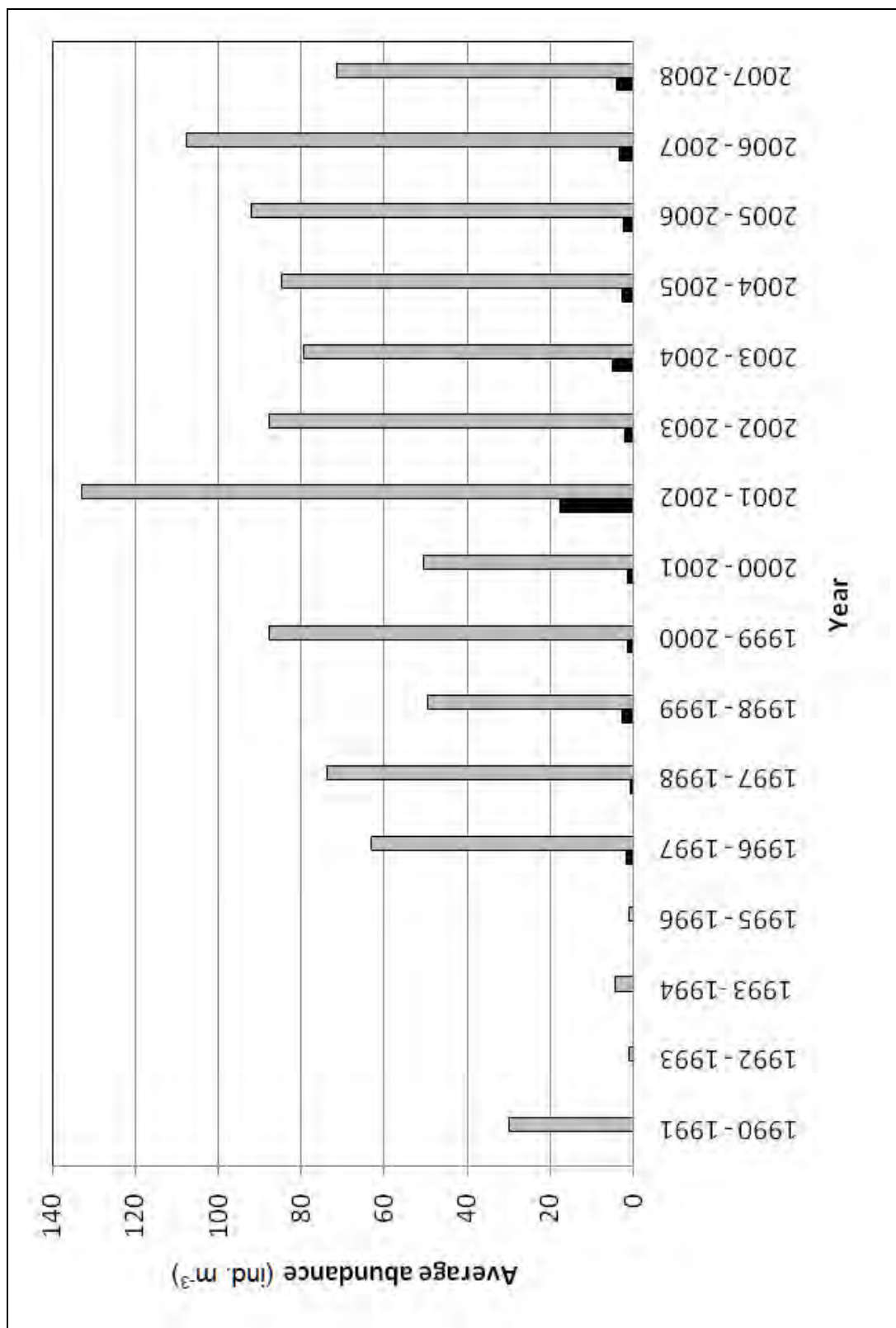


Figure 4.22. Annual comparison of average larvacean (black) abundances and total zooplankton (grey). Data from the SO-CPR Survey.

Table 4.13. Annual comparison of larvacean percentages compared to total zooplankton.

Year	%
1990 - 1991	0.0
1992 - 1993	0.0
1993 -1994	0.0
1995 - 1996	0.0
1996 - 1997	2.7
1997 - 1998	1.2
1998 - 1999	5.4
1999 - 2000	1.8
2000 - 2001	3.2
2001 - 2002	13.4
2002 - 2003	2.5
2003 - 2004	6.6
2004 - 2005	3.4
2005 - 2006	2.7
2006 - 2007	3.3
2007- 2008	5.9
Overall mean	5.2

By graphing the monthly mean abundance of larvaceans against total zooplankton (Figure 4.23 and 4.24), a two month lag for seasonality can be seen (maxima in December and February). The monthly mean abundances of larvaceans, as a percentage of total zooplankton (Table 4.14), show a higher ratio in both spring (October) and late summer (February). The highest abundance of larvaceans occurred in February. In this month, larvaceans formed 8.8 % of the total zooplankton population (Table 4.14).

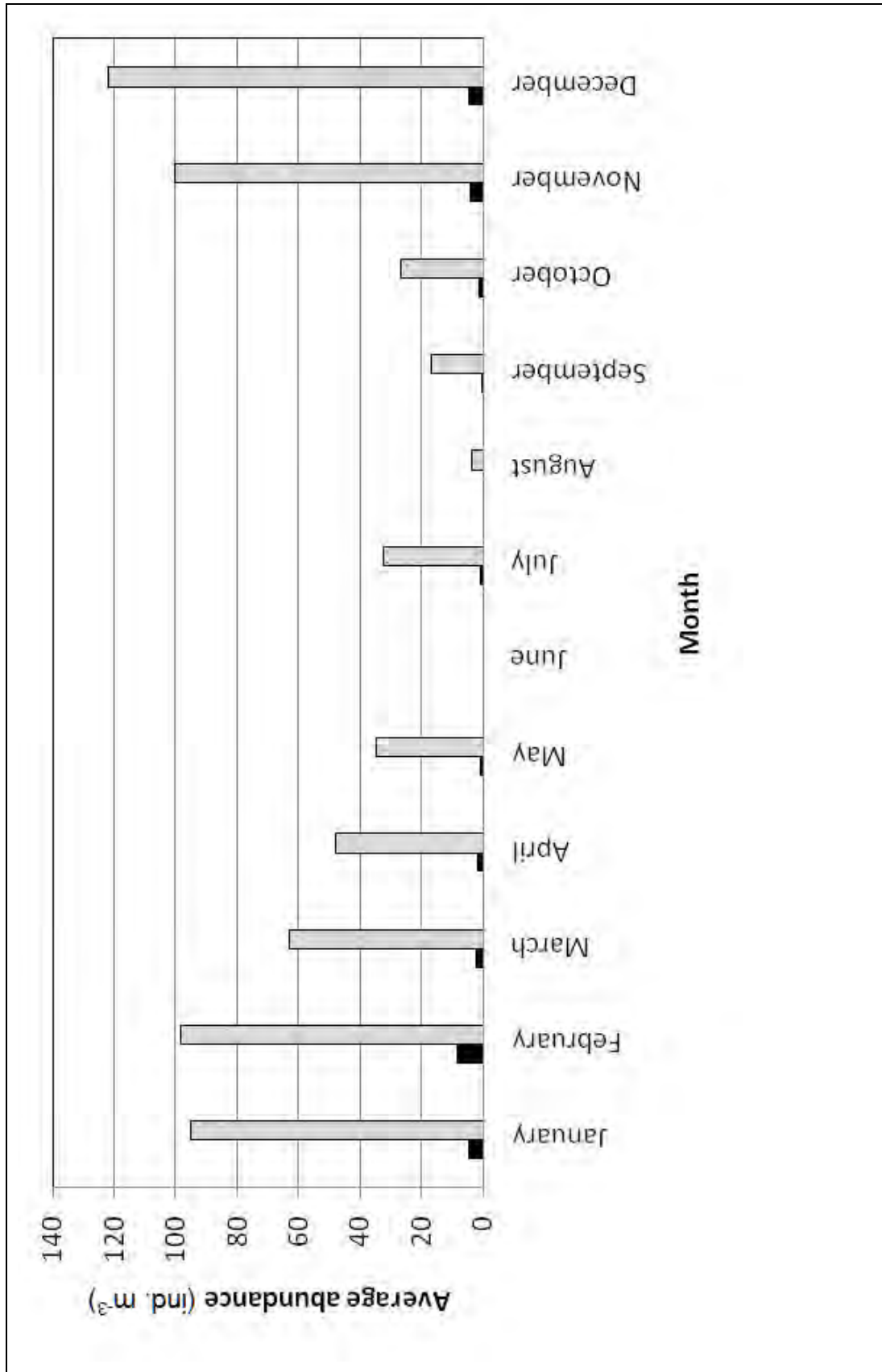


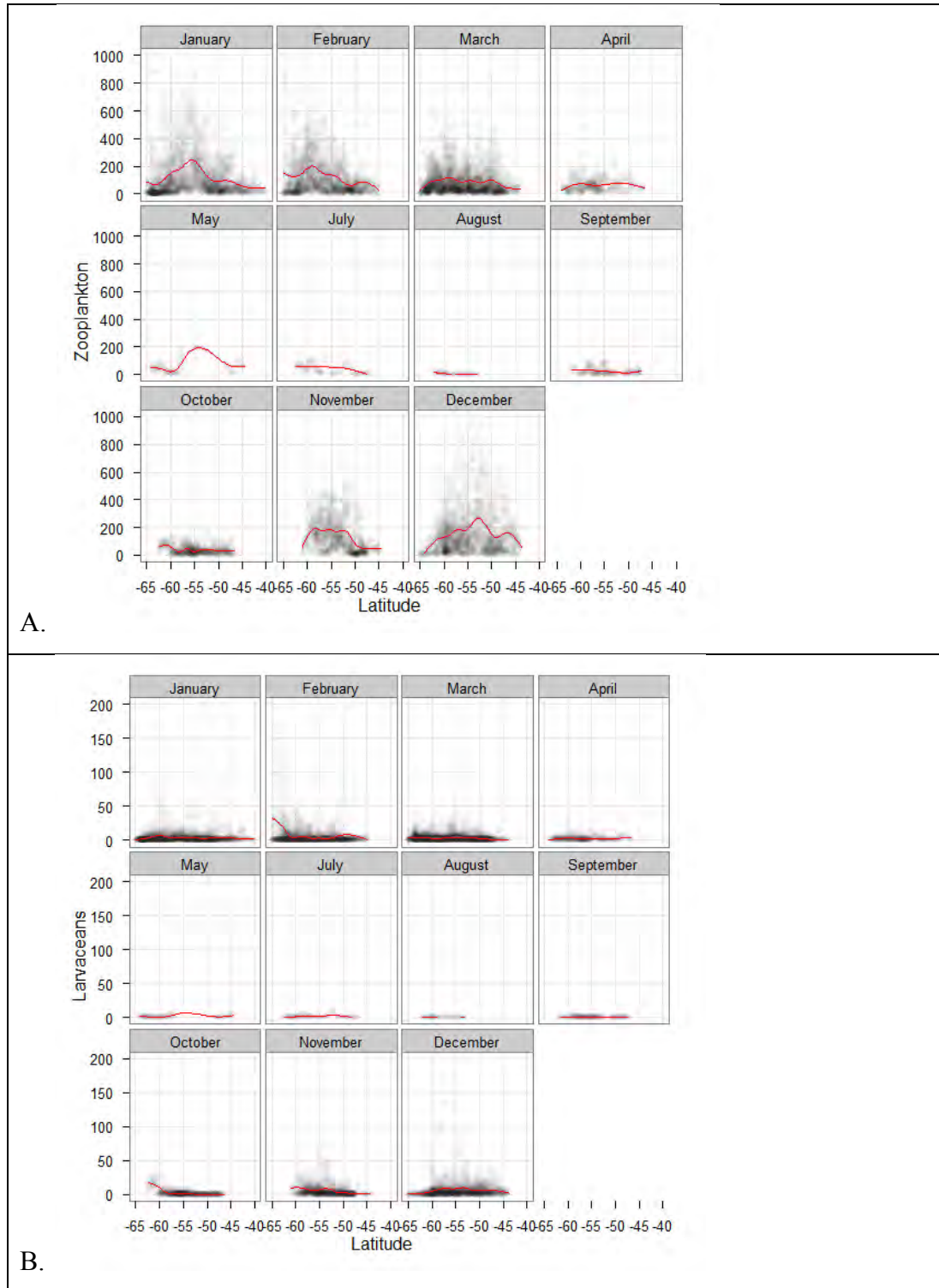
Figure 4.23. Monthly comparison of average larvacean (black) abundances and total zooplankton (white). Data from the SO-CPR Survey.

Table 4.14. Monthly seasonal comparison of larvacean percentages compared to total zooplankton.

Month	%
January	4.9
February	8.8
March	3.7
April	3.8
May	2.6
June	0.0
July	3.1
August	0.0
September	1.8
October	6.0
November	4.1
December	4.1
Overall mean	5.2

The visualisation of the monthly abundances of total zooplankton (Figure 4.24A), total larvacean (Figure 4.24B), *Oikopleura* sp. (Figure 4.24C) and *Fritillaria* sp. (Figure 4.24D) shows that all zooplankton abundances are higher in the austral summer months and larvaceans occur further south (down to -70°S) in February. The highest total zooplankton abundance occurred in December. Seasonality of larvaceans appeared to lag one month behind that of total zooplankton. Abundances of zooplankton declined during autumn, reaching lowest numbers in winter. Larvacean numbers began to increase in October (spring) through to November and December (late spring). Both larvacean species showed the same seasonal pattern though *Fritillaria* sp. occurred further south than *Oikopleura* sp. The two peaks that are visible in the larvacean graphs for January and February account for only 0.4% of the data points.

4. Large-scale distribution patterns determined from the CPR



4. Large-scale distribution patterns determined from the CPR

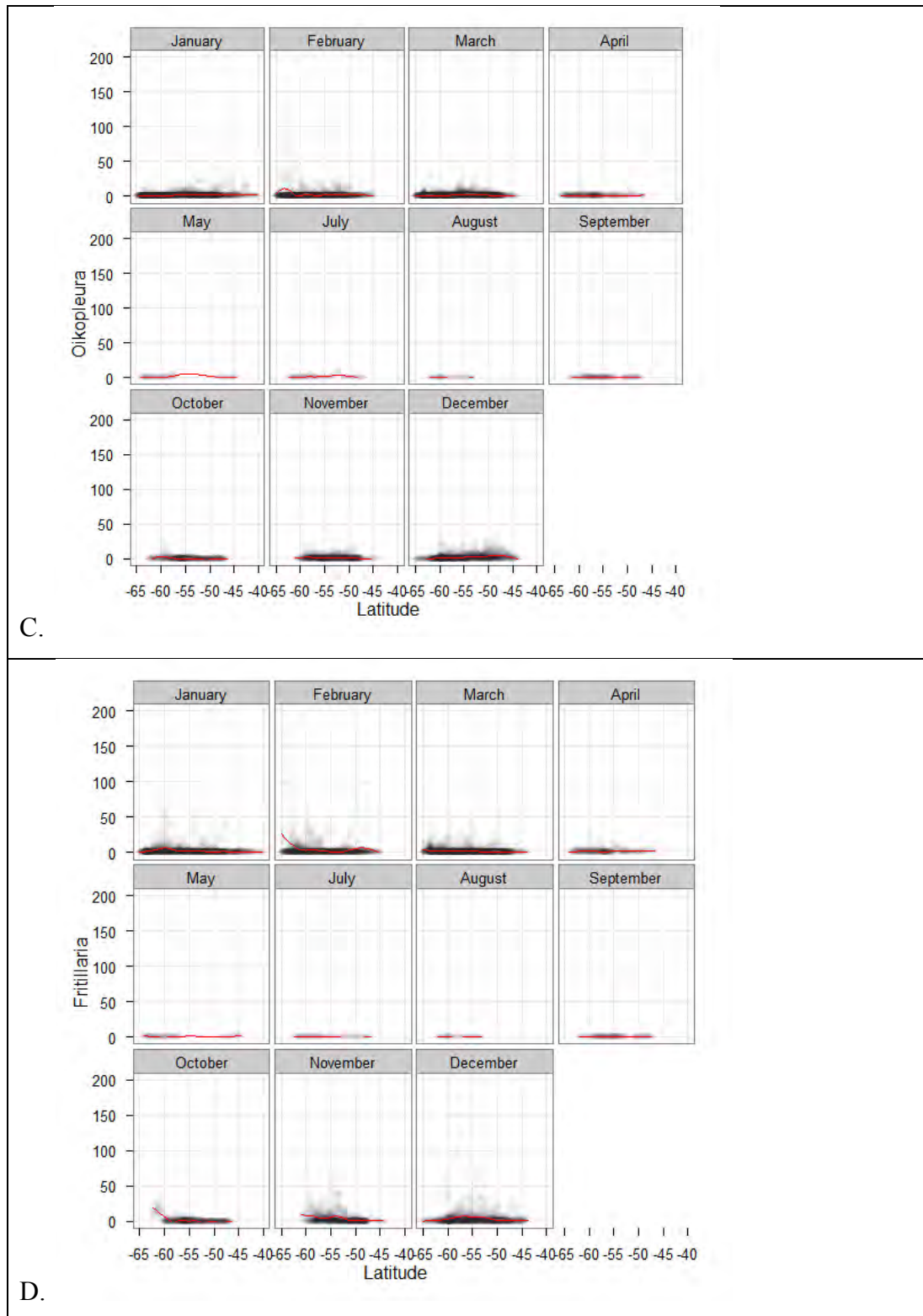


Figure 4.24. Visualisation of the monthly SO-CPR Survey (1991 – 2008) abundance (count per 5Nm) data for A) total zooplankton, B) total larvacean, C) *Oikopleura* sp. and D) *Fritillaria* sp. compared to latitude (°South). Note there is no data for June.

4.5.5 Southern Ocean physical parameters

Underway data obtained during SO-CPR Surveys was tabled according to season (Table 4.15), month (Table 4.16) and Southern Ocean zone (Table 4.17).

Table 4.15. Seasonal underway data from the SO-CPR Survey dataset 1990 – 2008

SEASON	Fluorescence		Salinity (psu)		Temperature (°C)		PAR ($\mu\text{Em}^{-2}\text{s}^{-1}$)	
	mean	std (\pm)	mean	std (\pm)	mean	std (\pm)	mean	std (\pm)
Survey period	11.4	27.5	33.7	2.5	4.1	3.4	267.6	385.1
1990 - 1991	37.9	31.1	33.6	0.2	1.1	1.1	162.3	187.6
1992 - 1993	298.2	121.4	33.6	0.3	0.2	0.1	394.7	365.5
1993 -1994	91.7	86.8	34.2	0.1	0.4	0.4	160.8	234.2
1995 - 1996			33.8	0.0	1.3	0.9	51.5	63.1
1996 - 1997					3.3	1.7	143.6	217.5
1997 - 1998	39.0	24.4	33.8	0.2	2.5	2.4	316.2	452.7
1998 - 1999	49.6	38.7	33.8	0.1	2.5	2.4	116.4	200.4
1999 - 2000	10.5	12.7	33.9	0.2	2.9	2.8	143.8	214.4
2000 - 2001	8.2	6.4	33.7	0.3	4.4	3.0	217.5	283.6
2001 - 2002	6.5	7.3	32.0	7.6	4.9	3.5	222.1	283.4
2002 - 2003	7.2	7.1	33.9	0.8	4.3	3.5	312.3	404.6
2003 - 2004	21.0	42.0	33.7	0.4	3.5	3.2	265.7	407.6
2004 - 2005	2.0	2.0	33.7	1.1	4.2	3.3	285.7	403.6
2005 - 2006	3.5	2.9	33.9	0.3	4.7	3.5	355.0	457.3
2006 - 2007	23.4	59.3	33.8	0.7	4.6	3.3	287.6	379.2
2007- 2008	2.3	2.1	34.0	0.3	5.1	3.8	297.5	427.9

Table 4.16. Monthly underway data from the SO-CPR Survey dataset 1990 – 2008. Std (\pm) is the standard deviation.

MONTH	Fluorescence		Salinity (psu)		Temperature ($^{\circ}$ C)		PAR (μ Em $^{-2}$ s $^{-1}$)	
	mean	std (\pm)	mean	std (\pm)	mean	std (\pm)	mean	std (\pm)
Annual	11.4	27.5	33.7	2.5	4.1	3.4	267.6	385.1
January	8.2	11.5	33.9	0.6	4.6	3.8	312.4	419.2
February	13.4	31.8	32.8	5.6	4.5	3.3	290.9	410.4
March	6.7	16.2	33.7	0.6	4.9	3.4	193.1	285.8
April	23.5	25.6	33.9	0.1	2.2	2.2	78.4	155.5
May	50.4	27.6	33.9	0.1	1.8	2.7	20.1	52.7
June								
July	11.8	4.0	34.0	0.4	3.1	4.0	34.9	81.0
August	12.3	0.7	33.9	0.1	0.6	1.3	42.4	63.2
September	13.9	18.6	33.9	0.4	3.6	3.1	149.6	256.1
October	31.4	66.7	34.0	0.3	3.7	3.1	213.6	310.2
November	7.7	11.9	34.0	1.3	3.4	3.1	365.1	457.1
December	10.4	29.8	33.9	0.2	3.6	3.0	349.5	424.9

Table 4.17. Southern Ocean zone underway data from the SO-CPR Survey dataset 1990 – 2008. Std (\pm) is the standard deviation.

CPR	Fluorescence		Salinity (psu)		Temperature ($^{\circ}$ C)		PAR (μ Em $^{-2}$ s $^{-1}$)	
	mean	std (\pm)	mean	std (\pm)	mean	std (\pm)	mean	std (\pm)
Southern Ocean	11.4	27.5	33.7	2.5	4.1	3.4	267.6	385.1
SIZ	19.1	41.8	32.5	6.1	0.9	1.2	215.0	288.1
POOZ	9.2	20.6	33.7	5.7	3.8	1.8	274.5	381.1
SAZ	11.0	33.1	34.3	0.4	10.6	3.0	330.7	506.8

Pearson's r correlations between SO-CPR Survey larvacean abundances (25,791 data points) and latitude, longitude, and underway data (PAR, fluorescence, water temperature and salinity) found no significant relationships (Table 4.18).

However, longitude was close to being significant.

Table 4.18. Pearson's r correlations between larvacean abundances and environmental parameters. UW = underway data, and **Bold** indicates a significant relationship (ns = not significant), $\alpha=0.05(2)$. Degrees of freedom (df) for are 1000 data points or ∞ .

Parameter	r	d	p
Continuous Plankton Recorder (CPR) (<i>critical $r = 0.062$</i>)			
Latitude	0.04	1000	ns
Longitude	0.06	1000	ns
UW - PAR	0.00	1000	ns
UW - Fluorescence	0.04	1000	ns
UW - Temperature	0.02	1000	ns
UW - Salinity	0.04	1000	ns

There was no significant relationship between the monthly average sea ice extent and abundances for total zooplankton and larvaceans. Though when the monthly average abundance (count per 5Nm) for total zooplankton (Figure 4.25A) and for total larvaceans (Figure 4.25B) were compared to the difference in latitude between sample location and the monthly average sea ice extent (diffSIcelat) it can be seen that zooplankton and larvaceans occur at and amongst the sea ice (when the latitudinal differences are in the negatives) in the summer months. This may be due to sampling as the CPR is not deployed amongst dense sea ice.

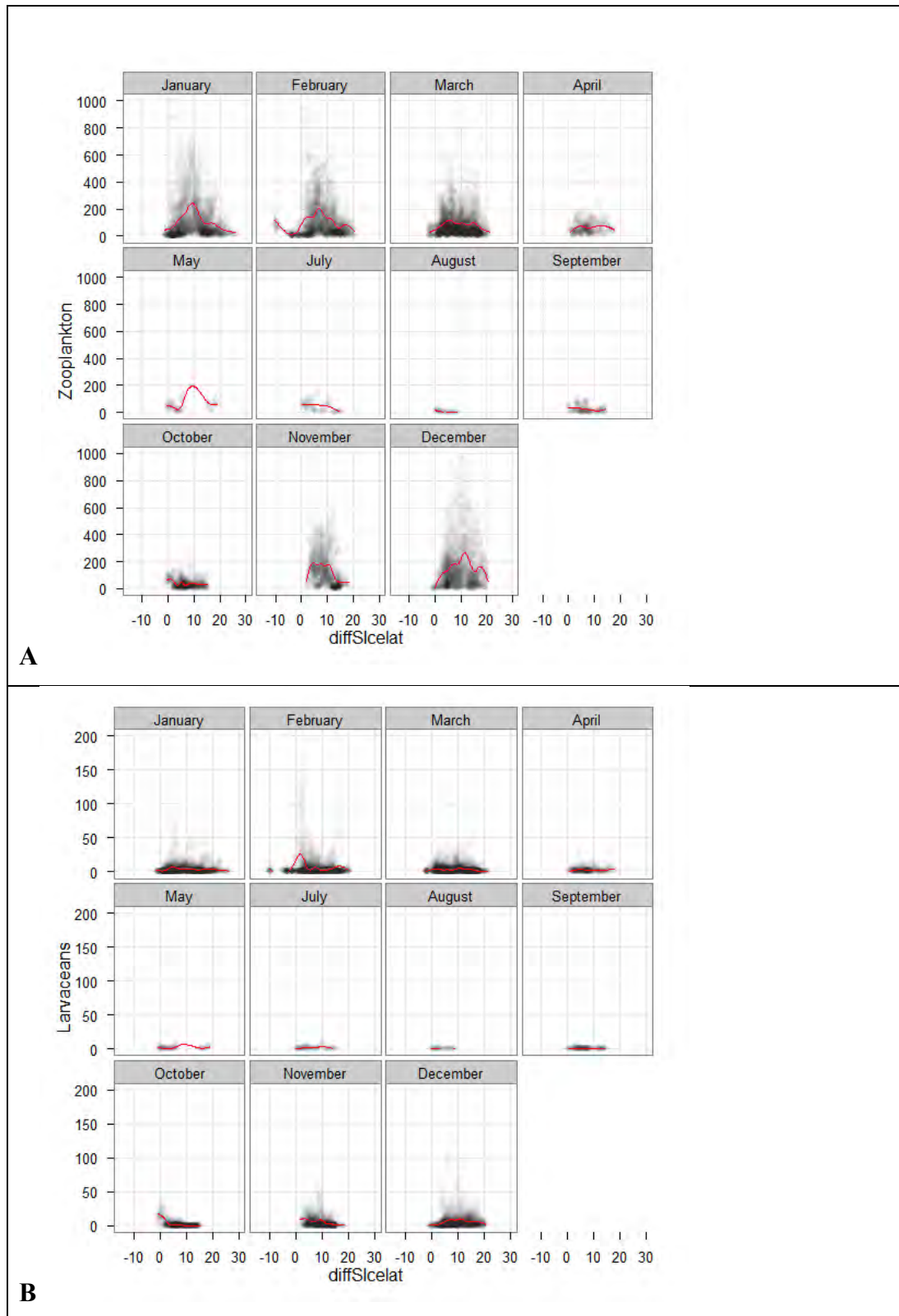


Figure 4.25. A) ggplot of the monthly average abundance (count per 5Nm) for total zooplankton compared to the difference in latitude between sample location and the sea ice extent (diffSIcelat). B) ggplot of the monthly average abundance (count per 5Nm) for total larvaceans compared to the difference in latitude between sample location and the sea ice extent (diffSIcelat). Transparency of both plots set at 0.01 and showing a smoothed mean (red line).

4.5.6 Summary of larvacean distribution and abundance in the Southern Ocean

The SO-CPR database showed that between 1990 and 2008, the mean abundance of *Oikopleura* sp. and *Fritillaria* sp. in the Southern Ocean was 1.9 ± 7.6 and 4.4 ± 28.2 ind. m^{-3} , respectively. Larvacean mean abundances from 1996 to 2008 were compared to total zooplankton, which had a mean abundance of 121.7 ± 171.6 ind. m^{-3} (Figure 4.22).

4.5.7 Larvacean CPR database 1991 – 2008 distribution and abundance according to Generalized Additive Mixed Models (GAMM)

Linear statistic models make the assumption that the response variables have a normal distribution and the predictor depends linearly on the parameters. They model univariate responses as the sum of linear terms and have a zero mean random error term that is, the data points, when measurements are repeated several times they are scattered about the true value. Generalized Additive Mixed Models (GAMM) combine Linear Mixed Effect models (LME) and an extension of Generalized Linear Models (GLMs), called Generalized Additive Models (GAM) (Wood, 2006).

The standard linear model (LM) assumes the response y is normally distributed about its mean μ with constant variance σ^2

$$y \sim N(\mu, \sigma^2)$$

and represents the mean as a linear combination of predictor variables x_1, x_2, \dots, x_m

$$\mu = \beta_0 + \beta_1 x_1 + \beta_2 x_2 + \dots + \beta_m x_m$$

where the β_i are regression coefficients to be estimated.

The generalized linear model (GLM) extends the general linear model in two important ways (McCullagh and Nelder 1989). The generalized linear model assumes the response is distributed about its mean

$$y \sim F(\mu)$$

according to a distribution F that is an exponential family. The predictors enter the model through the linear predictor η

$$\eta = \beta_0 + \beta_1 x_1 + \beta_2 x_2 + \cdots + \beta_m x_m$$

which is in turn related to the mean through a monotonic link function l ,

$$l(\mu) = \eta = \beta_0 + \beta_1 x_1 + \beta_2 x_2 + \cdots + \beta_m x_m.$$

Inference in the general linear model is based on the theory of the Normal and F distributions, and the associated hypothesis tests and confidence intervals are exact provided all model assumptions are met. Inference in the generalized linear model is based on the theory of maximum likelihood, and the associated hypothesis test and confidence intervals are only approximate.

In a generalized additive model (GAM) the response is again assumed to be distributed about its mean according to an exponential family F distribution

$$y \sim F(\mu)$$

but the predictors enter the model through a relation of the form

$$l(\mu) = \eta = f_1(x_1) + f_2(x_2) + \cdots + f_m(x_m)$$

where the f_i are arbitrary smooth functions of their arguments (Wood 2006).

Where a generalized linear model estimates the regression coefficients β_i , a generalized additive model estimates the smooth transformations f_i . The f_i are estimated by smoothing partial residuals, and have no specific functional form. So where the results of a GLM is represented as a table of coefficients, the results of a GAM must be represented as a sequence of plots of the estimated transformations f_i . The level of smoothing imposed is at the discretion of the analyst, but an appropriate level of smoothing can be determined by cross validation (Wood 2006).

In a GAM, inferences are based on the theory of maximum likelihood, and so are again only approximate, but are also conditional of the level of smoothing imposed.

The advantage of GAMs is that they can easily represent arbitrarily complex relationships between the response and individual predictors. The disadvantage is

that GAMs assume the effects of the predictors are additive, it is not possible to represent interactions between predictors.

In a mixed model, the linear predictor itself may contain one or more normally distributed random effects

$$\eta = \beta_0 + \beta_1 x_1 + \beta_2 x_2 + \cdots + \beta_m x_m + E$$

$$E \sim N(0, \sigma_E^2),$$

that are intended to represent the individual variability of sampling units in the design. Random effects may be incorporated into linear models, generalized linear models and generalized additive models. Introducing random effects to a linear model (LM) yields a linear mixed model, introducing random effects to a generalized linear model (GLM) results in a generalized linear mixed model (GLMM), and so on.

GAMM as a form of predictive multiple regression analysis is an appropriate analysis for the SO-CPR Survey database, when determining the relationship between the larvacean abundances and other parameters. This is because GAMMs fit smooth non-linear trends of abundance with physical variables (such as water temperature) in the marine ecosystem. GAMMs also simultaneously incorporates a number of non-physical variables as co-predictor variables such as latitude (by combining LMEs and GAMs). The theory of GAMMs is further explained in Appendix VI.

As in surveys of this nature with a response such as abundance counts to a number of co-varying predictor variables, fitting a multiple regression, or its extension to GAMMs and demonstrating the predictive model using partial plots and plots of observed and fitted values is a useful statistical practice. The severe limitations in inferences that can be drawn by plotting the response on each predictor variable one at a time and fitting one variable at a time need to be recognised in the case of co-varying predictors because these naive plots can show spurious trends or alternatively, have their real trends masked because of confounding relationships between parameters that are not included. The partial plots overcome this by conditioning on all other predictors while plotting the trend of the response with the remaining predictor and repeating this for each predictor variable in turn.

The difficulty for inference even with partial plots is determining which predictors are "driving" the abundance and which are merely correlated with the main driving variables.

Methods

GAMMs were applied to the CPR database using the statistical program 'R' and the *mgcv* package to determine if there was a relationship between each of the total zooplankton and larvacean abundances (counts per 5 Nm) and season, month and latitude and longitude and the physical parameters of fluorescence, salinity (psu), temperature (°C) and PAR ($\mu\text{Em}^{-2}\text{s}^{-1}$) from the underway data that was logged at one minute intervals by shipboard meters. The R code for *mgcv* used for the SO-CPR Survey data is included in Appendix VII.

The GAMM equation used for the total zooplankton and larvaceans was:

Predicted abundance of total zooplankton or larvaceans =

$$\exp(\hat{P}_L) \exp(\sum \hat{P}_{i, i \neq L} \text{ other} + \text{intercept})$$

Parameters are:

Season, Month, Latitude, Fluorescence,
Water temperature (°C) and PAR ($\mu\text{Em}^{-2}\text{s}^{-1}$)

The GAMM model output includes F values, p values and estimated degrees of freedom and the GAMM model output that plots the splines. The output and splines are explained in detail in Appendix VI. The y-axis is an ordinate scale of the variable being predicted. In this study, this is the abundance of total zooplankton or larvaceans and the x-axis is the variable that is being used as the predictor. For total zooplankton this is a GAMM ordinate scale between -4 and 4 and for larvaceans is between -8 and 10. The GAMM output was compared to scatter plots of the SO-CPR Survey data that show the x-axis as the parameter that is being used as the predictor and the y-axis is the observed abundance of the total zooplankton or larvaceans. When comparing the GAMM output to the scatter

plots the comparison needs to consider that GAMM includes all variables simultaneously while the scatter plots compare each parameter singularly and may be severely confounded by effects from another variable that correlate with the single variable plotted (e.g. temperature with latitude).

Results

To compare the SO-CPR Survey GAMM output and observations the fitted GAMM on top of total abundance (for each of total zooplankton (Figure 4.26 a) and total larvacean (Figure 4.26 b)) vs fitted GAMM values was plotted and is shown by the red points which form a red line. The green points are from the fitted loess smoother using the GAMM fitted value as the x-variable and the R-function loess. A loess smoother is a naive statistical curve which is independent of the individual GAMM components. The marginal R^2 values for each of total zooplankton (Figure 4.26 a) and total larvacean (Figure 4.26 b) are low though still significantly different at 0.0405 and 0.0098, respectively. The loess is naive in that (i) it is a simple least squares fit (not maximum quasi-likelihood as is the case for the GAMM fit assuming over-dispersed Poisson counts), and (ii) it does not take into account the random data effects as the GAMM does. However, the red and green points (lines) showed that the GAMM did have some predictive power but also that there was a huge amount of residual variation.

The single-variable-at-a time graphs (scatterplots) and R^2 values that were completed to compare with the GAMM model are only slightly more informative than the single pair wise *Pearson r* correlations, presented in detail in section 4.5.5.

Zooplankton CPR 1991-2008 analyses for the GAMM fitted values compared to actual abundance (counts per 5 Nm) (Figure 4.26) are shown for total zooplankton (A) and total larvaceans (B). This plot shows that the greater concentration of data occurred when the total zooplankton (81.5%) and larvaceans (99.6%) abundance were less than 200 counts per 5 Nm. Thus trends are present but are not strong due to the high variability in the data. The predictors are very limited in

the ability to predict abundances at the 5 Nm level relative to the highly localised concentrations, which occur randomly and are difficult to predict.

Total zooplankton (Figure 4.26a) and larvacean (Figure 4.26b) CPR 1991-2008 analyses for the total abundance GAMM fitted compared to actual larvacean abundance (counts per 5 Nm) shows that trends are present but due to the high variability in the data are not as statistically significant compared to the GAMMs for total zooplankton. The predictors are very coarse and the zooplankton have localised high concentrations due to random occurrences that are not yet understood. The estimated transect-level standard deviation for the Poisson GAMM (i.e. on the log scale of the linear predictor obtained from the LME) was 1.05. The Poisson over-dispersion parameter, ϕ , was estimated 59.74. The number of observations was 22, 165. There was therefore considerable variation (standard deviation) about predicted values. For example for a segment predicted to have a mean abundance of 100, the contribution to the variance of the random transect, σ , would be $\sim 1.054^2 \times 100^2 = 1.111 \times 10^4$, while that for the random segment would be $59.74 \times 100 = 0.597 \times 10^4$. Overall the standard deviation for a random segment (irrespective of transect) was 100 ± 130.7 .

Table 4.19 lists the approximate significance of smooth terms (splines) for GAMM analysis of total zooplankton abundances from the CPR database 1990-91 to 2008. The higher the F value (significance value) the more important the predictor value is, thus the zooplankton abundances from the CPR Survey could be predicted by using fluorescence ($F = 295.3$), water temperature ($F = 40.1$) and latitude ($F = 23.0$) and to a lesser degree the season ($F = 15.7$) and month ($F = 7.6$). Fluorescence is a variable that derives from highly-localised abundances of phytoplankton and in itself is difficult to predict from physical variables such as latitude and water temperature.

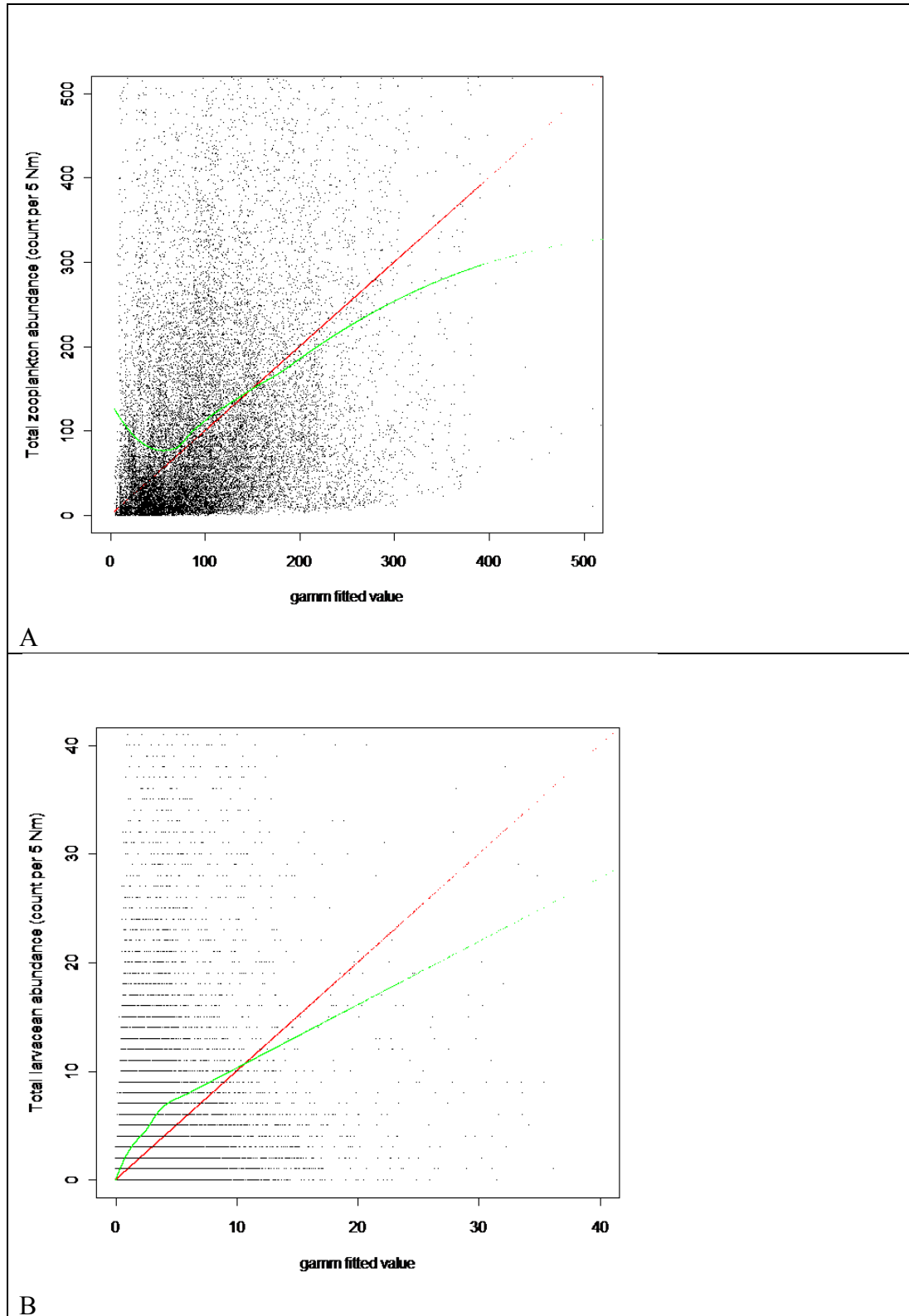


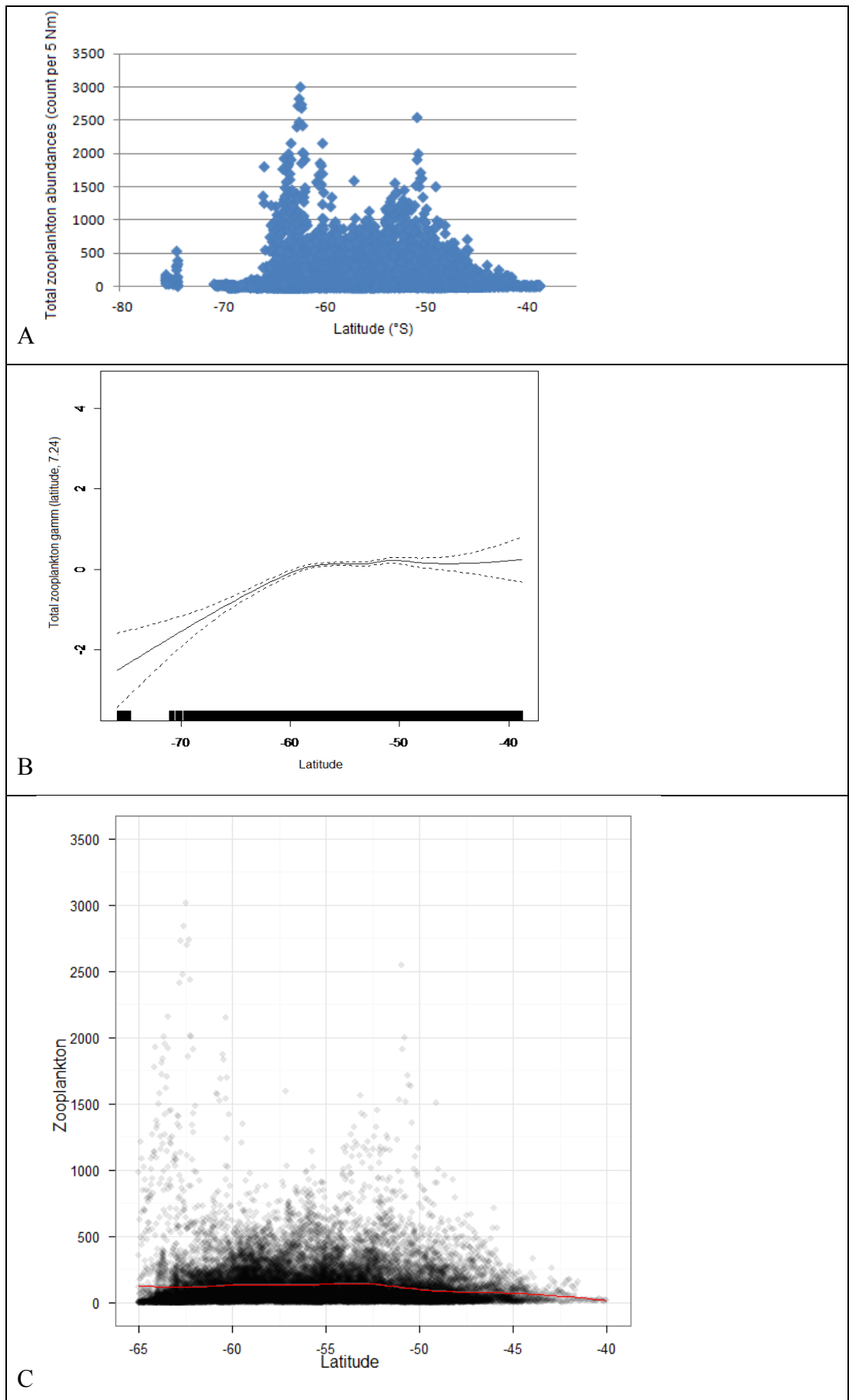
Figure 4.26. A plot of the fitted GAMM on top of total abundance (for each of total zooplankton (A) (marginal R^2 0.0405 $\sigma = 1.054$ $\phi = 59.741$) and total larvacean (B) (marginal R^2 0.0098 $\sigma = 1.432$ $\phi = 4.268$) vs fitted GAMM values shown by the red points which form a line. The green points are from the fitted loess smoother (which is independent of the individual GAMM components) using the GAMM fitted value as the x-variable and the R-function loess).

Table 4.19. Approximate significance of smooth terms for GAMM analysis of total zooplankton abundances from the CPR database 1990-91 to 2008 (n = 25,791).

	Estimated degrees of freedom	F value	p-value	significance	Figure for GAMM plots
Latitude	7.2	23.0	<2e-16	0.001	4.25
Water temperature	8.3	40.1	<2e-16	0.001	4.26
Fluorescence	9.0	295.3	<2e-16	0.001	4.27
Month	6.3	7.6	3.31 e-11	0.001	4.28
Season	2.8	15.7	4.59 e-09	0.001	4.29

The visualisation of the mean SO-CPR Survey data for total zooplankton abundances compared to latitude (Figure 4.27A) shows that zooplankton are likely to be found in higher abundances between 50 and 60°S in the POOZ and at 65°S in the SIZ. This is supported by the GAMM splines (Figure 4.27B) that are plotted with a 95% confidence band and show that zooplankton prefer latitudes between 50 and 65°S. The lines at the base of the figure show where data points for latitude and total zooplankton abundance occur. The gap south of 70°S is due to the CPR not being deployed amongst the sea ice. The two peaks of total zooplankton abundances that are greater than 1000 counts per 5 Nm represent 0.5% of the SO-CPR Survey data points. When the extreme 0.5% of data are removed (Figure 4.27D) the smoothed mean is reduced and the peaks no longer dominate the ggplots.

4. Large-scale distribution patterns determined from the CPR



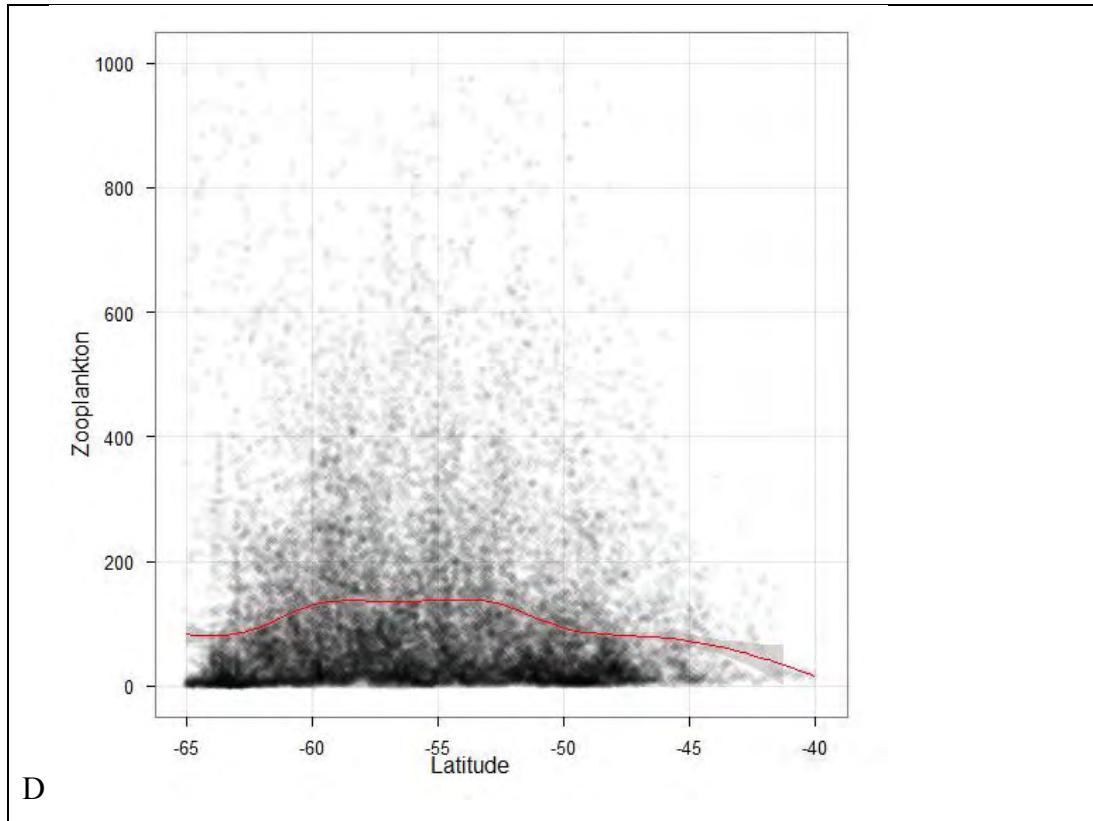


Figure 4.27. A) Visualisation of the SO-CPR Survey data (1991-2008). Total zooplankton abundance (counts per 5 Nm) compared to latitude (R^2 0.0014). B) GAMM output for zooplankton CPR 1991-2008 analyses Total zooplankton (ordinate scale estimated degrees of freedom (edf)) GAMM and latitude ($^{\circ}$ South). C) ggplot of total zooplankton abundance (0 – 3500 counts per 5 Nm) compared to latitude ($^{\circ}$ S). Transparency of data points set at 0.01 and showing a smoothed mean (red line). D) ggplot of total zooplankton abundance (0 – 1000 counts per 5 Nm) compared to latitude ($^{\circ}$ S). Transparency of data points set at 0.01 and showing a smoothed mean (red line).

The visualisation of the SO-CPR Survey data for total zooplankton abundances compared to water temperature (Figure 4.28 A and C) shows that the higher abundances of zooplankton occur in water temperatures between 0 and 5 $^{\circ}$ C and between 8 and 14 $^{\circ}$ C. This temperature preference is also shown in the total zooplankton GAMM and water temperature plot (Figure 4.28B).

The visualisation of the SO-CPR Survey data for total zooplankton abundances compared to fluorescence (Figure 4.29 A and C) shows that the majority of zooplankton occur when the fluorescence is between 0 and 5 and the highest abundance of zooplankton occur when the fluorescence is low. Fluorescence had the highest F value, thus as a predictor it is a statistically significant predictor of zooplankton abundances. Figure 4.29B shows what appears to be a threshold level

of the fluorescence of around 10-20 units below which abundance of zooplankton very rapidly declines to very low levels. Above this threshold region of fluorescence there is a gradual increase in zooplankton abundances in the GAMM output.

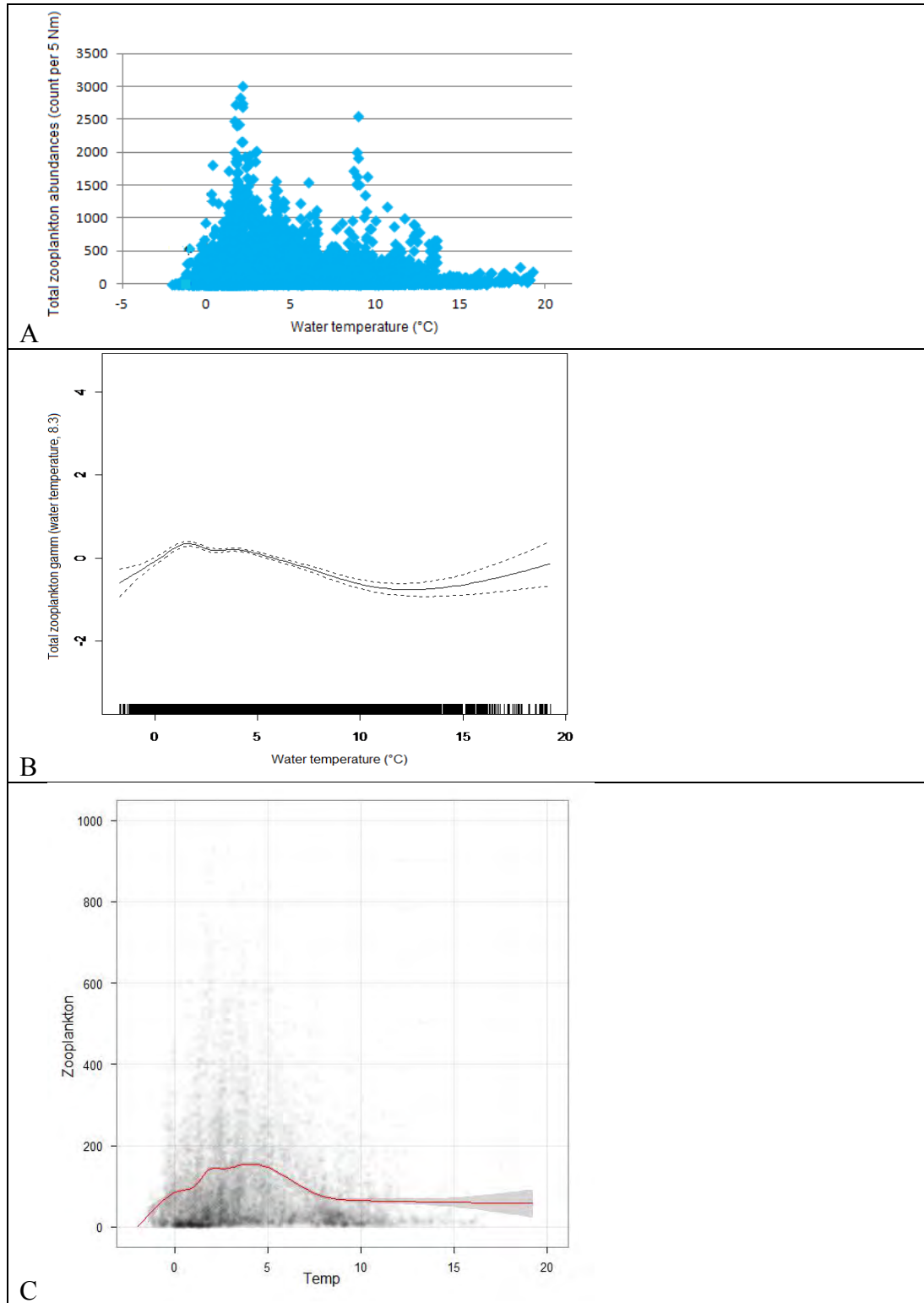


Figure 4.28. A) Visualisation of the SO-CPR Survey data (1991-2008). Total zooplankton abundance (counts per 5 Nm) compared to water temperature (°C) (R^2 0.0069). B) GAMM output for zooplankton CPR 1991-2008 analyses Total zooplankton (ordinate scale (edf)) GAMM water temperature (°C). C) ggplot of total zooplankton abundance (0 – 1000 counts per 5 Nm) compared to water temperature (°C). Transparency of data points set at 0.01 and showing a smoothed mean (red line).

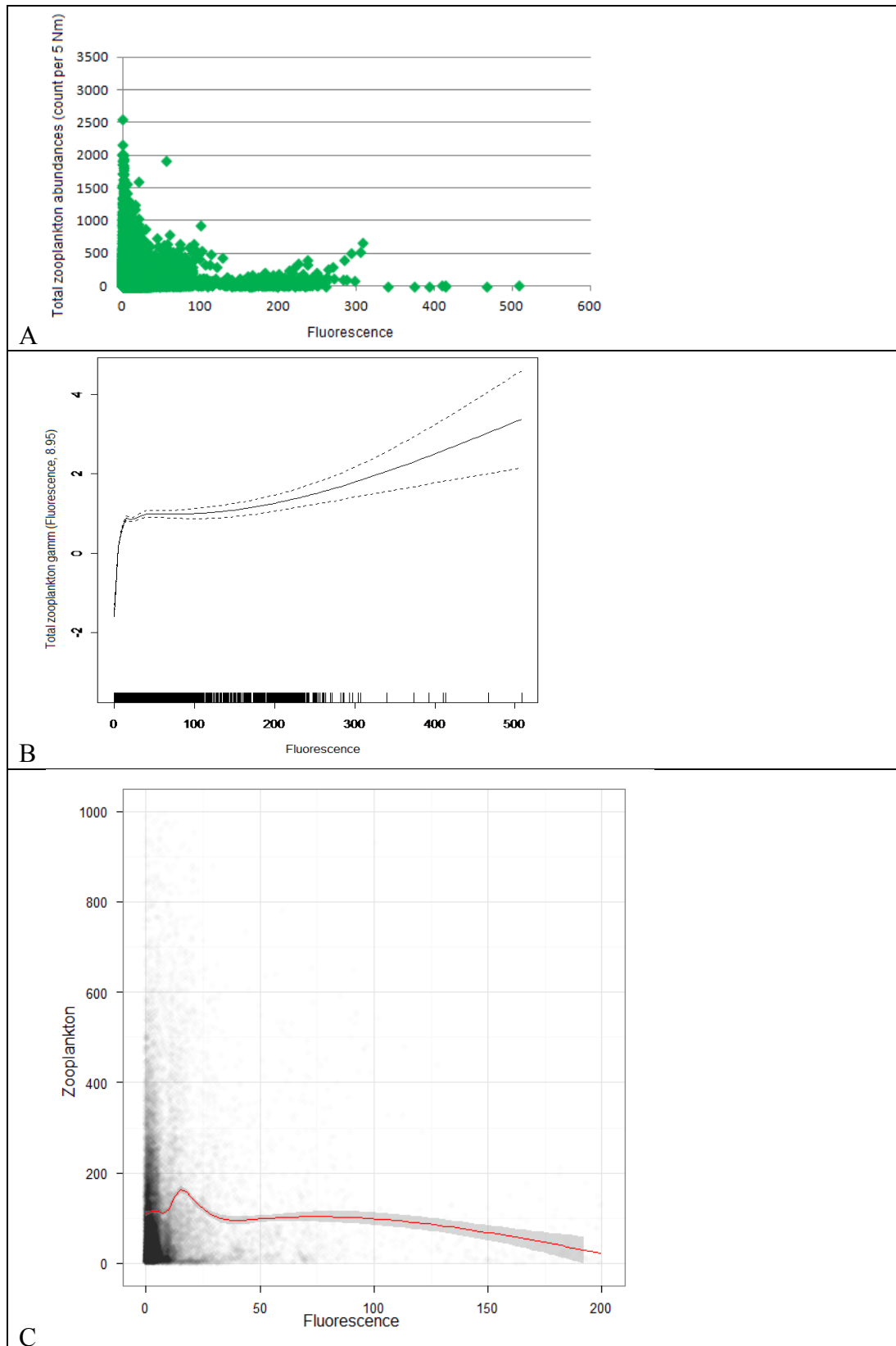


Figure 4.29. A) Visualisation of the SO-CPR Survey data (1991-2008). Total zooplankton abundance (counts per 5 Nm) compared to fluorescence (R^2 0.0015). B) GAMM output for zooplankton CPR 1991-2008 analyses Total zooplankton (ordinate scale (edf) GAMM fluorescence. C) ggplot of total zooplankton abundance (0 – 1000 counts per 5 Nm) compared to fluorescence. Transparency of data points set at 0.01 and showing a smoothed mean (red line).

The scatterplot and ggplot for salinity (Figure 4.30 A and B) shows that zooplanktons highest abundances occurred when salinity was between 33.5 and 34.0 psu. There was no GAMM output as the significance level of this visual pattern was not statistically significant.

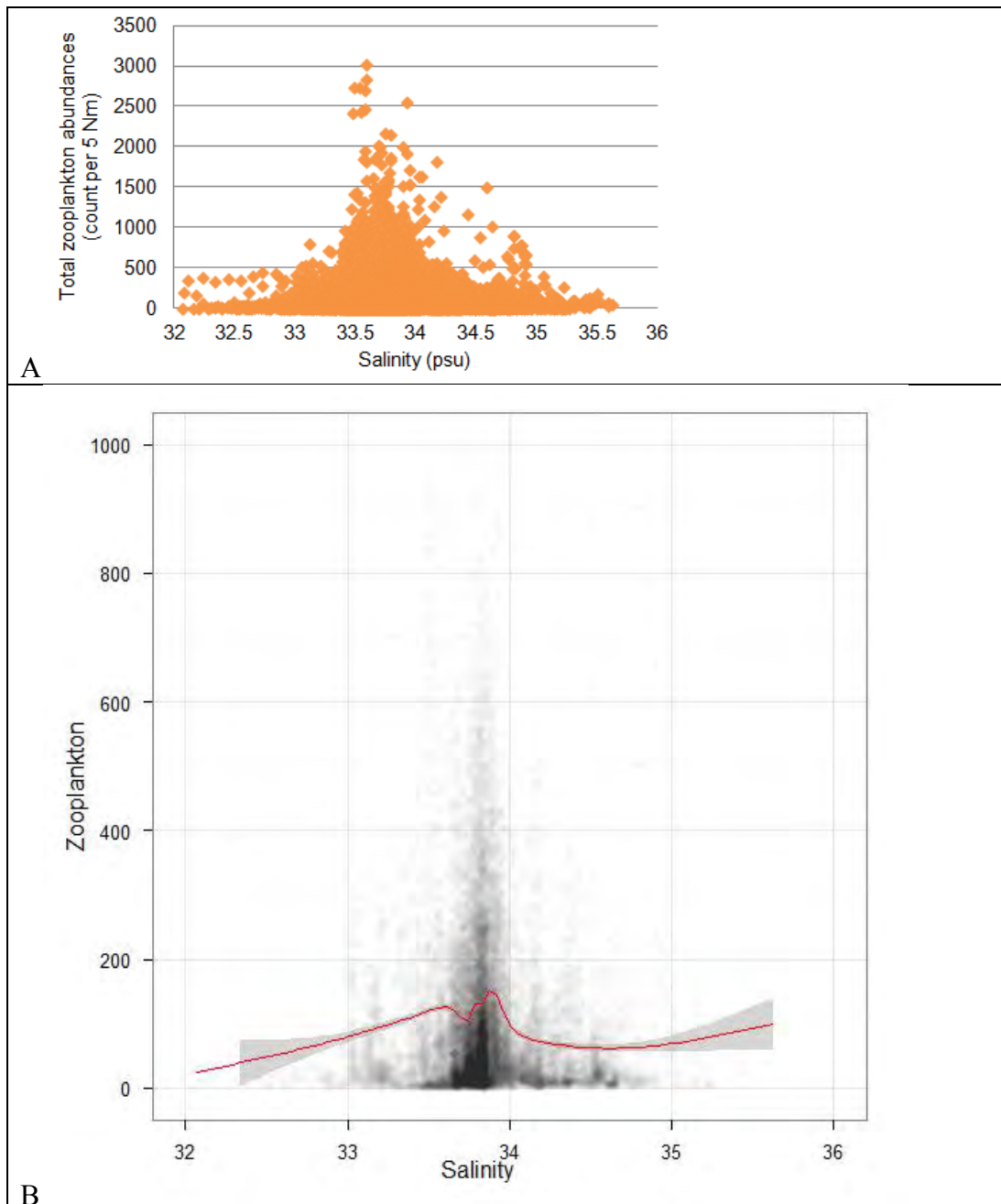


Figure 4.30. A) Visualisation of the SO-CPR Survey data (1991-2008). Total zooplankton abundance (counts per 5 Nm) compared to salinity (psu) (R^2 0.005). B) ggplot of zooplankton abundance (0 – 200 counts per 5 Nm) compared to salinity (psu). Transparency of data points set at 0.01 and showing a smoothed mean (red line).

The visualisation of the SO-CPR Survey data for total zooplankton abundances compared to month (Figure 4.24 and Figure 4.31 A and C) shows that zooplankton abundances are greater in the austral summer and this is supported by the GAMM output (Figure 4.31 B) though using the CPR Survey month as a predictor of zooplankton abundance had the lowest F value. Figure 4.31 B shows that the winter months are “noisy” (i.e. wide confidence bands) due to a low number of data points compared to the summer months which show that abundances of zooplankton increase in summer and then decrease at the onset of winter.

The scatter plot for season and total zooplankton abundances (Figure 4.32 A and C) shows that zooplankton abundances are greater between 2001-02 and 2004-05. The GAMM output (Figure 4. 32B) shows the season as a predictor indicates that the abundance of zooplankton in the Southern Ocean has increased from 1990-91 to 2008. The SO-CPR Survey data has not been standardised for sampling effort, area and time of sampling.

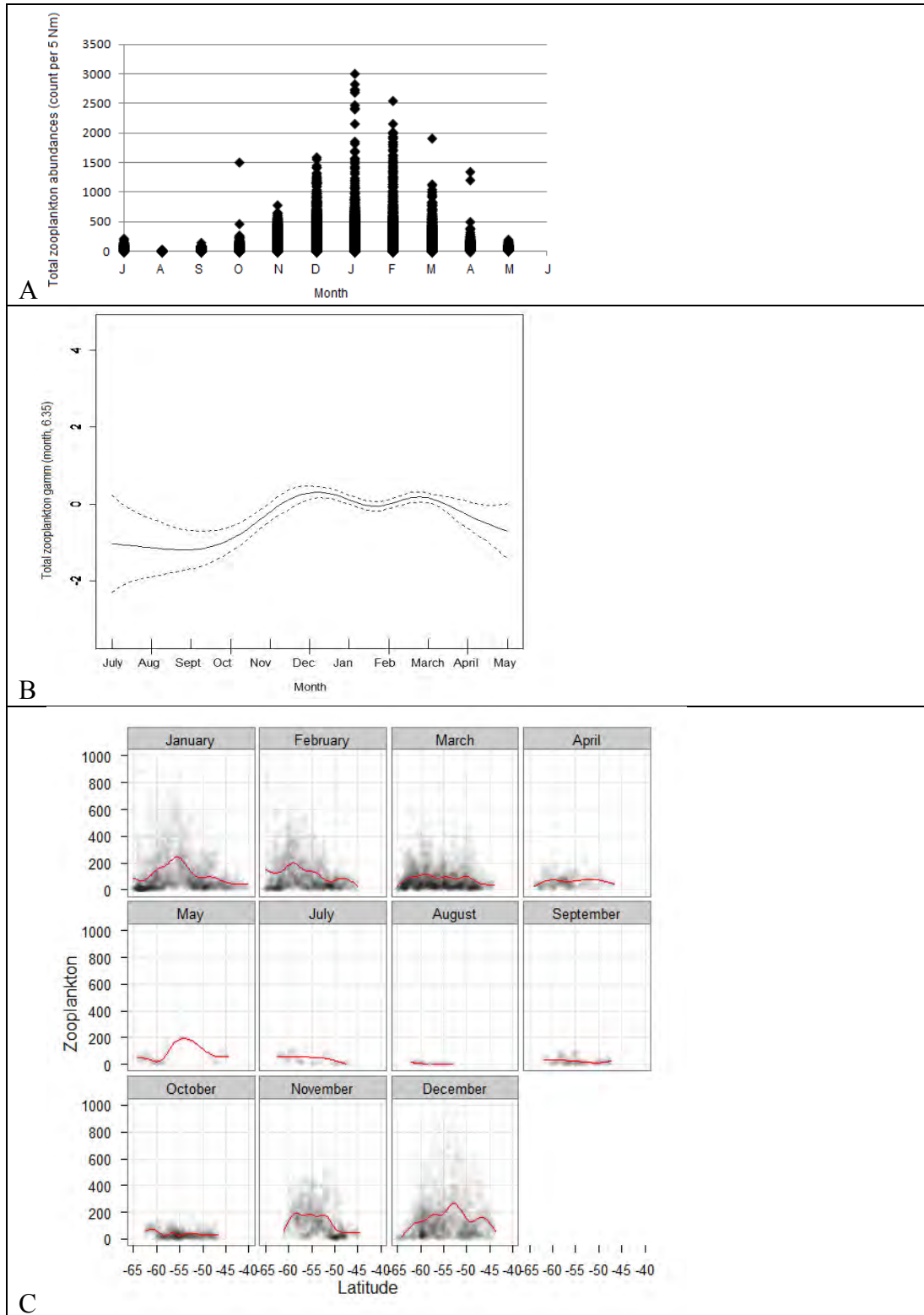


Figure 4.31. A) Visualisation of the SO-CPR Survey data (1991-2008). Total zooplankton abundance (counts per 5 Nm) compared to month (R² 4e-05). B) GAMM output for zooplankton CPR 1991-2008 analyses Total zooplankton (ordinate scale (edf)) GAMM month from July (no abundances for June). C) ggplot of total zooplankton abundance (0 – 1000 counts per 5 Nm) compared to months. Transparency of data points set at 0.01 and showing a smoothed mean (red line). Note no data for the month of June.

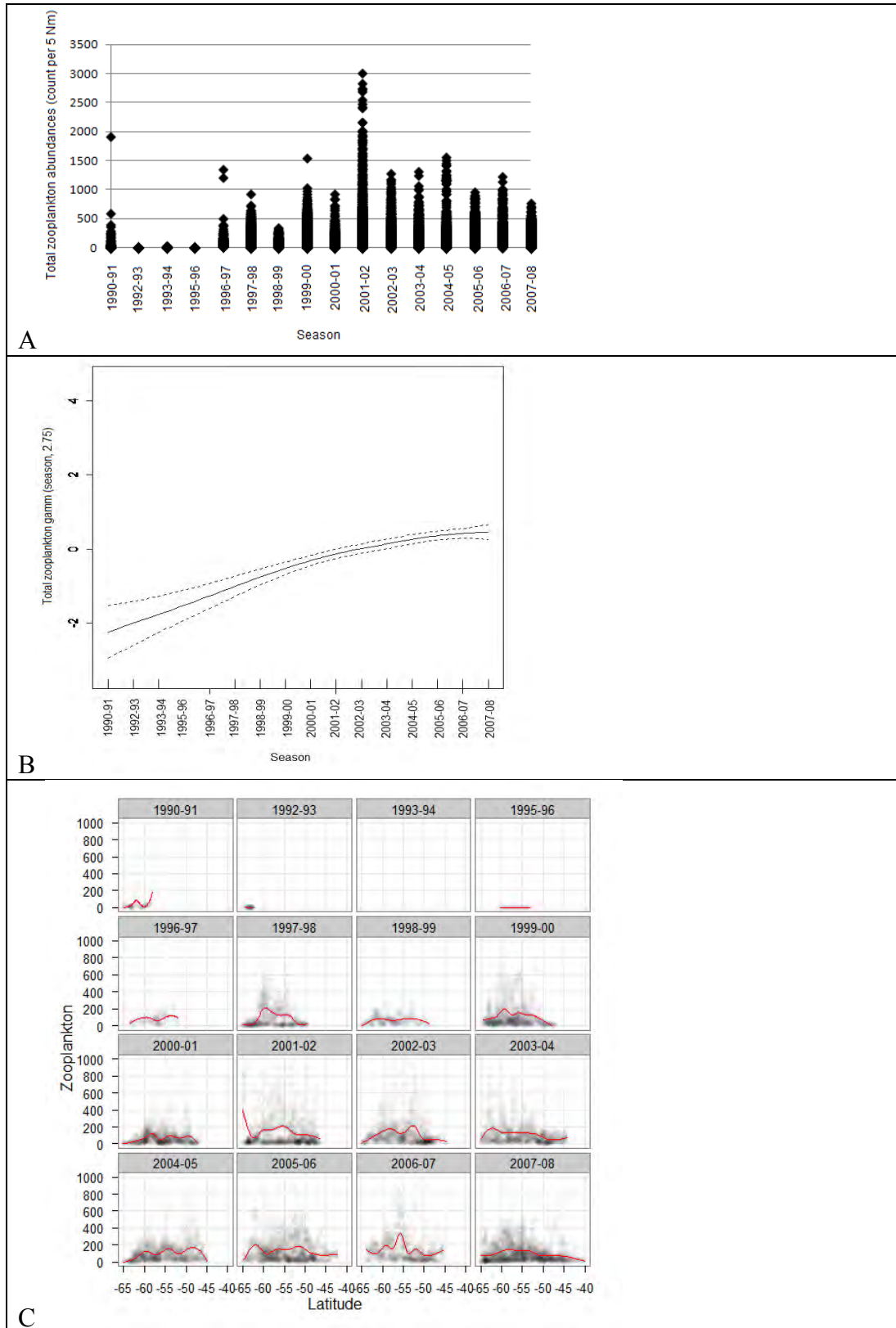


Figure 4.32. A) Visualisation of the SO-CPR Survey data (1991-2008). Total zooplankton abundance (counts per 5 Nm) compared to season (R^2 0.0018). B) GAMM output for zooplankton CPR 1991-2008 analyses Total zooplankton (ordinate scale (edf)) GAMM season. C) ggplot of total zooplankton abundance (0 – 1000 counts per 5 Nm) compared to seasons. Transparency of data points set at 0.01 and showing a smoothed mean (red line).

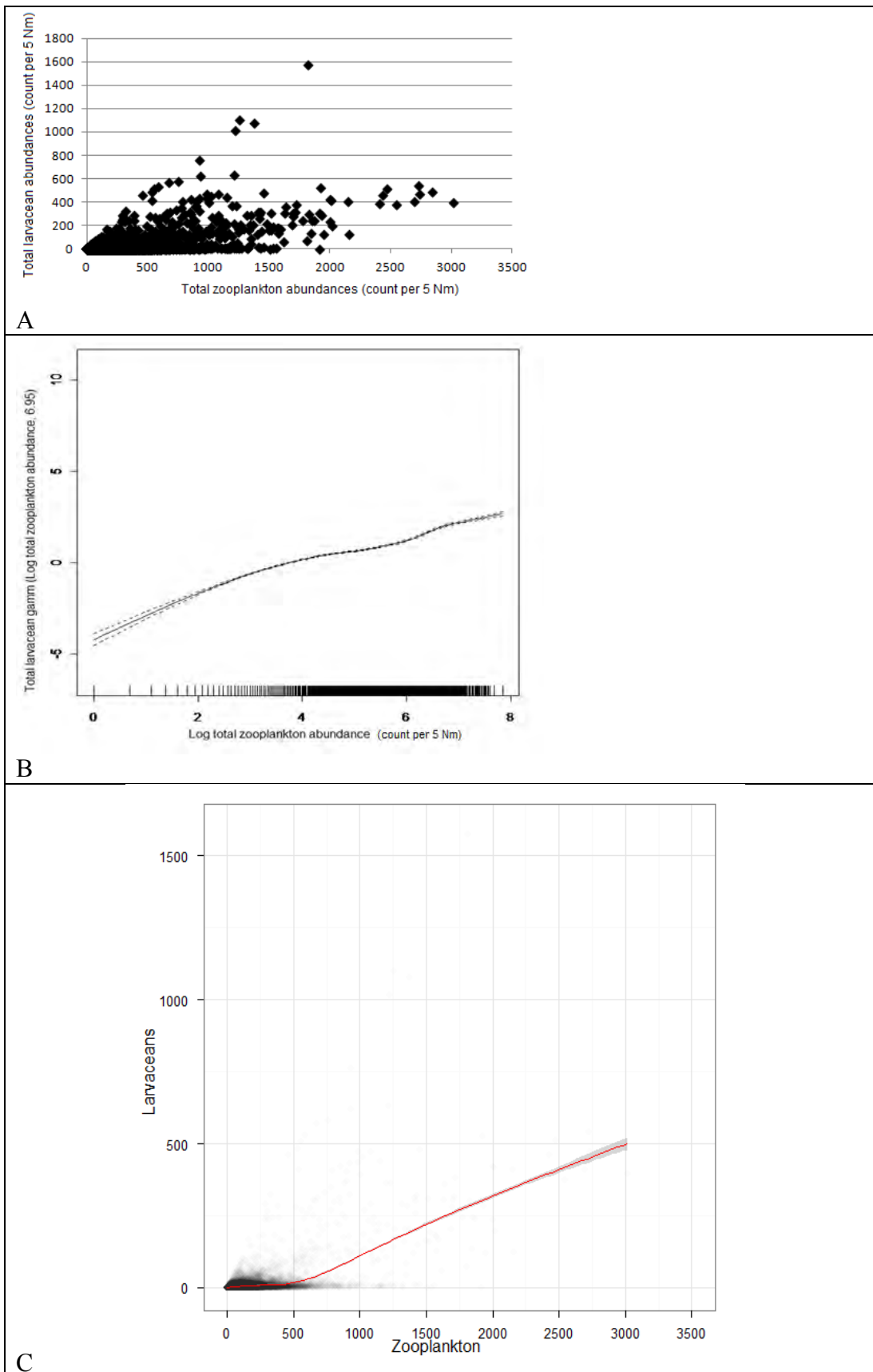
Table 4.20 lists the approximate significance of smooth terms for GAMM analysis of total larvacean abundances from the CPR database 1990-91 to 2008. The higher the F value the higher the predictor value is, thus the larvacean abundances from the CPR Survey could be predicted by using the log+1 transformed total zooplankton abundance ($F = 701.0$), latitude ($F = 131.2$) and water temperature ($F = 53.4$) and to a lesser degree the season ($F = 6.4$) and month ($F = 5.0$). There are no comparable fluorescence values for larvaceans as there was not a F value from the GAMM output that was statistically significant.

Table 4.20. Approximate significance of smooth terms for GAMM analysis of total larvacean abundances from the CPR database 1990-91 to 2008 ($n = 25791$).

	Estimated degrees of freedom	F value	p -value	significance	Figure
Log total zooplankton	7.0	701.0	<2e-16	0.001	4.31
Latitude	9.0	131.2	<2e-16	0.001	4.32
Water temperature	8.1	53.4	<2e-16	0.001	4.33
Month	5.1	5.0	1.16 e-06	0.001	4.35
Season	5.2	6.4	4.59 e-09	0.001	4.36

Figure 4.33 A and C shows the visualisation of the SO-CPR Survey data for the total larvacean abundances compared to the total zooplankton abundance (that includes total larvacean abundance) and shows that larvacean abundances increase with an increase in zooplankton abundances. This was the only scatterplot (Figure 4.33A) in section 4.5.7 that had a statistically significant r value. Figure 4.33D shows that the same pattern is visualised when 0.4% of the data points (i.e. those above 200 counts per 5Nm) are removed. Log transformed zooplankton abundances (Figure 4.33B) has the highest F value (701.0) and is therefore a statistically significant predictor of larvacean abundances in the Southern Ocean. As zooplankton abundances increase the larvacean abundances also increase. Therefore the effect of predictors of zooplankton abundances as demonstrated in

Figures 4.27 to Figures 4.32 should be taken into account when interpreting effects of these same predictors on larvacean abundances.



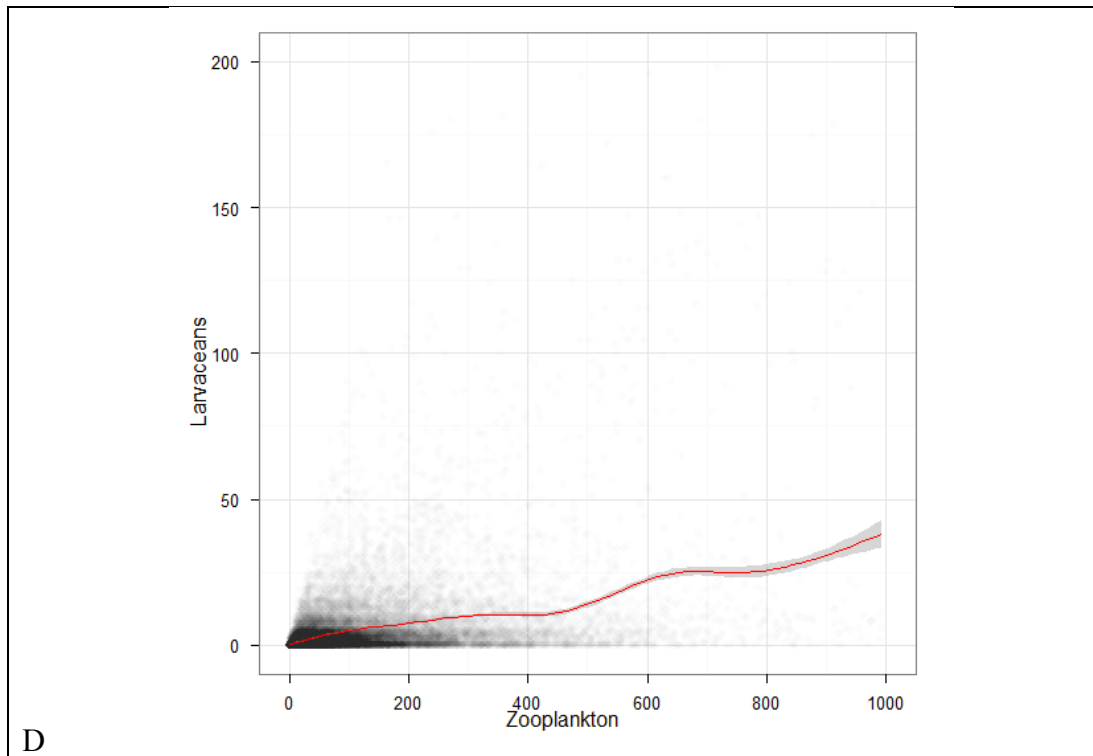


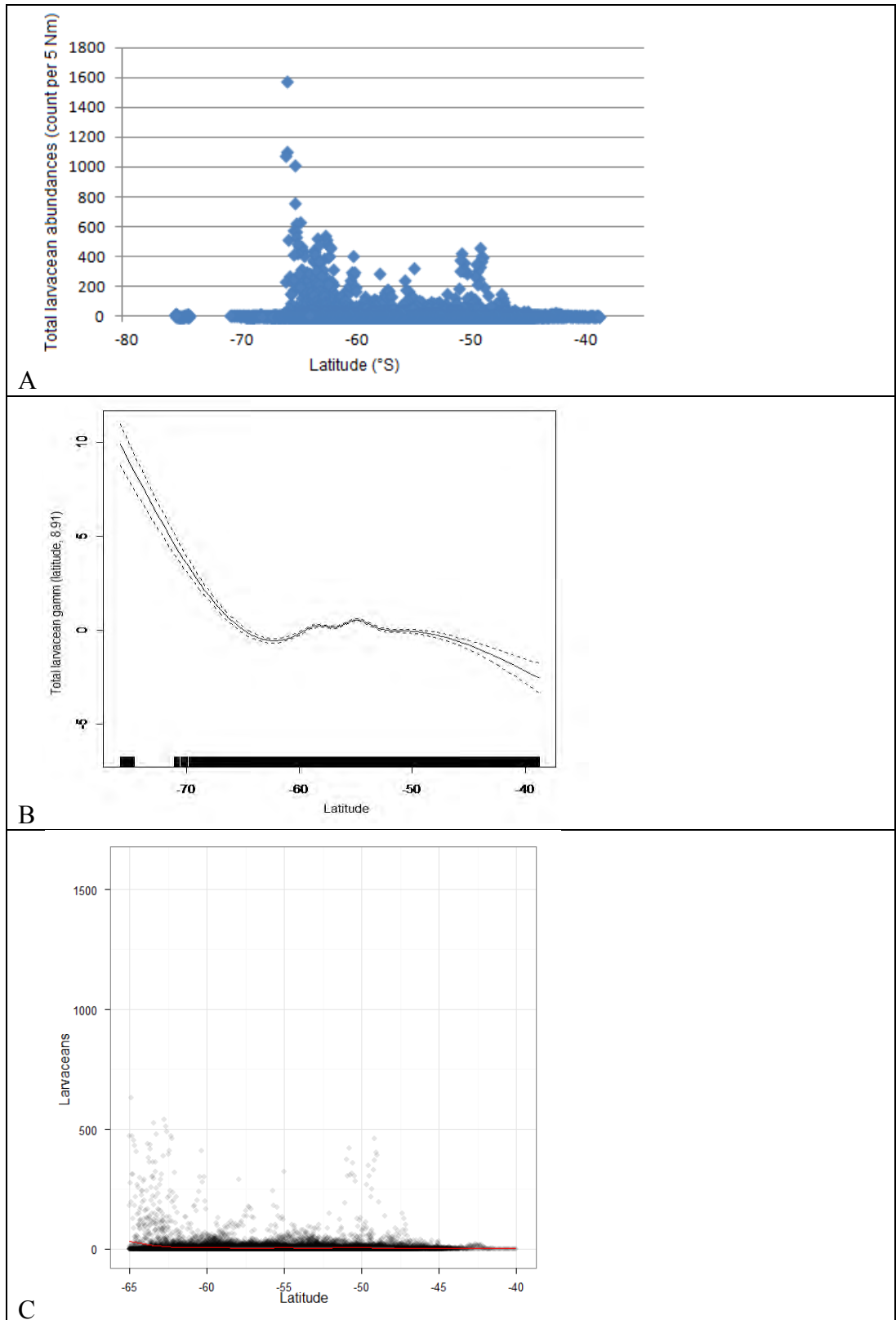
Figure 4.33. A) Visualisation of the SO-CPR Survey data (1991-2008). Total larvacean abundance (count per 5 Nm) compared to total zooplankton abundance (counts per 5 Nm) (R^2 0.2499). B) GAMM output for Larvacean CPR 1991-2008 analyses Total larvacean (Log count per 5 Nm) (ordinate scale (edf)) GAMM total Log link zooplankton (Log count per 5Nm). C) ggplot of total zooplankton larvaceans abundance (0 – 3500 counts per 5 Nm) compared to larvaceans abundance (0 – 1800 counts per 5 Nm). Transparency of data points set at 0.01 and showing a smoothed mean (red line). D) ggplot of total zooplankton larvaceans abundance (0 – 200 counts per 5 Nm) compared to larvaceans abundance (0 – 200 counts per 5 Nm). Transparency of data points set at 0.01 and showing a smoothed mean (red line).

The visualisation of the SO-CPR Survey data for total larvaceans abundances compared to latitude (Figure 4.34A) shows high abundances between 50 and 60 °S (POOZ) and the greatest concentration at 65 °S in the SIZ. Total larvaceans GAMM and latitude had a high F value of 131.2, thus latitude is a predictor of larvacean abundances. The plot for total larvaceans GAMM and latitude (Figure 4.34B) showed the model predicts that larvaceans, for a given value of other predictors, particularly total zooplankton abundances, have higher abundances at higher latitudes of the SIZ. Further, Figure 4.27 shows that total zooplankton abundances decreased at high latitudes and larvaceans abundances also decreased with a decrease in total zooplankton abundance (Figure 4.34). A conclusion is that at high latitudes higher abundance than expected occurred, given that total

zooplankton abundance was detected by the GAMM for larvacean abundance. The two peaks of total larvacean abundances that are greater than 200 counts per 5 Nm represent 0.4% of the SO-CPR Survey data points. By removing the 0.4% data points (Figure 4.34D?) the ggplot supports that greater abundances of larvaceans occurred at 65 °S.

The visualisation of the SO-CPR Survey data for total larvaceans abundances compared to water temperature (Figure 4.35 A and C) shows that the majority of larvaceans occur when the mean water temperature is between 0 and 4 °C. The total larvacean GAMM and water temperature plot (Figure 4.35 B) supports the visualisation the larvaceans in the Southern Ocean have a converse but weaker relationship with abundance and water temperature than total zooplankton (Figure 4.28B). If there is only a small or no effect of water temperature on larvacean abundance, this similar but weak relationship may simply be compensation in the GAMM empirically enforced by the inclusion of log zooplankton abundances as a predictor over the relationship seen in Figure 4.28.

4. Large-scale distribution patterns determined from the CPR



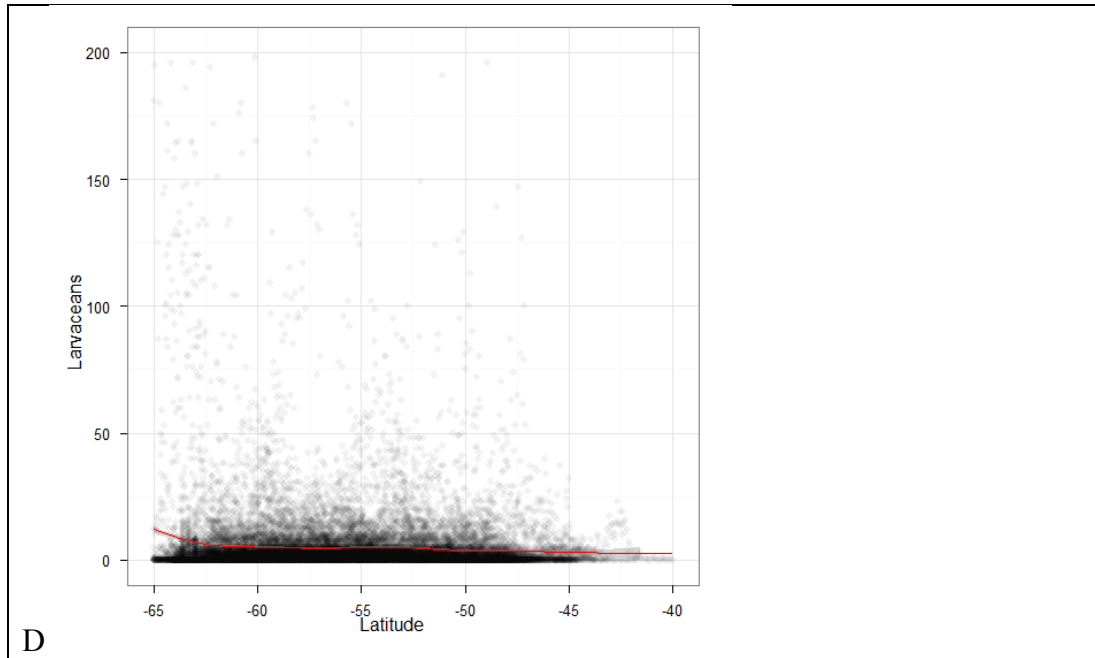


Figure 4.34. A) Visualisation of the SO-CPR Survey data (1991-2008). Total larvacean abundance (counts per 5 Nm) compared latitude ($^{\circ}$ South) (R^2 0.007). B) GAMM output for Larvacean CPR 1991-2008 analyses Total larvacean (ordinate scale (edf)) GAMM and latitude ($^{\circ}$ South). C) ggplot of larvaceans abundance (0 – 1800 counts per 5 Nm) compared to latitude ($^{\circ}$ S). Transparency of data points set at 0.1 and showing a smoothed mean (red line). D) ggplot of larvaceans abundance (0 – 200 counts per 5 Nm) compared to latitude ($^{\circ}$ S). Transparency of data points set at 0.05 and showing a smoothed mean (red line).

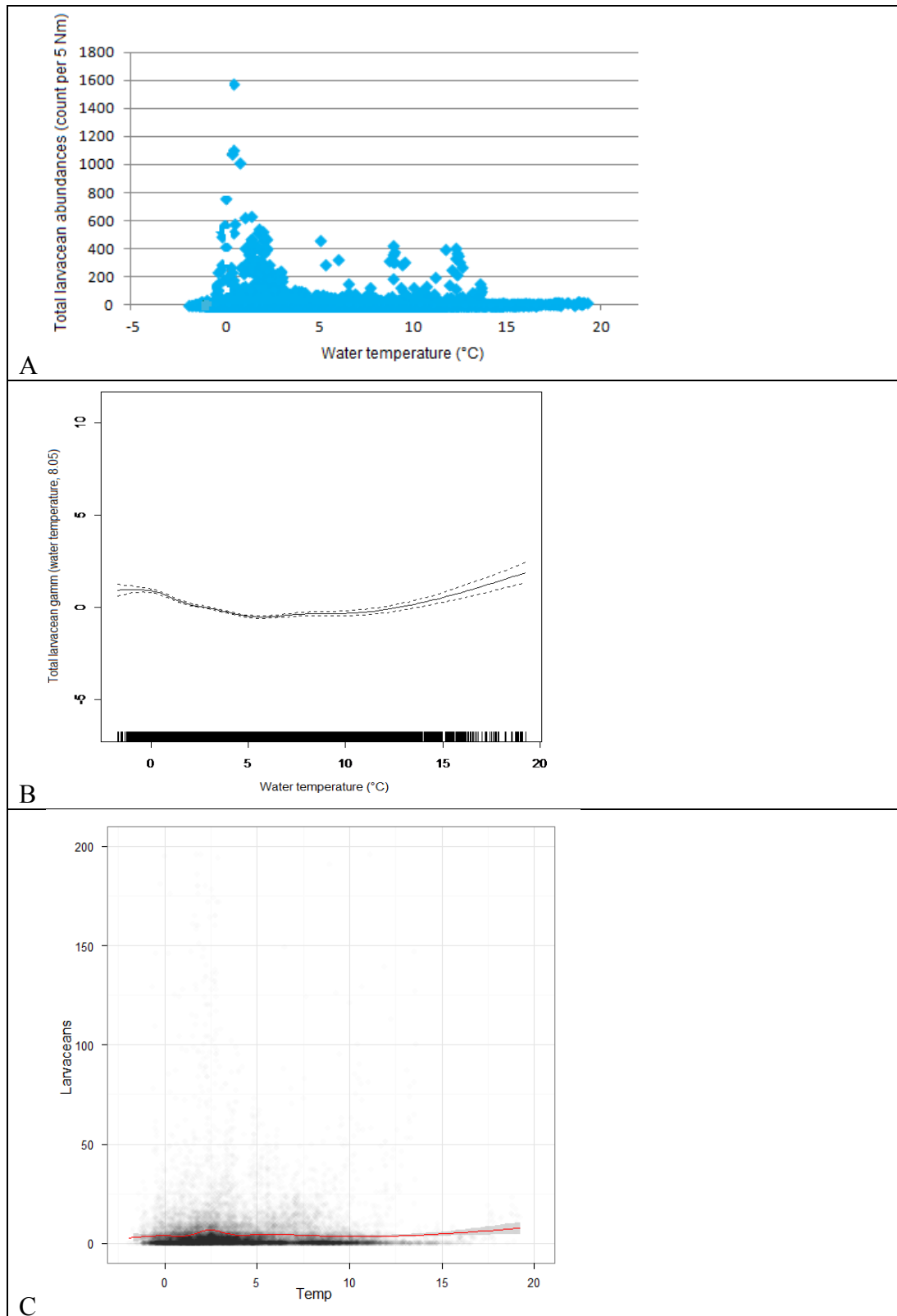


Figure 4.35. A) Visualisation of the SO-CPR Survey data (1991-2008). Total larvacean abundance (counts per 5 Nm) compared water temperature (°C) (R^2 0.001). B) GAMM output for Larvacean CPR 1991-2008 analyses Total larvacean (ordinate scale (edf)) GAMM water temperature (°C). C) ggplot of larvaceans abundance (0 – 200 counts per 5 Nm) compared to water temperature (°C). Transparency of data points set at 0.01 and showing a smoothed mean (red line).

The scatter plot shows that higher abundances of larvaceans occur when the mean fluorescence values were between 0 and 10 (Figure 4.36). The outliers could not be smoother adequately by the GAMM so there is no GAMM output for the total larvacean abundance and fluorescence as there was no statistically significant relationship.

Figure 4.37 shows that the greatest abundance of larvaceans occurred between 33.5 and 34.0 psu. The outliers could not be smoother adequately by the GAMM so there is no GAMM output for the total larvacean abundance and fluorescence as there was no statistically significant relationship.

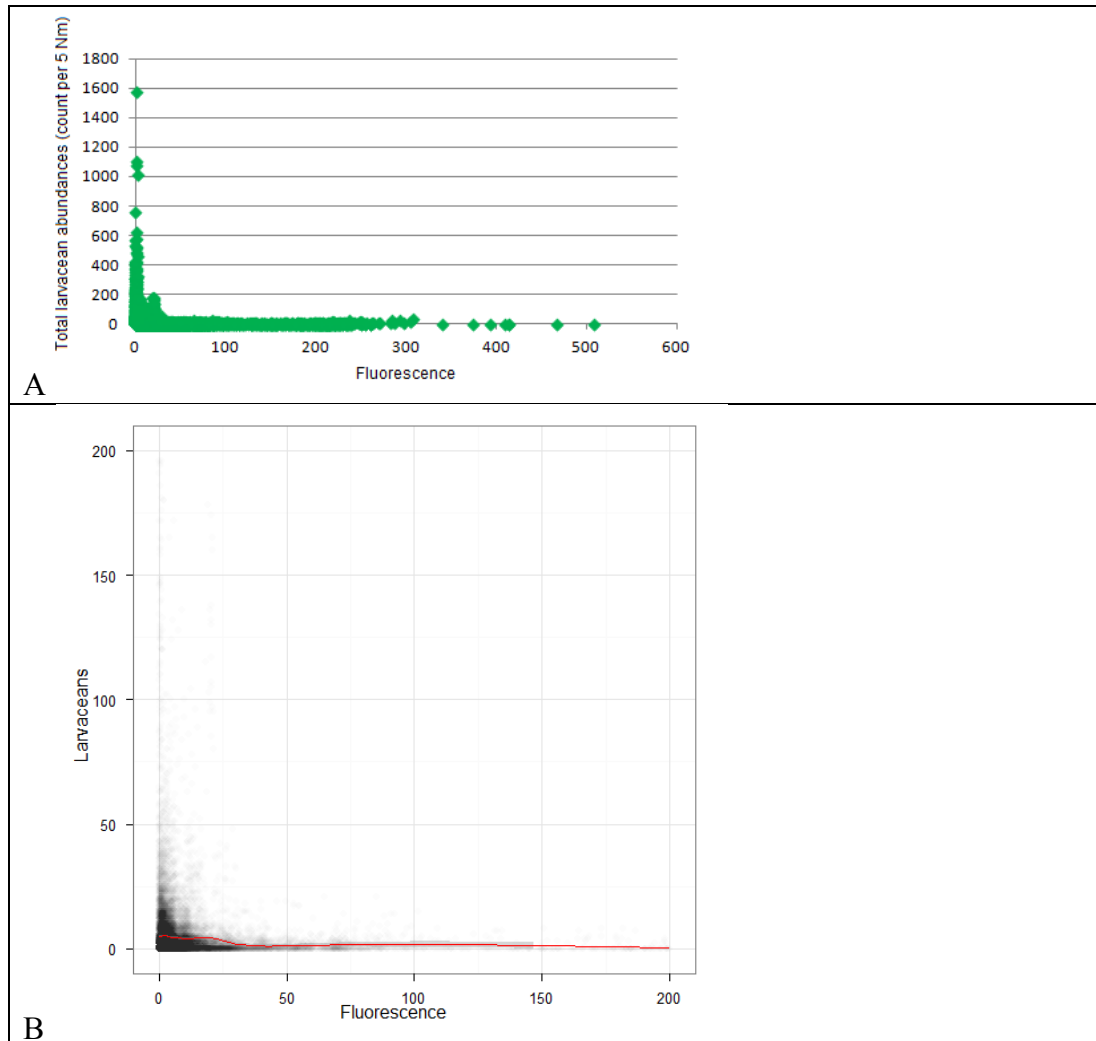


Figure 4.36. A) Visualisation of the SO-CPR Survey data (1991-2008). Total larvacean abundance (counts per 5 Nm) compared to fluorescence (R^2 0.0018). C) ggplot of larvaceans abundance (0 – 200 counts per 5 Nm) compared to fluorescence. Transparency of data points set at 0.01 and showing a smoothed mean (red line).

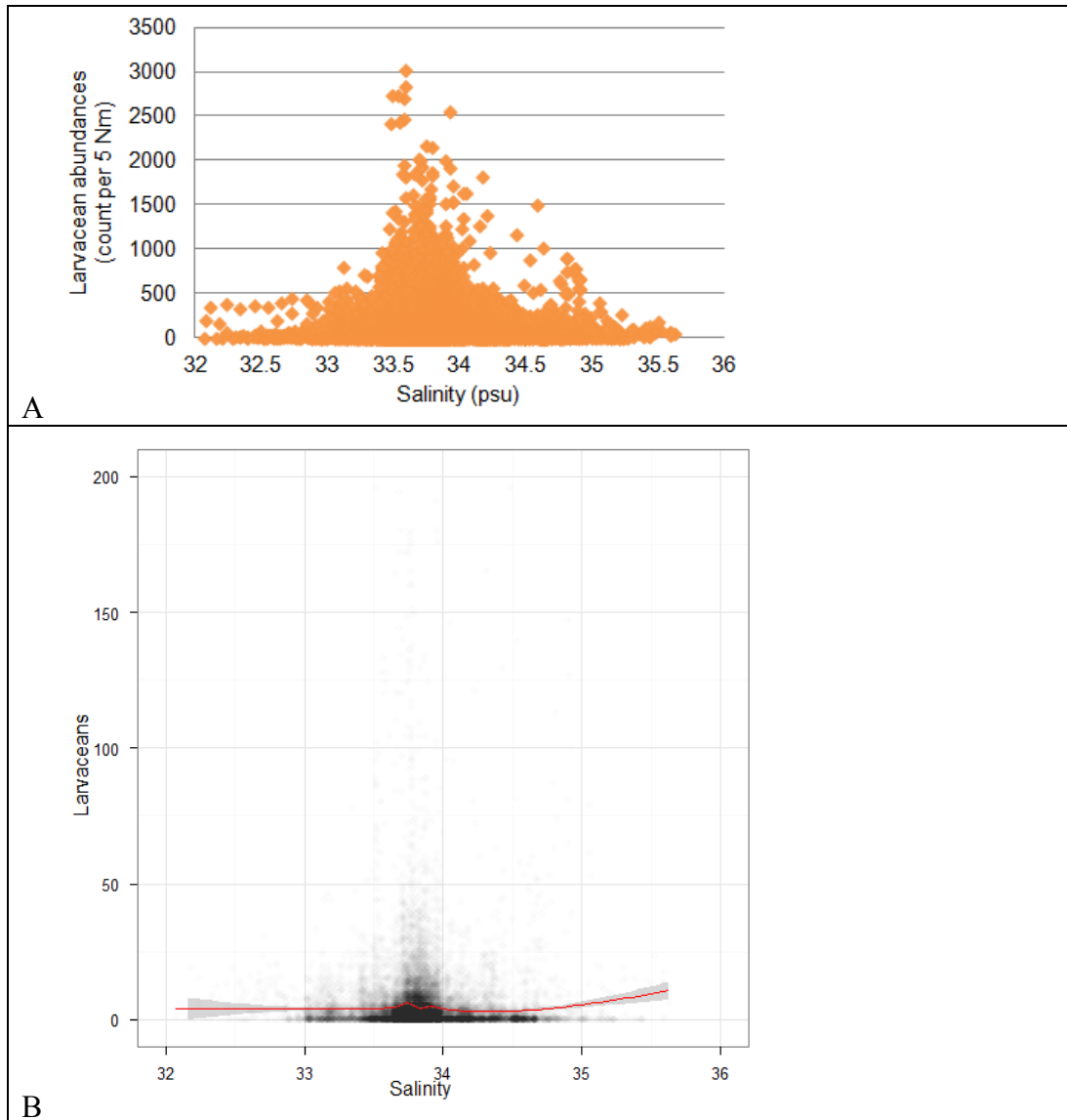
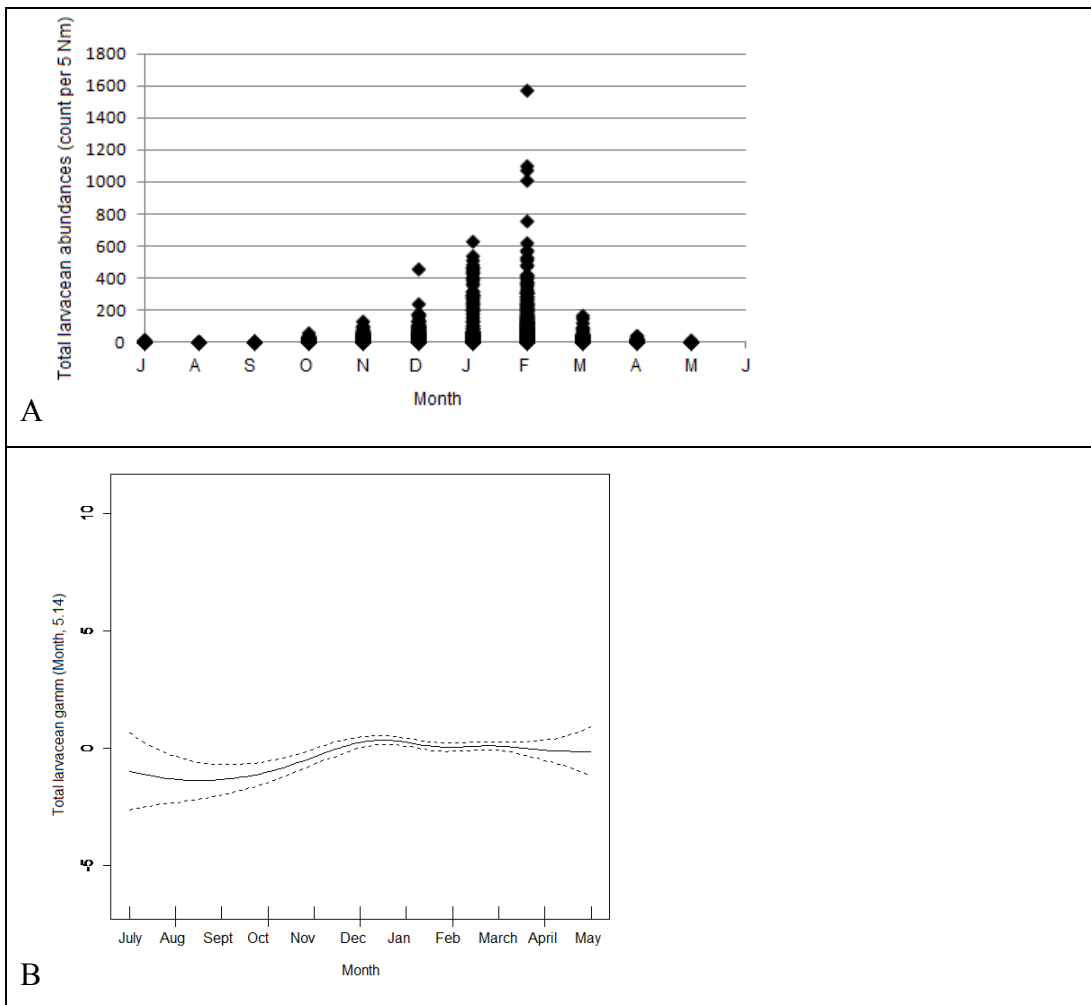


Figure 4.37. A) Visualisation of the SO-CPR Survey data (1991-2008). Total larvacean abundance (counts per 5 Nm) compared to salinity (psu) (R^2 0.005). B) ggplot of larvaceans abundance (0 – 200 counts per 5 Nm) compared to salinity (psu). Transparency of data points set at 0.01 and showing a smoothed mean (red line).

Figure 4.38 A and C shows that larvaceans predominantly were found between December and February. The CPR Survey month as a predictor of larvacean abundance had the lowest F value (5.0). The GAMM plot (Figure 4.38B) showed that abundances of larvaceans increase slightly in summer and autumn relative to winter and spring. The similar but stronger relationship trend between zooplankton abundance and months (Figure 4.24 and 4.31) and this trend for

larvacean abundance and month reinforces that larvaceans abundances are related to the abundance of zooplankton.

The majority of larvaceans (Figure 4.39 A and C) recorded in the SO-CPR Survey occurred in 2001-02 and there has been an increase in abundances since 1996-97. The GAMM output for the season (Figure 4.39B) as a predictor reveals that the abundance of larvaceans in the Southern Ocean has increased from 1990-91 to 2008. The data over the survey period has not been standardised for sampling effort, area and time of sampling. Tows in the early 1990s focussed on the SIZ which has low abundances whereas most tows today are in the permanent open ocean zone where abundances are higher. The peak in 2001-02 is due to the high larvacean abundances that were recorded during the New Zealand *Tangaroa* voyage. This high peak is possible due to sampling a bloom or sorting intensity with the “sorter” being able to clearly identify larvaceans on the CPR silks.



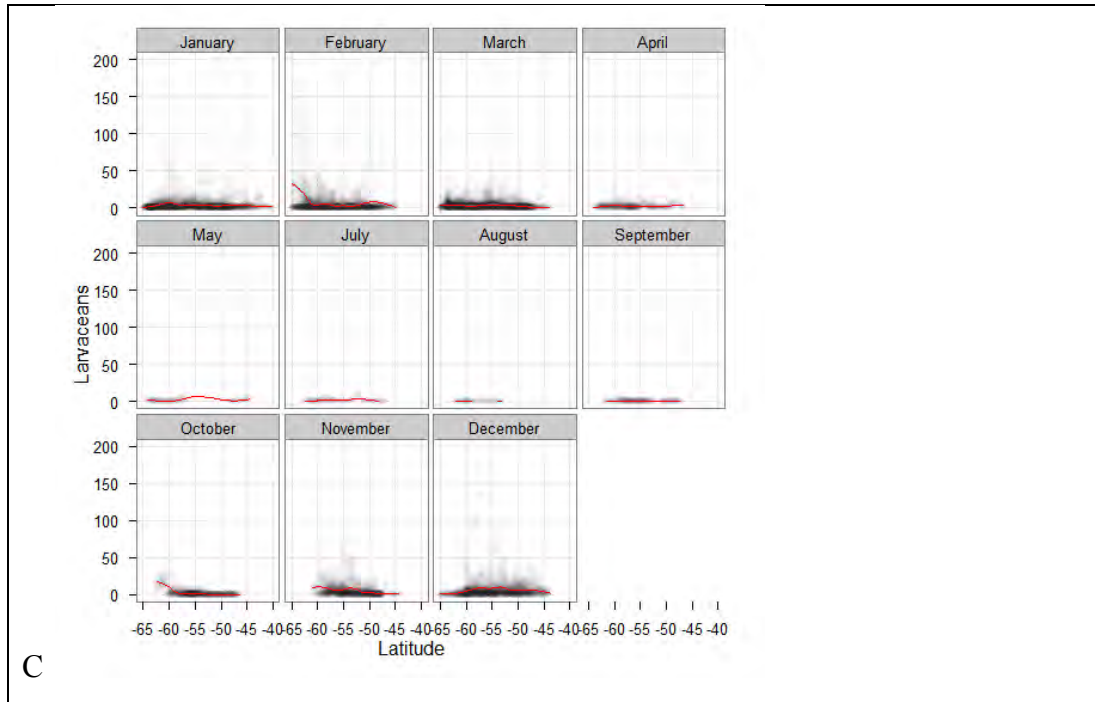


Figure 4.38. A) Visualisation of the SO-CPR Survey data (1991-2008). Total larvacean abundance (counts per 5 Nm) compared to month (R^2 0.0002). B) GAMM output for Larvacean CPR 1991-2008 analyses Total larvacean (ordinate scale (edf)) GAMM month from July. ggplot of larvaceans abundance (0 – 200 counts per 5 Nm) compared to months. Transparency of data points set at 0.01 and showing a smoothed mean (red line). Note no data for the month of June.

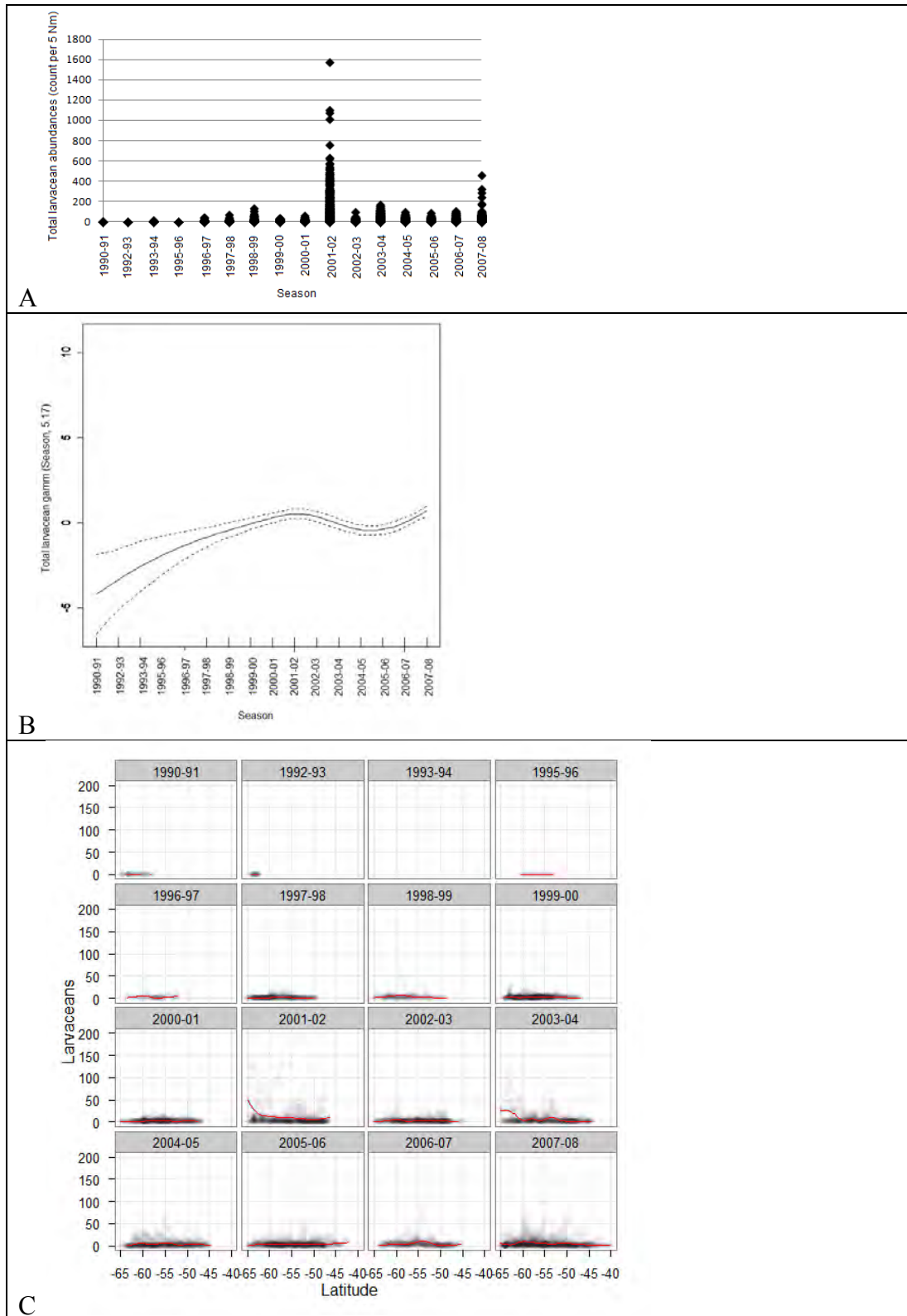


Figure 4.39. A) Visualisation of the SO-CPR Survey data (1991-2008). Total larvacean abundance (counts per 5 Nm) compared to season ($R^2 = 7e-05$). B) GAMM output for Larvacean CPR 1991-2008 analyses Total larvacean (ordinate scale (edf)) GAMM season. C) ggplot of larvaceans abundance (0 – 200 counts per 5 Nm) compared to seasons. Transparency of data points set at 0.01 and showing a smoothed mean (red line).

When comparing *Oikopleura* to *Fritillaria* directly there appears to be a transition between separate niches (Figure 4. 40), that is when *Oikopleura* occur in high abundances *Fritillaria* occur in low abundance. When *Fritillaria* and *Oikopleura* are compared to fluorescence, salinity, water temperature and irradiance the plots show the similar patterns to larvaceans as a total.

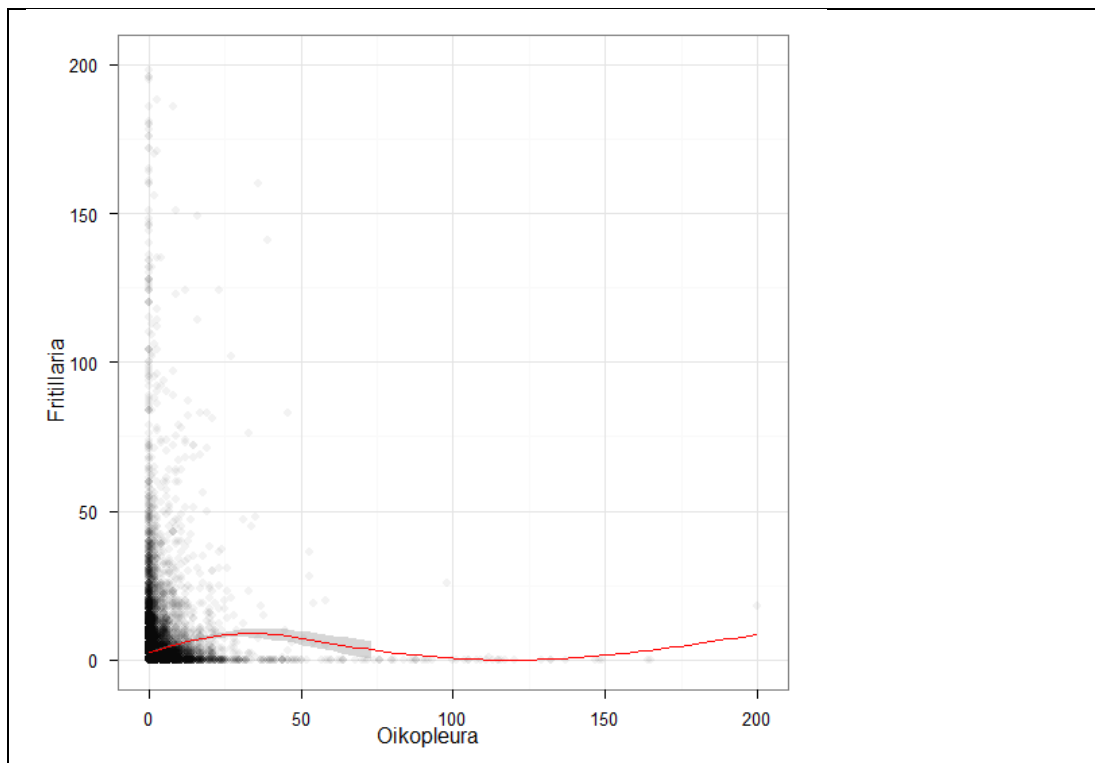


Figure 4. 40. ggplot of *Oikopleura* compared to *Fritillaria* abundance (0 – 200 counts per 5 Nm). Transparency of data points set at 0.01 and showing a smoothed mean (red line).

4.6 Discussion

Identification of larvaceans to species level was not possible in the SO-CPR Survey due to their often damaged condition, as was discussed in Chapter 3. Organisms were identified to genus or family at best. The CPR is best suited to the sampling of robust meso-zooplankton rather than gelatinous organisms. Hunt and Hosie (2003) identified that the CPR can under-sample some components of the zooplankton population, but the device provides a relatively consistent qualitative data set. Hence, the SO-CPR database is a long-term monitoring tool

that provides an ideal method for the identification of biogeographic zones in the Southern Ocean.

The CPR atlas map for total near-shore zooplankton showed in general that there were higher abundances of zooplankton in the SAZ and lower abundances in the SIZ. However, when comparing mean abundances of larvaceans to zooplankton distributions, this pattern was reversed. Larvaceans were distributed throughout the Southern Ocean, but had highest mean abundances in the SIZ (11.1 ± 49.3 ind. m^{-3}), followed by the POOZ (6.4 ± 29.7 ind. m^{-3}) and SAZ (1.9 ± 7.6 ind. m^{-3}). Tows in the early 1990s focussed on the SIZ which had low abundances whereas most tows since 1997 are in the permanent open ocean zone where abundances are higher.

Relative abundances of larvaceans compared to physical (latitude, longitude, temperature, salinity and light) and biological (fluorescence and total zooplankton) parameters are presented in Figure 4.41. This model shows that highest abundances of larvaceans occurred in the SIZ where total zooplankton was high, temperature was low, salinity and irradiance were low, and fluorescence was the highest. Tsujimoto et al. (2006) also reported high abundances of larvaceans in the SIZ using NORPAC nets. From SO-CPR Survey data, *Fritillaria* sp. was dominant with 4.4 ± 28.2 ind. m^{-3} , compared to 1.9 ± 7.6 ind. m^{-3} for *Oikopleura* sp.. Distribution and abundance data from the SO-CPR Survey showed that larvaceans were consistently present in the Southern Ocean and formed an important component of zooplankton populations.

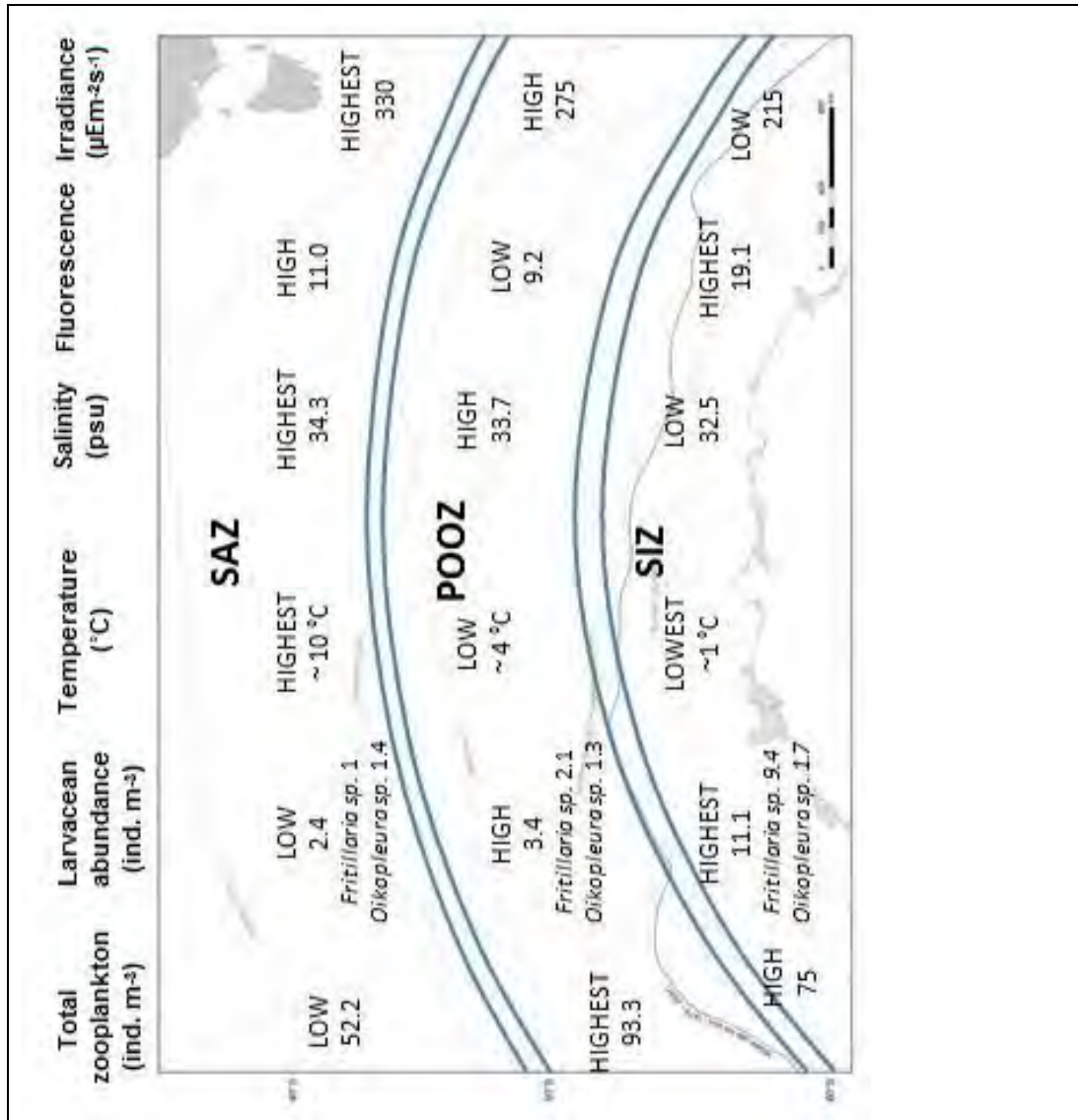


Figure 4.41. Relative abundances of larvaceans from the SO-CPR Survey compared to physical (latitude, longitude, temperature, salinity and irradiance (light)) and biological (fluorescence and total zooplankton) parameters.

Hunt and Hosie (2005) completed a 2150 km long CPR transect along 140 °E, between 47.02 °S and 66.36 °S, in the Southern Ocean to determine changes in zooplankton assemblages and the relationships with oceanic fronts. They identified six zooplankton assemblages that were strongly correlated with frontal/oceanographic zones. Larvaceans were found throughout the Southern Ocean but dominated the area south of the Southern Boundary. Mean abundances in this region were ~200 ind. m⁻³ during the night and ~ 50 ind. m⁻³ during the day. Total zooplankton mean abundances were ~310 ind. m⁻³ during the night and ~60 ind. m⁻³ during the day. Hosie and Hunt (2005) stated that the demarcation

between zooplankton assemblages was clear, though changes in oceanographic frontal zones could sometimes be subtle.

Between November 2001 and March 2002, Hunt and Hosie (2006a) repeatedly sampled along a 140° E transect, south of 62°S in the SIZ. Along this transect, they found that larvaceans were common throughout the season (occurring in >99 % of samples) and that larvaceans demonstrated a seasonal cycle similar to other zooplankton. This also indicated that larvaceans formed an important part of zooplankton populations. Larvaceans were identified as one of eight “peak species” that dominated the zooplankton community. Hunt and Hosie (2006a) explained that during periods of reduced sea-ice extent, low krill biomass, and relatively warm waters, high densities of small grazers, such as larvaceans, would develop in response to phytoplankton blooms.

Larvaceans also had a seasonal distribution with highest abundances occurring in summer and lowest abundances in winter. No larvaceans were recorded in the winter month of June. In 2003 – 2004 there was a statistically significant correlation of larvacean abundance with longitude, reflecting differences in the east and west of the surveyed region. In 2005 – 2006, niche separation appeared to occur with alternating distributions of *Oikopleura* and *Fritillaria* sp, that is when *Oikopleura* occur in high abundances *Fritillaria* are in low abundance. This may be an artefact that *Fritillaria* occur in far greater abundances than *Oikopleura*. When the families are graphed separately they both occur within the same latitude range. If the larvaceans are competing for the same food source they may have a patchy distribution within their geographic range. The difference in abundance may be due to different life cycles or temporal responses. When *Fritillaria* and *Oikopleura* are compared to fluorescence, salinity, water temperature and irradiance the plots show the same patterns as larvaceans in total.

Hunt and Hosie (2006b) surveyed the sub-Antarctic to Polar Frontal Zone, between 47- 54°S using CPR and NORPAC nets. They found that larvaceans were a major contributor (17%) to the zooplankton community. Highest mean zooplankton abundances occurred in February, with *Oithona similis* (copepod), foraminiferans and larvaceans (~ 110 ind. m⁻³) found to be the core taxa.

Combined, these organisms occurred in > 97% of samples, and contributing an average of 75% to total zooplankton abundance (634 ind. m⁻³). The Hunt and Hosie (2006b) findings were supported by this studies use of *Pearson r*, GAMM and scatterplots.

The partial plots for the various predictor variables, such as latitude, show significant trends, this indicates that the GAMM has some predictive power but the graphs showing observed and fitted values makes this clear using the sum of predictor-specific terms in the linear predictors. The GAMM allows a number of extensions to standard multiple regression. These (i) allow the fit to non-Gaussian (i.e. normal) non-constant variance exponential families such as the Poisson, (ii) can use a log link which gives multiplicative effects, (iii) allow smoothed nonlinear trends with continuous predictor variables to be fitted, and (iv) allow validation of random effects to more adequate model random departures from the fitted model.

Multiple regression or multiple predictors in GAMMs try to tease these effects out using this much more rigorous approach but even then often give less than a clear picture especially with such noisy data. The single-variable-at-a time graphs (scatterplots) and R² values that were completed to compare with the GAMM model are only slightly more informative than the single pair wise *Pearson r* correlations, presented in detail in section 4.5.5. The only scatterplot that had a statistically significant R² of 0.25 was Figure 4.32 A, total zooplankton compared to larvaceans.

The physical parameters used to determine reasons for distribution and abundances are not independent and it is difficult to determine which the stronger driver is. For example, a relationship with latitude may be influenced by the relationship with water temperature and/or salinity or the relationship with latitude and light (irradiance).

Larvaceans occur in higher abundances in similar conditions to when the total zooplankton abundances are high. High zooplankton abundances are predicted to occur where the parameters of fluorescence is between 0 and 5, when the water

temperature is between 0 - 4 °C, and salinity is between 33.5 and 34.0psu in the summer months and during the later CPR Survey seasons. This correlation and whatever affects total abundance also affects total larvacean counts, which is also part of the total zooplankton count. Therefore larvacean abundances can thus be predicted to occur in areas of the Southern Ocean where the water temperatures are low, in areas where the fluorescence is low between 10 and 20 and in the SIZ and POOZ.

There is possibly a constant background abundance of larvaceans upon which blooms occur sporadically. This occurs with phytoplankton when there is a background abundance of flagellates and small diatoms under oligotrophic conditions, when there are nutrient intrusion events, sporadic blooms of larger diatoms and dinoflagellates occur (*pers com* Wright). The statistics used in this study did not identify the triggers or the circumstances for the sporadic larvacean blooms. It is a possibility that the larvaceans higher abundances in areas of low fluorescence could be because the larvaceans had consumed all the chlorophyll prior to sampling.

4.7 Conclusions from Southern Ocean CPR

The correlations with environmental conditions for the SO-CPR Survey GAMM for zooplankton and larvaceans are present but are not strong due to the high variability in the data and the fact that zooplankton have localised high concentrations due to random occurrences. The high occurrences of zeros (i.e. absences or non-captures) also result in an inability to explain ecological patterns of co-occurrence to any reasonable degree of confidence, so modelling was limited to a response variable of the total abundance of both species combined. This inability to explain ecological patterns of co-occurrence was emphasised by the lack of *Pearson r* correlations with fluorescence or temperature. GAMM determined that a relationship for these parameters did occur for zooplankton and for larvaceans and water temperature. The GAMM for larvaceans includes the total zooplankton abundances as a predictor parameter, this approach shows that both experience the same or similar effect from environmental drivers. There was a correlation between larvaceans and total

zooplankton, which in turn correlates with fluorescence and water temperature. GAMM was not able to determine whether the increased abundances of larvaceans in the SIZ (high latitudes) is a reflection of a preference for the sea ice zones, sea ice edge, cold water or related to the concentration of available food in this zone. The peaks that appear to dominate the scatterplots have been identified to be from 0.5% of the zooplankton data and 0.4% of the larvacean data and are associated with the 2001/02 *RSV Tangaroa* data that is explained throughout the chapter. This has also resulted in the graphs that compare latitude and abundances not showing any significant patterns or relationships with the fronts.

The following chapter has been removed for
copyright or proprietary reasons

Chapter 5:

Distribution and abundance of Larvaceans in the Southern Ocean between 30° and 80°E.

Published in Deep-Sea Research II

[Lindsay, M. C. M.](#); [Williams, G. D.](#)

Deep Sea Research Part II: Topical Studies in Oceanography, v. 57, iss. 9-10, p. 905-915.

DOI: [10.1016/j.dsr2.2009.04.021](https://doi.org/10.1016/j.dsr2.2009.04.021)

CHAPTER 6.

**Fine-scale distribution patterns determined from
plankton nets**

6.1 Introduction

Chapter 5 detailed the distributions of larvaceans from the BROKE-West voyage, a summer voyage in the high Antarctic. This chapter expands on the distribution and abundance of larvaceans with similar data from CEAMARC–Pelagic, another summer voyage in the high Antarctic; SIPEX, a winter voyage in the high Antarctic sea-ice zone; and SAZ-SENSE, a summer voyage in the Sub-Antarctic zone. This chapter has three sections; Section 6.2 details methods, Section 6.3 determines the large-scale distribution and abundance of larvaceans in the Sub-Antarctic zone (SAZ), Southern Ocean Permanent Open Ocean Zone (POOZ) and the Seasonal Ice Zone (SIZ) from plankton net data obtained during each voyage. Section 6.4 examines fine-scale distribution patterns determined from plankton nets, through observation of variations with depth and time of day. Possible controls on larvacean distributions are also discussed through examination of associated physical (latitude, longitude, temperature, salinity and light) and biological (chlorophyll *a* and total zooplankton) distributions.

When undertaking studies on zooplankton, Omori and Ikeda (1984) explained that the careful consideration of sampling design and selection of sampling devices are important to meet the aims of the project. The sampling of zooplankton has many challenges due to differences in life stages, swimming capabilities, behaviour and habitats. Distribution and abundance estimates are influenced by many factors including the sampling device itself, frequency of sampling, net avoidance and horizontal/vertical migration of zooplankton.

A well-designed sample program increases the amount and usefulness of information available. For effective design, the main objectives of the study need to be considered and the target population defined so that the relevant sampling device can be used. A relevant location/habitat must also be surveyed. Most

statistical analyses require replicated samples. These are challenges that opportunistic sampling have to attempt to overcome. To investigate long-term variations in zooplankton, Omori and Ikeda (1984) stated that sampling devices and methods need to be standardised. The procedure needs to represent the region both quantitatively and qualitatively. Standardised sampling also enables comparisons of abundances of certain taxa and/or communities between locations and between different surveys undertaken at different times and years. A comprehensive study of nets and alternative sampling devices was provided by Wiebe and Benfield (2003).

Gelatinous zooplankton, including larvaceans, are widely distributed in high abundances throughout all oceans. Raskoff et al. (2003) explained that due to their fragility they are the least understood planktonic faunal group. Collection of gelatinous zooplankton requires minimal handling to reduce damage to individuals. Specialised sampling devices are used to collect gelatinous zooplankton and nets need to be deployed slowly to ensure that the animals are undamaged and remain alive after gear recovery. In addition, cod-ends need to be wide enough so that animals are not damaged upon entry. Nets that have been used to collect larvaceans include NORPAC nets (Tomita et al., 2003; Hunt and Hosie, 2003; Tsujimoto et al., 2006; Sato et al., 2008), Bongo nets (Hopcroft et al., 2005), opening and closing Tucker trawls (Choe and Deibel, 2008), Working Party 2 (WP2) nets (Vargas et al., 2002), purpose-built plankton nets (Selander and Tiselius, 2002), Continuous Plankton Recorders (CPR) (Hunt and Hosie, 2003, 2005, 2006a and 2006b), Niskin bottles (Jaspers et al., 2009) and Rectangular Mid-Water Trawls (RMT) (Hosie et al. 2000).

Live animals have been observed *in situ* by manned and remotely operated vehicles (ROV) (Youngbluth et al., 1990; Steinberg et al. 1994; Robison et al., 2005; Raskoff et al., 2005) and by Visual Plankton Recorders (VPR) (Lombard et al., 2010). Live animals have also been collected and observed *in situ* by snorkelling and SCUBA diving (Bochdansky and Deibel, 1999; Hamner, 1975; Alldredge, 1976). Individual larvaceans have been collected in wide sampling jars or with syringes (Hansen et al., 1996).

For this study, larvaceans were collected during four Southern Ocean voyages using a number of sampling devices; a purpose-built ring net, a Rectangular Mid-Water Trawl (RMT1), a Working Party 2 (WP2) net, a HYDRO-BIOS MultiNet, a Visual Plankton Recorder (VPR) and a Continuous Plankton Recorder (CPR). The nets that were used were selected for different taxonomic targets. The ring net targets larvaceans, the RMT targets krill (Euphausiacea) and other zooplankton, and the CPR is best suited for robust meso-zooplankton. The WP2 net targets small zooplankton and the VPR provides *in situ* observations of all visible taxa.

Observations and the collection of larvacean samples for this study were dictated by logistics and the workload of the research vessels involved, rather than by sampling design. This made it difficult to directly answer questions concerning the ecology of larvaceans in the Southern Ocean. Data is discussed within the context of these limitations that arose from the necessity to use opportunistic ship time for sampling.

6.2 Methods

6.2.1 Survey region

The three zones of the Southern Ocean that were surveyed during this study are described in Chapter 2, which also includes maps of the voyage tracks and survey sites. The Sub-Antarctic Zone (SAZ) was surveyed during the SAZ-Sense voyage in 2006/2007 (Figure 2.17), the Permanent Open Ocean Zone (POOZ) was surveyed during Leg 12 of the BROKE-West voyage (Figure 2.16) in 2005/2006, and the Seasonal Ice Zone (SIZ) was surveyed during the southern section of the BROKE-West voyage (2005/2006), the SIPEX voyage (Figure 2.18, 2007/2008) and the CEAMARC-Pelagic voyage (Figure 2.19, 2007/2008). Three of these voyages were conducted aboard RSV *Aurora Australis*; BROKE-West, SAZ-Sense and SIPEX. The CEAMARC–Pelagic voyage was conducted aboard TRV *Umitaka Maru*.

6.2.2 Plankton nets

Larvaceans were collected using a number of sampling devices including a ring net, Rectangular Mid-water Trawl 1 (RMT1, part of an RMT1+8 system), WP2, HYDRO-BIOS MultiNet and VPR. These devices were described briefly in the paper by Lindsay and Williams (2010) included in Chapter 5, but are expanded on here.

Ring net

The ring net was purpose built for this project with a mouth area of 0.8m^2 , $150\ \mu\text{m}$ mesh, and a 20 L, weighted (approximately 15kg), 0.3 m wide cod-end with windows (Figure 6.1). It was designed as a non-destructive sampling device to capture larvaceans in good condition, enabling delicate taxonomic features to be maintained for identification and Scanning Electron Microscope (SEM) imaging. The ring net was deployed from RSV *Aurora Australis*. It was hauled vertically from a depth of 20 m, providing a sampling volume of $16\ \text{m}^3$. This depth was selected based on Hunt and Hosie (2003) who noted that larvaceans were predominantly found at these depths in higher abundances. In order to reduce damage/contact with delicate gelatinous zooplankton, the ring net did not have a flow meter. Filtering efficiency was assumed to be 100%. The deployment speed of the net was determined by ocean conditions and the haul speed conducted as slowly as possible by the winch (approximately $0.5\ \text{m s}^{-1}$).

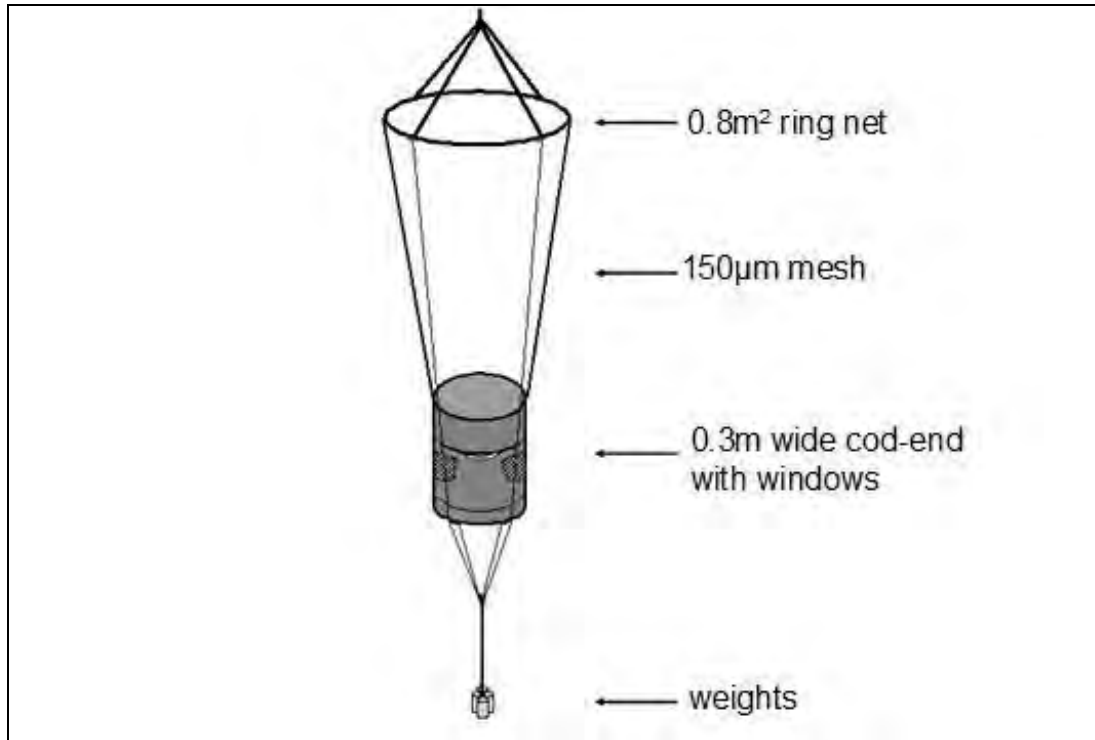


Figure 6.1. Ring net which was vertically deployed. Mouth area 0.8m^2 , $150\ \mu\text{m}$ mesh and a 20 L, weighted (approximately 15kg), 0.3 m wide cod-end with windows.

Ring net Subantarctic Zone (SAZ)

The ring net was deployed 29 times in total during SAZ-Sense. Six deployments were conducted at transit stations, 6 deployments conducted at process stations 1 and 2, and 9 deployments conducted at process station 3. Two deployments were not included due to net damage and station abandonment. Diel deployments were conducted at process stations over 24 hour periods with midnight hauls including three depths (20m, 50m, and 100m). The methods used during this voyage are to be published in Howard et al. (accepted).

Ring net Permanent open ocean Zone (POOZ)

The ring net was deployed in the POOZ 10 times during Leg 12 of the BROKE-west voyage. These results are detailed in Chapter 5.

Ring net Sea Ice Zone (SIZ)

During BROKE-West the ring net was deployed 108 times on the westbound and southbound transects whilst oceanographic stations were conducted. The ring net was hauled vertically from 20m. The results are also detailed in Chapter 5.

During SIPEX the ring net was also hauled from 20m. The first deployment was at 62° 00.82S, 129° 00.41E on the 9 September 2007. Additional ring nets were deployed at and between ice stations (15 ice stations in total). The 40th and final ring net was deployed on 11 October 2007 at 62° 09.38S, 124° 13.91E.

Rectangular Mid-water Trawl 1+8 (RMT)

The Rectangular Mid-water Trawl 1+8 (RMT1+8) is a net system used to sample macro- and meso-zooplankton. The RMT1 has a smaller mesh and sampling volume than the RMT8 (Figure 6.2). Mesh sizes that were used varied for different voyages according to the priority zooplankton group being targeted. When krill larvae were being targeted, the RMT1 mesh size was 300 µm (BROKE-West) or 330 µm (SIPEX). The RMT8 mesh size for these two voyages was 4.5 mm. During SAZ-Sense, a finer 150 µm mesh was used for the RMT1, and a mesh size of 2 mm for the RMT8. The SAZ-Sense voyage targeted groups such as pteropods and foraminifera, as well as larvaceans. For all voyages, nets were opened remotely at defined depths and towed obliquely from the surface to 200m, then horizontally for 15 minutes (Hosie, 1994).

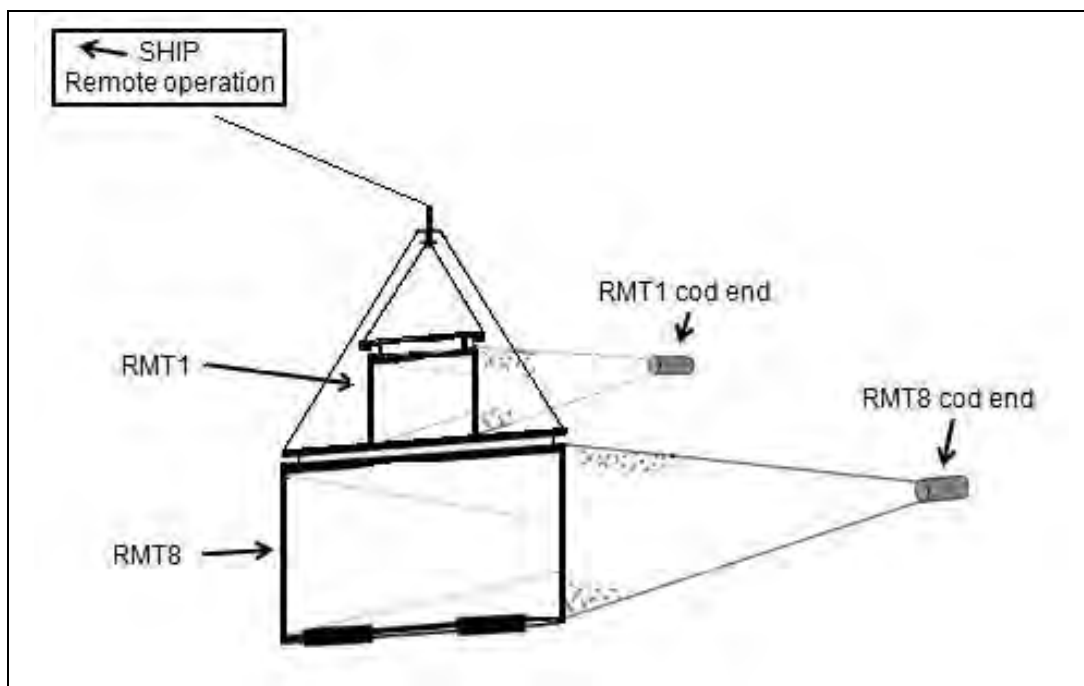


Figure 6.2. Generalised schematic of the Rectangular Mid-water Trawl 1 (RMT1), part of an RMT1+8 system.

RMT SAZ

During SAZ-Sense the RMT was deployed a total of 12 times at 8 stations. A deployment normally consisted of two 15 minute horizontal tows. However, for two deployments there was no second trawl, and on some occasions only one part of the net (either the RMT1 or RMT8) was working, with damage to the other net.

RMT1 tows were deployed between 20 and 150 m depending on the depth of the chlorophyll maximum. This variation in depth, combined with the small mesh size of 150 μm , meant that the formulae normally used to calculate volume filtered using mouth area (Roe et al., 1980; Pommeranz et al., 1982) could not be used. With a mesh size of 150 μm and horizontal tows at a minimum speed of 0.5 knots and a maximum speed of 1.9 knots, the nominal mouth area was assumed to be 1 m^2 . Therefore, volume filtered (m^3) was equal to the distance towed by RMT1 (m) multiplied by the mouth area of RMT1 (m^2). Distance towed and speed of the net in the water were calculated from a flow meter that was fitted to the RMT8 (8 m^2 net opening with 2 mm mesh). The filtering efficiency of RMT1 was approximately 85% (Ikeda et al., 1986) of the RMT8 when comparing a 300 μm

to 4.5 mm system. The methods used during this voyage are to be published in Howard et al. (accepted).

RMT SIZ

The RMT was deployed in the SIZ during the BROKE-West voyage. Larvacean data from this voyage were detailed in Chapter 5 and are also included in Swadling et al. (2010). The RMT was deployed 125 times and 20 of these trawls did not produce samples due to damage to the net and/or cod-end. The RMT1 net was fitted with 300 μm mesh and had a nominal opening of 1 m^2 when towed horizontally at 2 knots (Roe et al., 1980). Mouth area is affected by speed and trajectory. Ship speed was between 2 – 2.5 knots during oblique trawls. There were two types of trawls – routine and target. Routine trawls were deployed to 200 m at pre-determined sites and target trawls occurred at locations where acoustics detected aggregations of krill. Target trawl deployment depths ranged from 17 to 255 m. The RMT8 (8 m^2 net opening with 4.5 mm mesh) was fitted with a flow meter and the volume filtered was determined using the formula from Pommeranz et al. (1982). The filtering efficiency of the RMT1 was approximately 85 % (Ikeda et al., 1986) compared to the RMT8. Routine trawls predominantly occurred on the southbound transects while target trawl sites were determined by acoustic detection of krill on northbound transects. There were some additional target trawls on westbound and southbound transects.

Additional plankton nets and sampling devices

Larvaceans were also observed during the 15 day CEAMARC–Pelagic survey aboard *TRV Umitaka Maru*. A total of 23 sites were sampled using a combination of traditional and new technologies. This was a multi-disciplinary voyage examining pelagic communities, protists, plankton, fish and cephalopods throughout the water column. Traditional methods included CPR, plankton nets (WP2, North Pacific standard plankton net (NORPAC) and HYDRO-BIOS MultiNet) and the RMT. A new technology that was utilised was the Visual Plankton Recorder (VPR). It was used to obtain video images of zooplankton,

focusing on gelatinous forms and cephalopods that are poorly sampled in traditional nets.

The North Pacific standard plankton net (NORPAC) designed by Motoda (1957) has a 45cm mouth diameter and a conical net length of 180cm and mesh size of 0.33 mm). The NORPAC net has been used for numerous quantitative zooplankton studies including larvacean studies by Tomita et al. (2003) and Hunt and Hosie (2006a and b).

Working Party 2 (WP2) net

The WP2 (Figure 6.3) is generally used for long-term plankton research. On the *TRV Umitaka Maru* the WP2 net was fitted with a standard 200 μm mesh and was deployed between 0 – 200 m in vertical hauls. Larvaceans were recorded as present/absent when using the WP2 rather than quantitative records due to time constraints and project priorities.

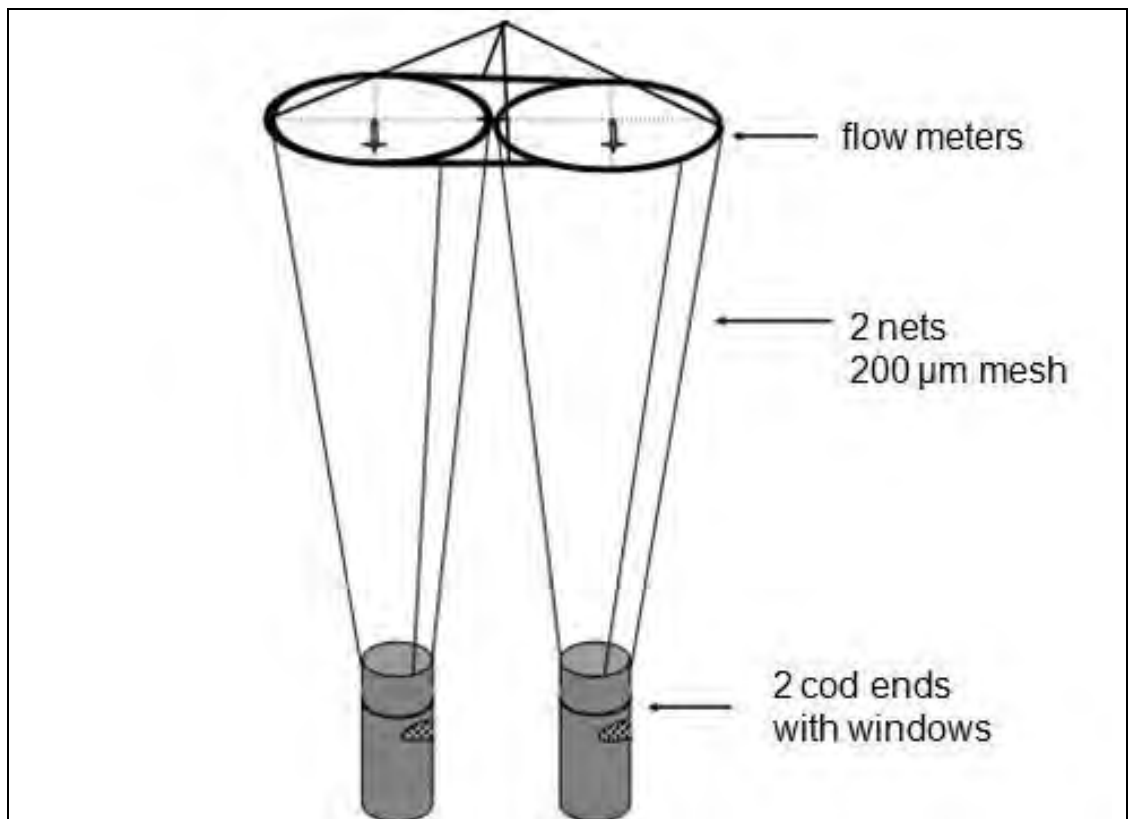


Figure 6.3. WP2 net with 200 μm mesh used during the CEAMARC – Pelagic voyage. Hauls were vertical between 0 – 200 m.

HYDRO-BIOS MultiNet

The HYDRO-BIOS MultiNet was deployed on the *TRV Umitaka Maru* and enabled the presence or absence of larvaceans in deeper water to be determined. The HYDRO-BIOS MultiNet consisted of 5 nets with 150 μ m mesh. Each net was remotely triggered at varying depths during horizontal trawls between the surface and bottom (Figure 6.4). The HYDRO-BIOS MultiNet was deployed 9 times at 8 stations with trawl depths dependent on bottom-depth. There were 6 successful deployments and retrievals with various sampling depths as listed in Table 6.1.

Table 6.1. Successful HYDRO-BIOS MultiNet deployment depths during CEAMARC. Depths in metres.

CEAMARC STATION	net 1	net 2	net 3	net 4	net 5
8	2000	1000	500	200	100
10	430	300	200	100	50
11	670	500	300	200	100
21	1775	1000	500	200	100
25	200	150	100	50	25
27	380	300	200	100	50

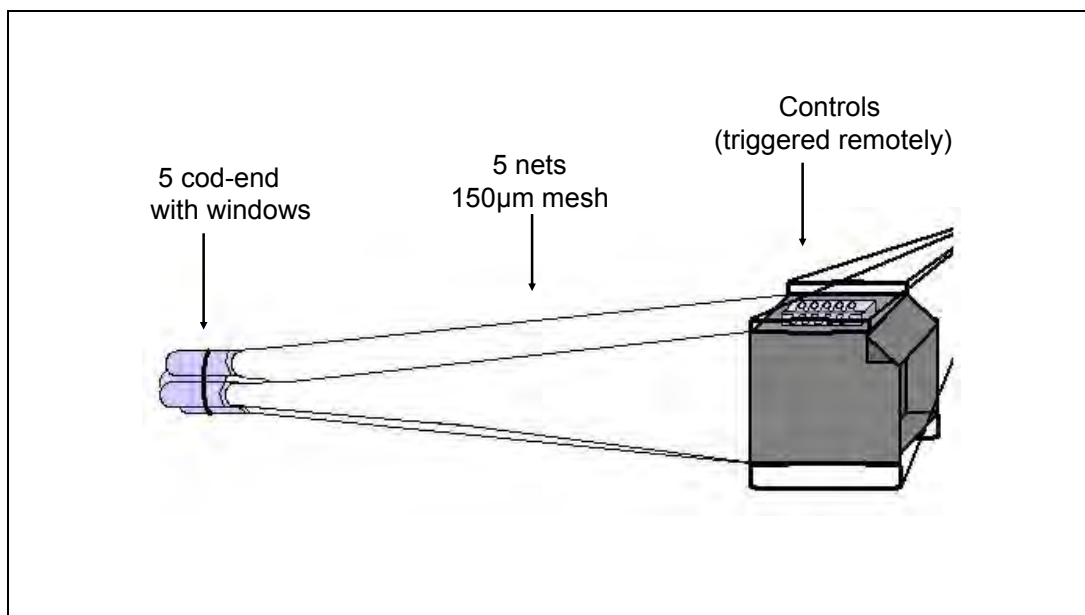


Figure 6.4. HYDRO-BIOS MultiNet with 150 μ m mesh. Horizontal trawls were conducted between the surface and bottom during the CEAMARC – Pelagic voyage.

Visual plankton recorder (VPR)

The VPR (Figure 6.5) provided *in situ* images of plankton in the water column and helped to determine the distribution of gelatinous zooplankton that are often damaged by other sampling devices. A stainless steel frame housed a CTD and two Autonomous Visual Plankton Recorders consisting of high definition video cameras and lights. VPR images were extracted from stations 10, 20 and 21 conducted aboard *TRV Umitaka Maru*. The images were extracted from the VPR hard drive and re-saved as JPEG2000 files using full frame extraction software (FFrExtr version 1.0.0.1, 20 June 2006 build) modified from the Auto Deck software (Seascan Video Plankton Recorder v.3.01 CTD:SeaBird49 or FSI NXIC). The JPEG2000 files are renamed and then converted into JPEG files using software Advanced Batch Converter (Version 3.9, build number 3.9.76, Gold Software Development) and then Particle analyses is applied to each image using Image-Pro Plus 6.3J (version 6.3.1.535, Media Cybernetics) using a macro routine developed by the Japan Agency for Marine-Earth Science and Technology (JAMSTEC). Auto Deck software (Seascan Video Plankton recorder v3.01 CTD: SeaBird49 or FSI NXIC) was used to extract ‘regions of interest’. Images of zooplankton were then identified by hand to taxon or species using an image browser (Thumbs Plus 6.0J).

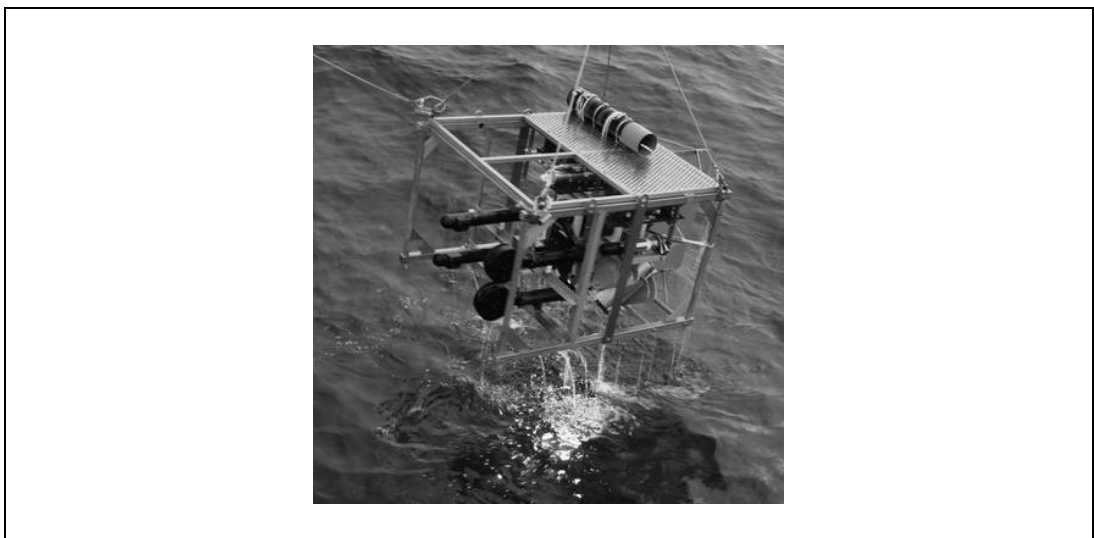


Figure 6.5. The Autonomous Video Plankton Recorder deployed during CEAMARC – Pelagic. It was housed in a stainless steel frame with cameras, lights and associated sensors. Photo: JAMSTEC

Continuous Plankton Recorder (CPR)

Details of the CPR are provided in Chapter 4. SO-CPR survey data included in this chapter was collected during the BROKE-West (2005/2006) and SIPEX (2007/2008) voyages aboard RSV *Aurora Australis*, and during the CEAMARC – Pelagic (2007/08) voyage aboard *TRV Umitaka Maru*.

CPR deployment on BROKE-West

The CPR was deployed eight times during this voyage (Figure 6.6). A 1200 Nm southbound transect was conducted between Fremantle, Western Australia (43.69°S, 93.03°E), and the BROKE-West survey region (60.53°S, 78.69°E). This consisted of three tows that were conducted in January 2006. An 1800 Nm transect was conducted on a northbound transect from the BROKE-West survey region (63.63°S, 80.12°E) to Hobart (47.40°S, 131.85°E). The northbound transect consisted of five tows and was conducted in March 2006 (Table 6.2).

Table 6.2. CPR tow details for BROKE-West

CPR	Start		Finish		Direction	Distance (Nm)
	Lat. (°S)	Long. (°E)	Lat. (°S)	Long. (°E)		
1	-43.69	93.03	-49.66	86.94	Sth	456.8
2	-49.77	86.93	-56.28	86.8	Sth	397.8
3	-56.38	86.82	-60.53	78.68	Sth	354.4
4	-63.62	80.12	-58.33	89.63	Nth	456
5	-58.29	89.8	-55.03	101.45	Nth	110
6	-54.98	101.65	-52.05	112.97	Nth	445.2
7	-52.01	113.13	-49.45	123.68	Nth	434
8	-49.42	123.83	-47.39	131.84	Nth	346.1

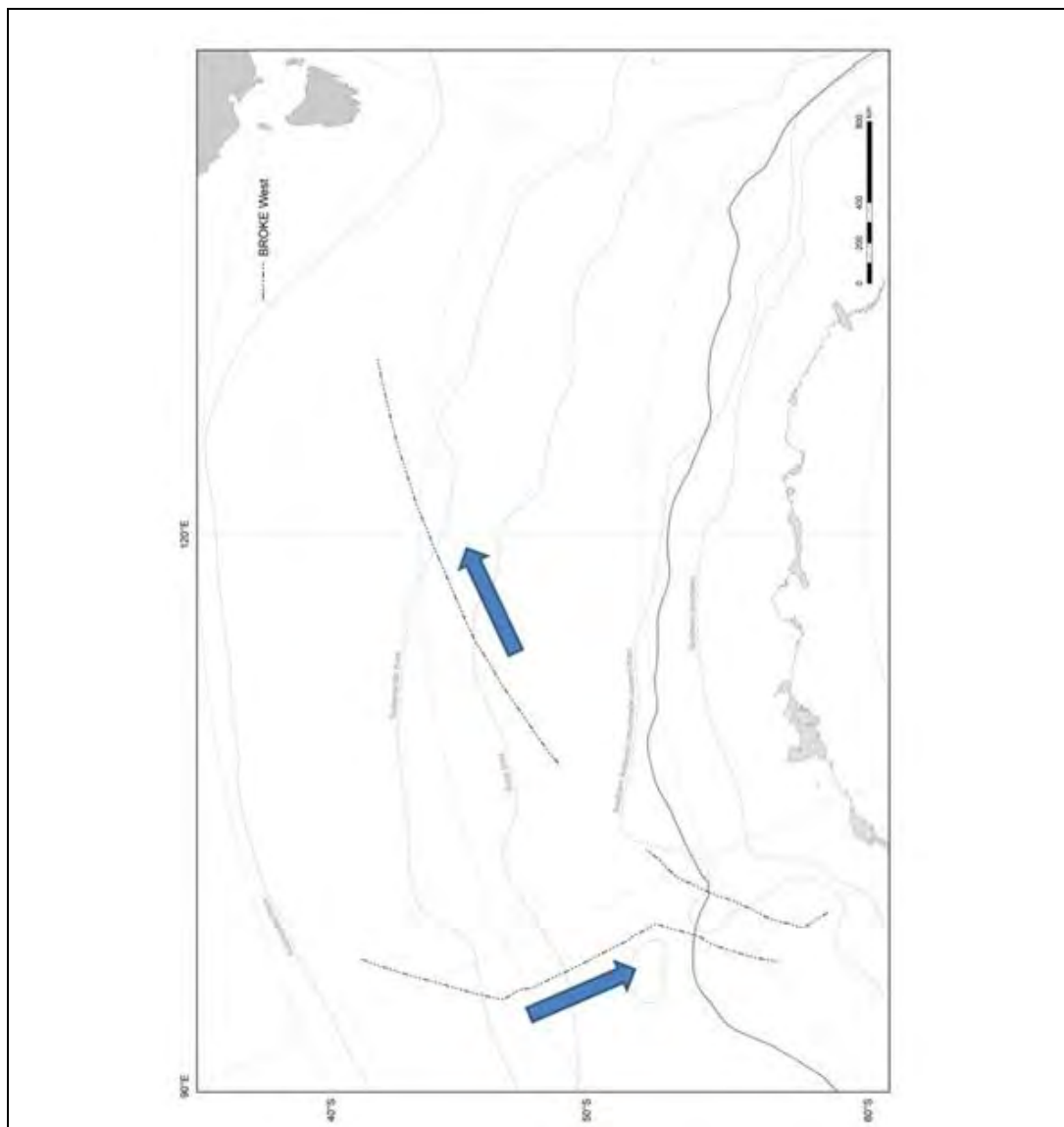


Figure 6.6. SO-CPR transects during the BROKE-West voyage aboard RSV *Aurora Australis*. The western transect was the southbound transect deployed in January 2006. The eastern transect was the northbound transect deployed in March 2006. A break in the northbound transect was due to the malfunction of a mechanism inside the CPR.

CPR deployment on SIPEX

The CPR was deployed six times during the SIPEX voyage aboard RSV *Aurora Australis* (Figure 6.7) covering a total of 1730 Nm. An 880 Nm southbound transect was conducted from Hobart (47.42°S, 144.52°E) to the start of the ice-edge/survey region (61.98°S, 129.03 °E). This consisted of three tows that were conducted in September 2007. An 850 Nm northbound transect was conducted from the survey region (58.84°S, 129.36°E) to Hobart (47.68°S, 142.81°E). This consisted of three tows conducted in October 2007 (Table 6.3).

Table 6.3. CPR tow details for SIPEX

CPR	Start		Finish		Direction	Distance (Nm)
	Lat. (°S)	Long. (°E)	Lat. (°S)	Long. (°E)		
1	-47.43	144.52	-50.5	141.65	Sth	242.9
2	-53.01	139.1	-58.89	132.57	Sth	423.5
3	-58.99	132.45	-61.98	129.03	Sth	210.4
4	-58.84	129.36	-52.26	137.86	Nth	493.1
5	-52.17	137.99	-51.32	138.85	Nth	65.7
6	-51.22	138.84	-47.68	142.81	Nth	291.9



Figure 6.7. SO-CPR transects during the SIPEX voyage aboard RSV *Aurora Australis*. The eastern transect was the southbound transect conducted in September 2007. The western transect was the northbound transect conducted in October 2007. A break in the southbound transect was due to the malfunction of a silk inside the CPR.

CPR deployment on CEAMARC

The CPR was deployed ten times during the CEAMARC–Pelagic voyage aboard *TRV Umitaka Maru* (Figure 6.8) covering 2600 Nm. A 1350 Nm southbound transect was conducted from Fremantle, Western Australia (42.86°S, 121.14°E) to the start of the survey region (61.99°S, 139.99°E). This consisted of four tows that were conducted in January 2008. A 1250 Nm transect was conducted on a northbound leg from the survey region (62.72°S, 143.61°E) to Hobart (44.85°S, 147.31°E). This consisted of six tows conducted in February 2008 (Table 6.4).

Table 6.4. CPR tow details for CEAMARC – Pelagic

CPR	Start		Finish		Direction	Distance (Nm)
	Lat. (°S)	Long. (°E)	Lat. (°S)	Long. (°E)		
1	-42.86	121.14	-47.91	125.38	Sth	359.7
2	-47.97	125.42	-53.13	130.14	Sth	366.5
3	-53.21	130.26	-57.94	135.13	Sth	335.5
4	-58.02	135.25	-61.99	139.99	Sth	283
5	-65.36	142.95	-62.79	143.56	Nth	160
6	-62.72	143.61	-60.52	144.25	Nth	139.1
7	-60.14	144.28	-55.03	145.32	Nth	331.8
8	-54.95	145.34	-51.05	146.17	Nth	240.8
9	-50.97	146.2	-49.73	146.49	Nth	80.2
10	-49.64	146.52	-44.85	147.31	Nth	294.8

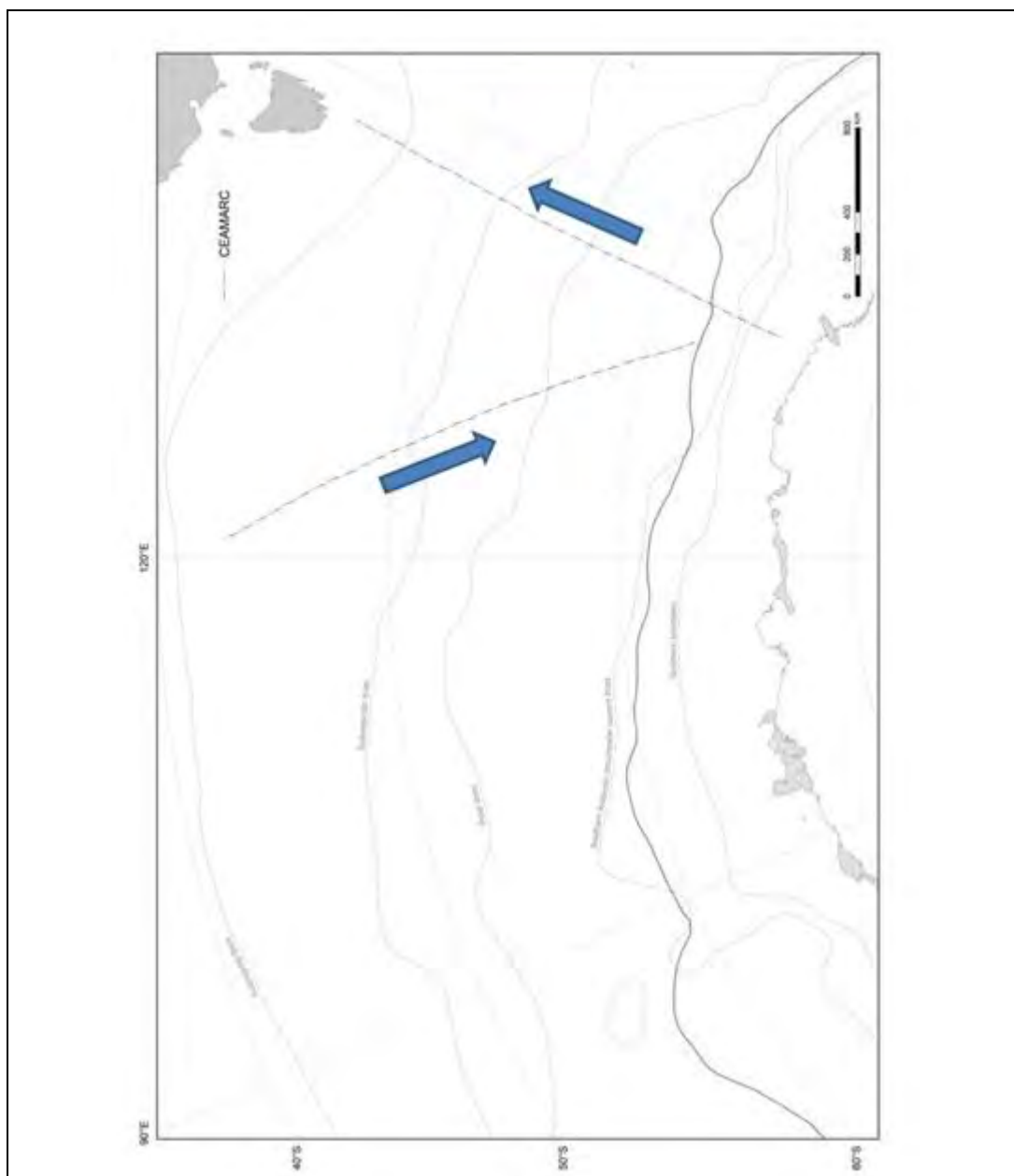


Figure 6.8. SO-CPR transects during the CEAMARC–Pelagic voyage aboard *TRV Umitaka Maru*. The western transect was the southbound transect deployed in January 2008. The eastern transect was the northbound transect deployed in February 2008.

6.2.3 Processing and preservation of samples

The ring net was rinsed with seawater before the cod-end was removed. The contents of the cod-end were then observed under light microscope. Visible larvaceans were separated and preserved in 5% buffered formalin and seawater during SAZ-Sense and SIPEX. During BROKE-West, larvaceans were preserved in 2.5 % buffered formalin and seawater (the change in percentage was due to recommendations from fellow zooplankton researchers) or absolute ethanol. Larvaceans abundance levels from the ring net were converted to ind. m⁻³ by dividing the larvacean count by the volume filtered by the ring net.

Cod-ends from RMT trawls during SAZ-Sense were processed similarly to ring net samples, with visible larvaceans separated and preserved in 5% buffered formalin and seawater, or in absolute ethanol. Entire RMT1 catches from BROKE-West were preserved without any sorting on board apart from the removal of large cnidarians and salps. This was because the target species, euphausiid larvae, were often caught up in mucous or body parts of other zooplankton. Proper identification and counting of larvaceans in the whole sample was later achieved using a stereo dissecting microscope in the laboratory. The identification level of larvaceans from the RMT1 was to genus, or recorded as ‘larvacean’ depending on the condition of the individual. Larvacean abundance levels were converted to ind. m⁻³ by dividing the RMT1 larvacean net count by the volume filtered.

A random selection of individual larvaceans from the BROKE-West voyage were prepared for Scanning Electron Microscopy (SEM); See Chapter 7 for details. In addition, the preservation and processing of CPR samples were detailed in Chapter 4.

6.2.4 Physical parameters

Physical oceanographic parameters were measured using a CTD at each oceanographic station. The CTD was a General Oceanics Mark II probe and sampled from the sea surface to near-bottom. The parameters measured included temperature, salinity, oxygen, fluorescence and photosynthetically active radiation (PAR). CTD data were extracted for similar depths to that of ring net deployments. Details of physical oceanographic data processing were presented in Rosenberg (2006).

The same parameters as measured using the CTD were also measured whilst the ship was underway using shipboard meters. Underway data provided surface values only and was logged at one minute intervals. For CPR data, larvacean abundance measurements were directly comparable to the physical oceanographic data logged at one minute intervals. For ring net deployments, ten minute averages of underway data were utilised. For the RMT1, underway data from the closest hour to deployment were utilised. PAR values measured on the port and starboard side of the ship were analysed to reduce the influence of ship shadow on measurements.

During SAZ-Sense, 12 CTD casts were able to be made at the same location as 12 RMT trawls and 18 ring net deployments. During BROKE-West, 118 CTDs were conducted and all corresponded with RMT and ring net deployments. During SIPEX, underway data was used for measurements of physical oceanography as the survey design did not have regular CTD deployments. For the CEAMARC–Pelagic voyage, only underway temperature data were available.

6.2.5 Data analysis

The abundance and distribution of larvaceans were compared with physical parameters using Pearson's r correlation. Relationships were examined according to the sampling device used, latitude, longitude, and available underway data (temperature, salinity, fluorescence and PAR). Ring net abundances were also tested for correlations with CTD data from corresponding depths. SAZ-Sense

larvacean abundances were also compared against chlorophyll *a* levels shown in Figure 6.9, as determined using SeaWiFS.

Larvacean distribution maps from CPR data were produced for each voyage undertaken. Each graduated symbol represents 5 Nm sections. Pearson's *r* correlations were again used to determine if there were significant linear relationships between larvacean abundances from CPR tows and latitude, longitude, and corresponding underway data (temperature, salinity, fluorescence and irradiance).

6.3 Results

6.3.1 Distribution and abundance of larvaceans from SAZ-Sense

Ring net deployments in the SAZ during the SAZ-Sense voyage (Figure 6.10) showed that larvacean abundances were high in the west and low in the east. RMT trawls showed a similar pattern (Figure 6.11) with the same relative abundances.

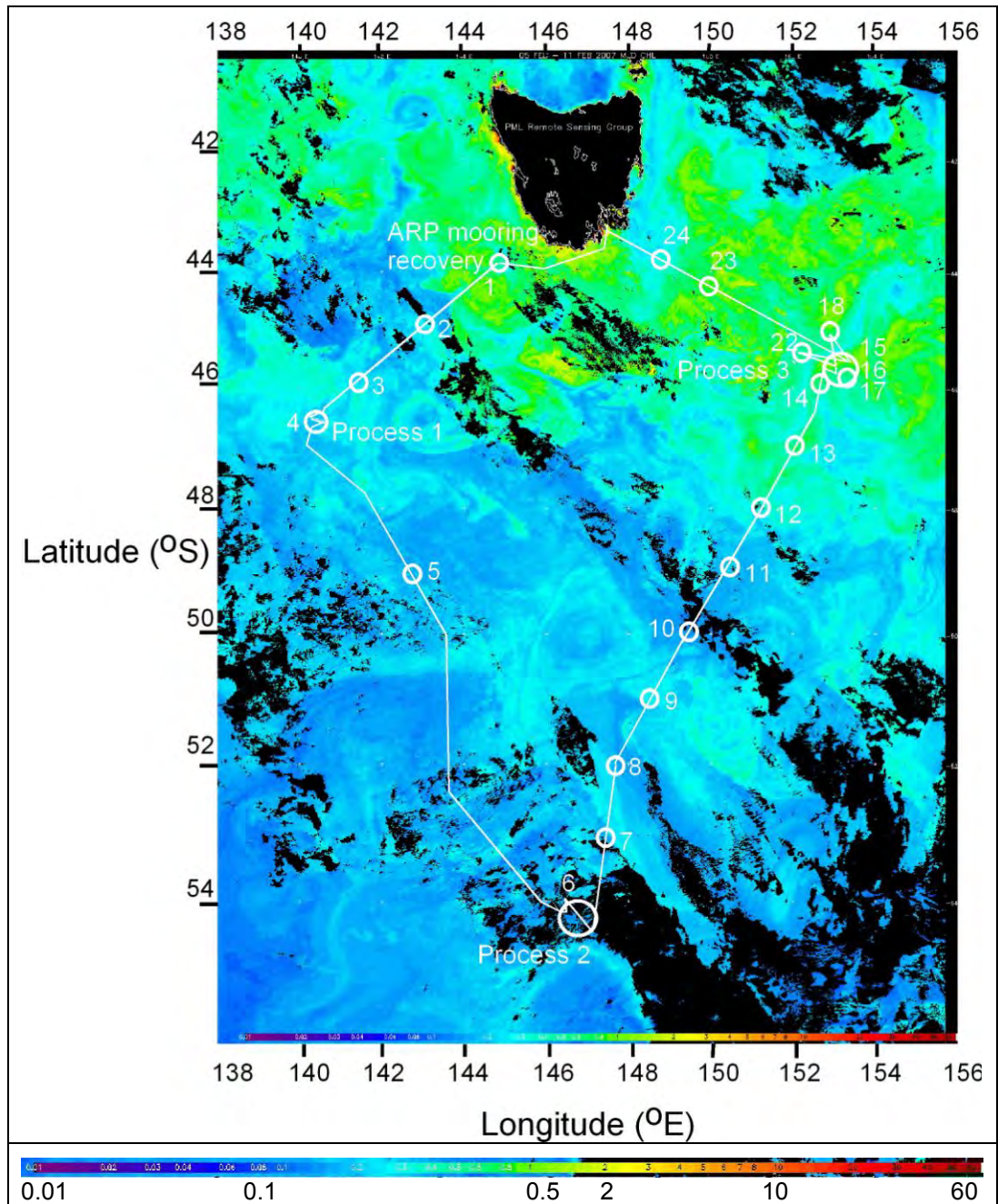


Figure 6.9. SAZ-Sense voyage track and sample sites (circles) overlaid on a MERIS ocean colour composite image (SeaWiFS) with 1 km resolution (ESA satellite). Data is for the period 5-11 February 2007 and was processed by the PML Remote Sensing Group. The colour scale at the bottom of the image is a logarithmic scale between 0.01 and 60 $\mu\text{g chlorophyll } a \text{ l}^{-1}$ (source Bowie et al., in press).

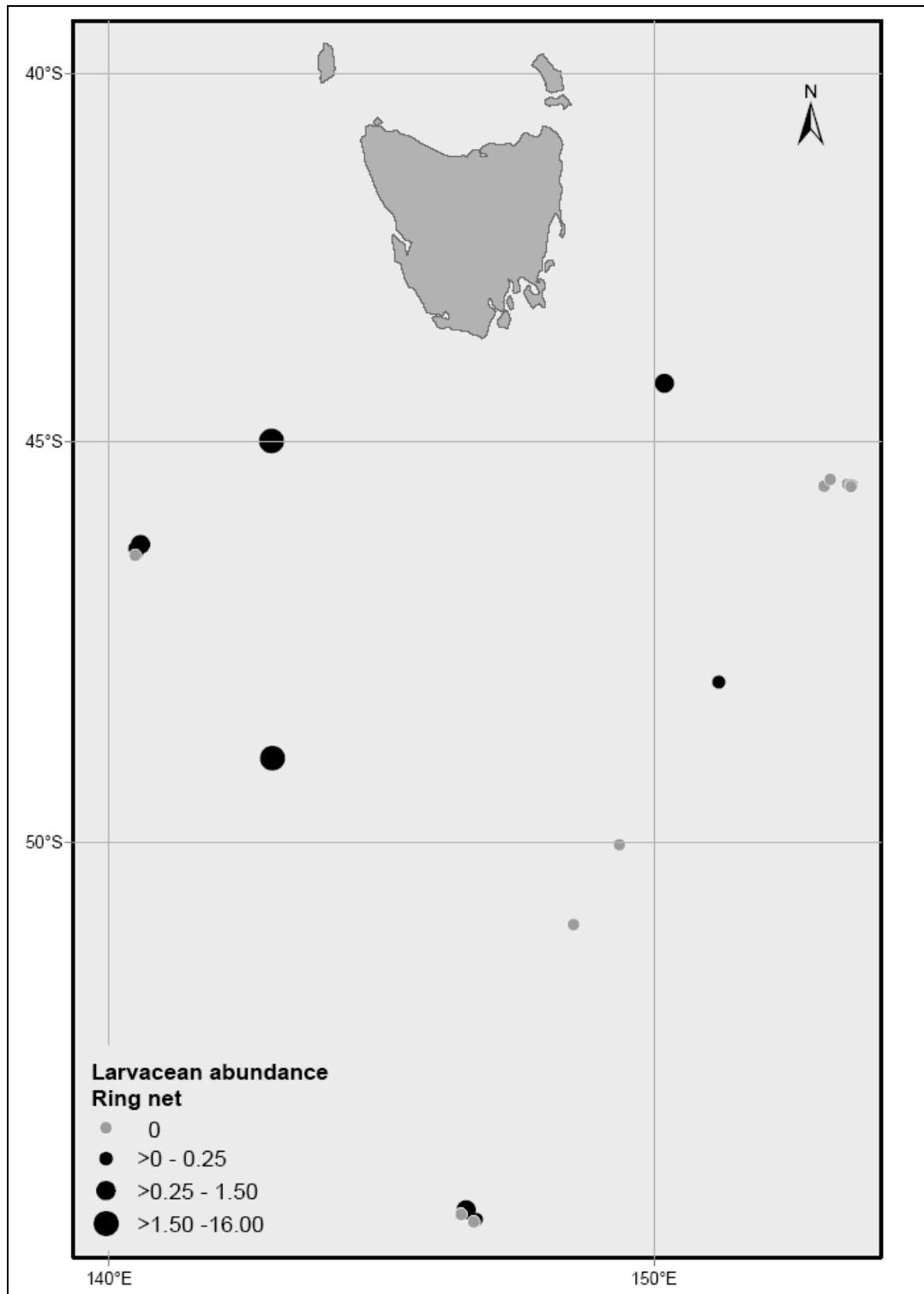


Figure 6.10. Larvacean abundances (ind. m^{-3}) determined using a ring net. Abundances were high in the west and low in the east. Data obtained during the SAZ-Sense voyage from 17 January to 20 February 2007, aboard RSV *Aurora Australis*. Figure adapted from the Australian Antarctic Data Centre.

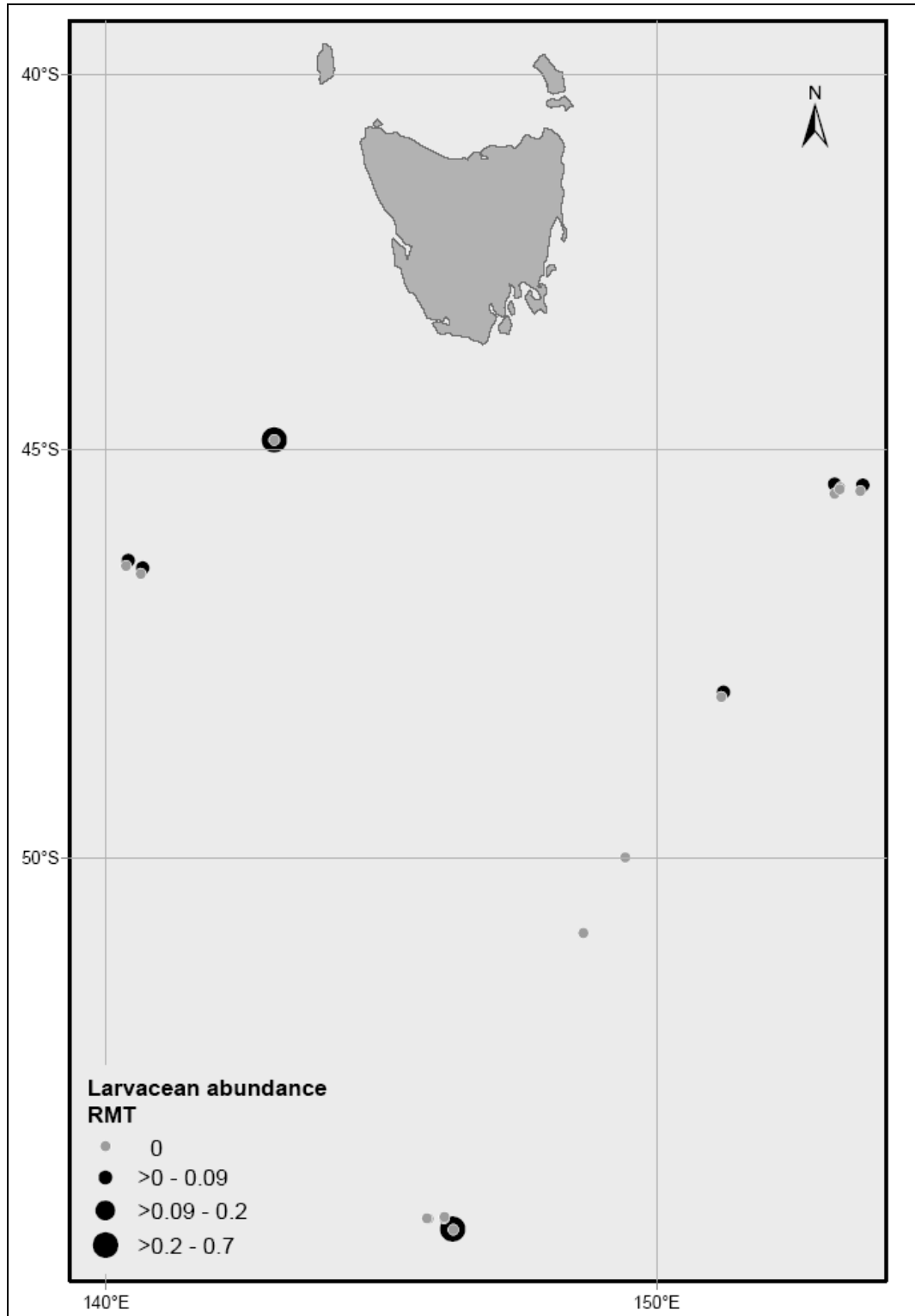


Figure 6.11 Larvaceans abundances (ind. m^{-3}) determined using RMT1 trawls. Abundances were high in the west and low in the east. Data obtained during the SAZ-Sense voyage from 17 January to 20 February 2007, aboard RSV *Aurora Australis*. Figure adapted from the Australian Antarctic Data Centre.

Diel distribution of larvaceans during SAZ-Sense

Diel studies of larvaceans were undertaken at three process stations shown in Chapter 2 (Figure 2.17). At process station one (Figure 6.12 A, Table 6.5) data from ring nets deployed to 20 m suggested that diel vertical migration did occur. The highest abundance was at midnight with 0.7 ind. m^{-3} . The abundance decreased to 0.25 ind. m^{-3} at both sunrise and midday. At sunset there were no larvaceans present. At process station 2, the highest abundance of larvaceans occurred at sunrise (Figure 6.12 B, Table 6.5). At process station 3 there were no larvaceans recorded.

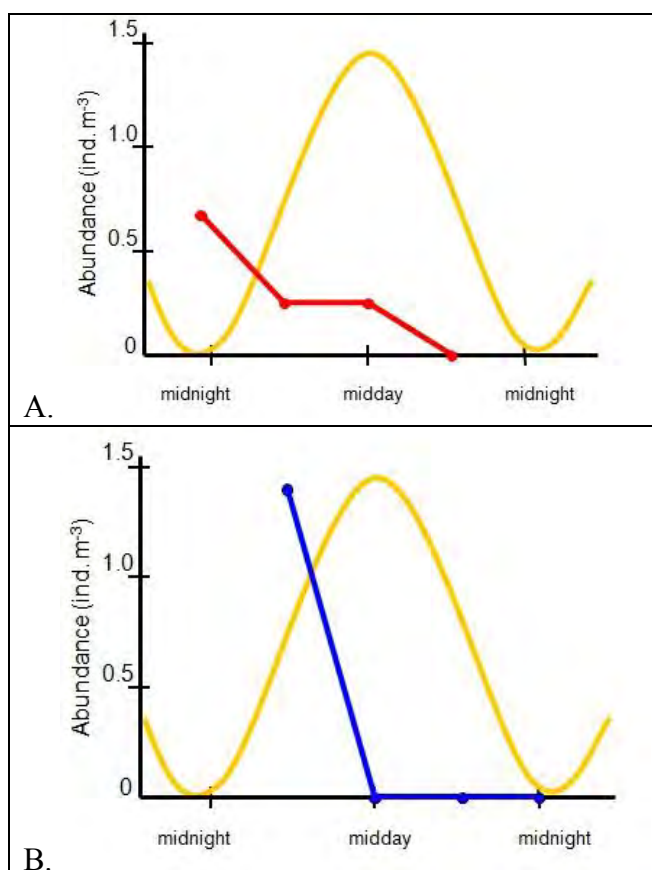


Figure 6.12. Diel abundance of larvaceans at 20 m during the SAZ-Sense voyage. (A) process station one (B) process station two. The curved yellow line represents light availability as a relative concentration to time.

Table 6.5. Diel vertical migration of larvaceans during SAZ-Sense

time	PROCESS 1 (ind. m ⁻³)	PROCESS 2 (ind. m ⁻³)	PROCESS 3 (ind. m ⁻³)
Sunset			0
Midnight	0.7		0
Sunrise	0.3	1.4	0
Midday	0.3	0	0
Sunset	0	0	0
Midnight		0	
	High abundance	Low abundance	No larvaceans

Stratified distribution of larvaceans during SAZ-Sense

Stratification was also examined at process stations during SAZ-Sense. At process station one, the highest abundance occurred from the ring net deployed to 20 m with 0.7 ind. m^{-3} . This decreased to 0.05 ind. m^{-3} at 50 m and $0.025 \text{ ind. m}^{-3}$ at 100 m (Figure 6.13 A, Table 6.6). In contrast, at process station two the highest abundance of larvaceans occurred at 100 m and there were none present at shallower depths (Figure 6.13 B, Table 6.6).

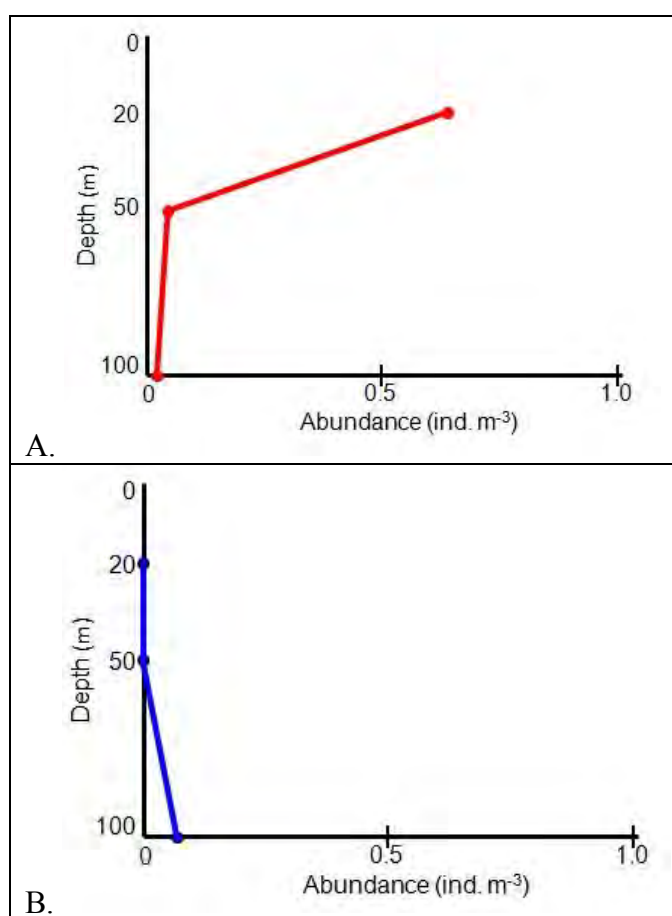


Figure 6.13. Abundance of larvaceans with depth during the SAZ-Sense voyage. (A) process station one (B) process station two.

Table 6.6. Abundance of larvaceans with depth during the SAZ-Sense voyage

depth	PROCESS 1 (ind. m ⁻³)	PROCESS 2 (ind. m ⁻³)	PROCESS 3 (ind. m ⁻³)
20	0.7	0	0
50	0.05	0	0
100	0.03	0.09	0

Physical and biological parameters during SAZ-Sense

There were no statistically significant linear relationships found between larvacean abundances and underway or CTD physical oceanographic data (Table 6.7), although, for ring net data there was almost a significant relationship with longitude.

Table 6.7. Pearson's r correlations between larvacean abundances from each sampling device, and environmental parameters measured during SAZ-Sense. UW = underway data, CTD = data measured using the CTD during ring net deployments. **Bold** indicates a significant relationship (ns = not significant), $\alpha=0.05(2)$.

Parameter	r	df	p
Ring Net (<i>critical r = 0.367</i>)			
Latitude	0.04	25	ns
Longitude	0.28	25	ns
UW - irradiance	0.03	25	ns
UW - Fluorescence			
UW - Temperature			
UW - Salinity	0.04	25	ns
CTD - Conductivity	0.06	25	ns
CTD - Temperature	0.08	25	ns
CTD - Salinity		25	ns
CTD - PAR	0.06	25	ns
CTD - Fluorescence		25	ns
CTD - Oxygen	0.02	25	ns
Rectangular Mid-water Trawl 1 (RMT1) (<i>critical r = 0.423</i>)			
Latitude	0.13	20	ns
Longitude	0.21	20	ns
UW - irradiance	0.18	20	ns
UW - Fluorescence	0.03	20	ns
UW - Salinity	0.09	20	ns
CTD - Conductivity	0.06	20	ns
CTD - Temperature	0.06	20	ns
CTD - Salinity	0.06	20	ns
CTD - PAR	0.25	20	ns
CTD - Fluorescence	0.03	20	ns
CTD - Oxygen	0.07	20	ns

6.3.2 Distribution and abundance of larvaceans from BROKE-West

Distribution and abundance maps of larvaceans from the BROKE-West voyage were shown in Chapter 5. A total of 47 ring net (Figure 5.4) deployments were undertaken. RMT1 trawls (Figure 5.5) were also conducted at the same sites and at a similar time of day. The abundance of larvaceans varied within the BROKE-West survey area, ranging from 0 - 5.4 ind. m⁻³ in ring net samples, and 0 - 57.8 ind. m⁻³ for RMT1 samples. Ring net samples generally returned significantly lower larvacean abundances than RMT1 samples. The average larvacean abundance from ring net samples was 0.5 (± 0.8) ind. m⁻³, and for RMT1 samples 6.7(± 8.2) ind. m⁻³.

BROKE-West CPR larvacean abundances were graphed in Figure 5.6 in Chapter 5. Two transects are also shown in Figures 6.14A and B below, with values presented in Table 6.8.

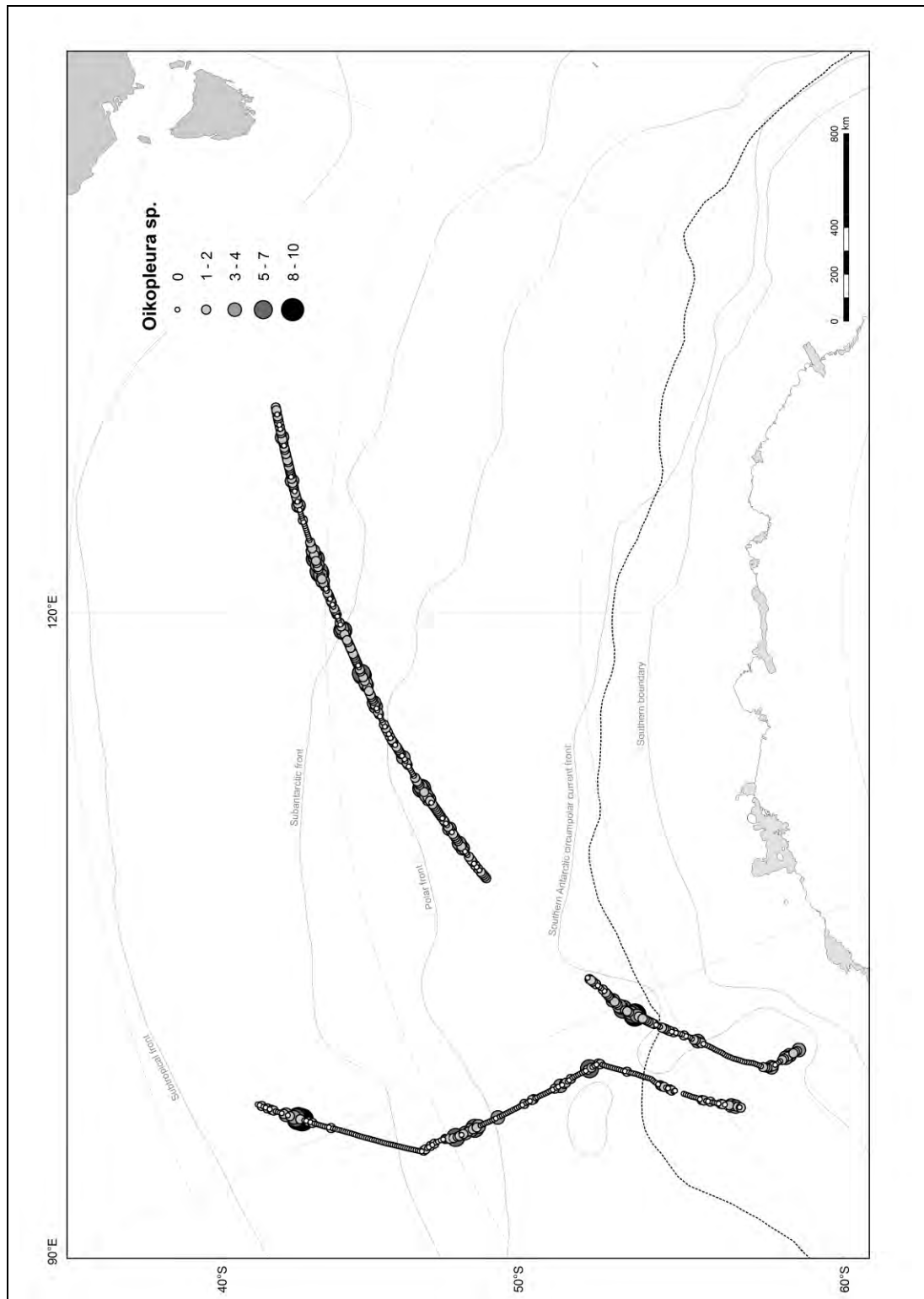


Figure 6.14 A. SO-CPR BROKE-West distribution and abundance maps of Southern Ocean *Oikopleura* sp. Abundance is in counts per 5 Nm.

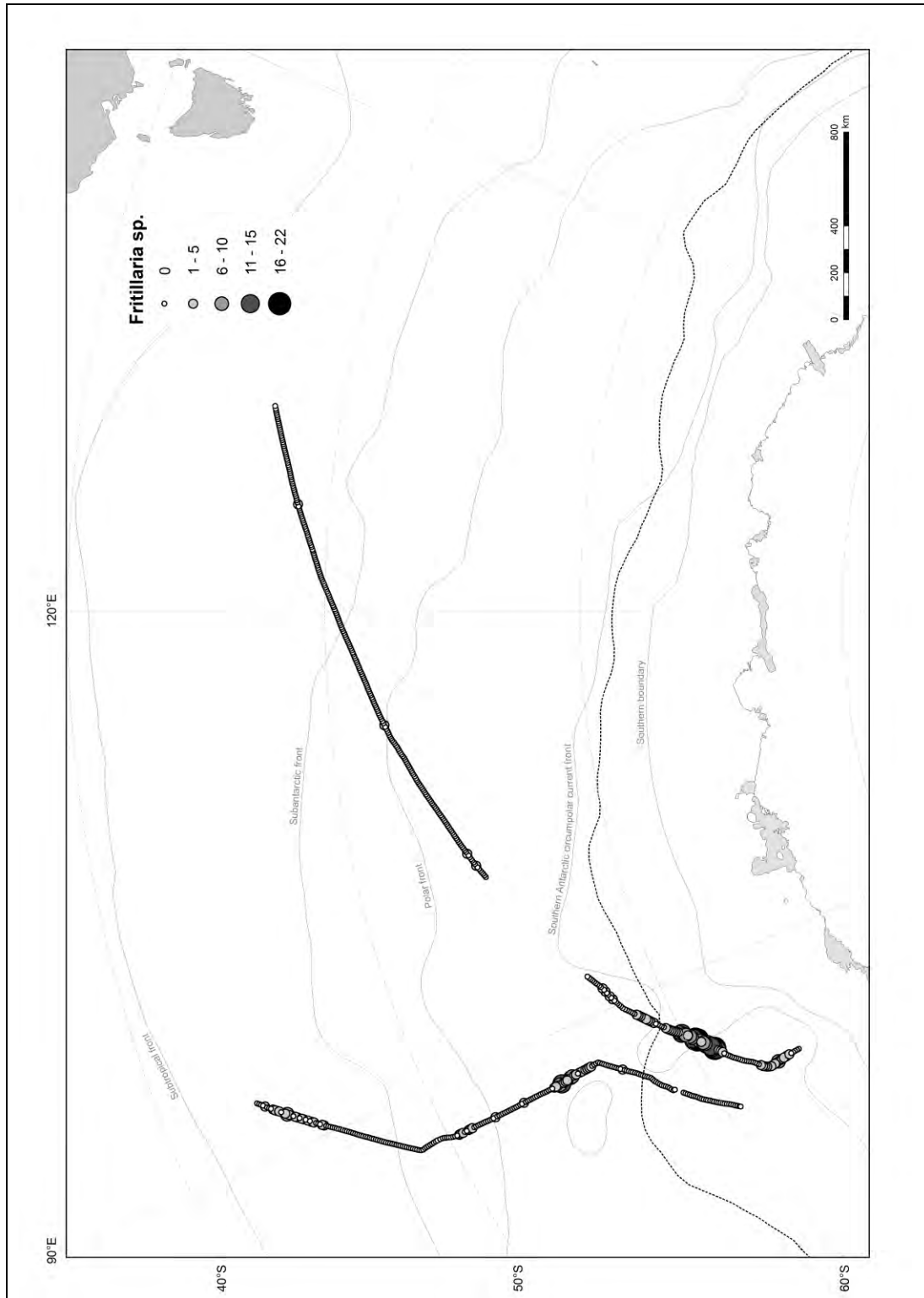


Figure 6.14 B. SO-CPR BROKE-West distribution and abundance maps of Southern Ocean *Fritillaria* sp. Abundance is in counts per 5 Nm.

Table 6.8. BROKE-West CPR transect summary

MONTH - Transect direction	<i>Fritillaria</i> sp.		<i>Oikopleura</i> sp.		Total larvaceans		Total zooplankton	
	ind. m ³	std (±)	ind. m ³	std (±)	ind. m ³	std (±)	ind. m ³	std (±)
January - southbound	0.4	1	0.4	0.9	0.8	1.5	126.3	109.8
March - northbound	0.6	1.9	0.8	0.9	1.4	2.1	66.7	76.1
Overall mean	0.5	1.6	0.7	0.9	1.2	1.9	90.8	95.7

Physical and biological parameters during BROKE-West

In Chapter 5 it was demonstrated that there were significant Pearson's r correlations between larvacean abundance and sampling location for the ring net and RMT. Physical parameters from underway and CTD data were also detailed in Chapter 5. In Table 6.9, parameters that were significant are again presented, showing that latitude had a significant effect on larvacean abundance, as determined from both ring net and RMT1 data.

Table 6.9. Pearson's r correlations between larvacean abundances and environmental parameters. Data collected using a ring net and RMT1. **Bold** indicates a significant relationship (ns = not significant), $\alpha=0.05(2)$.

Parameter	r	df	p
Ring Net (<i>critical r = 0.288</i>)			
Latitude	0.2944	45	0.02 < p < 0.05
UW - Fluorescence	0.2665	45	ns
Rectangular Mid-water Trawl 1 (RMT1) (<i>critical r = 0.288</i>)			
Latitude	0.4366	45	0.002 < p < 0.005
Longitude	0.4110	45	0.002 < p < 0.005

There were no significant relationships between larvacean abundances determined using CPR tows and environmental parameters determined from underway data (Table 6.10). This work is also shown in Lindsay and Williams (2010).

Table 6.10. Pearson's r correlations between larvacean abundances determined from eight CPR tows during BROKE-West, and environmental parameters determined from underway data. **Bold** indicates a significant relationship (ns = not significant), $\alpha=0.05(2)$.

Parameter	r	df	p
Continuous Plankton Recorder (CPR) (<i>critical r = 0.666</i>)			
Latitude	0.58	6	ns
Longitude	0.41	6	ns
Irradiance	0.26	6	ns
Fluorescence	0.63	6	ns
Temperature	0.39	6	ns
Salinity	0.40	6	ns

6.3.3 Distribution and abundance of larvaceans from SIPEX

The abundance and distribution of larvaceans determined using the ring net and RMT during the SIPEX voyage are mapped in Figure 6.15. Figures 6.16 and 6.17 show abundances for *Oikopleura* sp. and *Fritillaria* sp., respectively. The data shows that early and late in the voyage, larvacean abundances were very low at the eastern longitudes.

The abundance and distribution of *Oikopleura* sp. and *Fritillaria* sp. determined using CPR during the SIPEX voyage are shown in Figures 6.18 A and B, respectively. Table 6.11 lists larvacean and zooplankton abundances for each tow undertaken. Table 6.12 lists larvacean and zooplankton abundances averaged over each transect.

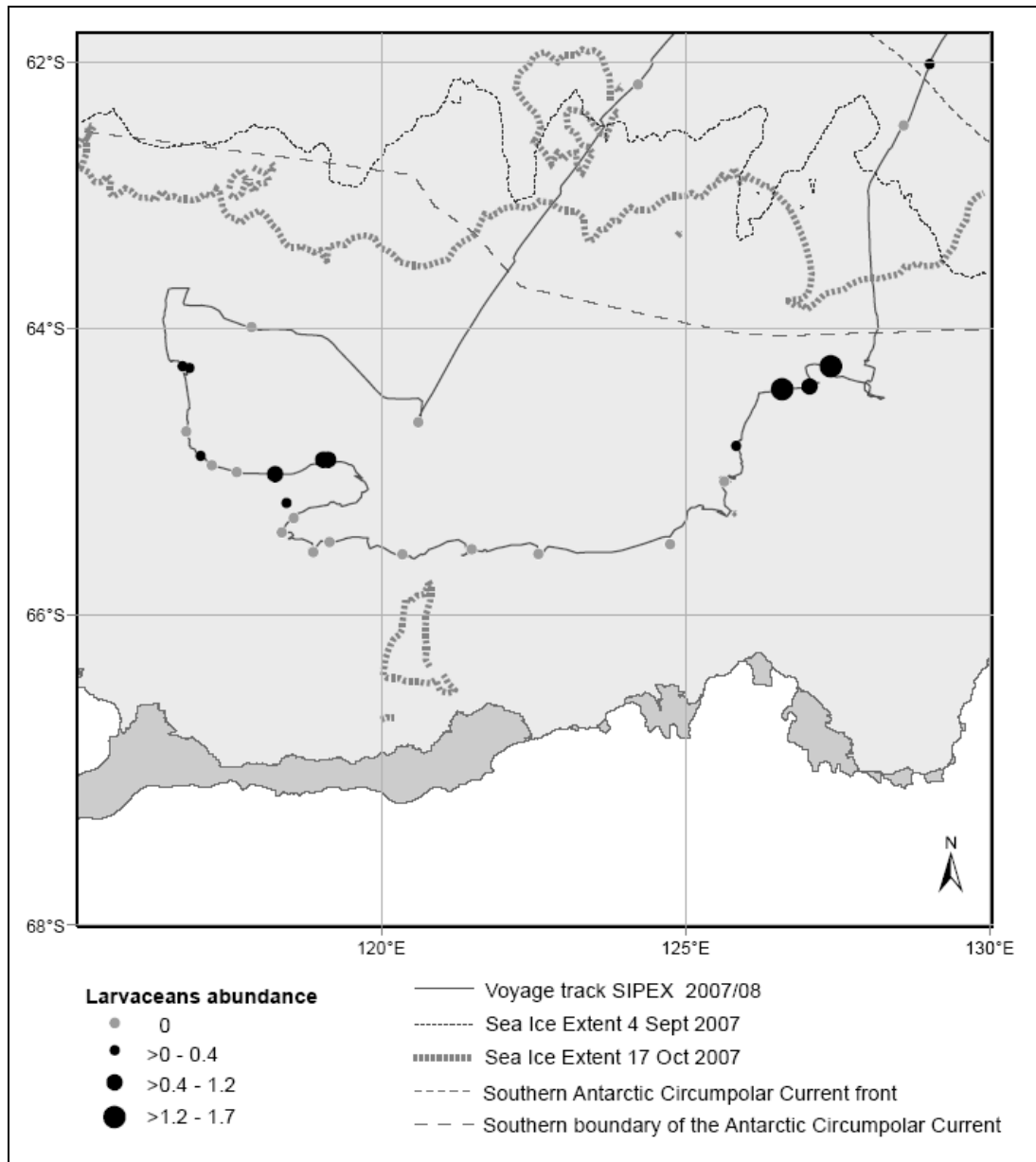


Figure 6.15. Larvacean abundances (ind. m^{-3}) determined from ring net samples during the SIPEX voyage. The voyage was conducted from 4 September to 17 October 2007 aboard RSV *Aurora Australis*. Figure adapted from the Australian Antarctic Data Centre.

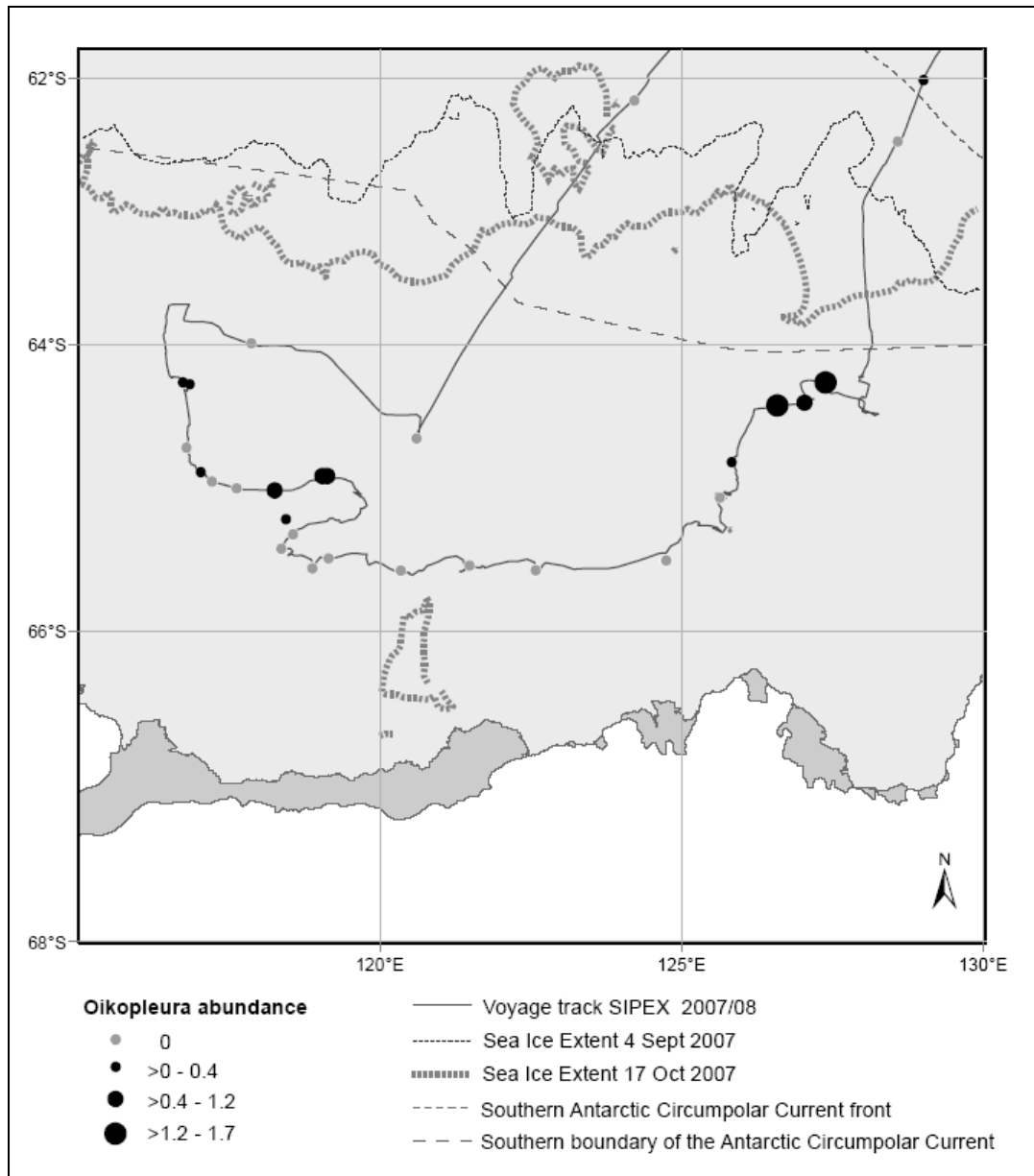


Figure 6.16. *Oikopleura* sp. abundances (ind. m⁻³) determined from ring net samples during the SIPEX voyage. The voyage was conducted from 4 September to 17 October 2007 aboard RSV *Aurora Australis*. Figure adapted from the Australian Antarctic Data Centre

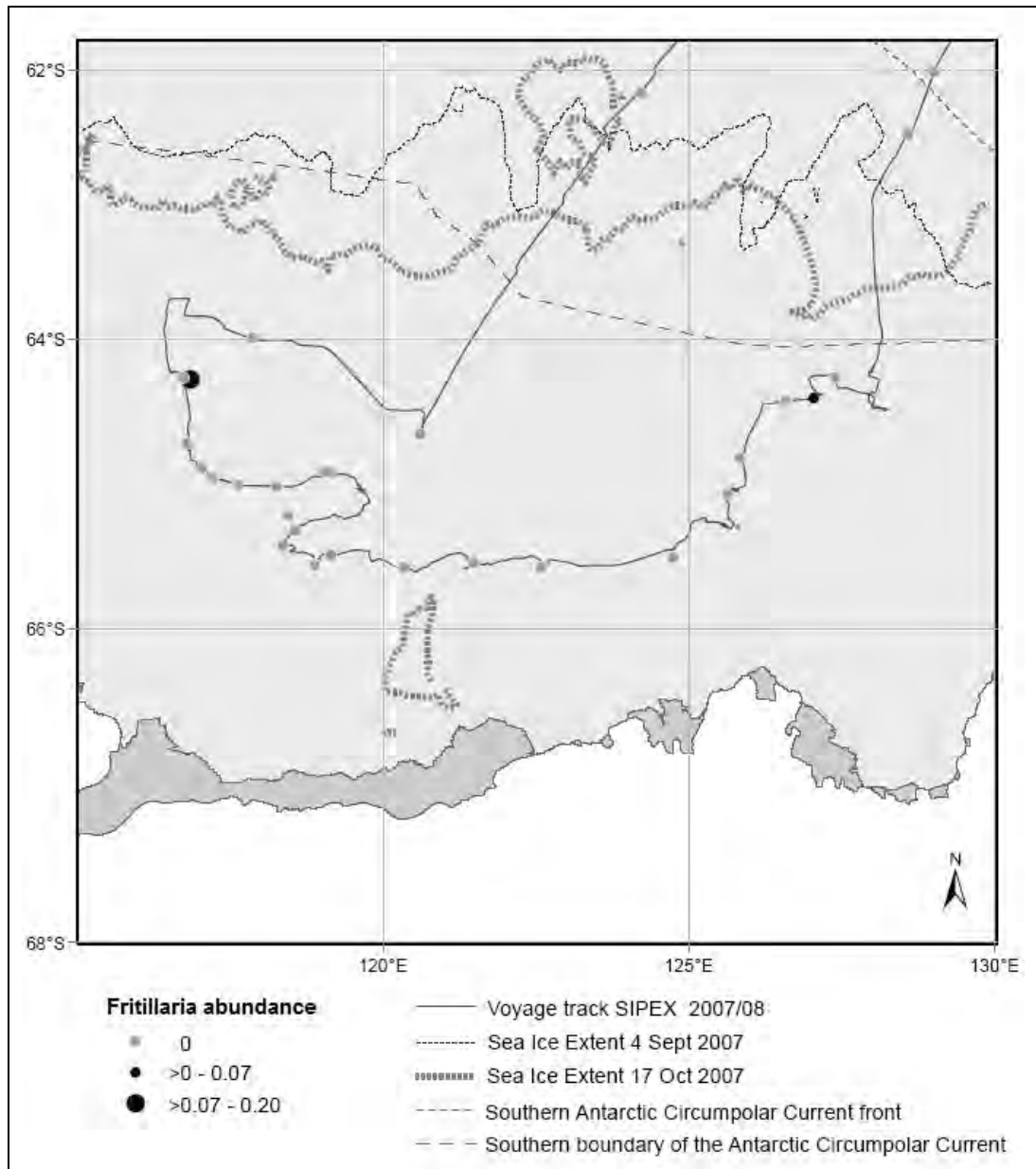


Figure 6.17. *Fritillaria* sp. abundances (ind. m⁻³) determined from the ring net samples during the SIPEX voyage. The voyage was conducted from 4 September to 17 October 2007 aboard RSV *Aurora Australis*. Figure adapted from the Australian Antarctic Data Centre

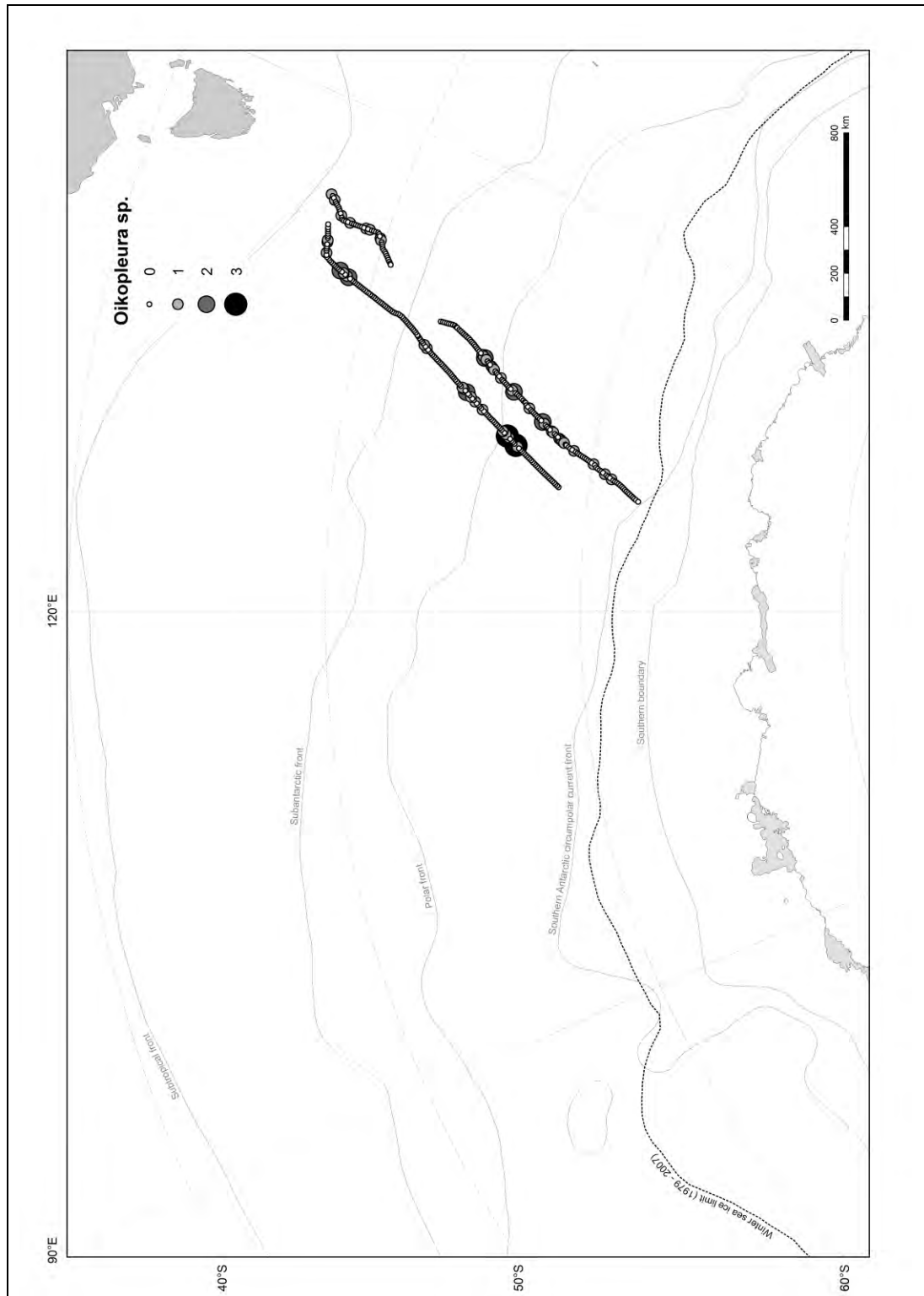


Figure 6.18 A. *Oikopleura* sp. abundances determined using CPR during the SIPEX voyage. Abundance is in counts per 5 Nm.

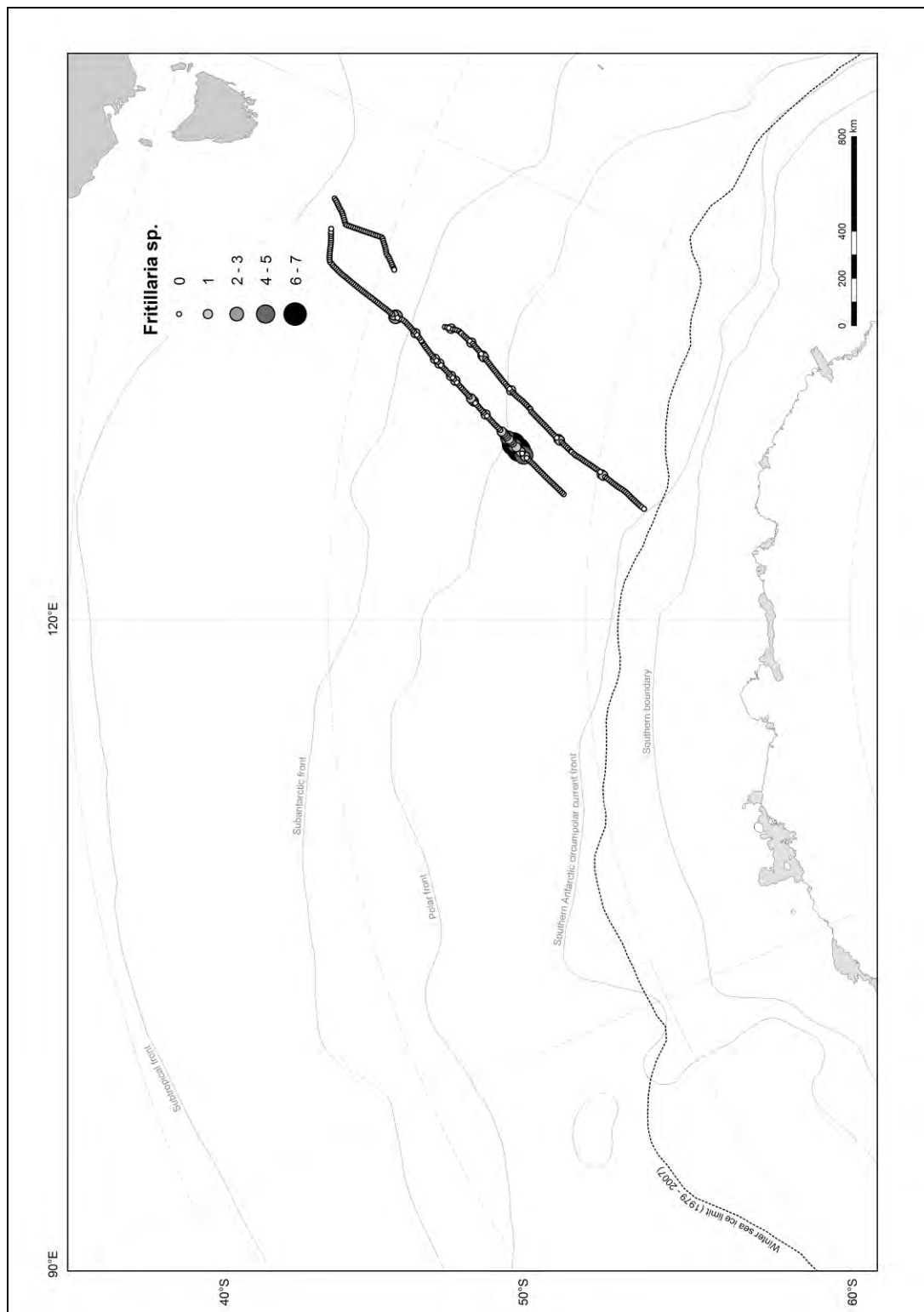


Figure 6.18 B. *Fritillaria* sp. abundances determined using CPR during the SIPEX voyage. Abundance is in counts per 5 Nm.

Table 6.11. Average *Fritillaria* sp., *Oikopleura* sp. and larvacean abundances determined using CPR during the SIPEX voyage. Data are shown for each tow undertaken.

CPR	Start		Finish		Distance (Nm)	<i>Fritillaria</i> sp. (ind. m ⁻³)	<i>Oikopleura</i> sp. (ind. m ⁻³)	Larvaceans (ind. m ⁻³)
	Lat. (°S)	Long. (°E)	(Nm)	Long. (°E)				
1	-47.43	144.52	-50.50	141.65	242.9	0.0	0.1	0.1
2	-53.01	139.10	-58.89	132.57	423.5	0.1	0.2	0.2
3	-58.99	132.45	-61.98	129.03	210.4	0.0	0.1	0.1
4	-58.84	129.36	-52.26	137.86	493.1	0.3	0.1	0.5
5	-52.17	137.99	-51.32	138.85	65.7	0.1	0.0	0.1
6	-51.22	138.84	-47.68	142.81	291.9	0.0	0.1	0.2

Table 6.12. Average *Fritillaria* sp., *Oikopleura* sp. and larvacean abundances determined using CPR during the SIPEX voyage. To determine transect averages, data from each tow within the same transect were pooled.

MONTH - Transect direction	<i>Fritillaria</i> sp.		<i>Oikopleura</i> sp.		Total larvaceans		Total zooplankton	
	ind. m ³	std (±)	ind. m ³	std (±)	ind. m ³	std (±)	ind. m ³	std (±)
September - southbound	0	0.2	0.1	0.3	0.2	0.3	22.5	18.7
October - northbound	0.2	0.7	0.1	0.3	0.3	0.8	50.5	43.6
Grand total	0.1	0.5	0.1	0.3	0.2	0.6	36.2	36.1

Physical and biological parameters during SIPEX

Significant relationships were found between larvacean abundances determined using a ring net and fluorescence, and irradiance (Table 6.13). The western area of the survey region (stations 7, 9, 10, 11 and 13; Figure 6.3) was sampled later in the season.

Table 6.13. Pearson's *r* correlations between larvacean abundances determined using a ring net, and environmental parameters during the SIPEX voyage. UW= underway data. **Bold** indicates a significant relationship (ns = not significant), $\alpha=0.05(2)$.

Parameter	<i>r</i>	df	<i>p</i>
Ring Net (<i>critical r</i> = 0.355)			
Latitude	0.17	29	ns
Longitude	0.34	29	ns
UW - irradiance	0.47	29	0.005 < ρ < 0.01
UW - Fluorescence	0.41	29	0.02 < ρ < 0.05
UW - Temperature	0.03	29	ns
UW - Salinity	0.08	29	ns

Larvacean abundances determined using CPR were significantly correlated with latitude, longitude, fluorescence, temperature and salinity (Table 6.14).

Table 6.14. Pearson's r correlations between larvacean abundances determined using CPR segments and environmental parameters determined from underway data during the SIPEX voyage. **Bold** indicates a significant relationship (ns = not significant), $\alpha=0.05(2)$.

Parameter	r	df	p
Continuous Plankton Recorder (CPR) (<i>critical r = 0.105</i>)			
Latitude	0.10	345	0.05 < p < 0.10
Longitude	0.14	345	0.005 < p < 0.01
Irradiance	0.09	345	ns
Fluorescence	0.18	345	0.001 < p
Temperature	0.11	345	0.02 < p < 0.05
Salinity	0.13	345	0.001 < p < 0.02

6.3.4 Distribution and abundance of larvaceans from CEAMARC-Pelagic

Larvaceans were present at 17 of 23 sites sampled within the CEAMARC – Pelagic survey region which was in the SIZ (Figure 6.19). Both *Fritillaria borealis* typica and *Oikopleura gaussica* were captured using the WP2. The HYDRO-BIOS MultiNet captured *Oikopleura gaussica*, as well as the deep species *Oikopleura vanhoffeni*. The VPR showed *Fritillaria* sp. at depth (larger than *F. borealis* typica). Overall, there was a decrease in diversity of larvaceans on the southern bound leg along 140°E, but an increase in phytoplankton. Most of the larvaceans were located at sites at or below the location of the shelf break.

Distribution and abundance maps for *Oikopleura* sp. and *Fritillaria* sp. determined using CPR during the CEAMARC-Pelagic voyage are shown in Figures 6.20A and 6.20B, respectively. These maps indicate that the highest abundances of both species occurred in the POOZ. Values for the abundance of these species averaged over each transect are presented in Tables 6.15 and 6.16.

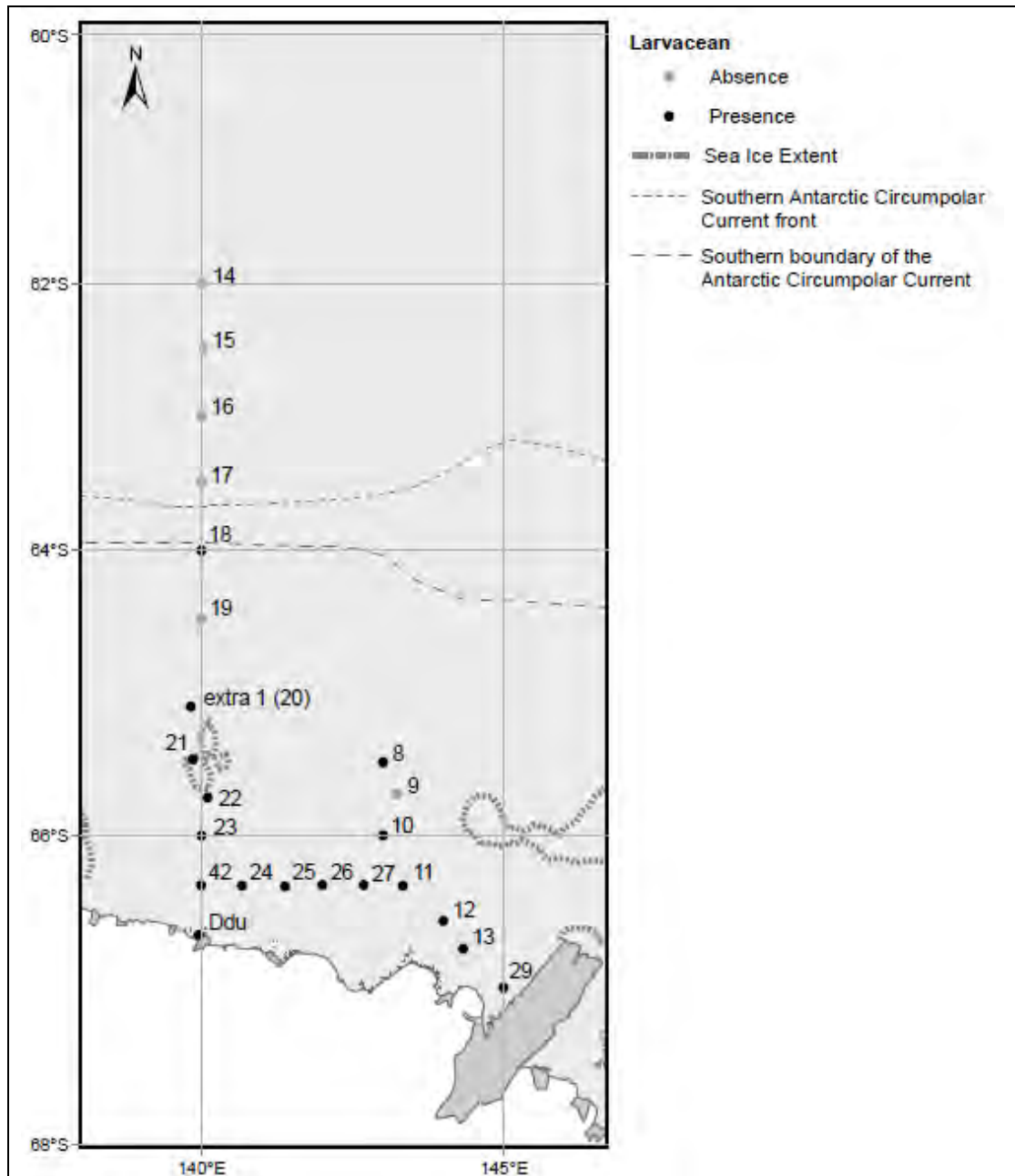


Figure 6.19. Presence or absence of larvaceans determined using the WP2 net, the HYDRO BIOS MultiNet and the VPR in the SIZ during the CEAMARC – Pelagic voyage. The voyage was conducted from 23 January to 17 February 2008 aboard *TRV Umitaka Maru*. Figure adapted from the Australian Antarctic Data Centre.

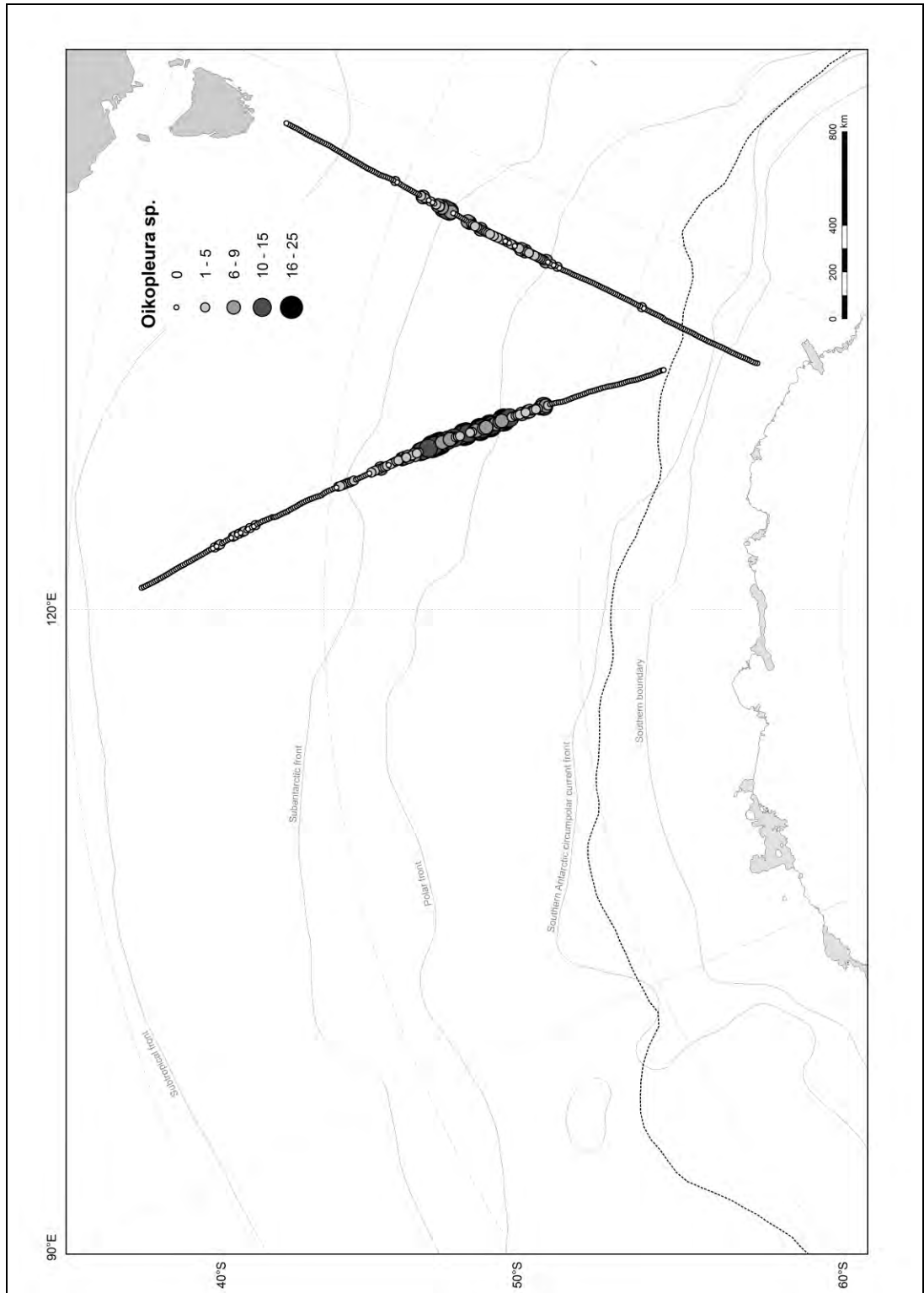


Figure 6.20 A. Abundance of *Oikopleura* sp. determined using CPR during the CEAMARC – Pelagic voyage. Abundance is in counts per 5 Nm.



Figure 6.20 B. Abundance of *Fritillaria* sp. determined using CPR during the CEAMARC – Pelagic voyage. Abundance is in counts per 5 Nm.

Table 6.15. Average *Fritillaria* sp., *Oikopleura* sp. and larvaceans abundances determined using CPR during the CEAMARC – Pelagic voyage. Data are shown for each tow undertaken.

CPR	Start		Finish		Distance (Nm)	<i>Fritillaria</i> sp.	<i>Oikopleura</i> sp.	Larvaceans (ind. m ⁻³)
	Lat. (°S)	Long. (°E)	Lat. (°S)	Long. (°E)		(ind. m ⁻³)	(ind. m ⁻³)	
1	-42.86	121.14	-47.91	125.38	359.7	0.1	0.1	0.2
2	-47.97	125.42	-53.13	130.14	366.5	1.0	0.9	2.2
3	-53.21	130.26	-57.94	135.13	335.5	1.1	6.3	10.1
4	-58.02	135.25	-61.99	139.99	283.0	20.2	0.0	20.2
5	-65.36	142.95	-62.79	143.56	160.0	4.4	0.0	4.4
6	-62.72	143.61	-60.52	144.25	139.1	0.0	0.0	0.0
7	-60.14	144.28	-55.03	145.32	331.8	17.0	0.5	20.5
8	-54.95	145.34	-51.05	146.17	240.8	1.5	2.4	4.4
9	-50.97	146.20	-49.73	146.49	80.2	0.5	0.4	1.7
10	-49.64	146.52	-44.85	147.31	294.8	0.2	0.0	0.3

Table 6.16. Average *Fritillaria* sp., *Oikopleura* sp. and larvacean abundances determined using CPR during the CEAMARC – Pelagic voyage. To determine transect averages, data from each tow within the same transect were pooled.

MONTH Transect direction	<i>Fritillaria</i> sp.		<i>Oikopleura</i> sp.		Total larvaceans		Total zooplankton	
	ind. m ³	std (±)	ind. m ³	std (±)	ind. m ³	std (±)	ind. m ³	std (±)
January - southbound	4.8	11	1.8	3.2	7.4	16.1	92	87.5
March - northbound	5.4	9	0.6	1.6	7	16.5	79.9	70.4
Grand total	5.1	10.1	1.3	2.6	7.2	16.3	86.2	79.9

Physical and biological parameters during CEAMARC – Pelagic

Water temperatures at stations sampled during the CEAMARC – Pelagic voyage were obtained from the observation log book aboard *TRV Umitaka Maru*.

Pearson's *r* correlations (Table 6.17) showed a significant relationship between the presence/absence of larvaceans and longitude, latitude and water temperature.

Table 6.17. Pearson's *r* correlations between larvacean abundances determined using a ring net, and environmental parameters recorded during the CEAMARC – Pelagic voyage. **Bold** indicates a significant relationship (ns = not significant), $\alpha=0.05(2)$.

Parameter	<i>r</i>	df	<i>p</i>
Ring Net (<i>critical r = 0.334</i>)			
Latitude	0.58	33	0.001 < <i>p</i>
Longitude	0.46	33	0.005 < <i>p</i> < 0.01
UW - Temperature	0.59	33	0.001 < <i>p</i>

For CPR data obtained during the CEAMARC – Pelagic voyage, there were significant relationships between larvacean abundance and latitude, longitude, fluorescence and temperature (Table 6.18).

Table 6.18. Pearson's r correlations between larvacean abundances determined from CPR segments, and environmental parameters determined from underway data during the CEAMARC – Pelagic voyage. **Bold** indicates a significant relationship (ns = not significant), $\alpha=0.05(2)$.

Parameter	r	df	p
Continuous Plankton Recorder (CPR) (<i>critical $r = 0.088$</i>)			
Latitude	0.27	517	$0.001 < p$
Longitude	0.11	517	$0.01 < p < 0.02$
Irradiance	0.02	517	ns
Fluorescence	0.17	517	$0.001 < p$
Temperature	0.27	517	$0.001 < p$
Salinity	0.03	517	ns

6.3.5 Net comparisons

The average abundance of larvaceans determined using various nets in this study was 1.4 ± 5.4 ind m^{-3} . The average abundance determined using CPR was 4.5 ± 14.9 ind m^{-3} . In a previous study, NORPAC net deployments were found to provide comparable zooplankton distributions to those obtained from CPR tows when the NORPAC net was hauled at ~ 1.5 m s^{-1} between 0 m and 20 m (Hunt and Hosie 2003). The main difference between NORPAC net hauls and CPR tows in the study by Hunt and Hosie (2003) was that larvacean abundances were different although distributions were similar. Zooplankton abundances in the NORPAC net were found to be three times less than the CPR. As per Hunt and Hosie (2003, 2006a and 2006b), distribution patterns of larvaceans in this study were similar, but larvacean abundances were different when comparing data obtained from the plankton nets and CPR.

6.3.6 Physical and biological parameters of the Southern Ocean

Possible controls on larvacean distributions were evaluated by comparing them to physical (latitude, longitude, temperature, salinity and light) and biological (chlorophyll and total zooplankton) distributions. Significant correlations occurred with latitude, longitude, fluorescence, irradiance and water temperature. Table 6.19 shows a summary of underway data for each oceanographic zone in the Southern Ocean during each voyage.

Table 6.19. Averages of underway data for each oceanographic zone in the Southern Ocean and during each research voyage.

CPR	Fluorescence		Salinity (psu)		Temperature (°C)		PAR ($\mu\text{Em}^{-2}\text{s}^{-1}$)	
	mean	Std dev (\pm)	mean	Std dev (\pm)	mean	Std dev (\pm)	mean	Std dev (\pm)
Southern Ocean	11.4	27.5	33.6	9.5	4.1	9.5	267.6	385.1
BROKE-West	0.7	0.8	34.0	0.3	4.5	3.1	366.9	500.2
SIPEX	0.5	0.3	34.0	0.3	4.4	2.9	185.6	326.5
CEAMARC	2.8	1.0	34.0	0.4	7.9	3.3	281.0	371.4
SAZ	11.0	33.1	34.3	0.4	10.6	3.0	330.7	506.8
POOZ	9.2	20.6	33.7	11.7	3.8	11.7	274.5	381.1
SIZ	19.1	41.8	32.5	6.1	0.9	1.2	215.0	288.1

6.4 Discussion

6.4.1 Summary of distributions and abundances of larvaceans in the Southern Ocean

Patterns of larvacean distributions in the Southern Ocean were complex to analyse given that a significant fraction of ring net hauls (55%) obtained no specimens at all. In contrast, other net hauls captured large numbers of larvaceans (maximum 57.8 ind. m⁻³ in the RMT) suggesting high spatial variability. The average abundance of larvaceans from the variety of nets used was 1.4 ± 5.4 ind m⁻³, and for the CPR was 4.5 ± 14.9 ind. m⁻³ (Table 6.20). A positive outcome from the study was that larvacean distributions were found to vary according to Southern Ocean oceanographic zones (Table 6. 21). Lowest abundances were found in the SAZ, high abundances in the SIZ, and highest abundances in the POOZ. Table 6.22 shows the mean abundance of larvaceans for each voyage in each oceanographic zone.

Table 6.20. Mean larvacean, *Oikopleura* sp. and *Fritillaria* sp. abundances for each sampling device used. Data from each research voyage were pooled. Sample size (n) represents number of net deployments.

NETS	n	Larvaceans (ind. m ⁻³)		Oikopleura sp. (ind. m ⁻³)		Fritillaria sp. (ind. m ⁻³)	
		mean	std. dev.	mean	std. dev.	mean	std. dev.
Ring net	158	0.5	1.6	0.1	0.3	0.2	0.7
RMT 1	147	2.4	7.6	0	0.1	3	8.3
VPR	3	present		present		present	
WP2	26	present		present		present	
HYDRO- BIOS							
MultiNet	6	present		present		present	
total		1.4	5.4	0.1	0.2	1.6	5.9
CPR	1464	4.5	14.9	1.1	2.5	3.0	9.4

Table 6.21. Mean larvacean, *Oikopleura* sp. and *Fritillaria* sp. abundances (ind. m⁻³) within each oceanographic zone determined from net samples (excludes CPR data). Data from each research voyage were pooled.

ZONE	Abundance statistics (ind.m-3)	Larvaceans (ind.m ⁻³)	<i>Oikopleura</i> sp.		<i>Fritillaria</i> sp.	
			(ind.m ⁻³)		(ind.m ⁻³)	
SAZ	mean	0.6				
	std. dev.	2.6				
	minimum	0.0				
	maximum	15.9				
	median	0.0				
	n	49				
POOZ	mean	2.8	0.1		2.8	
	std. dev.	10.6	0.1		10.6	
	minimum	0.0	0.0		0.0	
	maximum	57.8	0.5		57.8	
	median	0.0	0.0		0.0	
	n	49				
SIZ	mean	1.4	0.1		1.4	
	std. dev.	4.8	0.2		4.8	
	minimum	0.0	0.0		0.0	
	maximum	49.7	1.7		48.8	
	median	0.0	0.0		0.0	
	n	66				
Southern Ocean	mean	1.4	0.1		1.6	
	std. dev.	5.4	0.2		5.9	
	minimum	0.0	0.0		0.0	
	maximum	57.8	1.7		57.8	
	median	0.0	0.0		0.0	
	n	114				

Table 6.22. Mean larvacean abundance determined using nets for each voyage in each oceanographic zone.

VOYAGE	ZONE	Larvaceans		<i>Oikopleura</i> sp.		<i>Fritillaria</i> sp.	
		(ind. m ⁻³)		(ind. m ⁻³)		(ind. m ⁻³)	
		mean	std. dev.	mean	std. dev.	mean	std. dev.
SAZ Sense	SAZ	0.6	2.6				
BROKE-West	POOZ	2.8	10.6	0.1	0.1	2.8	10.6
	SIZ	1.6	5.1	0.1	0.2	1.6	5.1
	total	1.8	6.2	1.8	6.2	0.1	0.2
SIPEX	SIZ	0.2	0.5	0.2	0.5	0.0	0.0
CEAMARC	SIZ	present		present		present	
	Southern Ocean	1.4	5.4	0.1	0.2	1.6	5.9

Figures 6.21 and 6.22 (a repeat of Figure 2.15) show that temporal aliasing is not a confounding issue, because three voyages occurred in summer (e.g. February) and during these voyages all zones were surveyed. The exception may be the SIPEX SIZ data which is the only survey to occur in early spring.

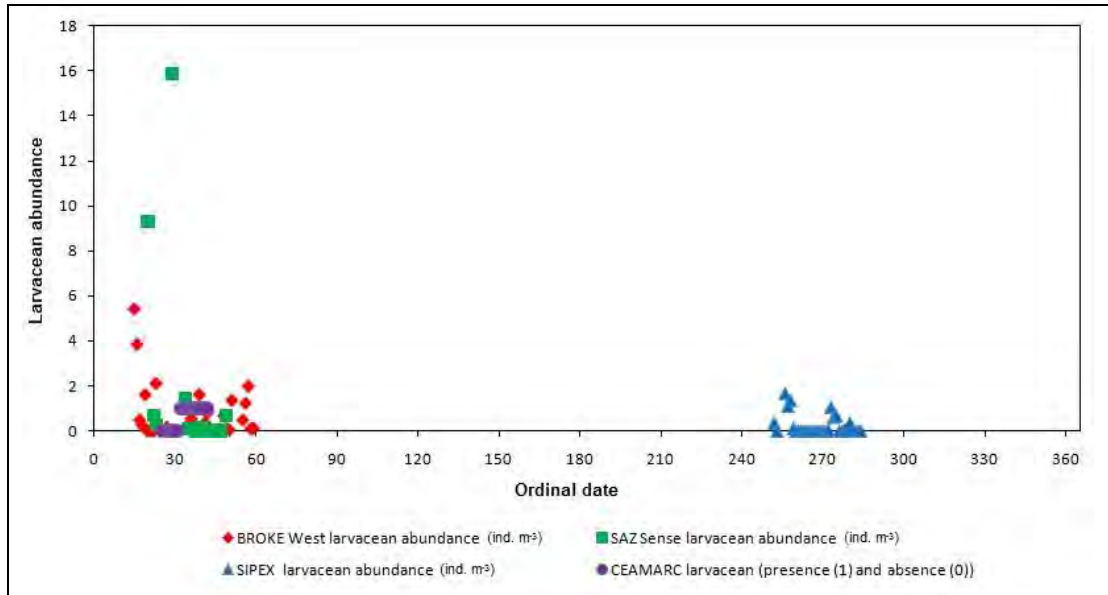


Figure 6.21 Graph showing ordinal date and larvacean abundance (BROKE-West (red), SAZ-Sense (green) and SIPEX (blue) abundances as ind. m^{-3} and CEAMARC (purple) recorded as presence (1) and absence (0)) for the voyages undertaken to collect larvaceans in the East Antarctic Southern Ocean. BROKE-West (red), SAZ-Sense (green), SIPEX (blue) and CEAMARC (purple).

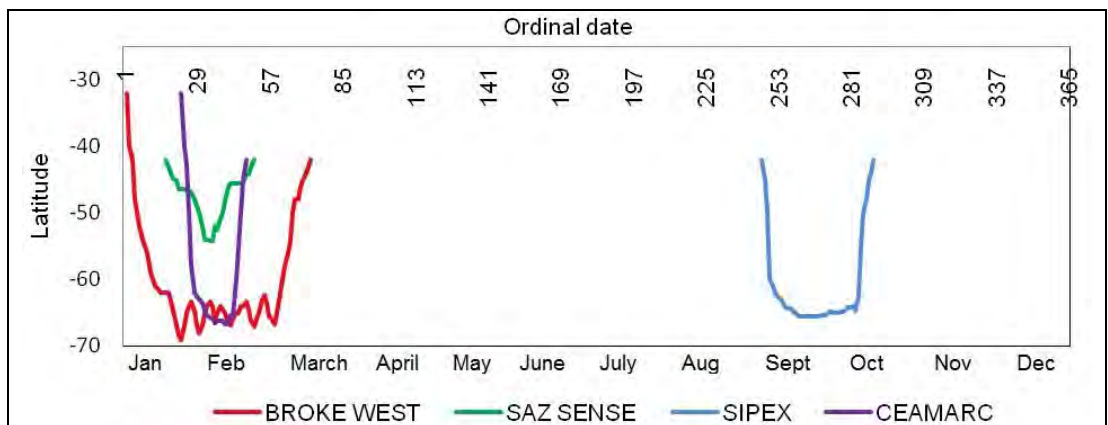


Figure 2.22 Graph showing ordinal date and latitude for the voyages undertaken to collect larvaceans in the East Antarctic Southern Ocean. BROKE-West (red), SAZ-Sense (green), SIPEX (blue) and CEAMARC (purple).

6.4.2 Sub Antarctic Zone (SAZ)

The SAZ had lowest mean total zooplankton (52.2 ind. m⁻³) and larvacean abundances (0.6 ind. m⁻³). This region had the highest water temperature, salinity and irradiance, and also had high fluorescence.

During the SAZ-Sense voyage there were no statistically significant relationships between larvacean abundances and underway or CTD physical oceanographic data. However, a SeaWiFS map (Figure 6.21) shows that chlorophyll *a* concentrations were high in the northern region and lower in the south during the SAZ-Sense voyage. Therefore, larvacean abundances and chlorophyll *a* seemed to have an inverse relationship. In Figure 6.23, a diagonal solid red line shows the separation of regions according to larvacean abundances and chlorophyll *a*. The inverse relationship supports temperate studies that suggest larvaceans occur in oligotrophic (low productivity) waters (Banse, 1996; Atkinson, 1998; Fiala *et al.*, 1998). It has been suggested that larvaceans do not cope when they are supersaturated with food as they are unable to replace their feeding houses at a sufficient rate for them to feed efficiently and survive (Flood and Deibel, 1998).

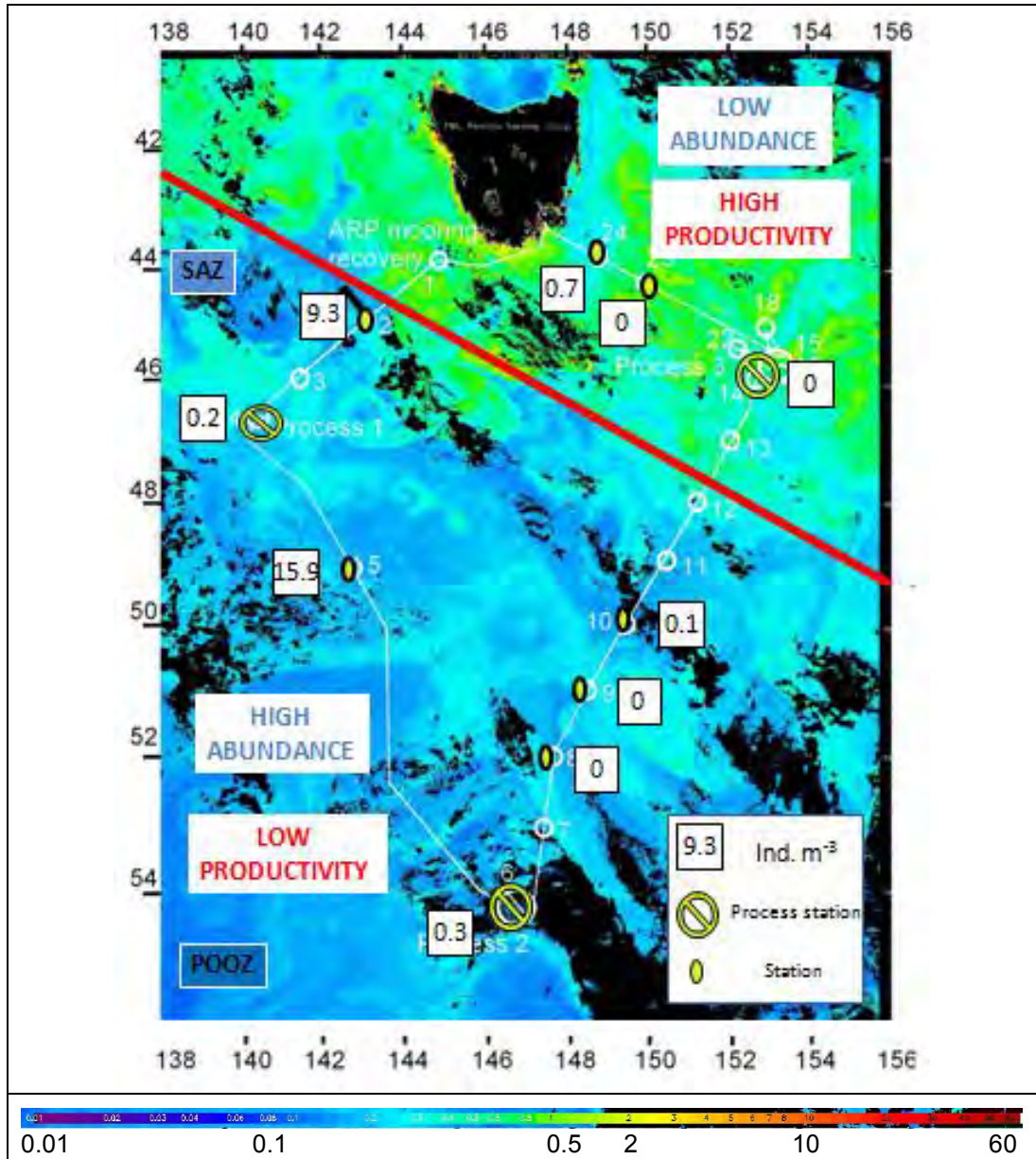


Figure 6.23. Larvacean abundances from ring net (ind.m⁻³) and chlorophyll *a* concentrations (coloured scale) during SAZ-Sense. The red line indicates the inverse relationship between larvacean abundance and chlorophyll *a*, as measure of productivity.

As net deployments for the capture of larvaceans were opportunistic during research voyages, only limited diel and stratification studies could be undertaken. These studies were restricted to process stations conducted during the SAZ-Sense voyage. For the stratification study, various depths were sampled at midnight. Data was not sufficiently strong to claim that larvaceans had a stratified distribution. There was also conflicting data as to whether vertical migrations occurred on a diel cycle. During process station 1, it appeared that a vertical migration did occur, with highest larvacean abundances at 20 m at midnight (0.7 ind. m^{-3}), decreasing to 0.25 ind. m^{-3} at both sunrise and midday, and 0.0 ind. m^{-3} at sunset. Abundances were expected to increase again the following midnight, but this was unable to be tested due to restrictions in ship time. At process station 2, highest larvacean abundances occurred at sunrise. However, the following three net deployments returned zero larvaceans, including a midnight deployment. These distribution patterns occurred despite process station 1 and 2 being located in the same low productivity zone (south of the red line in Figure 6.23). This may be due to biological factors that could not be examined during this study such as grazing and mortality.

6.4.3 Permanent Open Ocean Zone (POOZ)

The POOZ was surveyed for larvaceans during the east to west leg of the BROKE-West voyage (Chapter 5). This region was identified as the zone of highest larvacean abundance with a mean of 2.8 ind. m^{-3} . The POOZ also had the highest abundance of total zooplankton with a mean of 93.3 ind. m^{-3} , as determined using the CPR.

6.4.4 Sea Ice Zone (SIZ)

Larvacean abundance in the SIZ was high with an average of 1.4 ind. m^{-3} . High abundances in this region were also shown by Hunt and Hosie (2003, 2005 and 2006a) and Tsujimoto et al (2006). Larvacean abundances determined in the SIZ during the BROKE-West voyage using a ring net, RMT and CPR are explained in detail in Lindsay and Williams (2010) and Chapter 5. General distribution patterns of larvaceans were similar when sampling with the ring net and RMT. Larvacean

abundances generally corresponded to oceanographic zones and to the three climatology regions described in Schwartz et al. (2010). CPR tows undertaken during BROKE-West showed that abundances increased then decreased on the southwest bound transect. On the northeast bound transect back to Australia, the highest abundance of nearly 3 ind. m⁻³ occurred at the start of the transect. Abundances then decreased with decreasing latitude.

Early and late in the SIPEX voyage, larvaceans were present in very low abundances. They were also very low at the eastern longitudes. A significant relationship was found between larvacean abundance and longitude, as well as fluorescence and irradiance. The western area sampled later in the season was where the first significant algal densities were found (stations 7, 9, 10, 11 and 13, shown in Figure 6.24). This supports observations in the SIZ during BROKE-West, by Tsujimoto et al. (2006) and by Hunt and Hosie (2003, 2005 and 2006a). These all showed that larvaceans were present in high abundances in areas of high productivity. This is opposite to the larvacean distribution and abundances that were observed in the SAZ during the SAZ-Sense voyage and different to the published theory that larvaceans occur in oligotrophic waters (Banse, 1996; Atkinson, 1998; Fiala *et al.*, 1998 and Flood and Deibel, 1998). The occurrence of larvaceans in high abundances in the highly productive SIZ may be a feeding behaviour adaptation.

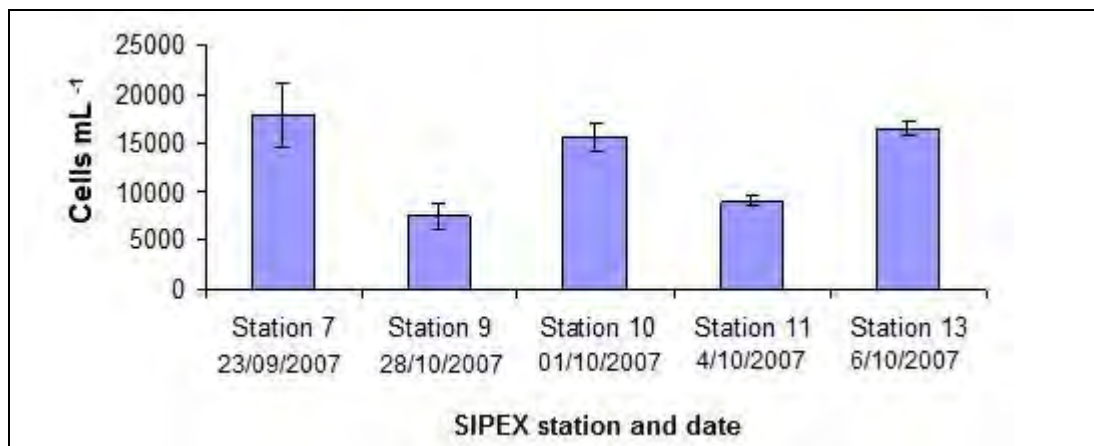


Figure 6.24. Sea ice algal cell density from the western area of the SIPEX voyage. Station 7 is the first station that significant algal densities occurred. Data from K. Petrou.

Larvaceans in the SIZ during the CEAMARC – Pelagic voyage were recorded as present or absent. Overall, there was a decrease in diversity on the south bound leg along 140°E, and an increase in phytoplankton. Most larvaceans were located at or below the shelf break location. In general, the abundance of larvaceans increased from north to south and decreased from west to east.

6.5 Conclusion

Oceanographic zones have a significant influence on the distribution and abundance of larvaceans in the Southern Ocean. The SAZ had the lowest abundance (0.6 ± 2.6 ind. m^{-3}), followed by the SIZ (1.4 ± 4.8 ind. m^{-3}) and the POOZ (2.8 ± 10.6 ind. m^{-3}). Correlations between larvacean abundances and environmental parameters identified that latitude, longitude, fluorescence, irradiance and water temperature had significant influences. A synthesis of these relationships according to oceanographic zones is shown in Figure 6.25.

Correlations were not consistently significant indicating that other factors were also likely to be influential. Chapter 7 investigates the feeding behaviour and food preferences of larvaceans in order to better understand the observed distribution and abundance patterns shown in this chapter.

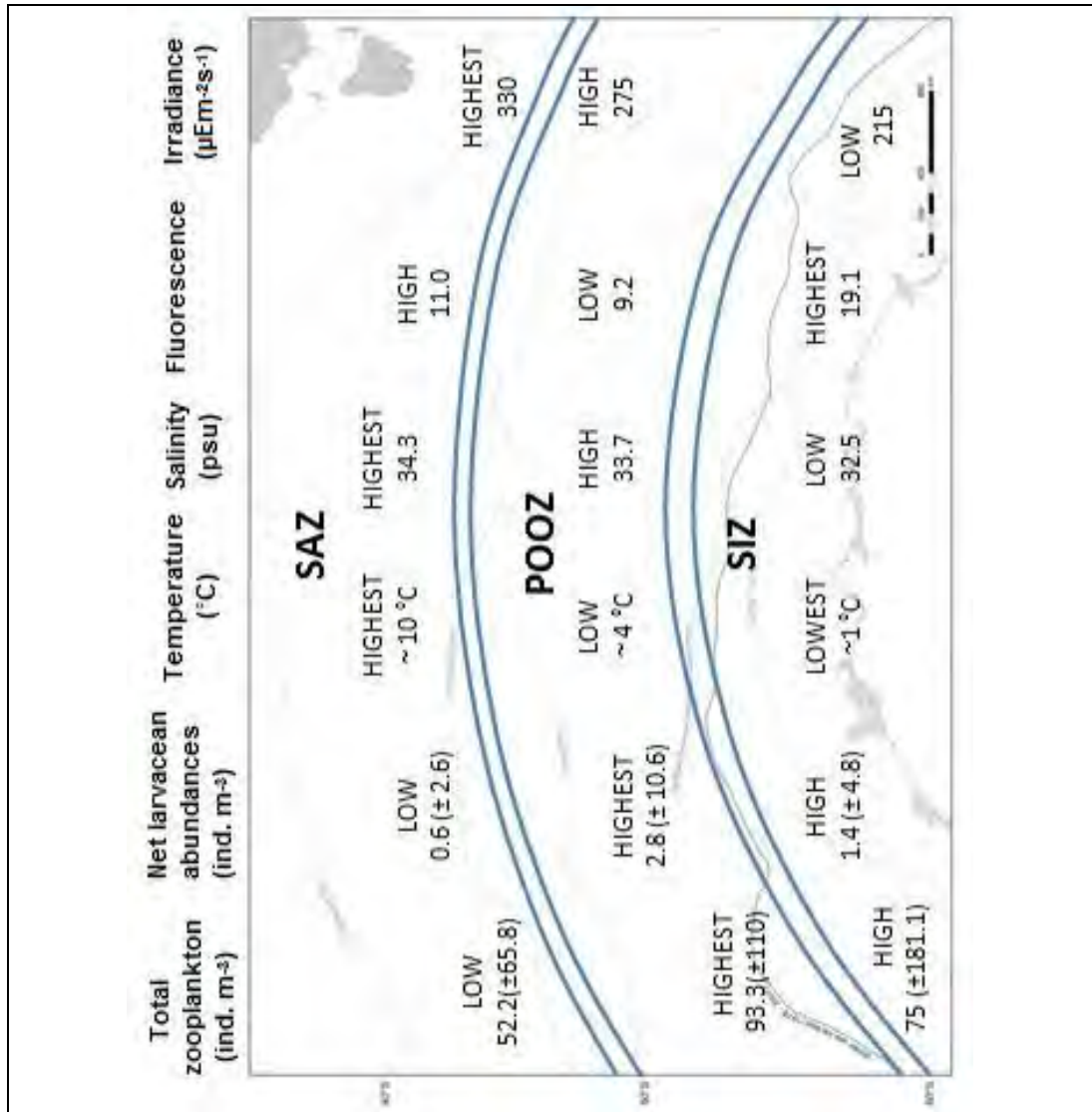


Figure 6.25. Relative abundances of larvaceans compared to physical (latitude, longitude, temperature, salinity and light) and biological (total zooplankton) distributions.

CHAPTER 7.

Feeding ecology

7.1 Introduction

At the inception of this project, it was planned that the diet of larvaceans would be studied directly by conducting feeding studies on live animals collected from the Southern Ocean. Despite a variety of nets employed, the larvacean bodies were too fragile to survive sampling and unfortunately no live animals were able to be collected on any voyage. Thus, it was not possible to directly examine feeding behaviour, house production rates, or faecal pellet production rates through experimentation. Ideally, if live larvaceans had been collected and cultivated successfully, faecal pellets would have contained the remains of protists and provided an indication of the diet of the larvaceans. The examination of discarded feeding houses would also have provided samples of protists that had been discriminately filtered according to the size of mucopolysaccharide feeding meshes.

In this chapter, scanning electron microscopy (SEM) was used to examine the surface and stomach contents of *Oikopleura gaussica*. In this way, the size and species of protists that had passed through inlet filters, and had been collected by food concentrating filters, could be determined. The material used for examination was collected during the 2005/2006 BROKE-West voyage. *O. gaussica* was examined as this was the largest and most numerous species, and samples were in a satisfactory condition for dissection and SEM.

Results from this study were compared with published data from non-Antarctic species to provide an estimate of the feeding capability of Southern Ocean larvaceans. An understanding of feeding ecology enables a better interpretation of larvacean distribution and the role of these organisms in the Southern Ocean ecosystem.

7.2 Background to larvacean feeding and ecology

Larvaceans form a gelatinous “house” through which they circulate seawater to filter very small particles onto mucopolysaccharide meshes. This concentrates sub-micron and micron-sized protists to 100 -1000 times greater than ambient concentrations (Flood and Deibel, 1998). The house is discarded when the meshes clog, and this occurs up to several times per day. Discarded feeding houses form a significant portion of accumulated detritus known as “marine snow” (Gorsky et al., 2005) which may sink and be an important component of carbon export from surface waters. Thus, larvaceans play an unusual role in the marine microbial food-web by transferring biological particulate matter across many orders of magnitude in size, and moving it into the ocean interior.

The capacity for larvaceans to build houses has always been considered an important characteristic. The genus name *Oikopleura* is derived from the Greek *Oikos* for “house” and *pleura* for “rib” or “side of the body”. It was coined by Mertens (1830), soon after the original description by Chamisso and Eysenhardt (1821). The house is very challenging to study due to its complex and fragile nature. Its function was unknown until Eisen (1874), who suggested that the house was used in the feeding process and that its function was “to introduce nutritional substances to the mouth opening”.

Most feeding ecology studies have been conducted on several Oikopleurid species, with fewer on Fritillariidae. Very little is known about the feeding ecology of the third larvacean family, Kowalevskiidae. The feeding ecology of Fritillariidae is very different to that of Oikopleurid species in that they have different house production and feeding mechanisms (Bone, 1998). The feeding houses for each larvacean family are described below.

Oikopleurid house and feeding behaviour

Structure and function of the feeding house has been studied in several Oikopleurid species, including *O. dioca*, *O. vanhoeffeni*, *O. cornutogastra*,

O. fusiformis, *O. intermedia*, *O. longicauda*, *O. refescens*, *Megalocerus huxleyi*, *Stergosoma magnum* and *O. labradoriensis* (Flood and Deibel, 1998). Flood and Deibel (1998) suggested that all Oikopleurid houses function in the same way given that they contain the same water passages, chambers, valves and filters.

However, the size of the feeding house varies between species, with the house diameter normally twice as large as the total length of the larvacean. The feeding house diameter for *O. dioca* is 4 mm and 6-7 cm for *O. vanhoeffeni* (Flood and Deibel, 1998).

The gelatinous feeding house is a delicate and complex mucopolysaccharide structure that allows water to be pumped through a number of filters which extract particles. Figure 7.1 is an explanatory diagram of the filtering structure and water flow in *O. labradoriensis*, as described by Flood and Deibel (1998). The muscular activity of the larvacean's tail pumps water through the structure. Water is sucked into the house through bilateral coarse-meshed inlet filters that prevent large particles accessing the interior as these may be harmful to the animal. The water is then forced through food concentrating filters by the tail. These filters have extremely small and regular pore sizes that trap living and dead particles and allow the now-filtered water to leave the house. The trapped particles, as small as 2 μm , flow into a food collecting duct that is located between the filters and the mouth of the animal.

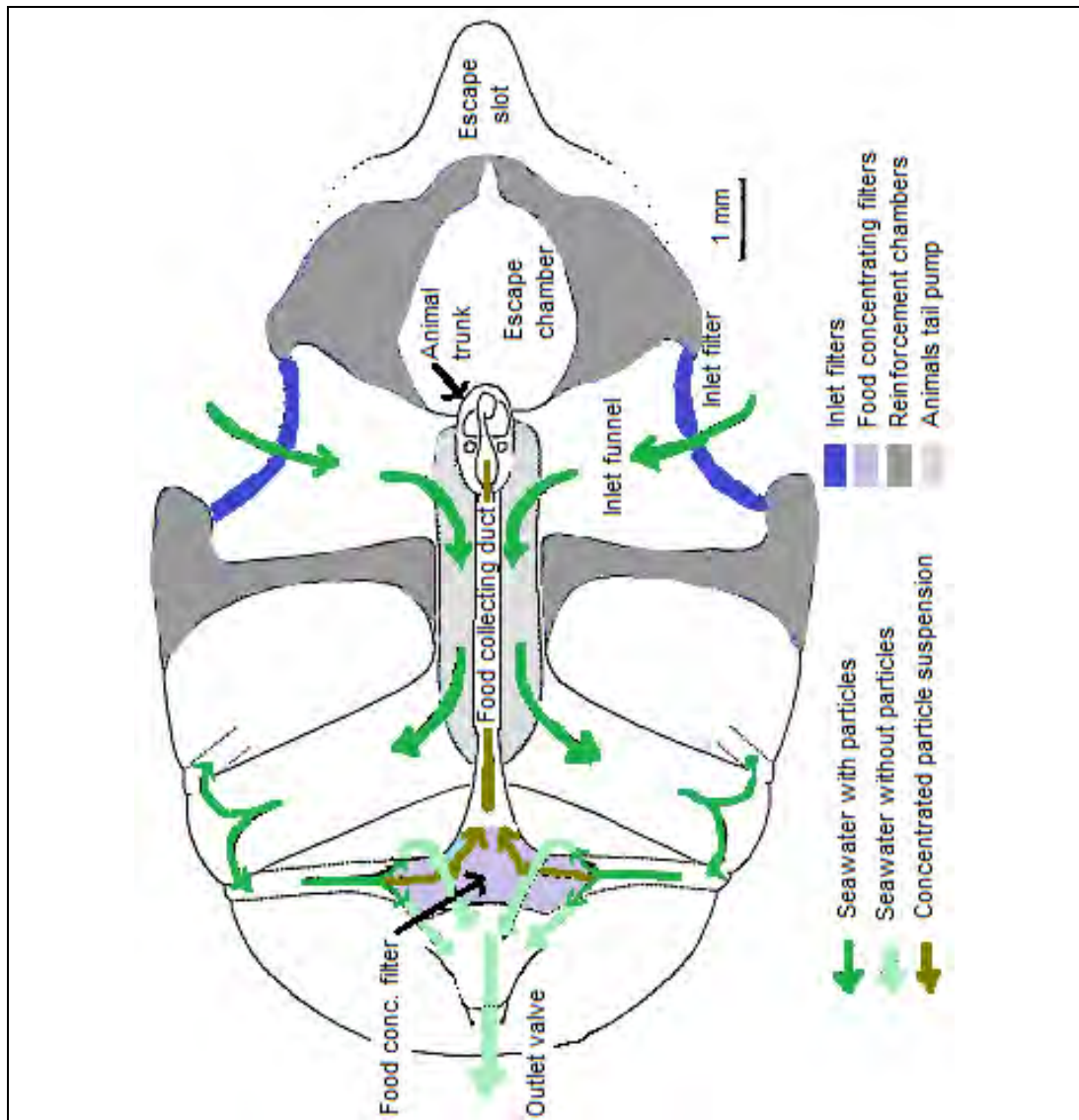


Figure 7.1. Diagram of the feeding house of *O. labradoriensis*. Dark green and light green arrows indicate water flow through the house before, and after, the passage of water through the food concentrating filter. Olive green arrow indicates the flow of trapped particles towards the mouth for consumption (modified from Flood and Diebel 1998).

After a feeding house has been discarded due to clogging, a replacement one is produced as a rudiment through the secretory activity of oikoblastic cells that cover the anterior trunk. Inflation of the new feeding house then occurs and for *O. labradoriensis* this takes about a minute (Deibel and Bone, 1998). Inflation is achieved in successive stages using water flow and tail pumping (Deibel and Bone, 1998, Figure 7.2). The first stage is that of the rudiment swelling, followed by the larvacean nodding to force water into the rudiment. The third stage

involves the larvacean withdrawing its tail into the house and then pumping the tail to inflate the house. The inflated house is approximately 300 times the volume of the rudiment, and the diameter is approximately twice the total length of the larvacean. *O. dioica* is known to drop its house and produce a new one every 4 h (Lohmann 1909). Larger species, and species living in low temperatures, retain their houses for longer. Riehl (1992) found that at temperatures between -0.6 and 5.8°C , house renewal rates for *O. vanhoeffeni* were 1.7 ± 0.78 houses day^{-1} and 2.32 ± 1.03 houses day^{-1} for *O. labradoriensis*.

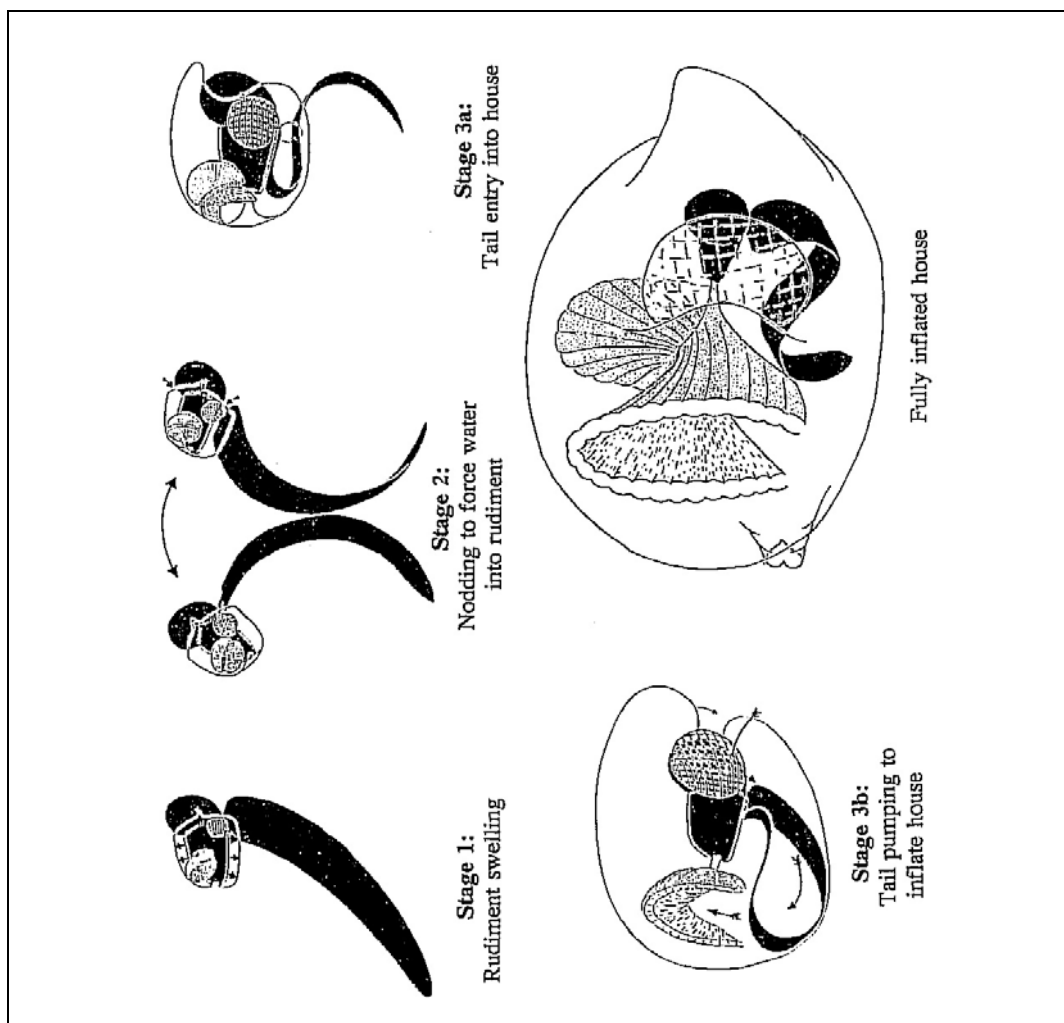


Figure 7.2. *O. labradoriensis* feeding house inflation in successive stages (Flood and Diebel, 1998)

Fritillariid house and feeding behaviour

Knowledge of house production by Fritillariids is derived from studies on *F. borealis*, *F. megachile* and *F. pellucid* (Flood and Deibel, 1998). A Fritillariid house is produced in a similar way to an Oikopleurid house with rudiments and inflation. However, the structure and function are different and the posterior half of the trunk is located outside the house (Figure 7.3). *F. borealis* has five phases associated with feeding house production and deployment (Figure 7.4):

- rudiment expansion phase,
- normal feeding cycle,
- house-jettison phase,
- phase of water outflow-obstruction-behaviour and
- free-swimming

During the normal feeding cycle, water enters directly into the tail chamber and is pumped through a coarse-meshed pre-filter before it enters a fine-meshed food concentrating trap. This trap has two-filtering membranes as seen in the Oikopleurids, though one of the Fritillariid membranes is external and forms the scalloped wall of the house through which the filtered water leaves. The second filtering membrane traces a scalloped, interior, mid-line chamber which appears to also serve as a water outlet. The Fritillariid house differs significantly from the Oikopleurid house in that it has the ability to efficiently backwash the coarse-meshed pre-filters. In addition, as soon as the larvacean stops pumping its tail the entire house collapses around the animal due to elasticity.

While not feeding or producing and deploying the feeding house the Fritillariid tail retracts into a fin-like prolongation of the tail chamber. This then acts as a paddle during the first tail strokes, moving the animal and its collapsed house a few millimetres before the house is reinflated. This allows the Fritillariid to move away from expelled coarse particles and from water depleted of food after each pumping cycle.

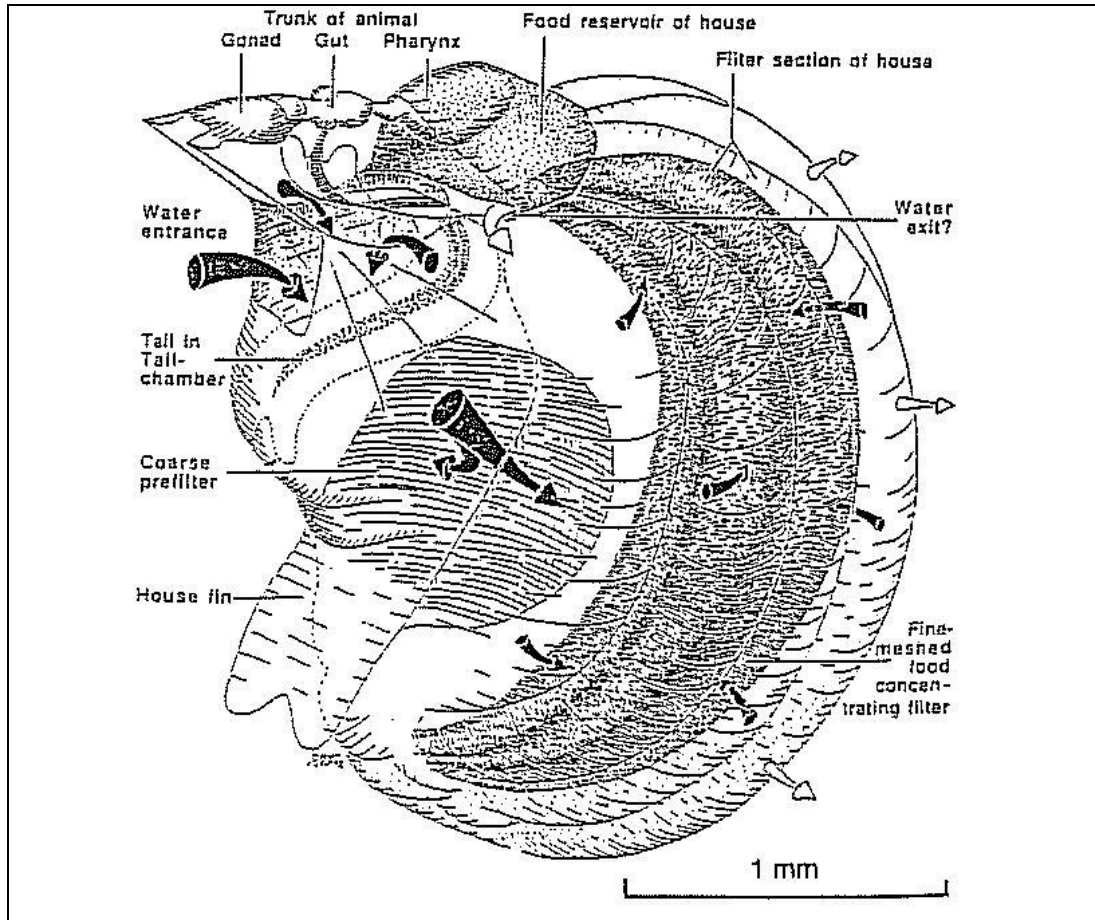


Figure 7.3. Diagram of the feeding house of *F. borealis*. Black and white arrows indicate water flow through the house before, and after, its passage through the food concentrating filter (Flood and Diebel, 1998).

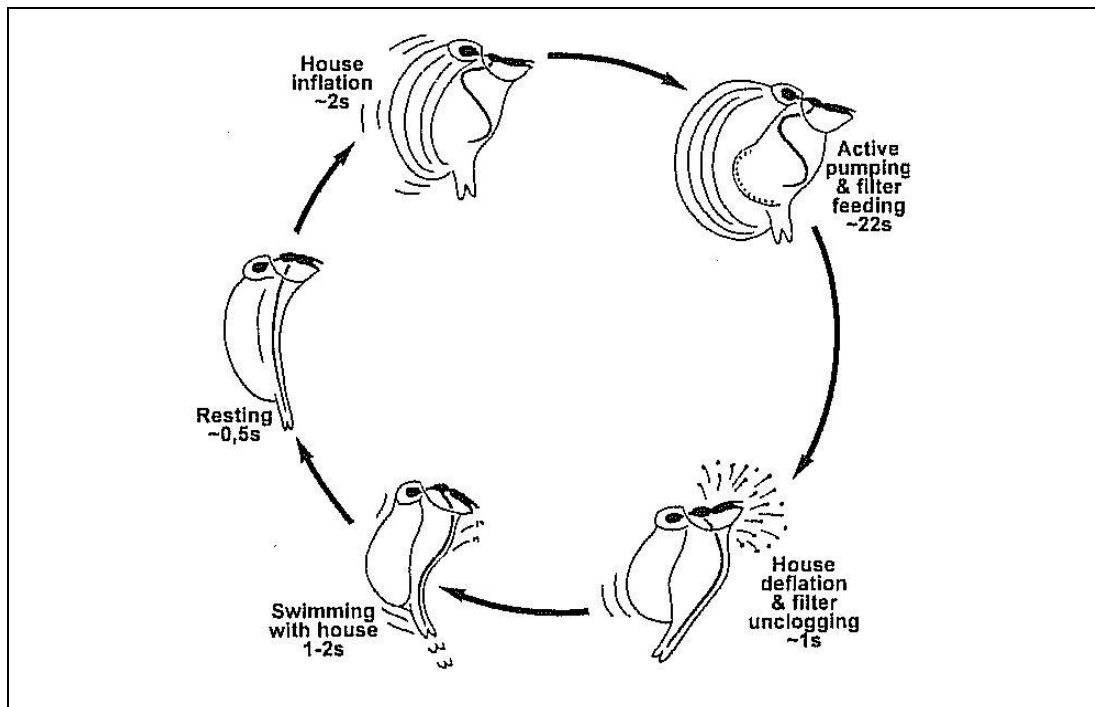


Figure 7.4. Typical feeding cycle of *F. borealis* in relation to the inflation and deflation of the house (Flood, 2003).

Kowalevskia house and feeding behaviour

The house of *Kowalevskia* differs greatly from that of Oikopleurids and Fritillariids. It has a flattened rotational ellipsoid shape with 24 – 28 evenly spaced vertical radial ridges (Figure 7.5). It has a single, centrally located water inlet that has a coarse meshed but fragile inlet filter. This opening is usually located downwards in the water-column. There have been no studies of *Kowalevskia* feeding behaviours to date.

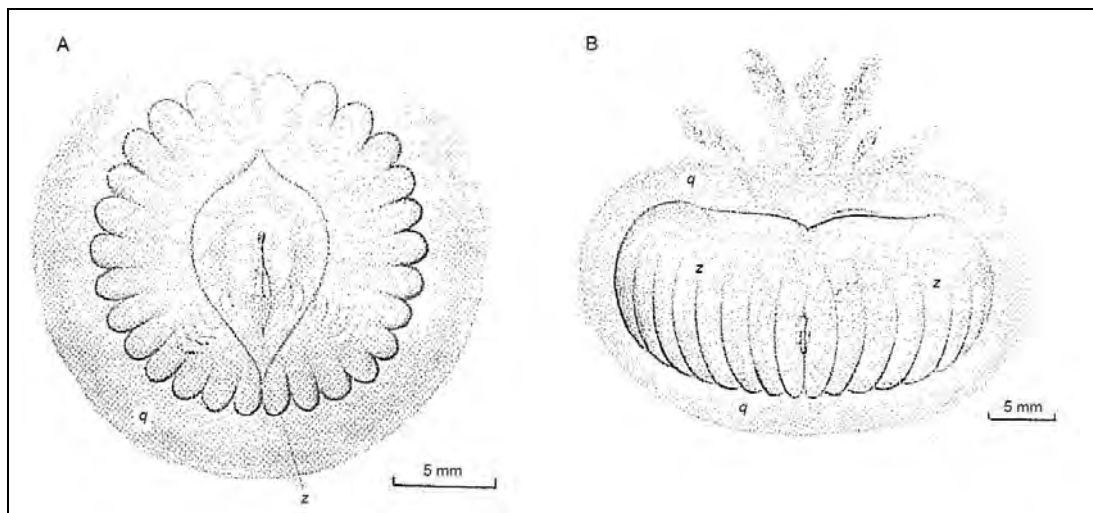


Figure 7.5. Line drawing of *Kowalevskia tenuis* house from A) below and B) side. Fol (1872) Notes: q, coquille (house); z, three-dimensional internal cavity (Flood and Deibel, 1998).

Feeding house filters

This section describes the movement of particulate matter through filters in the feeding house. Table 7.1 provides the length and width of rectangular pores in the inlet and food concentrating filters in the feeding houses of various temperate larvaceans. Water and particulate matter is filtered through a coarse-meshed inlet filter and two food concentrating filters: the fine-meshed upper filter and the finer-meshed lower filter (Figure 7.6). The rate of flow through larvacean houses generally ranges from 12 – 1500 ml h⁻¹ (Alldredge, 1977; Flood, 1991; Morris and Deibel, 1993). Particle clearance rates are within a similar range. Table 7.1 also shows that the clearance rate for *O. dioica* is 8.5 – 10 ml h⁻¹ and that the filtration

rate for *F. borealis* is 12 ml h⁻¹ (Flood and Diebel, 1998). Normal larvacean clearance rates range from <1% to > 60% of particles on a daily basis (Alldredge, 1981; Deibel, 1988; Knoechel and Steel-Flynn, 1989).

Table 7. 1. Numerical data on selected larvacean species and their houses, (U) Upper filter screen (L) Lower filter screen (extracted from Flood and Diebel, 1998). The filtration rate is the bulk flow of water pumped through the house. The clearance rate is the volume of water swept clear of particulate matter (or protists), which equates to the filtration rate times the particle retention efficiency. The open area fraction is a measure of porosity.

Species		<i>O. dioica</i>	<i>O. labradoriensis</i>	<i>O. vanhoeffeni</i>	<i>F. borealis</i>
Animal size	Trunk length (mm)	3.6	3.6	6.5	1.3
	Tail length (mm)	14.4	14.4	32.8	3
House diameter	(mean ± SD) (mm)	18	18	70	2.5
Inlet filter mesh	Width (mean ± SD) (µm)	12.7 ± 2.1	12.7 ± 2.1	81 ± 34	(<30)
	Length (mean ± SD) (µm)	74 ± 12	74 ± 12	163 ± 65	
	Length: Width ratio	5.8:1	5.8:1	2.0:1	
Food concentrating filter mesh	Width (mean ± SD) (µm)	180 ± 30 (U) 240 ± 30 (L)	180 ± 30 (U) 240 ± 30 (L)	0.2 ± 0.4	(<0.45)
	Length (mean ± SD) (µm)	690 ± 200 (U) 1430 ± 170(L)	690 ± 200 (U) 1430 ± 170(L)	0.1 ± 0.2	
	Length: Width ratio	3.8:1 (U) 6:1 (L)	3.8:1 (U) 6:1 (L)	4.7:1	
Open area fraction	(%)	95	95	91	
Filtration (F) or clearance rate (C)	(ml h ⁻¹)	35 (F)	35 (F)	182 (C)	12 (F)
House renewal rate	(houses day ⁻¹)	2.32 ± 1.03	2.32 ± 1.03	1.7 ± 0.78	

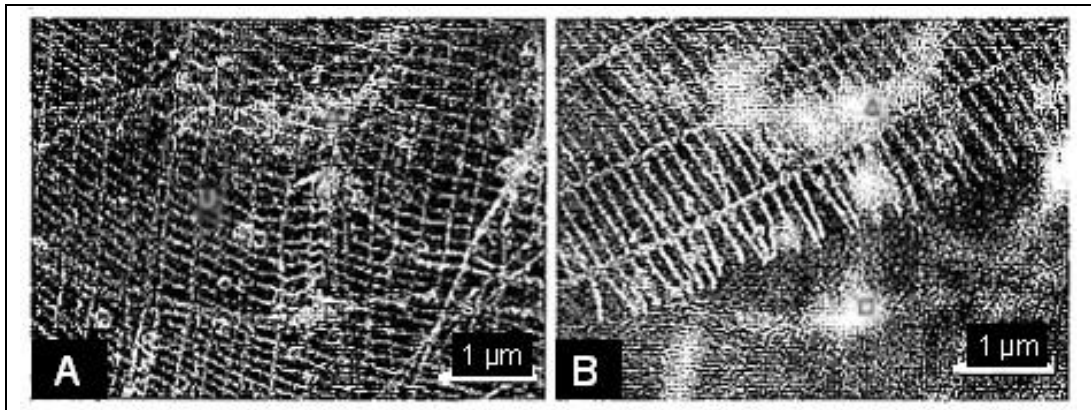


Figure 7.6. Scanning electron micrographs showing the different structures of A. upper, and B. lower food concentrating filters of *Oikopleura dioica*. Magnification x12,000 (adapted from Flood and Deibel 1998).

Figure 7.7 shows the flow of seawater through a feeding house, and the separation of particles into size classes. The first segregation of particles occurs at the inlet filter, with those that are too large attaching to the outside of the feeding house. These particles are discarded with the feeding house once it becomes clogged. Seawater with particles that have passed through the inlet filter then flow through the house to the food concentrating filter. Here, a second segregation occurs, with particles that are large flowing through the food collecting duct and into the stomach. Particles that are small are filtered through the feeding concentrating filter, with the remaining particle-free seawater exiting from the house. Waste is excreted after digestion as ellipsoid faecal pellets.

In this study, the identification of protists in the stomach of larvaceans was used as a method to estimate the mesh size of the inlet filter and the food concentrating filter. Protists were also identified on the surface of larvaceans and assumed to be rejected by the inlet filter, and therefore too large for filtration. However, their presence may also possibly have been an artefact of the sampling process.

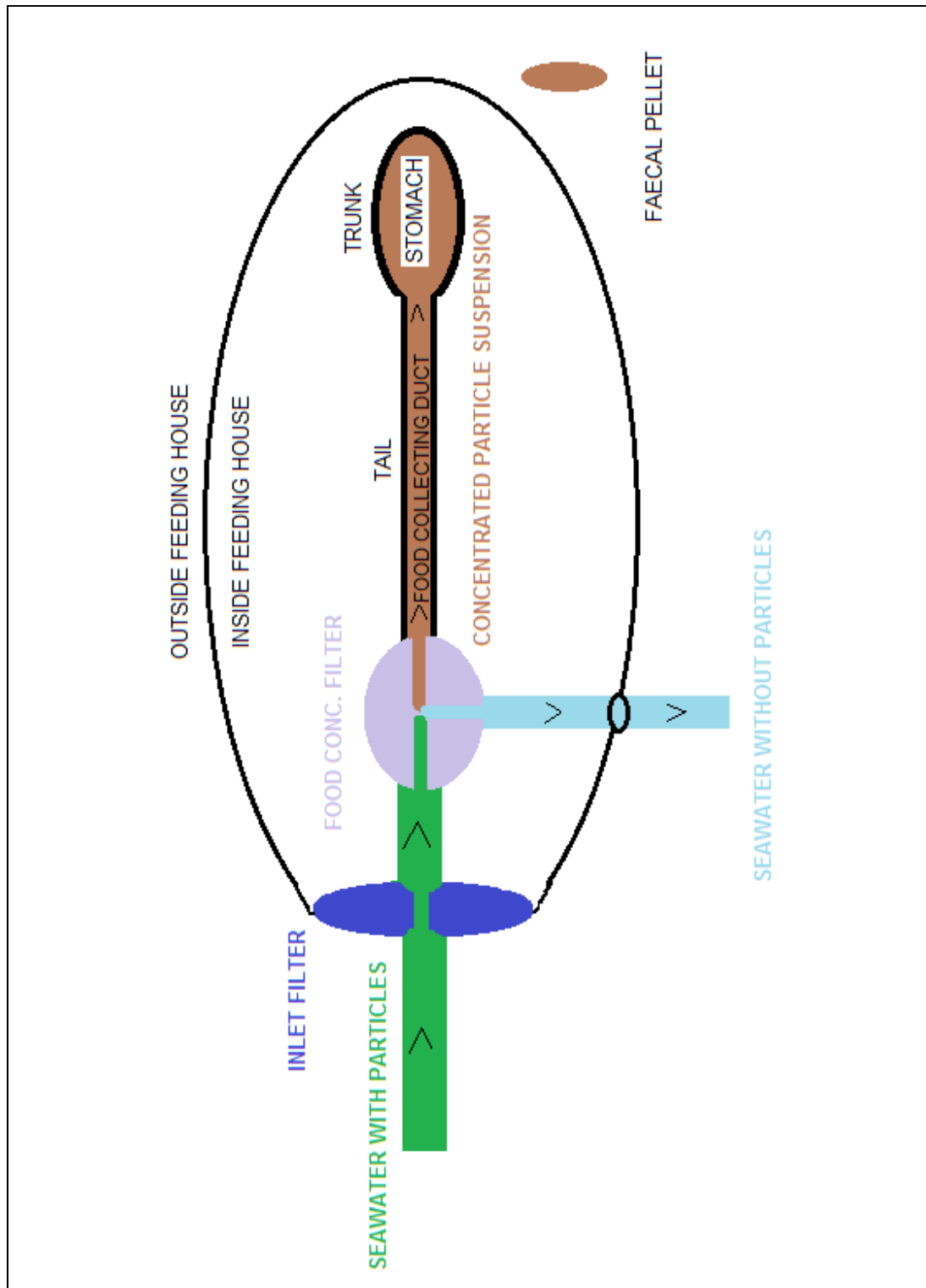


Figure 7.7. Schematic of generalised feeding house showing two filters and the flow of seawater. Dark green and light green arrows indicate water flow through the house before, and after, the passage of water through the food concentrating filter. Olive green arrow indicates the flow of trapped particles towards the mouth for consumption.

Role in carbon flux

The feeding houses of larvaceans (Figure 7.8) are discarded when the mesh becomes clogged. Clogging may occur through the accumulation of any particulate matter, including protozoans, autotrophs, heterotrophs, small metazoans, and organic/inorganic particulate matter. As much as 30% of filtered particulate and colloidal material remains trapped in the feeding house rather than being consumed (Gorsky, 1980). A sub-tropical species, *O. dioica*, can produce up to 16 houses per day and the discarded houses represent 490-1100% of its biomass per day (Sato et al., 2001). House production is a function of temperature, and is also regulated by the rate of clogging of the filters. When feeding houses are discarded, they gradually sink through the water-column with the sinking rate dependent on size and degree of collapse of the house. The sinking rate of discarded houses of *O. dioica* was determined in laboratory experiments by Silver and Alldredge (1981). At 5 °C, larger *O. dioica* houses sank at $64.6 \pm 5.8 \text{ m day}^{-1}$. At 16 °C, smaller *O. dioica* houses sank at $57 \pm 3.5 \text{ m day}^{-1}$. Assuming that similar sinking rates occur for cold-water species, this means that houses may sink below the euphotic zone in the Southern Ocean within a time period of two days.

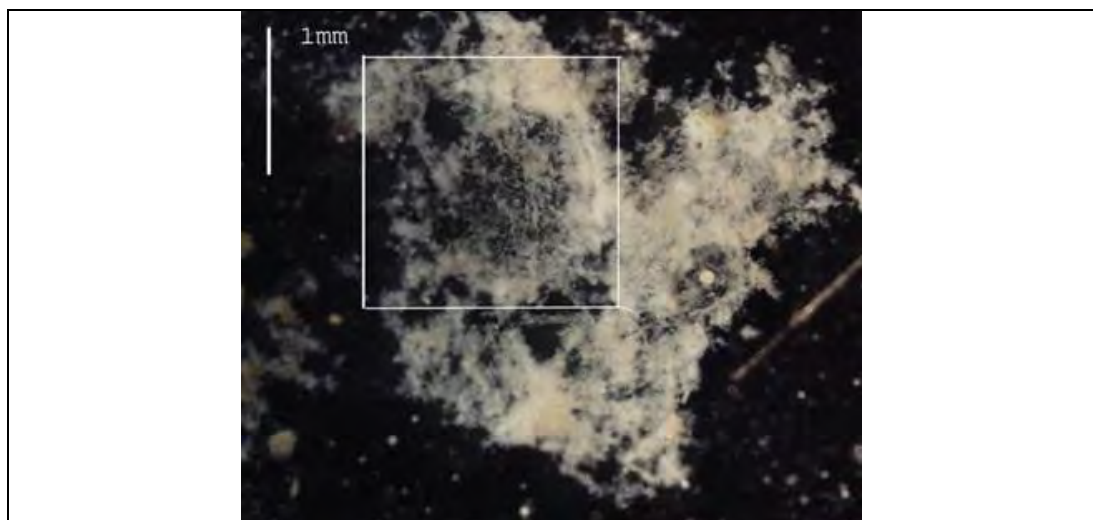


Figure 7.8. Discarded feeding house. Photo courtesy of Debbie Steinberg and Stephanie Wilson of the Virginia Institute of Marine Science. Scale bar = 1 mm.

Urban et al (1992) studied the contents of larvacean faecal pellets and confirmed that these organisms are “generalist suspension feeders”. The waste is excreted as compact ellipsoid faecal pellets (Figure 7.9), and Gorsky et al. (1984) showed that *O. dioica* produced 530 faecal pellets per individual per day. In the laboratory under optimal feeding conditions, Taguchi (1982) also showed that *O. longicauda* produced one faecal pellet every 146 s (*i.e.* ~590 /day at 26 °C). The sinking rate of faecal pellets is closely related to the density of the pellet and this is dependent on the composition and concentration of the protists consumed. Gorsky et al. (1984) found that the faecal pellet sinking rate of *O. dioica* was 25 – 166 m day⁻¹.



Figure 7.9. Larvacean faecal pellet size: <300 - 500 μm . Photos courtesy of Debbie Steinberg and Stephanie Wilson of the Virginia Institute of Marine Science

Role of larvaceans in the food web

The role of larvaceans in the food web is represented in Figure 7.10. This shows that larvaceans consume dissolved organic matter, nanoflagellates, ciliates, diatoms and dinoflagellates (represented in the box in Figure 7.10). In turn, larvaceans are consumed by larger carnivorous zooplankton, such as copepods and krill, and fish (Gorsky and Fenux, 1998). These predators also feed on the discarded feeding houses of larvaceans, their faecal pellets, and larvaceans that are without houses and in the process of inflating new ones (Figure 7.11).

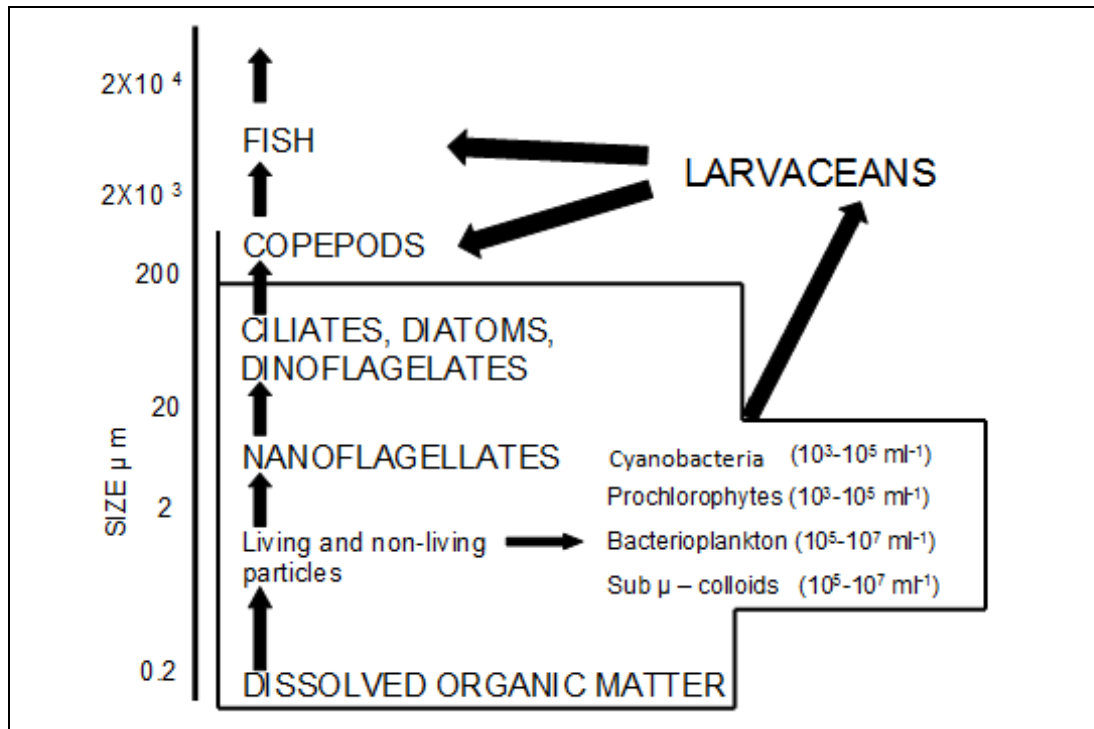


Figure 7.10. Role of larvaceans in marine ecosystem (adapted from Gorsky and Fenoux, 1998)

Gorsky et al. (2005) suggest that larvaceans are important in the structure, dynamics and resilience of the marine plankton community as a whole. Their wide distribution and high abundance means that they are of high trophic importance. Through their mechanism of feeding, larvaceans are able to package protists that would otherwise be too small for direct consumption by filter feeders and carnivores. This means that larvaceans are an important link between primary and secondary producers in the oceans. Larvaceans also have a high N and C content in their tissue, do not have a carapace, and have a relatively slow escape reaction to predators, making them an important fraction in the diet of pelagic predators (Gorsky and Fenoux, 1998).

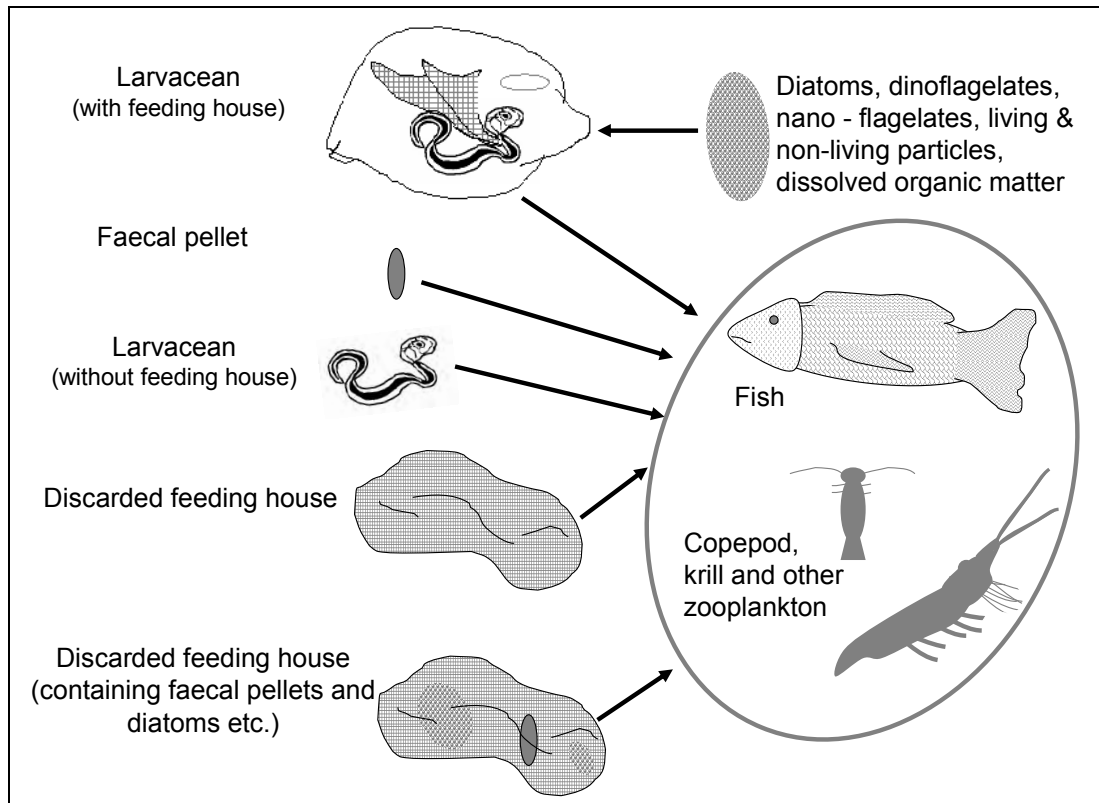


Figure 7.11. Larvaceans role in the food web.

The larvacean contribution to marine snow and the carbon cycle is shown in Figure 7.12. Unconsumed discarded feeding houses play an important role in the production of marine snow. They contain ~30% of sequestered filtered matter, and can also contain faecal pellets that adhere to the discarded house. This means that the houses have an energy and nutrient content that is favourable for colonisation by microbes associated with marine snow (Bedo et al, 1993). Marine snow is essentially a macroscopic aggregate and is therefore an agent for the transfer of carbon and organic matter from surface waters to the ocean interior, and potentially to the ocean floor through sinking (Gorsky and Fenaux, 1998; Robinson et al. 2005). Both discarded houses and faecal pellets have fast sinking rates and are therefore an important component of marine snow (Lopez-Urrutia and Acuna 1990, Sato et al. 2003 and Alldredge 2005). It has been estimated that the carbon concentration of marine snow is at least three orders of magnitude higher than surrounding waters (Silver and Alldredge, 1981). Other factors that may contribute to high carbon turnover in larvaceans include high growth rates (Hopcroft and Roff 1995), short life cycles (Fenaux 1976) and intensive feeding on small particles (Fernandez et al. 2004).

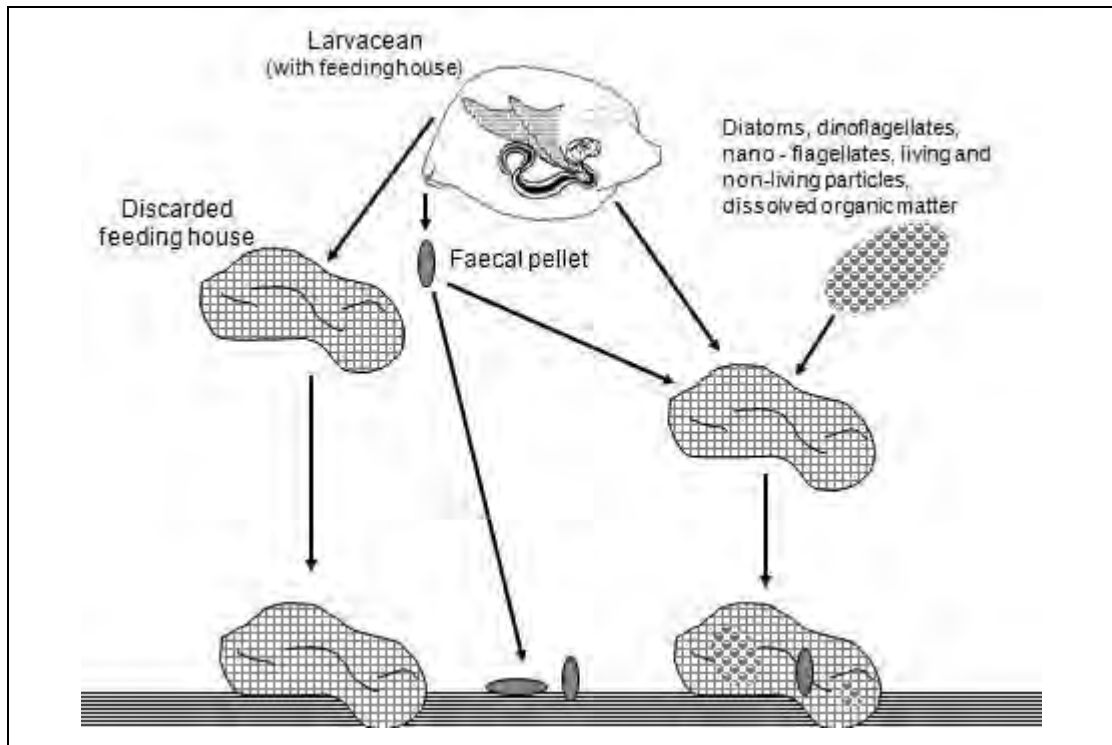


Figure 7.12. Larvaceans contribution to marine snow and carbon cycling.

The majority of published descriptions on the role of larvaceans in the marine environment are derived from tropical or temperate species. This study attempts to address the gap in knowledge for polar larvaceans, by determining the feeding preference, behaviour and role of Southern Ocean larvaceans in relation to carbon flux.

7.3 Methods

7.3.1 Survey region and sampling device

Samples were collected with a ring net (detailed in Chapter 6) during the BROKE-West voyage (Figure 7.13). Identification of larvaceans and descriptions of their distribution and abundance are presented in Lindsay and Williams (2008), and in Chapter 5. Observations of stomach contents and protists present on the surface of *Oikopleura gaussica* were made on organisms from two stations: 28 and 67. Data was compared with protists observed in the water-column close by at stations 25 and 65. Only two sites were able to be used as these were the only

locations where *O. gaussica* was in enough abundance and in a satisfactory condition for dissection and SEM.

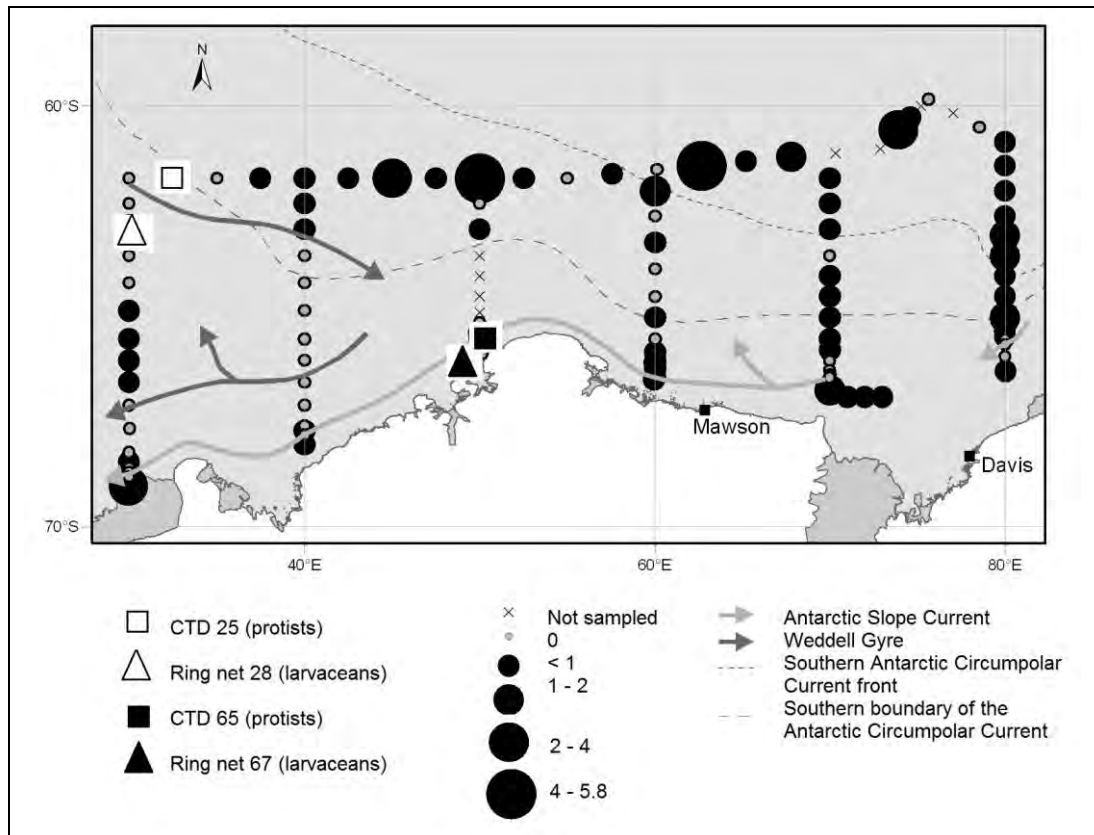


Figure 7.13. Abundance and distribution map of larvaceans that were captured using a ring net. The location of stations 25 and 65 (squares) where protists were sampled are shown. The location of stations 28 and 67 (triangles) where larvaceans were sampled for diet studies are also shown. Station 25 and Station 28 (white shapes) were at a similar location. Station 65 and Station 67 (black shapes) were also at a similar location.

Figure 7.14 is a schematic of the components related to the feeding ecology of Southern Ocean larvaceans that were utilised in this study. This figure also shows the features (e.g. feeding houses and faecal pellets) that eluded the sampling process.

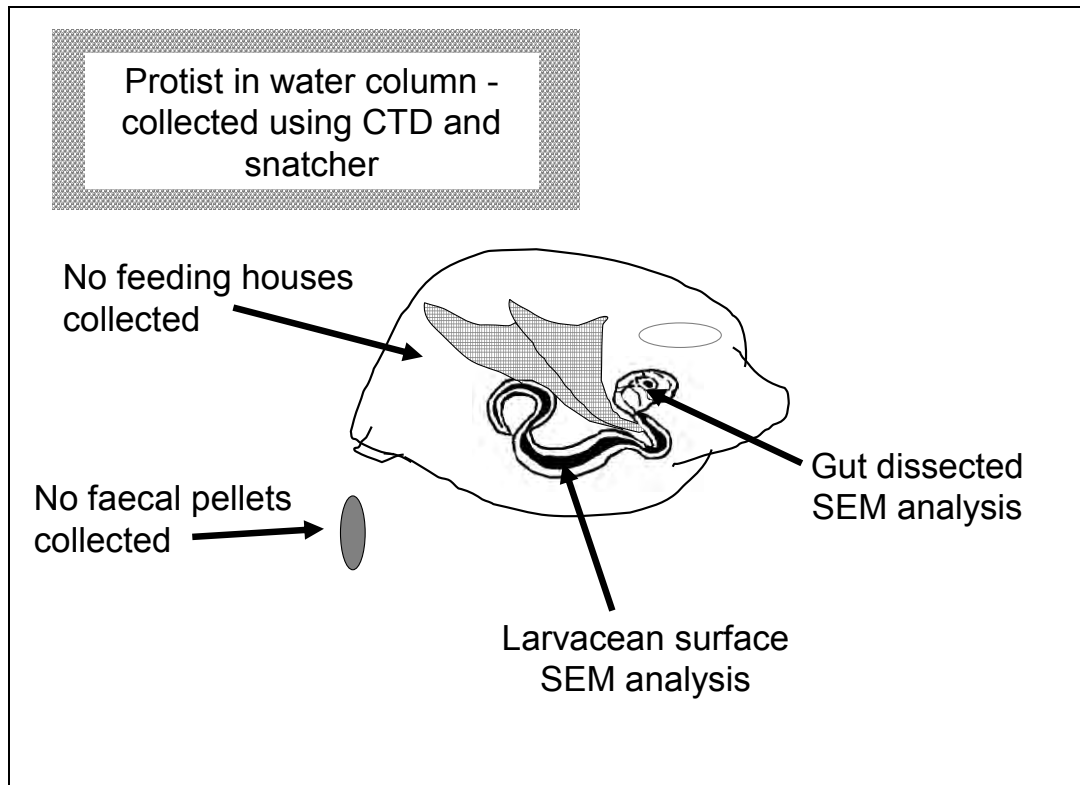


Figure 7.14. Schematic summary of the method used to determine Southern Ocean larvacean diet. Marine protists identified were from water samples collected using a CTD and a “snatcher” (a rosette of Niskin bottles that collected surface waters).

7.3.2. Protist sampling and quantification

The protistan community in surface waters within the BROKE-West survey region was examined using light and electron microscopy, High Performance Liquid Chromatography (HPLC), and flow cytometry. Sampling, preservation, identification and analysis methods are detailed in Davidson et al. (2010), Wright et al. (2010) and Thomson et al. (2010). Marine protists that were identified in the water-column by Davidson et al. (2010) at Stations 25 and 65, were compared with marine protists identified on the surface and in the stomachs of *O. gaussica* at Stations 28 and 67.

7.3.3. Sampling, preservation and SEM processing of larvaceans

A ring net (150 μm mesh) was used to collect quality specimens for identification of larvaceans from 0 - 20 m. Details of the deployment of the ring net are shown

in Chapter 6. The ring net was rinsed with seawater before the cod-end was removed. Larvaceans visible under stereo-dissecting microscope were counted, separated and preserved in 2.5% buffered formalin.

7.3.4 Analysis of stomach and gut contents

The diet of one species of Southern Ocean larvacean (*O. gaussica*) was determined by stomach dissections. This was the largest species collected, with some individuals up to 2 cm in size. Wet dissections of the stomachs were conducted after washing each larvacean in filtered seawater then drying with filter paper. The larvacean was then glued to a cavity slide on its side. A drop of filtered seawater was added to the cavity slide after the glue had dried, and the stomach dissected using forceps and needle. The stomach and gut contents were isolated and transferred with micropipettes to vials containing weak (1 – 2 %) gluteraldehyde in seawater.

SEM images were obtained using a method developed as part of this study. The *O. gaussica* specimens were fixed with osmium, dehydrated using a series of methanol, dry methanol and acetone, and then critically point dried before stud preparation. The stomach contents were split open onto the studs. The studs were then sputter coated with gold at 5 µm for 5 minutes. SEM images were taken of the surface and the guts of *O. gaussica* using a JEOL JSM 840. Protists within the stomach contents and on the surface of *O. gaussica* were identified using Scott and Marchant (2005).

7.3.5 Larvacean protist comparison to water column protists

Unfortunately CTD and net samples could not be collected simultaneously, as only one sampler could be in the water at the same time. For this reason, alternative CTD stations that were nearest to the larvacean sample sites were used. Protists identified within the stomach contents and on the surface of *O. gaussica* from CTD 28 were compared to protists in the water column from 20 m at CTD 25. Similarly, protists identified within the stomach contents and on the surface of

O. gaussica from CTD 67 were compared to protists in the water column at 20 m from CTD 65. The protist data from *O. gaussica* samples was based on presence/absence, while data from the water column is given in average cells L⁻¹.

7.3.6 Inferred mesh size

Larvacean inlet filter mesh size was inferred by comparing the size of protists observed in the stomach, with that of those on the surface of the organism, and in the water column. Protist size ranges were obtained from Scott and Marchant (2005). The apical axis is the long axis of a bilateral diatom, or the axis between the poles of the frustules (the silica-containing wall of the diatom). The pervalvar axis is the axis through the centre point of two valves, and there is also a transapical axis. The orientation of protists through filters has been found to follow the direction of water flow (Chamisso and Eysenhardt, 1821). Thus, filters do not always separate elongate species on the basis of their longest axial dimension. Rather, the size of a cell that passes through a mesh is determined by its smallest diameter, as the cells tend to align lengthways and are parallel to the flow (Runge and Ohman, 1982).

7.4 Results

By identifying and measuring marine protists within stomach contents and comparing the data to that from the water column, the mesh size of the inlet filter and the feeding concentrating filter were inferred.

7.4.1 Distribution of marine protists and larvaceans

The average *O. gaussica* abundance captured in the ring net at CTD 28 was 1.4 ind. m⁻³, while at CTD 67 it was 0.4 ind. m⁻³. The average abundance for the whole survey region was 0.1 ind. m⁻³. The number of protist species at CTD 25 was 30 species, compared to 26 species at CTD 65. The mean abundance of each species from CTDs 25 and 65 is listed in Appendix VII. The mean abundance of larvaceans and marine protist species associated with the diet of *O. gaussica* are shown in Table 7.2. Interestingly, CTD 28 had higher abundance of *O. gaussica*

than CTD 65 and was closer to waters with higher diversity of marine protists (Davidson et al., 2010). Figure 7.15A shows the northerly location of CTDs 28 and 25 along Leg 1, and Figure 7.15B the southerly location of CTDs 67 and 65 along Leg 5, in relation to chlorophyll *a* (Wright et al., 2010).

Table 7.2. Mean abundance of larvaceans and marine protist species associated with the diet of *O. gaussica* at the surveyed CTD sites.

Species	Mean abundance			
	CTD 25 (cells L ⁻³)	Ring net 28 (ind. m ⁻³)	CTD 65 (cells L ⁻³)	Ring net 67 (ind. m ⁻³)
Larvacean				
<i>O. gaussica</i>		1.4		0.4
Protist				
<i>Asteromphalus</i>			230000	
<i>Asteromphalus hookeri</i>	189.3			
<i>Eucampia antarctica</i> (var. <i>recta</i>)	946.7			
<i>Chaetoceros</i>	present		present	
<i>Chaetoceros dicaeta</i>	189.3		750	
<i>Rhizosolenia</i>	1136.0			
<i>Thalassiosira</i> 20-30 µmd			4350	
<i>Thalassiosira</i> 60 µmd			750	
<i>Thalassiosira gracilis</i>	1704.0		190	
<i>Fragilariopsis</i> 60 µml	1704.0		7000	
<i>Fragilariopsis curta/cylindrus</i>	378.7		1890	
<i>Fragilariopsis kerguelensis</i>	6816.0		14000	
<i>Fragilariopsis rhombica</i>	757.3		3400	
<i>Dictyocha speculum</i>	189.3			
<i>Corethron pennatum</i>	Present		Present	
Number of species	30		26	

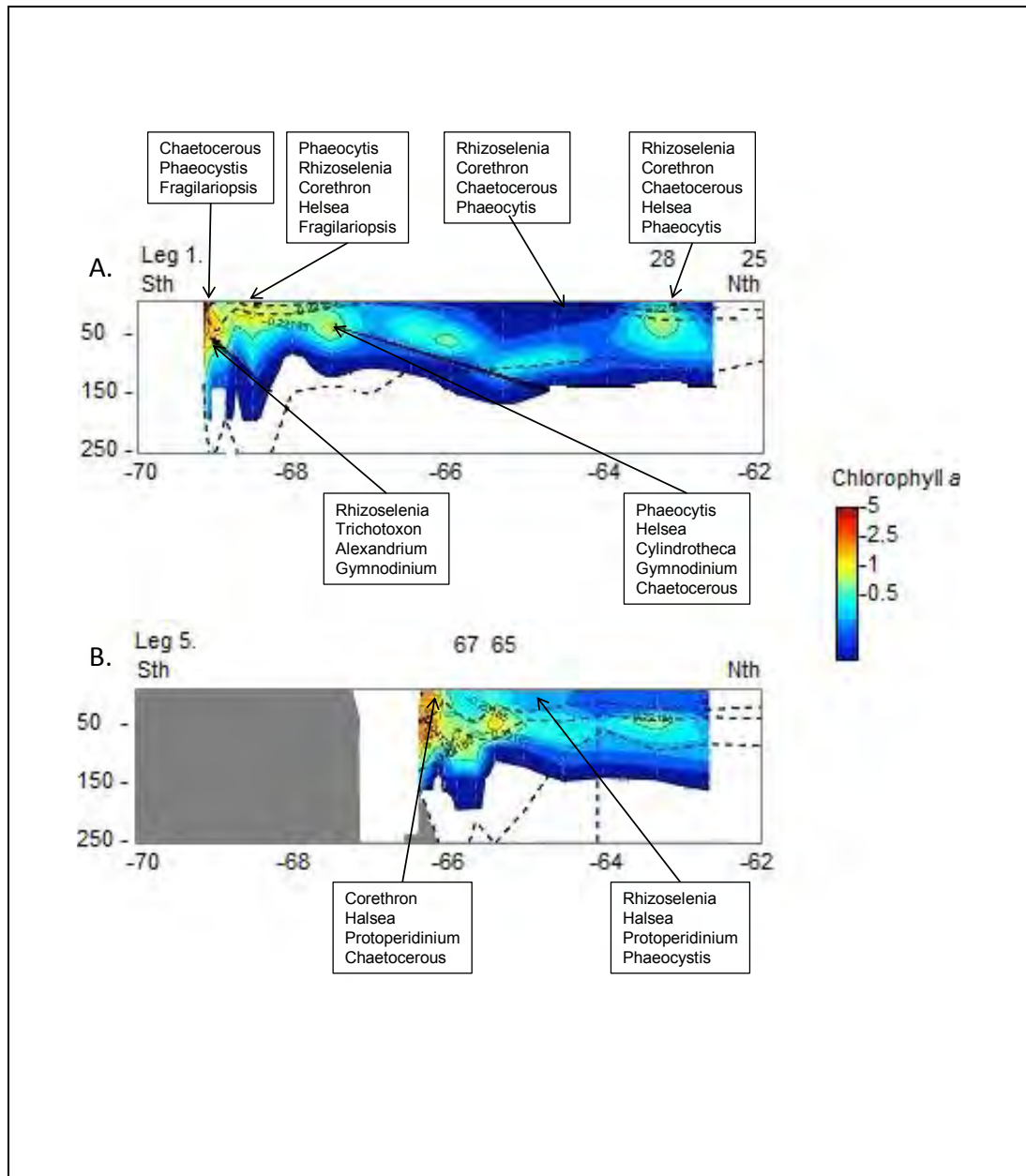


Figure 7.15. Marine protist distributions in relation to chlorophyll *a* (µg/L). A. Leg 1 showing the northerly location of CTDs 28 and 25, and B. Leg 5 showing the southerly location of CTDs 67 and 65 (modified after Wright et al., 2010).

7.4.2 Larvacean diet determined by scanning electron microscopy (SEM)

Protists associated with the diet of *O. gaussica* are listed in Table 7.3. Of the 14 marine protists associated with *O. gaussica*, 4 species occurred both within the stomach and on the surface: *Corethron pennatum* (Figure 7.16 A), *Thalassiosira gracilis* (Figure 7.16 B), *Fragilariopsis curta/cylindrus* and *F. kerguelensis* (Figure 7.16 C).

Marine protists that occurred only on the surface of larvaceans included *Asteromphalus*, *Asteromphalus hookeri*, *Eucampia antarctica* (var. *recta*), *Chaetoceros*, *Chaetoceros dichchaeta* and *Rhizosolenia*. These species were assumed to have been filtered through the inlet filter mesh, but were too large to be consumed. In some cases, the surface of *O. gaussica* was densely covered with *Rhizosolenia*, as shown in Figure 7.17.

Protists found within the stomach included *Corethron pennatum*, *Thalassiosira gracilis*, *Fragilariopsis curta/cylindrus*, *F. kerguelensis* and *F. rhombica*. These species were assumed to be consumed for sustenance and not in the stomach by accident. Figure 7.18 shows a low-magnification SEM image of stomach contents spread across the SEM stub.

Table 7.3. Protists found in the water column, on the surface of *O. gaussica*, or within the stomach of *O. gaussica* in the Southern Ocean. Those in **bold** occurred in all three scenarios.

Marine protist	Water column	STOMACH	SURFACE
<i>Asteromphalus</i>	X		X
<i>Asteromphalus hookeri</i>	X		X
<i>Eucampia Antarctica</i> (var. <i>recta</i>)	X		X
<i>Chaetoceros</i>	X		X
<i>Chaetoceros dichchaeta</i>	X		X
<i>Rhizosolenia</i>	X		X
<i>Thalassiosira</i>	X	X	X
<i>Thalassiosira gracilis</i>	X	X	X
<i>Fragilariopsis</i>	X	X	X
<i>Fragilariopsis curta / cylindrus</i>	X	X	X
<i>Fragilariopsis kerguelensis</i>	X	X	X
<i>Fragilariopsis rhombica</i>	X	X	
<i>Dictyocha speculum</i>	X		X
<i>Corethron pennatum</i>	X	X	X

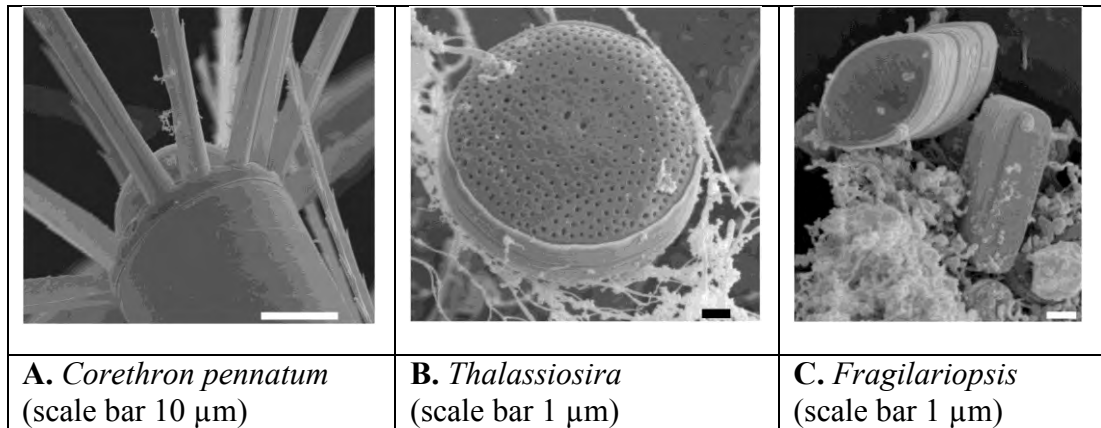


Figure 7.16. Antarctic marine protists found in the water column, on the surface of *O. gaussica*, or within the stomach of *O. gaussica*. A. *Corethron pennatum* (scale bar 10 μm) B. *Thalassiosira* (scale bar 1 μm) C. *Fragilariopsis* (scale bar 1 μm).

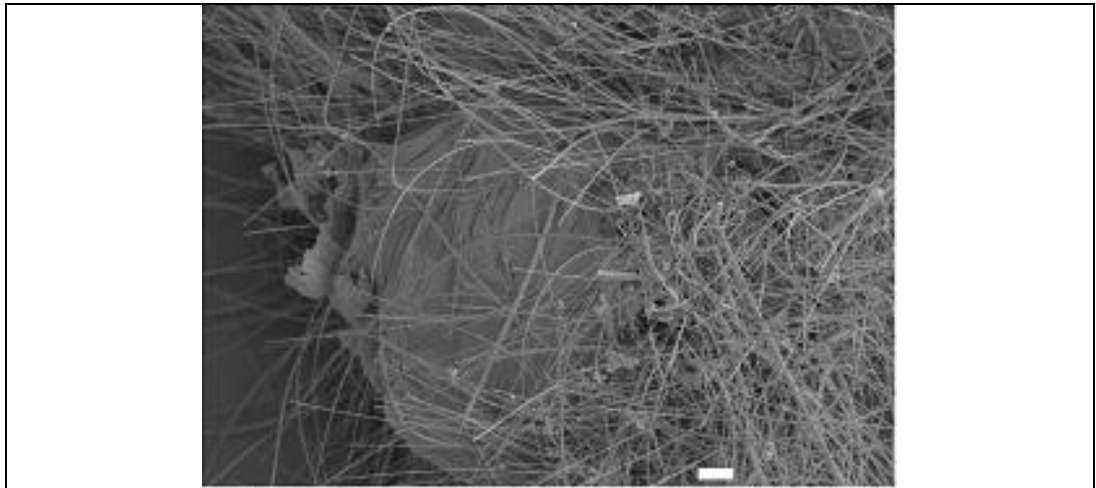


Figure 7.17. *Rhizosolenia* on the trunk of *O. gaussica* (scale bar 100 μm).

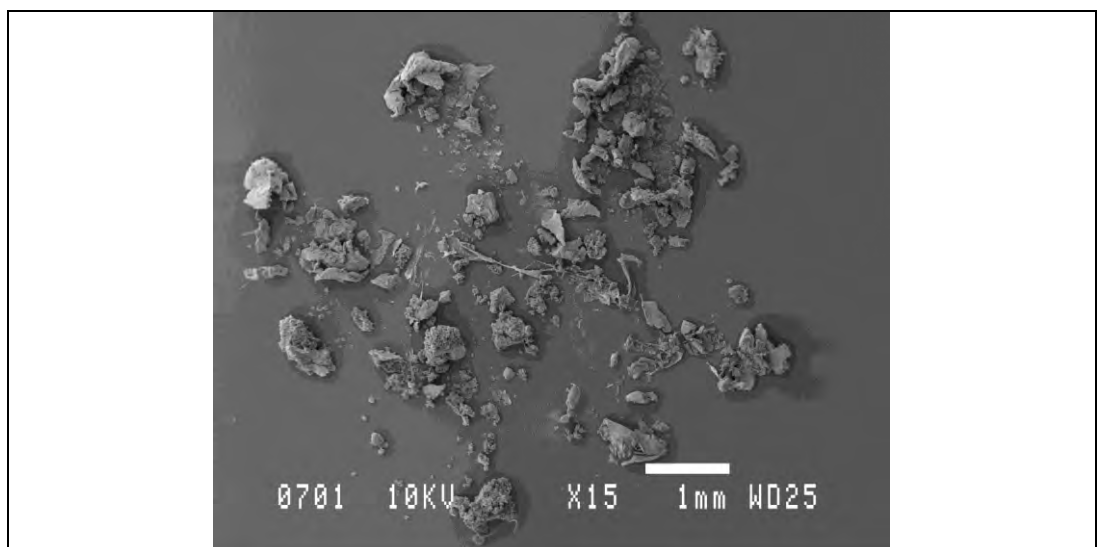


Figure 7.18. SEM stub showing gut content

7.4.3 Inferred mesh size

Table 7.4 shows the size of protists associated with the diet of *O. gaussica*. Figure 7.19 demonstrates a size comparison between a larvacean and its prey items. All sizes of protists identified in the water column, on the surface of *O. gaussica*, or within the stomach of *O. gaussica* are listed in Appendix VIII.

The mesh size of *O. gaussica* (2 cm body length) was inferred by considering the alignment and sizes of protists found on the surface of *O. gaussica*, within the stomach of *O. gaussica* or within the water column. The largest protist located within the stomach and on the surface of *O. gaussica* was *Corethron pennatum*. From SEM images of *C. pennatum* in the stomach, the long axis was unable to be measured as there were no images of the entire cell. The short axis was 600 μm inclusive of setae, and 34 μm not inclusive of setae. These measurements are comparable to Scott and Marchant (2005) who showed an apical axis from 5 to 82 μm and a perivalvar axis of 20 - 240 μm .

Table 7.4. Size of protists (from Scott and Marchant 2005) associated with the diet of *O. gaussica*. Those in **bold** occurred in the water column, on the surface of *O. gaussica*, and within the stomach of *O. gaussica*.

PROTISTS	SIZE (μm)	Apical axis (μm)	Pervalvar axis or transapical (μm)
<i>Asteromphalus</i>	22-120		
<i>Asteromphalus hookeri</i>	25-60		
<i>Eucampia antarctica</i> (var. <i>recta</i>)	39-116		
<i>Chaetoceros</i>	7-50		
<i>Chaetoceros dichchaeta</i>	7 - 40	7-50	10-40
<i>Corethron pennatum</i>	5 - 240	5-82	20-240
<i>Rhizosolenia</i>	2.5 - 400	2.5-57	400
<i>Thalassiosira gracilis</i>	5-28		3.5-9.5
<i>Thalassiosira</i>	5-71		
<i>Fragilariopsis curta / cylindrus</i>	2 - 42	10-42 / 9-12	3.5-6 / 2-4
<i>Fragilariopsis kerguelensis</i>	5 - 76	10-76	5-11
<i>Fragilariopsis rhombica</i>	7 - 53	8-53	7-13
<i>Fragilariopsis</i>	2-76		
<i>Dictyocha speculum</i>	70 diameter		

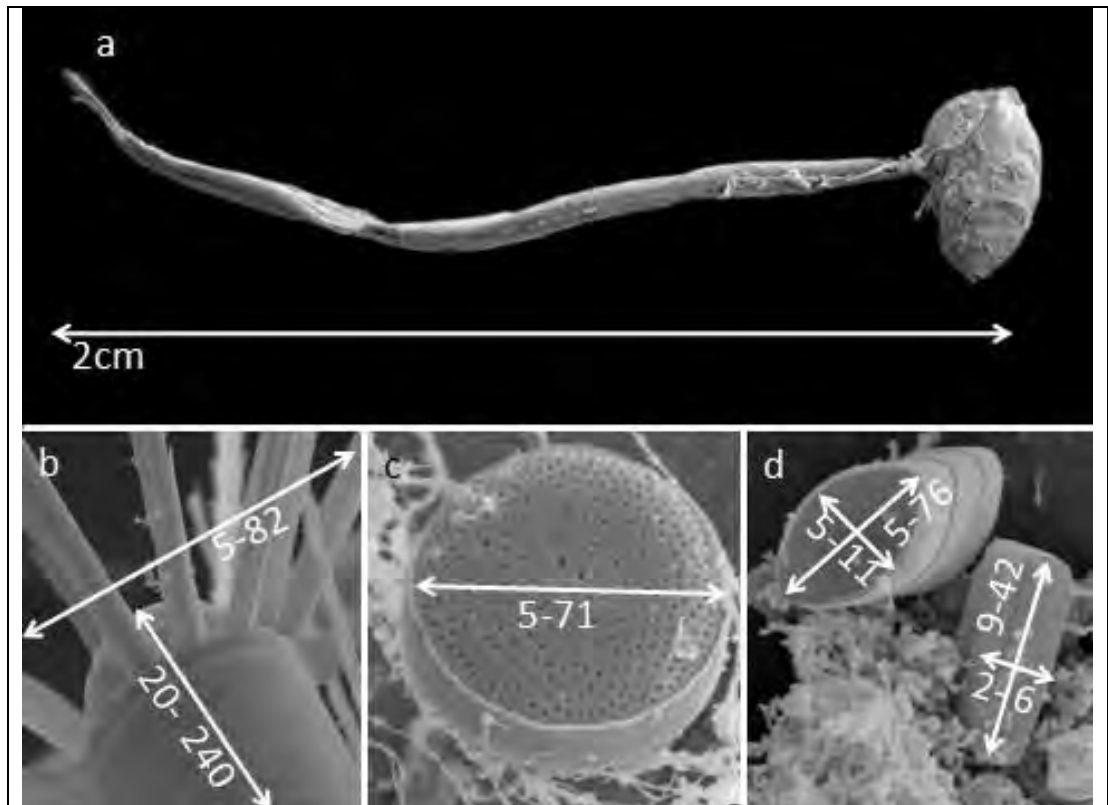


Figure 7.19. Size comparison between a. *O. gaussica* and b. *Corethron pennatum* (axis size range in μm) c. *Thalassiosira* (axis size range in μm) d. *Fragilariopsis* (axis size range in μm).

Figure 7.20 shows the alignment of *C. pennatum* that would be required for *O. gaussica* to be able to filter this species through its feeding mesh. Runge and Ohman (1982) identified that the size of a cell that passes through a mesh is determined by its smallest diameter. This is because cells tend to align lengthways and parallel to the water flow through a pore. The suggested alignment for *C. pennatum* cells requires a pore size between 5 and 82 μm .

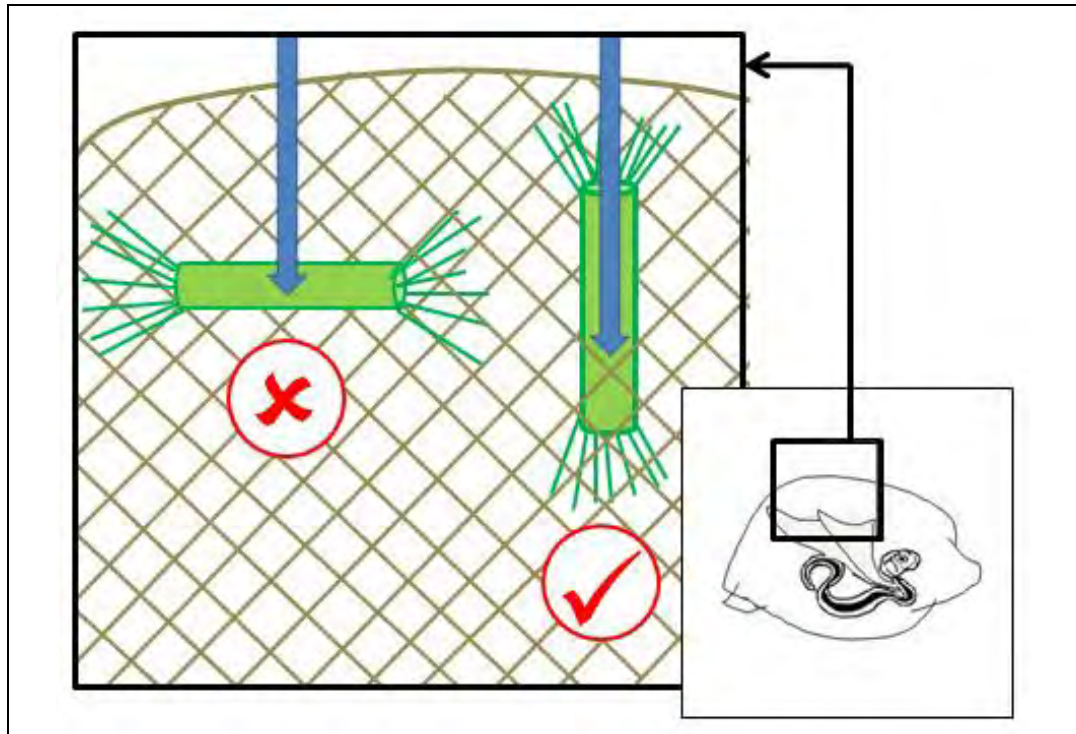


Figure 7.20. The alignment of *Corethron pennatum* cells required for ingestion by *O. gaussica*. The inferred feeding-mesh size from this alignment is between 5 and 82 μm given the known dimensions of the protist.

7.5 Discussion

The feeding ecology of *O. gaussica* from the Southern Ocean was determined by using SEM. Unfortunately, the ring net did not capture any larvaceans in their feeding houses, but marine protists on the surface of *O. gaussica*, within the stomach of *O. gaussica*, and in the water column from CTDs were able to be compared. Marine protists on the surface of the larvaceans were assumed to have been filtered through the coarse-meshed inlet filters of the feeding house, and through the finer food concentrating filters. Marine protists within the stomach essentially provided a ‘snapshot’ of what the larvaceans had consumed and therefore filtered. Protists in the water column were all assumed to be possible food sources for *O. gaussica* due to the general filter feeding method utilised by larvaceans.

This study identified that *O. gaussica* consumed a number of marine protists and these are listed in Table 7.3. Protists found within the stomach included *Corethron pennatum*, *Thalassiosira gracilis*, *Fragilariopsis curta/cylindrus*, *F. kerguelensis*

and *F. rhombic*. These protists were assumed to be consumed for sustenance. The smaller Southern Ocean larvacean *Fritillaria sp.* may consume different protists due to the smaller size of its food concentrating mesh. In the Southern Ocean, there is a low abundance of picoplankton (Wright et al., 2009), so that bacteria may instead be the dominant group consumed by this group.

Spines of *Corethron pennatum* were located in the stomach of *O. gaussica*. It was thought that these spines would have been filtered out in the feeding house due to the presence of barbs and because the setae are the widest part of the protist. The setae of *C. debile* (a temperate filamentous diatom species) is approximately 95% of the width of the species. However, during filtration the spines either bend, but remain intact, or the tips break off (Chamisso and Eysenhardt, 1821).

Approximately 30% of filtered particulate matter remains in the feeding house of larvaceans (Gorsky, 1980). This is then discarded with the house when it clogs. In this study it was found that some of the filtered protists remained on the surface of larvaceans suggesting that not all filtered material was discarded. Alternatively, the protists that were attached to the surface of the larvaceans may have been due to dislodgement and disturbance during the capture process.

During the BROKE-West voyage, there were high abundances of *O. gaussica* found in areas with high concentrations of *Rhizosolenia*. Figure 7.16 is an SEM image of *Rhizosolenia* on the trunk of *O. gaussica*. It is possible that the larvaceans were actively feeding on *Rhizosolenia* during the bloom. However, they may also have starved due to high saturation clogging of the feeding houses before adequate digestion could occur (Flood and Deibel, 1998). Larvacean abundances can be high in oligotrophic (or low productivity) zones (Banse, 1996; Atkinson, 1998; Fiala *et al.*, 1998). Unfortunately, these questions remain unanswered due to the inability to capture live animals or the present study.

As the capture of live larvaceans was unsuccessful during this study, mesh sizes, feeding rates and clearance rates were inferred for *O. gaussica* and *Fritillaria sp.* using estimates from literature. Numerical data on selected larvacean species and their houses were presented in Table 7.1. Due to similar body sizes between

O. labradoriensis (temperate distribution) and *O. gaussica* (Southern Ocean distribution) the published mesh size for *O. labradoriensis* (Table 7.5) was compared to that calculated in this study for *O. gaussica*. For *O. labradoriensis* the inlet filter width and length is 13 x 74 μm (Flood and Diebel, 1998). These values are within the range of that calculated for *O. gaussica* (5 - 82 μm). The food concentrating filters of *O. labradoriensis* are 0.18 μm width x 0.69 μm length for the upper filter, and 0.34 μm width x 1.430 μm length for the lower filter. These food concentration filters are finer than the assumed mesh size for *O. gaussica*.

The filtration rate for *O. labradoriensis* is 35 ml h^{-1} and the house renewal rate is 2.32 ± 1.03 houses per day (Flood and Diebel, 1998). This was assumed to be similar for *O. gaussica*. Filtration rates are temperate dependent, but given that *O. labradoriensis* is also a cold water species, the rates are likely to be similar.

The methods applied to determine the feeding ecology of *O. gaussica* in this study could not be applied to *Fritillaria sp.* due to its small cell size and difficulty with dissections. In addition, it was not in adequate abundance or in a satisfactory condition at any station. The similar size of Southern Ocean *Fritillaria sp.* to *F. borealis* allows the assumption that it has a similar filtration rate and feeds on similar sized protists. *F. borealis* can feed efficiently on particles < 0.45 μm in diameter and filters particles < 30 μm (Flood and Diebel, 1998).

Table 7.5. Numerical data on feeding behaviour of *O. labradoriensis* and *F. borealis* (Flood and Diebel, 1998) compared to *O. gaussica* and *Fritillaria* sp. (this study). (U) Upper filter screen (L) Lower filter screen. **Bold** values are assumptions due to similar size.

Species		<i>O. labradoriensis</i>	<i>O. gaussica</i>	<i>F. borealis</i>	<i>Fritillaria</i> sp.
Animal size	Trunk length (mm)	3.6	5	1.3	0.5
	Tail length (mm)	14.4	15	3	1.5
House diameter	(mean \pm SD) (mm)	18	20	2.5	2
Inlet filter mesh	Width (mean \pm SD) (μ m)	12.7 \pm 2.1	5 - 82	(<30)	(<30)
	Length (mean \pm SD) (μ m)	74 \pm 12			
	Length: Width ratio	5.8:1			
Food concentrating filter mesh	Width (mean \pm SD) (μ m)	180 \pm 30 (U) 240 \pm 30 (L)	5 - 82	(<0.45)	(<0.45)
	Length (mean \pm SD) (μ m)	690 \pm 200 (U) 1430 \pm 170(L)			
	Length: Width ratio	3.8:1 (U) 6:1 (L)			
Open area fraction	(%)	95			
Filtration (F) or clearance rate (C)	(ml h ⁻¹)	35	35	12 (F)	12 (F)
House renewal rate	(houses day ⁻¹)	2.32 \pm 1.03	2.32 \pm 1.03		

7.6 Conclusion

The experimental phase of this project was originally conceived to include both a survey of the distribution and abundance of larvaceans in the Southern Ocean and direct measurements of their feeding behaviour and carbon flux.

The distribution and abundance data from Chapters 4, 5 and 6 determined that larvaceans occur throughout the Southern Ocean in varying abundances, depending on oceanographic zone. This chapter attempted to determine the feeding behaviour in relation to distribution and abundance. However, given that no live animals were able to be captured, data on their feeding behaviour was

instead determined using SEM and comparing this with published data on similar larvaceans. It was estimated that *O. gaussica* has a clearance rate of 35 ml h⁻¹ and an inferred mesh size between 5 and 82 µm. In smaller *Fritillaria sp.*, filtration rate was inferred as 12 ml h⁻¹ with inlet filters < 30 µm and food concentration filters <0.45 µm. In Chapter 8, these parameters are utilised to examine the contribution of larvaceans to carbon flux in the Southern Ocean.

CHAPTER 8.

Conclusions

8.1 Overview

This thesis was undertaken to examine the ecological role of Southern Ocean larvacean species and to determine their contribution to carbon flux in the Southern Ocean. As noted in the introduction (Chapter 1), initial estimates from existing Continuous Plankton Recorder (CPR) surveys from limited regions suggested the possibility of a large biomass of larvaceans in this region. This, combined with the ability of these organisms to ingest particulate matter across many orders of magnitude in size, suggested that larvaceans may contribute significantly to carbon transfer from surface waters to the deep ocean. Larvaceans may also play an unusual role in the Antarctic food-web through the provision of an alternative path of carbon flow between protists and higher trophic levels. In this final chapter, a summary of the estimates of distribution and abundance from Chapters 4, 5 and 6 is provided. This is then coupled with inferred feeding rates from Chapter 7 to estimate the overall grazing impact and contribution to carbon flux from larvaceans in the Southern Ocean.

8.2 Abundance and distribution of larvaceans

Larvaceans were collected during four marine science voyages (BROKE-West, SAZ-Sense, SIPEX and CEMARC- Pelagic) that surveyed different oceanographic zones during different seasons in the Southern Ocean. Sampling devices that were used to capture/observe larvaceans included a purpose-built ring net, a Rectangular Mid-Water Trawl (RMT1), a Working Party 2 (WP2) net, a HYDRO-BIOS MultiNet, a Visual Plankton Recorder (VPR) and a Continuous Plankton Recorder (CPR). The two dominant genera collected were *Oikopleura* and *Fritillaria*. The main species were *O. gaussica*, *O. vanhoeffeni*, *F. drygalski*, *F. borealis* typica, and a *Fritillaria* sp. that was larger than *F. borealis* typica.

The surveys revealed that larvaceans were present throughout all Southern Ocean zones. Their distributions were difficult to characterise, with many net hauls

recovering no individuals (55%), and others returning high abundances (up to 57.8 individuals m^{-3}). Individual voyages indicated correlations with temperature, phytoplankton biomass (indicated by fluorescence) or other water column parameters (Table 8.1), but these did not apply consistently across the combined data set. The grouping of results according to oceanographic zones was the simplest and most robust approach for data interpretation. The major patterns are summarized in Figure 8.1 with the results assigned to 3 zones – the Subantarctic Zone (SAZ), the Permanently Open Ocean Zone (POOZ), and the Sea Ice Zone (SIZ). In all three zones, *Fritillaria* sp. was in higher abundance than *Oikopleura* sp.

Figure 8.1 indicates that the relative abundance of larvaceans in the different oceanographic zones may depend on the sampling method utilised, with differences observed between net haul and CPR results. The average abundance for nets hauls over the four voyages was 1.4 ± 5.4 ind m^{-3} , and for the CPR was 6.4 ± 29.7 ind. m^{-3} . The net hauls returned highest larvacean abundances in the POOZ (2.8 ± 10.6 ind. m^{-3} , maximum = 57.8 ind. m^{-3}), intermediate abundances in the SIZ (1.4 ± 4.8 ind. m^{-3} , maximum = 49.7 ind. m^{-3}) and lowest abundances in the SAZ (0.6 ± 2.6 ind. m^{-3} , maximum = 15.9 ind. m^{-3}). In contrast, the CPR surveys suggested that highest abundances occurred in the SIZ (Figure 8.1). This discrepancy may reflect different spatial and temporal coverage using each method, although the sparseness of sampling prevents rigorous examination of this issue. The difference in abundances between plankton nets and the CPR also occurred when Hunt and Hosie (2003) compared zooplankton abundances and distributions from NORPAC net and CPR samples in the Southern Ocean. That study found that zooplankton had similar distributions, but the CPR found higher abundances. Based on the temporal coverage of CPR sampling, peak abundances of larvaceans were found to occur in February (austral summer) across all zones.

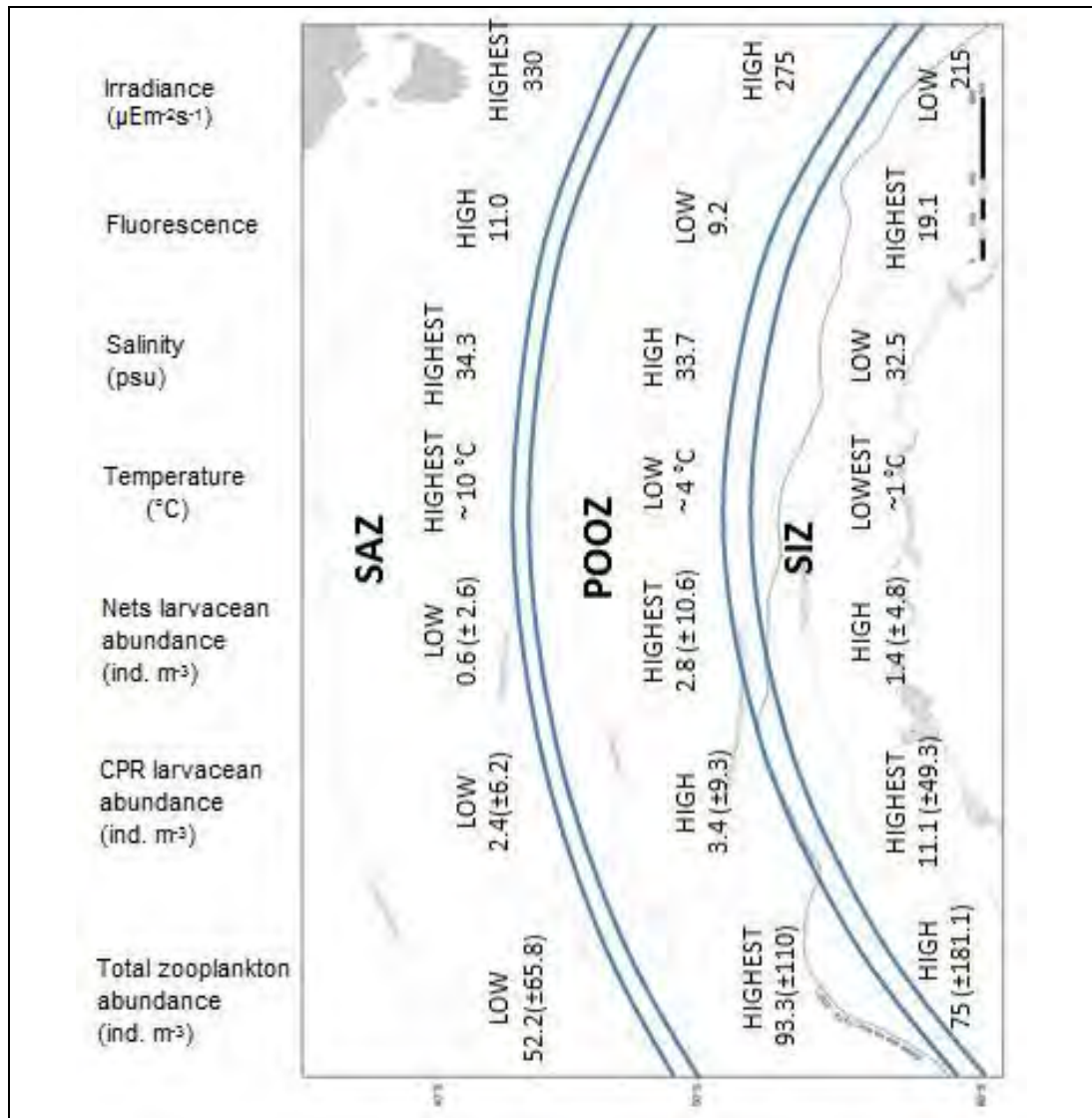


Figure 8.1 Relative abundances of larvaceans in the Southern Ocean compared to physical (latitude, longitude, temperature, salinity and light) and biological (total zooplankton) distributions.

Table 8.1. Physical parameters that were significantly correlated with larvacean abundances for each voyage. Data was analysed using Pearson's r correlations.

Parameter	Voyage	Sample device	Chapter
Latitude	BROKE West	Ring net	5 and 6
	BROKE West	RMT	5 and 6
	SIPEX	CPR	6
	CEAMARC	Nets	6
	CEAMARC	CPR	6
Longitude	BROKE West	RMT	5 and 6
	SIPEX	CPR	5 and 6
	CEAMARC	Nets	6
	CEAMARC	CPR	6
Fluorescence	SIPEX	Ring net	6
	SIPEX	CPR	6
	CEAMARC	CPR	6
Irradiance	SIPEX	Ring net	6
Water temperature	SIPEX	CPR	6
	CEAMARC	Nets	6
	CEAMARC	CPR	6
Salinity	SIPEX	CPR	6

8.3 Feeding ecology of larvaceans

Scanning electron microscopy (SEM) was conducted on stomach dissections from larvaceans collected using a ring net during BROKE-West. Observations suggested that larvaceans consume protists ranging in size from 3.5 μm – 240 μm . This was consistent with earlier results from Deibel (1998) who suggested that the diet of larvaceans includes picoplankton (<2 μm), nanoplankton (~2 – 20 μm), large diatoms and dinoflagellates (100 μm).

Studies in temperate areas (Banse, 1996; Atkinson, 1998; Fiala *et al.*, 1998) have shown that larvaceans prefer oligotrophic waters given that high abundances tend to occur in regions of low productivity. When larvaceans are supersaturated with food, it is thought that they are unable to replace their feeding houses at a fast enough rate to enable them to feed efficiently and therefore survive. Observations from the Southern Ocean during this study were consistent with this view, e.g. high larvacean abundances were found in low productivity regions within the SAZ-Sense survey area (chlorophyll $a < 0.8 \mu\text{g L}^{-1}$). However, during BROKE-West, *Fritillaria* sp. were found in high abundances in the SIZ in waters that were highly concentrated with phytoplankton (chlorophyll $a > 2 \mu\text{g L}^{-1}$). Hopcroft et al.

(2005) suggested that larvaceans in polar Arctic waters are adapted to boom and bust cycles of productivity. Results from the SIZ during BROKE-West suggest that the same pattern may occur in Antarctica.

For the purposes of the calculations that follow in section 8.4, the diet of *Fritillaria* sp. in the Southern Ocean was assumed to be similar to that of *F. borealis*. Unfortunately, attempts to maintain *Fritillaria* sp. in culture were unsuccessful so that direct grazing rates were unable to be determined. *F. borealis* has been shown to feed efficiently on particles < 0.45 μm in diameter and filters particles < 30 μm (Flood and Diebel, 1998). These sizes are comparable with the stomach dissection results obtained in Chapter 7, lending some support to this approach.

8.4 Larvacean biomass and grazing estimates, and their possible contribution to carbon fluxes to the ocean interior.

For initial calculations of the biomass of larvaceans in the Southern Ocean, a conservative NORPAC net abundance of 5 ind m^{-3} (Hunt and Hosie, 2003) was assumed, with an even distribution of individuals in the upper 150 m of the ocean. The approximate area of the Southern Ocean is 50 million km^2 . Assuming that the individual wet weight of a larvacean is 1 mg (Sato, 2005), the biomass of larvaceans in the Southern Ocean would be ~37.5 million tonnes. This is comparable to approximately 100 million tonnes of krill and 250 million tonnes of copepods (Wright, 2010). However, if the average estimate of larvacean abundance obtained from net samples during this study is used (1.4 ind m^{-3}), the larvacean biomass estimate is reduced to ~10.5 million tonnes.

To convert larvacean biomass into carbon units, a body carbon weight of 10 μg C per individual was used (Table 8.2). This yielded a total carbon biomass of 0.1 million tonnes. As a comparison, the total carbon biomass of a copepod-dominated zooplankton populations in the Southern Ocean is 23.5 million tonnes, assuming the copepod body carbon weight of 94 μg C per individual, the upper

end of the estimate provided in Table 8.2. Therefore, larvaceans contribute ~0.4 % of total zooplankton biomass in the Southern Ocean.

To gain perspective on the efficiency of carbon processing by larvaceans in the Southern Ocean, estimates for rates of grazing, production of faecal pellets and the discarding of polysaccharide houses are required. These are all pathways for carbon flow and were summarised in Chapter 7 (Figure 7.12). New estimates of carbon processing were unable to be obtained given that no larvaceans were able to be maintained in culture. Therefore, estimates from previous studies in temperate and tropical waters were used, as summarised by Sato et al. (2005) and presented in Table 8.2.

Sato et al. (2005) determined the ingestion rates and clearance rates of three temperate and tropical larvaceans. Ingestion efficiencies were affected both by temperature and the concentration of particulate matter. Feeding houses were found to clog at a greater rate for *O. rufescens* compared to *O. fusiformis* and *O. langicauda*. Clearance rates have also been shown to be affected by temperature, as well as body size, with faster clearance rates observed for *O. dioica* with a larger body size at higher temperature (Broms and Tiselius, 2003). The weight-specific clearance rate of a cold water species, *O. vanhoeffeni*, was found to be slower than temperate and tropical species, though it was faster at lower temperatures rather than slower (Knoechel and Steel-Flynn, 1989).

Table 8.2 suggests that clearance rates for larvaceans are similar to, or higher than krill, copepods and salps. Although larvaceans contribute a relatively small proportion to zooplankton biomass in the Southern Ocean, their relatively high clearance rate means that they may have an impact on the food-chain several times higher than would be expected from biomass alone.

Table 8.2. Carbon-based weight specific clearance rates and ingestion rates (source Sato et al. 2005).

Species	Body carbon weight (μg)	Weight specific clearance rate ($\text{ml } \mu\text{gC}^{-1}\text{h}^{-1}$)	Weight specific ingestion rate ($\text{pgChl.a } \mu\text{gC}^{-1}\text{h}^{-1}$)	Reference
Copepoda	3 - 94	0.6	362	Sato et al. 2005
<i>E. superb</i>	18000 – 56000	0.00003 – 3.7		Morris 1984; Ikeda and Mitchell 1982
<i>Salpa thompsoni</i>	2440	0.1		Huntly et al. 1989
<i>O. dioica</i>	10	0.6		King et al. 1980
	10	1.8		Paffenhofer 1976
	10	1.4		Allredge 1988
<i>O. vanhoeffeni</i>	10	2.0		Deibel 1988
(cool water)	10	1.5		Morris and Deibel 1993, Deibel 1986
			813	Acuna et al. 1999
<i>O. longicauda</i>	10	2.7 – 6.2	398 - 4342	Sato et al. 2005
<i>O. rufescens</i>	10	1.9 – 5.0	683 - 2300	Sato et al. 2005
<i>O. fusiformis</i>	10	6.3 – 12.9	854 - 5284	Sato et al. 2005

This perspective was recently championed by Jaspers et al. (2009), who found that larvacean production (taken as one-third of measured ingestion rate) was significant despite low abundance and biomass estimates. This was due to high grazing rates which can exceed that of copepods.

Discarded feeding houses are a potentially major source of sinking carbon in the Southern Ocean because of their large size, high abundance and rapid production rate. The contribution of discarded larvacean houses to the flux of particulate organic carbon (POC) from oceanic surface waters was studied by Allredge (2005). Calculations included abundances of *O. dioica* and *O. longicauda*, frequency distributions, size-specific carbon content of discarded houses and house sinking rates. The potential flux of particulate carbon was found to range from < 1 to over $1200 \text{ mg C m}^{-2} \text{ d}^{-1}$. The wide range resulted from high variation in larvacean abundances (from 1 to $20\,000 \text{ ind. m}^{-3}$). The maximum contribution to POC flux from discarded houses ranged from 12 to 83 %, though the majority of values were between 28 – 39%. This included both eutrophic coastal and oligotrophic oceanic regions.

In more recent work, the contribution to POC flux by larvaceans was estimated to be less than 1% of available carbon biomass (Lombard et al., 2010). This estimate was based on outputs from a multi-species ecophysiological model that included four larvacean species from the English Channel in the North Atlantic: *O. dioica*, *O. longicauda*, *O. fusiformis* and *O. rufescens*. The model found that there were high rates of consumption of the feeding houses whilst sinking through the water-column, thus reducing carbon export. It also found that 0.6% of available particulate carbon was grazed by larvaceans when present in high abundance (135 ind. m⁻³). Of this grazed material, 21% was used for growth, 14% was respired and 65% was lost as detritus.

Measured abundances of a few individuals per cubic meter in this thesis, suggest that contributions to carbon flux were towards the lower end of values estimated by Alldredge (2005) and Lombard et al. (2010). It was likely that the contribution is in the order of 1 mg C m⁻² d⁻¹ or less. This equates to 1% of primary production in the Southern Ocean as determined by an algorithm from satellite remote sensing of phytoplankton productivity (Arrigo et al., 1998). However, this estimate is clearly uncertain owing to the lack of direct measures of the rates of grazing, faecal pellet production, and mucopolysaccharide house renewal for Southern Ocean larvaceans.

8.5 Conclusion

The aim of this research was to determine the ecological role of Southern Ocean larvacean species and to determine their level of importance in relation to carbon contribution in the Southern Ocean. This was examined by determining larvacean distribution and abundances, and relating the results to biological and physical parameters as well as feeding ecology. Four main hypotheses were tested:

1. That the distribution and abundance of larvaceans have distinct zonation, as well as seasonal and annual variation.
2. That the distribution and abundance of larvaceans is related to physical (latitude, longitude, temperature, salinity and light) and biological (chlorophyll *a* and total zooplankton) influences.

3. That the diet of Southern Ocean larvaceans is selective.
4. That larvaceans contribute significantly to carbon flux in the Southern Ocean.

Based on multiple voyages undertaken during this research, Southern Ocean larvacean distributions were grouped into three oceanographic zones; the Sub-Antarctic zone (SAZ), the Permanent Open Ocean Zone (POOZ), and the Sea Ice Zone (SIZ). Within individual voyages, abundances showed correlations with latitude, longitude, fluorescence, irradiance, water temperature and salinity. However, seasonal and inter-annual variations were large and no strong environmental determinant of abundance emerged for the Southern Ocean overall.

Limited studies of stomach contents of *O. gaussica* during BROKE-West showed that *Corethron pennatum*, *Thalassiosira gracilis*, *Fragilariopsis curta/cylindrus*, *F. kerguelensis* and *F. rhombica* had been ingested. The estimated size of the food concentrating mesh was between 5 and 82 μm based on known dimensions of the largest ingested species, *Corethron pennatum*.

This study provides an initial baseline estimate of the role played by larvaceans in the Antarctic marine ecosystem. Calculations using measured abundances and inferred clearance rates showed that larvaceans are an important component of zooplankton trophodynamics in the Southern Ocean.

8.6 Recommendations for future studies

Future surveys should include other regions around Antarctica, including open waters north of the SIZ where larvaceans have also been shown to be prominent (Hunt and Hosie, 2003; 2006b). Further studies on feeding ecology to assess grazing impacts and secondary production, particularly in regards to their nutritional ecology and the role they may play in benthic-pelagic coupling, are also required. A major drawback to this study was the difficulty in capturing live larvaceans and appropriate techniques to do so need to be developed. Cultivation

of live larvaceans will enable the determination of feeding and breeding behaviours. With the development of *in situ* sampling and observation devices, the role of larvaceans in the food-web could be better understood. Live experiments would also enable a more accurate calculation of the contribution of larvaceans to carbon flux and trophodynamics, by determining life expectancy and rates of feeding house and faecal pellet production and sinking and tolerance to a variety of physical parameters (temperature, salinity, etc).

In addition to live experiments, the latest DNA methods could be used to identify Southern Ocean larvaceans and stable isotope analysis could be used to determine if resource partitioning exists between larvacean species in the Southern Ocean.

To determine how larvacean feeding house “flux” estimates from this study relate to the actual primary production rates and POC flux measurements, sediment traps samples deployed in the Southern Ocean (eg. Trull et al., 2001 in the SAZ and Pilskałn et al., 2004 in Prydz Bay) could be used. Larvacean houses are recognised primarily by their filters and these filters are very difficult to resolve in the mix of material in sediment trap samples (Silver and Gowin. 1991). Gel traps were deployed during the SAZ Sense voyage but only one larvacean was identified and therefore not included in this study.

References

- Aida, T. 1907. Appendicularia of Japanese waters. *Journal of the College of Science*. Imperial University, Tokyo, Japan **23** 1 -25.
- Allredge, A.L., Silver, M.W. 1988. Characteristics, dynamics and significance of marine snow. *Progress Oceanography*. **20**:41-82.
- Allredge, A. 2005. The contribution of discarded appendicularian houses to the flux of particulate organic carbon from oceanic surface waters *in* Response of Marine Ecosystems to Global Change – Ecological Impacts of Appendicularians. Gordon and Breach Scientific Publishers. 309 – 326.
- Arrigo, K.R., Worthen, D., Schnell, A. and Lizotte, M.P., 1998. Primary production in Southern Ocean waters. *Journal of geophysical research* **103**, 15587 – 15600.
- Atkinson, A. 1998. Life cycle strategies of epipelagic copepods in the Southern Ocean. *Journal of Marine Systems*, **15**, 289 - 31
- Atkinson, A., Siegel, V., Pakhomov, E., & Rothery, P. 2004. Long-term decline in krill stock and increase in salps within the Southern Ocean. *Nature*, **432**, 100 - 103.
- Australian Antarctic Data Centre. revised 2009. SCAR Southern Ocean Continuous Plankton Recorder Survey data (<http://data.aad.gov.au/aadc/cpr/>).
- Banse, K. 1996. Low seasonality of low concentrations of surface chlorophyll in the Subantarctic water ring: underwater irradiance, iron, or grazing? *Progress in Oceanography*, **37**, 241 – 291.
- Bedo, A.W., Acuna, J.L., Robins, D., Harris, R.P. 1993. Grazing in the micron and the sub-micron particle size range: the case of *Oiklopeura dioica* (Appendicularia). *Bulletin of Marine Science*, **53**, 2 - 14.
- Blain S., Quéguiner, B., Armand, L., Belviso, S., Bombled, B., Bopp, L., Bowie, A., Brunet, C., Brussaard, C., Carlotti, F., Christaki, U., Corbière, A., Durand, I., Ebersbach, F., Fuda, J. L., Garcia, N., Gerringa, L., Griffiths, B., Guigue, C., Guillerm, C., Jacquet, S., Jeandel, C., Laan, P., Lefèvre, D., Lomonaco, C., Malits, A., Mosseri, J., Obernosterer, I., Park, Y.-H., Picheral, M., Pondaven, P., Remenyi, T., Sandroni, V., Sarthou, G., Savoye, N., Scouarnec, L., Souhaut, M., Thuiller, D., Timmermans, K., Trull, T., Uitz, J., van-Beek, P., Veldhuis, M., Vincent, D., Viollier, E., Vong, L., and Wagener, T. 2007. Impacts of natural iron fertilisation on the Southern Ocean. *Nature* **446**: 1070-1074, doi:10.1038/nature05700.
- Boyd P. W., Jickells, T., Law, C. S., Blain, S., Boyle, E. A., Buesseler, K. O., Coale, K. H., Cullen, J. J., d. Baar, H. J. W., Follows, M., Harvey, M., Lancelot, C., Levasseur, M., Owens, N. P. J., Pollard, R., Rivkin, R. B., Sarmiento, J., Schoemann, V., Smetacek, V., Takeda, S., Tsuda, A., Turner, S., and Watson, A.

- J. 2007. Mesoscale Iron Enrichment Experiments 1993-2005: Synthesis and Future Directions. *Science* **315**: 612 - 617, DOI: 610.1126/science.1131669
- Boyd, P.W., Doney, S. C., Strzepek, R., Dusenberry, J., Lindsay, K., and Fung, I. 2008. Climate-mediated changes to mixed-layer properties in the Southern Ocean: assessing the phytoplankton response. *Biogeosciences*. **5**, 847–864.
- Bone, Q. 1998. *The Biology of Pelagic Tunicates* Oxford University Press, Oxford. p. xiii.
- Bochdansky, A. and Deibel, D. 1999. Measurement of in situ clearance rates of *Oikopleura vanhoeffeni* (Appendicularia: Tunicata) from tail beat frequency, time spent feeding and individual body size. *Marine Biology* **133** 37 – 44.
- Boero, F., Bouillion, J., Gravili, C., Milietta, M., Parsons, T., Piraino, S., 2008. Gelatinous plankton: irregularities rule the world (sometimes). *Marine Ecology Progress Series* **356**: 299 – 310.
- Bouquet, J., Spriet, E., Troedsson, C., Ottera, H., Chourrout, D. and Thompson, E. 2009. Culture optimization for the emergent zooplanktonic model organism *Oikopleura dioica*. *Journal of Plankton Research* **31**: 4 359 – 370.
- Bowie A. R., Lannuzel, D., Remenyi, T. A., Wagener, T., Lam, P. J., Boyd, P. W., Guieu, C., Townsend, A. T., and Trull, T. W. 2009. Biogeochemical iron budgets of the Southern Ocean south of Australia: Decoupling of iron and nutrient cycles in the subantarctic zone by the summertime supply. *Global Biogeochemical Cycles* **23**: GB4034, doi:4010.1029/2009GB003500.
- Bowie, A.R., Griffiths, F.B., Dehairs, F. and Trull, T.W. (in prep) Oceanographic setting of the Sub-Antarctic zone south of Australia – introduction to *Deep Sea Research SAZ-Sense special edition*.
- Bückmann, A., 1969. APPENDICULARIA. *Electronic Document Collection of ICES Identification Leaflets for Plankton*. **7**, 1 -9.
- Broms, F. and Tiselius, P., 2003. Effect of temperature and body size on the clearance rate of *Oikopleura dioica*. *Journal of Plankton Research* **25** (5) 573 – 577.
- Capitanio, F.L, Daponte, M.C., Esnal, G.B., 2003. The classification of Antarctic appendicularians: the *Oikopleura gaussica* group. *Antarctic Science* **15** (4), 476-482.
- Chamisso, A. von & Eysenhardt, C.W., 1821. De animalibus quisbusdam e classe Vermium Linneana. In, *Circumnavigatione Terrae, auspicante Comite N. Romanzoff, duce Ottone de Kotzbue, annis 1815–1818, peracta. observatio. Fasciculus secundus, reliquos vermes continens. Nova Acta Acad. Leop.-Carol* 10(2): 543–574 pl. Xxxi

- Choe, N. and Deibel, D. 2008. Temporal and vertical distributions of three appendicularian species (Tunicata) in Conception Bay, Newfoundland. *Journal of Plankton Research* **30** 9: 969 - 979
- Constable A J, Nicol S and Strutton P.G. 2003. Southern ocean productivity in relation to spatial and temporal variation in the physical environment. *Journal of Geophysical Research* **108**(C4) 8079, doi:10.1029/2001JC001270
- Davidson, A.T., Scott, F.J., Nash, G.V., Wright, S.W., Raymond, B., 2010. Physical and biological control of protistian community composition, distribution and abundance in the seasonal ice zone of the Southern Ocean between 30 and 80° E. *Deep Sea Research II*, **57**, 9-10, 828 – 848.
- Davoll, P.J., and Silver, M.W. 1986. Marine snow aggregates: life history sequence and microbial community of abandoned larvacean houses from Monterey Bay, California. *Marine Ecology Progress Series*, **33**, 111 - 120.
- Deibel, D., 1998. Feeding and metabolism of appendicularians. In Q. Bone, The Biology of Pelagic Tunicates, (pp 139-149). Oxford: Oxford University Press.
- de Baar H. J. W., de Jong, J. T. M., Bakker, D. C. E., Loscher, B. M., Bathmann, U., and Smetacek V. 1995. Importance of iron for phytoplankton blooms and carbon dioxide drawdown in the Southern Ocean. *Nature* **373**: 412-415.
- Eisen, A.G., 1874. *Vexillaria speciosa* n. sp. ett bidrag till Appendiculariornas Anatomi. *K. Sven. Vetensk.-Akad. Handl. (ser. 4)***12**(9): 1–15 pls i–iii [1].
- Esnal, G.B., 1999. Appendicularia. In South Atlantic Zooplankton (ed D. Boltovskoy). Vol. 2, pp. 1375 - 1399. Backhuys Publishers, Leiden.
- Esnal, G., Capitanio, F., and Simone, L. 1996. Concerning intraspecific taxa in *Fritillaria borealis* Lohmann (Tunicata, Appendicularia). *Bulltin Marine Science* **59** 461 – 468.
- Essenberg, C. 1926. Copelata from the San Diego region. *University California publication Zoology*. **28** 399 - 521
- Fenaux, R. 1998. Anatomy and functional morphology of the Appendicularia. In Q. Bone, The Biology of Pelagic Tunicates, (pp 25 - 34). Oxford: Oxford University Press.
- Fenaux, R. 1998. Life history of the Appendicularia. In Q. Bone, The Biology of Pelagic Tunicates, (pp 151-159). Oxford: Oxford University Press.
- Fenaux, R. 1998. The classification of Appendicularia. In Q. Bone, The Biology of Pelagic Tunicates, (pp 295 - 306). Oxford: Oxford University Press.

- Fenaux, R., Bone, Q., and Deibel, D., 1998. Appendicularia distribution and zoogeography. In Q. Bone, *The Biology of Pelagic Tunicates*, (pp 253 -264). Oxford: Oxford University Press.
- Fenaux, R and Youngbluth, M. 1990. A new mesoplelagic appendicularian, *Mesochordaeus bahamasi* gen. Nov. *Journal of Marine Biology Association* **70** 755 – 760.
- Fenaux, R and Youngbluth, M. 1991. Two new mesoplegic appendicularians: *Inopinata inflata* gen nov., sp. nov., *Mesopelagica caudaornata* gen nov., sp. nov., *Journal of Marine Biology Association* **71** 613 - 621.
- Fiala, M., Semeneh, M., and Oriol, L. 1998. Size-fractionated phytoplankton biomass and species composition in the Indian sector of the Southern Ocean during austral summer. *Journal of Marine Systems*, **17**, 179 - 194
- Fortier, L., Le Fevre, J., and Legendre, L., 1994. Export of biogenic carbon to fish and to the deep ocean: the role of large planktonic microphages. *Journal of Plankton Research*, **16**, 809 - 839.
- Foxton, P. 1966. The distribution and life history of *Salpa thompsoni* Foxton with observations on a related species, *Salpa gerlachii* Foxton. *Discovery Reports* **34** 1 – 116.
- Flood, P.R., 1991. Architecture of, and water circulation and flow rate in, the house of the planktonic tunicate *Oikopleura labradoriensis*. *Marine Biology*, **111**, 95–111.
- Flood, P. 2000. A new appendicularian, *Oikopleura gorskyi* n.sp. (Tunicata) from Norwegian fjords. *Beaufortia*, **50** 69 - 77
- Flood, P. 2003. House formation and feeding behaviour of *Fritillaria borealis* (Appendicularia: Tunicata). *Marine Biology* **143** 467 – 475.
- Flood, P and Deibel, D. 1998. The Appendicularian house. In Q. Bone, *The Biology of Pelagic Tunicates*, (pp 105 - 124). Oxford: Oxford University Press.
- Garstang, W. and Georgeson, E. 1935. Report on the Tunicata. Part II – Copelata. *British Antarctic “Terra Nova” Expedition, 1910, Natural History Report, Zoology* **4** 263 – 282.
- Gorsky, G., 1998 – 2001. European Appendicularian EURAPP. The Impact of Appendicularians in European Marine Ecosystems. www page <http://www.obs-vlfr.fr/~eurapp/> .
- Gorsky G, Youngbluth MJ, Deibel D 2005. Response of marine ecosystems to global change: ecological impact of appendicularians. Gordon and Breach Scientific Publishers. p. 3-8.

- Gorsky, G., Chretiennot-Dinet, M.J., Blanchot, J., and Palazzoli, I. 1999. Picoplankton and nanoplankton aggregation by appendicularians: Fecal pellet contents of *Megalocercus huxleyi* in the equatorial Pacific. *Journal of Geophysical Research*, **104**, 3381 - 3390
- Gorsky, G. and Fenaux, R. 1998. The role of appendicularians in marine food webs. In Q. Bone, *The Biology of Pelagic Tunicates*, (pp 161-169). Oxford: Oxford University Press
- Hays, G., Richardson, A., and Robinson, C. 2005. Climate change and marine plankton. *Trends in Ecology and Evolution* **20** (6): 337 - 344
- Hamner, W. and Robison, B. 1992. *In situ* observation of giant appendicularians in Monterey Bay. *Deep Sea Research Part A* **39** 7-8: 1299 – 1313.
- Hansen, J., Kiorboe, T., and Alldredge, A. 1996. Marine snow derived from abandoned larvacean houses: sinking rates, particle content and mechanisms of aggregate formation. *Marine Ecology progress Series* **141** 205 - 215
- Herdman, W.A., 1888. Report upon the Tunicata collected during the voyage of H.M.S. "Challenger" during the years 1873-76. III. Ascidae, Salpiformes, Thaliacea, Larvacea. *Challenger Expedition*. **27**:1-663, Pls. 1 – 11.
- Heywood, K. R., Sparrow, M. D., Brown, J., and Dickson, R. R., 1999. Frontal structure and Antarctic Bottom Water flow through the Princess Elizabeth Trough, Antarctica. *Deep-Sea Research I* **46**, 1181–1200.
- Hunt, B.P.V., and Hosie, G.W., 2003. The Continuous Plankton Recorder in the Southern Ocean: a comparative analysis of communities sampled by the CPR and vertical net hauls along 140°E. *Journal of Plankton Research* **12**, 1561-1579
- Hunt, B.P.V., and Hosie, G.W., 2005. Zonal structure of zooplankton communities in the Southern Ocean South of Australia: results from a 2150 km continuous plankton recorder transect. *Deep-Sea Research Part I*, 1241 - 1271.
- Hunt, B.P.V., and Hosie, G.W., 2006a. The seasonal succession of zooplankton in the Southern Ocean south of Australia, part 1: The seasonal ice zone. *Deep-Sea Research I* **53** 1182 – 1202.
- Hunt, B.P.V., Hosie, G.W., 2006b. The seasonal succession of zooplankton in the Southern Ocean south of Australia, part 2: The Sub-Antarctic to Polar Frontal Zones. *Deep-Sea Research I* **53** 1203 – 1223.
- Hopcroft, R, Clarke, C., Nelson, R. and Raskoff, K. 2005. Zooplankton communities of the Arctic's Canada Basin: the contribution by smaller taxa. *Polar Biology* **28**: 198 – 206.
- Hopcroft, R., Roff, J., Bouman, H. 1998. Zooplankton growth rates: the larvaceans *Appendicularia*, *Fritillaria* and *Oikopleura* in tropical waters. *Journal of Plankton Research* **20** 3: 539 – 555.

- Hopcroft, R and Robison, B. 1999. A new mesoplelagic larvacean, *Mesochordaeus erythrocephalus*, sp.nov., from Monterey Bay, with description of its filtering house. *Journal Plankton Research* **21** 1923 – 1937.
- Hosie, G. W. 1994. The macrozooplankton communities in the Prydz Bay region, Antarctica. In S. Z. El-Sayed (Ed.), *Southern Ocean Ecology: The BIOMASS Perspective* (pp. 93–123). Cambridge: Cambridge University Press.
- Hosie, G.W., Fukuchi, M., and Kawaguchi, S., 2003. Development of the Southern Ocean Continuous Plankton Recorder Survey. *Progress in Oceanography* **58**, 263 – 283.
- Hosie, G,W,. 2004 Tackling fundamental issues in Southern Ocean plankton ecology – Japan and Australia’s collaborative achievements. *Plankton Biology and Ecology* **51** (2), 57 -70.
- Hosie, G.W., 2007. The truth: Southern Ocean biomass. PowerPoint presentation,
- Hosie, G.W., Schultz, M.B., Kitchener, J.A. Cochran, T.G., and Richards, K. 2000. Macrozooplankton community structure off East Antarctica (80 – 150 E) during the Austral summer of 1995/1996. *Deep Sea Research II* **47**: 2437 – 2463.
- Hosie, G., Koubbi, P., Riddle, M., Ozouf-Costaz, C., Moteki, M., Fukuchi, M., Ameziane, N., Ishimaru, T., and Goffart, A. 2011. CEAMARC the Collaborative east Antarctic Marine census for the Census of Antarctic Marine Life (IPY # 53): An overview. *Polar Science* **5**: 75 – 87.
- Howard W.R., Roberts D., Moy A.D., Lindsay M.C.M., Hopcroft R.R., Trull T.W., and Bray S.G. Distribution, abundance and seasonal flux of pteropods in the Sub-Antarctic Zone. *Deep Sea Research II SAZ-SENSE special issue* (accepted).
- Ikeda, T., Hosie, and G., Stolp., 1986. SIBEX II cruise krill/zooplankton data. *ANARE Research notes* 32. Antarctic Division Department of Science.
- Ishikawa, A., Wright, S., van den Enden, R., Davidson, A., and Marchant, H., 2002. Abundance, size structure and community composition of phytoplankton in the Southern Ocean in austral summer 1999/2000. *Polar Biology Science* **15**, 11-26.
- Jaspers, C., Nielsen, T., Carstensen, J., Hopcroft, R., and Moller, E. 2009. Metazooplankton distribution across the Southern Indian Ocean with emphasis on the role of Larvaceans. *Journal of Plankton Research*. **31**: 5 525 – 540.
- Knoechel, R. and Steel-Flynn, D. 1989. Clearance rates of *Oikopleura* in cold coastal Newfoundland waters: a predictive model and its trophodynamic implications. *Marine Ecology Progress Series* **53**, 257 – 266.

- Knox, G. 2007. *Biology of the Southern Ocean* second edition. CRC Press. *Marine Biology Series*. USA.
- Kramp, P. 1957. Hydromedusae from Discovery collections. *Discovery Reports* **29** 1 – 128.
- Lindsay, M and Williams, G., 2010. Distribution and abundance of Larvaceans in the Southern Ocean between 30 and 80 E longitude. *Deep Sea Research II* **57** 905-915.
- Liu, H., Ciannelli, L., Decker, M., Ladd, C. And Chan, K. 2011. Nonparametric Threshold Model of Zero-Inflated Spatio-Temporal Data with Application to Shifts in Jellyfish Distribution. *Journal of Agricultural, Biological and Environmental Statistics*. **16**: 2, 185 – 201.
- Lohmann, H. 1909. Copelata und Thaliacea. pp. 143–149 in Michaelsen, W. & Hartmeyer, R. (eds) *Die Fauna Südwest-Australiens*. 2(10) Jena : Fischer.
- Lombard, F., Legendre, L. Picheral, M., Sciandra, A., and Gorsky, G. 2010. Prediction of ecological niches and carbon export by appendicularians using a new multispecies ecophysiological model. *Marine Ecology progress Series* **389** 109 – 125.
- Longhurst A. 1998. *Ecological geography of the sea*. San Diego: Academic Press.
- Mann, K.H. and Lazier, J.R.N. 1991 *Dynamics of marine ecosystem. Biological – Physical Interactions in the Oceans* Blackwell Scientific Publications USA.
- Marchant HJ, Davidson AT, Wright SW. 1987. The distribution and abundance of chroococcoid cyanobacteria in the Southern Ocean. Proc NIPR Symp *Polar Biology* **1**:1–9.
- McCullagh, P. and Nelder, J.A. 1989. *Generalized Linear Models*. Chapman and Hall, London.
- McLeod, D.J., Hosie, G.W, Kitchener, J.A, Takahashi, K.T. and Hunt, B.P.V. 1991-2008. *In Press Zooplankton Atlas of the Southern Ocean: The SCAR SO-CPR Survey* *Polar Science* doi:10.1016/j.polar.2010.03.004.
- McLeod, D.J., Hosie, G.W, Kitchener, J.A. 2009. ‘Using Southern Ocean zooplankton as canaries’. Poster.
- Meiners, K., Norman, L., Granskog, M., Krell, A., Heil, P. and Thomas, D. (in prep) Physico-ecobiogeochemistry of East Antarctic pack ice during the winter-spring transition.
- Meijers, A. J. S., Klocker, A., Bindoff, N. L., Williams, G. D., and Marsland, S. J., 2008. The circulation and water masses of the Antarctic shelf and continental slope between 30 and 80°E. *Deep-Sea Research Part II* **57** 9 – 10: 723 – 737.

- Mengesha, S., Dehairs, F., Fiala, M., Elskens, M., and Goryens, L., 1998. Seasonal variation of phytoplankton community structure and nitrogen uptake regimes in the Indian Sector of the Southern Ocean. *Polar Biology*. **20**, 259 – 272.
- Mertens, C.H., 1830. Beschreibung der *Oikopleura*, einer neuen Mollusken-Gattung. *Mém. Acad. Imp. Sci. St Pétersburg* 6(1)2: 205–220 2 pls.
- Moore J. K., and Abbott, M. R. 2000. Phytoplankton chlorophyll distributions and primary production in the Southern Ocean. *Journal of Geophysical Research* **105**: 28,709 – 28,722.
- Motoda, S. 1957 North Pacific standard plankton net. *Information Bulletin Plankton Japan* **4**, 13-15.
- NASA, 2010.
http://earthobservatory.nasa.gov/Features/WorldOfChange/sea_ice_south.php
- Nicol, S, Pauly, T. Bindoff, N. L., Wright, S. Thiele, D. Woehler, E. Hosie, G. and Strutton, P. 2000. Ocean circulation off East Antarctica affects ecosystem structure and sea-ice extent. *Nature* **406**, 504-507.
- Nicol, S., Meiners, K. and Raymond, B. 2010. BROKE-West, A large ecosystem survey of the South West Indian Ocean sector of the Southern Ocean (CCAMLR Division 58.4.2). *Deep-Sea Research II* **57** 9 – 10: 693 – 700.
- Odate, T., and Fukuchi, M., 1995. Distribution and community structure of picophytoplankton in the Southern Ocean during the late austral summer of 1992. *NIPR Symposium Polar Biology*. **8**, 86 – 100.
- Omori, M. and Ikeda, T. 1984. *Methods in Marine Zooplankton Ecology*. Wiley-Interscience, United States of America.
- Orloci, L. 1975. *Multivariate analysis in vegetation research*. 1st edititon. W.Junk, The Hague.
- Orsi, A. H., Whitworth, T., and Nowlin, W. 1995. On the meridional extent and fronts of the Antarctic Circumpolar Current. *Deep-Sea Research Part I*, **42**, 641-673.
- O'Sullivan, D., 1983. A guide to the Pelagic Tunicates of the Southern Ocean and Adjacent Waters. *Antarctic Division Department of Science and Technology, Kingston, Tasmania*.
- Paffenhöfer, G.A., 1973. The cultivation of an Appendicularian through Numerous Generations. *Marine Biology* **22**, 183 – 185.
- Petrou, K., Hill, R., Brown, C., Campbell, D., Doblin, M. And Ralph, P. 2010. Rapid photoprotection in sea-ice diatoms from the East Antarctic pack ice. *Limnology Oceanography*. **55** (3) doi:10.4319/lo.2010.55.3.0000.

- Pilskaln, C.H., Manganini, S.J., Trull, T.W., Armand, L., Howard, W., Asper, V.L., Massom, R. 2004. Geochemical particle fluxes in the Southern Indian Ocean seasonal ice zone: Prydz Bay region, East Antarctica. *Deep-Sea Research I*. **51**: 307 – 332.
- Pinkerton, M. H., Smith, A. N. H., Raymond, B., Hosie, G.W., Sharp, B., Leathwick, J. R., and Bradford-Grieve, J. M. 2010. Spatial and seasonal distribution of adult *Othiona similis* in the Southern Ocean: Predictions using boosted regression trees. *Deep-Sea Research I*. **57**: 469 – 485.
- Pollard R. T., Salter, I., Sanders, R. J., Lucas, M. I., Moore, C. M., Mills, R. A., Statham, P. J., Allen, J. T., Baker, A. R., Bakker, D. C. E., Charette, M. A., Fielding, S., Fones, G. R., French, M., Hickman, A. E., Holland, R. J., Hughes, J. A., Jickells, T. D., Lampitt, R. S., Morris, P. J., Nédélec, F. H., Nielsdóttir, M., Planquette, H., Popova, E. E., Poulton, A. J., Read, J. F., Seeyave, S., Smith, T., Stinchcombe, M., Taylor, S., Thomalla, S., Venables, H. J., Williamson, R., and Zubkov M. V. 2009. Southern Ocean deep-water carbon export enhanced by natural iron fertilization. *Nature* **457**: 577-580, doi:510.1038/nature07716.
- Pommeranz, T., Hermann, C., and Kühn, A., 1982. Mouth angle of the Rectangular Midwater Trawl (RMT1+8) during paying out and hauling. *Meeresforschung* **29**: 267-274.
- Pugh, P. 1989. Gelatinous zooplankton – the forgotten fauna. *Progress in underwater science*. **14** 67 – 78.
- RAMS. 2010. Larvacea. Accessed through: De Broyer, C.; Clarke, A.; Koubbi, P.; Pakhomov, E.; Scott, F.; Vanden Berghe, E. and Danis, B. (Eds). The SCAR-MarBIN Register of Antarctic Marine Species (RAMS) at <http://www.scarmarbin.be/rams.php?p=taxdetails&id=17446> on 2010-05-10.
- Raskoff, K.A., Sommer, F., Hamner, W. and Cross, K. 2003. Collection and Culture Techniques for Gelatinous Zooplankton. *Biological Bulletin* **204**: 68 – 80.
- Raskoff, K.A., Purcell, J.E., and Hopcroft, R., 2005. Gelatinous zooplankton of the Arctic Ocean: in situ observations under the ice. *Polar Biology*, **28**, 207 - 217.
- Ritz, D., Swadling, K., Hosie, G., and Cazassus, F., 2003. Guide to the Zooplankton of south eastern Australia. Fauna of Tasmania Committee, University of Tasmania, Hobart.
- Roe, H.S.J., Baker, A. de C., Carson, R.M., Wild, R., and Shale, D.M. 1980. Behaviour of the Institute of Oceanographic Science's rectangular midwater trawls: theoretical aspects and experimental observations. *Marine Biology* **56**: 247-259.
- Rosenberg, M.A., 2006 BROKE-West Hydrology analysis. *Antarctic Climate and Ecosystems CRC Research Report*. Hobart, Australia.

- Sallée, J. B., Speer, K. G, and Rintoul, S. R. 2010 Zonally asymmetric response of the Southern Ocean mixed-layer depth to the Southern Annular Mode. *Nature Geoscience* **3**:4, 273-279.
- SAZ Sense voyage website (<http://www.cmar.csiro.au/datacentre/saz-sense/>).
- Sato, R., Tanaka, Y., and Ishimaru, T. 2001. House production by *Oikopleura dioica* (Tunicata, Appendicularia) under laboratory conditions. *Journal of Plankton Research*, **23**, 415 – 423.
- Sato, R., Tanaka, Y. and Ishimaru, T. 2005. Clearance and ingestion rates of three appendicularian species, *Oikopleura longicauda*, *O. rufescens* and *O. fusiformis* in Response of Marine Ecosystems to Global Change – Ecological Impacts of Appendicularians. Gordon and Breach Scientific Publishers 189 – 205.
- Scott, F. and Marchant, H. 2005. Antarctic Marine Protists. Australian Biological Resources Study, Canberra and Australian Antarctic Division, Hobart.
- Silver, M. and Gowing, M. 1991. The “Particle” flux: Origins and biological components. *Progress in Oceanography* **26**, 75 – 113.
- SIPEX. Web site for the Sea Ice Physics & Ecosystem eXperiment voyage. www.acecrc.sipex.aq
- Slawyk, G., 1979. ¹³C and ¹⁵N uptake by phytoplankton in the Antarctic upwelling area: Results from the Antiope 1 cruise in the Indian Ocean sector. *Australian Journal of Marine and Freshwater Research*. **30**, 431 – 448.
- Sokolov, S., and S. R. Rintoul, 2007. Multiple jets of the Antarctic Circumpolar Current south of Australia. *Journal of Physical Oceanography*. **37**, 1394–1412.
- Southern Ocean Continuous Plankton Recorder (SO-CPR) Survey database, unpublished 2007. Located at Australian Antarctic Division, Kingston, Australia.
- Spreen, G., Kaleschke, L., and Heygster, G. 2008. Sea ice remote sensing using AMSR-E 89 GHz channels, *Journal of Geophysics Research*. **113**, C02S03, doi:10.1029/2005JC003384.
- Steinberg, D., Silver, M., Pilskaln, C., Coale, S., and Paduan, J. 1994. Midwater zooplankton communities on pelagic detritus (giant larvacean houses) in Monterey Bay, California. *Limnology Oceanography* **39** 7: 1606 – 1620.
- Swadling, K., Kowaguchi, S., and Hosie, G.W., 2010. Zooplankton community structure during the BROKE-West survey. *Deep-Sea Research II* **57**, 9-10, 887 – 904.
- Takahashi, K.T., Kawaguchi, S., Kobayashi, M. Hosie, G.W., Fukuchi, M., and Toda, T., 2002. Zooplankton distribution patterns in relation to the Antarctic Polar Front Zones recorded by Continuous Plankton Recorder (CPR) during 1999/2000 *Kaiyo Maru* cruise. *Polar Bioscience* **15**, 97-107.

- Thompson, H., 1948. Pelagic Tunicates of Australia. Commonwealth Council for Scientific and Industrial Research, Melbourne, Australia.
- Tiselius, P., Petersen, J.K., Nielsen, T.G., Maar, M., Moller, E.F., Satapoomin, S., Tonnesson, K., Zervoudaki, T., Christou, E., Giannakourou, A., Sell, A., and Vargas, C.A. 2003. Functional response of *Oikopleura dioica* clogging due to exposure to algae of different sizes. *Marine Biology*, **142**, 253 - 261.
- Tomita, M. Shiga, N., and Ikeda, T. 2003. Seasonal occurrence and vertical distribution of appendicularians in Toyama Bay, southern Japan Sea. *Journal of Plankton Research* **25** 6: 579 – 589.
- Tokioka, T., 1961. Appendicularians of the Japanese Antarctic Research Expedition. *Bulletin of Marine Biological Station of Asamushi* **5**, 241 - 245.
- Tokioka, T., 1964. Taxonomic Studies of Appendicularians. Collected by the Japanese Antarctic Research Expedition 1957. *JARE 1956-1962 Scientific Reports Series E*, **21E**, 1 - 16.
- Totton, A. 1954. Siphonophores of the Indian Ocean, together with systematic and biological notes on related species from other areas. *Discovery Reports* **27** 1 – 162.
- Treguer, P., and Jacques, G. 1992. Dynamics of nutrients and phytoplankton, and fluxes of carbon, nitrogen, and silicon in the Antarctic Ocean. *Polar Biology* **12**, 149-162.
- Trull T. W., S. R. Rintoul, M. Hadfield, and E. R. Abraham. 2001. Circulation and seasonal evolution of Polar waters south of Australia: Implications for iron fertilisation of the Southern Ocean. *Deep Sea Research II* **48**: 2439-2466.
- Trull T. W., P. N. Sedwick, F. B. Griffiths, and S. R. Rintoul. 2001. Introduction to special section: SAZ Project. *Journal of Geophysical Research* **106**: 31425 - 31430.
- Trull, T.W., Bray, S.G., Manganini, S.J., Honjo, S., Francois, R. 2001. Moored sediment trap measurements of carbon export in the Subantarctic and Polar frontal Zones of the Southern Ocean, south of Australia. *Journal of Geophysical Research*. **106** (C12): 31489 – 31509.
- Tsujimoto, M., Takahashi, K.T., Hirawake, T., Fukuchi, M., 2006. Unusual abundance of appendicularians in the seasonal ice zone (140°E) of the Southern Ocean. *Polar Bioscience* **19**, 133-141.
- Tynan, C. 1998. Ecological importance of the Southern Boundary of the Antarctic Circumpolar Current. *Nature* **392**, 708 – 710.
- Vargas, C.A., Tonnesson, K., Sell, A., Maar, M., Moller, E.F., Zervoudaki, T., Giannakourou, A., Christou, E., Satapoomin, S., Petersen, J.K., Nielsen, T.G., and

- Tiselius, P. 2002. Importance of copepods versus appendicularians in vertical carbon fluxes in a swedish fjord. *Marine Ecology Progress Series*, **241**, 125 – 138.
- Wiebe, P. and Benfield, M. 2003. From the Hensen net toward four-dimensional biological oceanography. *Progress in Oceanography* **56**: 7 – 136.
- Williams, G. D., Nicol, S., Raymond, B., and Meiners, K., 2008. Summertime mixed layer development in the marginal sea ice zone off the Mawson Coast, East Antarctica. *Deep-Sea Research II* (2008), doi:10.1016/j.dsr2.2007.11.2007.
- Williams, G. D., Nicol, S., Bindoff, N. L., Aoki, S., Meijers, A. J. S., Marsland, S. J., Klocker, A., and Iijima, Y., 2008. The surface oceanography of BROKE-West, along the Antarctic Margin of the South-West Indian Ocean (30° – 80°E) *Deep Sea Research II* **57** 9 – 10: 738 – 757.
- Wood, S. 2006. Generalized Additive Models – An Introduction with R. *Chapman & Hall/CRC America*.
- Wood, S. 2011. Package ‘mgcv’ Version 1.7-6. GAMs with GCV/AIC/REML smoothness estimation and GAMMs by PQL <http://cran.r-project.org/web/packages/mgcv/mgcv.pdf> (accessed September 2011).
- Worby A. P., R. A. Massom, I. Allison, V. I. Lytle, and P. Heil. 1998. East Antarctic Sea Ice: a review of its structure, properties and drift. *Antarctic Research Series* **74**: 41-67.
- Wright, S. 2010. Microbial Ecosystems in the Southern Ocean: threats from climate change. Australian Antarctic Division seminar series.
- Wright, S., Davidson, A., Scott, F., Nash, G., Raymond, B. and Westwood, K. 2008. Preliminary presentation of marine protist distribution from SAZ Sense. Australian Antarctic Division seminar series.
- Wright, S., Ishikawa, A., Marchant, H., Davidson, A., van den Enden, R., and Nash, G. 2009. Composition and significance of picophytoplankton in Antarctic waters. *Polar Biology* **32**:797–808 DOI 10.1007/s00300-009-0582-9.

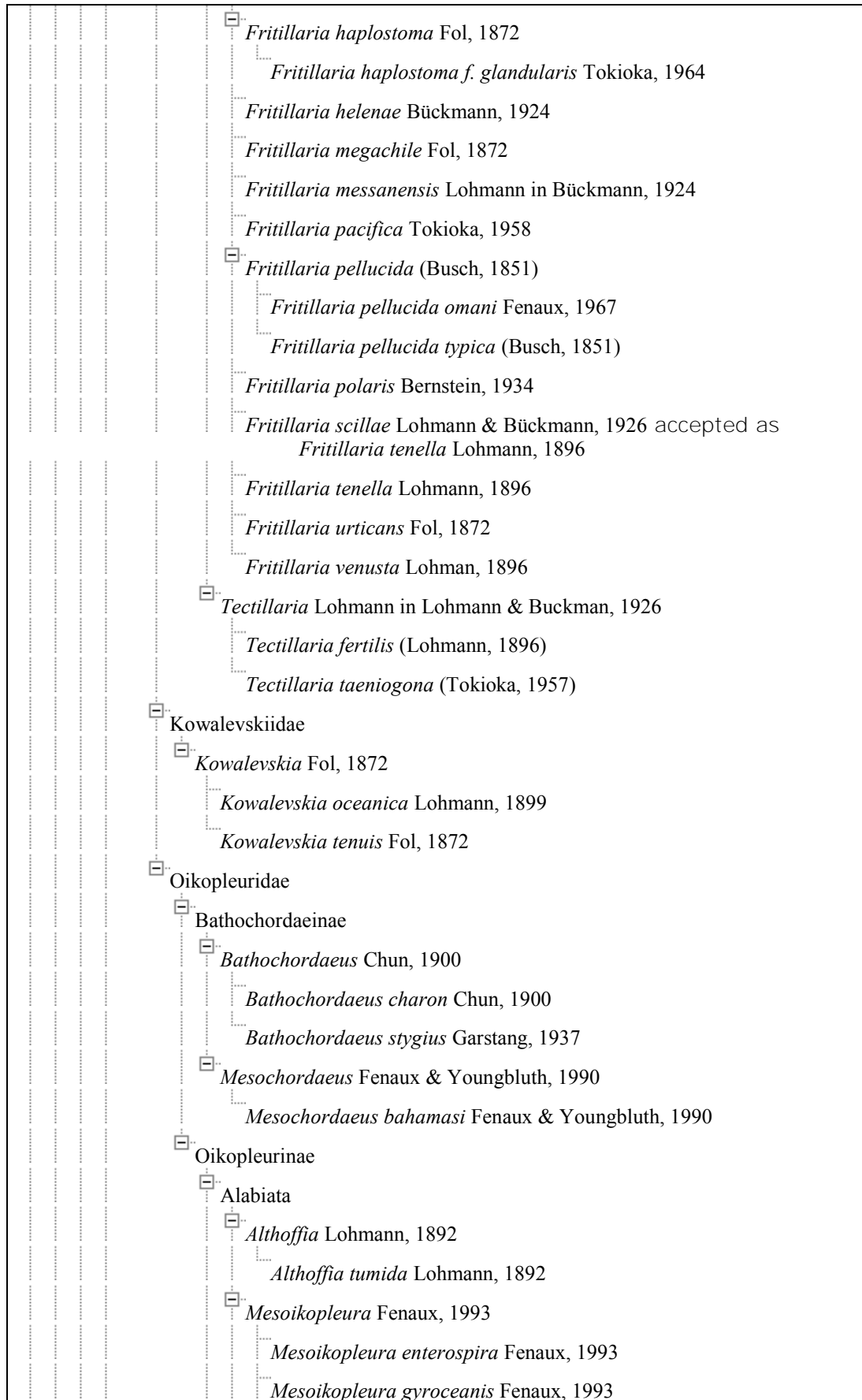
List of Appendices

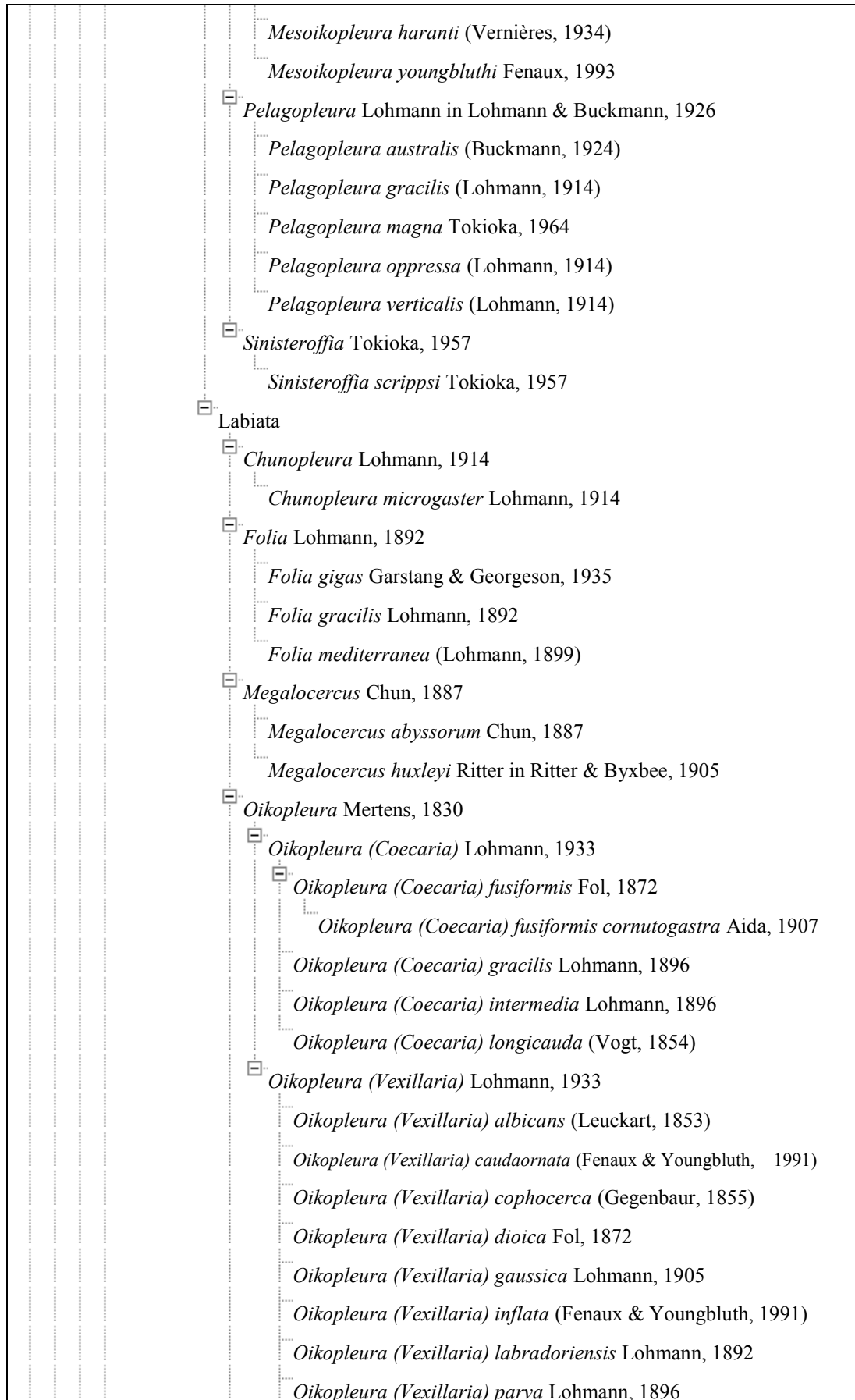
Appendix I. Larvacean species list (RAMS, 2010)	288
Appendix II. Larvacean taxonomic tree (RAMS, 2010)	290
Appendix III . Larvacean images submitted to SCARmarBIN	294
Appendix IV. Larvacean images submitted to WoRMS	298
Appendix V. SO-CPR Survey annual and seasonal maps	302
Appendix VI. Generalized Additive Mixed Models (GAMM) theory	323
Appendix VII. R code for mgcv	327
Appendix VIII. Mean abundances of marine protists. Raw data from Fiona Scott.	334
Appendix IX. Sizes of marine protist. (from Scott and Marchant 2005)	335
Appendix X. PDF of Lindsay, M. and Williams, G. 2010. Distribution and abundance of Larvaceans in the Southern Ocean between 30° and 80°E. <i>Deep-Sea Research II</i> 57 905–15	337

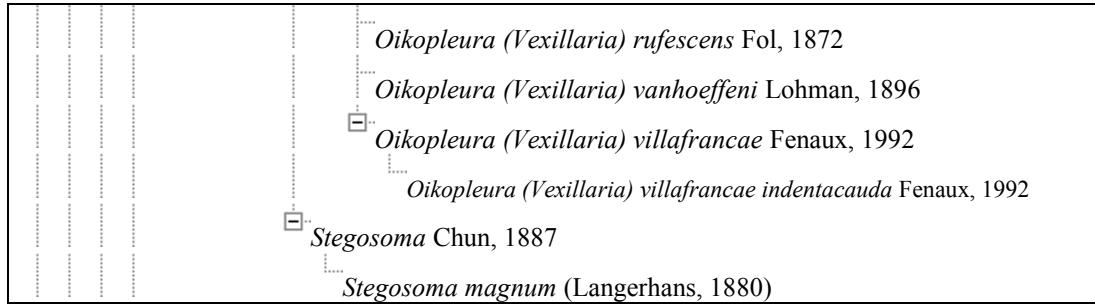
Appendix I**List of larvacean species****Larvacean species list (RAMS, 2010).**

- Althoffia tumida* Lohmann, 1892
Appendicularia sicula Fol, 1874
Appendicularia tregouboffi Fenaux, 1960
Bathochordaeus charon Chun, 1900
Bathochordaeus stygius Garstang, 1937
Chunopleura microgaster Lohmann, 1914
Folia gigas Garstang & Georgeson, 1935
Folia gracilis Lohmann, 1892
Folia mediterranea (Lohmann, 1899)
Fritillaria aberrans Lohmann, 1896
Fritillaria abjornseni Lohmann, 1909
Fritillaria aequatorialis Lohmann, 1896
Fritillaria antarctica Lohmann, 1905
Fritillaria arafuera Tokioka, 1956
Fritillaria borealis Lohmann, 1896
Fritillaria borealis intermedia Lohmann, 1905
Fritillaria borealis sargassi Lohmann, 1896
Fritillaria borealis typica Lohmann, 1896
Fritillaria charybdae Lohmann in Lohmann & Buckmann, 1926
Fritillaria drygalskii Lohmann in Bückmann, 1923
Fritillaria fagei Fenaux, 1961
Fritillaria formica Fol, 1872
Fritillaria formica digitata Lohmann in Lohmann & Buckmann, 1926
Fritillaria formica tuberculata Lohmann in Lohmann & Buckmann, 1926
Fritillaria fraudax Lohmann, 1896
Fritillaria gracilis Lohmann, 1896
Fritillaria haplostoma Fol, 1872
Fritillaria haplostoma f. glandularis Tokioka, 1964
Fritillaria helenae Bückmann, 1924
Fritillaria megachile Fol, 1872
Fritillaria messanensis Lohmann in Bückmann, 1924
Fritillaria pacifica Tokioka, 1958
Fritillaria pellucida (Busch, 1851)
Fritillaria pellucida omani Fenaux, 1967
Fritillaria pellucida typica (Busch, 1851)
Fritillaria polaris Bernstein, 1934

- Fritillaria scillae* Lohmann & Bückmann, 1926 accepted as *Fritillaria tenella* Lohmann, 1896
Fritillaria tenella Lohmann, 1896
Fritillaria urticans Fol, 1872
Fritillaria venusta Lohman, 1896
Kowalevskia oceanica Lohmann, 1899
Kowalevskia tenuis Fol, 1872
Megalocercus abyssorum Chun, 1887
Megalocercus huxleyi Ritter in Ritter & Byxbee, 1905
Mesochordaeus bahamasi Fenaux & Youngbluth, 1990
Mesoikopleura enterospira Fenaux, 1993
Mesoikopleura gyroceanis Fenaux, 1993
Mesoikopleura haranti (Vernières, 1934)
Mesoikopleura youngbluthi Fenaux, 1993
Oikopleura (Coecaria) fusiformis Fol, 1872
Oikopleura (Coecaria) fusiformis cornutogastra Aida, 1907
Oikopleura (Coecaria) gracilis Lohmann, 1896
Oikopleura (Coecaria) intermedia Lohmann, 1896
Oikopleura (Coecaria) longicauda (Vogt, 1854)
Oikopleura (Vexillaria) albicans (Leuckart, 1853)
Oikopleura (Vexillaria) caudaornata (Fenaux & Youngbluth, 1991)
Oikopleura (Vexillaria) cophocerca (Gegenbaur, 1855)
Oikopleura (Vexillaria) dioica Fol, 1872
Oikopleura (Vexillaria) gaussica Lohmann, 1905
Oikopleura (Vexillaria) inflata (Fenaux & Youngbluth, 1991)
Oikopleura (Vexillaria) labradoriensis Lohmann, 1892
Oikopleura (Vexillaria) parva Lohmann, 1896
Oikopleura (Vexillaria) rufescens Fol, 1872
Oikopleura (Vexillaria) vanhoeffeni Lohman, 1896
Oikopleura (Vexillaria) villafrancae Fenaux, 1992
Oikopleura (Vexillaria) villafrancae indentacauda Fenaux, 1992
Pelagopleura australis (Buckmann, 1924)
Pelagopleura gracilis (Lohmann, 1914)
Pelagopleura magna Tokioka, 1964
Pelagopleura oppressa (Lohmann, 1914)
Pelagopleura verticalis (Lohmann, 1914)
Sinisteroffia scrippsi Tokioka, 1957
Stegosoma magnum (Langerhans, 1880)
Tectillaria fertilis (Lohmann, 1896)
Tectillaria taeniogona (Tokioka, 1957)







Appendix III

SCAR MarBIN larvacean images

The screenshot shows the SCAR-MarBIN website interface. At the top, there is a navigation bar with links for Home, Species, Geography, Services, Datasets, and Outreach. The main content area is titled "Photo Gallery" and displays a single image of a larva. Below the image, there is a detailed description and metadata for the specimen, including the author's name and contact information. The footer of the page contains logos for SCAR, OBIS, CENSUS OF MARINE LIFE, Biodiversity.be, mus-um, VLIZ, and the Belgian Science Policy.

Regional OBIS Node for the Antarctic

SCAR-MarBIN

OBIS OCEAN BIOGEOGRAPHIC INFORMATION SYSTEM

Home Species Geography Services Datasets Outreach

Not logged in [Log in]

Photo Gallery

Photo Gallery > SCAR-MarBIN Species > Appendicularians

◀ Previous Next ▶



17.01.2006

Add to cart

Olkopleura
Description: Olkopleura under the light microscope
Author: Margaret Lindsay (Margaret.Lindsay@aad.gov.au)
JPG file - 6 kB - 347 x 307 pixels
added on 2007-04-20 - 953 views
RAMS Taxa on this image:
Olkopleura Mertens, 1830

This work is licensed under a Creative Commons Attribution-NonCommercial-Share Alike 3.0 License

Click here to return to thumbnails.

[Add an image] [Add comment] [RSS] [Search]

SCAR OCEAN BIOGEOGRAPHIC INFORMATION SYSTEM

CENSUS OF MARINE LIFE

Biodiversity.be

mus-um

VLIZ

Belgian Science Policy

Project implemented by the Belgian Biodiversity Platform, Webportal hosted and maintained by Flanders Marine Institute (VLIZ) - Contact info@scarmarbin.be
Total number of visitors: 759929 - Total hits: 5319386 (since 2005-10-26) - page generated: 2010-05-10 08:56:53

http://www.scarmarbin.be/photo_gallery.php?album+482&pic=10290

Regional OBIS Node for the Antarctic

SCAR-MarBIN

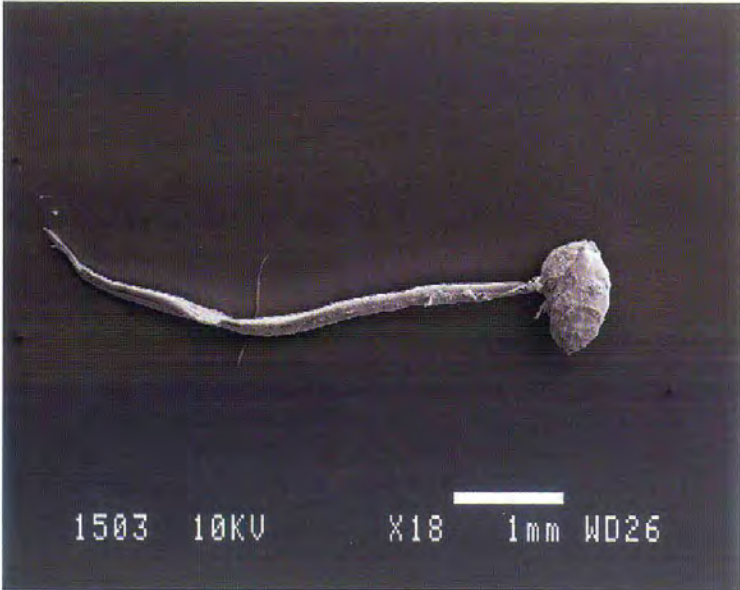
Home Species Geography Services Datasets Outreach

Not logged in [Log in]

Photo Gallery

Photo Gallery > SCAR-MarBIN Species > Appendicularians


< Previous Next >



1503 10KV X18 1mm WD26








[Add to cart](#)

Olkopleura Scanning electron microscopy
Description: Olkopleura Scanning electron microscopy
scale bar 1mm
Author: Margaret Lindsay (Margaret.Lindsay@aad.gov.au)
JPG file - 426 kB - 1024 x 819 pixels
added on 2007-04-20 - 1241 views
[RAMS Taxa on this image:](#)
Olkopleura Mertens, 1830

 This work is licensed under a Creative Commons Attribution-Noncommercial-Share Alike 3.0 License

[Click here to return to thumbnails.](#)

[\[Add an image\]](#) [\[Add comment\]](#) [\[RSS\]](#) [\[Search\]](#)

Project implemented by the Belgian Biodiversity Platform, Webportal hosted and maintained by Flanders Marine Institute (VLIZ) - Contact info@scarmarbin.be
Total number of visitors: 759929 - Total hits: 5319381 (since 2005-10-26) - page generated: 2010-05-10 06:56:00

http://www.scarmarbin.be/photo_gallery.php?album+482&pic=10291

The screenshot shows the SCAR-MarBIN website interface. At the top, there is a navigation bar with links for Home, Species, Geography, Services, Datasets, and Outreach. The main content area is titled "Photo Gallery" and shows a single image of a larva, identified as *Fritillaria*. Below the image, there is a description, author information, and a Creative Commons license. The footer contains logos for SCAR, OBIS, Census of Marine Life, biodiversity.be, mus.um, VLIZ, and Belgian Science Policy, along with project implementation details and visitor statistics.

Regional OBIS Node for the Antarctic

SCAR-MarBIN

OBIS
OCEAN BIOGEOGRAPHIC INFORMATION SYSTEM

Home Species Geography Services Datasets Outreach

Not logged in [Log in]

Photo Gallery

Photo Gallery > SCAR-MarBIN Species > Appendicularians

< Previous Next >



Add to cart

Fritillaria
Description: Fritillaria under light microscope
Author: Margaret Lindsay (margaret.lindsay@aad.gov.au)
JPG file - 3 kB - 284 x 214 pixels
added on 2007-04-20 - 940 views
RAMS Taxa on this image:
Fritillaria Fol, 1872

This work is licensed under a Creative Commons Attribution-NonCommercial-Share Alike 3.0 License

Click here to return to thumbnails.

[Add an image] [Add comment] [RSS] [Search]

SCAR OBIS CENSUS OF MARINE LIFE biodiversity.be mus.um VLIZ Belgian Science Policy

Project implemented by the Belgian Biodiversity Platform, Webportal hosted and maintained by Flanders Marine Institute (VLIZ) - Contact info@scarmarbin.be
Total number of visitors: 759929 • Total hits: 5319390 (since 2005-10-26) - page generated: 2010-05-10 06:57:33

http://www.scarmarbin.be/photo_gallery.php?album+482&pic=10288

Regional OBIS Node for the Antarctic

SCAR-MarBIN

OBIS
OCEAN BIOGEOGRAPHIC
INFORMATION SYSTEM


Home Species Geography Services Datasets Outreach

Not logged in [Log in]

Photo Gallery

Photo Gallery > SCAR-MarBIN Species > Appendicularians


« Previous Next »



0501 10KV X120 100µm WD26








Add to cart

Fritillaria Scanning Electron Microscopy
Description: Fritillaria Scanning Electron Microscopy
scale bar 100 microns
Author: Margaret Lindsay (Margaret.L.Lindsay@aad.gov.au)
JPG file - 386 kB - 1024 x 819 pixels
added on 2007-04-20 - 1309 views
[RAMS Taxa on this image:](#)
Fritillaria Fol, 1872

 This work is licensed under a Creative Commons Attribution-Noncommercial-Share Alike 3.0 License

[Click here to return to thumbnails.](#)

[Add an image] [Add comment] [RSS] [Search]

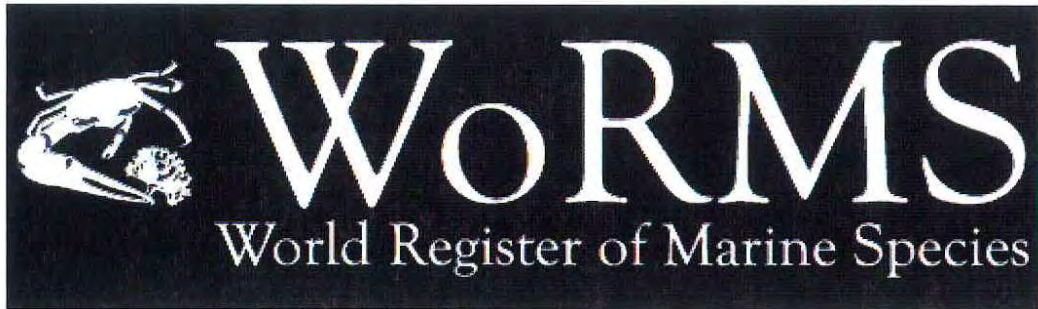
      

Project implemented by the Belgian Biodiversity Platform, Webportal hosted and maintained by Flanders Marine Institute (VLIZ) - Contact info@scarmarbin.be
Total number of visitors: 759929 - Total hits: 5319388 (since 2005-10-26) - page generated: 2010-05-10 06:57:12

http://www.scarmarbin.be/photo_gallery.php?album+482&pic=10289

Appendix IV

WoRMS larvacean images



[WoRMS Photogallery > Tunicata \(sea squirts\)](#)

[« Previous](#)

[Next »](#)



Oikopleura

Description: Oikopleura under the light microscope

Author: Margaret Lindsay (Margaret.Lindsay@aad.gov.au)

JPG file - 6 kB - 347 x 307 pixels

added on 2007-04-20 - 1032 views

WoRMS Taxa on this image:

Oikopleura Mertens, 1830



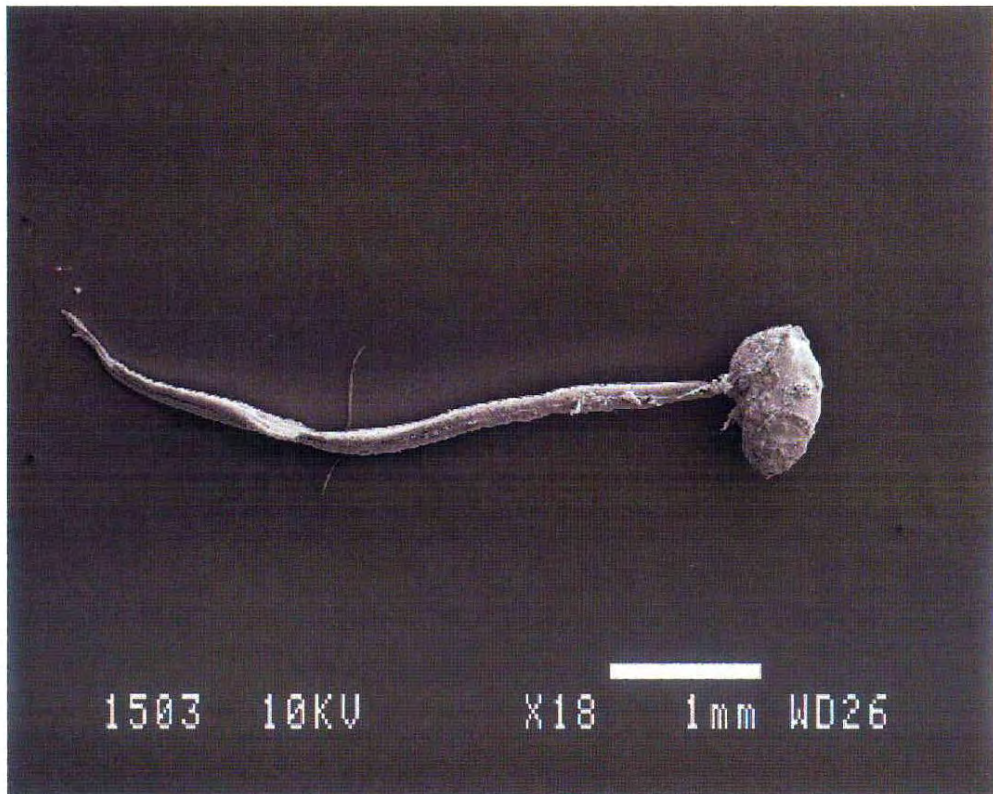
This work is licensed under a Creative Commons Attribution-Noncommercial-Share Alike 3.0 License

<http://www.marinespecies.org/photogallery.php?album=669&pic=10290>

WoRMS Photogallery > Tunicata (sea squirts)

« Previous

Next »



Oikopleura Scanning electron microscopy

Description: Oikopleura Scanning electron microscopy
scale bar 1mm

Author: Margaret Lindsay (Margaret.Lindsay@aad.gov.au)

JPG file - 426 kB - 1024 x 819 pixels

added on 2007-04-20 - 1360 views

WoRMS Taxa on this image:

Oikopleura Mertens, 1830



This work is licensed under a Creative Commons Attribution-NonCommercial-Share Alike 3.0 License

<http://www.marinespecies.org/photogallery.php?album=669&pic=10291>

WoRMS Photogallery > Tunicata (sea squirts)

[« Previous](#)

[Next »](#)



Fritillaria

Description: Fritillaria under light microscope

Author: Margaret Lindsay (Margaret.Lindsay@aad.gov.au)

JPG file - 3 kB - 284 x 214 pixels
added on 2007-04-20 - 980 views

WoRMS Taxa on this image:

[Fritillaria Fol, 1872](#)



This work is licensed under a Creative Commons Attribution-NonCommercial-Share Alike 3.0 License

<http://www.marinespecies.org/photogallery.php?album=669&pic=10288>

WoRMS Photogallery > Tunicata (sea squirts)

« Previous



Fritillaria Scanning Electron Microscopy

Description: Fritillaria Scanning Electron Microscopy
scale bar 100 microns

Author: Margaret Lindsay (Margaret.Lindsay@aad.gov.au)

JPG file - 386 kB - 1024 x 819 pixels

added on 2007-04-20 - 1407 views

[WoRMS Taxa on this image:](#)

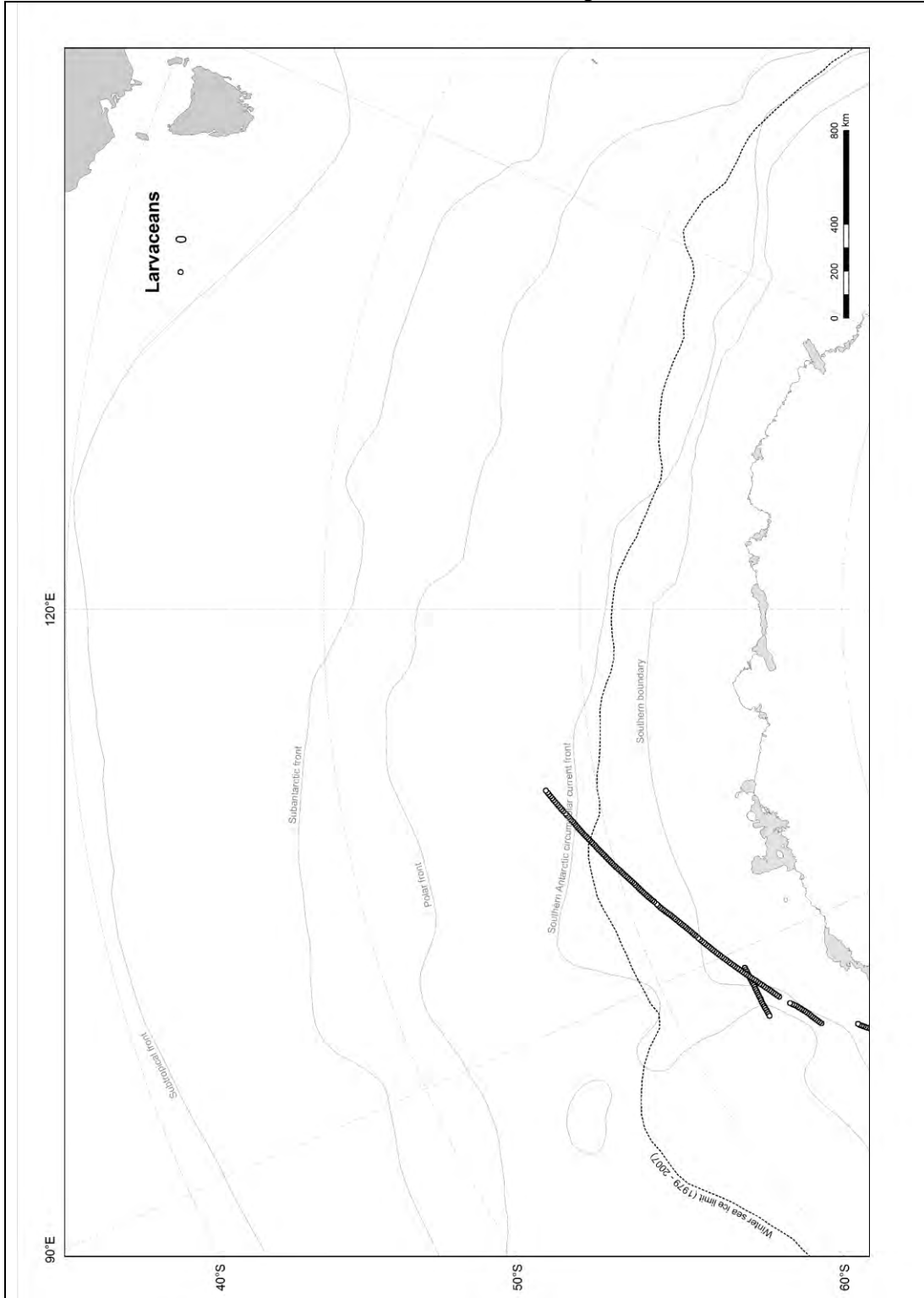
Fritillaria Fol, 1872

<http://www.marinespecies.org/photogallery.php?album=669&pic=10289>

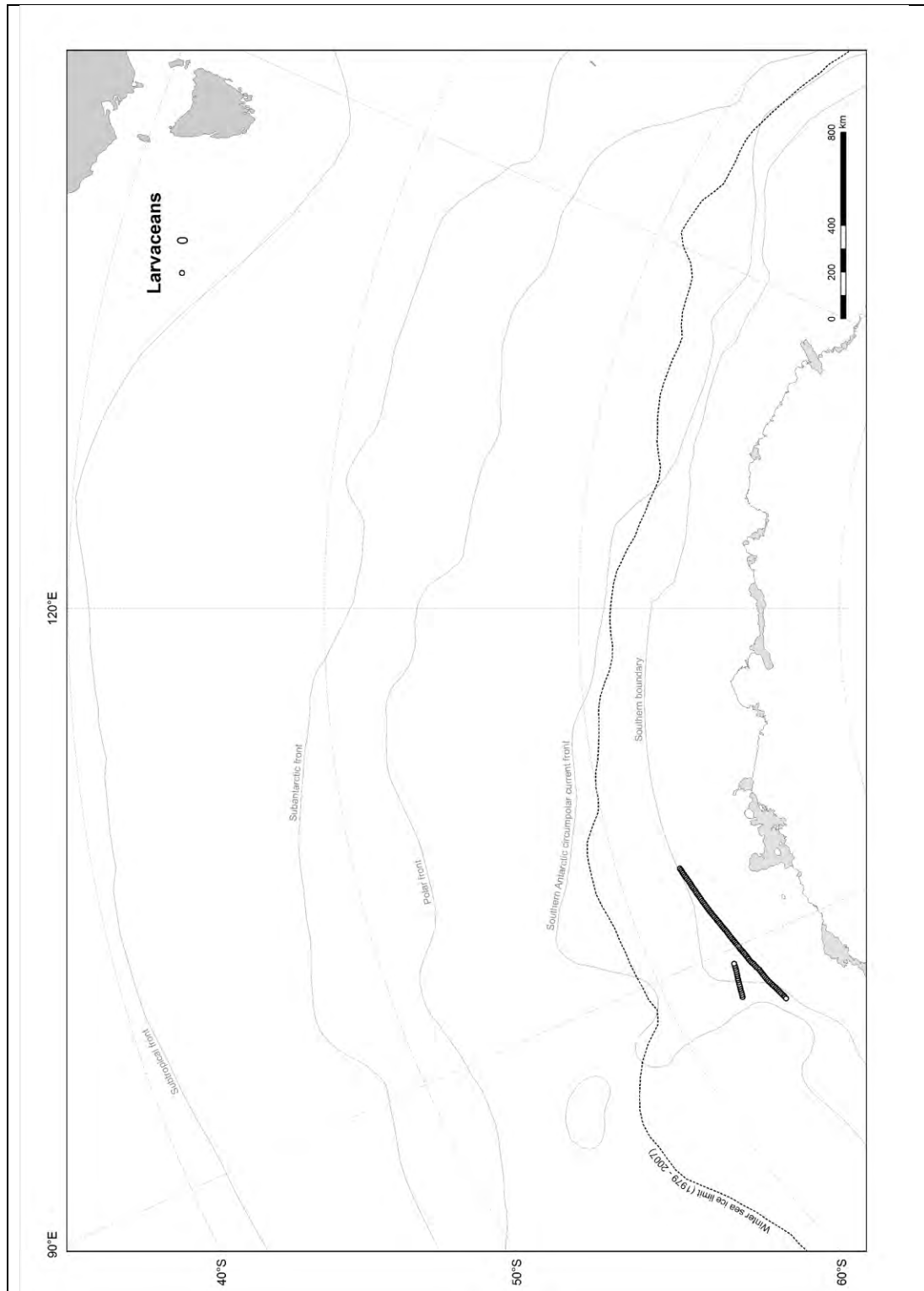
Appendix V

**Continuous Plankton Recorder (CPR)
maps**

Annual SO-CPR Distribution and abundance maps

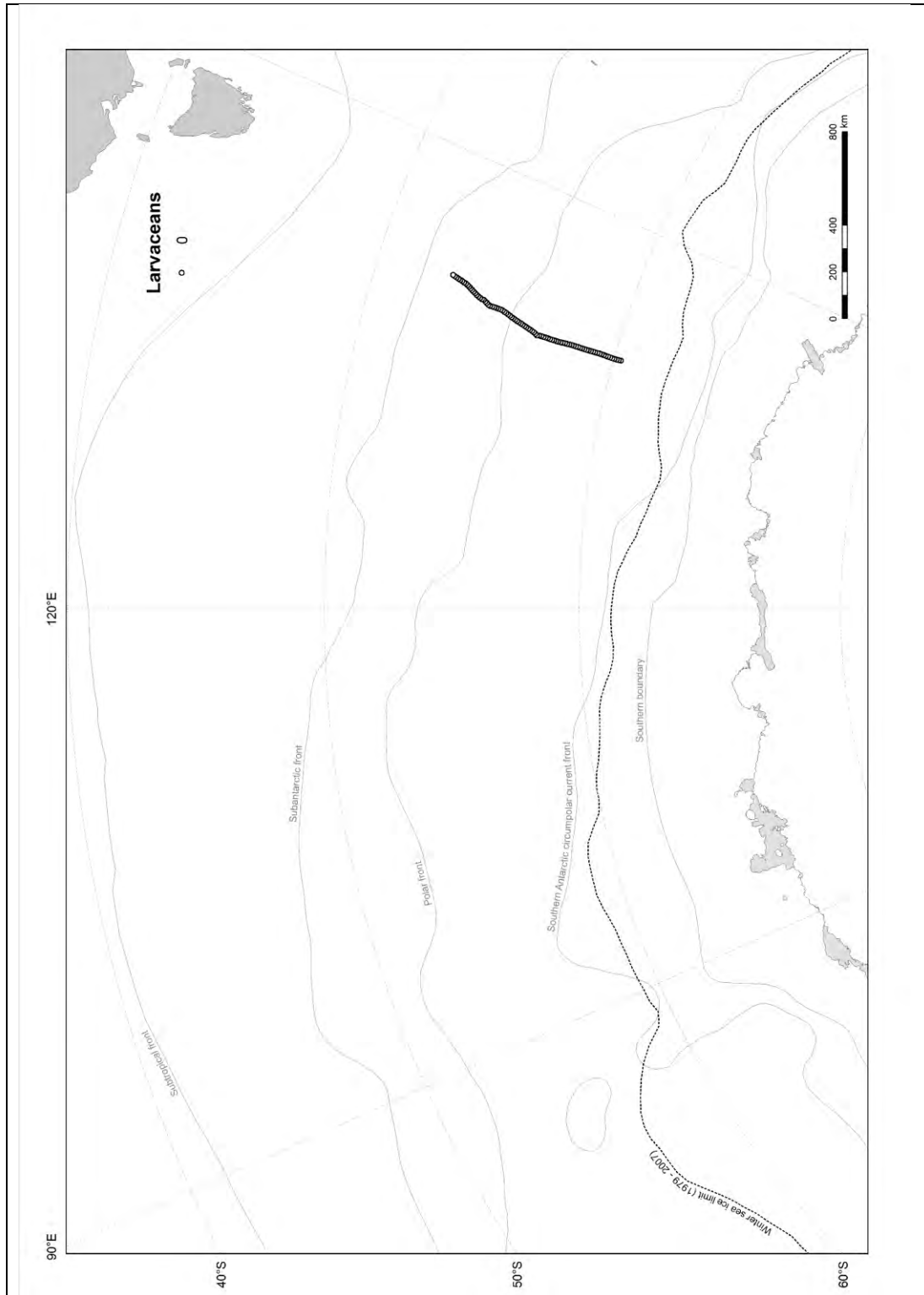


Appendix V.1. 1990-1991 No larvaceans recorded mapped to show transect location. Abundance is in counts per 5 Nm.



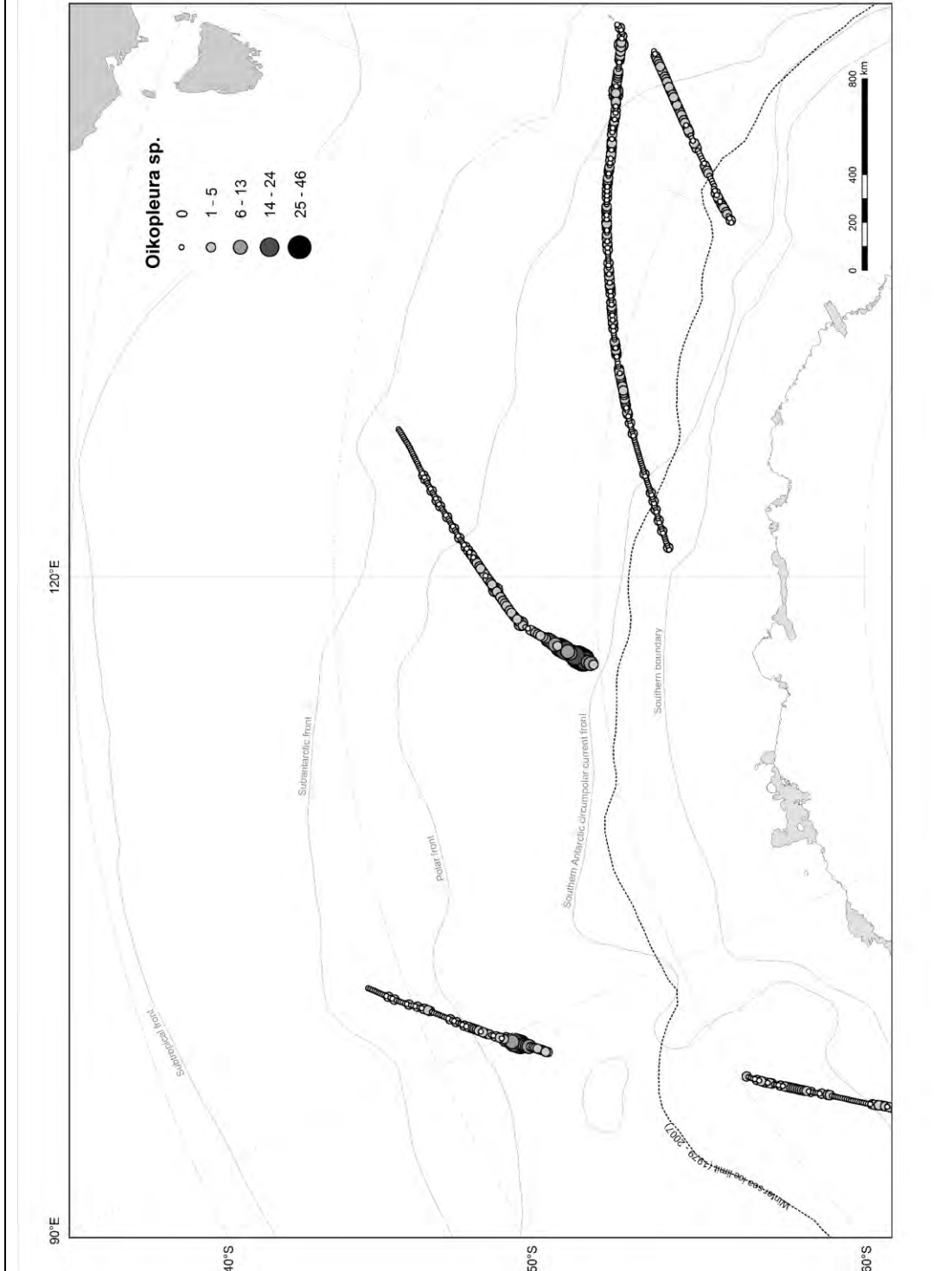
Appendix V.2. 1992-1993 No larvaceans recorded mapped to show transect location. Abundance is in counts per 5 Nm.

1993 -1994 had no CPR deployments in the area mapped



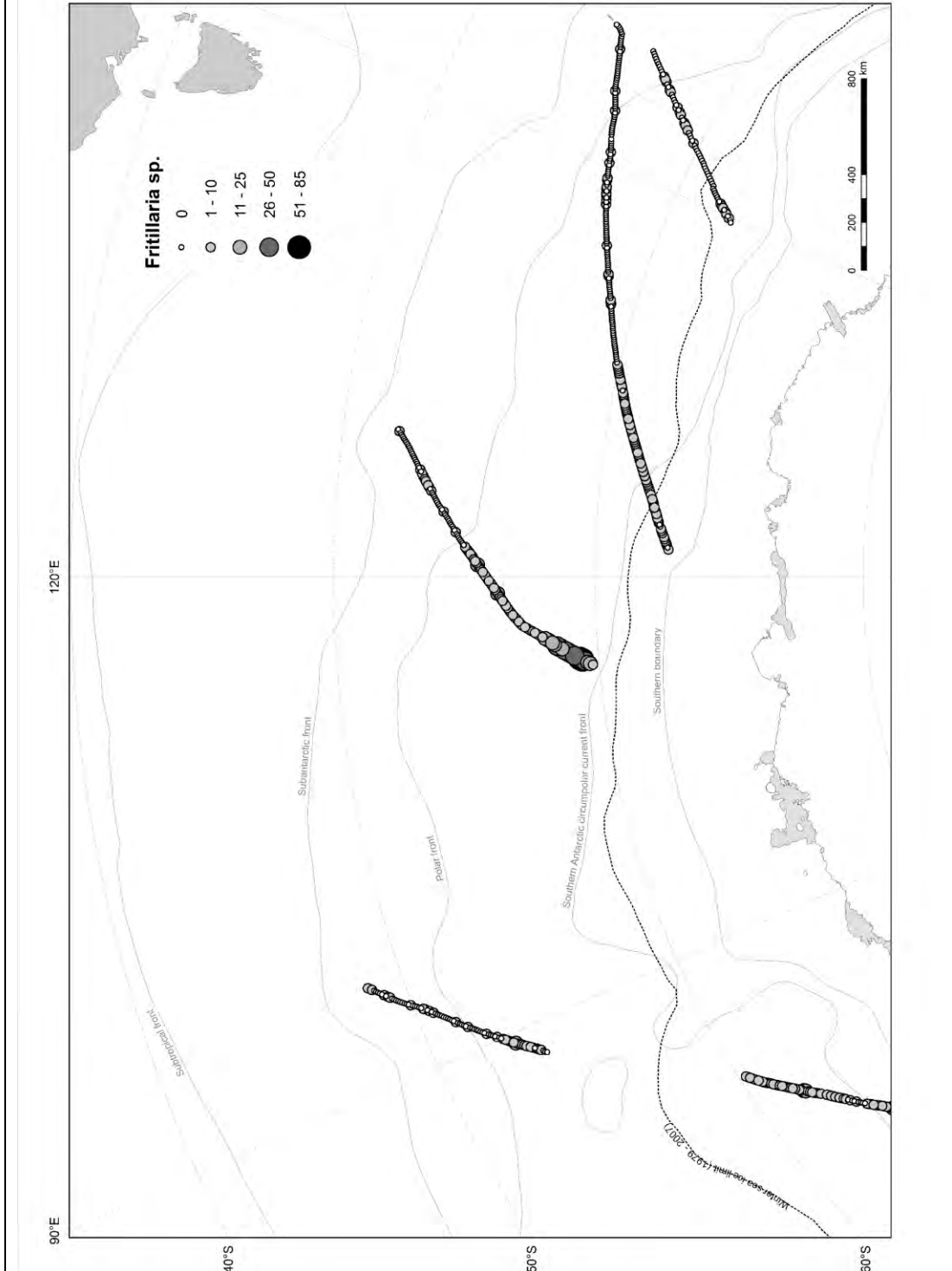
Appendix V.3. 1995- 1996 No larvaceans recorded mapped to show transect location. Abundance is in counts per 5 Nm.

A. *Oikopleura* sp.



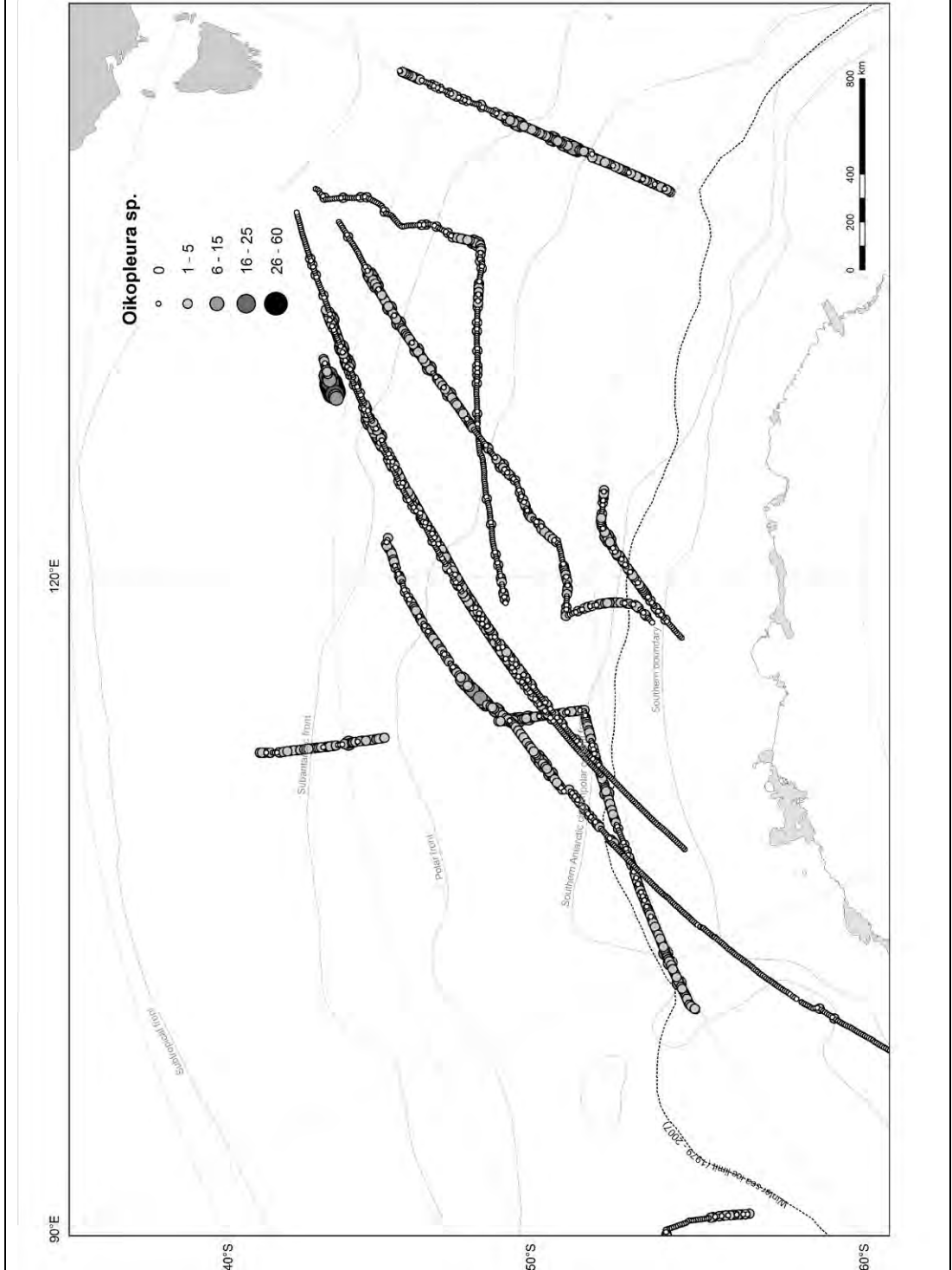
Appendix V. 4.A 1998 – 1999 Lower abundances of *Oikopleura* sp. compared to *Fritillaria* sp. though they have a similar distribution and abundance pattern. Abundance is in counts per 5 Nm.

B. *Fritillaria* sp.



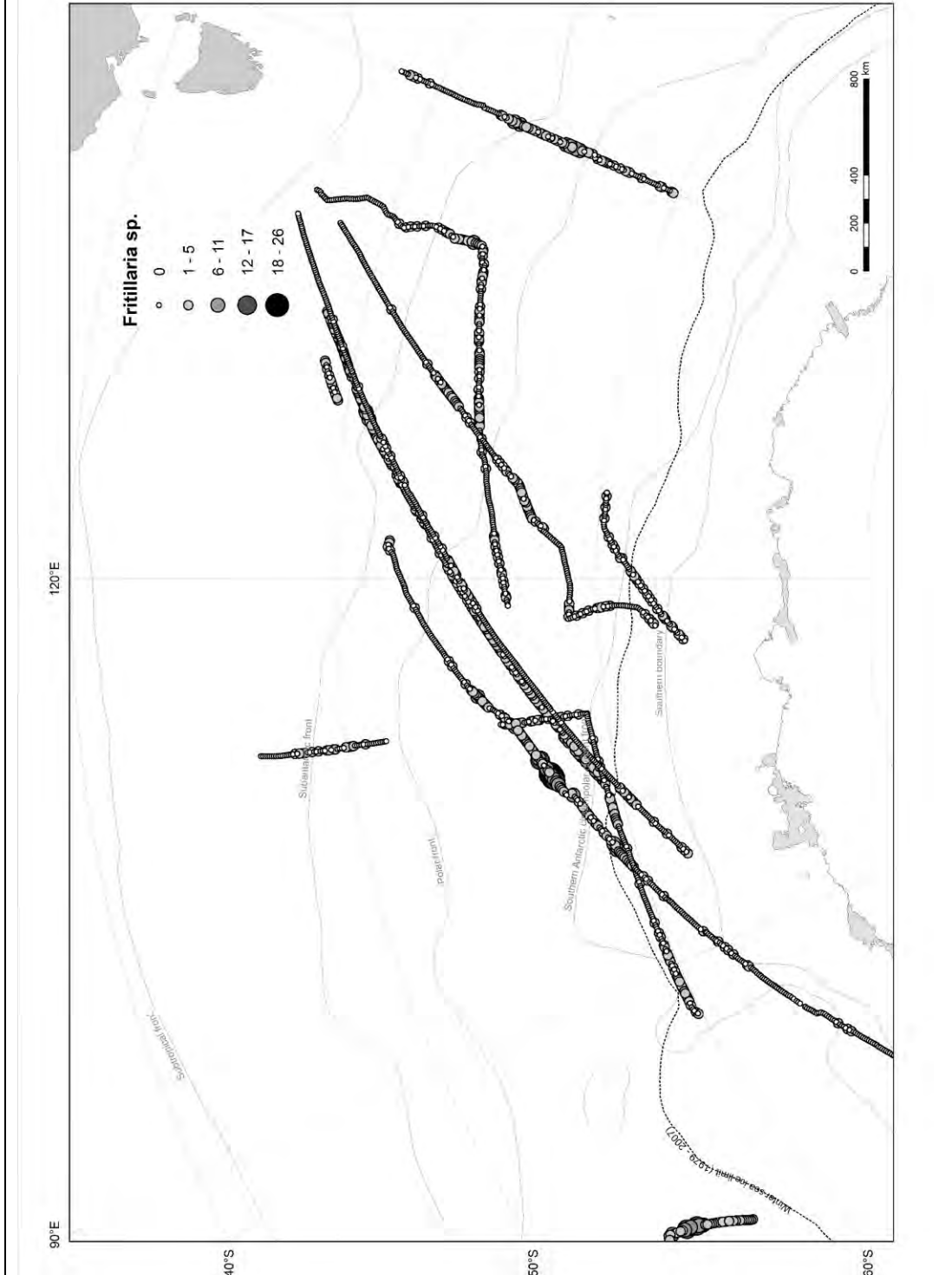
Appendix V. 4. B.1998 – 1999 Lower abundances of *Oikopleura* sp. compared to *Fritillaria* sp. though they have a similar distribution and abundance pattern. Abundance is in counts per 5 Nm.

A. *Oikopleura* sp.



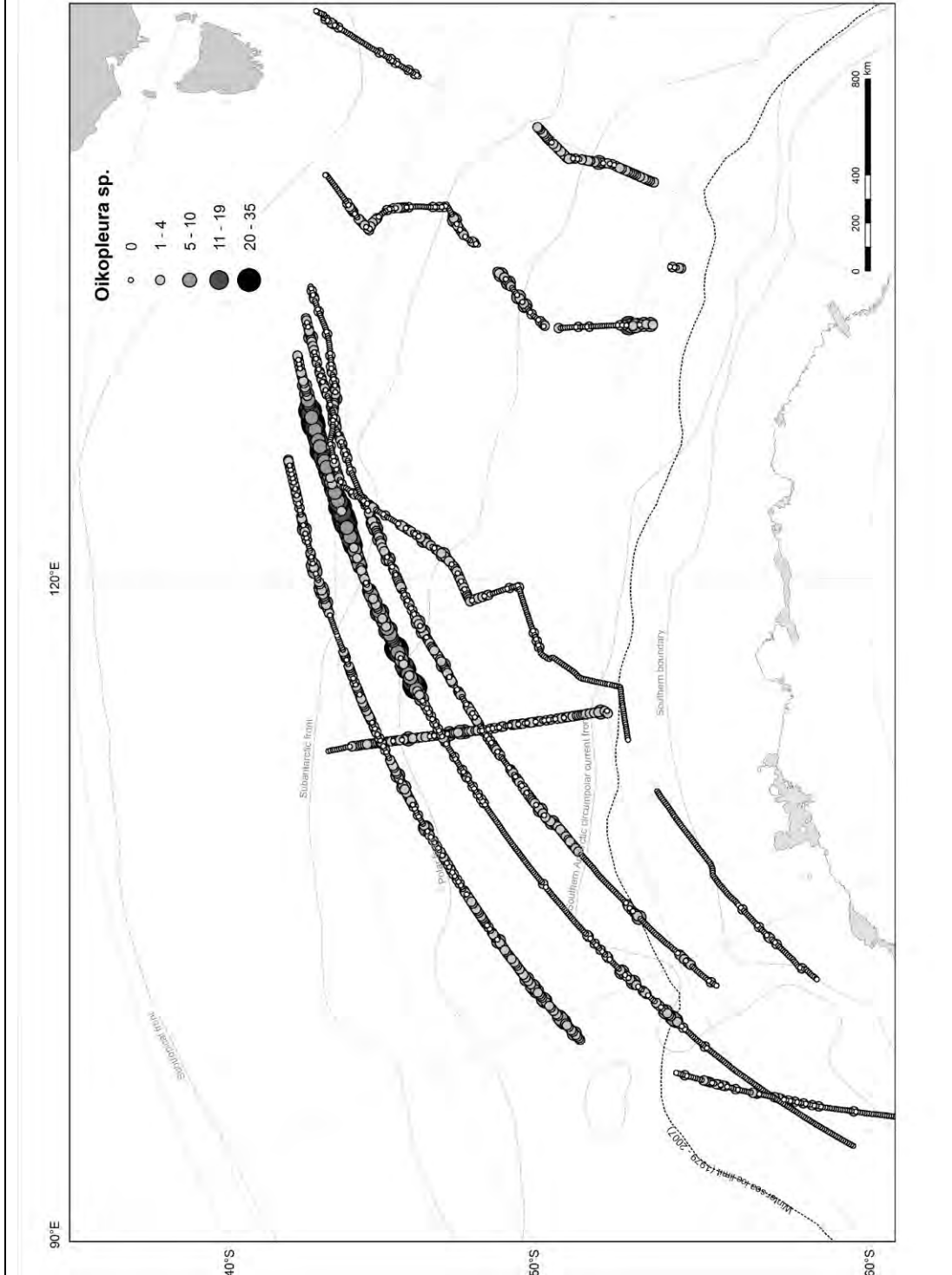
Appendix V.5.A. 2000 – 2001 Higher *Oikopleura* sp. abundances found in the north east compared to the lower abundances of *Fritillaria* sp. that have a south westerly distribution. Abundance is in counts per 5 Nm.

B. *Fritillaria* sp.



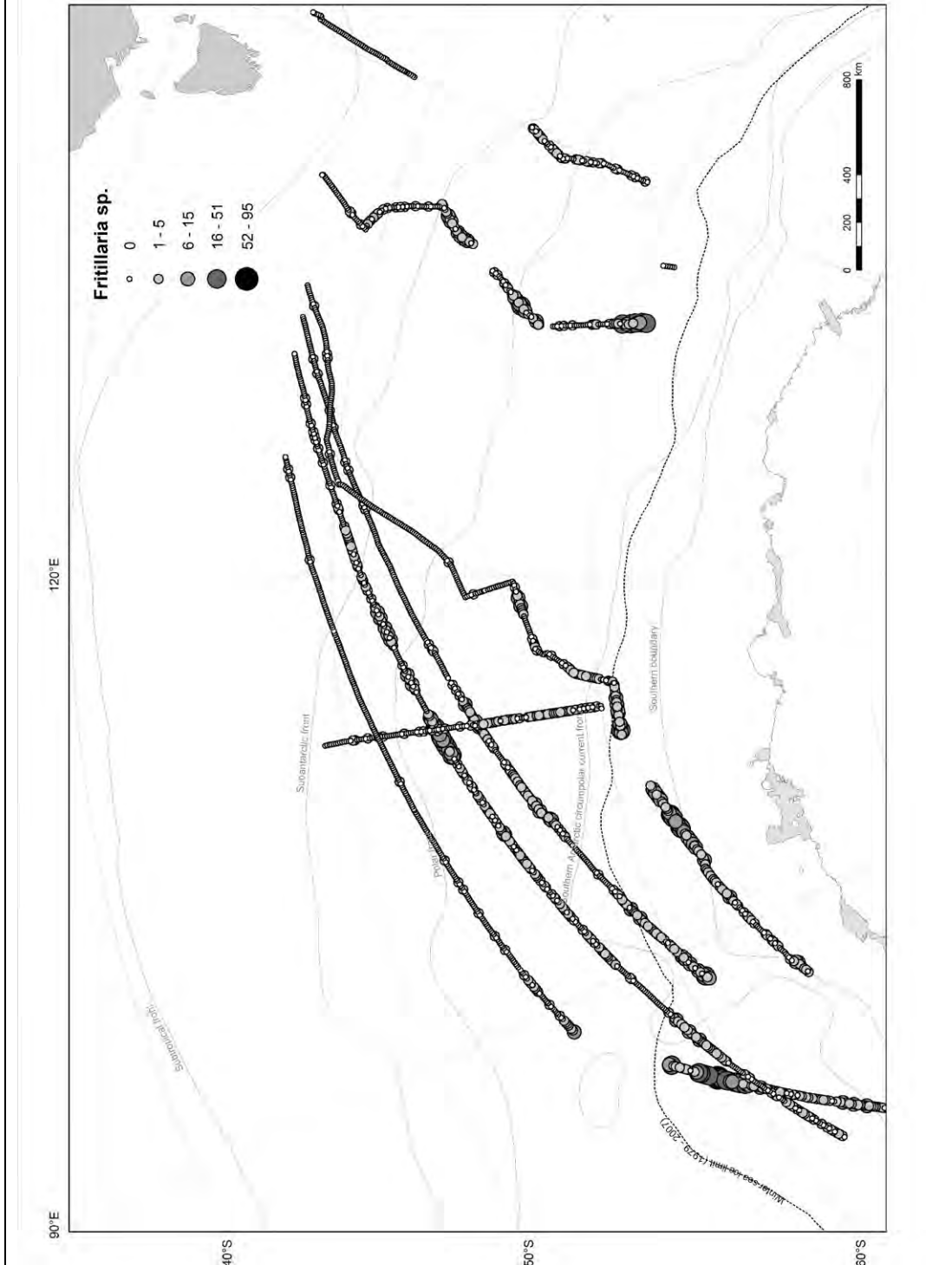
Appendix V.5.B. 2000 – 2001 Higher *Oikopleura* sp. abundances found in the north east compared to the lower abundances of *Fritillaria* sp. that have a south westerly distribution. Abundance is in counts per 5 Nm.

A. *Oikopleura* sp.



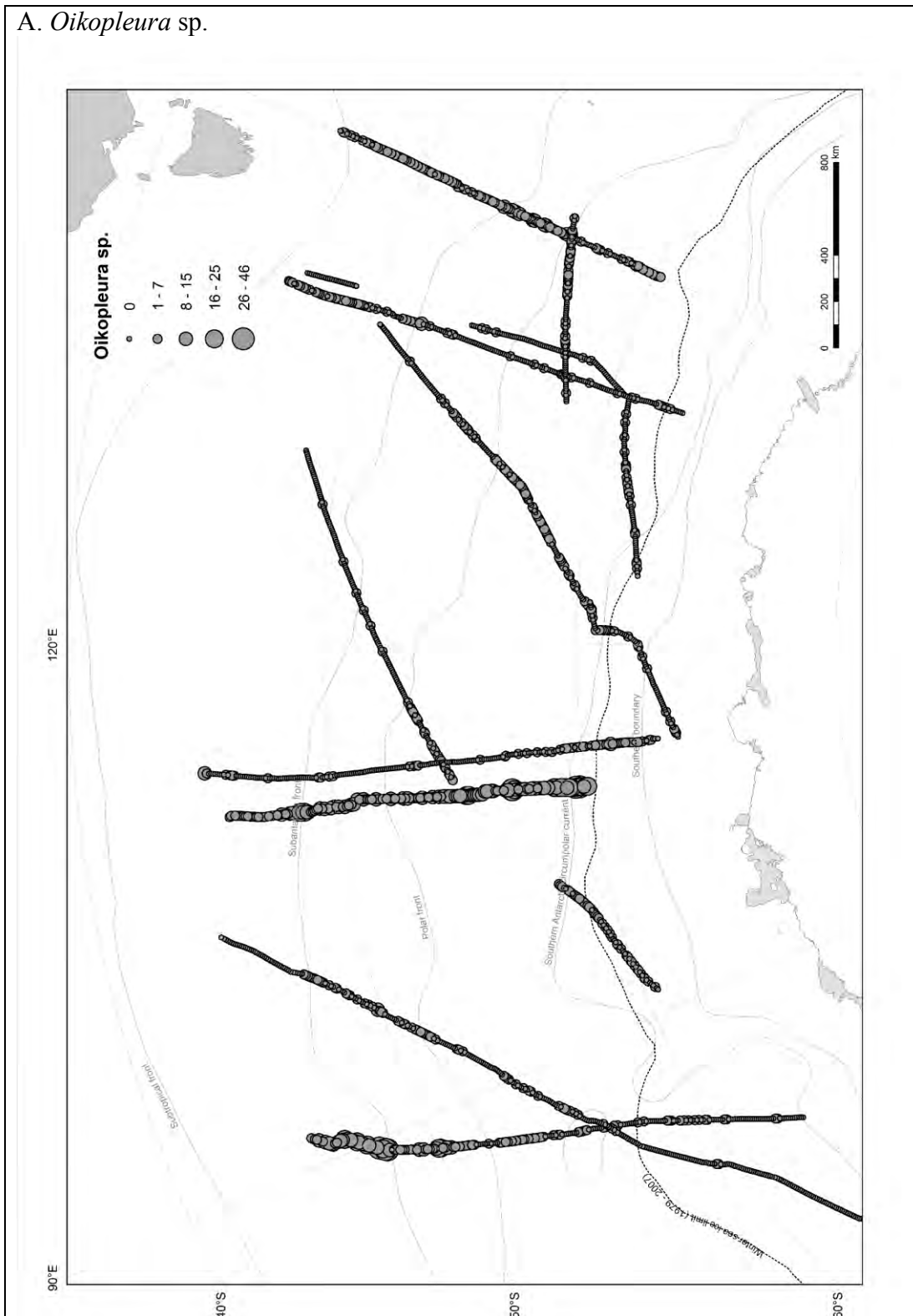
Appendix V.6.A. 2002 – 2003 Lower *Oikopleura* sp. compared to the *Fritillaria* sp. that have a south west distribution. In the POOZ between the Subtropical front and the Southern Antarctic Circumpolar Current the distribution nearly alternates between the *Oikopleura* sp. and *Fritillaria* sp. Abundance is in counts per 5 Nm.

B. *Fritillaria* sp.



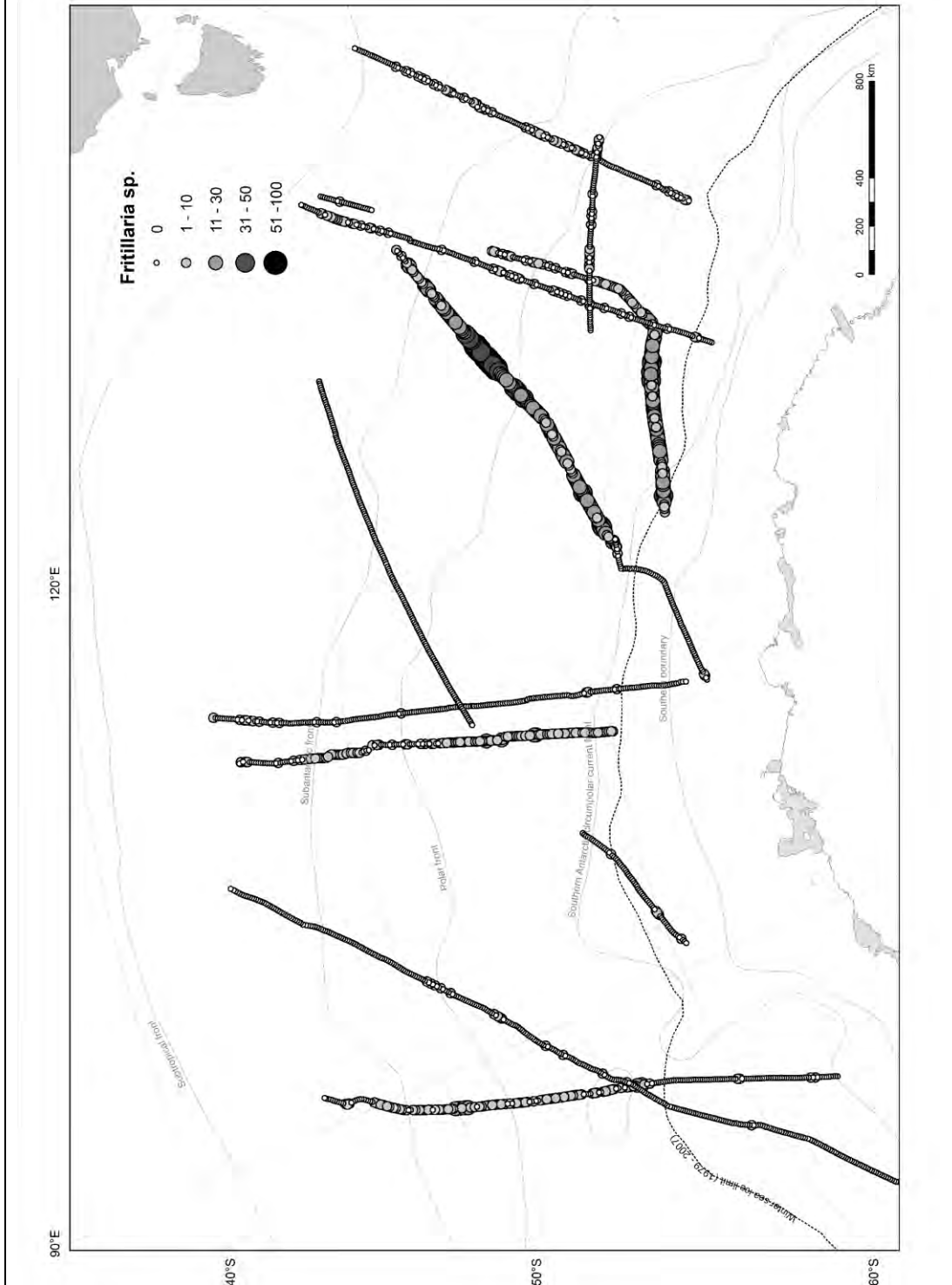
Appendix V.6.B. 2002 – 2003 Lower *Oikopleura* sp. compared to the *Fritillaria* sp. that have a south west distribution. In the POOZ between the Subtropical front and the Southern Antarctic Circumpolar Current the distribution nearly alternates between the *Oikopleura* sp. and *Fritillaria* sp. Abundance is in counts per 5 Nm.

A. *Oikopleura* sp.



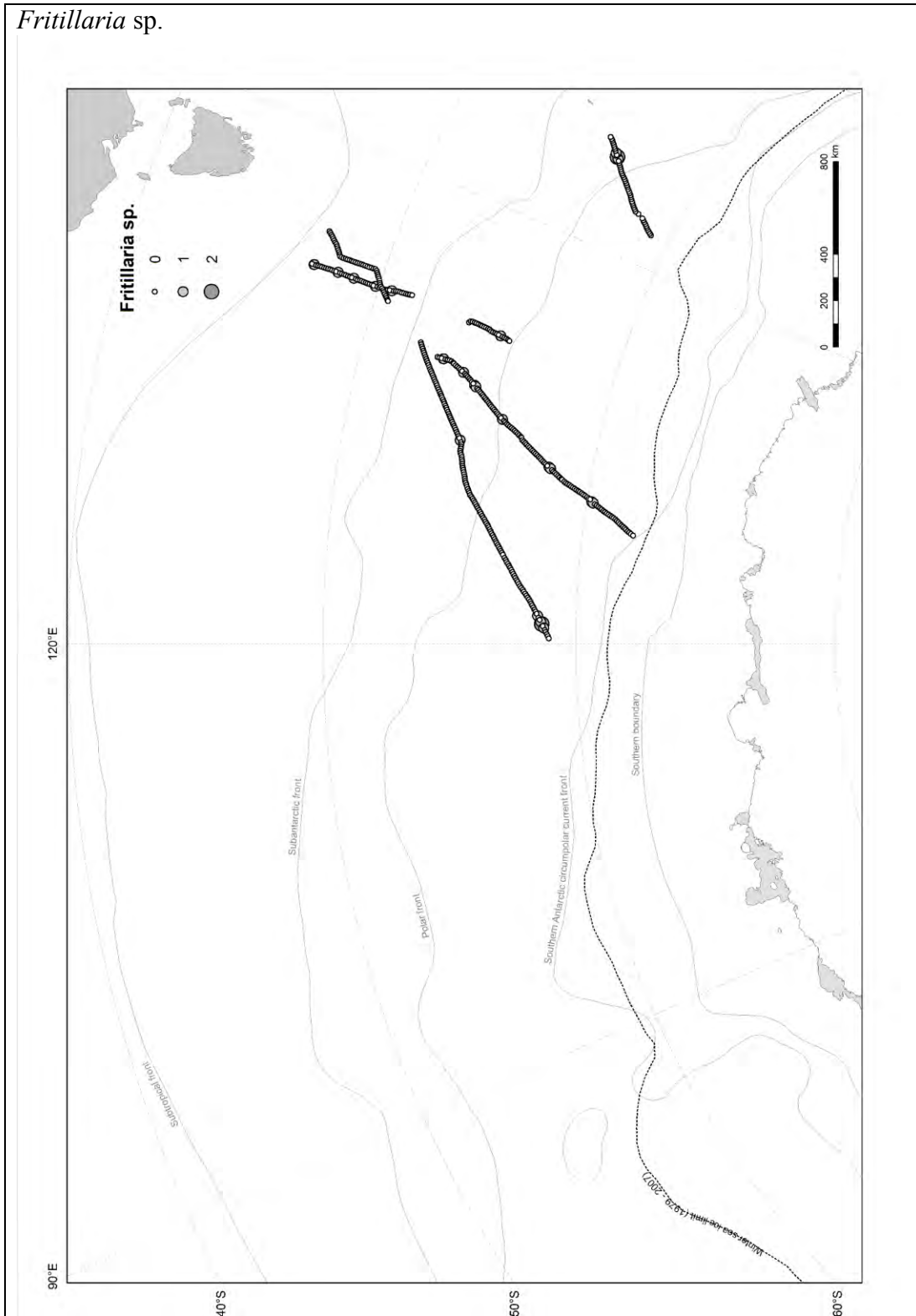
Appendix V.7.A. 2004 – 2005 Lower *Oikopleura* sp. abundances compared to the abundances of the *Fritillaria* sp. The distribution was similar for some transects though the *Fritillaria* sp. dominate. Abundance is in counts per 5 Nm.

B. *Fritillaria* sp.



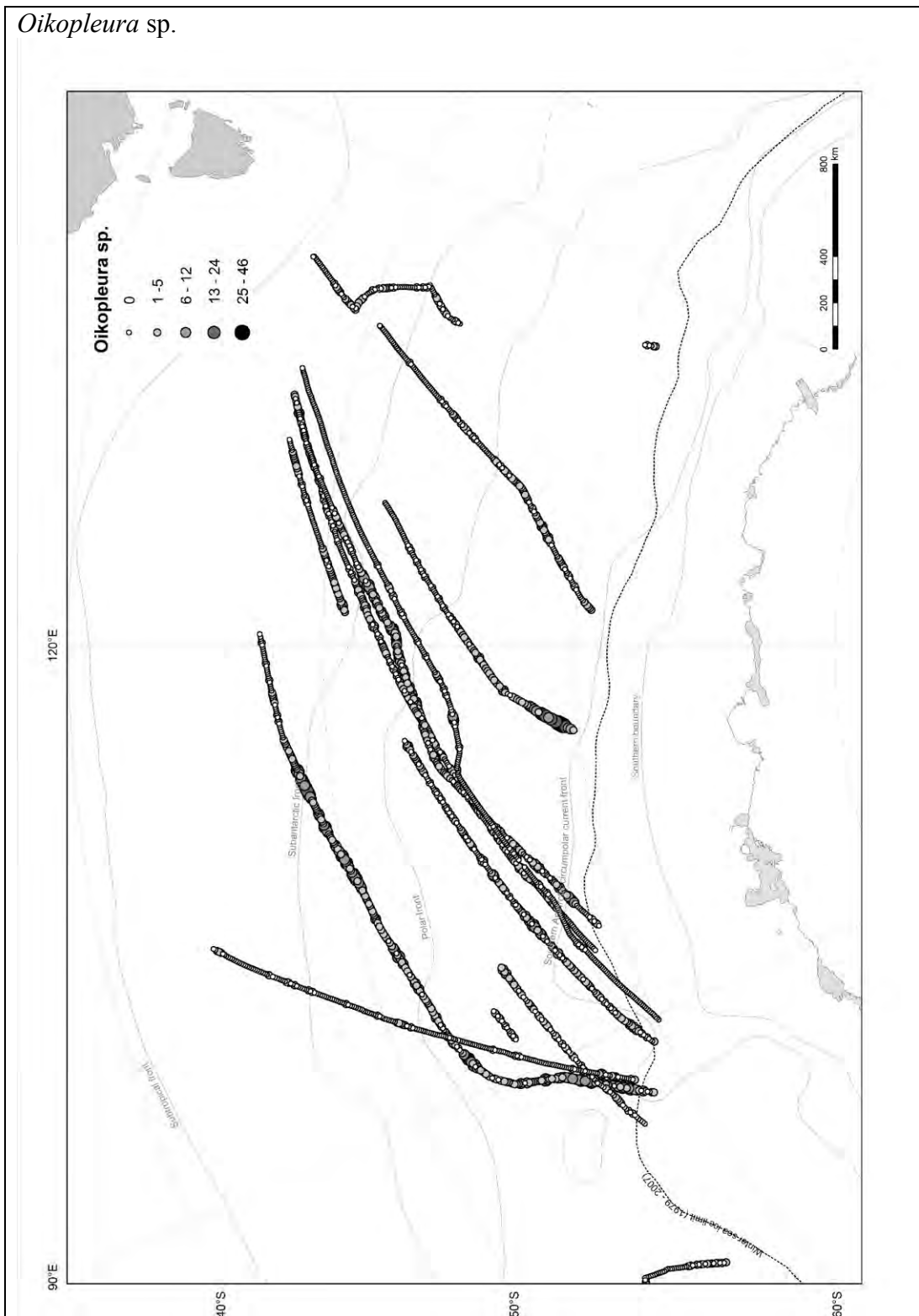
Appendix V.7.B. 2004 – 2005 Lower *Oikopleura* sp. abundances compared to the abundances of the *Fritillaria* sp. The distribution was similar for some transects though the *Fritillaria* sp. dominate. Abundance is in counts per 5 Nm.

Seasonal SO-CPR Distribution and abundance maps



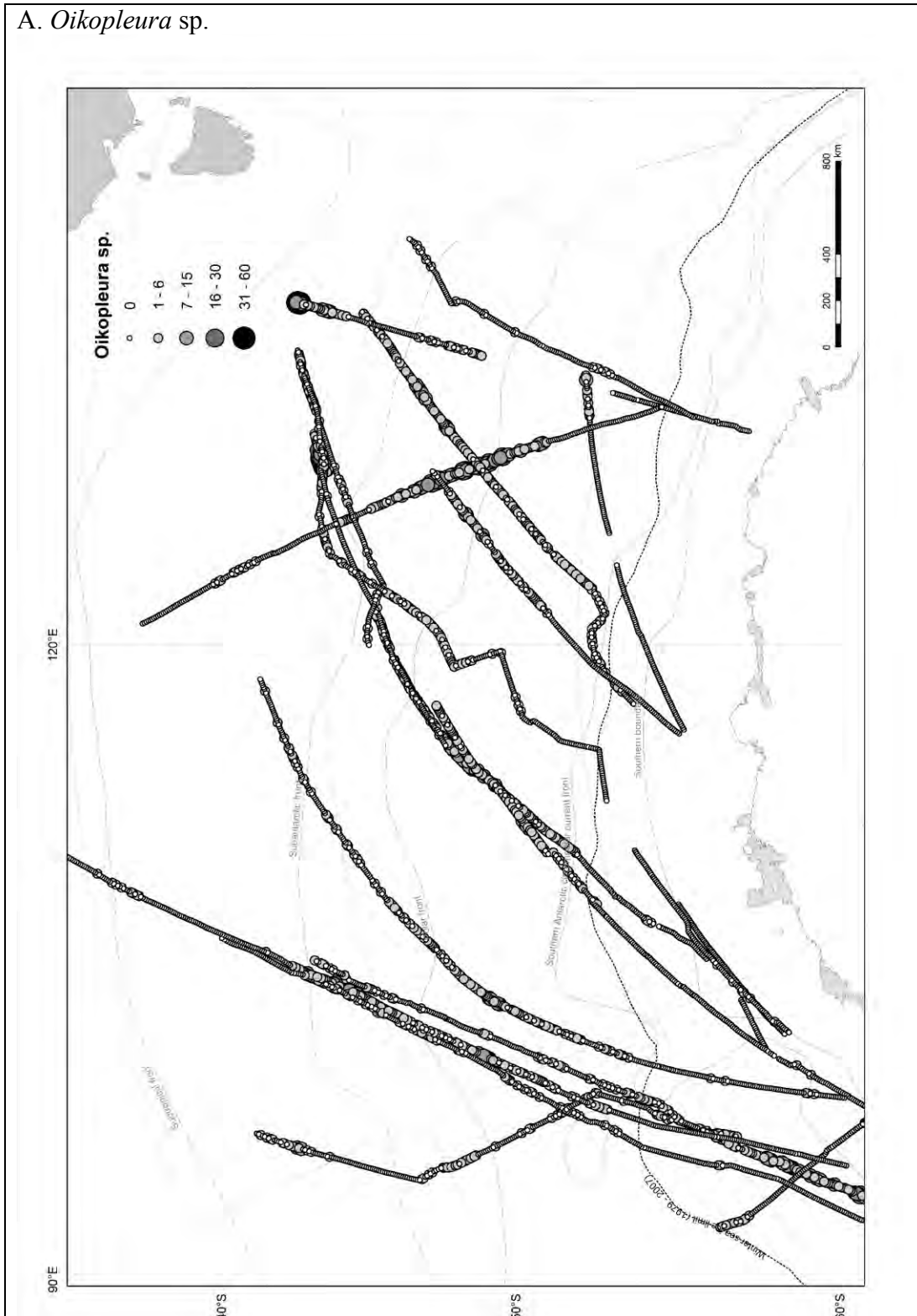
Appendix V.8. September (spring) low abundances of *Fritillaria* sp. at only 1-2 individuals per 5Nm and no recorded *Oikopleura* sp. Abundance is in counts per 5 Nm.

Oikopleura sp.



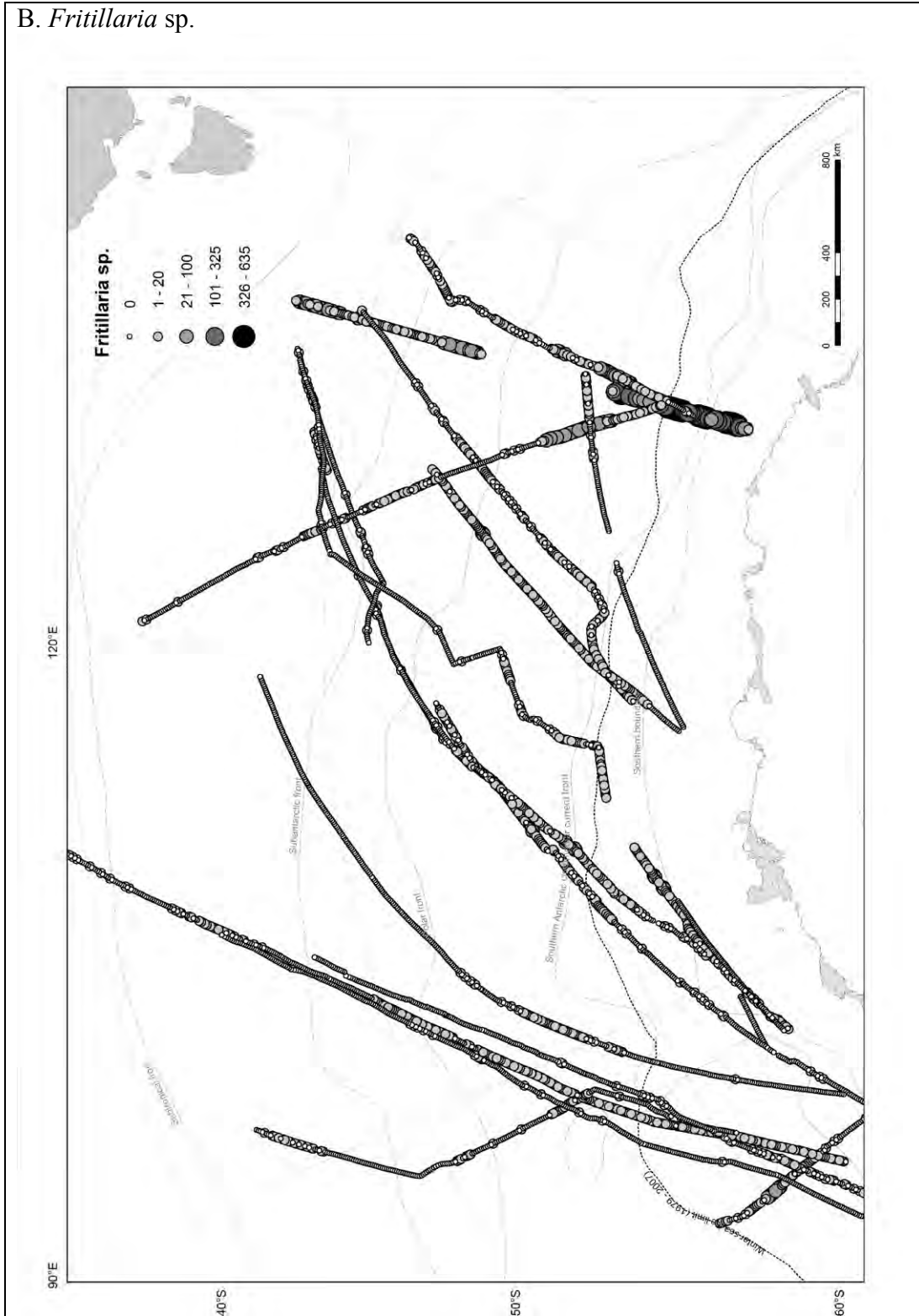
Appendix V.9. November (late spring) *Oikopleura* sp. have higher abundances in the south compared to the north of the tows and there was no recorded *Fritillaria* sp. Abundance is in counts per 5 Nm.

A. *Oikopleura* sp.



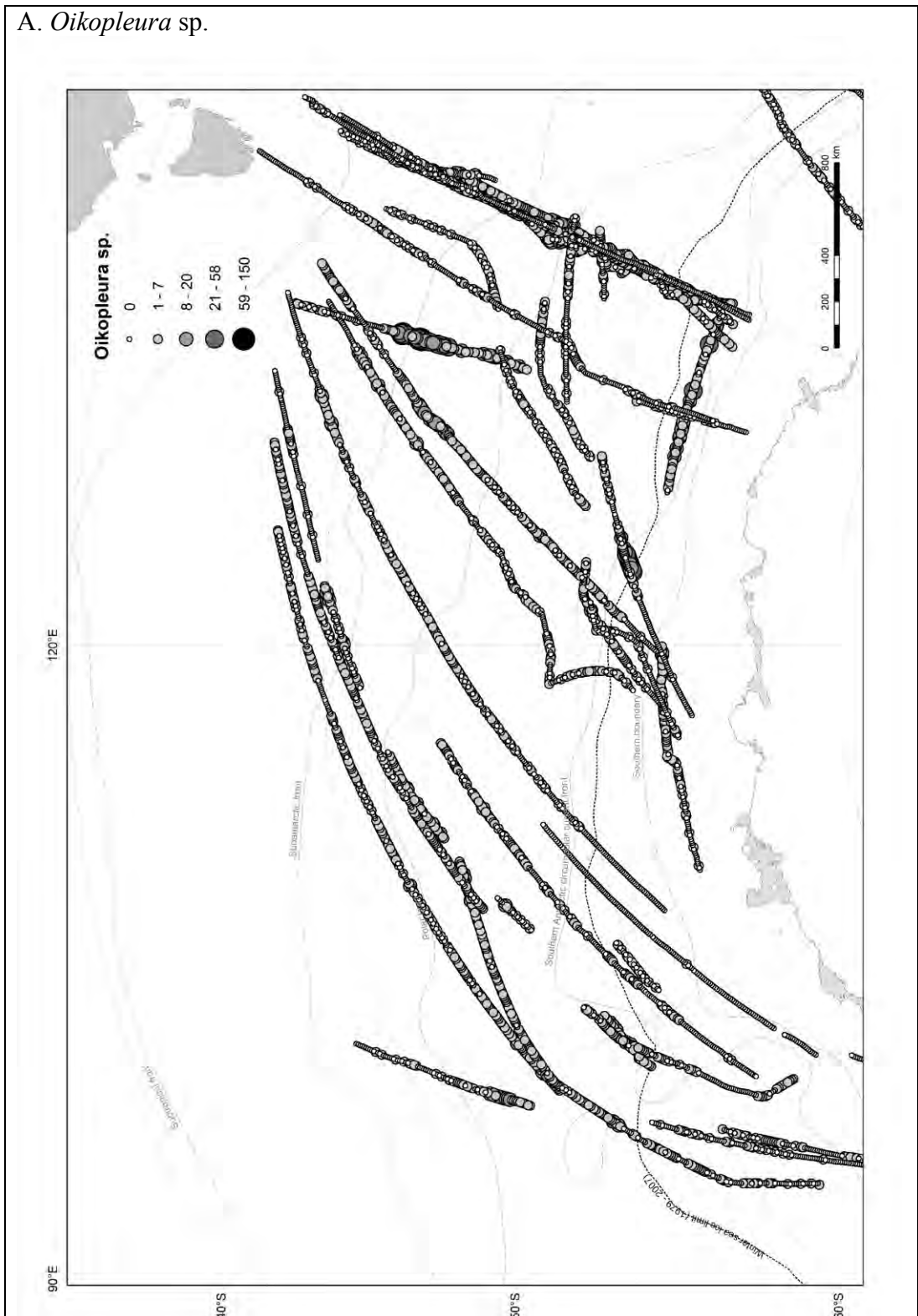
Appendix V.10.A. January (summer) higher abundance of the southerly *Fritillaria* sp. compared to the northerly *Oikopleura* sp. Though along some transects there appears to be an alternate distribution. Abundance is in counts per 5 Nm.

B. *Fritillaria* sp.



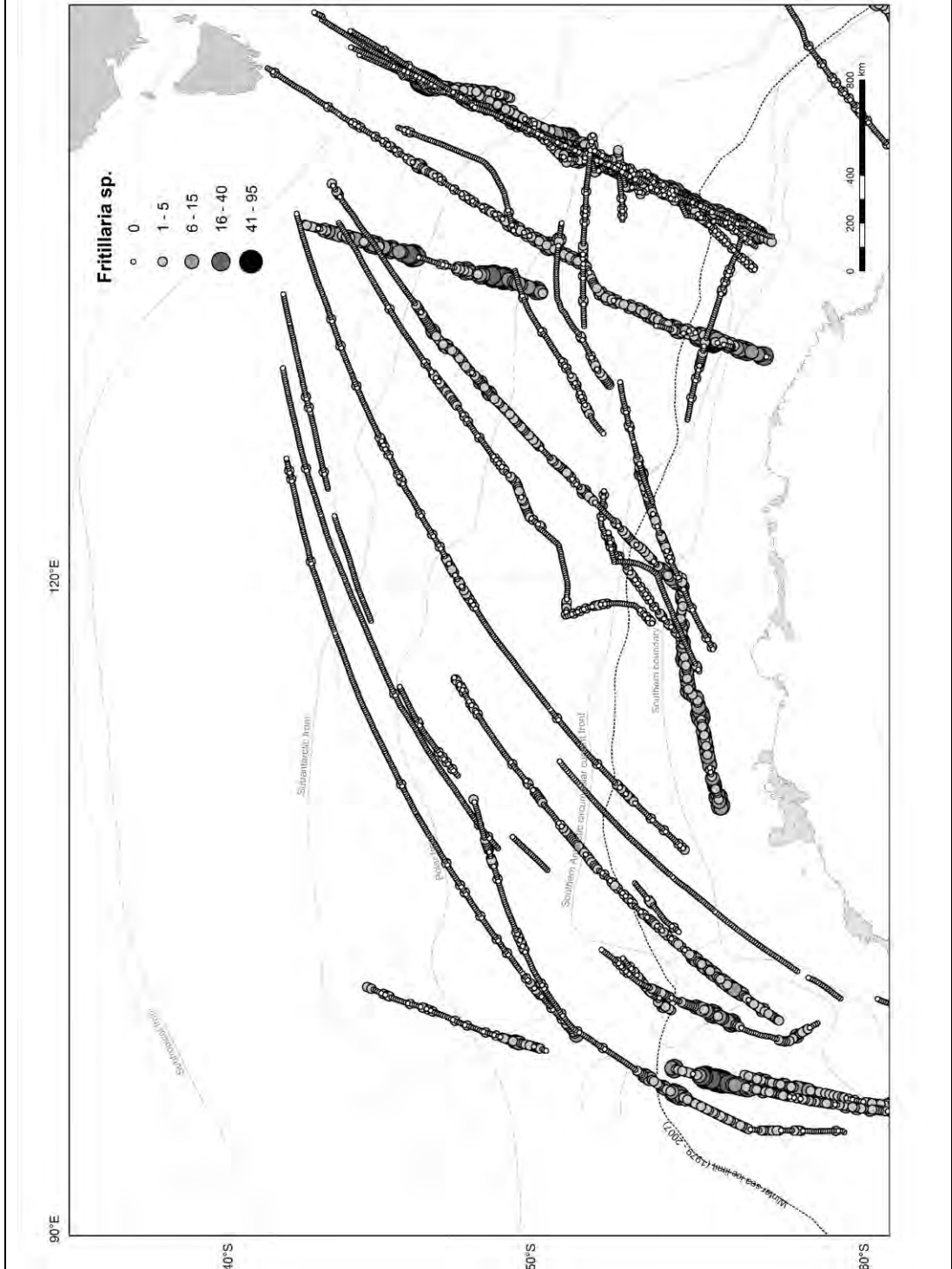
Appendix V.10.B. January (summer) higher abundance of the southerly *Fritillaria* sp. compared to the northerly *Oikopleura* sp. Though along some transects there appears to be an alternate distribution. Abundance is in counts per 5 Nm.

A. *Oikopleura* sp.



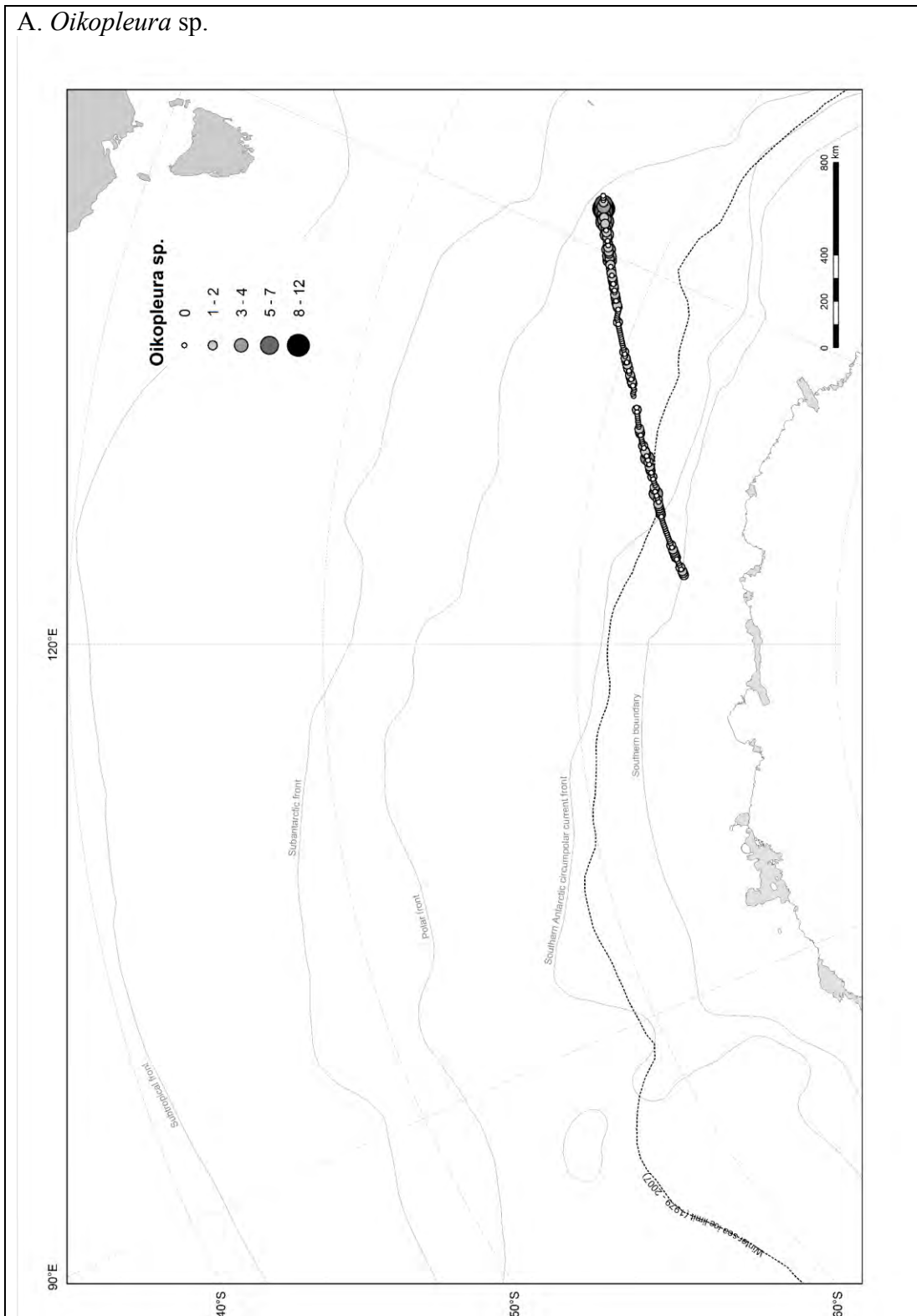
Appendix V.11.A. March (autumn) The abundances are reducing compared to the previous month and now *Oikopleura* sp. dominate. The distribution of both species has a similar pattern. Abundance is in counts per 5 Nm.

B. *Fritillaria* sp.



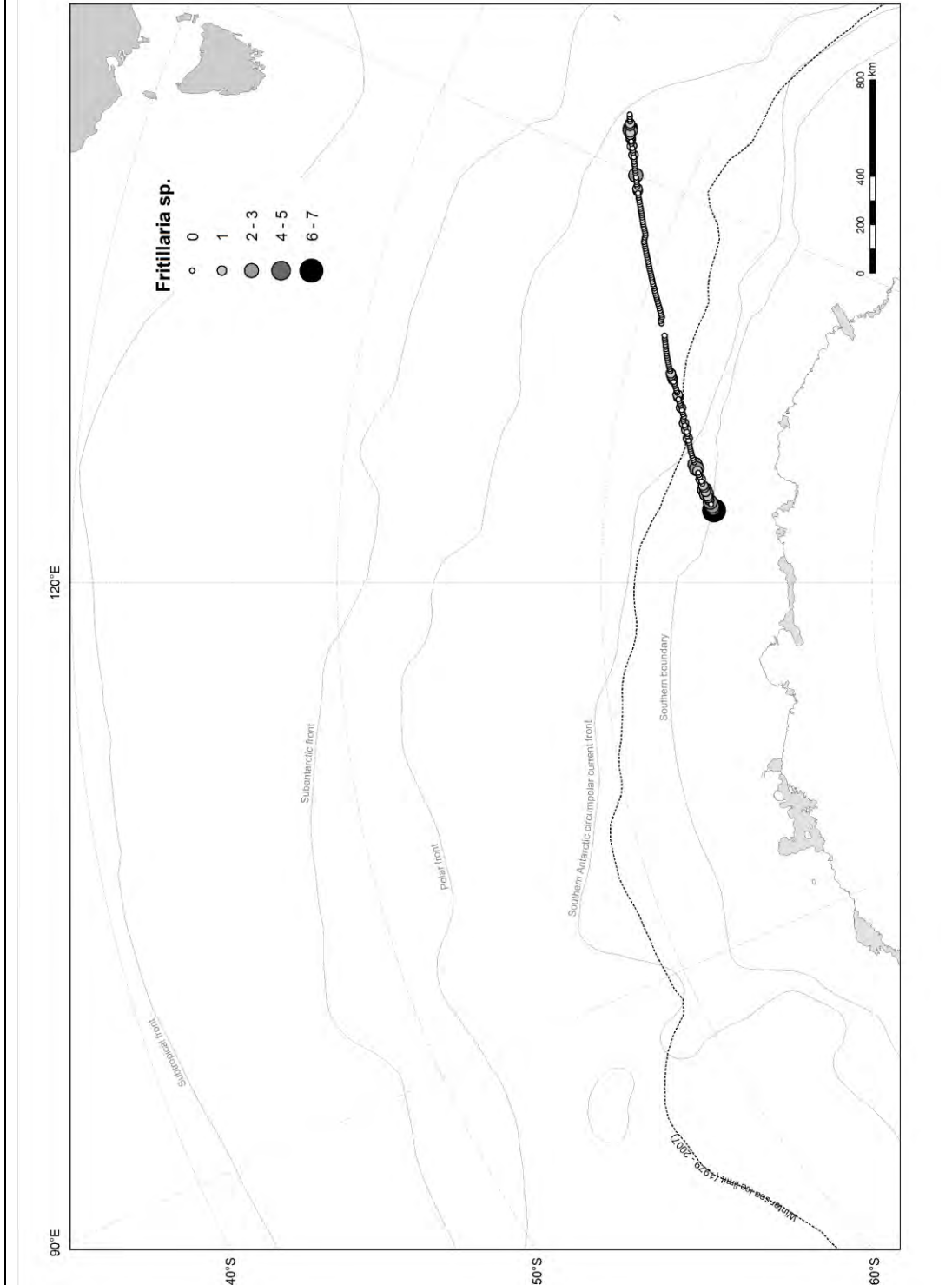
Appendix V.11.B. March (autumn) The abundances are reducing compared to the previous month and now *Oikopleura* sp. dominate. The distribution of both species has a similar pattern. Abundance is in counts per 5 Nm.

A. *Oikopleura* sp.



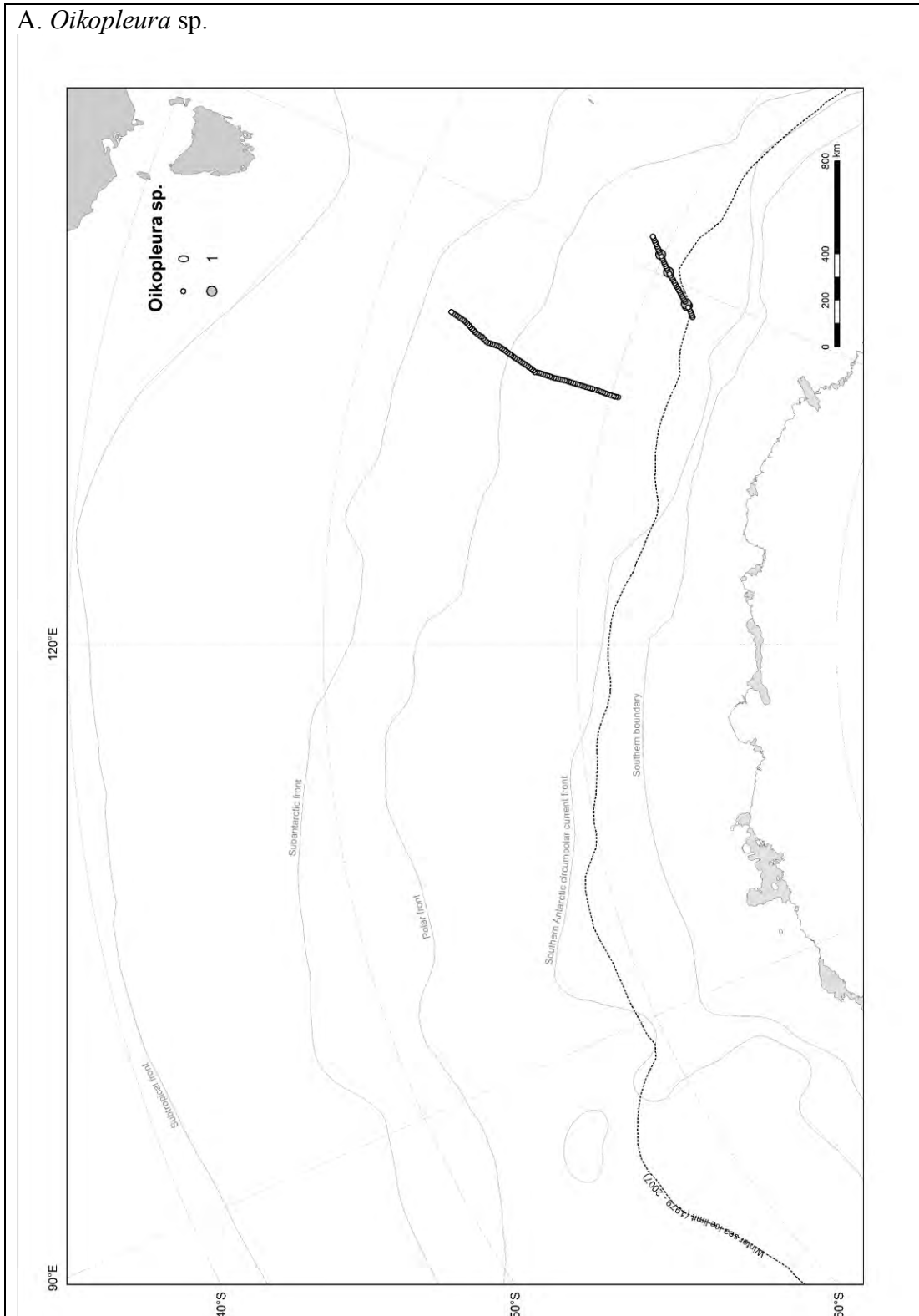
Appendix V.12.A. May (winter) Low abundances for both species in winter with the abundance of the northerly distributed *Oikopleura* sp. doubling that of the southerly distributed *Fritillaria* sp. Abundance is in counts per 5 Nm.

B. *Fritillaria* sp.



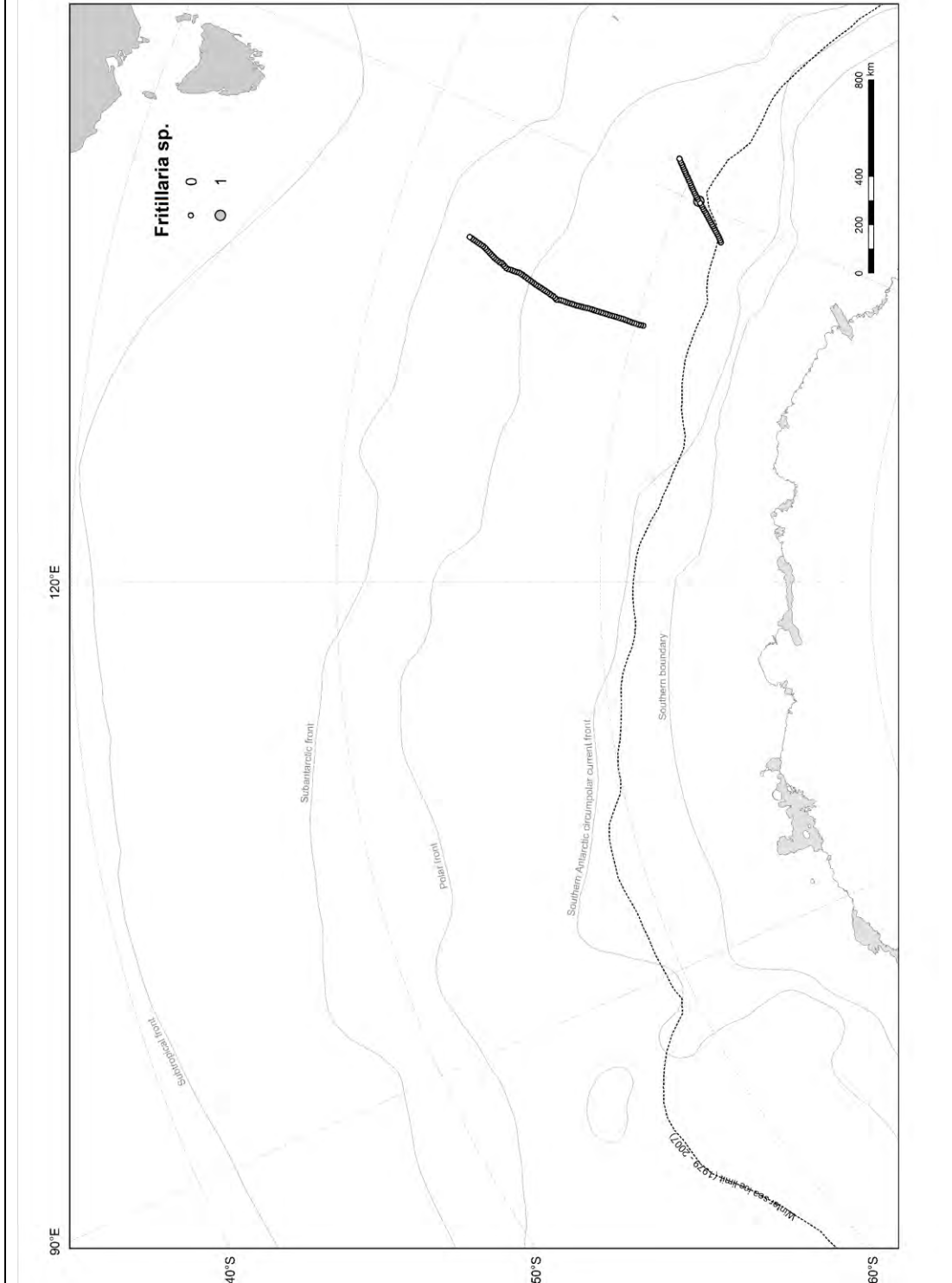
Appendix V.12.B. May (winter) Low abundances for both species in winter with the abundance of the northerly distributed *Oikopleura* sp. doubling that of the southerly distributed *Fritillaria* sp. Abundance is in counts per 5 Nm.

A. *Oikopleura* sp.



Appendix V.13. A. August (winter) Both *Oikopleura* sp. and *Fritillaria* sp. occur north of the winter sea ice limit in very low abundances at 1 individual per 5 Nm. Abundance is in counts per 5 Nm.

B. *Fritillaria* sp.



Appendix V.13.B August (winter) Both *Oikopleura* sp. and *Fritillaria* sp. occur north of the winter sea ice limit in very low abundances at 1 individual per 5 Nm. Abundance is in counts per 5 Nm.

Appendix VI

Generalized Additive Mixed Models (GAMM) theory

Linear statistic models make the assumption that the response variables have a normal distribution and the predictor depends linearly on the parameters. They model univariate responses as the sum of linear terms and have a zero mean random error term, that is, the data points, when measurements are repeated several times are scattered about the true value. Generalized Additive Mixed Models (GAMM) combine Linear Mixed Effect models (LME) and an extension of Generalized Linear Models (GLMs), called Generalized Additive Models (GAM) (Wood, 2006).

GAMM as a form of predictive multiple regression analysis is the most appropriate analysis for the SO-CPR Survey database, when determining the relationship between the larvacean abundances and other parameters. GAMMs fit smooth non-linear trends of abundance with physical variables in the marine ecosystem. GAMMs also simultaneously incorporates a number of non-physical variables as co-predictor variables such as latitude, water temperature etc. (by combining LMEs and GAMs).

Linear Mixed models (LME) are limited compared to GAMMs in the flexibility of the shape of relationships between the expected value of the response and the continuous predictor variables, such as latitude, that can be fitted. GAMMs also allow more realistic distributions for the response of abundance than a normal distribution, particularly the Poisson, given that random effect estimates are included in the linear predictor. Generalized Linear Models (GLMs) “relax” the linearity assumptions of linear models by allowing the expected value of the responses to depend on a smooth monotonic function of the linear predictor (i.e. a Poisson log "link" function). A Generalized Additive Model (GAM) is a GLM that has part of the linear predictor specified in terms of a sum of smooth functions of predictor variables. These smooth trends are known as splines. The GAMM function in the *mgcv* R-library (Wood, 2006) iterates between a GAM fit,

and an LME fit where a "working" response variable is supplied to the LME function from the GAM fit and random effects and their variance along with other more complex variance structures can then be estimated by LME.

An alternate statistical analysis was the Principal Components Analysis (PCA), a dimensionality-reduction ordination technique typically used in community ecology studies when there are a substantial number of species required to be jointly modelled and can be used in indirect gradient analysis or by modelling the most important principal components (i.e. ranked in order of their contribution to the sum of variances over all species) as a function of predictor variables (Orloci, 1975). PCA constructs linear combinations of species abundances (or their transform) whereas other ordination techniques such as Non-metric Multidimensional Scaling do not require derived dimensions to be such linear combinations. PCA was considered to not be a suitable statistical analysis tool in this study as a predictive model was required to predict the abundance of two larvacean species (not the substantial number of species that the PCA requires) from a number of parameters (latitude, season, month, fluorescence, salinity (psu), temperature (°C) and PAR ($\mu\text{Em}^{-2}\text{s}^{-1}$)).

The GAMM model fits, smooth but flexible nonlinear relationships as described above and typically models a single response variable (even though multivariate responses can theoretically be modelled, GAMMs fitted by *mgcv* are limited to a single response variable). This study focused on two larvacean species (not a community) from the SO-CPR Survey. The abundances of the two individual species of larvaceans both had an extreme numbers of zeros. This high occurrences of zeros (i.e. absences) resulted in an inability to explain ecological patterns of co-occurrence to any reasonable degree of confidence, so modelling was limited to a response variable defined as the total abundance of both species combined. LME was also used but it cannot model the nonlinear nature of relationships as GAMM was able to do. These data did not support estimation models of greater complexity (e.g. a constrained zero-inflated generalized additive model (COZIGAM) Liu et al. (2011)).

The GAMM model output includes F values, *p* values and estimated degrees of freedom. The GAMM output uses F values to determine the level of statistical

significance between the predictor variable and the abundance of total zooplankton or larvaceans. In GAMM the F values are comparable (i.e. relative) to the other F values from the same output and dataset. The F values are influenced by the estimated degrees of freedom and due to this the higher the F value the lower the p value. The estimated degrees of freedom is the number of values in the final calculation of a statistic that are free to vary (Wood, 2011). The GAMM output for each predictor also includes a graph (i.e. ‘partial’ plots) where the y-axis is an ordinate scale of the variable being predicted. In this study, this is the abundance of total zooplankton or larvaceans on the log scale (i.e. since a log link function was used in the GAMM) and the x-axis is the parameter that is being used as the predictor.

The GAMM splines are presented as a plots using a ordinate scale that represents the contribution to linear predictor, \hat{P}_L . Exponentiation of the ordinate gives a multiplicative factor to scale predictors for the intercept plus other predictors, that is the :

$$\text{Predicted abundance} = \exp(\hat{P}_L) \exp(\sum \hat{P}_{i, i \neq L} \text{ other} + \text{intercept})$$

This is for the log-link Poisson GAMM, which is a smooth monotonic function of the linear predictor, \hat{P}_L = is the predicted contribution of variable L where latitude is given by the x axis while holding the other predictors each at a constant value (e.g. their mean values) and the *other* are the other predictors in the model. For example, the ordinate scale for the predicted total zooplankton abundance using the zooplankton CPR 1991-2008 analyses Total zooplankton GAMM and latitude (Figure 4.25) shows \hat{P}_L versus L = latitude is: Predicted total zooplankton abundance = $\exp(\hat{P}[\text{latitude}]_L) \exp(\sum \hat{P} [\text{water temperature, fluorescence, month and season}] + \text{intercept})$.

The spline (solid smoothed line) is flanked by dashed lines that indicate the 95% confidence interval. When the 95% confidence intervals (dashed lines on the graphs) are close to the splines (solid line) the confidence in the estimate of the spline is greater. The GAMM output shows if there is a statistically significant

trend (or relationship) between the zooplankton or larvacean abundances (counts per 5 Nm) and the predictor variable such as latitude.

The over dispersion parameters for the Poisson error given the random effects from the data points is denoted ϕ , i.e. while the random effect standard deviation on the linear predictor scale is denoted σ .

Appendix VII**R code for mgcv**

R code for mgcv

```
# Margaret's Larvacean CPR data

library(lattice)
library(asreml)
library(chron)
library(mgcv)
library(lme4)
library(nlme)

data <- read.csv(file="CPR larvacean 1991-2008.csv")

summary(data)

dim(data)

data <- data[!is.na(data$Flu_Value),]

summary(data)

dim(data)

data <- data[!is.na(data$W_Temp_Hi),]

data <- data[data$W_Temp_Hi>-5,]

summary(data)

data$Season.i <- as.integer(data$Season)
tapply(data$Season.i, INDEX=data$Season, FUN=mean)

levels(data$Month)

dim(data)

Month.im <- outer(data$Month, levels(data$Month), FUN=="==")

dim(Month.im)
Month.im[,1,]

Month.i <- Month.im %*% matrix(data=c(10,2,6,8,7,1,9,11,5,4,3), nrow=11, ncol=1)

length(Month.i)
tapply(Month.i, INDEX=data$Month, FUN=mean)
```

```

data$Month.i <- Month.i

rm(Month.i,Month.im)

data$Tow_Number <- as.factor(data$Tow_Number)

data$Segment_No.f <- as.factor(data$Segment_No.)

data$Time <- as.character(data$Time)

#t1 <- chron(times = data$Time, format = c(times = "h:m"))

asreml.01 <-asreml(fixed = Total_larvacean_abundance ~ Season + Month + Flu_Value
+ W_Temp_Hi , data=data,
  random = ~ Tow_Number, family=asreml.poisson(link="log",dispersion=NA))

asreml.01 <-asreml(fixed = Total_zooplankton_.abundance ~ Season + Month +
Flu_Value + W_Temp_Hi , data=data,
  random = ~ Tow_Number, family=asreml.poisson(link="log",dispersion=NA))

asreml.01 <-asreml(fixed = Total_larvacean_abundance ~ Season + Month + Flu_Value
+ W_Temp_Hi , data=data,
  random = ~ Tow_Number)

#asreml.01 <-asreml(fixed = Total_larvacean_abundance ~ Season + Flu_Value +
W_Temp_Hi , data=data,
#   random = ~ Tow_Number)

asreml.01 <-asreml(fixed = Total_larvacean_abundance ~ Season + Latitude + Month +
Flu_Value + W_Temp_Hi , data=data,
  random = ~ Tow_Number + spl(Latitude))

#asreml.01 <-asreml(fixed = Total_larvacean_abundance ~ Season + Latitude + Month +
Flu_Value + W_Temp_Hi , data=data,
#   random = ~ Tow_Number, family=asreml.poisson(link="log",dispersion=NA))

asreml.01 <-asreml(fixed = Total_zooplankton_.abundance ~ Season + Latitude +
Month + Flu_Value + W_Temp_Hi , data=data,
  random = ~ Tow_Number)

#asreml.01 <-asreml(fixed = Total_zooplankton_.abundance ~ Season + Latitude +
Month + Flu_Value + W_Temp_Hi , data=data,
#   random = ~ Tow_Number, rcov=~ Tow_Number:exp(Segment_No.))

anova(asreml.01)
summary(asreml.01)$coef.fixed
summary(asreml.01)$varcomp

asreml.01 <-asreml(fixed = log(Total_zooplankton_.abundance+1) ~ Season + Month +
Flu_Value + W_Temp_Hi , data=data,
  random = ~ Tow_Number)

```

```

asreml.01 <- asreml(fixed = Total_zooplankton_.abundance ~ Season + Month +
  Flu_Value + W_Temp_Hi , data=data,
  random = ~ Tow_Number, family=asreml.poisson(link="log",dispersion=NA))

length(levels(data$Tow_Number))

anova(asreml.01)
summary(asreml.01)$coef.fixed
summary(asreml.01)$varcomp

Tow_Number <- data$Tow_Number
gamm.01 <- gamm(formula=Total_zooplankton_.abundance ~ Season + Month +
  s(Flu_Value,bs="cr") + s(W_Temp_Hi,bs="cr"),
  random=list(Tow_Number= ~1), family=poisson(link="log"), data=data)

summary(gamm.01)

summary(gamm.01$lme)

summary(gamm.01$gam)

plot(gamm.01$gam)

gamm.01 <- gamm(formula=Total_zooplankton_.abundance ~ Season + Month +
  s(Latitude,bs="cr") +
  s(Flu_Value,bs="cr") + s(W_Temp_Hi,bs="cr"),
  random=list(Tow_Number= ~1), family=poisson(link="log"), data=data)

gamm.01 <- gamm(formula=Total_zooplankton_.abundance ~ s(Season.i,bs="cr") +
  s(Month.i,bs="cr") + s(Latitude,bs="cr") +
  s(Flu_Value,bs="cr") + s(W_Temp_Hi,bs="cr"),
  random=list(Tow_Number= ~1), family=poisson(link="log"), data=data)

gamm.01 <- gamm(formula=Total_zooplankton_.abundance ~ s(Season.i,bs="cr") +
  s(Month.i,bs="cr") + s(Latitude,bs="cr") +
  s(Flu_Value,bs="cr") + s(W_Temp_Hi,bs="cr"),
  random=list(Tow_Number= ~1), correlation=corLin(form= ~ Segment_No. |
  Tow_Number),
  family=poisson(link="log"), data=data,
  control=nlme::lmeControl(tolerance=1e-4, msTol=1e-5,
  niterEM=0,optimMethod="L-BFGS-
  B"),niterPQL=15,verbosePQL=TRUE,method="ML")

gamm.01 <- gamm(formula=Total_zooplankton_.abundance ~ s(Season.i,bs="cr") +
  s(Month.i,bs="cr") + s(Latitude,bs="cr") +
  s(Flu_Value,bs="cr") + s(W_Temp_Hi,bs="cr"),
  correlation=corLin(form= ~ Segment_No. | Tow_Number, nugget=TRUE),
  family=poisson(link="log"), data=data,
  control=nlme::lmeControl(tolerance=1e-4, msTol=1e-5,
  niterEM=0,optimMethod="L-BFGS-
  B"),niterPQL=2,verbosePQL=TRUE,method="ML")

```

```

gamm.01 <- gamm(formula=Total_zooplankton_abundance ~ s(Season.i,bs="cr") +
s(Month.i,bs="cr") + s(Latitude,bs="cr") +
s(Flu_Value,bs="cr") + s(W_Temp_Hi,bs="cr"),
correlation=corLin(form= ~ Segment_No. | Tow_Number, nugget=TRUE),
data=data, control=nlme::lmeControl(tolerance=1e-4, msTol=1e-5,
niterEM=0,optimMethod="L-BFGS-
B"),niterPQL=12,verbosePQL=TRUE,method="ML")

```

```

gamm.01 <- gamm(formula=Total_zooplankton_abundance ~ s(Season.i,bs="cr") +
s(Month.i,bs="cr") + s(Latitude,bs="cr") +
s(Flu_Value,bs="cr") + s(W_Temp_Hi,bs="cr"),
correlation=corLin(form= ~ Segment_No. | Tow_Number),
family=poisson(link="log"), data=data,
control=nlme::lmeControl(tolerance=1e-5, msTol=1e-5,
niterEM=0,optimMethod="L-BFGS-
B"),niterPQL=10,verbosePQL=TRUE,method="ML")

```

```

gamm.01 <- gamm(formula=Total_zooplankton_abundance ~ s(Season.i,k=3,bs="tp") +
s(Month.i,k=3,bs="tp") + s(Latitude,k=8,bs="tp") +
s(Flu_Value,k=8,bs="tp") + s(W_Temp_Hi,k=8,bs="tp"),
random=list(Tow_Number= ~1), family=poisson(link="log"), data=data,
control=nlme::lmeControl(niterEM=0,optimMethod="L-BFGS-B"),
niterPQL=10,verbosePQL=TRUE,method="ML")

```

```

lme.01 <- lme(fixed=Total_zooplankton_abundance ~ Season.i + Month.i + Latitude +
Flu_Value + W_Temp_Hi, random= ~ 1 | Tow_Number,
correlation=corLin(form= ~ Segment_No. | Tow_Number, nugget=TRUE),
data=data, method="ML")

```

```

summary(lme.01)
anova(lme.01)

```

```

lme.02 <- lme(fixed=Total_zooplankton_abundance ~ Season.i + Month.i + Latitude +
Flu_Value + W_Temp_Hi, random= ~ 1 | Tow_Number,
data=data, method="ML")

```

```

summary(lme.02)
anova(lme.02)

```

```

summary(gamm.01)

```

```

summary(gamm.01$lme)

```

```

summary(gamm.01$gam)

```

```

plot(gamm.01$gam)

```

```

summary(gamm.01$gam)
names(gamm.01$gam)

names(gamm.01$lme)

summary(gamm.01$gam$fitted.values)
summary(gamm.01$lme$residuals)
summary(gamm.01$lme$fitted[,1])
lme.fitted.re <- gamm.01$lme$fitted %*% matrix(data=rep(1,7), nrow=7, ncol=1)

lme.fitted <- gamm.01$lme$fitted %*% matrix(data=c(rep(1,6),0), nrow=7, ncol=1)

plot(y=lme.fitted.re, x=data$Total_zooplankton_.abundance, ylim=c(0,50),
xlim=c(0,500))

plot(y=lme.fitted, x=data$Total_zooplankton_.abundance, ylim=c(0,50), xlim=c(0,500))

plot(y=gamm.01$gam$fitted.values, x=data$Total_zooplankton_.abundance)

plot(y=gamm.01$gam$fitted.values, x=data$Total_zooplankton_.abundance,
ylim=c(0,500), xlim=c(0,500))

gamm.01 <- gamm(formula=Total_larvacean_abundance ~ s(Season.i,k=3,bs="tp") +
s(Month.i,k=3,bs="tp") + s(Latitude,k=8,bs="tp") +
s(Flu_Value,k=8,bs="tp") + s(W_Temp_Hi,k=8,bs="tp"),
random=list(Tow_Number= ~1), family=poisson(link="log"), data=data,
control=nlme::lmeControl(niterEM=0,optimMethod="L-BFGS-B"),
niterPQL=10,verbosePQL=TRUE,method="ML")

gamm.01 <- gamm(formula=Total_larvacean_abundance ~ s(Season.i,k=3,bs="tp") +
s(Month.i,k=3,bs="tp") + s(Latitude,k=8,bs="tp") +
s(Flu_Value,k=8,bs="tp") + s(W_Temp_Hi,k=8,bs="tp"),
random=list(Tow_Number= ~1), family=poisson(link="log"), data=data)

gamm.01 <- gamm(formula=Total_larvacean_abundance ~ s(Season.i,bs="cr") +
s(Month.i,bs="cr") + s(Latitude,bs="cr") +
s(Total_zooplankton_.abundance,bs="cr") + s(W_Temp_Hi,bs="cr"),
random=list(Tow_Number= ~1), family=poisson(link="log"), data=data)

data$LTtotal_zoo <- log(data$Total_zooplankton_.abundance+1)

gamm.01 <- gamm(formula=Total_larvacean_abundance ~ s(Season.i,bs="cr") +
s(Month.i,bs="cr") + s(Latitude,bs="cr") +
s(LTtotal_zoo,bs="cr") + s(W_Temp_Hi,bs="cr"),
random=list(Tow_Number= ~1), family=poisson(link="log"), data=data)

```



```

.Random.seed <- 0.4541872

summary(gamm.01)

summary(gamm.01$lme)

summary(gamm.01$gam)

summary(gamm.01$gam$fitted.values)

plot(gamm.01$gam)

lme.fitted.re <- gamm.01$lme$fitted %**% matrix(data=rep(1,7), nrow=7, ncol=1)

lme.fitted <- gamm.01$lme$fitted %**% matrix(data=c(rep(1,6),0), nrow=7, ncol=1)

plot(y=gamm.01$gam$fitted.values, x=data$Total_larvacean_abundance, ylim=c(0,100),
xlim=c(0,100))

plot(y=gamm.01$gam$fitted.values, x=data$Total_larvacean_abundance, ylim=c(0,20),
xlim=c(0,20))

plot(y=lme.fitted.re, x=data$Total_larvacean_abundance)

plot(y=lme.fitted, x=data$Total_larvacean_abundance)

asreml.mv01 <-asreml(fixed =
cbind(Total_zooplankton_.abundance,Total_larvacean_abundance) ~ trait + trait:Season
+ trait:Month +
  trait:Flu_Value + trait:W_Temp_Hi , data=data,
  random = ~ trait:Tow_Number, rcov= ~ units:diag(trait))

asreml.mv01 <-asreml(fixed =
cbind(Total_zooplankton_.abundance,Total_larvacean_abundance) ~ trait + trait:Season
+ trait:Month +
  trait:Flu_Value + trait:W_Temp_Hi , data=data,
  random = ~ trait:Tow_Number, rcov= ~ units:us(trait))

anova(asreml.mv01)
summary(asreml.mv01)$coef.fixed
summary(asreml.mv01)$varcomp

asreml.mv01 <-asreml(fixed =
cbind(Total_zooplankton_.abundance,Fritillaria_sp,Oikopleura_sp) ~ trait + trait:Season
+ trait:Month +

```

```
trait:Flu_Value + trait:W_Temp_Hi , data=data,  
random = ~ trait:Tow_Number, rcov= ~ units:us(trait))  
  
anova(asreml.mv01)  
summary(asreml.mv01)$coef.fixed  
summary(asreml.mv01)$varcomp
```

Appendix VIII**Mean abundance of marine protists**

Mean abundance of Antarctic marine protists from the water column of CTD 25 (-61.996S 32.485E) and 65 (-65.380S 49.998E) from BROKE West. Those in **bold** occur in the water column and on the surface and in the stomachs of *O. gaussica*. Raw data from Fiona Scott.

CTD 025	mean (cells L ⁻³)	CTD 065	mean (cells L ⁻³)
un ID HET (Phaeocystis gametes)	15714.7	un ID HET (Phaeocystis)	7384.0
<i>Asteromphalus parvulus</i>	73840.3	<i>Asteromphalus</i> 30 umd	230230.2
<i>Asteromphalus hookeri</i> 30 umd	189.3	<i>Chaetoceros bulbosus</i>	2840.0
<i>Asteromphalus roperianus</i>	2650.7	<i>Chaetoceros dichaeta</i>	757.3
<i>Chaetoceros dichaeta</i>	189.3	<i>Chaetoceros hendeyi</i>	2082.7
<i>Chaetoceros hendeyi</i>	6437.4	<i>Chaetoceros peruvianus</i>	1893.3
<i>Chaetoceros peruvianus</i>	3408.0	<i>Coscinodiscus</i> 40 umd	189.3
<i>Dactyliosolen</i>	378.7	<i>Thalassiosira gracilis</i> 10 umd	189.3
<i>Eucampia antarctica</i>	946.7	<i>Thalassiosira</i> 20-30 umd	4354.7
<i>Melosira adeliae</i>	189.3	<i>Thalassiosira</i> 60 umd	757.3
<i>Rhizosolenia</i>	1136.0	<i>Cylindrotheca closterium</i>	189.3
<i>Thalassiosira gracilis</i> 10 umd	1704.0	<i>Fragilariopsis curta</i> / <i>cylindrus</i>	1893.3
<i>Thalassiosira maculata</i>	6816.0	<i>Fragilariopsis kerguelensis</i>	14010.7
<i>Thalassiosira</i> 60 umd	2272.0	<i>Fragilariopsis rhombica</i>	3408.0
<i>Cylindrotheca closterium</i>	757.3	<i>Fragilariopsis</i> sp. 60 uml	7005.4
<i>Fragilariopsis curta</i> / <i>cylindrus</i>	378.7	<i>Membraneis challengerii</i>	568.0
<i>Fragilariopsis kerguelensis</i>	6816.0	<i>Navicula</i> 60 uml	1514.7
<i>Fragilariopsis pseudonana</i>	21016.1	<i>Pseudonitzschia</i> 90 uml	1893.3
<i>Fragilariopsis rhombica</i>	757.3	<i>Trichotoxon reinboldii</i>	8330.7
<i>Fragilariopsis</i> 60 uml	1704.0	<i>Alexandrium</i>	3597.3
<i>Halsea trompii</i>	4354.7	<i>Gymnodinium</i> 12 uml	568.0
<i>Membraneis challengerii</i>	189.3	<i>Oxytoxum criophilum</i>	1325.3
<i>Navicula</i> 60 uml	189.3	<i>Prorocentrum</i>	378.7
<i>Pseudonitzschia</i> 90 uml	2082.7	<i>Protoperidinium</i> het 60 umd	757.3
<i>Trichotoxon reinboldii</i>	5490.7	<i>Codonellopsis</i>	568.0
<i>Alexandrium</i>	10034.7	ciliate sp un-ID	189.3
<i>Gymnodinium</i> 12 uml	2840.0		
<i>Oxytoxum criophilum</i>	946.7		
<i>Prorocentrum</i>	568.0		
<i>Dictyocha speculum</i>	189.3		
<i>Tontonia</i>	378.7		

Appendix IX**Marine protists size**

The sizes of the protists (Scott and Marchant, 2005) identified in the water column and on or in the larvacean, *O. gaussica*. Those in **bold** occur in the water column and on the surface and in the stomachs of the larvacean.

	PROTISTS	SIZE (µm)	Setae (µm)	Apical axis (µm)	Pervalvar axis or transapical (µm)
	in ID auto				
Prymnesiales	un ID HET (Phaeocystis gametes)	5-10			
	Phaeocystis (in colony)	5-10			
Coccolithophore	<i>coccolithophorid</i> un-ID	3-12			
Diatoms	<i>Asteromphalus</i>	22-120			
	<i>Asteromphalus elegans</i>				
	<i>Asteromphalus parvulus</i>	22-48			
	<i>Asteromphalus hookeri</i> 30 umd	25-60			
	<i>Asteromphalus roperianus</i>	80-120			
	<i>Eucampia Antarctica</i> (var. <i>recta</i>)	39-116			
	<i>Chaetoceros</i>	7-50			
	<i>Chaetoceros atlanticus</i>		200	10-46	12-40
	<i>Chaetoceros bulbosus</i>		20	40-50	10-25
	<i>Chaetoceros curvatus</i>			15-36	10-15
	<i>Chaetoceros dichchaeta</i>			7-50	10-40
	<i>Chaetoceros hendeyi</i>			14-27	11.5-16
	<i>Chaetoceros neglectus</i>			8.5-15	5.5-10
	<i>Chaetoceros peruvianus</i>			10-32	13-20
	<i>Coscinodiscus</i> 40 umd	40			
	<i>Corethron pennatum</i>			5-82	20-240
	<i>Dactyliosolen</i>			13-90	-140
	<i>Melosira adeliae</i>			15-24	9-25
	<i>Rhizosolenia</i>			2.5-57	-400
	<i>Thalassiosira gracilis</i>	5-28			3.5-9.5
	<i>Thalassiosira maculata</i>	23-71			
	<i>Thalassiosira</i>	5-71			
	<i>Thalassionema</i>			10-80	2 (-7)
	<i>Cylindrotheca closterium</i>			30-400	
	<i>Fragilariopsis curta</i> / <i>cylindrus</i>			10-42/9-12	3.5-6/2-4
	<i>Fragilariopsis kerguelensis</i>			10-76	5-11
	<i>Fragilariopsis pseudonana</i>			4-20	2.5-5
	<i>Fragilariopsis rhombica</i>			8-53	7-13
	<i>Fragilariopsis</i>	2-76			

Appendix IX. Marine protist size

	<i>Halsea trompii</i>			70-160	10-14
	<i>Manguinea fusiformis</i>			49-135	11
	<i>Membraneis challengerii</i>			85-270	33
	<i>Navicula</i> 60 uml			28-60	6-10
	<i>Pseudonitzschia</i> 90 uml			18-70	4-11
	<i>Trichotoxon reinboldii</i>			800-3600	3-10
Dinoflagellates	<i>Alexandrium</i>	20-44 long 16-36 diameter			
	<i>Dinophysis ovum</i>	40-58 long 30-45 diameter			
	<i>Gymnodinium</i> 12 uml	5			
	<i>Gyrodinium lachryma</i>	60-135 long 28-50 wide			
	<i>Oxytoxum criophilum</i>	56-61 long 33-36 wide			
	<i>Prorocentrum</i>	15-22 long 15-25 diameter			
	<i>Protoperidinium</i> het 60 umd	30-50			
Silicoflagellates	<i>Dictyocha speculum</i>	70 diameter			
Chaonoflagellates	<i>Acanthocorbis unguiculata</i>	12 long 11 diameter			
Ciliates	<i>Codonellopsis</i>	69-136 x 45-80			
	<i>Myrionecta rubra</i>	10-70 x 10-50			
	un-ID ciliate	20-200			
	<i>Tontonia</i>	55-80 x 50-75			
Urgo	Urgo				
	Mesh/feeding house filters				

Appendix 10 has been removed for
copyright or proprietary reasons

Appendix X

**Lindsay, M. and Williams, G. (2010).
Distribution and abundance of Larvaceans in the
Southern Ocean between 30° and 80°E.
Deep-Sea Research II 57 (2010) 905–15**

